Université d'Ottawa · University of Ottawa

Seismic Evaluation and Retrofit of Existing Reinforced Concrete Bridge Columns

by

Cem Yalçın

A thesis submitted to
the Faculty of Graduate Studies and Research
in partial fulfillment of
the requirements for the degree of

Doctor of Philosophy

Department of Civil Engineering

The Doctor of Philosophy Program in Civil Engineering
is a joint program with the Carleton University,
administered by The Ottawa-Carleton Institute for Civil Engineering

University of Ottawa
Ottawa, Ontario, Canada
September 1997

Abstract

Bridges like other important lifeline structures must remain in service when they are subjected to strong earthquakes. Many existing bridges, especially those built before the 1970s, are vulnerable to seismic damage since a number of deficiencies with regard to low design force levels, inadequate column confinement and lack of shear capacity were discovered during recent earthquakes.

Bridge columns are expected to withstand seismically induced inertia forces without a significant loss of strength. This can be achieved in old columns through external retrofitting. Many reinforced concrete bridge columns in California were already retrofitted with steel jackets to enhance flexural ductility and shear resistance. Although this retrofitting technique is highly effective, it is also time consuming and costly, especially in view of the fact that high number of columns are yet to be retrofitted. Therefore, a new retrofitting technique has been developed through experimental research that involves external prestressing of bridge columns for improved deformability and shear strength. The supporting experimental work involved testing of 1485 mm high two 550 mm square and five 610 mm diameter circular cantilever columns. The columns were retrofitted with post-tensioned external hoops and high-strength steel straps at different spacing and stress levels. The results indicated that transverse prestressing of shear-dominant columns improved ductility and changed the mode of behavior from a brittle shear response to a ductile flexural behavior.

The research project also included analysis of columns to establish lateral drift demands and capacities for bridge columns in Canada. A comprehensive survey of existing bridges in Canada was conducted to identify and classify common types of

existing bridges in terms of their numbers, types, age, and structural and geometric properties. This information proved to be helpful in establishing column drift capacities and demands. A computer software DRAIN-RC, developed for non-linear dynamic analysis of reinforced concrete structures, was used to determine the drift demands of columns under various ground motions. Drift capacities were computed by a computer program COLA, developed by the author. The program COLA uses proper material models such as confinement of core concrete, extension of longitudinal reinforcement in tension, and buckling of re-bars in compression. The decision for retrofitting depended on the capacity of a column when demand exceeded its capacity.

Acknowledgment

I would like to express my gratitude to Dr. Murat Saatçıoğlu, thesis supervisor, for his guidance, encouragement, and financial support throughout the course of this study. Many thanks to Mongi Grira, laboratory technician and fellow graduate student, for his great effort in my experimental work. Also, many thanks to my other fellow graduate students, Brent Cotter at the Machine Shop and other support staff for many fruitful discussion and help.

I am grateful to the engineers at the Bridge Engineering Department, Ministry of Transportation of all the provinces for providing me crucial bridge inventory information, as well as to Central Precast of Ottawa for donating prestressing cables for this research.

Special appreciation is extended to my parents for their patience and support.

Contents

List of Tables

List of Figures

Notations

A_b Cross-sectional area of longitudinal reinforcing steel.

A_c Core cross-sectional area of concrete column.

A_d Cross-sectional area of bridge deck.

A_g Gross cross-sectional area of concrete column.

A_{hoop} Cross-sectional area of external hoop.

A_e Effective shear area of member.

A_{sh} Total cross-sectional area of transverse reinforcement of circular columns.

A_v Total cross-sectional area of transverse reinforcement of rectangular columns.

AR Aspect ratio (full column height to cross-sectional dimension) of column.

b_c Core dimension measured center-to-center of perimeter hoop.

b_{cx} Core dimension measured center-to-center of perimeter hoop along x-direction of a rectangular column.

b_{cy} Core dimension measured center-to-center of perimeter hoop along y-direction of a rectangular column.

c Depth of neutral axis.

D Diameter of column.

d Effective depth of tension reinforcement.

d_b Diameter of longitudinal reinforcing steel.

E_c Modulus of elasticity of plain concrete.

E_s Modulus of elasticity of reinforcing steel.

E_{sec} Secant modulus of elasticity of confined concrete.

EI_{cr} Stiffness of concrete member at cracking.

EI_c Elastic stiffness of concrete member.

f_c Stress in concrete.

f'_c Cylinder compressive strength of concrete specimen.

f'_{cc} Confined concrete compressive strength in member.

f'_{co} Unconfined concrete compressive strength in member.

f_l Lateral pressure in columns.

f_{le} Equivalent lateral pressure that produces the same effect as uniformly applied pressure.

f_{lex} Equivalent lateral pressure that produces the same effect as uniformly applied pressure in x-direction of a rectangular column.

f_{ley} Equivalent lateral pressure that produces the same effect as uniformly applied pressure in y-direction of a rectangular column.

f_s Stress in reinforcing steel.

f'_s Stress in reinforcing steel.

f_{sh} Strain-hardening stress of reinforcing steel.

$f_{S/Du}$ Limiting stress in compression reinforcing steel.

f_y Yield stress of reinforcing steel.

f_{yh} Yield strength of transverse reinforcement.

f_u Ultimate stress of reinforcing steel.

F_{pb} Yield shear force of an elastomeric bearing with lead plugs.

f_{py} Yield strength of prestressing wire.

f_{pu} Ultimate strength of prestressing wire.

g Gravitational acceleration.

H_L Height of the lugs on the longitudinal reinforcing bar.

I_g Gross sectional moment of inertia.

K Coefficient used in Equation 3.33.

k Concrete confinement coefficient defined in Equation 3.4.

k_1 Concrete confinement coefficient defined in Equation 3.5.

k_2 Concrete conf. coefficient for circular columns defined in Equations 3.7 and 3.8.

k_3 Concrete confinement coefficient defined in Equation 3.19.

k_4 Concrete confinement coefficient defined in Equation 3.21.

k_c Stiffness coefficient used in Equation 4.6.

k_d Post-elastic stiffness of an elastomeric bearing with lead plugs.

k_u Elastic stiffness of an elastomeric bearing with lead plugs.

L Shear span of column.

L_c Column height.

l_d Development length of longitudinal reinforcing steel.

L_e Elastic length of longitudinal reinforcing steel.

L_{pc} Pullout-cone length of longitudinal reinforcing steel.

L_s Span length of bridge structure.

L_{sh} Strain-hardening length of longitudinal reinforcing steel.

L_{yp} Yield length of longitudinal reinforcing steel.

m Mass of bridge structure.

M_y Yield moment of member.

M_{cr} Cracking moment of member.

M_{ult} Ultimate moment of member.

n Nominal shear strength coefficient.

n_c Number of columns.

p' Spiral transverse reinforcement ratio.

P Applied axial load.

P_0 Axial load capacity of a column.

r Coefficient defined in Equation 3.15.

r_c Coefficient defined in Equation 3.49.

s Spacing of transverse reinforcement in longitudinal direction.

s_{hoop} Spacing of external hoops in longitudinal direction.

S_L Spacing of the lugs on the longitudinal reinforcing bar.

s_l Spacing of longitudinal reinforcing laterally supported by the corner of a hoop or the hook of a cross tie.

T Period of a structure.

t_d Thickness of bridge deck.

u_{ACI} Average elastic bond stress proposed by ACI Committee 408.

u_e Elastic bond stress.

u_f Frictional bond stress.

V_c Concrete contribution to nominal shear strength.

V_d Nominal shear strength.

V_{fle} Nominal shear strength calculated by software COLA.

V_{hoop} Shear resistance of external hoops.

V_p Axial load contribution to nominal shear strength.

$V_{prob.}$ Shear force corresponding to probable flexural resistance.

V_s Steel contribution to nominal shear strength.

V_{shear} Nominal shear strength calculated by Equation 3.40.

W Dead weight of bridge superstructure.

W_d Width of bridge deck.

α Angle formed between column axis strut from application point of axial load to center of compression zone in plastic hinging region.

α_f Ratio of initial prestressing strength to yield strength of external hoop.

ε_1 Strain corresponding to peak stress of confined concrete.

ε_{01} Strain corresponding to peak stress of unconfined concrete.

ε_{85} Strain corresponding to 85% of peak stress of confined concrete on the descending branch.

ε_{085} Strain corresponding to 85% of peak stress of unconfined concrete on the descending branch.

ε_c Strain in concrete.

ε_{cu} Ultimate concrete strain.

ε_s Strain in reinforcing steel.

ε_{sh} Strain-hardening strain of reinforcing steel.

$\varepsilon_{S/Du}$ Limiting strain in compression reinforcing steel.

ε_u Ultimate strain of reinforcing steel.

ε_y Yield strain of reinforcing steel.

Δf_s Incremental longitudinal steel stress within the yield region.

Δ_{tip} Lateral tip displacement of column.

δ_{ext} Total extension of longitudinal steel.

ϕ_c Concrete strength factor.

ϕ_s Steel strength factor.

μ_Δ Displacement ductility of column.

θ Critical shear cracking angle.

θ_e Rotation due to extension of reinforcing steel.

ρ Transverse reinforcement ratio.

ρ_l Longitudinal reinforcement ratio.

ρ_s Spiral transverse reinforcement ratio.

ρ_v Volumetric transverse reinforcement ratio.

Chapter 1

Introduction

1.1 General

Bridge structures typically have little or no redundancy in their framing systems. Therefore, the alternate load paths to allow for redistribution of stresses may not be available as in the case of a multi-story, multi-bay, continuous building structures. While the simple layout of a bridge structure makes the prediction of structural response easier, it increases the vulnerability of the bridge to structural collapse, especially under seismic attack. This was evident in the case of bridges that suffered damage during recent earthquakes, especially those in Western United States (California), Central and South America (Mexico, Chile), Middle Asia (Turkey, Armenia, Iran) and Pacific Rim (Japan).

Seismic damage to lifeline structures has recently gained importance, especially after the Loma Prieta earthquake (magnitude of 7.1) of 1989. Among the previous earthquakes, the 1987 Whitter Narrows (magnitude of 5.9) and 1971 San Fernando (magnitude of 6.6) earthquakes also caused considerable damages, leading to revisions of design codes (Bruneau 1990; Mitchell, et al. 1991; Tarakji 1991). San Fernando earthquake revealed a number of deficiencies in design of bridge structures with regard to low design force levels, inadequate column confinement, lack of restrainers between expansion joints, insufficient seat widths at joints, and inadequate anchorage of longitudinal reinforcement. More recently, the 1994 Northridge earthquake (magnitude 6.8) once again proved the vulnerability of old and nonductile structures (Saatcioglu 1994;

Mitchell, et al. 1995; Mitchell, et al. 1995). Lessons learned from previous earthquakes, as well as recent research on seismic response of bridges, have led to revised bridge codes. The revised code provisions incorporate both the design of new structures, and retrofitting existing and old structures. Figures 1.1 through 1.4 illustrate observed damage in bridge columns during recent earthquakes.

The deficiencies in old bridges are direct results of the elastic seismic design methodology that was adopted for almost all bridges prior 1971. The elastic approach resulted in an underestimation of seismic deflections, since member stiffnesses were calculated on the basis of gross cross-sections rather than cracked-sections. Low seismic force levels have resulted in inadequate member capacities and inaccurate estimation of inflection points in members. A direct consequence of this was lack of reinforcement and insufficient development lengths in critical regions of members. Furthermore, inelastic behavior, which is crucial for dissipation of seismic induced energy, was not considered. Thus, potential hinging regions were not detailed to resist seismic forces, resulting in brittle flexural or shear failures.

Development of seismic retrofitting programs that started in the early 70's mainly involved the connection systems in bridges. Subsequently, it was extended to cover the entire bridge superstructure. Consequently, the structures designed by more recent code provisions behaved well in the Loma Prieta earthquake. Much of the current research since the Loma Prieta event has focused on retrofitting older structures, especially the lifeline structures such as bridges. Since then, many bridge columns were retrofitted with steel jackets to enhance flexural ductility and shear resistance.

Many California bridges built before 1971 have inadequate seismic resistance due to non-ductile members and poor connectivity of superstructure elements. The California Department of Transportation (CALTRANS) initiated an extensive seismic retrofitting program. Phase I of this program was implemented prior to 1989 and dealt with tying the superstructure. Phase II of the same program started after 1989 and included seismic analysis of the entire bridge structure, including retrofitting techniques for the whole bridge structure. Retrofitting bridges not only included tying of superstructures to prevent span unseating, but also steel jacketing of columns to increase strength and ductility of

columns and other areas where problems occurred during past earthquakes. It was suggested that liquefaction and abutment slumping could be reduced through site densification or reduction of pore-water pressure buildup; cap beam strength could be increased using external tendons anchored against end blocks; column-cap beam or column-footing joints could be retrofitted using heavily reinforced knee-joint concrete jackets; footings could be retrofitted by increasing plan dimensions and providing additional piles; and finally, old bearings could be replaced by seismic isolation bearings in order to dissipate energy.

It is clear that a great majority of existing bridges in seismically active regions are vulnerable during earthquakes. Therefore, more research is needed to expand knowledge on seismic behavior and design of bridge structures. This research program was directed towards solving some of the problems associated with seismic performance of reinforced concrete bridge columns. More specifically, inelastic deformation demands and capacities of concrete bridge columns were investigated and a new retrofitting technique was developed for those columns that have lower capacities than the estimated demands.

1.2 Review of Previous Research

Review of previous research on seismic performance of bridges was conducted in two parts, to be consistent with the scope of current research. These include, "modeling and dynamic analysis of bridges," and "bridge retrofitting."

1.2.1 Literature Review on Modeling and Dynamic Analysis of Bridges

Ghobarah and Tso (1974) were among earlier researchers who analyzed bridges for seismic excitations. They investigated the behavior of skewed bridges that were damaged in the San Fernando earthquake. The researchers used a beam model with flexural and torsional characteristics. The equation of motion was applied and the mode shapes were obtained. Analytical results showed good agreement with observed bridge damage patterns. It was observed that the contribution of torsional stresses caused considerable deformations of the deck. Furthermore, the columns away from the centerline of bridge deck were found to be more vulnerable due to the leverage action.

Takizawa and Aoyama (1976) studied the effect of biaxial flexure due to two-dimensional earthquake excitation on reinforced concrete columns, and proposed a model. Degrading tri-linear stiffness model was used in bridge analysis. Biaxial effects were found to be significant especially for reinforced concrete materials when a comparison was made with experimental data. However, the same effect was found to be small for non-degrading inelastic cases.

Meyer et al. (1983) analyzed reinforced concrete frame members by considering the finite size of plastic regions. They suggested that a thorough understanding of the behavior of reinforced concrete structures was needed prior to application to bridges. They concluded that it was necessary to form a mathematical model that could simulate the behavior of such structures with reasonable accuracy when compared with test results. As well, the model should be of the type that could be implemented to any non-linear structural software, working efficiently to make non-linear dynamic analysis feasible. It was indicated that the behavior of reinforced concrete members subjected to cyclic loading was controlled by a large number of variables which made accurate modeling a difficult task. For this reason, it was concluded that it would be advantageous to isolate flexural behavior from shear and bar slip. Meyer (1989) also stated that non-linear structural behavior may be caused either by geometric or material non-linearity. Geometric non-linearity is associated with large deformations in the structure, whereas material non-linearity is associated with inelastic behavior of members.

Wilson (1986) formed a 3-D finite element model to correlate measured and calculated bridge responses. Some California bridges have been monitored and the actual response data obtained have been compared with analytical results. The objective was to minimize the correlation factor, J, which was a normalized integral mean square ranging between 0.0 and 1.0. Multi-span simply supported bridges were modeled with a pin joint at one end of the span and a roller joint at the other end. The analyses showed variations in response. Thus, a second model was designed with roller joints replaced with pin joints to account for accumulated debris and high degree of corrosion at the rollers. Furthermore, since the abutment bearings were locked against translation, the adjacent span became an integral part of the abutment, and a soil spring was needed to

accommodate displacements along the longitudinal axis. This ultimately changed the bridge response and produced low J values or better correlation with measured response. This indicates that, when analyzing bridges, it is important to consider not only the design conditions but also the actual conditions in practice.

Somani (1987) investigated the influence of horizontally propagating waves on seismic behavior of long-span bridges. A two-dimensional mathematical model was formed considering soil-structure interaction at the bases of piers. The mass of superstructure was lumped at the top of the column which was integral to the deck. It was concluded that, due to the soil-structure interaction, the fundamental frequency was found to be smaller than the case of fixed-base bridges, and bridges with hinged columns were found to be more vulnerable than those with columns integrally built with the deck.

Ghobarah and Ali (1988) compared seismic response of isolated and non-isolated highway bridges. They analyzed bridges by ignoring the vertical component of earthquake motion. Furthermore, the deck was assumed to be rigid and no soil-structure interaction was considered. The nodes at the piers were allowed to displace in the transverse direction and rotate about the longitudinal axis. For the longitudinal loading, the nodes at the piers were allowed to displace in the longitudinal direction and to rotate about the transverse axis. Clough's degrading stiffness model was used for non-isolated bridges. The analyses were carried out using a step-by-step numerical integration technique with four actual earthquake records accounting for various site conditions, intensity, and frequency content. The selected records were the 1940 El Centro S90W, 1966 Parkfield N65W, 1971 San Fernando S74W, and 1985 Mexico City N90W. It was found that the seismic response of non-isolated bridges showed large inelastic deformations, requiring high ductility design. However, the use of lead plugs in isolation devices proved to be an efficient energy dissipation system. It was also concluded that shearing forces at piers could be reduced by locating the lead plugs at abutments only.

Liu et al. (1989) analyzed a two-span bridge in order to check their newly developed non-linear analysis program, SEISAB-II (SEISmic Analysis of Bridges) which was a new version of SEISAB. The program evolved from the original NEABS (Nonlinear Earthquake Analysis of Bridge Structures) computer program which was

developed by Tseng and Penzien (1973). They included elasto-plastic column element and non-linear expansion joint elements. Later, Imbsen and Penzien (1984) upgraded the program to NEABS-II while including kinematic strain hardening in the column element and one-dimensional bilinear energy-absorbing elements for the expansion joints. Computer programs, SEISAB and SEISAB-II, were developed by the authors. They included some improvements in order for the program to convergence faster and to provide better efficiency.

Saiidi and Ghusn (1989) described a five-spring element (5-SE) model which idealized the plastic region of a column by five axial springs, representing the effects of both concrete and steel. The springs were located at the base of the column. The analysis was carried out using a computer software NEABS-86. The concrete spring, which was located at the centerline of the column, took only compression, whereas the remaining four springs were placed in the corners and acted in compression (composite action consisting concrete and steel) and in tension (steel only). Also, stiffnesses of composite springs were specified as elastic and post yield stiffnesses in tension and compression. In the five-spring element model, foundations were assumed to be rigid and abutments were modeled as pinned or roller elements. Generally, the damping ratio was assumed to be 5%, which was common for almost all the models.

Saadeghvaziri and Foutch (1989) investigated the effect of vertical accelerations on structures. They concluded that the assumption of vertical acceleration being small and always smaller than the maximum horizontal acceleration was a major deficiency in seismic design of buildings and bridges. According to the researchers, modeling of a bridge deck required a 3-D analysis with the vertical component of earthquake motion considered. Thus, bridge decks could be idealized as a grid model with beam elements. Columns could be modeled using inelastic isoparametric plane stress elements to represent concrete and elasto-plastic bar elements to model reinforcing steel. This type of a model could simulate the behavior of reinforced concrete members under non-proportional axial and lateral loads. Here, inelastic properties of both concrete and reinforcing steel were used. The analysis showed that when the transverse motion was considered alone, the columns remained almost elastic. However, when the combined effect of vertical and transverse

motions were considered, higher inelasticity was observed and the possibility of shear failure prevailed.

Kunnath et al. (1990) studied the use of hysteretic models for bridge analysis. The researchers indicated that the earlier hysteretic models were bilinear elasto-plastic models, and essentially represented the behavior of steel members. A degrading stiffness approach was needed to simulate the behavior of reinforced concrete structures. Among the stiffness degrading models, those proposed by Clough and Johnston in 1966, and Takeda et al. in 1970 with a more complex set of hysteretic rules were considered. The researchers concluded that reinforced concrete depended on numerous structural parameters that affected deformation and energy-absorbing characteristics of components, such as concrete strength, steel content, axial stress level, and shear span-to-depth ratio. Thus, a versatile model was required to simulate the behavior in terms of stiffness degradation, strength degradation, pinching behavior, and the variability of hysteresis loop areas at different deformation levels. This would enable the estimation of energy and strength reserves in structures before collapse.

Spyrakos (1990) investigated the significance of soil-structure interaction of short span bridges in seismic analysis. The analysis focused on bridge piers where a single degree of freedom model was used with horizontal and rotational soil springs and damping at the column base. The tributary mass for each pier was obtained by dividing the mass of entire bridge superstructure by the number of piers, and was lumped at pier top. Foundations and piers were assumed massless. The base shear was evaluated including soil-structure interaction with easy-to-use procedures that were recommended to practicing bridge designers.

Zelinski and Dubovik (1991) indicated that there were two different models, namely compression and tension models that could be used to simulate non-linear response of bridges. The researchers simulated non-linear response by using an iterative procedure that utilized a linear elastic program, STRUDL. A series of linear analyses were performed with the end conditions being changed and the analysis repeated. This was done to simulate hinging of columns at the base. The model had its hinge joints released in order to show bridge response that would simulate the "pulling apart" of

hinges. The compression model had these joints pinned together to simulate the bridge movement with hinges closed. Computer generated elastic moment and shear forces were compared with calculated member capacities to determine demand-to-capacity ratios and ductility demands.

Zelinski (1991) investigated the use of elastic response spectra. The researcher indicated that the maximum elastic force demands on structures could be determined using linear response spectra or modal analysis. Among the linear programs considered were STRUDL, ABACUS, SAP 90, and BSAP, which were also widely used by consultants. The author further indicated that CALTRANS retrofit philosophy was based on designing columns elastically for 25% of the maximum elastic force derived from linear dynamic analysis. Harper (1991) also investigated the use of elastic spectra and concluded that CALTRANS' ARS spectra could be used with a bedrock acceleration of $0.7g$ and alluvial material deeper than 150 feet, to perform dynamic analyses of bridges. A linear computer program such as STRUDL could be used and iterated to take into account the non-linear behavior of structures and to capture stiffness degradation. If the ductility demand exceeded the ductility capacity of the column, the joint behavior was assumed to behave more like a pin rather than a fixed end condition. Therefore, the model's end conditions were changed accordingly.

Akkari and Hoffman (1993) studied modeling and analysis of bridges. They indicated that a bridge superstructure could be modeled with a pin on one side of the bent cap and a roller on the other side, with a cable element across the cap. Bottom of the column could be assumed as rigid or fixed to the footing so that it could also be modeled as a pin connection, assuming a plastic hinge has formed.

Eberhard et al. (1996) used DRAIN-2DX, a version developed by Prakash et al. in 1993, to study the effectiveness of seismic restrainers. The researchers investigated relative displacements at hinges, abutments and simple supports, and developed restrainer design methods.

Kunnath and Gross (1996) analyzed a damaged bridge structure using IDARC, an inelastic damage analysis program. They modeled Cypress Viaduct, which collapsed during the 1989 Loma Prieta earthquake. IDARC features a distributed flexibility model

to represent the spread of plasticity, a hysteretic force-deformation model which represents stiffness degradation, strength deterioration, and pinching effect, and a shear panel element to model inelastic flexure and shear independently. Each bent of the viaduct was modeled separately as a two dimensional structure. Lumped masses were assigned to each node of the beam element in order to obtain the response of vertical accelerations in flexure. The results of time-history analyses showed that the collapse of the bent was initiated by the shear failure of pedestal regions, which was the observed failure mechanism during actual earthquake response.

1.2.2 Literature Review on Bridge Retrofitting

Literature review on bridge retrofitting was conducted while keeping one of the main objectives of the proposed research in mind i.e., development of a new retrofitting technique for bridge columns. Therefore, while the available literature on bridge retrofitting in general was reviewed, the emphasis was placed on bridge columns.

The concept of confining existing reinforced concrete bridge columns started in the mid 80s when bridges were severely damaged by earthquakes due to non-ductile column behavior. Retrofitting bridge columns to increase concrete confinement was intended to improve ductility under combined axial compression and flexure to dissipate seismic energy while maintaining inelastic strength capacity. Retrofitting techniques were also developed to increase shear strength of bridge columns, especially for short columns and columns under-designed in shear.

Early research on concrete confinement was conducted by Richart et al. (1928, 1929). The study included plain concrete cylinders subjected to uniform fluid pressure. The research program later extended to include concrete cylinders confined by circular spirals. The researchers established a relationship between lateral pressure and concrete strength. King (1946) subsequently studied the effect of confinement on strength of reinforced concrete columns. The stress-strain relationship of confined concrete was studied by various researchers (Chan 1955, Roy and Sozen 1963, and Kent and Park 1971). Their proposed models included size, strength, amount, and spacing of lateral reinforcement as confinement parameters. The effect of distribution of longitudinal

reinforcement and the resulting tie arrangement was first discussed by Park and Paulay (1975), and investigated by Vallenas et al.(1977), and Sheikh and Uzumeri (1980, 1982). Sheik and Uzumeri, for the first time, showed experimentally that the effect of tie arrangement on concrete confinement was significant, and developed an analytical model incorporating this parameter. More recently, Saatcioglu and Razvi (1992) conducted an extensive investigation on concrete confinement and developed a general analytical model for square, circular and rectangular columns.

Roberts (1991) reported that common details of circular and square columns in bridges constructed prior to 1971 consisted of #4 (12.7 mm diameter) transverse hoops at 12" to 18" (304.8 mm to 457.2 mm) on centers, regardless of column size and area of main reinforcement. The extension of dowels into the foundation, and lap-splices in potential hinge regions were found to be inadequate. Columns built after 1971 typically had #6 (19.1 mm) hoops or spirals at 3" (76.2 mm) pitch. Improvements were also made in dowel lengths and splicing. Roberts also indicated that the most common form of retrofitting concrete columns was steel shells placed around the columns. It was mentioned that other techniques, such as wrapping cables or fiber reinforcing, were under development. Initial results on the fiber-wrap technique were reported to be encouraging. Finally, tests indicated that steel encasement significantly increased shear strength and ductility of columns.

Zelinski and Dubovik (1991) reported that damages observed in bridges usually occurred in single-column bridges since they possessed less redundancy. It was indicated that tests of round and elliptical steel casings, fiber-wrap, and wire-wrap were being conducted as part of an ongoing research program at the University of California at San Diego. Test results showed that circular steel casings produced a displacement ductility of about 8 compared to non-retrofit columns which showed about 1.5. Also, fiber-wrapped and steel-wrapped columns exhibited displacement ductility ratios of 6 and 7, respectively.

Zelinski (1991) investigated causes of bridge damage observed during earthquakes. It was reported that non-ductile columns, inadequate cap bar development, low capacity pin connections, poor foundations, lap splice column connections, low capacity footing connections, limited torsional capacity in outriggers, knee joints without sufficient

ductility, and short transverse bearing seats constituted major structural deficiencies. The author reported that the collapse of Cypress Viaduct during the Loma Prieta earthquake heightened the awareness of retrofitting multiple-deck structures. Retrofitting with horizontal and vertical prestressing, steel jacketing, and bracing with dampers included some of the suggested techniques.

Harper (1991) indicated that the most common retrofit scheme for circular piers was the steel encasement. The steel encasement provided a composite action to increase strength, and confinement to improve ductility and toughness. The steel jackets used in present practice have a thickness of 3/8" (9.5 mm), covering the entire plastic hinging region. Polystyrene material was wrapped around the column first, and grout was injected between the column and the steel casing. Two types of retrofit by steel jacketing exist. The first type involves full column retrofit where the purpose of the casing is to increase confinement and shear capacity, but not the moment capacity. Therefore, a gap of 2" (50.8 mm) is provided at the ends of the column assuming that the footing is capable of maintaining probable plastic moment of the column. The second type involves partial column retrofit for columns having excessive ductility demands. In this case the steel casings are placed at the ends of columns where plastic hinges occur without leaving any gap. The steel casing increases confinement of the column after the spalling of cover concrete.

Jones and Schroeder (1991) investigated the collapse of Cypress Viaduct in order to develop an appropriate retrofit scheme. Two retrofit schemes were selected. The first included clamping structural steel beams around the existing columns, while the second required bolting structural steel plates around the columns. Weak areas were retrofitted by steel confinement plates, tightened by external prestressing rods.

Rodriguez and Park (1991) explained the strengthening techniques and elements used in Japan to increase strength and ductility of bridges. Accordingly, to increase strength; infill walls such as cast-in-place concrete panels, precast concrete wall panels, and concrete block wall panels are used. Bracing elements, such as tension and compression cross bracing (steel or concrete), tension cross bracing (steel), and K-bracing (steel or concrete) are also used. To increase strength together with ductility infill walls,

bracing elements, steel jacketing (circular and rectangular), steel straps, and welded wire fabrics are used. To increase ductility alone; columns are reinforced. Test results showed that frame structures with retrofitted columns, using the techniques described above, did not increase the flexural strength significantly but certainly enhanced the shear strength and ductility. Also, steel jackets consisting of added concrete with longitudinal and transverse reinforcement improved axial and shear strengths of columns, while both the flexural strengths of columns and strengths of beam-column joints remained the same. The connection of the retrofitted column to the floor could not be achieved properly since it was difficult to pass the steel casing or wire fabric through the floor. Therefore, the flexural capacity of the column could not be augmented as much as its axial and lateral strengths. The concrete cover was chipped and roughened prior to jacketing to increase bond between the old and new concretes. Square columns, retrofitted with steel casings and straps with structural angles in corners, were also tested.

Chai et al. (1991) investigated all possible sources of seismic damage in bridges. They indicated that structural inadequacies in many older bridge columns were due to inadequate flexural strength caused by low lateral seismic force coefficients specified in design codes prior to 1971. This also resulted in higher ductility demands and inadequate flexural ductility. Furthermore, bridges constructed before 1971 contained insufficient transverse reinforcement where columns had #4 transverse reinforcement at 12" regardless of the column sectional dimension. Many bridges were spliced by a development length of 20 times the bar diameter with footing dowels. This lap length was found to be insufficient for developing the yield strength of longitudinal bars, especially when large diameter-bars were involved. Other problems included inadequate shear strength and inadequate anchorage of transverse reinforcement which resulted in brittle shear failures. Short columns exhibited low ductility and poor energy-absorption characteristics. Bridge footings were identified as other elements with inadequate performance. Pile caps and footings in older bridges were often provided with only a bottom mat of reinforcement assuming that only the gravity load was resting on the footing and that the lateral seismic force would cause no disturbance. Joint regions, either at column-footing or column-bent cap beam connections, were also identified as potentially critical regions due to high shear

stresses expected during strong earthquakes. However, these regions in old bridges were not designed to resist such stresses. Tests of rectangular columns with oval steel shells, used for shear strength enhancement, showed similar performance as circular columns. Column tests conducted by the authors showed that closely spaced lateral confinement increased the ultimate compressive strain from 0.005 to 0.03 and higher, with displacement ductility factors of more than 6.

Coffman et al. (1993) acknowledged the absence of seismic resistance in long circular concrete bridge columns built between 1950 and mid 1970. Many of these bridges have unconfined longitudinal bar splices in potential plastic hinge zones due to minimal transverse ties. The researchers tested columns that were retrofitted by wrapping individual hoops around the column face. The specimens were 3048 mm long and 457 mm in diameter. A scale factor of 1/2 was used to ensure normal reinforced concrete behavior. A constant axial load was applied ranging between 700 KN and 490 KN, accompanied by lateral loads. The results showed that retrofitting did not alter the stiffness of the column and did not significantly increase the strength. However, a significant increase in energy dissipation was observed.

Ersoy et al. (1993) tested columns retrofitted by jacketing. The columns were jacketed by enlarging the existing cross section with a new layer of concrete that was reinforced with both longitudinal and transverse reinforcement. Test results showed that under uniaxial loading, repaired and strengthened square columns behaved well when the jacketing was done after unloading. About 80% to 90% of the capacity of the reference specimen was achieved in these columns. Columns strengthened under load also behaved well. However, columns repaired under load developed only 50% of the capacity. Repaired and strengthened columns under cyclic loading showed 90% of the reference specimen's capacity.

Valluvan et al. (1993) performed tests on square columns subjected to cyclic loading to study the effects of splicing and methods of strengthening. They indicated that the columns sometimes failed due to low splice tensile strength. Two approaches for strengthening column splices were tested. First, the spliced bars were made continuous so that forces could be transferred directly without relying on the bond strength between

spliced bars and surrounding concrete, and secondly, by improving confinement with additional ties in the column splice region. Test results showed that providing continuity in the splice region by welding longitudinal bars enabled columns to yield in tension under reversed cyclic loading. Also, additional internal ties were required in order to prevent the outward thrust produced by the eccentricity between spliced bars. On the other hand, adding internal ties may likely reduce the splice strength due to the micro cracking caused by removal of concrete cover. The grouted angles and straps constituted the best retrofit technique, but it was found to be impractical. Therefore, it was concluded that retrofitting of square columns by using external ties was an easy and cost-effective retrofit scheme.

Priestley et al. (1993) conducted tests of half scale retrofitted cap-beam column joints. Square columns were replaced by well-confined circular columns. End-regions of cap-beams were replaced by unbonded prestressing tendons to increase flexural and shear strength of the existing and replaced portions of the cap-beam. Strength and stiffness properties were accurately predicted from a cracked-section analysis. A reduction of 25% in design loads could be achieved without affecting the overall stability of the structure. The damage was limited to the spalling of concrete and the measured plastic hinge length agreed well with its predicted value.

Mitchell et al. (1994) described common deficiencies that exist among reinforced concrete columns such as inadequate development of vertical bars, splicing of column bars, dowels being short, insufficient amount of transverse reinforcement resulting poor confinement, insufficient shear strength, poor detailing of confinement reinforcement, insufficient flexural strength and ductility. Various retrofitting solutions were suggested in order to minimize the adverse effects of the above problems. It was reported that the most common practice was to install steel jacketing which would provide passive confinement, increase shear strength, reduce tendency of buckling of the vertical bars, and improve ductility. It was further reported that rectangular steel jackets were not as effective as circular or elliptical jackets. It was recommended that steel jackets be stopped above the footing level in order to avoid excessive demands on the footing. Alternate solutions, such as prestressed wire wraps, pressure-grouted fiber glass sleeves, and

jacketing by reinforced concrete of existing columns were also suggested. It was indicated that the latter schemes were still being investigated.

Stanton et al. (1996) retrofitted a square reinforced concrete column using carbon fiber wrapping. They acknowledged the effectiveness of steel jacketing, while claiming that it was somewhat restrictive due to roadway clearances and difficulties in site welding. Their test specimen was based on an existing building column built in 1971, and typically laterally reinforced with #3 hoops at 18". The original dimension was 22" and 34" square. It was sized down to 11" and contained four #5 longitudinal bars. The column was subjected to cyclic loading with an axial load level of 33% of its concentric load capacity. Up to 5% drift was achieved after retrofitting. The failure of the fiber sheet occurred at the column corner. It was noted that fiber wrapping did not increase the column flexural stiffness and strength, whereas, steel jacketing provided vertical strength, increasing the moment capacity and hence the shear demand on the column.

Jaradat et al. (1996) reported the deficiencies in confinement of pre-1971 reinforced concrete bridge columns as having very little transverse reinforcement, typically, #3 or #4 hoops at 12", regardless of the column size. Xiao and Ma (1996) developed an analytical model to predict lateral force and displacement of reinforced concrete bridge columns having lap-splices, considering both flexural and bond slip deformations. They also recommend a retrofit design procedure for steel jacketing of columns. The following steps were recommended for the retrofit design:

1. Analyze the force-displacement response and find ductility capacity.
2. Compare the computed ductility factor with the ductility demand estimated from structural analysis.
3. Carry out retrofitting if the calculated ductility is less the estimated ductility.
4. Assume a thickness of the steel jacket and a target ductility.
5. Perform calculations until desired ductility at a certain thickness is achieved.

Gamble et al. (1996) tested nine full-scale 1220 mm and 1370 mm diameter bridge columns with longitudinal reinforcement ratios ranging from 1.6% to 1.9%. The bridges built in late 1960's had $30d_b$ lap-splices and minimum lateral reinforcement of #3 at 12" with lack of positive end anchorage by hooks or other means. The columns were

retrofitted by externally tensioned steel bands, externally tensioned prestressing strands, thin fiberglass jacketing laid up of cloth and epoxy resin, and thicker fiberglass jacketing made of four pre-formed layers which were glued to the column, as well as to each other. The prestressing strands were 15.24 mm in diameter and stressed to about 186 KN. All retrofitting techniques were successful. No difference was observed between stressed or "active" systems, and fiberglass or "passive" systems, in terms of load-deflection relationships. The amount of stressing and the temperature effects for fiber sheets were reported to be examined in the future.

Buckle and Mayes (1989) reviewed the effect of seismic isolation at bent cap level which involved separation of the superstructure from its substructure. They indicated that the seismic isolation increased the fundamental period of vibration and thus the structure was subjected to lower earthquake forces. The analysis of six bridges showed that the demand for non-isolated bents were much higher than their capacities. It was suggested that the application of seismic isolation to bridge structures, especially to those built before 1971 would result in significant improvements of column connections, strength and ductility of columns and substructures, and seat widths for girders.

The importance of retrofitting was investigated by Selna et al. (1989, 1989) in terms of its cost. The researchers concluded that retrofitting formed only a fraction of what a new construction would cost and thus recommended as the only logical choice. Also, a full scale model of a box girder deck was tested to investigate the behavior of restrainers. The test results showed that the measured capacity of the retrofitted system was slightly grater than the design yield load for the restrainers. The actual failure occurred in the reinforced concrete diaphragms due to combined bending and punching shear.

Ehsani and Saadatmanesh (1990) investigated the effectiveness of glass-fiber-reinforced-plastic (GFRP) plates in terms of their adhesion and strength when bonded to tension flanges. The GFRP consisted of 70% glass (type E) by weight. Its ultimate strength and the modulus of elasticity were 380 MPa and 37200 MPa, respectively. It was found that the success of this material depended to a great extent on the type of the epoxy employed. The viscosity of the epoxy used was similar to that of the cement paste applied

in practice, and yielded good results. Up to 100% increase in applied load was observed for the same mid-span deflection.

Yashinsky (1991) suggested that the protection of weak columns could be achieved by changing the stiffness of some bridge elements, making columns pinned in the longitudinal direction while strengthened in the transverse direction. Furthermore, it was indicated that stiffening the abutments could reduce the period of the structure and draw forces from nearby columns into the abutments.

Seismic evaluation of Golden Gate bridge was conducted by Seim and Rodriguez (1993). The results of their seismic analyses showed that a major earthquake on a nearby San Andreas or Hayward faults would likely to cause severe damages. The suggested retrofitting techniques included providing dampers between the main span and the towers, constructing new ductile concrete walls inside the pylons, strengthening of base plates of the towers to overcome the uplift motion, and installing of post-tensioning tendons at the top of the piers to provide confinement since the piers were subjected to high bearing stresses under uplift conditions. Astaneh-Asl and Shen (1993) suggested an alternate retrofit technique to the Golden Gate Bridge where the base of the pier could be allowed to rotate or rock. Elastic analysis was conducted and the rocking effect was designed so that the particular retrofit plan would result in an "almost elastic" response.

Akkari and Hoffman (1993) summarized the proposed retrofitting methods to be used for the San Francisco Bayshore Freeway Viaduct. The retrofitting strategy included tying the superstructure for its continuity, retrofitting the columns with additional vertical main reinforcement, and circular steel jackets, retrofitting multi-column bents with cross bracings, and finally retrofitting footings to accommodate transverse forces at the bents due to cross bracing.

Lobo et al. (1993) investigated the impact of viscoelastic braces on frame structures since they have an ability to dissipate energy while the structure remains elastic. One of the characteristics of reinforced concrete structures was stated to be their inelasticity and ability to develop permanent deformations. Viscoelastic dampers would provide a good solution to minimize this behavior. It was reported that scaled model experiments showed viscoelastic dampers to reduce overall structural response.

Alcocer (1993) and Alcocer et al. (1993) experimented the behavior of a jacketed slab-beam-column joint. The specimen was scaled to 2/3 of the original section. Bi-directional cyclic load history was applied and inter-story drift angles were found. The load history was applied in displacement control mode. Joint confinement was provided by a cage comprised of structural steel angles at the corners, and flat steel bars in the middle. Tests indicated that jacketing was effective to rehabilitate existing structures. The rehabilitated specimens showed better stiffness, strength, and high energy dissipation compared to existing structures.

1.2.3 Conclusions From Previous Study

The following conclusions may be drawn from the review of previous research presented in the preceding section.

- No literature was found on the inventory of existing bridges in Canada describing their numbers, types, age, and most importantly their classifications in terms of structural and geometric properties. This information is important in identifying common types of bridges so that their seismic vulnerability can be assessed.
- Many researchers showed that two dimensional modeling and planar analysis produce acceptable results in assessing dynamic response of bridge structures. Some researchers used linear dynamic analysis software, such as, STRUDL, ABACUS, SAP90, BSAP, and simulate the non-linear effects by iterating changes in the geometry of structure for each time step. Programs such as NEABS, SEISAB, IDARC, or ADINA can be used for non-linear analysis. But, both linear and non-linear programs have deficiencies in estimating the behavior of reinforced concrete members accurately due to lack of proper hysteretic models.
- Most bridges built prior to 1971 have structurally deficient columns. These columns lack either sufficient confinement or shear capacity, both resulting from inadequate transverse reinforcement.
- Among the retrofitting techniques considered for bridge columns, steel jacketing appears to satisfy all the requirements. However, this technique may be labor and

material intensive, providing a costly solution. A more practical and economical alternative may be necessary for extensive retrofitting of existing bridge columns.

- Retrofitting bridge columns using prestressing hoops or external strapping can be an alternative technique to steel encasement since all the material is readily available and its cost can be very low when compared with steel jacketing.
- Most of the previous experiments on bridge columns were conducted on flexure-dominant elements. It is necessary to consider shear-dominant columns as they suffered more damage during recent earthquakes.

1.3 Research Needs

It has become clear from the review of previous literature that more research is needed to mitigate seismic vulnerability of existing bridges in Canada. More specifically, the following areas need to be researched:

- Inventory of existing bridges in Canada with well established structural characteristics so that a classification of bridges can be made for further study.
- Capacities of existing bridge columns in terms of strength and inelastic deformability.
- Deformation demands of existing bridge columns through dynamic inelastic analysis, based on actual earthquake records.
- New and improved retrofitting techniques for bridge columns in order to achieve superior performance during earthquakes.

1.4 Objectives and Scope

The objective of the research project reported here is to assess seismic vulnerability of typical or most common types of bridges in Canada in terms of their strength and deformation capacities, as well as deformation demands. The objective also includes development of methods by which the capacity of existing reinforced concrete columns can be augmented through retrofitting.

The following scope is employed to achieve the stated objectives:

- Survey of existing bridges in Canada to identify common types of bridges. These bridges are then classified according to their geometric and structural properties for determination of their deformation capacities and demands.
- Development of a computer software to establish strength and deformation capacities of bridge columns.
- Determination of maximum drift demands of columns through dynamic inelastic response history analysis.
- Testing of large-scale bridge columns to develop retrofitting schemes to improve shear and flexural response of existing columns in the inelastic range of deformations.
- Presentation of results.

1.5 Major Tasks of the Research Program

The research program consists of four major tasks as outlined below. The details of each task are presented in Chapters 2 through 5.

- Survey of existing highway bridges in Canada.
- Computation of column strength and deformation capacities.
- Dynamic inelastic analysis and prediction of drift demands.
- Experimental research to develop retrofitting techniques.

Figure 1.1 Columns of Bull Creek Channel Overpass at Hwy. 118 damaged during the 1994 Northridge Earthquake. (Saatcioglu, 1994)

Figure 1.2 Columns of Foothill Boulevard Undercrossing damaged during the 1971 San Fernando Earthquake. (Bertero, 1985)

Figure 1.3 Column shear failure of Bull Creek Channel Overpass at Hwy. 118 damaged during the 1994 Northridge Earthquake. (Saatcioglu, 1994)

Figure 1.4 Column failure of Interstate 10 highway bridge undercrosing at Lacienega and Venice during the 1994 Northridge Earthquake. (Saatcioglu, 1994:)

Chapter 2

Bridge Survey

2.1 General

A comprehensive survey of Canadian highway bridges was initiated by the author. The survey was conducted to identify common types of reinforced concrete bridges used in Canada, in terms of their geometric and structural properties. This information allows categorization of bridges according to their types. Bridges in each type can then be analyzed for capacity and demand calculations, and the results can be generalized within each group.

The inventory of existing highway bridges was obtained from the Ministries of Transportation of Provinces. The data which was analyzed was sent originally in the form of spreadsheet files. This information is briefly summarized in the following sections.

2.2 Ontario Bridges

There are about 16,000 bridges and culverts in Ontario. Approximately 25% of this quantity represents culverts. A database of about 7,000 bridges obtained from the Ministry of Transportation of Ontario revealed the following results:

- 87% of all bridges have concrete deck, 1% have steel deck, and 12% have timber deck.
- 46% of all bridges have their main girders in concrete, 49% have steel, and 5% have timber.

- About a half of all bridges having their main beams concrete are simply supported while the other half is continuous.
- In the case of steel main beam bridges, about 80% of them are simply supported and the remaining 20% are continuous.
- Large majority of timber bridges are simply supported.
- Among concrete bridges, 37% have 1 span, 16% have 2 spans, 27% have 3 spans, and 20% have 4 or more spans.
- In steel bridges, 63% have 1 span, while 10% have 2 spans, 14% have 3 spans, and 13% have 4 or more spans.
- 84% of timber bridges have 1 span.
- 67% of all bridges having 2 or more spans have concrete columns, 2% have steel columns, and the rest are listed as "unknown".

Table 2.1 and Figure 2.1 summarize the classification of Ontario bridges.

2.3 Alberta Bridges

There are more than 14,000 bridges and culverts in Alberta. Approximately 60% of this quantity represents culverts. A database of about 6,000 bridges obtained from the Ministry of Transportation of Alberta revealed the following results:

- 74% of all bridges have their main beams in concrete, 13% have steel, and 13% have timber.
- 95% of all bridges having their main beams concrete are simply supported while the other 5% is continuous.
- About 70% of steel main beam bridges are simply supported and the remaining 30% are continuous.
- All timber bridges are simply supported.
- Among the concrete bridges; 50% have 1 span, 9% have 2 spans, 34% have 3 spans, and 7% have 4 or more spans.
- In steel bridges, 30% have 1 span, 12% have 2 spans, 36% have 3 spans, and 23% have 4 or more spans.

- 61% of all timber bridges have 1 span, the remaining 13% have 2 spans, 17% have 3 spans, and 9% % have 4 or more spans.
- Only 27% of all bridges with more than 2 spans have concrete columns and 19% have steel columns while the rest 53% are timber columns.

Table 2.2 and Figure 2.2 summarize the classification of bridges in Alberta.

2.4 British Columbia Bridges

The information obtained from the Province of British Columbia was not as detailed as those presented earlier. The bridges in British Columbia can be classified as 70% one-span, 20% two-span, and 5% three or more span bridges. Among all the existing bridges, 61% consists of stringer type spans and 12% have box girders.

2.5 Saskatchewan Bridges

There are 3183 bridges in Saskatchewan. Of this number, 29 % are concrete, 4% are steel, 66% are timber and 1% are culverts. Among concrete bridges; 17% are cast-in-place, 24% are precast, and 59% are prestressed. Among steel bridges; 52% are steel girder type, 48% are truss, and remaining 5% are classified as other types.

2.6 New Brunswick Bridges

There are 3160 bridges in New Brunswick. Of this number, 26 % are concrete, 24% are steel, 24% are timber, 24% are culverts, and remaining 2% are classified as other types. Among concrete bridges, 55% are cast-in-place, 2% are precast, 38% are prestressed and 5% are post-tensioned type bridges. Among steel bridges, 84% are steel girder type, 11% are truss, and remaining 5% are classified as "other types."

2.7 Prince Edward Island Bridges

In the province of Prince Edward Island there are 157 bridges. 46% of them are concrete, and 54% are timber bridges. Among the concrete bridges, 69% have 1 span, and 33% of all concrete bridges have circular columns while the rest are supported by steel tubes or piles. Among the steel bridges, 64% have a single span.

2.8 Bridges in Other Provinces

No information was obtained regarding bridge inventory and column details from the provinces of Quebec, Nova Scotia, Newfoundland and Northwest Territories.

2.9 Classification of Bridges and Their Columns

In addition to the bridge statistics presented in the preceding sections, about 300 bridge drawings were obtained from the ministries of Ontario, British Columbia, and Alberta to further study bridge design details used in Canada. Following results were obtained from these drawings and the Canada-wide bridge inventory survey:

2.9.1 Bridge Superstructure

The following statistical conclusions were obtained from the bridge survey conducted, relative to the bridge superstructure:

- Common bridge types are 2, 3 and 4-span continuous and simply supported bridges with 2, 3 and 4 traffic lanes. Figures 2.3 and 2.4 illustrate most common bridge types found from the survey.
- Each bent consists of 1 or 2 columns for 2 or 3-lane bridges; 3 columns for 4-lane bridges.
- Average deck width for a 2-lane bridge is 12 m with a standard deviation of 2.0 m.
- Average deck width for a 3-lane bridge is 16 m with a standard deviation of 1.5 m.
- Average deck width for a 4-lane bridge is 20 m with a standard deviation of 2.0 m.
- Round-voided post-tensioned decks have:
  - An average span length of 34 m with a standard deviation of 5.8 m.
  - An average axial load of 11.7% of column concentric capacity, with a standard deviation of 3.3%.
  - $t_d = 0.035L_s + 160$ (2.1)
  - $A_d = 1096W_d - 3078592$ (2.2)
- Rectangular-voided post-tensioned decks have:

- An average span length of 50 m with a standard deviation of 7.8 m.
- An average axial load ratio of 13.4 % of column concentric capacity with a standard deviation of 5.8 %.
- $t_d = 0.035L_s + 259$ (2.3)
- $A_d = 748W_d + 1382678$ (2.4)

- Slab-on-girder decks have:
  - Span length varies between 10 m to 60 m.
  - $t_d = 0.038L_s + 630$ (2.5)
  - $A_d = 579W_d + 1611000$ (2.6)

where t_d is the deck thickness in mm; L_s is the span length in mm; A_d is the cross sectional area of deck in mm^2; W_d is the width of deck in mm. The above equations are obtained through linear regression analysis. Figures 2.5 to 2.7 show plots of above linear regression analysis.

2.9.2 Bridge Columns

Column details from above mentioned provinces show a typical design pattern where bridges designed before the 70s have poorly confined columns. Usually #3 or #4 reinforcement, depending on the longitudinal reinforcement bar size, were used for transverse reinforcement at a minimum spacing of 12", regardless of the column dimensions. The most common detail in circular columns designed in that era was the use of individual hoops with lapped ends. Columns designed before the 60s had a hoop spacing of 18". Bridges built after the 70s have spirally reinforced circular columns with a pitch of 3", and after the 80s the pitch was reduced to 50 mm. Square or rectangular columns usually had a tie spacing of 300 mm, even after the 70s, and has not changed until present. Pre-70s bridges show insufficient cross ties and 90° hooks in rectangular columns. Since then, the tie detailing has improved with 90° hooks replaced by 135° hooks. Furthermore, more cross ties are being added as transverse reinforcement to improve concrete confinement. More bridges that were built in recent years had circular columns. The concrete strengths indicated in the drawings were changed over the years, as well. Pre-70s bridges had 20-25 MPa

concretes. Currently, 30-35 MPa concretes are used for bridge piers. Reinforcing steel strength also changed from 260 MPa to 400 MPa. Some of the above mentioned column details were shown in Appendix B. Figure 2.8 shows a typical hoop spacing used in bridge columns.

Aspect ratio of columns plays an important role in dictating the mode of behavior in columns, and can be defined as the ratio of full column height to its width. The average aspect ratio of the columns surveyed was found to be 5.44, with a standard deviation of 1.26. When the column ends were fixed, the aspect ratio reduced to one half the above average value, i.e., 2.72. Figure 2.9 shows the range of aspect ratio taken from a sample of about 200 columns.

Sectional diameter of circular columns was found to vary between 1000 mm and 2000 mm, with an average diameter of 1650 mm in rectangular-voided decks and 1350 mm in round-voided decks.

2.10 Evaluation of Material Strengths According to Ontario Highway Bridge Design Code (OHBDC), 1991, Third Edition

When concrete and reinforcing steel strengths were not readily available, or not clear from the bridge drawings surveyed, the values recommended by the Ontario Highway Bridge Design Code (OHBDC 1991) were adopted as representative values of practice. Accordingly, The minimum yield strength of reinforcing steel was estimated to be 210 MPa for bridges built before 1914, 230 MPa for bridges built between 1914 and 1972, 275 MPa for bridges built between 1972 and 1978, and 350 MPa for bridges built since 1978.

If the concrete had no visible sign of deterioration, concrete strengths of 15 MPa for substructure, 20 MPa for superstructure, and 25 MPa for prestressed concrete beams were suggested by OHBDC for structural evaluation purposes. These values were adopted when necessary. It may be of interest to note that, if the concrete had visible signs of deterioration, tests of drilled cores having a diameter of not less than 100 mm were required by OHBDC to verify the concrete strength.

2.11 American Association of State Highways and Transportation Officials (AASHTO) Requirements for Column Reinforcement

The American Association of State Highways and Transportation Officials (ASSHTO) requirements for column reinforcement were reviewed based on years of practice. This code has been used in Canada, and is still commonly referred to as a source document. In the 1957 edition of ASSHTO, the requirement for longitudinal reinforcement ratio for spirally reinforced columns was between 0.01 to 0.08, and the volumetric ratio of the spiral reinforcement was defined as

$$p' = 0.45\left(\frac{A_g}{A_c} - 1\right)\frac{f_c'}{f_s'} \tag{2.7}$$

The transverse reinforcement size used in columns with diameters of 18" or less was #3, otherwise #4. Maximum clear spiral pitch was 3". The longitudinal reinforcement ratio for tied columns varied between 0.01 and 0.04. The maximum lateral tie spacing was 12", although for very large columns or pier shafts the spacing could be greater than 12'. Additional cross ties were provided to support intermediate longitudinal bars whose distance from any tied bar exceeded 2'.

The 1977 edition of ASSHTO had the same provisions for longitudinal reinforcement as those specified in the 1957 edition. The ratio of spiral reinforcement ρ_s was changed as;

$$\rho_s = 0.45\left(\frac{A_g}{A_c} - 1\right)\frac{f_c'}{f_y} \tag{2.8}$$

where the yield strength f_y was specified as 414 MPa. The maximum clear spacing of spiral was 3", which was the same as that specified in the 1957 edition. The vertical spacing of ties was taken as the least dimension of column section or 12", whichever was smaller. The first tie was to be placed at half vertical spacing above the footing. The tie bend was to have a 135° hook at the end. In seismic areas, columns were detailed to provide adequate strength and ductility, however, no specific procedure was mentioned.

Seismic design provisions were first mentioned in the 1983 edition of ASSHTO. The transverse reinforcement for confinement at plastic hinges was defined for spiral reinforcement as

$$\rho_s = 0.45\left[\frac{A_g}{A_c} - 1\right]\frac{f_c'}{f_{yh}} \tag{2.9}$$

or

$$\rho_s = 0.12\frac{f_c'}{f_{yh}} \tag{2.10}$$

whichever was greater. The total cross sectional area of rectilinear hoop was to be

$$A_{sh} = 0.30sb_c\frac{f_c'}{f_{yh}}\left[\frac{A_g}{A_c} - 1\right] \tag{2.11}$$

or

$$A_{sh} = 0.12sb_c\frac{f_c'}{f_{yh}} \tag{2.12}$$

whichever was greater, where s is vertical spacing of hoops in inches with a maximum of 4", and b_c is the core dimension of tied column in inches.

2.12 Ontario Highway Bridge Design Code (OHBDC) Requirements for Column Reinforcement

First OHBDC came out in 1983. AASHTO code had been used until then as a guide for the design of highway bridges in Canada. The OHBDC 1983 edition refers to the seismic provisions specified in CSA Standard CAN-A23.3-M77, Code for the Design of Concrete Structures for the buildings.

The OHBDC 1991 edition refers seismic detailing to CSA Standard CAN3-A23.3-M84, Design of Concrete Structures for buildings. Hence, the longitudinal reinforcement ratio is to vary between 1% and 6%. The transverse reinforcement requirement is the same as that of the 1983 edition of AASHTO code. Accordingly, the transverse reinforcement is to be spaced not to exceed one-quarter of the minimum member dimension, 100 mm, or 6 times the diameter of the smallest bar. In the recent concrete code for buildings, CSA Standard A23.3-94, the value 0.12 in Equation 2.6 was replaced with 0.09. All other provisions remained the same.

Table 2.1 Summary of bridges in the Province of Ontario.

Province: Ontario			Superstructure (Main Beam)															
			Concrete					Steel					Timber					
Bridge	Substructure		Number of Spans					Number of Spans					Number of Spans					
Support	Column	Col. Type	1	2	3	≥ 4	Total	1	2	3	≥ 4	Total	1	2	3	≥ 4	Total	Total
Simple	Concrete	Circular		50	121	67	238		34	25	53	112		0	0	0	0	350
		Rectangular		3	2	1	6		5	2	6	13		0	0	0	0	19
		Wall		4	5	7	16		28	32	47	107		0	0	0	0	123
		Cir. & Wall		0	2	1	3		0	4	1	5		0	0	0	0	8
		Rec. & Wall		0	1	10	11		0	52	61	113		0	0	0	0	124
		Total		57	131	86	274		67	115	168	350		0	0	0	0	624
	Steel	Tube Pile		0	0	2	2		6	4	1	11		0	0	0	0	13
		H - Pile		2	0	1	3		0	0	0	0		0	0	0	0	3
		Total		2	0	3	5		6	4	1	11		0	0	0	0	16
	Timber			0	0	0	0		0	2	1	3		0	0	0	0	3
	Other			31	14	17	62		88	58	48	194		24	4	9	37	293
	Total		1145	90	145	106	1486	2056	161	179	218	2614	278	24	4	9	315	4415
Continuous	Concrete	Circular		103	435	246	784		25	88	47	160		0	0	0	0	944
		Rectangular		34	62	108	204		14	19	14	47		0	0	0	0	251
		Wall		7	13	14	34		25	52	26	103		0	1	0	1	138
		Cir. & Wall		0	9	9	18		0	10	5	15		0	0	0	0	33
		Rec. & Wall		0	11	6	17		0	68	17	85		0	0	0	0	102
		Total		144	530	383	1057		64	237	109	410		0	1	0	1	1468
	Steel	Tube Pile		0	0	2	2		0	15	13	28		0	0	0	0	30
		H - Pile		2	8	8	18		0	0	0	0		0	0	0	0	18
		Total		2	8	10	20		0	15	13	28		0	0	0	0	48
	Timber			0	3	1	4		2	2	0	4		0	0	0	0	8
	Other			243	140	86	469		66	53	54	173		6	3	3	12	654
	Total		0	389	681	480	1550	0	132	307	176	615	0	6	4	3	13	2178
Other			0	0	6	27	33	0	2	6	48	56	0	0	0	2	2	91
Total			1145	479	832	613	3069	2056	295	492	442	3285	278	30	8	14	330	6684

Notes: 1. "Continuous Bridge" includes continuous and semi-continuous (continuous for live load) bridges.
2. "Other Bridge" includes rigid frame, arch, suspension, cable stayed, bascule, lift, swing, articulated (slung span), mix (some spans simply supported, some spans continuous), culvert, and trestle bridges.
3. "Other Substructure" includes concrete hammer head, timber crib, and masonry columns.

Table 2.2 Summary of bridges in the Province of Alberta.

Province: Alberta			Superstructure (Main Beam)															
			Concrete					Steel					Timber					
Bridge	Substructure		Number of Spans					Number of Spans					Number of Spans					
Support	Column	Col. Type	1	2	3	≥ 4	Total	1	2	3	≥ 4	Total	1	2	3	≥ 4	Total	Total
Simple	Concrete	Cir. & Rec.		58	85	73	216		3	23	22	48		0	0	0	0	264
		Wall		59	115	57	231		20	50	45	115		0	0	0	0	346
		Total		117	200	130	447		23	73	67	163		0	0	0	0	610
	Steel	Tube Pile		19	246	75	340		8	20	2	30		0	0	0	0	370
		H - Pile		13	52	10	75		7	11	3	21		0	0	0	0	96
		Total		32	298	85	415		15	31	5	51		0	0	0	0	466
	Timber			181	804	27	1012		20	50	7	77		94	125	62	281	1370
	Other			0	1	1	2		0	1	2	3		0	0	0	0	5
	Sum		2083	330	1303	243	3959	212	58	155	81	506	437	94	125	62	718	5183
Continuous	Concrete	Cir. & Rec.		7	4	14	25		3	12	10	25		0	0	0	0	50
		Wall		8	9	11	28		7	35	54	96		0	0	0	0	124
		Total		15	13	25	53		10	47	64	121		0	0	0	0	174
	Steel	Tube Pile		3	21	15	39		3	14	5	22		0	0	0	0	61
		H - Pile		2	4	2	8		3	7	7	17		0	0	0	0	25
		Total		5	25	17	47		6	21	12	39		0	0	0	0	86
	Timber			23	68	5	96		10	40	14	64		0	0	0	0	160
	Other			0	0	0	0		1	3	0	4		0	0	0	0	4
	Total			43	106	47	196		27	111	90	228		0	0	0	0	424
Other				0	0	9	9		0	0	0	0		0	0	0	0	9
Total			2083	373	1409	299	4164	212	85	266	171	734	437	94	125	62	718	5616

Notes: 1. "Continuous Bridge" includes continuous and semi-continuous (continuous for live load) bridges.
2. "Other Bridge" includes rigid frame, arch, suspension, cable stayed, bascule, lift, swing, articulated (slung span), mix (some spans simply supported, some spans continuous), culvert, and trestle bridges.
3. "Other Substructure" includes concrete hammer head, timber crib, and masonry columns.

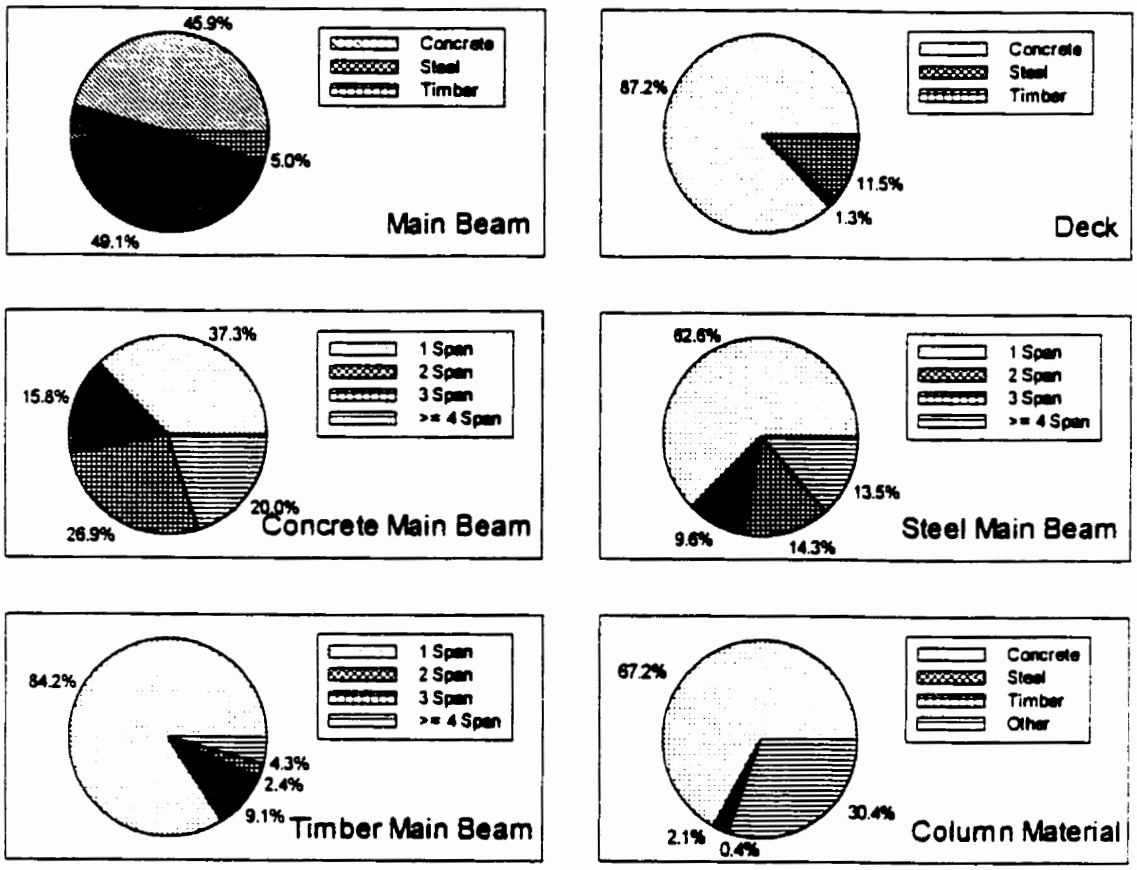

Figure 2.1 Classification of Ontario Bridges.

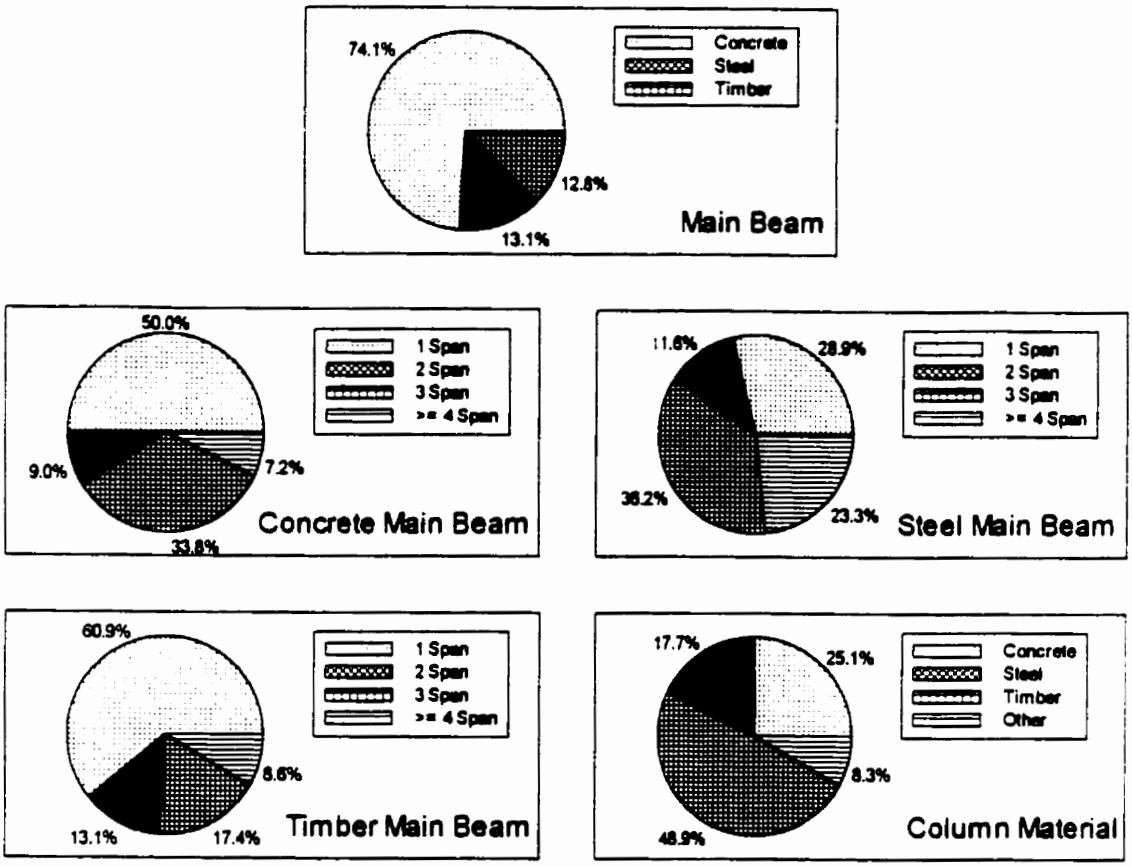

Figure 2.2 Classification of Alberta Bridges.

Bridge Name	2-D Representation
2S-SS	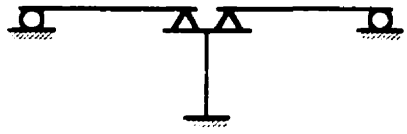
3S-SS-I	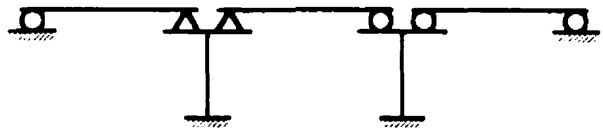
3S-SS-II	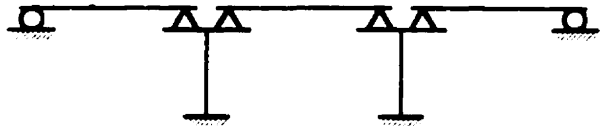
4S-SS	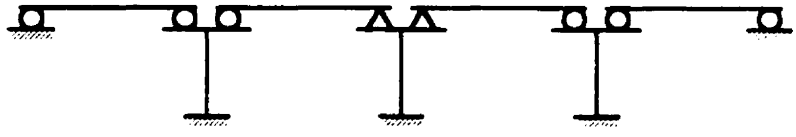

Figure 2.3 Schematic drawing of common simply-supported bridge types.

Bridge Name	2-D Representation
2S-C-I	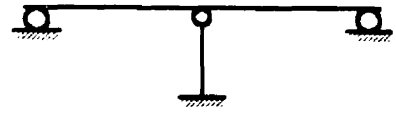
2S-C-II	
3S-C-I	
3S-C-II	
4S-C-I	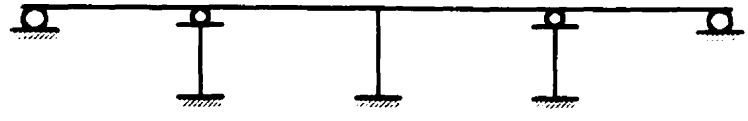
4S-C-II	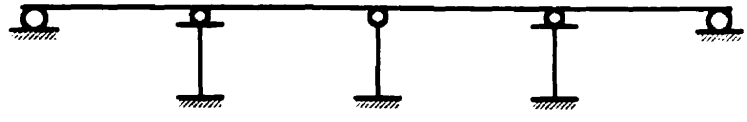

Figure 2.4 Schematic drawing of common continuous bridge types.

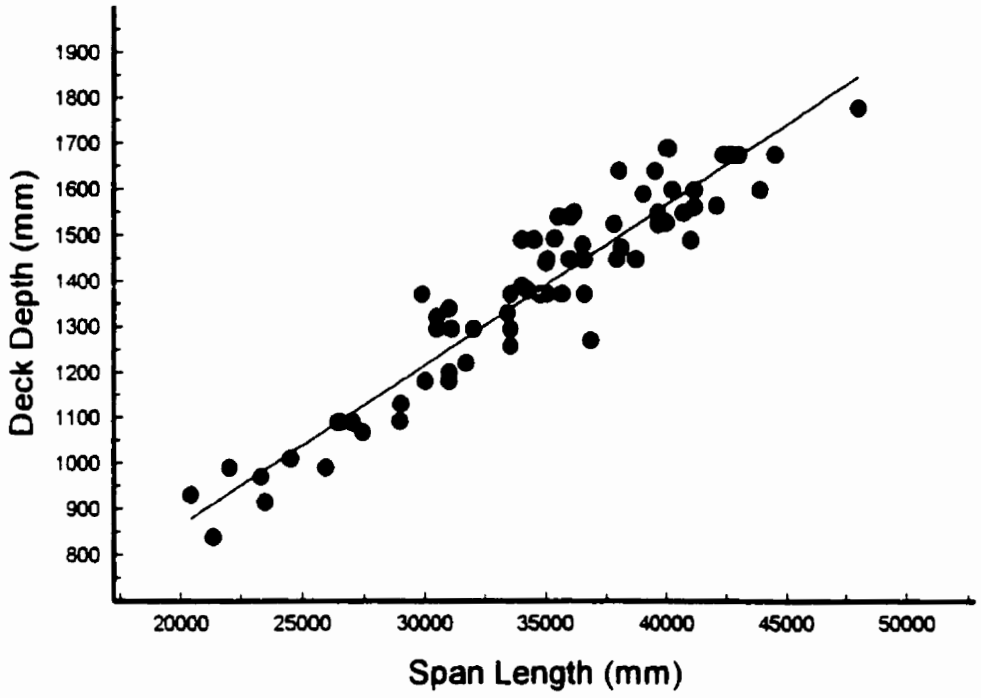

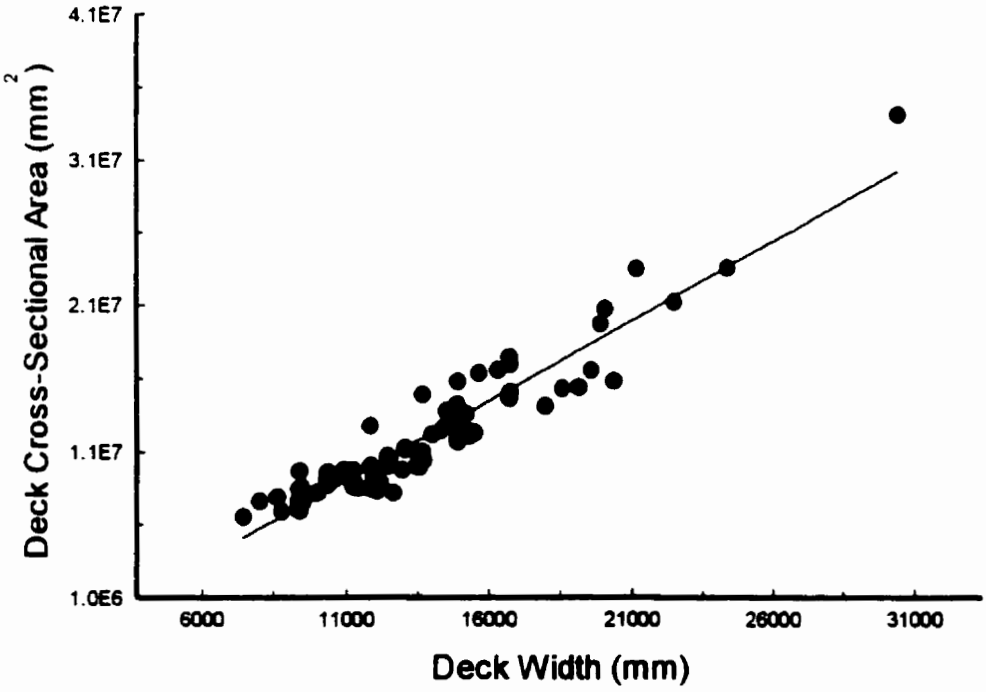

Figure 2.5 Statistical analysis of round-voided post-tensioned decks.

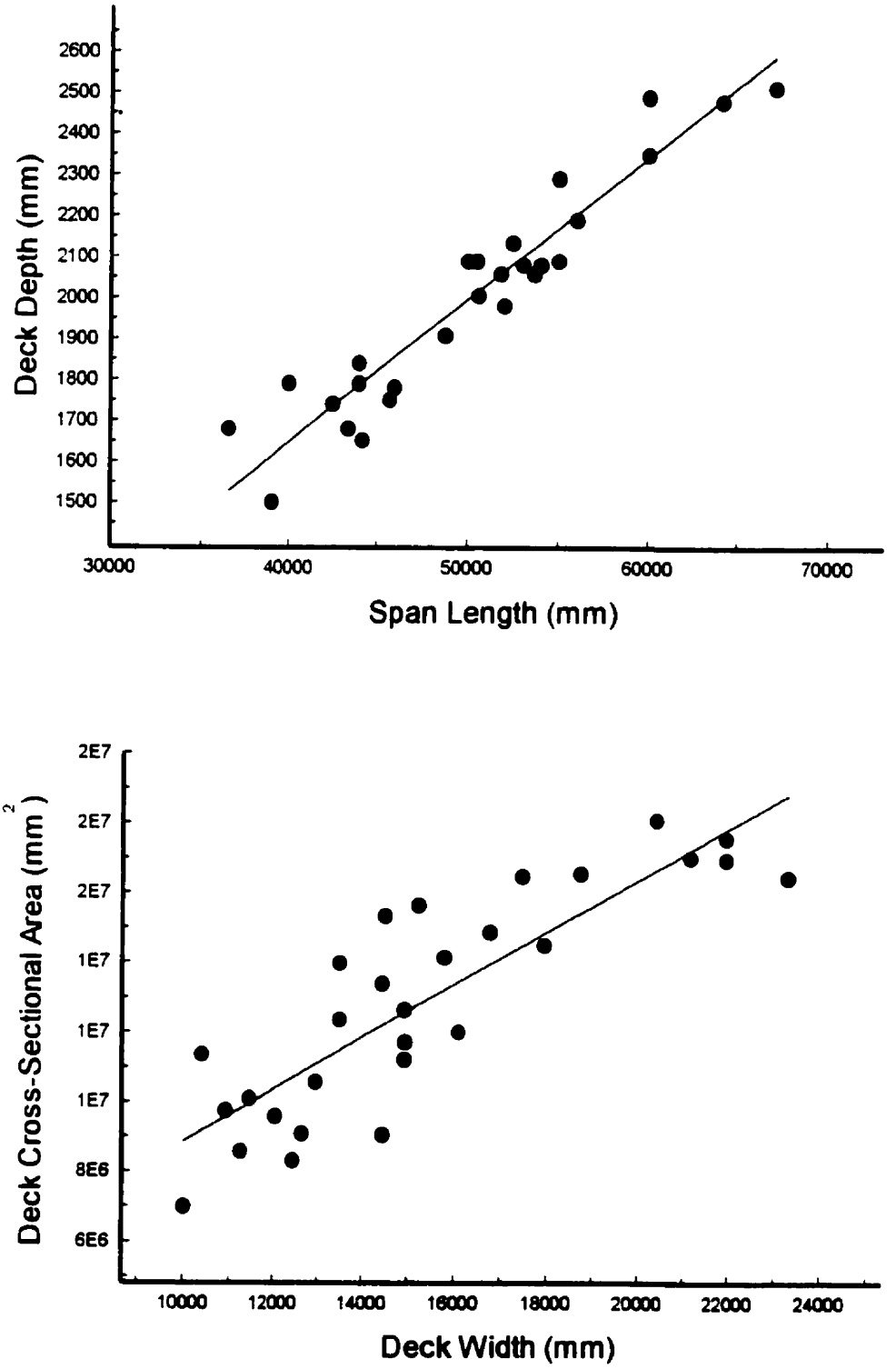

Figure 2.6 Statistical analysis of rectangular-voided post-tensioned decks.

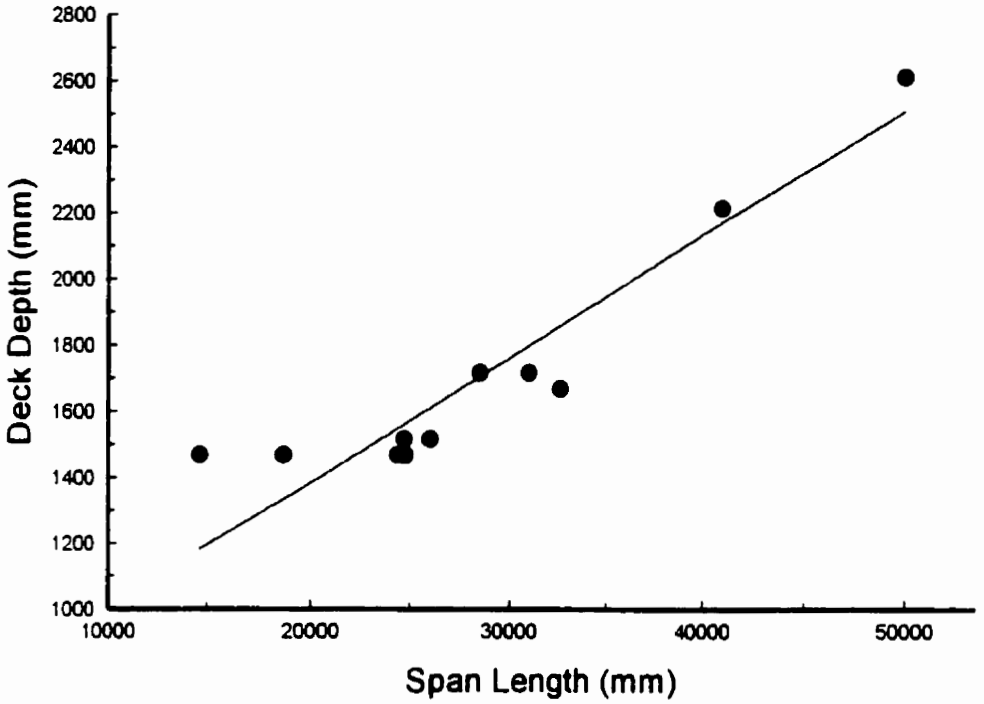

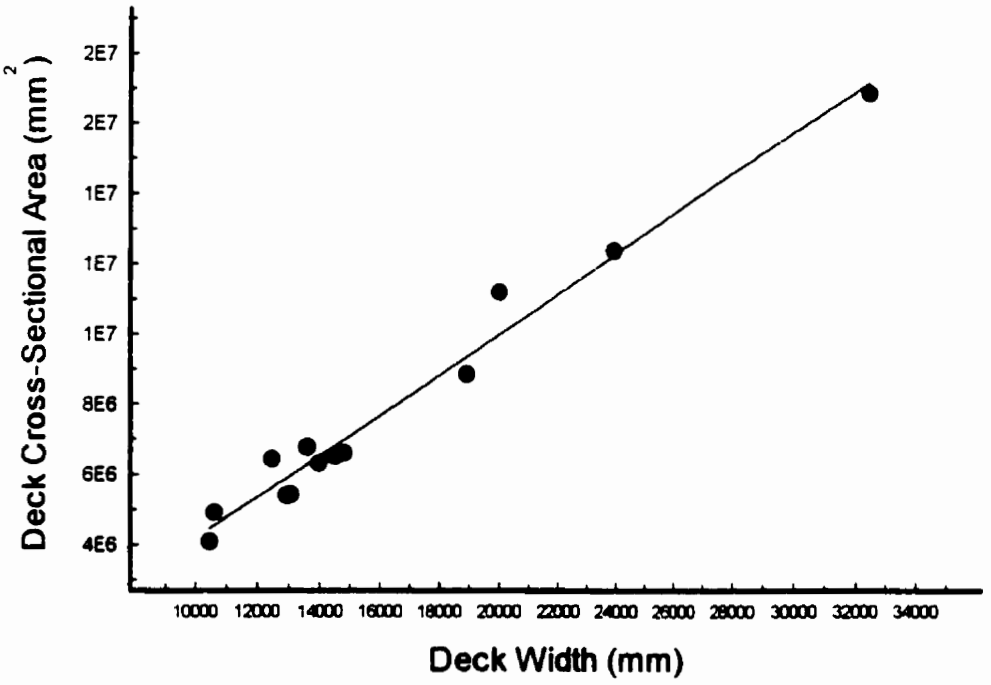

Figure 2.7 Statistical analysis of slab-on-girder decks.

(a) Spalling of cover concrete.

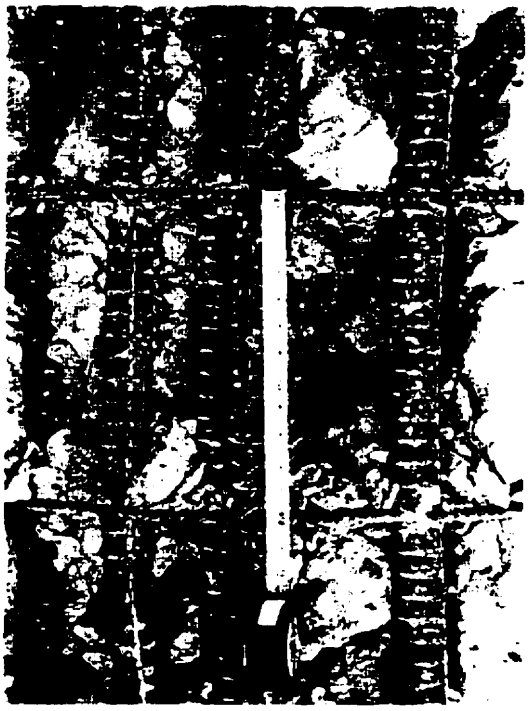

(b) Close-up view.

Figure 2.8 Column of a highway bridge at Interstate 10 that was damaged during the 1994 Northridge Earthquake. (Saatcioglu, 1994)

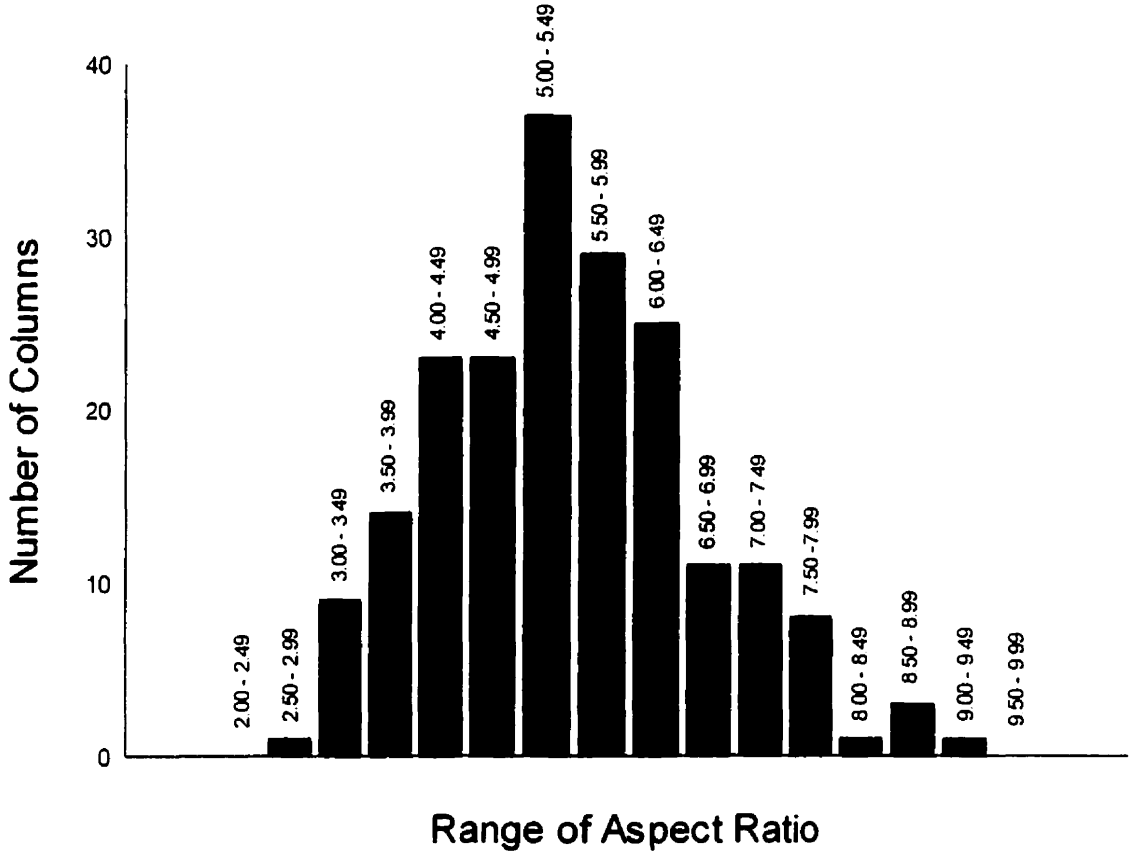

Figure 2.9 Range of aspect ratio (full column height to cross-sectional dimension) of bridge columns.

Chapter 3

Column Drift Capacity

3.1 General

Design of a structure for seismic effects becomes important due to extreme loads and greater risks associated with such loading. It is usually preferable to design a structure based on large inelastic deformation capacity rather than elastic action since the latter becomes uneconomical. Therefore, structures are expected to maintain their strengths during inelastic response to earthquakes. This brings up the problem of ductility. Ductility may be defined as the ability of structures or structural components to withstand inelastic deformation reversals without a significant loss in strength. Flexural response is known to be more ductile than shear and compression. For concrete and masonry structures, the required shear strength must exceed the required flexural strength by selecting a suitable structural configuration, detailing of potential plastic hinging locations, and making sure that inelastic deformations do not occur elsewhere in the structure. The same approach can also be taken for the design of seismic resistant bridge components.

Ductility of a column can be assessed by computing its deformation capacity within the inelastic range. Column deformation capacity can be computed if proper inelastic material models are utilized and all the relevant components of inelastic deformations are considered. The drift of a column can then be calculated as the ratio of its lateral displacement corresponding to maximum allowable strength decay to its height in percentage.

3.2 Computation of Inelastic Column Deformations

Inelastic deformations of reinforced concrete columns consist of three components; flexure, shear and anchorage slip (Saatcioglu and Ozcebe 1989). The shear component of a typical bridge column, with a high shear-span-to-depth ratio, usually forms only a fraction of total inelastic displacement. Unless a column is under-designed in shear, or falls into the short column category, the shear component can be neglected in inelastic displacement calculations. Columns that are critical in shear exhibit brittle behavior, and are usually classified as non-ductile columns. Deformations due to anchorage slip, on the other hand, are direct consequences of flexural response, and can not be ignored in certain columns, especially in bridge columns where axial compression due to gravity loads is low.

Analysis of reinforced concrete bridge columns requires proper material models, such as confinement, anchorage slip and buckling of longitudinal bars; consideration and modeling of inelastic hinges; and computation of all major components of response. This can be achieved by employing a computer software incorporating these features. One such software, entitled "Column Analysis (COLA)," was developed by the author to establish inelastic force deformation relationships. COLA computes deformation capacities of rectangular and circular columns under constant axial load and monotonically increasing lateral force. The analysis starts at the sectional level, through a moment-curvature analysis. Inelasticity and inelastic curvature distribution along column height are established, and deflections corresponding to lateral force capacities are calculated. Lateral deformations are found from deflections caused by flexure and anchorage slip.

3.2.1 Program Algorithm

COLA was programmed using Borland's Turbo Pascal compiler, version 6.0, and designed as a user friendly and interactive software. There are two input files to define the parameters of a column. The first input file consists of geometric data, and includes circular, square or rectangular column parameters where dimensions, amount and location of longitudinal reinforcement, and arrangement of transverse reinforcement are defined. The second input file essentially consists of material data, and includes unconfined concrete and

reinforcing steel models, as well as, axial load and names of data files to be produced after the analysis. The confined concrete stress-strain model is generated based on the input data.

The program first calculates moment and curvature at cracking. Beyond cracking, the analysis is conducted for each value of assumed extreme compressive fiber strain. The neutral axis location is assumed for each strain profile, and internal forces in reinforcing steel and unconfined and confined concrete are calculated. The equilibrium of forces is checked by also considering the axial load. If the equilibrium is not satisfied, the neutral axis location is revised until the equilibrium is satisfied within a desired range of accuracy. The analysis is conducted by using a circular cross-section for all columns. The section is first divided into rectangular strips. Radial coordinates are used to define the location of each strip. For square and rectangular sections, equivalent strip widths are calculated using the ratio of section width to cord width. Figure 3.1 shows typical strips of a cross-section and forces acting on that cross-section.

When the tensile steel reaches its ultimate fracturing stress, or the extreme compressive fiber strain reaches its pre-defined final value as specified in the input file, the program displays an appropriate failure message, and proceeds to the calculation of deformations due to flexure and anchorage slip, as well as axial force-moment interaction relationship, as explained in the following sections. The confined concrete model assumes a constant stress resistance beyond an 80% strength drop beyond peak. Hence the program continues calculations following this model until one of the above failure condition is encountered. Similarly, the bar buckling model adopted assumes zero resistance upon buckling. Therefore, should buckling of a longitudinal reinforcement occur, the program continues calculations with zero stress in that particular reinforcement, until failure. Finally, the output file and all data files are produced for plotting. Figure 3.2 shows a typical graphical output. The program flowchart is illustrated in Figure 3.3. The source code of COLA is shown in Appendix A.

3.2.2 Displacements due to Flexure

Inelastic displacements due to flexure is computed starting from section analysis. Plane section analysis of the column section is first conducted to construct the moment-curvature relationship. This requires confined and unconfined stress-strain relationships of

concrete, and a complete stress-strain relationship of reinforcing steel, including strain hardening in tension and compression.

3.2.2.1 Constitutive Model for Unconfined and Confined Concrete

The constitutive model used for concrete was developed by Saatcioglu and Razvi (1992) for confined concrete. The model covers a range of columns, between unconfined and well confined columns, and is depicted in Figure 3.4. For unconfined concrete it reduces to Hognestad's model (1951) with an ascending branch described by a second degree parabola, and a descending branch linearly changing to a strain corresponding to 20% of the peak. The slope of the descending branch is defined based on strain and stress values corresponding to 85% of the peak. This relationship is used for unconfined concrete in the cover. The following expressions describe the stress-strain relationship for unconfined concrete:

$$f_c = f'_{co}\left[2\frac{\varepsilon_c}{\varepsilon_{o1}} - \left(\frac{\varepsilon_c}{\varepsilon_{o1}}\right)^2\right] \qquad \text{for } \varepsilon_c \le \varepsilon_{o1} \qquad (3.1)$$

$$f_c = f'_{co} - (\varepsilon_c - \varepsilon_{o1})\left(\frac{0.15 f'_{co}}{\varepsilon_{o85} - \varepsilon_{o1}}\right) \qquad \text{for } \varepsilon_{o1} < \varepsilon_c \le \varepsilon_{cu} \qquad (3.2)$$

where f'_{co} is the unconfined concrete strength in MPa; ε_{01}, and ε_{085} are the strains at peak and 85% of peak unconfined stresses, respectively.

When the member is confined, the characteristics of stress-strain curve changes. Confinement produces significant enhancements in strength and ductility. As lateral confinement pressure increases with increased volumetric ratio and/or grade of lateral steel, and efficiency of confinement reinforcement, then the confined concrete becomes stronger and more ductile. The lateral confinement pressure was quantified in the confinement model in terms of section geometry and material properties. The following expressions define the ascending branch of the stress-strain model for confined concrete.

$$f_c = f'_{cc}\left[2\frac{\varepsilon_c}{\varepsilon_1} - \left(\frac{\varepsilon_c}{\varepsilon_1}\right)^2\right]^{\left(\frac{1}{1+2k}\right)} \qquad \text{for } \varepsilon_c \le \varepsilon_1 \qquad (3.3)$$

$$k = \frac{k_1 f_{le}}{f'_{co}} \tag{3.4}$$

$$k_1 = 6.7(f_{le})^{-0.17} \tag{3.5}$$

The equivalent uniform lateral pressure, f_{le}, is a function of the average lateral pressure f_l and reinforcement arrangement, as described in Figure 3.5. The reinforcement arrangement is reflected through coefficient k_2, which describes the efficiency of confinement reinforcement. For closely spaced circular spirals the efficiency of confinement is the highest, with approximately uniform passive pressure generated through hoop tension. In this case k_2 is equal to 1.0. For columns with rectilinear reinforcement, the efficiency of reinforcement depends on the spacing s, as well as the spacing of laterally supported longitudinal reinforcement s_l. Coefficient k_2 for this case assumes a value of 1.0 or smaller, depending on the arrangement. A simplified version of expression for k_2 is given below (Razvi and Saatcioglu 1996).

$$f_{le} = k_2 f_l \tag{3.6}$$

$$k_2 = 1.0 \qquad \text{(For closely spaced circular spirals)} \tag{3.7}$$

$$k_2 = 0.15\sqrt{\frac{b_c^2}{ss_l}} \qquad \text{(For rectilinear reinforcement)} \tag{3.8}$$

$$f_l = \frac{\sum A_{sh} f_{yh}}{b_c s} \tag{3.9}$$

$$\varepsilon_1 = \varepsilon_{ol} + (1 + 5k) \tag{3.10}$$

The descending branch of the confined concrete model is obtained by defining the strain corresponding to 85% of peak stress. This is specified below.

$$\varepsilon_{85} = 260\rho\varepsilon_1 + \varepsilon_{085} \tag{3.11}$$

$$\rho = \frac{\sum A_{sh}}{s(b_{cx} + b_{cy})} \tag{3.12}$$

where, $\sum A_{sh}$ is the total area of transverse reinforcement in both cross-sectional directions, in mm^2; f_{yh} is the yield strength of transverse reinforcement in MPa, s is the center to center spacing between ties in mm; b_{cx} and b_{cy} are core concrete dimensions measured center-to-center of the perimeter hoop in mm, in x and y directions, respectively.

The equivalent lateral pressure, f_{le} for rectangular sections and square sections with unequal confinement pressure in orthogonal directions, can be expressed as follows.

$$f_{le} = \frac{f_{lex} b_{cx} + f_{ley} b_{cy}}{b_{cx} + b_{cy}} \tag{3.13}$$

where the subscripts x and y refer to the two cross-sectional directions.

Although the confinement mode, as described above is applicable to normal-strength concrete columns, recent research by Razvi and Saatcioglu (1996) showed that certain modifications may be necessary when high-strength concrete, in the range of 60 MPa to 130 MPa, is used. Furthermore, it was also concluded that the exponential curve proposed by Popovics (1973) provided a better correlation with experimental data for both high-strength and normal-strength concretes. Therefore, Popovics's curve was also adopted here to describe the ascending branch of the stress-strain relationship. This is shown in the following expressions.

$$f_c = \frac{f'_{cc}\left(\frac{\varepsilon_c}{\varepsilon_1}\right)r}{r - 1 + \left(\frac{\varepsilon_c}{\varepsilon_1}\right)^r} \tag{3.14}$$

$$r = \frac{E_c}{E_c - E_{sec}} \tag{3.15}$$

where f'_{cc} is confined concrete strength in MPa; ε_1, and ε_{85} are strains at peak and 85% of peak stress, respectively; E_{sec} is the secant modulus of elasticity of concrete as expressed below.

$$E_{sec} = \frac{f'_{cc}}{\varepsilon_1} \tag{3.16}$$

E_c is the modulus of elasticity of unconfined concrete and it is defined as

$$E_c = 3320\sqrt{f'_c} + 6900 \tag{3.17}$$

Both E_{sec} and E_c are expressed in MPa. Modifications involved to accommodate high-strength concrete are illustrated in the following expression:

$$f'_{cc} = f'_{co} + (k_1 f_{le}) \tag{3.18}$$

$$k_3 = \frac{40}{f'_{co}} \leq 1.0 \tag{3.19}$$

$$\varepsilon_1 = \varepsilon_{o1} + (1 + 5k_3 k) \tag{3.20}$$

$$k_4 = \frac{f_{yh}}{500} \tag{3.21}$$

$$\varepsilon_{85} = 260 k_3 \rho \varepsilon_1 \left[1 + 0.5 k_2 (k_4 - 1)\right] + \varepsilon_{085} \tag{3.22}$$

where k, k_1, k_3, and k_4 are dimensionless factors. In the absence of experimental data ε_{01} and ε_{085} can be taken as $2f'_c/E_c$ or 0.0038, respectively.

Both the original, and modified confinement models are incorporated in the computer program with a user specified option.

3.2.2.2 Constitutive Model for Steel in Tension

The stress-strain relationship used for reinforcing steel in tension has three branches. The elastic and yield portions of the curve are linear while the strain-hardening portion is represented by a parabolic curve as illustrated in Figure 3.6. The following expressions define the complete curve:

$$f_s = E_s \varepsilon_s \qquad \text{for } \varepsilon_s \leq \varepsilon_y \tag{3.23}$$

$$f_s = f_y + (\varepsilon_s - \varepsilon_y)\left(\frac{f_{sh} - f_y}{\varepsilon_{sh} - \varepsilon_y}\right) \qquad \text{for } \varepsilon_y < \varepsilon_s \leq \varepsilon_{sh} \tag{3.24}$$

$$f_s = f_y + (f_u - f_y)\left[2\frac{\varepsilon_s - \varepsilon_{sh}}{\varepsilon_u - \varepsilon_{sh}} - \left(\frac{\varepsilon_s - \varepsilon_{sh}}{\varepsilon_u - \varepsilon_{sh}}\right)^2\right] \qquad \text{for } \varepsilon_{sh} < \varepsilon_s \leq \varepsilon_u \tag{3.25}$$

where f_y, f_{sh}, f_u are the yield, strain-hardening and ultimate stresses in MPa; ε_y, ε_{sh}, ε_u are the corresponding strains.

3.2.2.3 Proposed Constitutive Model for Steel in Compression

Stress-strain relationship of reinforcing steel in compression is the same as that in tension, if the stability of reinforcement can be maintained under compression. However, depending on the size of compression bars and the spacing of ties, the stress-strain relationship in compression can be quite different. Under unfavorable lateral restraint

conditions the compression reinforcement can loose its stability prior to developing full strain hardening. If the slenderness ratio of re-bar is very high, the stress-strain relationship may show unloading immediately after yielding.

Stability of compression reinforcement can be expressed in terms of bar aspect ratio, where the aspect ratio is defined as the ratio of unsupported bar length between two ties to its diameter. Mau and El-Mabsout (1989), and Mau (1990) predicted the behavior of reinforcing bars under compression using finite element analysis. They compared their results with experimental data which showed good agreement. Stress-strain relationships for reinforcing bars in compression were given only for certain aspect ratios in the form of plots. No general expressions were suggested relating the effect of aspect ratio to the behavior of reinforcing bars.

The observations made from analytical and experimental research reported by previous researchers were used in this investigation to derive empirical relationships. The expressions were developed as a function of bar aspect ratio. Figure 3.7 illustrates stress-strain relationships for compression reinforcement as a function of bar aspect ratio.

- **Aspect Ratio ≥ 8.0:**

When the aspect ratio is greater than 8.0, the bars become unstable as soon as the yield point is attained. The stress in steel drops linearly as strains increase. Thus, the slope of the descending branch of stress-strain curve depends on the aspect ratio. The aspect ratio of 8.0 is taken as the limiting value for bar stability where the reinforcement can maintain its stability with zero slope upon yielding. For aspect ratios of greater than 8.0, the slope becomes negative. As the aspect ratio increases, the negative slope increases until limiting values of $f_{S/Du}$ and $e_{S/Du}$ are reached. The following expressions describe this behavior:

$$f_s = f_y - (\varepsilon_s - \varepsilon_y)\left[-23000 + 11000\ln\left(\frac{s}{d_b}\right)\right] \qquad \text{for } \varepsilon_y < \varepsilon_s \le \varepsilon_{S/Du} \qquad (3.26)$$

$$f_{S/Du} = 28\left(\frac{s}{d_b}\right)^{-1.7} f_y \qquad (3.27)$$

$$\varepsilon_{S/Du} = \left[40 - 6\ln\left(\frac{s}{d_b}\right)\right]\varepsilon_y \tag{3.28}$$

where $f_{S/Du}$ is the limiting value of stress in MPa and $\varepsilon_{S/Du}$ is the limiting value of strain.

- **4.5 < Aspect Ratio ≤ 8.0:**

The stress-strain relationship within this range exhibits strain-hardening. The strain-hardening curve is lower than that for tension curve. As the aspect ratio decreases the strain-hardening curve approaches to that of tension reinforcement. The following expressions can be used in this range:

$$f_s = f_y + (f_{S/Du} - f_{sh})\left[2\frac{\varepsilon_s - \varepsilon_{sh}}{\varepsilon_{S/Du} - \varepsilon_{sh}} - \left(\frac{\varepsilon_s - \varepsilon_{sh}}{\varepsilon_{S/Du} - \varepsilon_{sh}}\right)^2\right] \qquad \text{for } \varepsilon_s > \varepsilon_{sh} \tag{3.29}$$

$$f_{S/Du} = f_{sh} + (f_u - f_{sh})\left[48e^{-0.9\left(\frac{s}{d_b}\right)}\right] \tag{3.30}$$

$$\varepsilon_{S/Du} = \varepsilon_{sh} + (\varepsilon_u - \varepsilon_{sh})\left[6e^{-0.4\left(\frac{s}{d_b}\right)}\right] \tag{3.31}$$

- **Aspect Ratio < 4.5:**

When the aspect ratio is in excess of 4.5 the stress-strain relationship becomes identical to that in tension, with complete strain hardening.

3.2.3 Displacements Due to Anchorage Slip

Deformations due to anchorage slip occur because of the slippage and/or extension of longitudinal reinforcement in adjoining members. The source of these deformations occur outside the member, and hence their effects are not included in flexural analysis. The slip component usually forms a small portion of anchorage slip, and can be avoided through proper anchorage. The penetration of yielding into the adjacent member and extension of tension reinforcement in the adjoining member can not be prevented if the critical section is to occur near the adjoining member. Therefore, bar extension was computed as the only source of

anchorage slip in columns. The penetration of yielding and the resulting bar extension increase when the level of axial compression is low, as typically is the case for bridge columns. Bridge columns are usually subjected to 10% to 20% of their concentric capacities.

Deformations due to anchorage slip was computed based on the model proposed by Alsiwat and Saatcioglu (1992). The extension of reinforcing bar in the adjoining member is defined as the area under the strain diagram. It is therefore essential to establish the strain distribution along the embedment length. This can be done by estimating bond stress between the steel and concrete and applying equilibrium of forces. The stressed portion of the embedment length consists of four segments as illustrated in Figure 3.8. These segments are discussed below.

- **Elastic Region:**

The bar in this region remains elastic. The average bond stress, proposed by ACI Committee 408, is applicable in the elastic range.

$$u_e = u_{ACI} = \frac{f_y d_b}{4 l_d} \tag{3.32}$$

and

$$l_d = \frac{440 A_b}{K\sqrt{f_c'}} \frac{f_y}{400} \geq 300 \tag{3.33}$$

where u_e is the elastic bond stress in MPa, d_b is the bar diameter in mm, A_b is the area of bar in mm^2, l_d is the development length in mm, and coefficient K is equal to 3 times the bar diameter. From the elastic bond stress, the elastic length, L_e, can be calculated as follows:

$$L_e = \frac{f_s d_b}{4 u_e} \tag{3.34}$$

- **Yield Plateau Region:**

In this region the bar is stressed beyond its yield strength. The length of the yield plateau region can be determined from equilibrium. Frictional bond stress, as given below, can be used in this region.

$$u_f = \left(5.5 - 0.07\frac{S_L}{H_L}\right)\sqrt{\frac{f'_{co}}{27.6}} \tag{3.35}$$

where S_L and H_L are the spacing and height of the lugs on the bar, respectively. Thus, the length of the yield plateau, L_{yp}, can be expressed as

$$L_{yp} = \frac{\Delta f_s d_b}{4u_f} \tag{3.36}$$

where, Δf_s is the incremental bar stress within the yield region. For reinforcement with perfect yield plateau the incremental increase in steel stress between yield and strain-hardening approaches zero. Therefore, the length of yield plateau region becomes insignificant, and is equal to zero in most cases.

- **Strain-Hardening Region:**

The same principles that apply to the yield plateau region also applies to the strain hardening region. The frictional bond stress is used with force equilibrium to compute the length of this segment. This time however, Δf_s represents the incremental stress between the beginning and end of the strain-hardening region.

- **Pullout-Cone Region:**

Pullout-cone occurs when the concrete cover breaks loose in tension, forming a constant stress and strain zone (L_{pc}). The pullout-cone can be prevented by reinforcing the potential cone region with transverse steel. Since in most reinforced concrete joints there is sufficient reinforcement to prevent the pullout cone, the length of this region may be taken equal to zero.

Once all stressed lengths in different regions are calculated, the total bar extension, δ_{ext}, can be determined from the following expression:

$$\delta_{ext} = \varepsilon_s L_{pc} + 0.5(\varepsilon_s + \varepsilon_{sh})L_{sh} + 0.5(\varepsilon_{sh} + \varepsilon_y)L_{yp} + 0.5\varepsilon_y L_e \tag{3.37}$$

The resulting rotation due to bar extension can be calculated as

$$\theta_e = \frac{\delta_{ext}}{d - c} \tag{3.38}$$

where d is the reinforcement depth, and c is the height of compression block, both in mm. Once the rotation due to bar extension is obtained, the tip column deflection can be computed as shown below.

$$\Delta_{np} = L(\theta_e) \tag{3.39}$$

where, L is the column shear span.

3.2.4 Calculation of Plastic Hinge Length

The variation of curvatures along column height can be determined from moment-curvature analysis. However, the distribution of curvatures in the hinging region becomes a challenging task, and can be established by an algorithm which was developed by Razvi and Saatcioglu (1996). This algorithm can be used to define the formation and progression of plastification within the column hinging region. The length of the hinging region and the magnitude of inelastic curvatures within this region can be computed. Once the curvature distribution is established, inelastic flexural rotations and displacements can be calculated as the area and moment of the area under the diagram, respectively. Figure 3.9 shows the progression of plastic hinging in a typical column.

3.3 Prediction of Drift Capacity for Bridge Columns

The procedures described in preceding sections can be used to establish lateral drift capacities of bridge columns when the governing mode of behavior is flexure. These procedures have been implemented in computer software COLA.. The software provides inelastic force-displacement relationships under monotonically increasing lateral loads. Although columns subjected to earthquake effects develop reversed cyclic loading, the envelope of hysteretic force-deformation relationship is very similar to force-deformation relationship computed by COLA under monotonically increasing lateral load. Figures 3.10 through 3.15 illustrate the actual behavior of columns recorded under reversed cyclic loading and predictions by COLA.

During strong earthquakes well confined columns survive beyond their elastic limits until a noticeable decay in their lateral load capacity is observed. In multistory multi-bay frame systems some strength decay is tolerable before the column is considered

to have failed. One criterion for establishing column inelastic displacement capacity is to compute column displacement at 20% strength decay (Saatcioglu 1989; Razvi and Saatcioglu 1996). Although bridge structures do not have as much redundancy in the system as building structures, they may experience some redistribution of forces among the supporting elements. It may be unduly conservative to limit the deformation capacity of bridge columns to those corresponding to peak loads, as peak loads often occur immediately after yielding. Therefore, it may be appropriate to adopt the same failure criterion of 20% strength decay to bridge columns, in order to establish the maximum tolerable displacement beyond the onset of strength decay. This criterion is adopted here for the purpose of determining inelastic deformation capacities of bridge columns.

While the concern in earthquake resistant bridge columns is to improve inelastic deformability and associated energy dissipation capacity, this can be achieved if the member behaves predominantly in ductile flexural mode while brittle modes of failure are suppressed through proper design and detailing. It was previously found in the bridge survey conducted that the bridge columns designed prior to 1970s and some designed more recently lack adequate shear resistance. These columns are likely to fail prematurely in a brittle manner, prior to developing their flexural capacity and inelastic deformation capacity that was discussed earlier in this section. Therefore, the current earthquake design practice calls for sufficiently high shear capacity so that ductile flexural response can be developed. Since the majority of existing bridge columns were not designed following this design philosophy, it becomes essential that shear strength of these columns be evaluated prior to any improvement in flexural deformability is assessed. An approached proposed by previous investigators is summarized in the next section for the evaluation of shear strength.

3.3.1 Shear Strength of Bridge Columns

The shear strength of a reinforced concrete column can be estimated using a recently developed approach by Priestley et al. (1994). Accordingly, the nominal shear strength, V_d consists of three components as shown below.

$$V_d = V_c + V_s + V_p \tag{3.40}$$

where, V_c, V_s and V_p are concrete, steel and axial load contributions, respectively. The concrete contribution is a function of column displacement ductility ratio, μ_Δ, within the plastic hinging region. It is defined below.

$$V_c = n\sqrt{f_c'}A_e \tag{3.41}$$

where A_e is the effective shear area in mm^2, and is taken as 80% of gross cross sectional area. This quantity is equal to $0.628D^2$ for circular columns, where D is the diameter of column section. The coefficient n depends on displacement ductility ratio, and is expressed in MPa. This coefficient is defined below for uniaxial loading.

$$n = 0.29 \qquad \text{for } \mu_\Delta \le 2 \tag{3.42}$$

$$n = 0.29 - 0.095(\mu_\Delta - 2) \qquad \text{for } 2 < \mu_\Delta \le 4 \tag{3.43}$$

$$n = 0.1 - 0.015(\mu_\Delta - 4) \qquad \text{for } 4 < \mu_\Delta \le 8 \tag{3.44}$$

$$n = 0.04 \qquad \text{for } \mu_\Delta > 8 \tag{3.45}$$

The steel contribution, V_d, is derived from truss analogy, with a variable angle θ. The expression for circular columns is given below.

$$V_s = \frac{\pi}{2}\frac{A_{sh}f_{yh}b_c}{s}\cot\theta \tag{3.46}$$

Where, θ is the critical angle where inclined shear cracking occurs, and it is taken as 30°. The same expression becomes as follows for rectangular columns.

$$V_s = \frac{A_v f_y b_c}{s}\cot\theta \tag{3.47}$$

The shear strength is enhanced with the contribution of axial compressive load, P, resulting from diagonal compression strut. This contribution, V_p is given below.

$$V_p = P\tan\alpha \tag{3.48}$$

Where, angle α is formed between column axis and the line of action of the strut. For a cantilever column loaded laterally by a tip force, the line of action of strut can be taken from the point of load application to the center of the flexural compression zone at the critical section.

The shear strength determined by the above procedure can be used to establish adequacy of columns for shear. The capacity is then compared with applied shear force

associated with flexural capacity. If the shear capacity is lower than that corresponding to flexure, the column is classified as inadequate, and must be retrofitted to increase its shear resistance. Otherwise, the adequacy of inelastic deformability in flexure is investigated. Software COLA can be used to establish inelastic deformation capacity of the column. Alternatively, charts developed in the following section may be used to estimate the deformation capacity expressed in terms of lateral drift. The drift capacity can then be compared with lateral drift demands established through dynamic inelastic analysis, discussed in Chapter 4. If the drift capacity determined in this Chapter is less than the drift demand established in Chapter 4, the column needs to be retrofitted. One potential retrofitting procedure, developed as part of this investigation, is outlined in Chapter 5.

3.3.2 Effects of Design Parameters on Column Deformability

The significance of structural parameters on column deformability was assessed analytically through a parametric investigation. This was done to explore the possibility of reducing total number of variables by eliminating some of the less significant parameters and combining others so that design aids can be prepared to establish drift capacities. Since concrete confinement was the primary mechanism to improve deformability, the parameters of confinement were included as the primary variables. The parameters considered for circular included the volumetric ratio, spacing, and grade of transverse reinforcement, concrete strength, axial compression, and column aspect ratio. Computer software COLA was used to conduct the analysis. The results of the bridge survey was used to consider realistic ranges of parameters employed in practice. The survey revealed geometric and material properties of bridge columns. Table 3.1 provides a summary of structural parameters considered.

The first parameter considered was the volumetric ratio. Columns with the same geometry and material properties, but with different volumetric ratios of transverse reinforcement, ρ_v, were analyzed to establish the effect of ρ_v on drift capacity. Figures 3.15 and 3.16 show that the volumetric ratio plays a significant role on drift capacities of columns with different levels of axial compression and longitudinal reinforcement ratios. Figure 3.16 also illustrates that drift capacity decreases with the level of constant axial

compression. This observation conforms to previously reported experimental data. Figure 3.17 shows the significance of longitudinal reinforcement ratio. It can be observed in this figure that column drift capacity increases as the percentage of longitudinal reinforcement increases. Additional analyses were also conducted to establish the significance of some of the geometric parameters. Figure 3.18 depicts the significance of column aspect ratio. It may be concluded from this figure that column aspect ratio plays an important role and must be considered in establishing drift capacities. Similarly, it is shown in Figure 3.19 that the ratio of gross cross-sectional area to core area is an important parameter that can not be ignored, since this ratio reflects the relative contribution of confined concrete to overall column behavior.

Deformability of confined concrete improves with increasing lateral pressure. The lateral pressure is affected by the volumetric ratio and grade of reinforcement. Higher grade reinforcement, within the limits used in practice, develop higher hoop tension, which in turn translates into higher confinement pressure. It is conceivable that a trade off exists between the volumetric ratio, ρ_v, and grade, f_{yh}, so that a smaller ρ_v can be used in columns with a proportionately higher f_{yh}. This was investigated by analyzing columns with different ρ_v and f_{yh}, such that the product $\rho_v f_{yh}$ remained constant. The results are compared in Figure 3.20, and show similar drift capacities. This implies that the volumetric ratio and grade need not be considered separately so long as the product $\rho_v f_{yh}$ is used as a parameter, within the practical ranges of volumetric ratio and grade of reinforcement.

Concrete strength, f'_c, was another parameter that was investigated. It is well known that deformability of concrete decreases with increasing strength. Therefore, higher strength concretes require higher confinement pressure ($\rho_v f_{yh}$). The relationship between f'_c and $\rho_v f_{yh}$ was investigated by analyzing columns with different strength concretes and different confinement pressures. Figure 3.21 illustrates that the adverse effects of an increase in concrete strength can be compensated by a proportional increase in the confinement pressure. It was observed that at higher aspect ratios, $\rho_v f_{yh} / f'_c$ yields a difference of about 0.5% drift between columns with 20 MPa and 40 MPa concretes.

However, at aspect ratios of less than 6.0, the $\rho_s f_{yh}/f'_c$ ratio yields same drift capacities, regardless of concrete strength.

The amount of cover concrete was also investigated by the considering columns with different ratios of gross-to-core cross sectional area. Figure 3.22 shows that as long as the product of $\rho_s f_{yh}/f'_c(A_g/A_c-1)^{-1}$ remains constant, similar drifts are obtained.

A similar parametric investigation was conducted by Razvi and Saatcioglu (1996) for rectilinear building columns. Their results are equally applicable to rectilinear bridge columns for appropriate levels of axial force, cover-to-core area ratio and percentage of longitudinal reinforcement. Therefore, the emphasis on the current parametric investigation was placed on circular bridge columns especially in view of the fact that a great majority of bridge columns have circular cross-section.

3.3.3 Approximate Determination of Column Drift Capacities

Deformability of concrete bridge columns can best be established by using the computer software COLA developed as part of this investigation. However, design charts can also be developed for approximate determination of drift capacities. The parametric investigation reported in the previous section revealed that the effects of the volumetric ratio and grade of transverse reinforcement, as well as concrete strength and gross-to-core area ratio of concrete can be merged into one single parameter, r_c, as defined below.

$$r_c = \rho_v \frac{f_{yh}}{f'_c} \frac{1}{\left(\frac{A_g}{A_c} - 1\right)} \tag{3.49}$$

This was shown to be especially true for columns with aspect ratios of less than 8. Therefore, design charts can be established, showing relationships between coefficient "r_c" and column drift capacity for different percentages of longitudinal reinforcement and levels of axial compression. Sample charts are shown in Figures 3.23 through 3.25. Also, all analytical results obtained from the parametric study were presented in Tables 3.2 through 3.4.

Although drift ratio is a convenient and a preferred way of expressing overall column deformability, it does not reflect the degree of inelasticity in the column.

Inelasticity in columns can be expressed in terms of a ductility ratio. Displacement ductility ratio has been selected here to express overall behavior of columns. The displacement ductility ratio is defined as the ratio of maximum column displacement at failure (20% strength drop beyond peak resistance) to displacement at yield. Since, the same maximum displacement quantity is also used in computing column drift, there exists a strong relationship between drift and ductility ratios. This is illustrated in Figure 26.

Although column drift capacity can be determined by using the computer software COLA or approximately from the charts given in Figures 3.23 through 3.25, these drift quantities are meant for flexure dominant columns. The majority of bridge columns in practice do fall in this category. However, short columns and shear deficient columns also exist in practice. Their behavior is effected by their shear capacity which may be lower than the shear force corresponding to flexural capacity. A discussion of shear resistance of bridge columns was provided earlier in this Chapter. Shear capacity is controlled by the amount of transverse reinforcement, which is one of the major parameters included in coefficient "r_c." Therefore, in order to indicate the mode of failure, the relationship between the ratio of shear capacity to shear force associated with flexural failure was computed and presented in Figure 3.27. The computed shear capacities included in this figure were obtained from the expressions recommended by Priestley et al. (1994) as discussed in section 3.3.1. Those corresponding to flexural failure were obtained by computer program COLA. When the shear ratio is less than 1.0 in Figure 3.27, the column is likely to fail in shear. If this ratio is greater than 1.0, the column may develop its full flexural capacity.

Table 3.1 Parameters of bridge columns used in the analysis.

Cross-sectional dimensions	Circular columns: 1000 mm and 2000 mm.
Shear span to cross-sectional dim. ratio	2.5, 5.0 and 10.0
Axial load ratio	10% and 20%
Longitudinal steel ratio	1%, 2% and 3%
Yield strength of steel	200 MPa and 400 MPa
Gross area to core area ratio	1.2 and 1.4

Table 3.2 Drift capacity for circular columns (ρ_l= 1 %).

			10 % P_0			20 % P_0		
L / D	**A_g / A_c**	**r_c**	**% Drift**	**Ductility**	**V_{shear}/V_{flo}**	**% Drift**	**Ductility**	**V_{shear}/V_{flo}**
2.5	1.2	0.876	> 7.20	> 8.00	2.08	> 7.20	> 8.00	1.87
		0.584	> 7.20	> 8.00	1.61	3.54	5.06	1.62
		0.438	> 7.20	> 8.00	1.35	2.88	4.50	1.42
		0.219	3.67	4.77	1.15	1.98	3.54	1.24
		0.146	3.17	4.46	1.03	1.76	3.32	1.21
		0.088	2.78	4.48	0.90	1.60	3.08	1.14
	1.4	0.473	> 7.20	> 8.00	2.06	3.71	7.00	1.91
		0.316	> 7.20	> 8.00	1.59	2.79	5.17	1.62
		0.237	4.72	6.74	1.42	2.36	4.45	1.43
		0.118	3.29	5.22	1.13	1.84	3.47	1.28
		0.079	2.91	4.85	1.01	1.70	3.21	1.25
		0.047	2.64	4.63	0.90	1.58	3.04	1.16
5.0	1.2	0.876	> 12.67	> 8.00	3.94	3.25	3.25	4.26
		0.584	> 12.67	> 8.00	2.93	2.75	2.67	3.84
		0.438	4.23	3.58	3.38	2.50	2.43	3.56
		0.219	3.38	3.07	2.93	2.16	2.18	3.06
		0.146	3.12	2.89	2.81	2.04	2.13	2.88
		0.088	2.93	2.93	2.53	1.94	2.09	2.68
	1.4	0.473	4.40	4.36	4.34	2.39	2.60	4.66
		0.316	3.86	4.11	3.40	2.26	2.40	4.03
		0.237	3.48	3.70	3.17	2.19	2.31	3.67
		0.118	3.05	3.28	2.76	2.04	2.15	3.13
		0.079	2.92	3.14	2.62	1.97	2.10	2.95
		0.047	2.81	3.02	2.49	1.90	2.07	2.73
10.0	1.2	0.876	3.35	2.08	14.29	2.58	1.80	12.75
		0.584	3.35	1.96	12.11	2.51	1.72	10.80
		0.438	3.33	1.92	10.87	2.46	1.66	9.72
		0.219	3.08	1.76	8.94	2.34	1.55	7.99
		0.146	2.97	1.70	8.27	2.27	1.50	7.40
		0.088	2.87	1.69	7.70	2.21	1.46	6.82
	1.4	0.473	3.00	1.83	14.39	2.29	1.58	12.69
		0.316	2.95	1.72	12.09	2.29	1.56	10.79
		0.237	2.91	1.68	10.90	2.27	1.52	9.75
		0.118	2.84	1.63	9.06	2.23	1.49	8.10
		0.079	2.80	1.60	8.42	2.20	1.46	7.53
		0.047	2.76	1.62	7.89	2.16	1.43	6.97

Table 3.3 Drift capacity for circular columns (ρ_l= 2 %).

			10 % P_0			20 % P_0		
L / D	A_g / A_c	r_c	% Drift	Ductility	V_{shear}/V_{flo}	% Drift	Ductility	V_{shear}/V_{flo}
2.5	1.2	0.876	> 7.20	> 8.00	1.35	> 7.20	> 8.00	1.40
		0.584	> 7.20	> 8.00	1.05	4.07	5.81	1.20
		0.438	> 7.20	> 8.00	0.90	3.21	5.10	1.05
		0.219	4.02	5.09	0.76	2.07	3.57	0.94
		0.146	3.22	4.54	0.69	1.80	3.21	0.92
		0.088	2.62	3.97	0.64	1.60	2.96	0.86
	1.4	0.473	> 7.20	> 8.00	1.38	> 7.20	> 8.00	1.42
		0.316	> 7.20	> 8.00	1.07	3.52	6.07	1.21
		0.237	> 7.20	> 8.00	0.91	2.77	4.69	1.08
		0.118	3.27	4.48	0.81	1.92	3.31	1.03
		0.079	2.78	4.15	0.72	1.73	3.04	0.98
		0.047	2.41	3.95	0.67	1.58	2.82	0.92
5.0	1.2	0.876	> 12.67	> 8.00	2.57	4.13	3.47	3.04
		0.584	> 12.67	> 8.00	1.90	3.24	2.82	2.77
		0.438	4.82	3.11	2.44	2.83	2.60	2.55
		0.219	3.64	2.76	2.12	2.34	2.23	2.26
		0.146	3.32	2.72	1.97	2.20	2.16	2.11
		0.088	3.05	2.70	1.83	2.06	2.12	1.95
	1.4	0.473	> 12.67	> 8.00	2.55	3.05	2.96	3.31
		0.316	> 12.67	> 8.00	1.90	2.58	2.46	3.00
		0.237	4.17	3.09	2.50	2.43	2.31	2.76
		0.118	3.32	2.74	2.20	2.21	2.13	2.38
		0.079	3.11	2.78	1.99	2.12	2.08	2.21
		0.047	2.92	2.83	1.81	2.01	2.03	2.06
10.0	1.2	0.876	4.58	2.36	8.83	3.04	1.72	9.17
		0.584	4.44	2.27	7.39	2.86	1.58	7.75
		0.438	4.09	2.08	6.87	2.77	1.51	6.96
		0.219	3.58	1.81	5.74	2.60	1.49	5.73
		0.146	3.43	1.74	5.31	2.52	1.45	5.27
		0.088	3.27	1.69	4.96	2.42	1.40	4.84
	1.4	0.473	3.99	2.06	9.30	2.64	1.55	9.32
		0.316	3.66	1.88	7.88	2.61	1.51	7.93
		0.237	3.55	1.81	7.12	2.59	1.49	7.15
		0.118	3.37	1.71	5.92	2.52	1.43	5.96
		0.079	3.27	1.66	5.50	2.47	1.40	5.49
		0.047	3.17	1.62	5.16	2.40	1.37	5.09

Table 3.4 Drift capacity for circular columns (ρ_l= 3 %).

			10 % P_0			20 % P_0		
L / D	A_g / A_c	r_c	% Drift	Ductility	V_{shear}/V_{flo}	% Drift	Ductility	V_{shear}/V_{flo}
2.5	1.2	0.876	> 7.20	> 8.00	1.03	> 7.20	> 8.00	1.13
		0.584	> 7.20	> 8.00	0.81	> 7.20	> 8.00	0.91
		0.438	> 7.20	> 8.00	0.69	3.37	5.11	0.86
		0.219	4.39	6.10	0.56	2.10	3.50	0.78
		0.146	3.22	4.95	0.52	1.80	3.10	0.77
		0.088	2.45	4.15	0.49	1.56	2.79	0.72
	1.4	0.473	> 7.20	> 8.00	1.07	> 7.20	> 8.00	1.16
		0.316	> 7.20	> 8.00	0.83	> 7.20	> 8.00	0.93
		0.237	> 7.20	> 8.00	0.71	3.01	4.85	0.89
		0.118	3.39	5.06	0.61	1.93	3.22	0.86
		0.079	2.77	4.33	0.56	1.71	2.90	0.84
		0.047	2.29	3.82	0.54	1.53	2.64	0.78
5.0	1.2	0.876	> 12.67	> 8.00	1.96	> 12.67	> 8.00	1.98
		0.584	> 12.67	> 8.00	1.45	3.54	2.90	2.20
		0.438	5.36	3.60	1.64	3.06	2.68	2.02
		0.219	3.85	3.10	1.48	2.44	2.26	1.81
		0.146	3.45	2.95	1.40	2.27	2.18	1.69
		0.088	3.08	2.88	1.32	2.10	2.10	1.57
	1.4	0.473	> 12.67	> 8.00	1.97	3.80	3.45	2.48
		0.316	> 12.67	> 8.00	1.46	2.92	2.61	2.37
		0.237	4.67	3.68	1.65	2.64	2.36	2.22
		0.118	3.52	2.98	1.58	2.31	2.14	1.93
		0.079	3.24	2.87	1.49	2.20	2.08	1.81
		0.047	2.99	2.74	1.43	2.07	2.01	1.68
10.0	1.2	0.876	5.36	2.59	6.33	3.43	1.77	7.18
		0.584	5.14	2.38	5.38	3.16	1.60	6.06
		0.438	4.55	2.10	5.07	2.99	1.51	5.43
		0.219	3.85	1.84	4.26	2.77	1.41	4.48
		0.146	3.65	1.76	3.94	2.67	1.38	4.12
		0.088	3.47	1.72	3.69	2.56	1.36	3.78
	1.4	0.473	4.65	2.22	6.82	2.90	1.50	7.40
		0.316	4.38	2.08	5.84	2.85	1.45	6.30
		0.237	3.96	1.87	5.35	2.81	1.42	5.68
		0.118	3.63	1.71	4.45	2.70	1.36	4.73
		0.079	3.52	1.68	4.14	2.64	1.34	4.37
		0.047	3.40	1.65	3.87	2.56	1.32	4.03

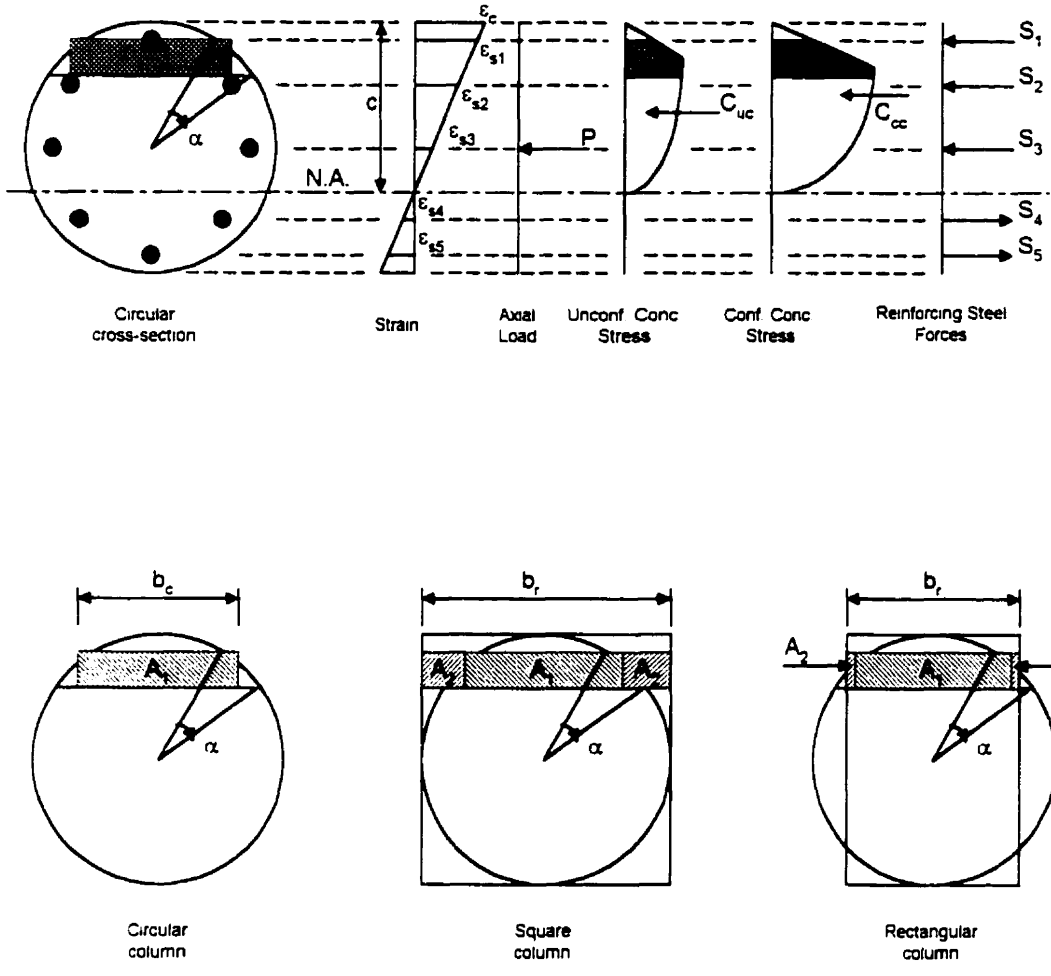

Figure 3.1 Sectional analysis.

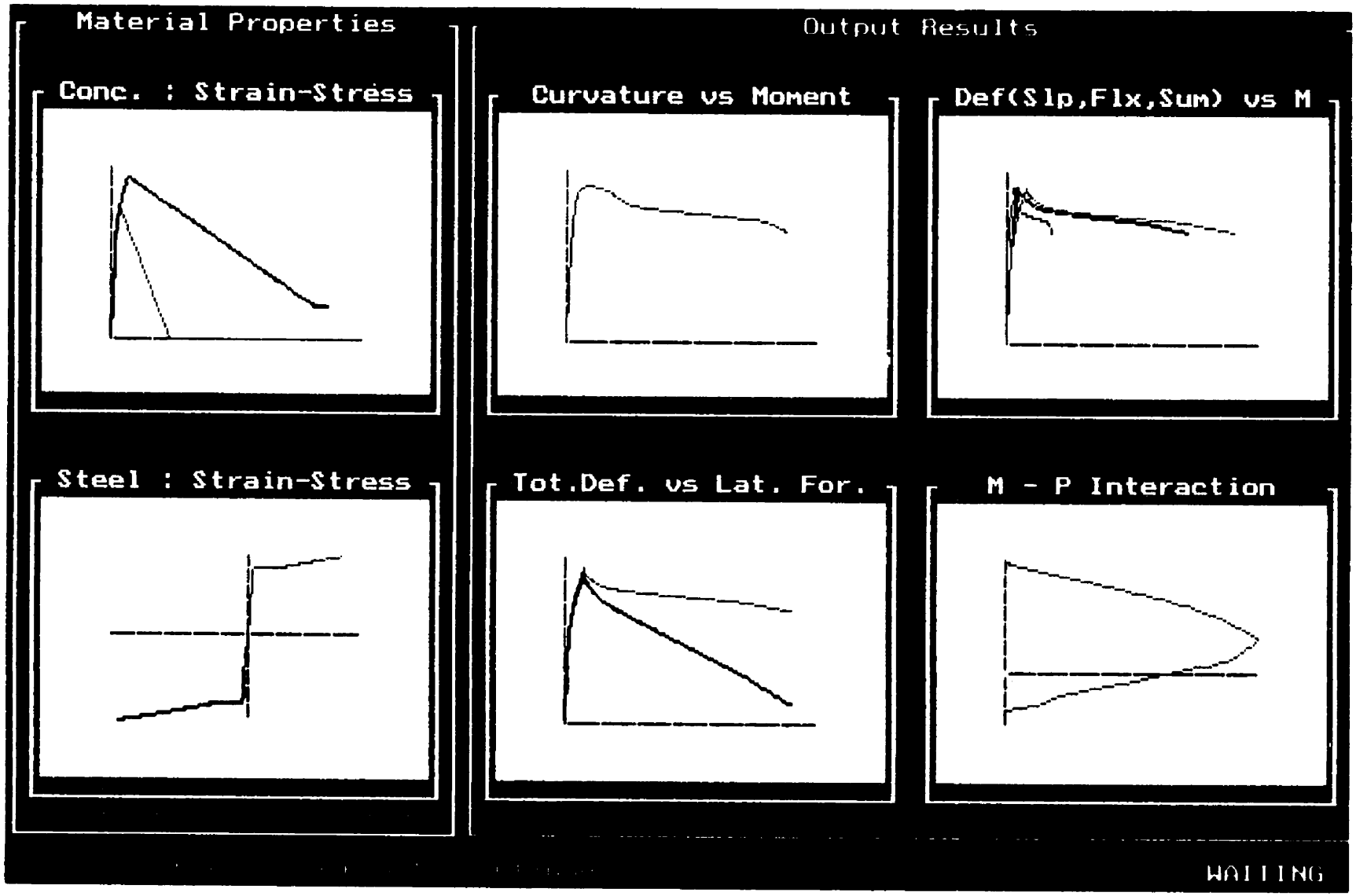
Material Properties
Conc. : Strain-Stress
Steel : Strain-Stress
Output Results
Curvature vs Moment
Def(Slp,Flx,Sum) vs M
Tot.Def. vs Lat. For.
M - P Interaction
WAITING

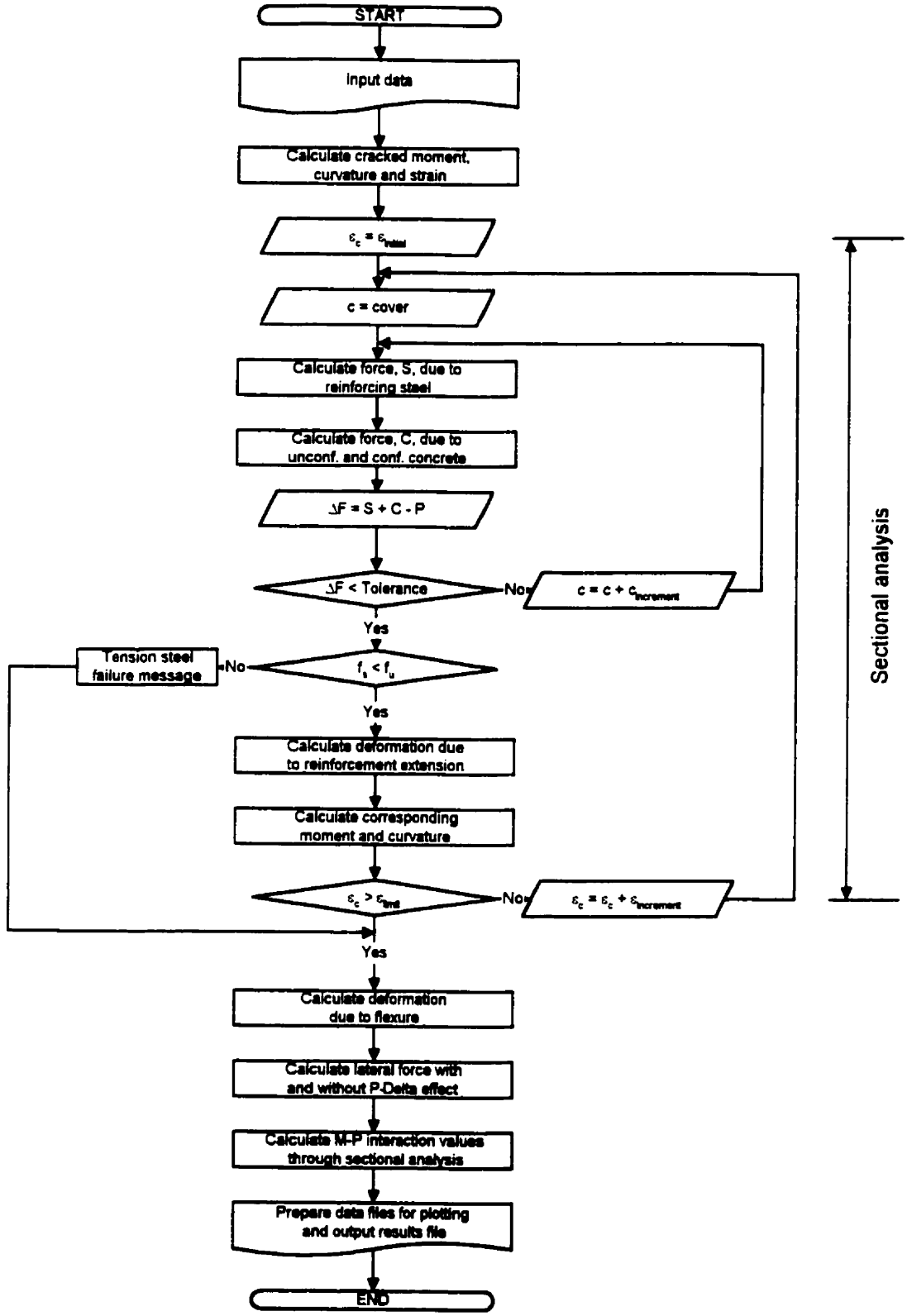

Figure 3.3 Flowchart of software COLA.

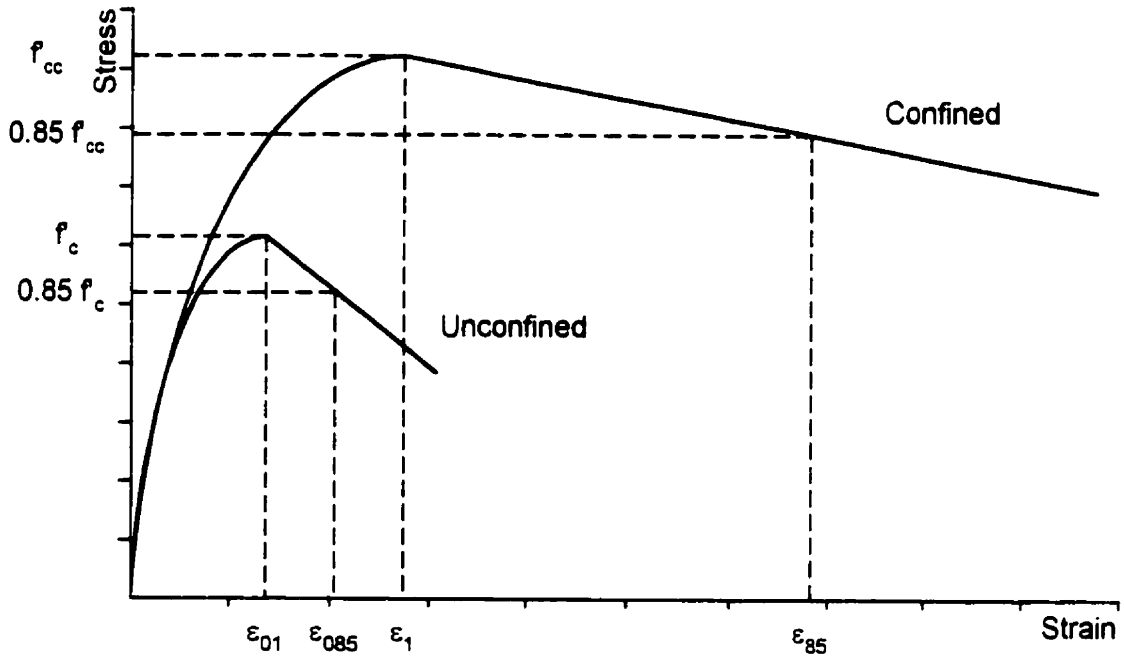

Figure 3.4 Stress-strain relationship for unconfined and confined concrete.

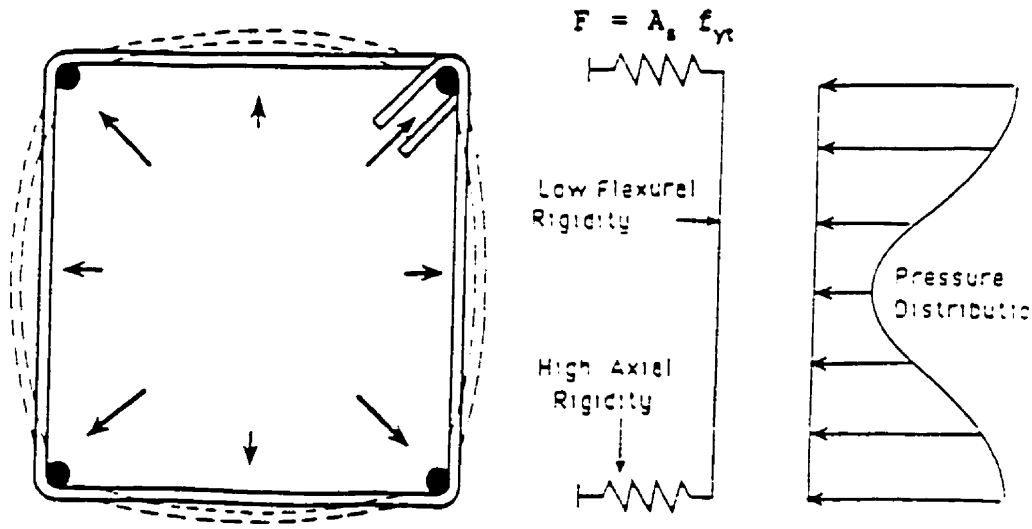

(a) Lateral pressure built-up in a square column

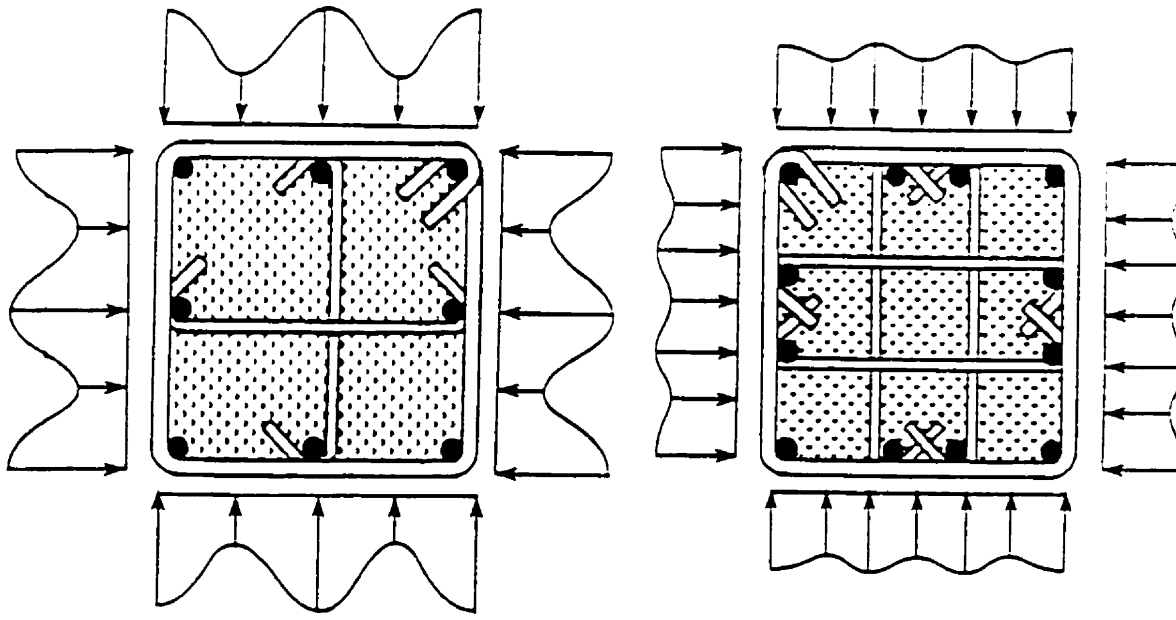

(b) Pressure distributions resulting from different reinforcement arrangements

Figure 3.5 Passive confinement pressure generated by transverse reinforcement.

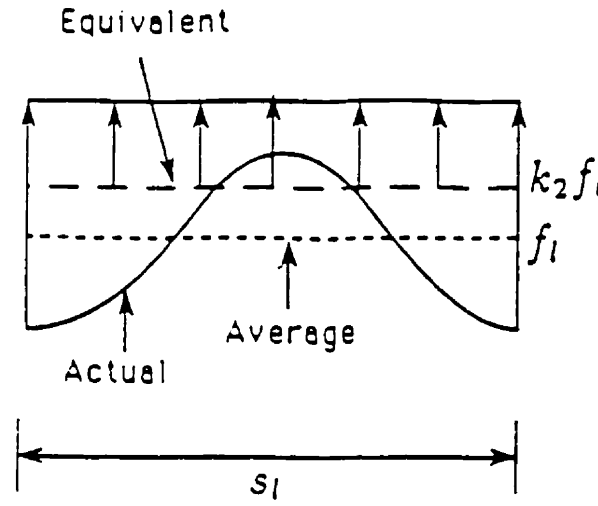

(c) Actual, average and equivalent lateral pressures

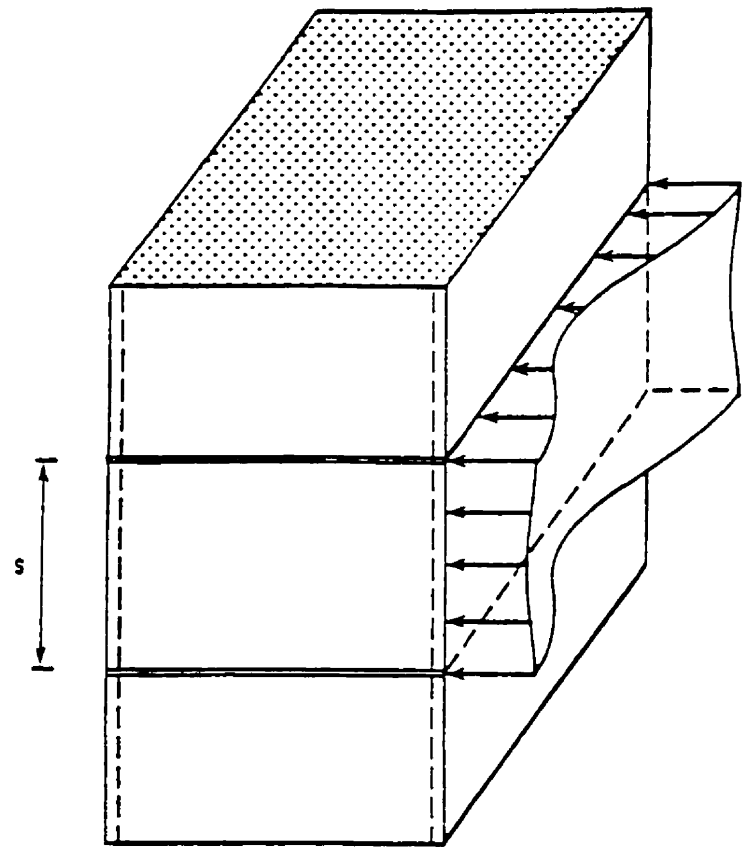

(d) Distribution of lateral pressure along member length.

Figure 3.5 (Continued).

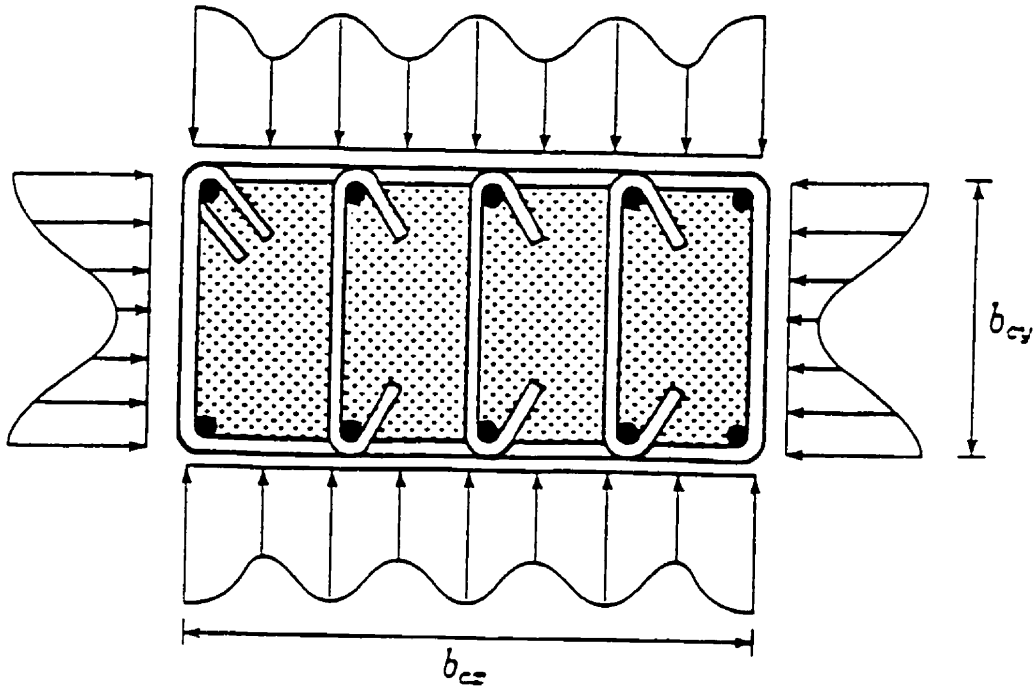

(e) Lateral pressure distribution in a rectangular column

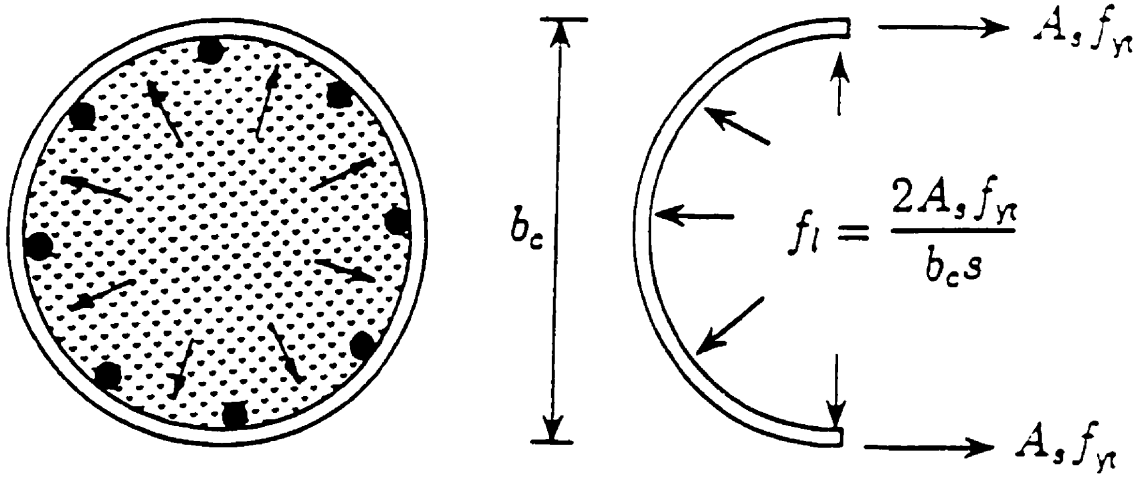

(f) Uniform pressure built-up in a circular column with closely spaced circular spirals

Figure 3.5 (Continued).

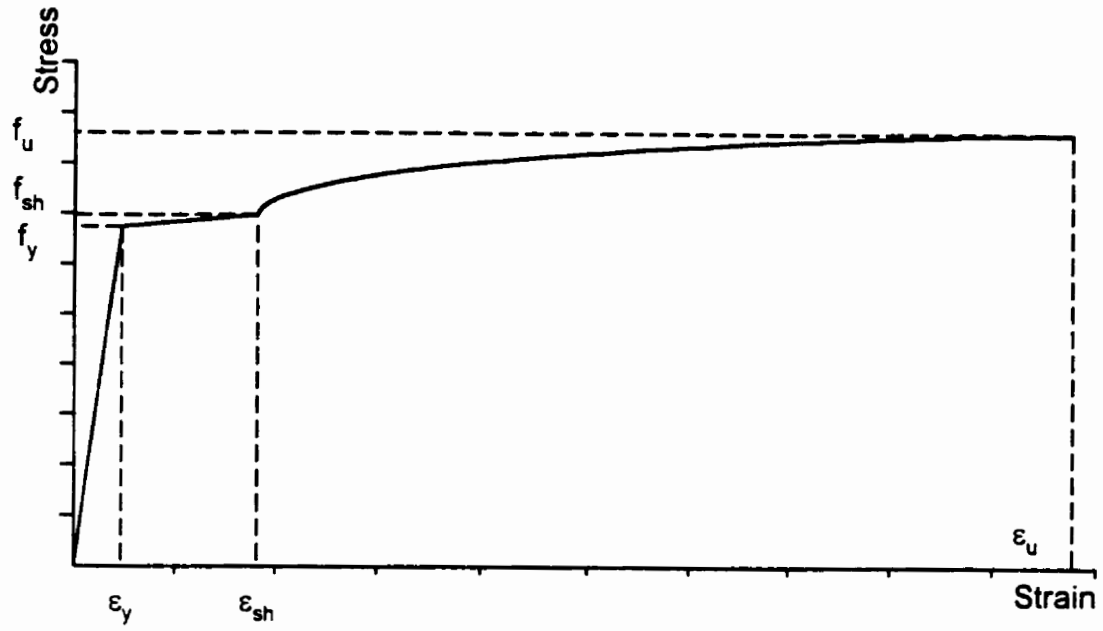

Figure 3.6 Stress-strain relationship for reinforcing steel in tension.

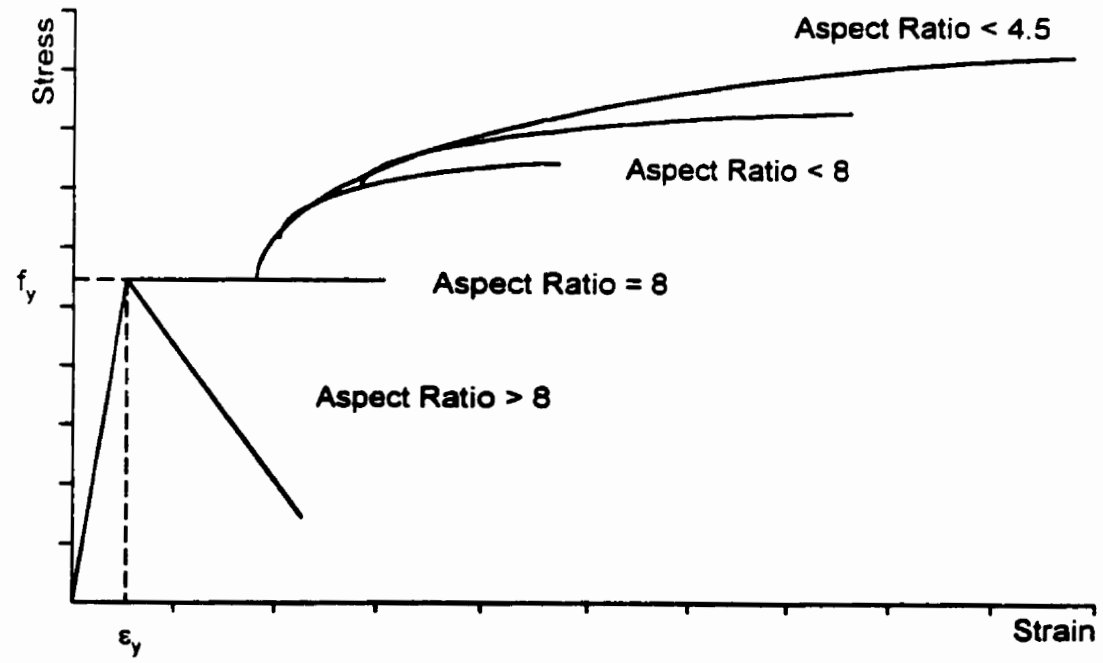

Figure 3.7 Stress-strain relationship for reinforcing steel in compression.

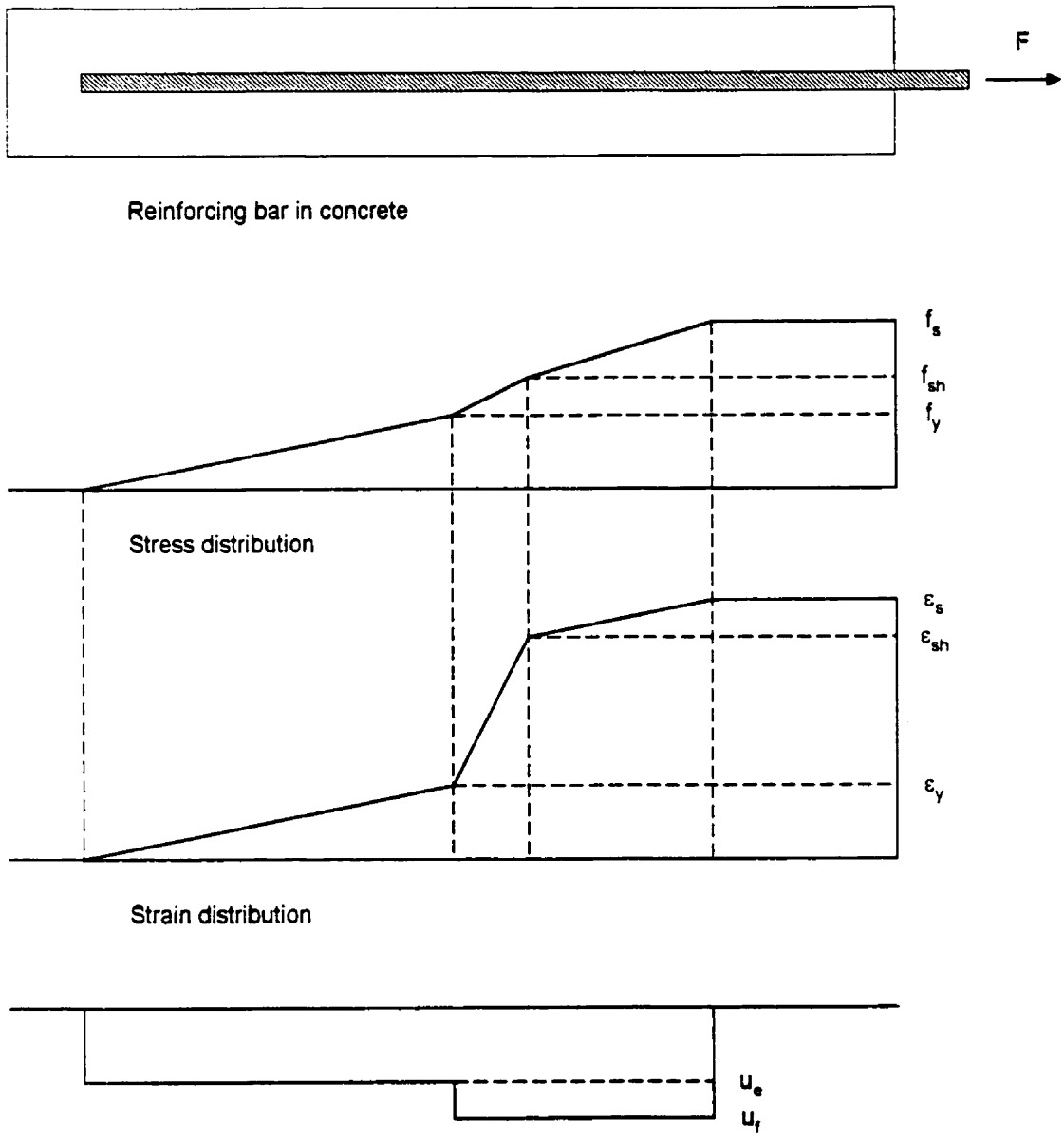

Figure 3.8 Stress and strain distributions of extension of reinforcing steel.

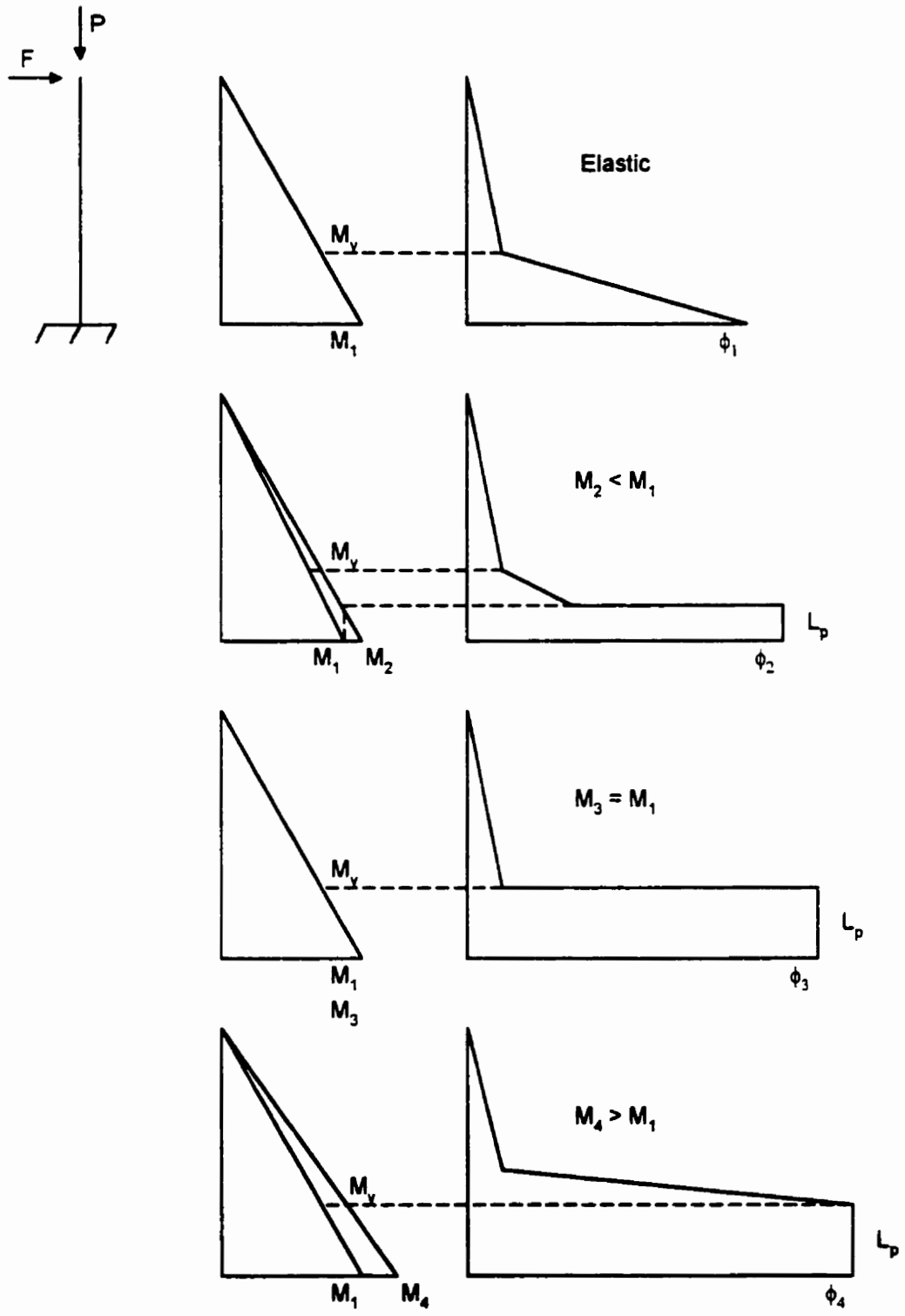

Figure 3.9 Progression of plastic hinging.

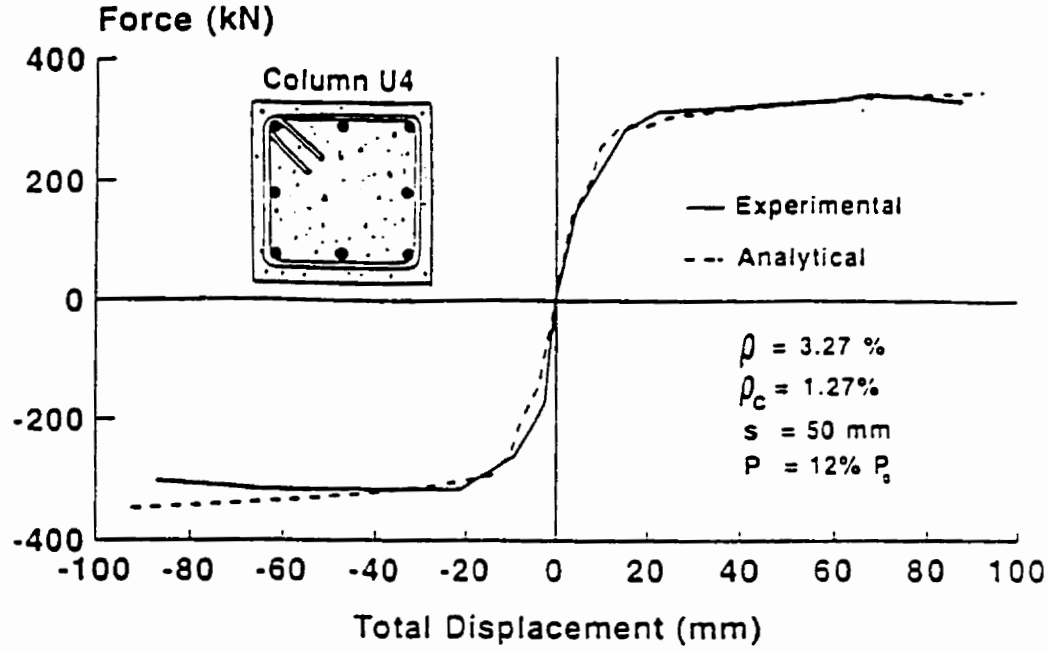

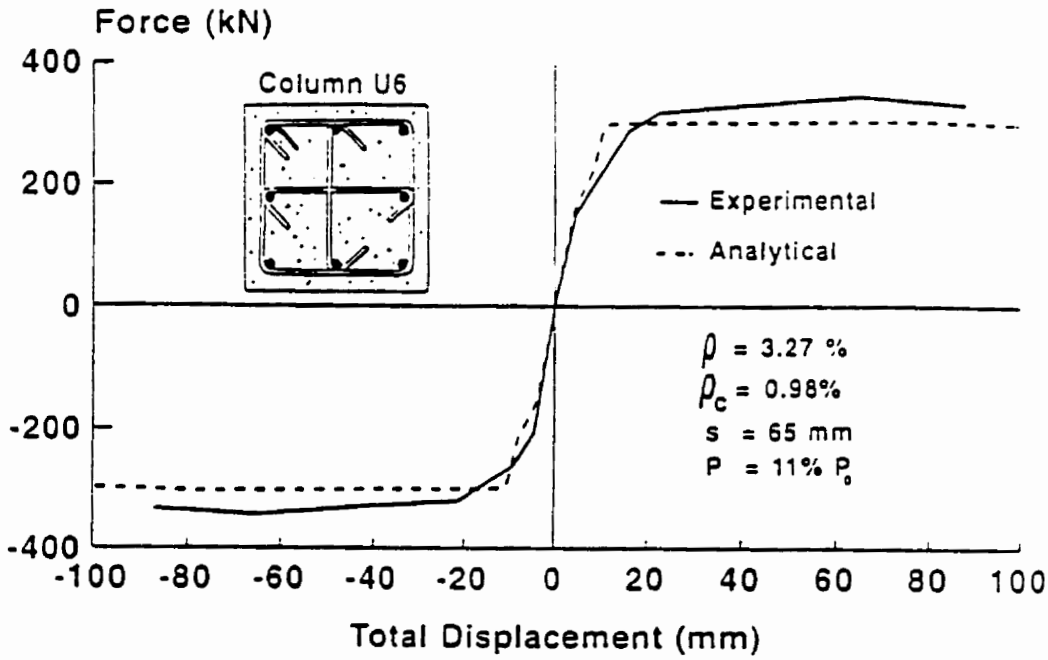

Figure 3.10 Comparisons of analytical and experimental lateral force-displacement relationships for columns tested by Saatcioglu and Ozcebe.

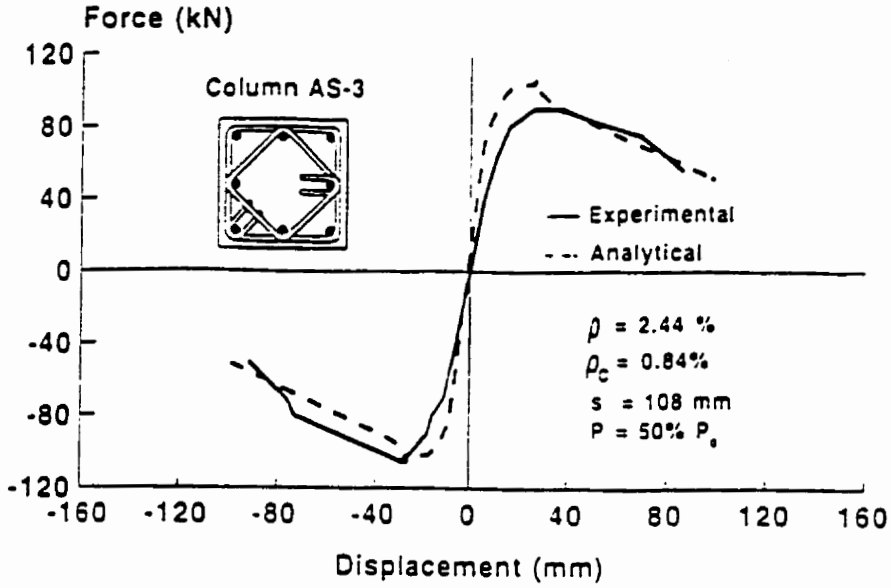

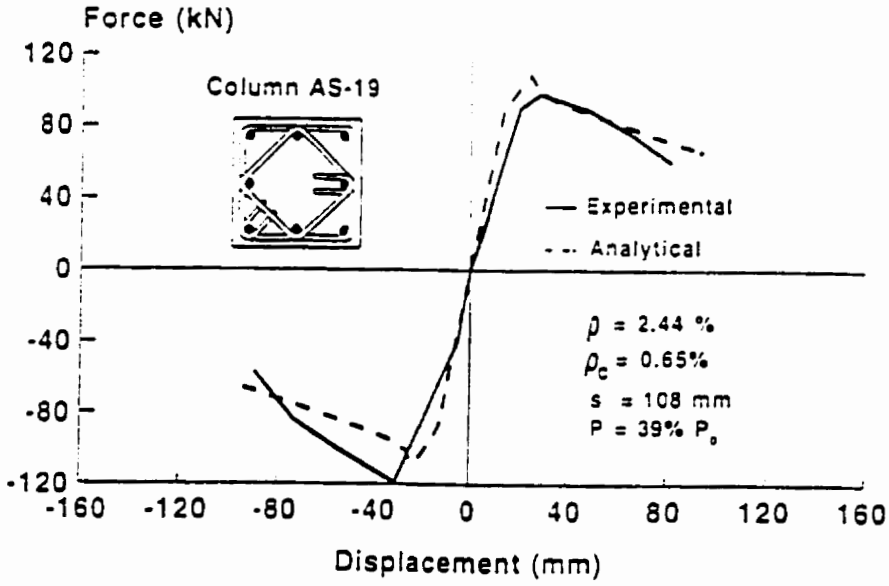

Figure 3.11 **Comparisons of analytical and experimental lateral force-displacement relationships for columns tested by Sheikh and Khoury.**

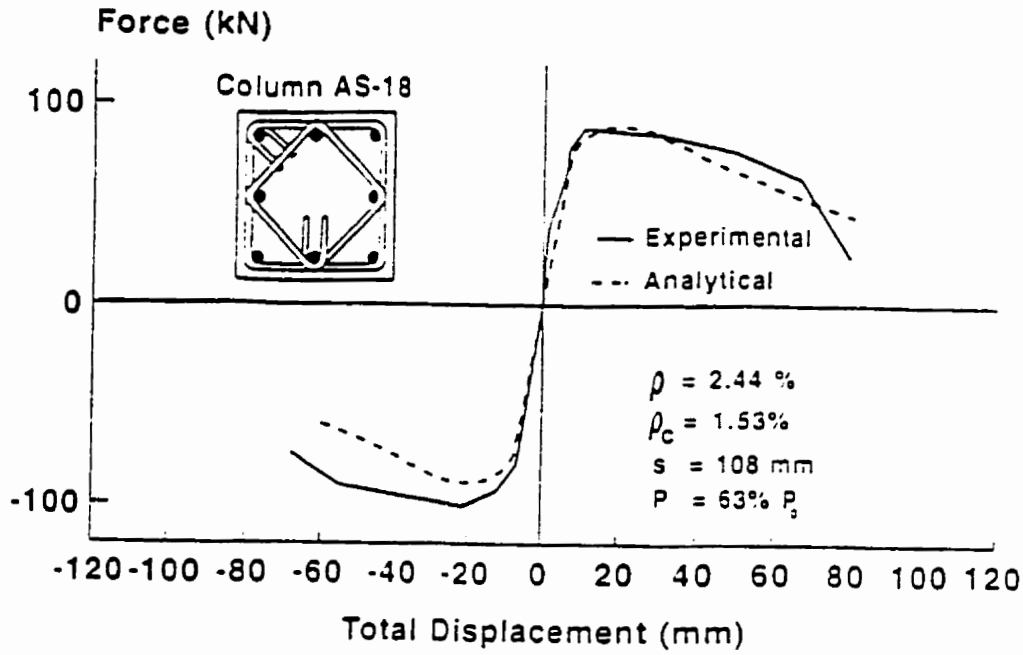

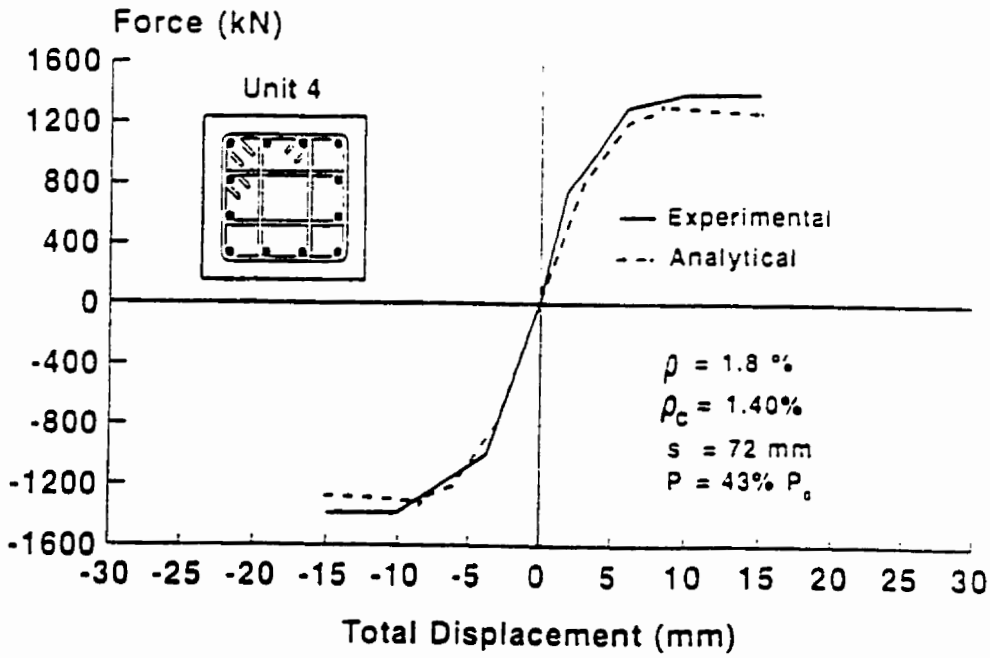

Figure 3.12 Comparisons of analytical and experimental lateral force-displacement relationships for columns tested by Sheikh and Khoury; Park, Priestley and Gill.

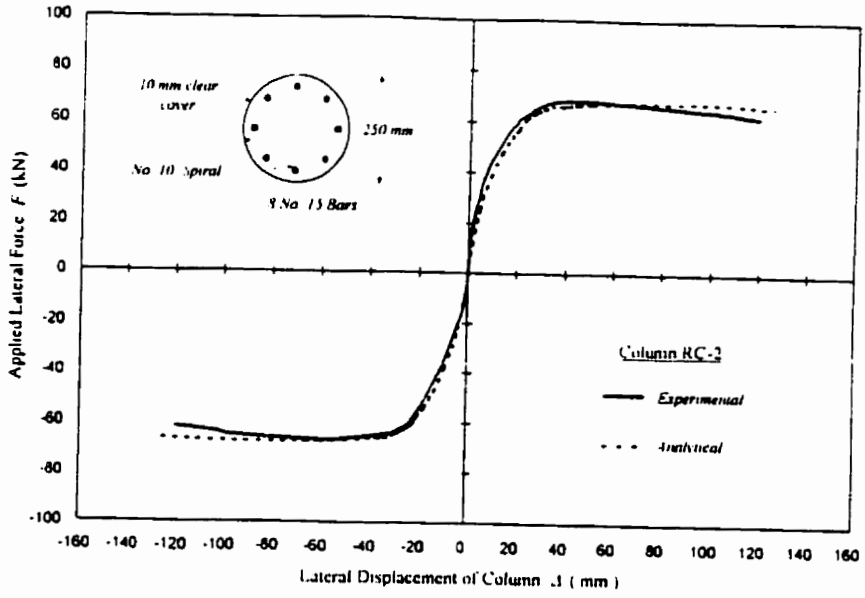

Comparison of Force - Displacement Relationships for Columns RC-2
(Experimental and Analytical - Without P-Δ effect)

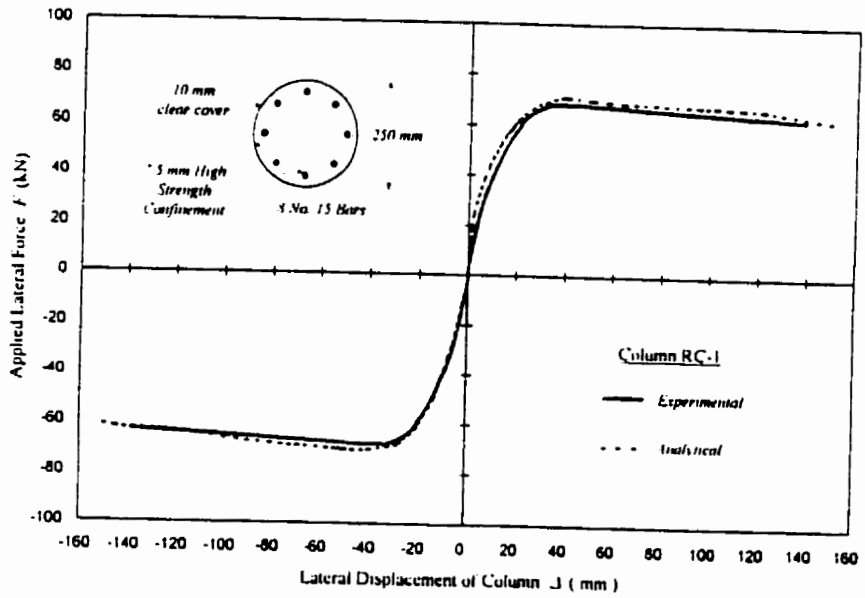

Comparison of Force - Displacement Relationships for Columns RC-1
(Experimental and Analytical - Without P-Δ effect)

Figure 3.13 Comparisons of analytical and experimental lateral force-displacement relationships for columns tested by Saatcioglu and Baingo.

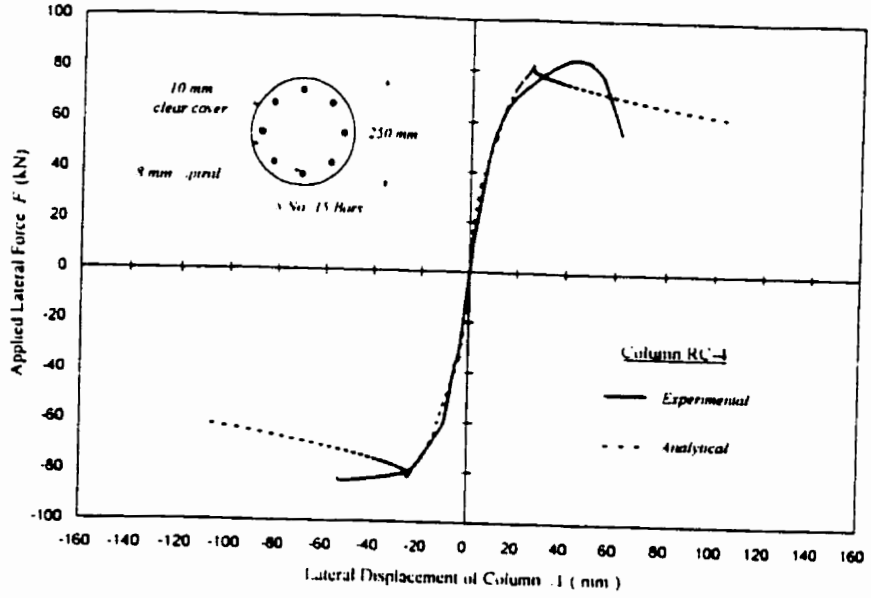

Lateral Displacement of Column 4 (mm)

Comparison of Force - Displacement Relationships for Columns RC-4
(*Experimental and Analytical - Without P-Δ effect*)

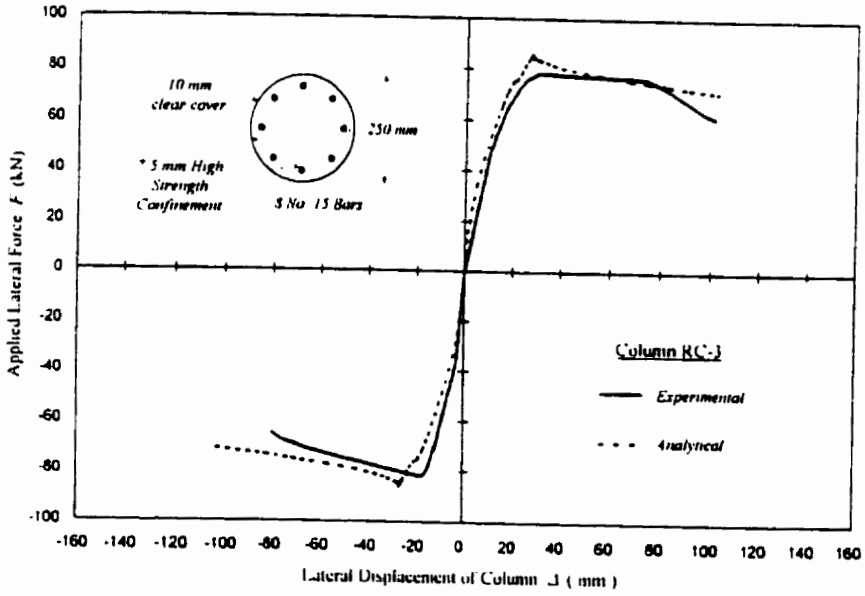

Lateral Displacement of Column 3 (mm)

Comparison of Force - Displacement Relationships for Columns RC-3
(*Experimental and Analytical - Without P-Δ effect*)

Figure 3.14 Comparisons of analytical and experimental lateral force-displacement relationships for columns tested by Saatcioglu and Baingo.

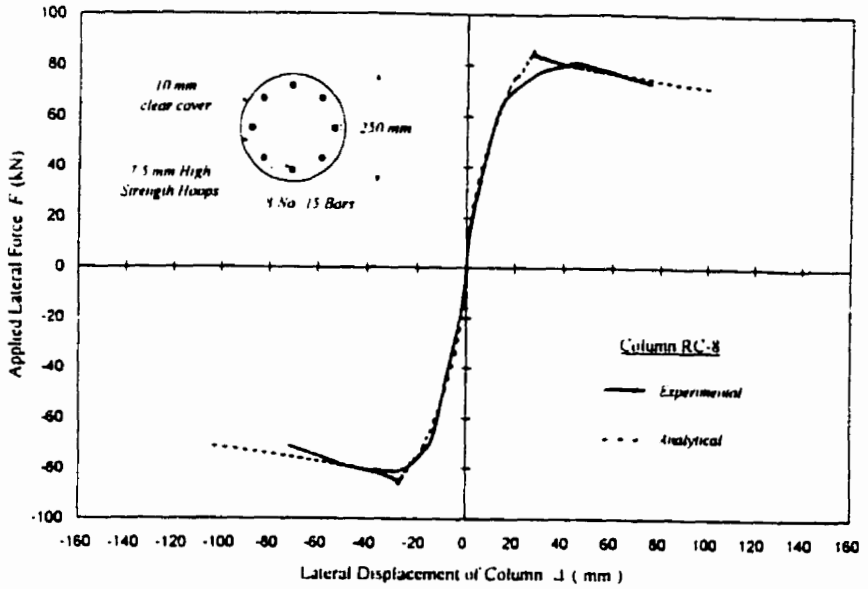

Comparison of Force - Displacement Relationships for Columns RC-8
(*Experimental and Analytical - Without P-Δ effect*)

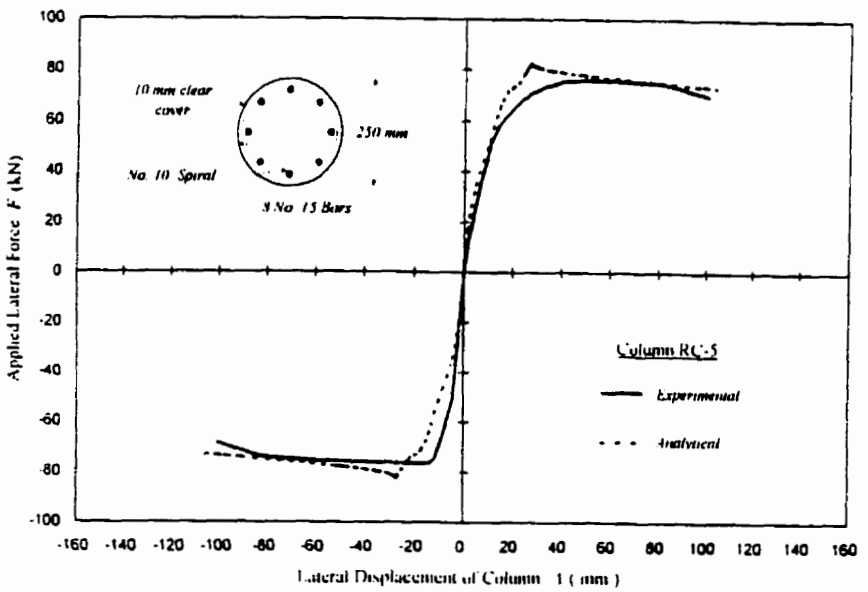

Comparison of Force - Displacement Relationships for Columns RC-5
(*Experimental and Analytical - Without P-Δ effect*)

Figure 3.15 Comparisons of analytical and experimental lateral force-displacement relationships for columns tested by Saatcioglu and Baingo.

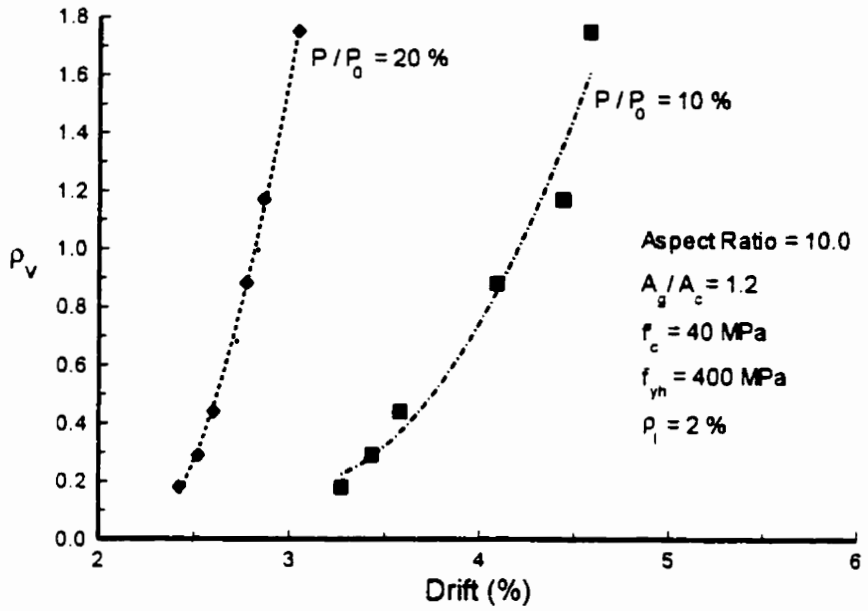

Figure 3.16 Effect of axial load ratio on drift capacity of columns.

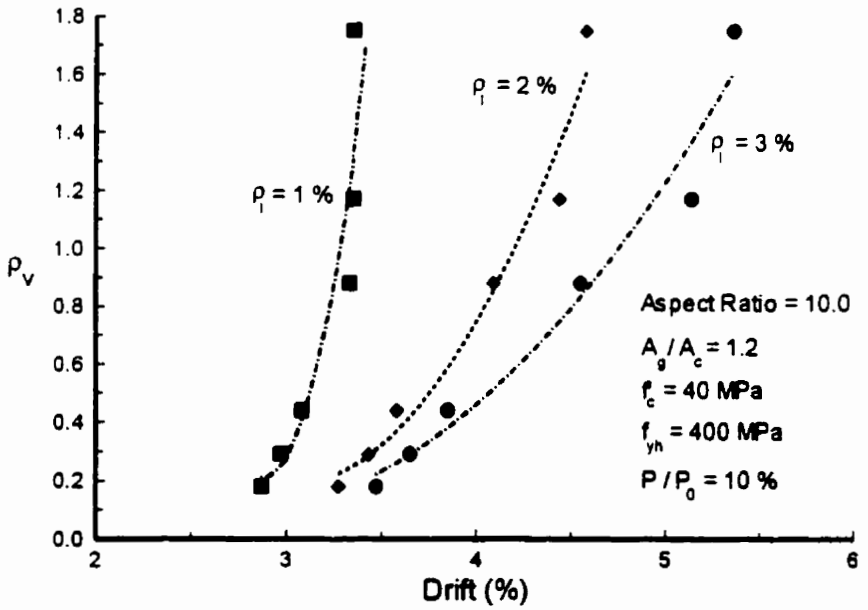

Figure 3.17 Effect of longitudinal reinforcement ratio on drift capacity of columns.

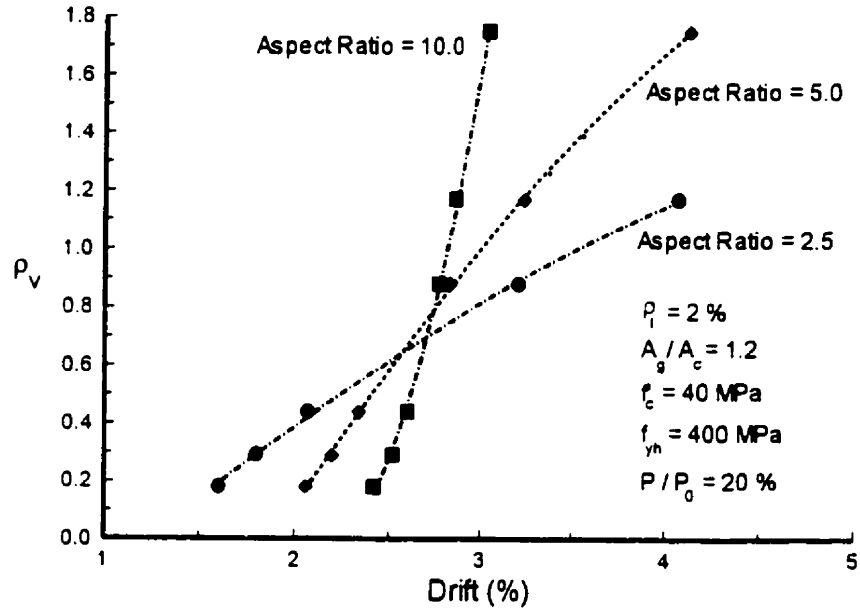

Figure 3.18 Effect of axial load ratio (cantilever length to cross-sectional dimension) on drift capacity of columns.

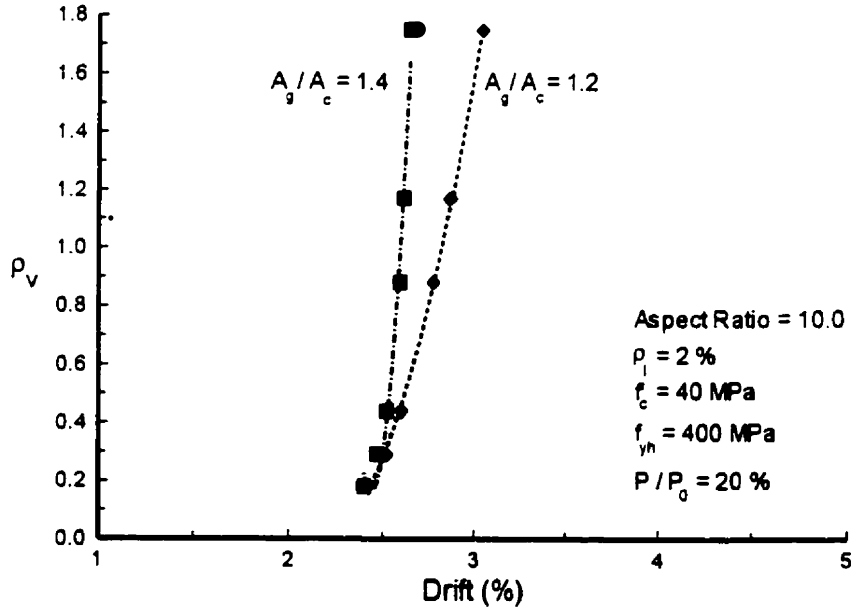

Figure 3.19 Effect of column gross area to core area ratio on drift capacity of columns.

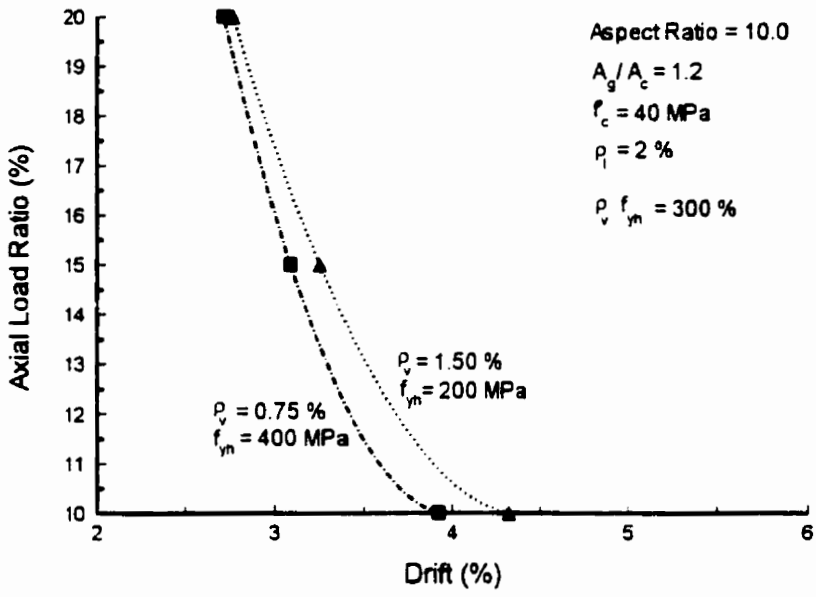

Figure 3.20 Effect of the product of volumetric transverse reinforcement ratio and hoop steel yield stress on drift capacity of columns.

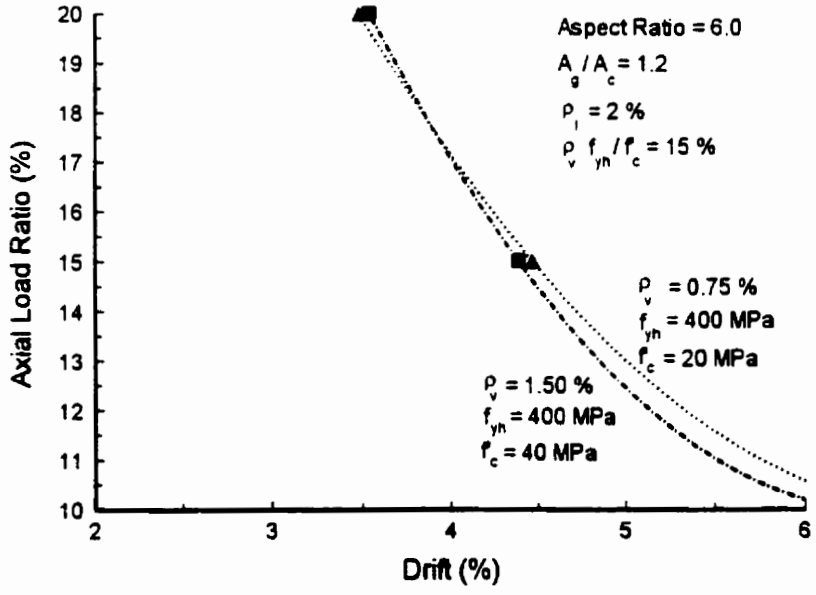

Figure 3.21 Effect of aspect ratio and the product of volumetric transverse reinforcement ratio, hoop steel yield stress and compressive strength of concrete on drift capacity of columns.

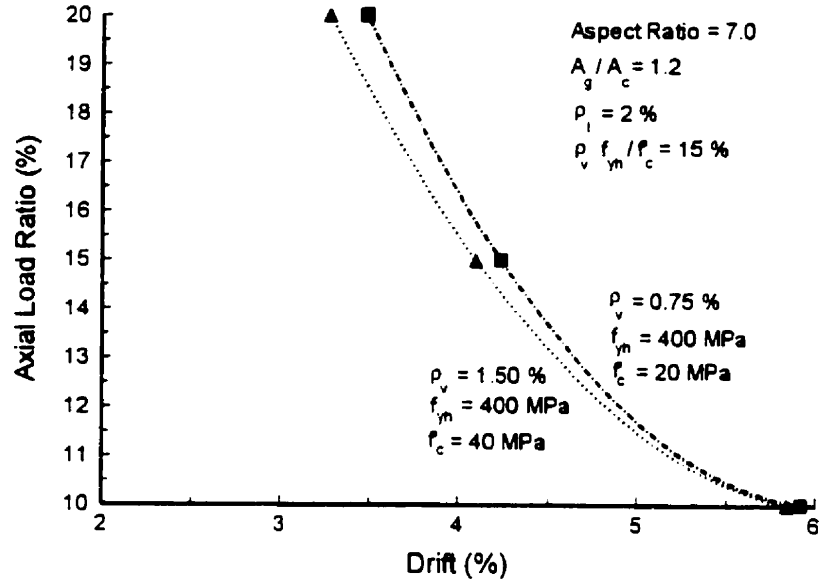

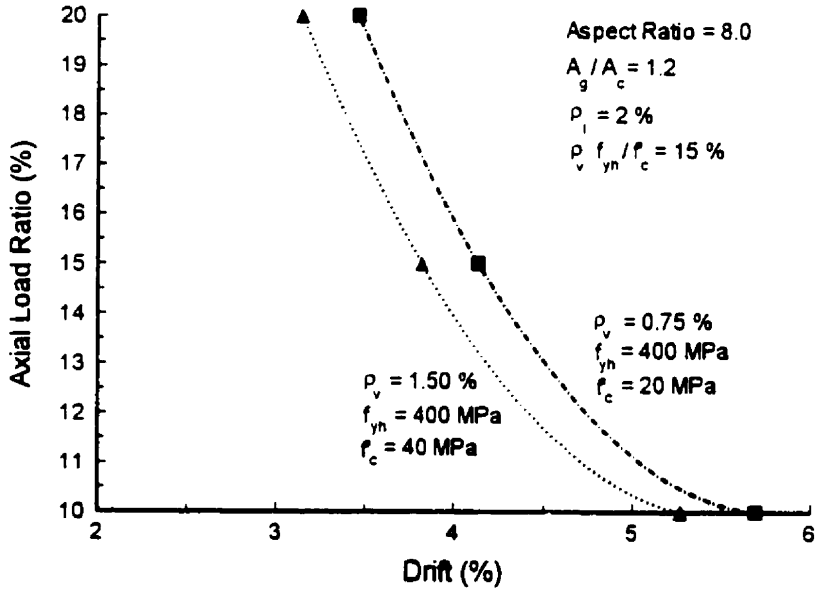

Figure 3.21 (Continued).

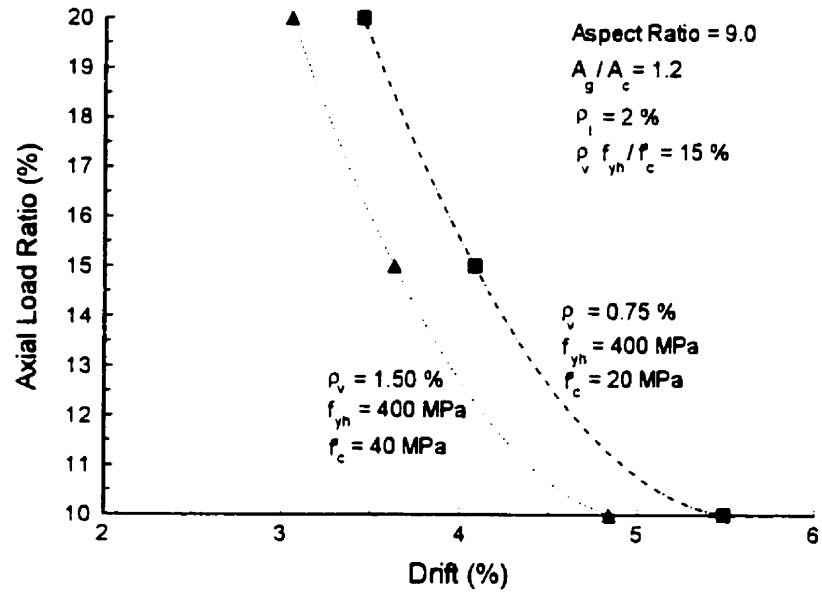

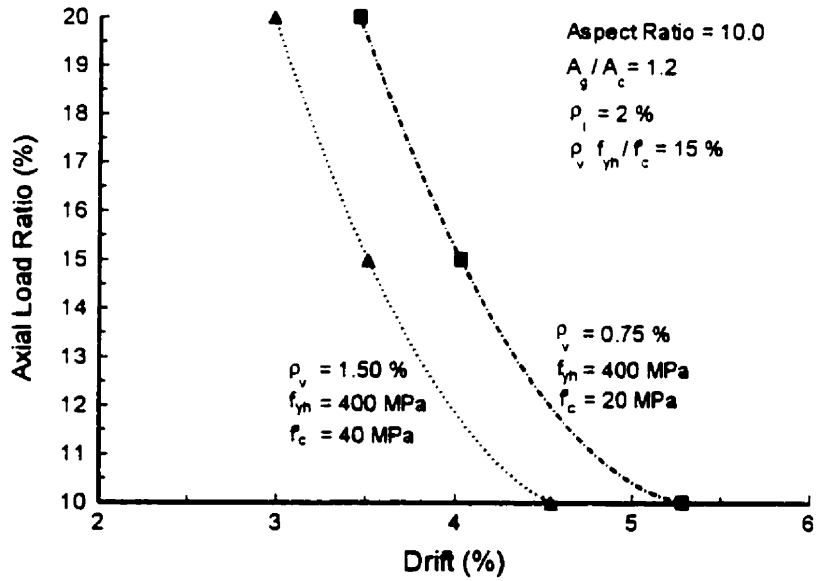

Figure 3.21 (Continued).

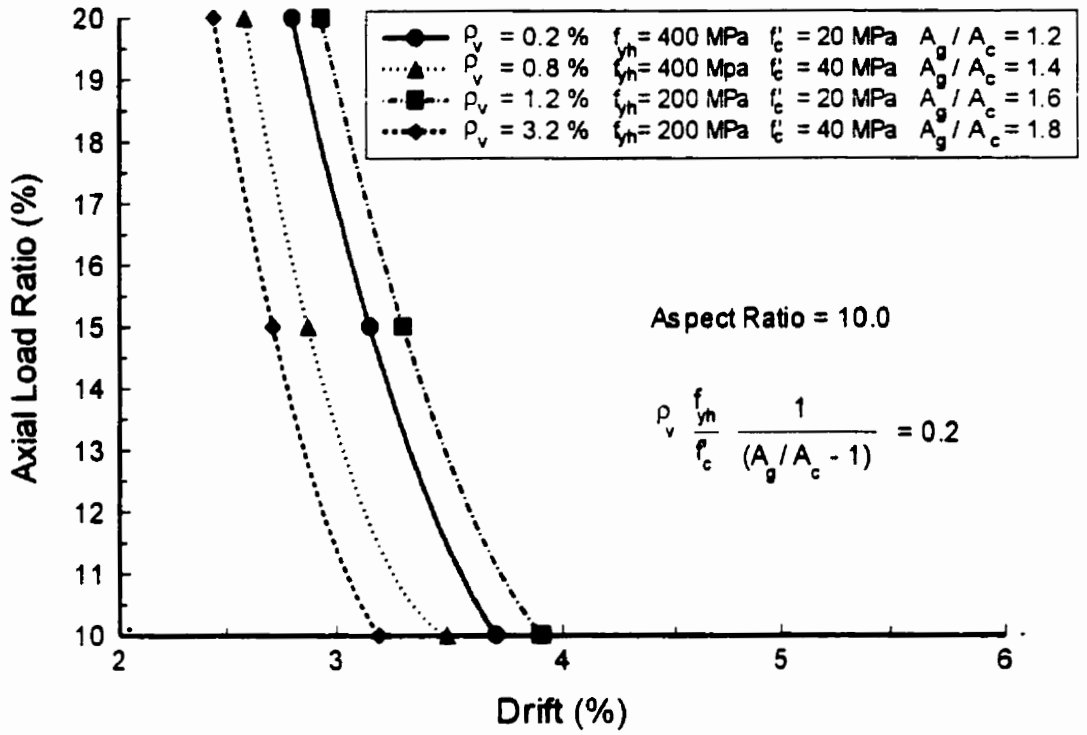

Figure 3.22 Effect of different concrete covers and different levels of confinement on drift capacity of columns.

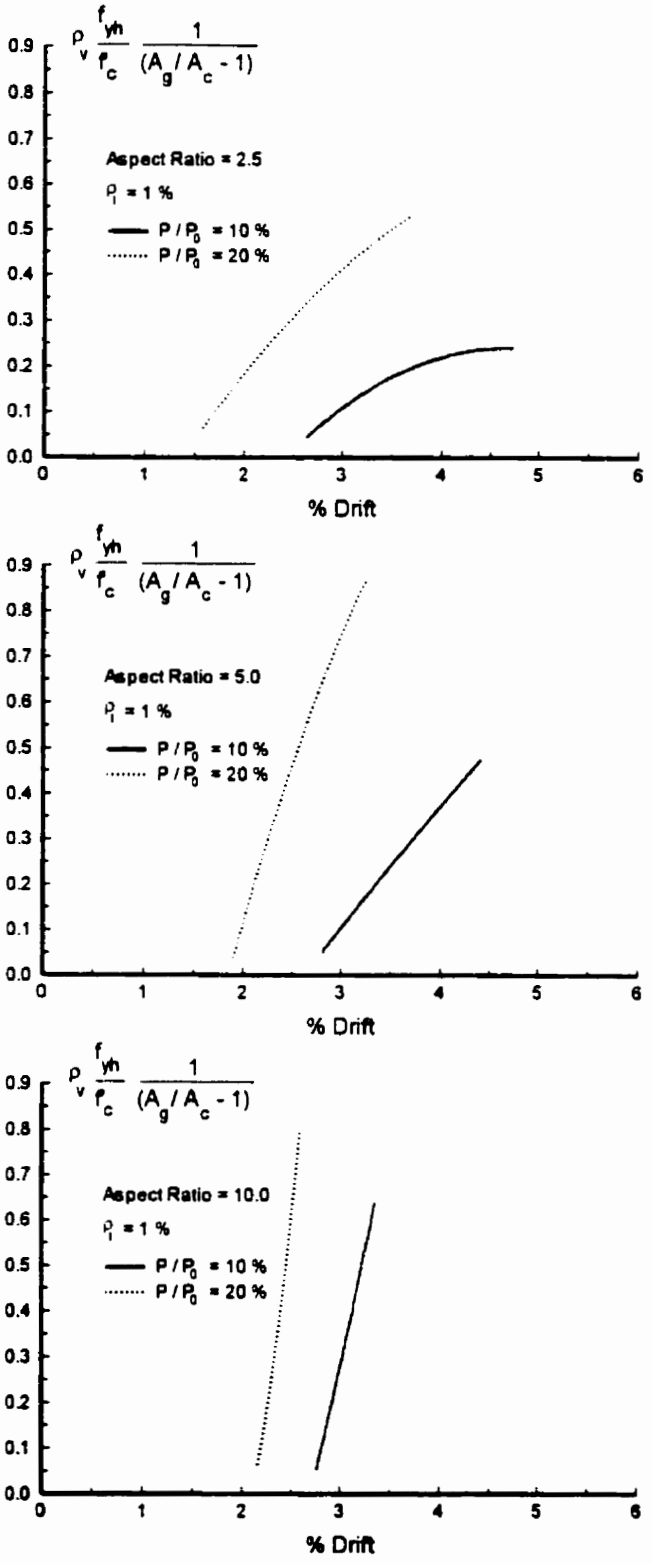

Figure 3.23 Design charts for circular columns (ρ_l = 1 %).

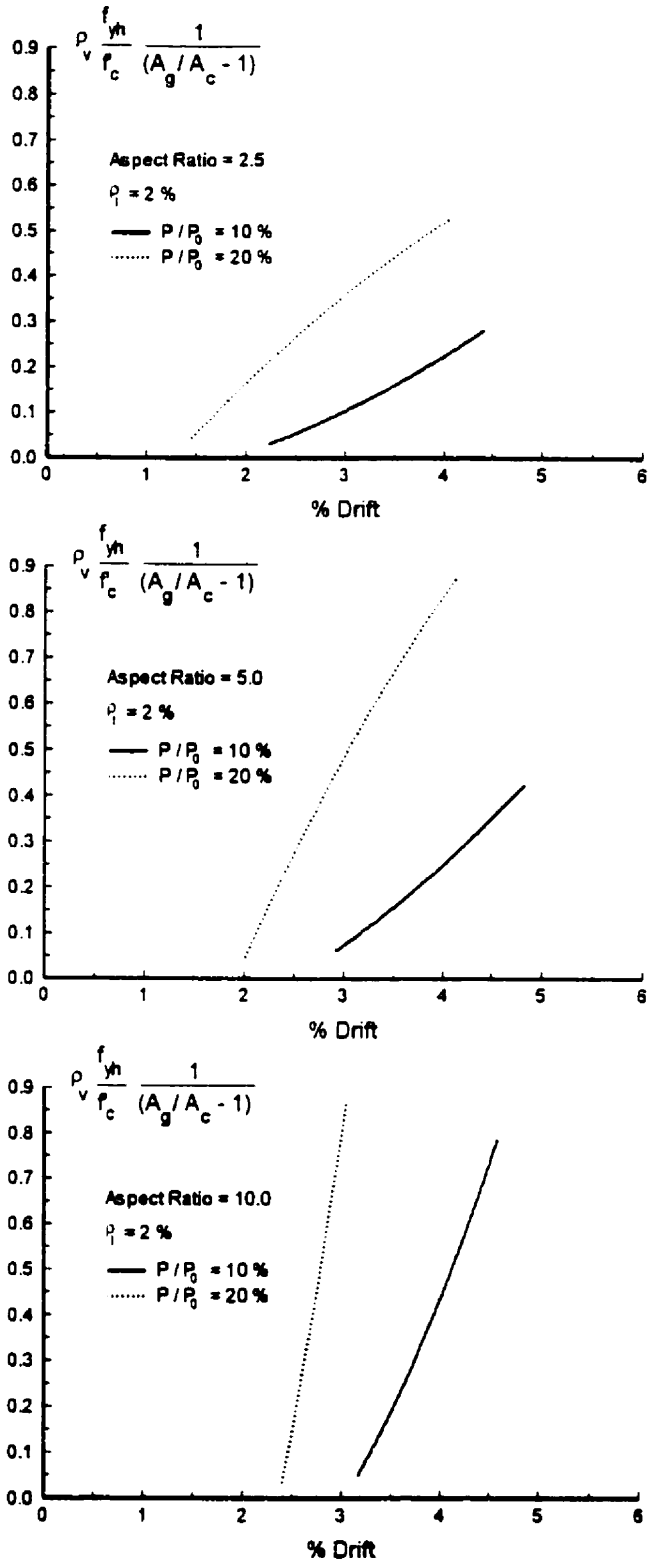

Figure 3.24 Design charts for circular columns ($\rho_l = 2$ %).

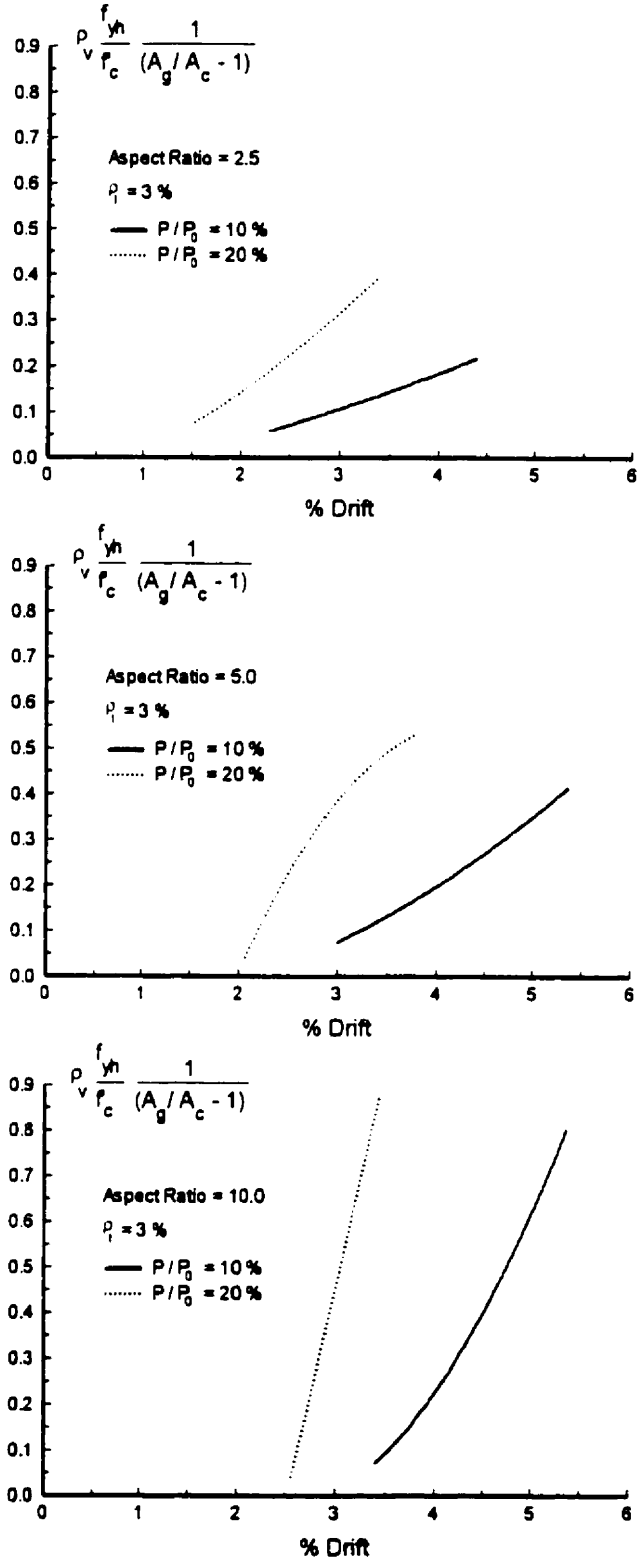

Figure 3.25 Design charts for circular columns (ρ_l = 3 %).

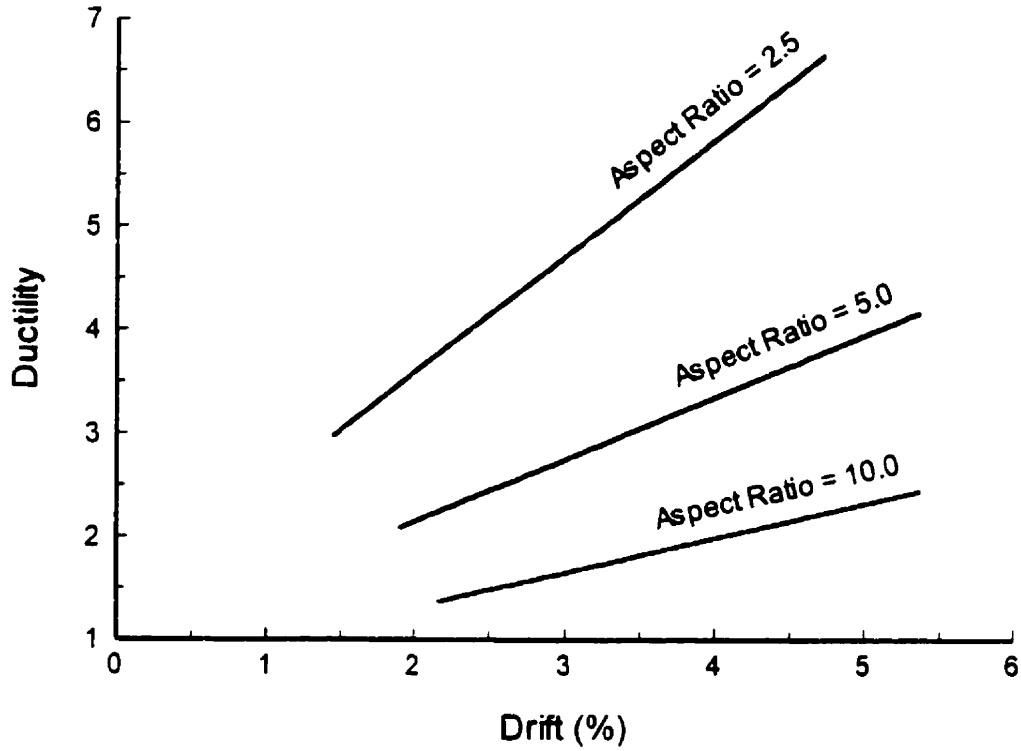

Figure 3.26 Relationship between ductility and drift capacity of columns for various aspect ratios.

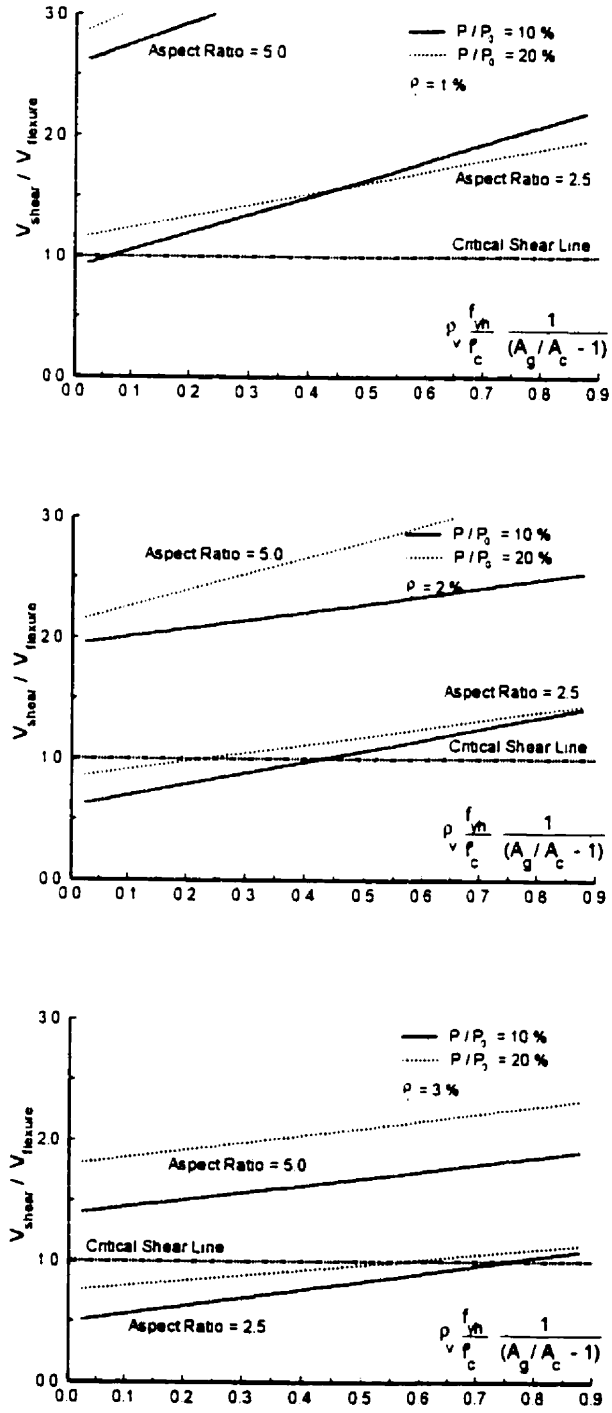

Figure 3.27 Charts for prediction of shear and flexural behavior of columns for various longitudinal reinforcement.

Chapter 4

Drift Demands

4.1 General

It is uneconomical to design structures to remain elastic during strong earthquakes. Therefore, structures are designed to experience inelastic deformations in critical regions. Inelastic deformation requirements in such structures must be established before rational design methods for new structures and retrofit techniques for existing structures can be employed. Thus, it is important to establish inelastic deformation demands of structures located in different seismic regions in Canada. Since the objective of this research project concerns reinforced concrete bridge columns, the emphasis is placed on inelastic drift demands of these columns.

Drift demands of bridge columns were investigated through dynamic inelastic response history analyses. A computer software, DRAIN-RC was chosen for this purpose. DRAIN-RC was developed at the University of Ottawa (Saatcioglu et al. 1997), as a modified version of general purpose computer software, DRAIN-2D, originally developed at the University of California, Berkeley (Kannan and Powell 1973). A brief description of the computer program and analysis scheme are discussed in the following sections.

4.2 Description of Computer Software, DRAIN-RC

DRAIN-RC is intended for planar dynamic inelastic response history analysis of reinforced concrete structures. It contains hysteretic models suitable for reinforced concrete

structures, including those for flexure, with and without axial load-moment interaction, shear, anchorage slip, infill panels, and truss elements. The hysteretic model for flexure was developed by Takeda et al. (1970) and has degrading stiffness characteristics. The model was later modified by Saatcioglu et al. (1983) to introduce the interactive effects of axial force with flexure and the resulting changes in strength and stiffness during response. Inelastic shear effects are modeled by a hysteretic model developed by Ozcebe and Saatcioglu (1989) and includes pinching of loops during reloading. Anchorage slip, consisting of the extension and slippage of reinforcement in the adjoining member, is modeled following the hysteretic model proposed by Saatcioglu and Alsiwat (1992). Infill panels can be assigned a hysteretic model that was developed by Klinger and Bertero (1978), simulating the behavior of diagonal ties and struts in wall panels. The program also has capabilities of conducting "Push-Over" analysis. Furthermore, it has an option to consider P-Δ effects. Dynamic loading is introduced in terms of horizontal and vertical ground motions.

The structure to be analyzed must first be modeled with discrete elements between nodes. Each node has three degrees of freedom, two translational, and one rotational. Structural mass is lumped at the nodes. The dynamic response is determined using a step-by-step integration technique, assuming constant acceleration during each time step. Therefore, non-linear response is divided into linear responses between two time intervals, and the stiffness of each element is updated at the end of each interval for the following time step.

Each element is modeled as an elastic member with three point springs at the ends for flexure, shear and anchorage slip components of inelastic deformations. Hysteretic models are assigned to these springs to simulate cyclic behavior. Primary curves for inelastic springs are specified as input. Loading, unloading and reloading branches of hysteresis loops are generated by following the rules incorporated in each model. The three hysteretic models assigned to the member end springs are shown in Figure 4.1.

The program calculates ductility factors based on chord angle. Ductility factors, defined as maximum chord angle divided by the angle at initial yield, are listed for each deformation component, i.e., flexure, shear and anchorage slip, as well as for total deformation. The program further calculates energy dissipation factors as the ratio of plastic to elastic

energy, where the energy is computed as the area under the force-deformation hysteretic relationship.

4.3 Modeling of Bridges

Structural response can be determined reasonably accurately under ideal conditions which involve well established material models, earthquake ground motion records, and computerized analysis tools. However, in reality, the unknown nature of boundary conditions often yields different results than what is found using deterministic mathematical models. The objective of modeling a structure for the purpose of analysis is to simulate actual conditions as realistically as possible. In order to achieve this objective one has to make certain simplifying assumptions since the connections between individual frame elements and the supports, including bearings at columns and abutments, may require complex modeling techniques which often can not be justified since their behavior are not well established.

The response of a prototype bridge structure can be described in terms of discrete mathematical elements with properly defined boundary conditions. There are various levels of discretization of mathematical models ranging from single degree of freedom (SDOF) lumped-mass models to detailed three-dimensional finite-element models.

It is generally believed that bridge models used for seismic analysis should be kept simple. Global bridge models are often used for single frame structures. Individual frame models are used when the bridge structure has movement joints between spans. The frame-by-frame analysis usually provides designers an upper-bound response of the portion considered. Individual structural members can be modeled as line elements, plates and shells, or solid elements depending on the type of general bridge model (Priestley et al. 1996).

In this investigation the emphasis was placed on drift demands on bridge columns to assess their seismic vulnerability. Therefore, an upper-bound approach was sought for drift demands. This was accomplished by idealizing the bridge structure as a single-degree-of-freedom system, both in longitudinal and transverse directions. Typical bridge structures were selected from the bridge survey conducted earlier, as schematically shown in

Figures 2.3 and 2.4. Global computer models corresponding to these common types of bridges were constructed assuming rigid decks, and simulating bearings as inelastic springs with elasto-plastic models. These analytical models are shown in Figures 4.2 an 4.3. These models are all single-degree-of-freedom (SDOF) models with abilities to have inelastic support resistances at different support locations. They can all be represented by a SDOF lumped-mass model as shown in Figure 4.4. The lumped-mass model consists of a column element which is fully fixed at the base, representing all the columns; mass, representing total bridge mass; and two attached springs, one representing the stiffness of abutment bearings while the other representing the stiffness of pier bearings. The bearings have the option of providing no lateral restraint, as in the case of frictionless rollers; elastic or elasto-plastic resistance with a finite rigidity, as in the case of elastomeric bearings; and a rigid resistance followed by yielding, as in the case of rusted rollers or rollers with debris providing initial resistance.

4.4 Dynamic Analysis Using DRAIN-RC

The SDOF lumped-mass analytical model, shown in Figure 4.4, was used to conduct dynamic inelastic analyses of bridges with different structural and ground motion parameters. The bridges were analyzed under actual ground motions, as well as artificial ground motions that represent seismic activities of Eastern and Western Canada. A total of 17 different actual and artificial ground motion records were considered as summarized in Table 4.1. Analyses of bridges were conducted assuming a planar response. Therefore, torsion was not considered. Ground motion was applied only in the horizontal direction. Vertical motion was neglected.

4.4.1 Preparation of Input Data

The structural properties were computed from the actual bridge design drawings reviewed as part of the bridge survey conducted, with proper ranges of variation for each bridge type considered. Tables 4.2 and 4.3 provide a summary of the range of structural properties considered for different bridge types. These data, corresponding to different span lengths, number of spans, and number of lanes (representing span width), were used to calculate structural mass, stiffness and strength.

4.4.1.1 Column Spring Properties

Computer software COLA was utilized to calculate primary force-displacement relationships required as input information for DRAIN-RC. This information was computed for both flexural and anchorage slip springs. The following relationships were derived for the column element, for elastic, effective elastic (including cracking), and post-yield stiffnesses and strengths.

For $P / P_0 = 10\%$ $\quad EI_{cr} / EI_e = 0.50 \quad M_y / M_{cr} = 3.60$ (4.1)

For $P / P_0 = 15\%$ $\quad EI_{cr} / EI_e = 0.60 \quad M_y / M_{cr} = 3.25$ (4.2)

For $P / P_0 = 20\%$ $\quad EI_{cr} / EI_e = 0.65 \quad M_y / M_{cr} = 2.95$ (4.3)

where the elastic concrete stiffness is defined according to CSA Standard A23.3-94, "Design of Concrete Structures," as follows:

$$EI_e = 4500\sqrt{f_c'} I_g \tag{4.4}$$

Also, the relationship between ultimate and yield moment was found as

$$M_{ult} / M_y = 0.87 \tag{4.5}$$

Using above relationships, moment-curvature relationship of a reinforced concrete section can be easily established knowing the gross section inertia, I_g, and the cracked section moment, M_{cr}.

For the shear spring, a value of 0.5 is assumed for the ratio of post-cracking to elastic shear stiffness. All post yielding stiffness values were assumed to be 0.05 of the elastic stiffness.

4.4.1.2 Fundamental Period of Bridge Structure

Effective elastic stiffness was used to calculate the period of a bridge. Depending on the bridge type, some columns were integral with the deck, while others had bearings between the column and the deck. Assuming the column was fixed at the foundation level, the following equation was used to estimate the fundamental period of a bridge structure:

$$T = 2\pi \sqrt{\frac{m}{\sum_{1}^{n_c} k_c \frac{EI_{cr}}{L_c^3}}} \tag{4.6}$$

where, T is the period in seconds; m is the total mass of bridge superstructure in kg; L_c is the column height in m; n_c is the number of columns; k_c is a stiffness coefficient depending on the boundary conditions of column with a value of 12 for fix-fix columns and 3 for fix-hinge columns; EI_{cr} is the cracked section rigidity in N/m^2.

The superstructure mass can be estimated using Equations 2.2, 2.4, and 2.6, derived from the bridge survey, depending on the type of bridge structure. Thus, mass can be expressed as;

$$m = \left[\frac{24}{9.81}10^{-6}\right] L_s A_d \tag{4.7}$$

where, L_s is the span length in mm and A_d is the deck area in mm^2.

4.4.1.3 Bearing Properties

Bearings provide connections between bridge superstructure and substructure, and transmit forces between these two media. Thus, they play an important role in the analysis of bridges and may dictate the behavior during a seismic activity. Therefore, they must be modeled properly.

There are basically five types of bearing used in bridges (OHBDC 1991). They are as follows:

- *Elastomeric Bearings*: This type of bearing can either be a plain bearing consisting of only elastomer, or a laminated bearing consisting of layers of elastomer and steel with or without lead plugs. The force-displacement relationship of an elastomeric bearing without lead plugs is mainly elastic. However, an elastomeric bearing with lead plugs exhibits a bilinear relationship with elastic and post-elastic stiffness branches. Figure 4.5 shows a typical hysterisis behavior of an elastomeric bearing with lead plugs. The following typical properties were suggested by Robinson (1982) for a typical elastomeric bearing with lead plugs.

  $$k_d = (1 \text{ to } 2)W \tag{4.8}$$

  $$F_{pb} = (0.05 \text{ to } 0.1)W \tag{4.9}$$

  Where k_d is the post-elastic stiffness in N/mm, W is the dead weight of bridge structure in N, and F_{pb} is the shearing force at yield in N. The elastic stiffness, k_u, was found to be in

the range of 5 to 15 times the post-elastic stiffness. According to experimental studies, the ratio of the elastic to post-elastic stiffness is close to 10 (Ghobarah 1988).

Horizontal crawling of elastomeric bearings may occur due to significant amounts of movement and inadequate bearing attachments. The coefficient of friction may be taken between 0.1 and 0.2 depending on the sliding surface condition.

- *Pot Bearings*: This type of a bearing consists of a circular non-reinforced rubber pad which is totally enclosed and sealed by a piston. They are manufactured as fixed bearings, uni-directional sliding bearings, and multi-directional sliding bearings. Uni- and multi-directional bearings have sliding surfaces and guiding systems. The coefficient of friction of the system can be taken between 0.06 and 0.03 for a contact pressure ranging between 10 MPa and 30 MPa. Any given contact pressure value or coefficient of friction can be linearly interpolated.
- *Disc Bearings*: This type of bearings rotate through differential deflection while accommodating horizontal forces by a shear-restriction mechanism. The shear-restriction mechanism accommodates horizontal forces and allows vertical deflection and rotation. They resemble to pot bearings in terms of their classification, and sliding and guiding characteristics.
- *Spherical Bearings*: These bearings are designed to allow movement in any direction. Thus, it is a type of multi-directional and non-guided system. Sliding characteristics are similar to pot bearings.
- *Roller and Rocker Bearings*: These types of bearings are not recommended for new structures due to the corrosion of bearings and steel sliding surfaces. The corrosion produces uneven distribution of the load. These bearings are usually considered to be frozen up to a point where horizontal forces exceed the capacity of frozen bearings. The friction coefficient in this case is related to the degree of corrosion as determined by an engineer. The hysteretic behavior of this type of bearing or any bearing subjected to horizontal crawling is shown in Figure 4.5.

4.4.1.4 Damping Property

The bridges were analyzed for 5% of critical damping, which is a commonly used value among researchers.

4.4.2 Parametric Investigation

Parametric investigation of bridges was conducted in three stages. The first stage involved the selection of critical ground motion parameters. Hence, dynamic inelastic analyses were carried out to select one actual and one artificial earthquake record representing Western and Eastern Canadian regions. Earthquake intensities were also studied to examine the variation of column tip deflection with increasing earthquake intensity. The second stage included the confirmation that the lumped mass model selected was representative of the different global bridge models derived for different bridge types obtained form the bridge survey. Finally, inelastic time history analyses of bridges were conducted under critical earthquake motions, with different intensities and bearing yielding levels, to determine drift and ductility demands of bridges within a typical range of fundamental periods.

4.4.2.1 Ground Motion Parameters

The effects of frequency content and intensity of ground motion on bridge response were investigated by considering a total of 17 earthquake records. The earthquake records were classified as representatives of Eastern and Western Canadian seismic activity, as summarized in Table 4.4. The artificial records were those generated by Atkinson and Beresnev (1997) to yield approximately the same response as that based on the uniform hazard response spectra with a 10% probability of exceedance in 50 years, proposed for NBCC year 2000 code. Hence, the response generated by these records may be viewed as those that are compatible with code-recommended design earthquakes.

The artificial records were used with their respective intensities to establish the most critical record, as a representative ground motion compatible with code level seismic forces. The previously recorded earthquake records were first normalized to give peak ground accelerations equal to 30% of the gravitational acceleration, g. This was done to eliminate

intensity as a parameter. Figure 4.6 shows displacement response of a SDOF system, representing all bridge types subjected to these earthquake records. The results indicate that Artificial Event #2 for East and West were critical among the artificial records. Saguenay and El Centro records governed response in the east and west, respectively. These records were then used as critical earthquake motions in subsequent analyses. The results are tabulated in Table 4.5.

The effect of the intensity of ground motion on bridge response was studied based on the peak ground acceleration. The critical earthquake records were normalized to give 30%, 60% and 90% of g. Selected bridges were analyzed under different intensities of ground motion for a period of 1.5 sec. The results are plotted in Figure 4.7. It becomes clear from these figures that displacement response varies approximately linearly with peak ground acceleration. This relationship was found to hold true even for bridges with different levels of inelasticity. The results are tabulated in Table 4.6.

4.4.2.2 Structural Parameters

Structural parameters of a SDOF bridge consists of strength, stiffness and mass. In the inelastic range, post-yield properties and ductility characteristics also gain importance. For elastic response, stiffness and mass can be combined and represented in the form of fundamental period. The period of a typical highway bridge falls between 0.7 second and 4.8 seconds with an average period range of 1.5 to 2.0 seconds. Ghobarah and Ali (1988) also stated that bridges have typically a period range of 1 to 2 seconds. This is illustrated in Tables 4.2 and 4.3, which summarize fundamental periods of different types of bridges with different geometric properties and support conditions, as obtained from the survey of existing bridges in Canada. The bridges listed in these Tables include two to four spans, two to four lanes, with simple and rigid column connections at the deck level. Although there appears to be an infinite number of cases with different bridge types, geometric parameters and support conditions, it is possible to group all the bridges with respect to their periods, so long as the structural response obtained is only affected by the period. This point was investigated by analyzing bridges with different types and properties, but the same fundamental period. Table 4.6 shows geometric parameters of different bridges having the same period of 2.5 seconds. They were subjected to

the 1940 El Centro earthquake with different intensities. The analysis showed similar response for different bridge types as long as their periods remained constant. This was true for a wide range of ductility ratios. The results are plotted in Figure 4.8. The difference in response was nearly ±5% between the average and absolute maximum response. This indicates that all bridges can be grouped in terms of their periods and analyzed using the SDOF lumped-mass model.

4.4.2.3 Drift Demands of Columns

Once the SDOF model was adopted to represent all bridge types, the analysis was then focused on the tip deflections of columns and their ductility demands subjected to Eastern Long Artificial Event #2, Saguenay, Western Long Artificial Event #2 and El Centro earthquakes. The earthquake records were used as they were, as well as after being normalized with respect to the gravitational acceleration to have peak ground accelerations of 30% and 60% of g. The analysis also included the combined stiffness of bearings in terms of the percentage of superstructure weight. Accordingly, bridges were analyzed with bearing restraints providing frictional forces of 5% and 20% of the superstructure weight. The non-linear frictional resistance was modeled as a truss element where the elastic slope of force-deformation curve was very large until the dynamic force reached to the required frictional force. Then, the truss element yielded with no further strength gain. Also, another set of analyses were carried out using elastomeric bearings with lead plugs. They were modeled applying average values derived from Equations 4.8 and 4.9. Thus, post-elastic stiffness was taken as 1.5 times the dead load of bridge superstructure, the yield force was taken as 0.075 times the dead load of bridge superstructure, and the ratio of elastic to post-elastic stiffness was taken as 10. The results are presented in Tables 4.7 through 4.12, and Figures 4.9 through 4.20.

Table 4.1 Ground Motion Data.

Ground Motion Record	Number of Ground Motion Pairs	Time Step (second)	Max. Recorded Acceleration (m/s^2)	% of g	Scale Factor for 30% of g	Scale Factor for 60% of g	Scale Factor for 90% of g
New Brunswick	2010	0.005	2.44710	24.94%	1.203	2.405	3.608
Saguenay	4168	0.005	1.23070	12.55%	2.391	4.783	7.174
Eastern Short Artificial Event #1	1000	0.010	1.75000	14.27%	1.682	3.363	5.045
Eastern Long Artificial Event #1	2600	0.010	1.31000	9.35%	2.247	4.493	6.740
Eastern Short Artificial Event #2	1000	0.010	1.90000	15.49%	1.549	3.098	4.647
Eastern Long Artificial Event #2	2600	0.010	1.23000	8.78%	2.393	4.785	7.178
Taft	3102	0.020	1.52705	15.57%	1.927	3.854	5.782
El Centro	1002	0.020	1.82100	18.56%	1.616	3.232	4.848
San Fernando	3702	0.020	1.47625	15.05%	1.994	3.987	5.981
Northridge #1	1345	0.020	4.28080	43.64%	0.687	1.375	2.062
Northridge #2	1345	0.020	5.70028	58.11%	0.516	1.033	1.549
Northridge #3	1345	0.020	4.20405	42.85%	0.700	1.400	2.100
Northridge #4	1345	0.020	5.47490	55.81%	0.538	1.075	1.613
Western Short Artificial Event #1	800	0.010	1.64000	18.39%	1.795	3.589	5.384
Western Long Artificial Event #1	2000	0.010	1.07000	8.73%	2.750	5.501	8.251
Western Short Artificial Event #2	800	0.010	2.00000	22.43%	1.472	2.943	4.415
Western Long Artificial Event #2	2000	0.010	1.04000	8.48%	2.830	5.660	8.489

Table 4.2 Structural parameters of different simply-supported bridge types.

Bridge Model	Span Length (mm)	Number of Lanes	No. of Columns per Bent	Column Aspect Ratio	Column Height (m)	P/P_0 Per Column	Superstructure Weight (kg)	Column EI_{cr} x 10^3 ($N \cdot m^2$)	Period (Second)
2S-SS	20,000	2	1	5.0	4.730	15%	837,578	640,626	1.349
	40,000	3	2	5.0	5.040	15%	1,901,798	827,126	1.392
	60,000	4	3	5.0	5.742	15%	3,702,606	1,402,585	1.481
	20,000	3	1	5.0	5.040	15%	950,900	827,126	1.392
	40,000	4	3	5.0	4.688	15%	2,468,404	622,128	1.339
	60,000	2	2	10.0	11.586	15%	2,512,734	1,508,939	4.128
	20,000	4	3	10.0	6.630	15%	1,234,202	156,182	3.178
	40,000	2	1	10.0	13.378	15%	1,675,156	2,667,789	4.448
	60,000	3	2	10.0	12.345	15%	2,852,698	1,863,595	4.353
3S-SS	20,000	2	1	5.0	4.730	15%	1,256,367	640,626	1.169
	40,000	3	2	5.0	5.040	15%	2,852,697	827,126	1.205
	60,000	4	3	5.0	5.742	15%	5,553,909	1,402,585	1.282
	20,000	3	1	10.0	10.080	15%	1,426,350	827,126	3.409
	40,000	4	3	10.0	9.376	15%	3,702,606	622,128	3.280
	60,000	2	2	10.0	11.586	15%	3,769,101	1,508,939	3.575
	20,000	4	3	10.0	8.120	10%	1,851,303	325,299	2.585
	40,000	2	1	10.0	16.385	10%	2,512,734	5,168,184	3.751
	60,000	3	2	10.	15.119	10%	4,279,047	3,761,418	3.596
4S-SS	20,000	2	1	5.0	4.730	15%	1,675,156	640,626	1.102
	40,000	3	2	5.0	5.040	15%	3,803,596	827,126	1.136
	60,000	4	3	5.0	5.742	15%	7,405,212	1,402,585	1.209
	20,000	3	1	10.0	10.080	15%	1,901,800	827,126	3.214
	40,000	4	3	10.0	9.376	15%	4,936,808	622,128	3.092
	60,000	2	2	10.0	11.586	15%	5,025,468	1,508,939	3.371
	20,000	4	3	10.0	5.742	20%	2,468,404	105,524	2.545
	40,000	2	1	10.0	11.586	20%	3,350,312	1,606,451	3.772
	60,000	3	2	10.0	10.691	20%	5,705,396	1,221,355	3.538

Table 4.3 Structural parameters of different rectangular-voided continuous bridge types.

Bridge Model	Span Length (mm)	Number of Lanes	No. of Columns per Bent	Column Aspect Ratio	Column Height (m)	P/P_o Per Column	Superstructure Weight (kg)	Column EI_{cr} x 10^3 ($N \cdot m^2$)	Period (Second)
2S-C-I	40,000	2	1	5.0	7.359	15%	2,027,387	3,912,550	0.824
	50,000	2	2	5.0	5.818	15%	2,534,233	1,523,221	0.734
	50,000	3	1	10.0	17.603	15%	2,900,227	8,030,720	2.546
	60,000	3	1	10.0	19.283	15%	3,480,272	11,512,289	2.670
	60,000	4	3	5.0	6.385	15%	4,578,254	2,231,310	0.765
2S-C-II	50,000	2	1	5.0	8.228	15%	2,534,233	6,148,660	1.738
	40,000	2	2	5.0	5.204	15%	2,027,387	979,187	1.386
	40,000	3	1	10.0	15.745	15%	2,320,182	5,127,660	4.821
	60,000	3	2	5.0	6.818	15%	3,480,272	2,880,336	1.587
	50,000	4	3	5.0	5.828	15%	3,815,212	1,531,902	1.471
3S-C-I	60,000	2	1	5.0	9.013	15%	4,561,620	8,816,872	0.998
	60,000	2	2	5.0	6.373	15%	4,561,620	2,119,488	0.856
	50,000	3	1	5.0	8.802	15%	4,350,341	8,030,720	0.986
	40,000	3	2	5.0	5.567	15%	3,480,273	1,357,158	0.763
	40,000	4	3	5.0	5.213	15%	4,578,254	985,360	0.760
3S-C-II	40,000	2	1	5.0	7.359	10%	3,041,080	3,912,550	1.428
	50,000	2	2	5.0	5.818	10%	3,801,350	1,523,221	1.272
	60,000	3	1	5.0	9.642	10%	5,220,409	11,512,289	1.635
	40,000	3	2	5.0	5.567	15%	3,480,273	1,357,158	1.206
	50,000	4	3	5.0	5.828	15%	5,722,818	1,531,902	1.274
4S-C-I	50,000	2	1	5.0	8.228	15%	5,068,467	6,148,660	1.004
	60,000	2	2	5.0	6.373	15%	6,082,159	2,119,488	0.903
	40,000	3	1	5.0	7.872	15%	4,640,363	5,127,660	0.984
	50,000	3	2	5.0	6.224	15%	5,800,454	1,914,350	0.895
	60,000	4	3	5.0	6.385	20%	9,156,508	2,231,310	0.884
4S-C-II	60,000	2	1	5.0	9.013	20%	6,082,159	8,816,872	1.488
	40,000	2	2	5.0	5.204	20%	4,054,773	979,187	1.131
	50,000	3	1	5.0	8.802	20%	5,800,454	8,030,720	1.470
	60,000	3	2	5.0	6.818	20%	6,960,545	2,880,336	1.296
	40,000	4	3	5.0	5.213	20%	6,104,339	985,360	1.133

Table 4.4 SDOF response of Eastern and Western Earthquakes.

	T = 0.5 s L/D = 2.110 L_c = 3.803 m		T = 1.5 s L/D = 4.387 L_c = 7.908 m		T = 2.5 s L/D = 6.167 L_c = 11.116 m		T = 3.5 s L/D = 7.718 L_c = 13.912 m		T = 4.5 s L/D = 9.125 L_c = 16.448 m	
Earthquake	Δ	μ	Δ	μ	Δ	μ	Δ	μ	Δ	μ
New Brunswick	1.05	0.058	0.86	0.015	0.84	0.008	0.82	0.005	0.82	0.004
Saguenay	11	0.610	12	0.202	12	0.115	17	0.107	21	0.096
East Artificial Short Event #1	10	0.543	22	0.388	13	0.127	14	0.088	19	0.086
East Artificial Long Event #1	29	1.945	42	0.735	59	0.567	80	0.506	87	0.403
East Artificial Short Event #2	10	0.559	20	0.356	29	0.277	22	0.142	17	0.080
East Artificial Long Event #2	29	1.978	88	1.957	137	1.574	104	0.662	161	0.745
Taft	48	3.247	116	2.826	146	1.718	223	1.765	400	2.954
El Centro	62	4.864	342	9.834	372	5.670	446	4.380	573	4.092
San Fernando	51	3.913	84	1.843	128	1.410	219	1.714	252	1.317
Northridge #1	82	6.571	222	6.121	379	5.797	512	5.155	525	3.682
Northridge #2	56	4.352	159	4.156	257	3.663	377	3.571	375	2.380
Northridge #3	111	9.179	180	4.800	331	4.948	310	2.783	304	1.762
Northridge #4	84	6.820	125	3.108	331	4.954	245	2.020	234	1.158
West Artificial Short Event #1	29	1.955	93	2.100	146	1.731	123	0.780	99	0.461
West Artificial Long Event #1	71	5.606	262	7.357	401	6.184	646	6.731	776	5.853
West Artificial Short Event #2	49	3.695	154	3.985	111	1.115	123	0.777	214	0.993
West Artificial Long Event #2	135	11.26	367	10.61	540	8.615	707	7.447	1021	7.980

Table 4.5 SDOF response of critical Eastern and Western Earthquakes at a period of 1.5 s.

	Without P-Δ Effect						With P-Δ Effect					
	30% g		60% g		90% g		30% g		60% g		90% g	
Earthquake	Δ	μ	Δ	μ	Δ	μ	Δ	μ	Δ	μ	Δ	μ
Saguenay	12	0.202	23	0.404	35	0.607	11	0.190	22	0.381	33	0.574
East Artificial Long Event #2	88	2.0	180	4.8	277	7.8	93	2.1	175	4.7	297	8.3
El Centro	342	9.8	622	18.5	1183	35.9	357	10.3	765	22.9	1677	51.2
West Artificial Long Event #2	367	10.6	768	23.0	1553	47.4	497	14.6	1020	30.8	2537	77.8

Table 4.6 Column tip deflections for different 2.5-second-period bridge types subjected to various intensities of El Centro Eq.

Bridge Model	Span Length (mm)	Num. of Lanes	Number of Columns per Bent	Column Aspect Ratio	Column Height (m)	P/P_o Per Column	Superstructure Weight (kg)	Column EI_{cr} x 10^3 ($N \cdot m^2$)	Period (Second)	As Rec. (mm)	30% of g (mm)	60% of g (mm)	90% of g (mm)
2S-SS	40,000	2	1	6.8	9.151	15%	1,675,156	2,667,789	2.5	348	396	947	1670
	60,000	3	1	6.3	10.929	15%	2,852,697	7,762,139	2.5	356	426	912	1625
3S-SS	60,000	4	3	8.0	11.181	10%	5,553,908	2,692,842	2.5	329	561	725	1377
4S-SS	40,000	3	1	7.6	9.357	20%	3,803,596	2,162,892	2.5	363	420	929	1645
2S-C-I	50,000	2	2	11.4	13.206	15%	2,534,233	1,523,221	2.5	318	423	871	1580
	60,000	3	1	9.6	18.512	15%	3,480,272	11,512,289	2.5	309	476	777	1460
	60,000	4	3	11.1	14.110	15%	4,578,254	2,231,310	2.5	317	437	849	1551
2S-C-II	60,000	2	1	6.2	11.158	15%	3,041,080	8,816,872	2.5	354	422	905	1617
3S-C-I	40,000	3	1	9.7	15.225	15%	3,480,273	5,127,660	2.5	308	479	803	1488
3S-C-II	40,000	2	1	7.3	10.729	15%	3,041,080	3,912,550	2.5	336	481	816	1504
4S-C-I	40,000	2	1	9.6	14.056	15%	4,054,773	3,912,550	2.5	327	529	757	1420
	60,000	3	1	8.7	16.834	15%	6,960,545	11,512,289	2.5	333	509	806	1484
4S-C-II	40,000	2	1	7.6	11.156	15%	4,054,773	3,912,550	2.5	336	514	785	1459
	50,000	3	1	7.2	12.586	15%	5,800,454	8,030,720	2.5	351	471	841	1534
									Average	335	467	837	1530
									Max.	363	561	947	1670
									Min.	308	396	725	1377
SDOF	-	-	1	6.2	11.116	15%	3,041,080	8,794,058	2.5	331	372	967	1696

Table 4.7 Eastern Earthquake response with elastomeric bearings.

Saguenay Earthquake

Period (s)	Without P-Δ Effect						With P-Δ Effect					
	As Recorded		30% g		60% g		As Recorded		30% g		60% g	
	Δ (mm)	μ	Δ (mm)	μ	Δ (mm)	μ	Δ (mm)	μ	Δ (mm)	μ	Δ (mm)	μ
0.5	5.139	0.286	12	0.669	20	1.229	5.123	0.285	12	0.667	20	1.221
1.5	4.995	0.087	12	0.215	20	0.342	4.973	0.086	12	0.215	20	0.339
2.5	5.490	0.052	13	0.120	18	0.174	5.494	0.052	13	0.119	18	0.170
3.5	5.697	0.036	12	0.077	17	0.109	5.684	0.035	12	0.076	17	0.108

Eastern Artificial Long Event #2 Earthquake

Period (s)	Without P-Δ Effect						With P-Δ Effect					
	As Recorded		30% g		60% g		As Recorded		30% g		60% g	
	Δ (mm)	μ	Δ (mm)	μ	Δ (mm)	μ	Δ (mm)	μ	Δ (mm)	μ	Δ (mm)	μ
0.5	6.974	0.391	22	1.422	44	3.310	7.168	0.401	23	1.426	44	3.320
1.5	11.000	0.191	24	0.411	64	1.211	11	0.189	24	0.410	65	1.227
2.5	10.000	0.099	25	0.235	74	0.704	10	0.095	25	0.234	74	0.704
3.5	9.212	0.058	25	0.160	78	0.495	9.133	0.057	25	0.158	79	0.492

Table 4.8 Western Earthquake response with elastomeric bearings.

El Centro Earthquake

Period (s)	Without P-Δ Effect						With P-Δ Effect					
	As Recorded		30% g		60% g		As Recorded		30% g		60% g	
	Δ (mm)	μ	Δ (mm)	μ	Δ (mm)	μ	Δ (mm)	μ	Δ (mm)	μ	Δ (mm)	μ
0.5	30	2.093	44	3.263	79	6.386	31	2.119	43	3.249	81	6.478
1.5	29	0.503	46	0.808	177	3.259	29	0.504	47	0.811	180	3.365
2.5	32	0.303	55	0.523	199	2.644	32	0.301	56	0.529	200	2.652
3.5	33	0.208	62	0.393	208	1.588	33	0.206	63	0.395	210	1.581

Western Long Event #2 Earthquake

Period (s)	Without P-Δ Effect						With P-Δ Effect					
	As Recorded		30% g		60% g		As Recorded		30% g		60% g	
	Δ (mm)	μ	Δ (mm)	μ	Δ (mm)	μ	Δ (mm)	μ	Δ (mm)	μ	Δ (mm)	μ
0.5	6.198	0.346	32	2.268	111	9.109	6.175	0.344	33	2.310	118	9.716
1.5	12	0.205	56	0.978	297	8.437	12	0.203	57	0.992	302	8.571
2.5	13	0.120	95	0.905	357	5.411	13	0.120	96	0.913	361	5.463
3.5	13	0.085	109	0.689	386	3.682	14	0.085	110	0.689	389	3.692

Table 4.9 Saguenay Earthquake response with roller and rocker bearings.

Saguenay Earthquake, f = 0.05 W

Period (s)	Without P-Δ Effect						With P-Δ Effect					
	As Recorded		30% g		60% g		As Recorded		30% g		60% g	
	Δ (mm)	μ	Δ (mm)	μ	Δ (mm)	μ	Δ (mm)	μ	Δ (mm)	μ	Δ (mm)	μ
0.5	0.924	0.051	7.682	0.431	19	1.163	1.087	0.060	9.187	0.517	19	1.159
1.5	1.376	0.024	10	0.171	18	0.315	2.308	0.040	10	0.174	18	0.313
2.5	0.882	0.008	11	0.102	19	0.183	1.417	0.014	9.452	0.089	12	0.111
3.5	1.883	0.012	11	0.072	22	0.141	1.134	0.007	10	0.063	25	0.155

Saguenay Earthquake, f = 0.20 W

Period (s)	Without P-Δ Effect						With P-Δ Effect					
	As Recorded		30% g		60% g		As Recorded		30% g		60% g	
	Δ (mm)	μ	Δ (mm)	μ	Δ (mm)	μ	Δ (mm)	μ	Δ (mm)	μ	Δ (mm)	μ
0.5	1.542	0.086	2.420	0.135	6	0.345	1.367	0.076	3	0.140	9	0.527
1.5	2.765	0.048	3.000	0.052	11	0.195	2.863	0.050	3.146	0.055	10	0.170
2.5	2.157	0.021	4.440	0.042	8.564	0.082	2.966	0.028	4.619	0.044	8.872	0.084
3.5	1.559	0.010	1.936	0.012	11	0.069	1.718	0.011	3.156	0.020	8.593	0.054

Table 4.10 Eastern Artificial Long Event #2 Earthquake response with roller and rocker bearings.

Eastern Artificial Long Event #2 Earthquake, f = 0.05 W

Period (s)	Without P-Δ Effect						With P-Δ Effect					
	As Recorded		30% g		60% g		As Recorded		30% g		60% g	
	Δ (mm)	μ	Δ (mm)	μ	Δ (mm)	μ	Δ (mm)	μ	Δ (mm)	μ	Δ (mm)	μ
0.5	1.747	0.097	16	0.890	42	3.140	1.437	0.080	16	0.894	43	3.236
1.5	2.132	0.037	23	0.405	84	1.821	2.828	0.049	23	0.391	74	1.519
2.5	2.608	0.025	22	0.211	94	0.903	2.415	0.023	24	0.224	98	0.925
3.5	3.656	0.023	27	0.171	102	0.646	3.210	0.020	27	0.167	87	0.546

Eastern Artificial Long Event #2 Earthquake, f = 0.20 W

Period (s)	Without P-Δ Effect						With P-Δ Effect					
	As Recorded		30% g		60% g		As Recorded		30% g		60% g	
	Δ (mm)	μ	Δ (mm)	μ	Δ (mm)	μ	Δ (mm)	μ	Δ (mm)	μ	Δ (mm)	μ
0.5	0	0	5.707	0.318	18	0.995	0	0	5.766	0.321	18	1.060
1.5	0	0	8.321	0.145	35	0.606	0	0	7.567	0.131	35	0.609
2.5	0	0	10	0.097	49	0.466	0	0	12	0.111	40	0.378
3.5	0	0	12	0.075	46	0.290	0	0	12	0.075	26	0.163

Table 4.11 El Centro Earthquake response with roller and rocker bearings.

El Centro Earthquake, f = 0.05 W

Period (s)	Without P-Δ Effect						With P-Δ Effect					
	As Recorded		30% g		60% g		As Recorded		30% g		60% g	
	Δ (mm)	μ	Δ (mm)	μ	Δ (mm)	μ	Δ (mm)	μ	Δ (mm)	μ	Δ (mm)	μ
0.5	30	2.089	42	3.135	153	12.804	30	2.060	42	3.138	166	13.903
1.5	38	0.657	126	3.131	443	12.968	39	0.683	139	3.526	439	12.818
2.5	58	0.555	230	3.184	469	7.362	60	0.570	237	3.299	542	8.623
3.5	63	0.400	243	1.998	598	6.171	66	0.413	227	1.786	676	7.056

El Centro Earthquake, f = 0.20 W

Period (s)	Without P-Δ Effect						With P-Δ Effect					
	As Recorded		30% g		60% g		As Recorded		30% g		60% g	
	Δ (mm)	μ	Δ (mm)	μ	Δ (mm)	μ	Δ (mm)	μ	Δ (mm)	μ	Δ (mm)	μ
0.5	7.55	0.423	12	0.702	87	7.021	7.587	0.424	13	0.717	90	7.314
1.5	12	0.208	32	0.557	94	2.141	14	0.249	32	0.552	101	2.350
2.5	13	0.120	31	0.295	113	1.144	12	0.109	31	0.291	118	1.220
3.5	8.184	0.052	30	0.192	162	1.050	11	0.069	30	0.189	167	1.083

Table 4.12 Western Artificial Long Event #2 Earthquake response with roller and rocker bearings.

Western Long Event #2 Earthquake, f = 0.05 W

Period (s)	Without P-Δ Effect						With P-Δ Effect					
	As Recorded		30% g		60% g		As Recorded		30% g		60% g	
	Δ (mm)	μ	Δ (mm)	μ	Δ (mm)	μ	Δ (mm)	μ	Δ (mm)	μ	Δ (mm)	μ
0.5	3.983	0.222	45	3.385	254	21.632	2	0.137	45	3.416	262	22.231
1.5	5.122	0.089	127	3.169	438	14.187	8	0.140	126	3.127	449	13.141
2.5	7.279	0.069	150	1.792	605	9.747	10	0.098	154	1.850	607	8.228
3.5	7.432	0.047	200	1.496	710	7.486	8	0.048	208	1.558	724	7.627

Western Long Event #2 Earthquake, f = 0.20 W

Period (s)	Without P-Δ Effect						With P-Δ Effect					
	As Recorded		30% g		60% g		As Recorded		30% g		60% g	
	Δ (mm)	μ	Δ (mm)	μ	Δ (mm)	μ	Δ (mm)	μ	Δ (mm)	μ	Δ (mm)	μ
0.5	0	0.000	11	0.594	65	5.131	0	0	10	0.576	58	4.916
1.5	0	0.000	16	0.273	102	2.388	0	0	20	0.352	100	2.325
2.5	0	0.000	30	0.285	149	1.783	0	0	14	0.136	146	1.702
3.5	0	0.000	21	0.133	156	0.992	0	0	31	0.191	173	1.147

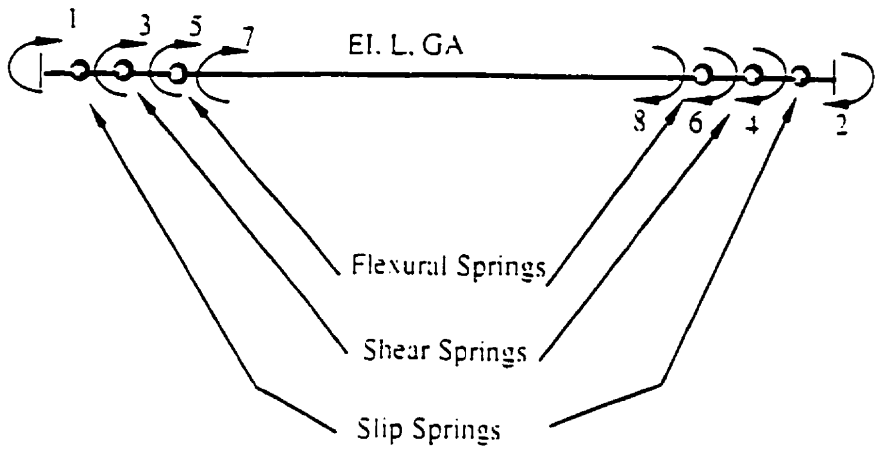

Modified One Component Model

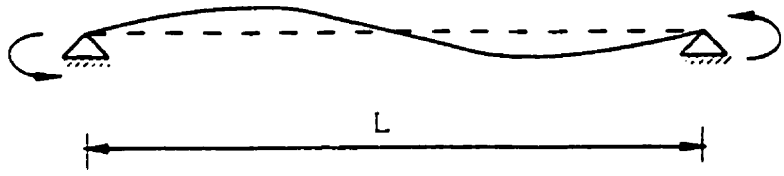

Beam

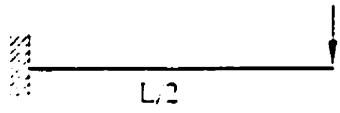

Actual Cantilever

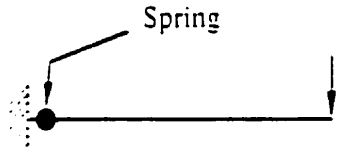

Idealized Cantilever

Figure 4.1 Flexural, shear and slip spring models.

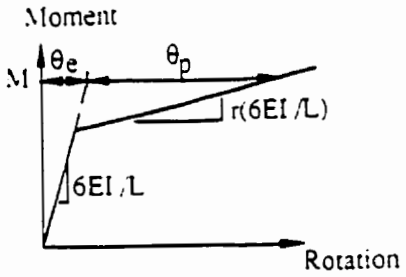

M - θ Relationship for the Cantilever

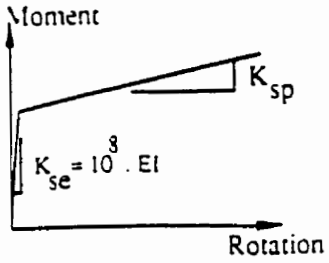

M - θ Relationship for the Spring

Derivation of Flexural Spring Stiffness

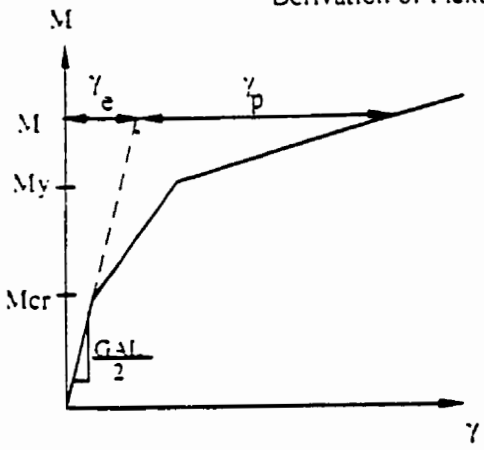

M - γ Relationship

Derivation of Shear Spring Stiffness

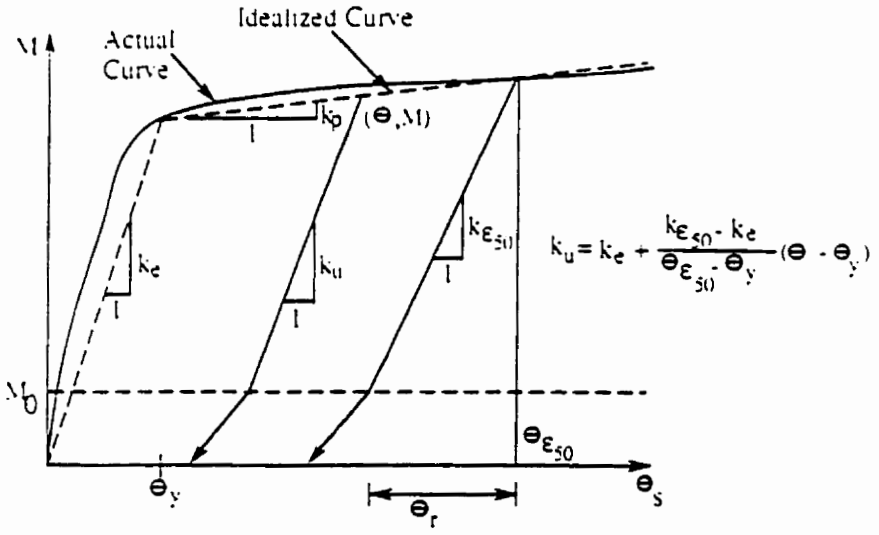

Idealized Primary Moment-Slip Relationship

Figure 4.1 Flexural, shear and slip spring models.

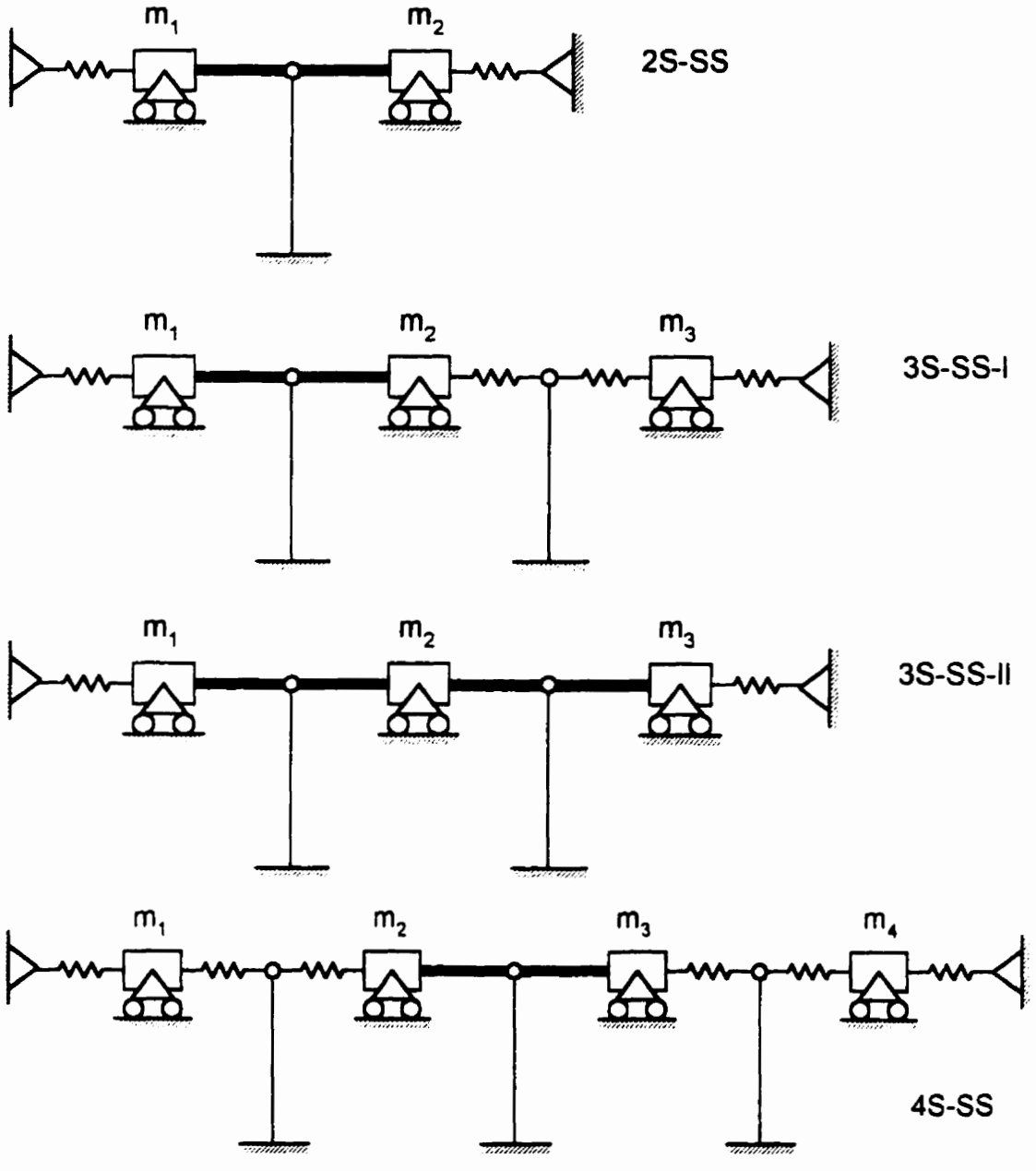

Figure 4.2 Global bridge models for simply-supported bridges.

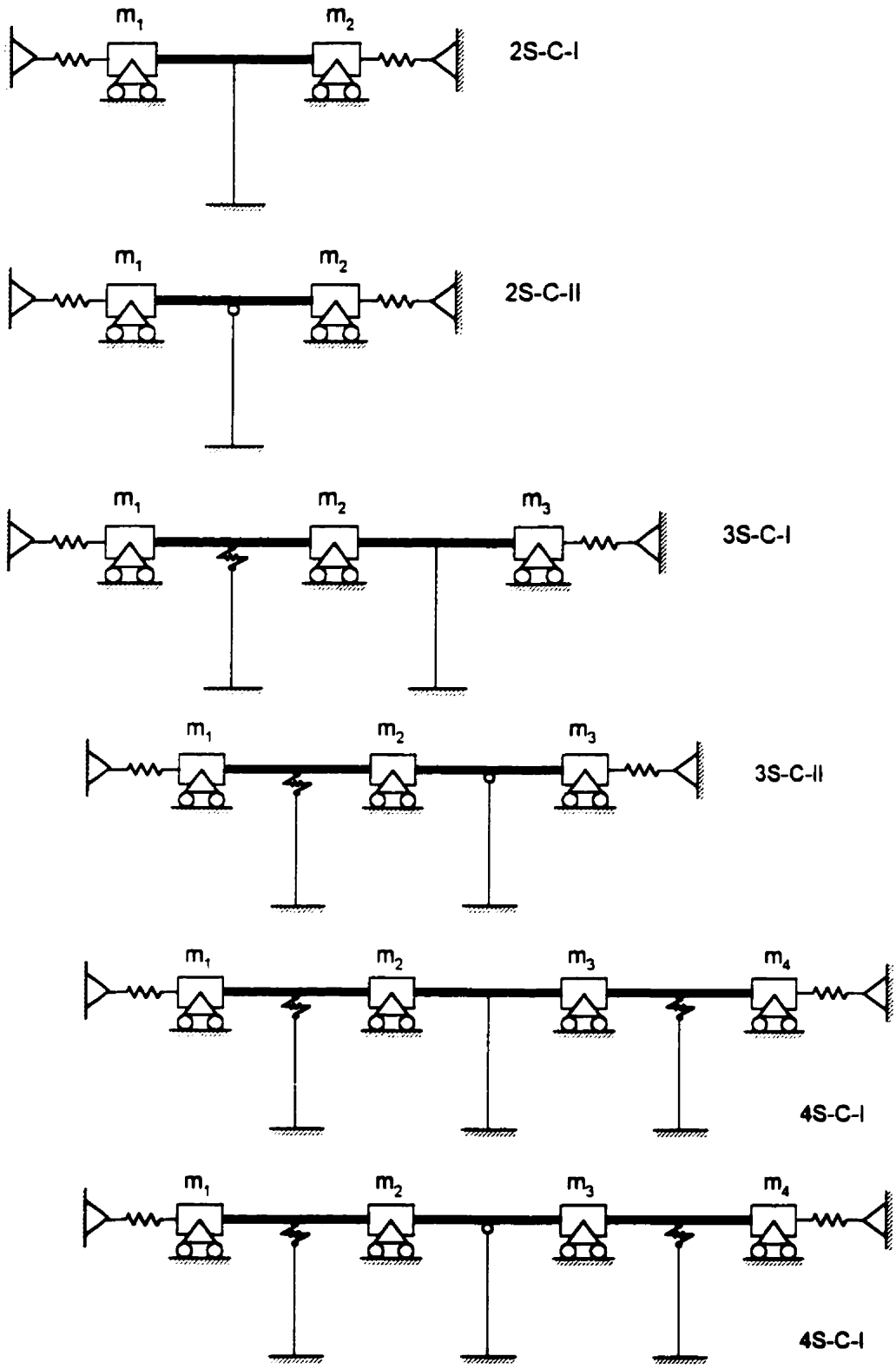

Figure 4.3 Global bridge models for continuous bridges.

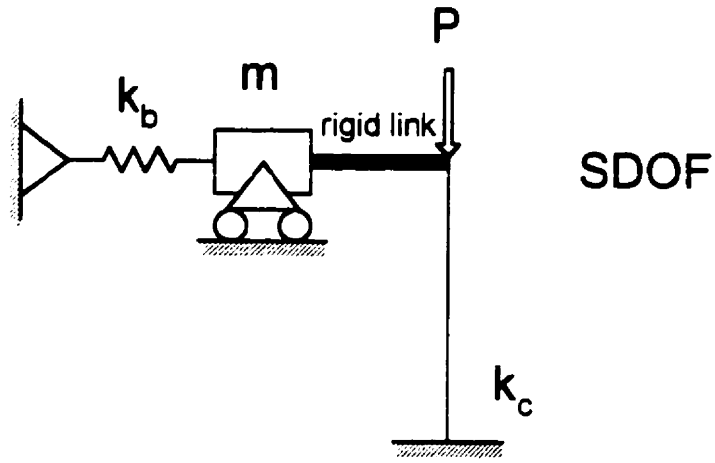

m: superstructure mass

P: concentrated superstructure load

k_b: bearing stiffness

k_c: column stiffness

Figure 4.4 Single degree of freedom model.

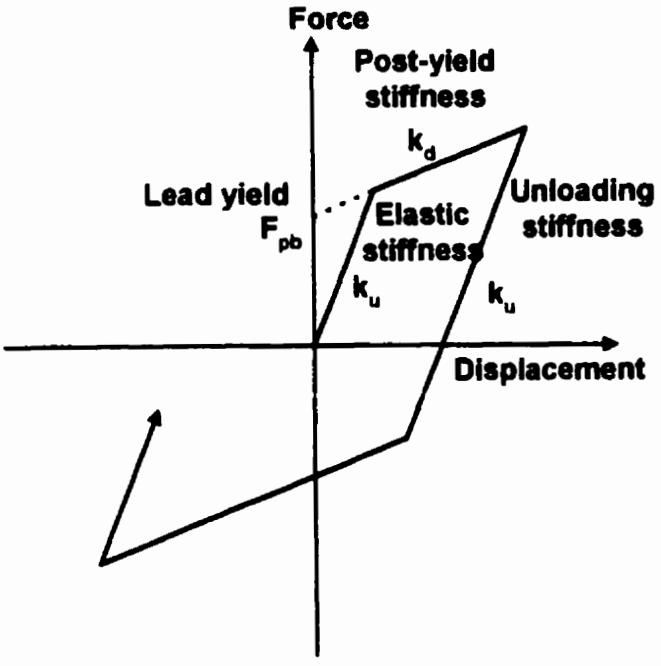

a) Bilinear hyteretic loop for lead-rubber bearings

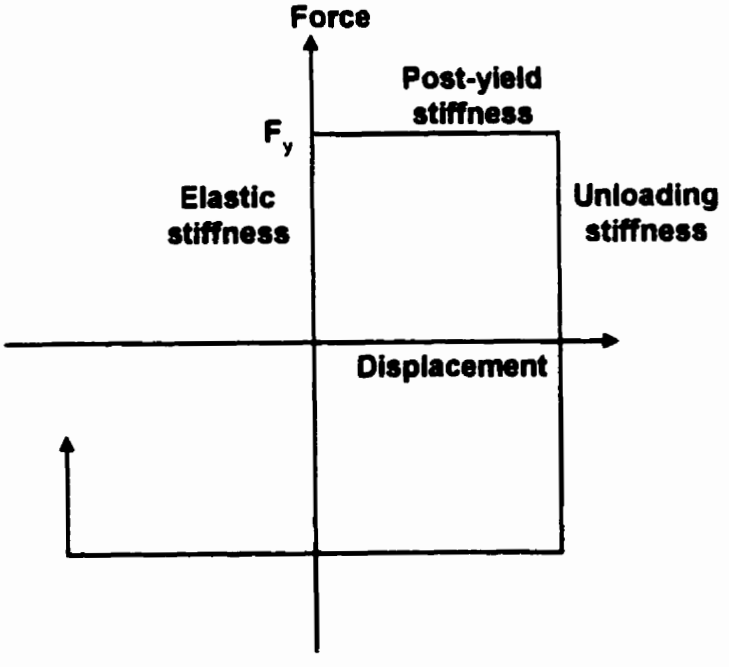

b) Bilinear hyteretic loop for roller and rocker bearings

Figure 4.5 Elasto-plastic models of bearing types.

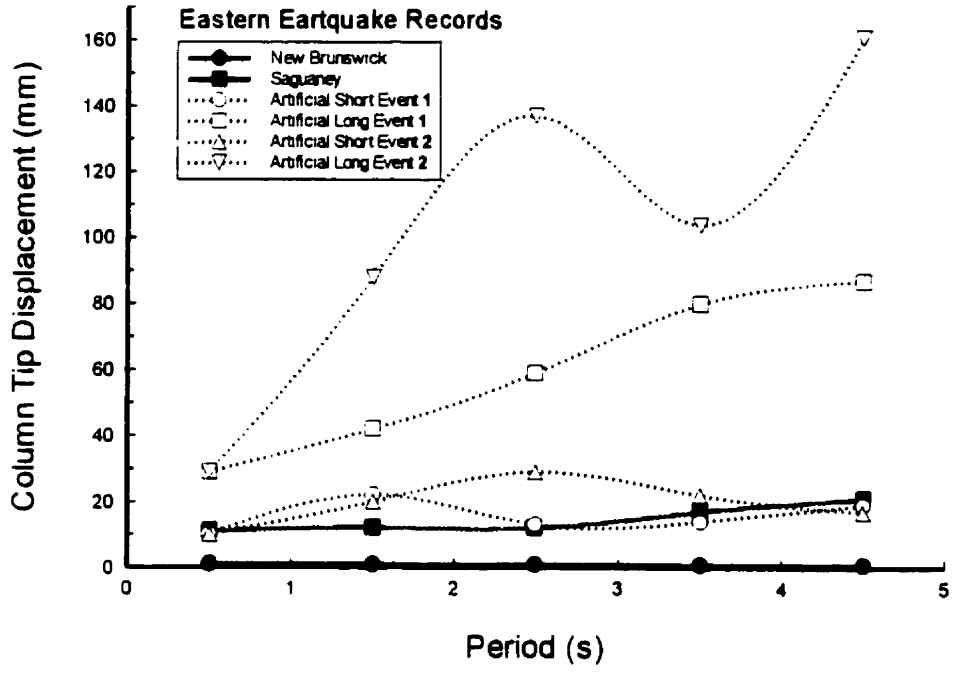

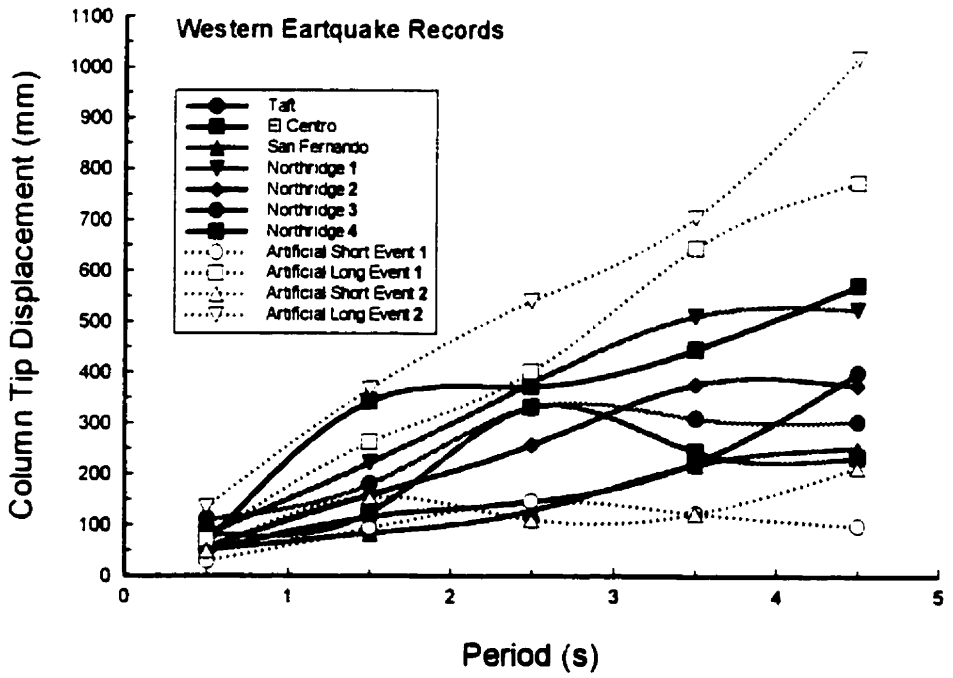

Figure 4.6 SDOF analysis of Eastern and Western Earthquake records normalized to 30% of g.

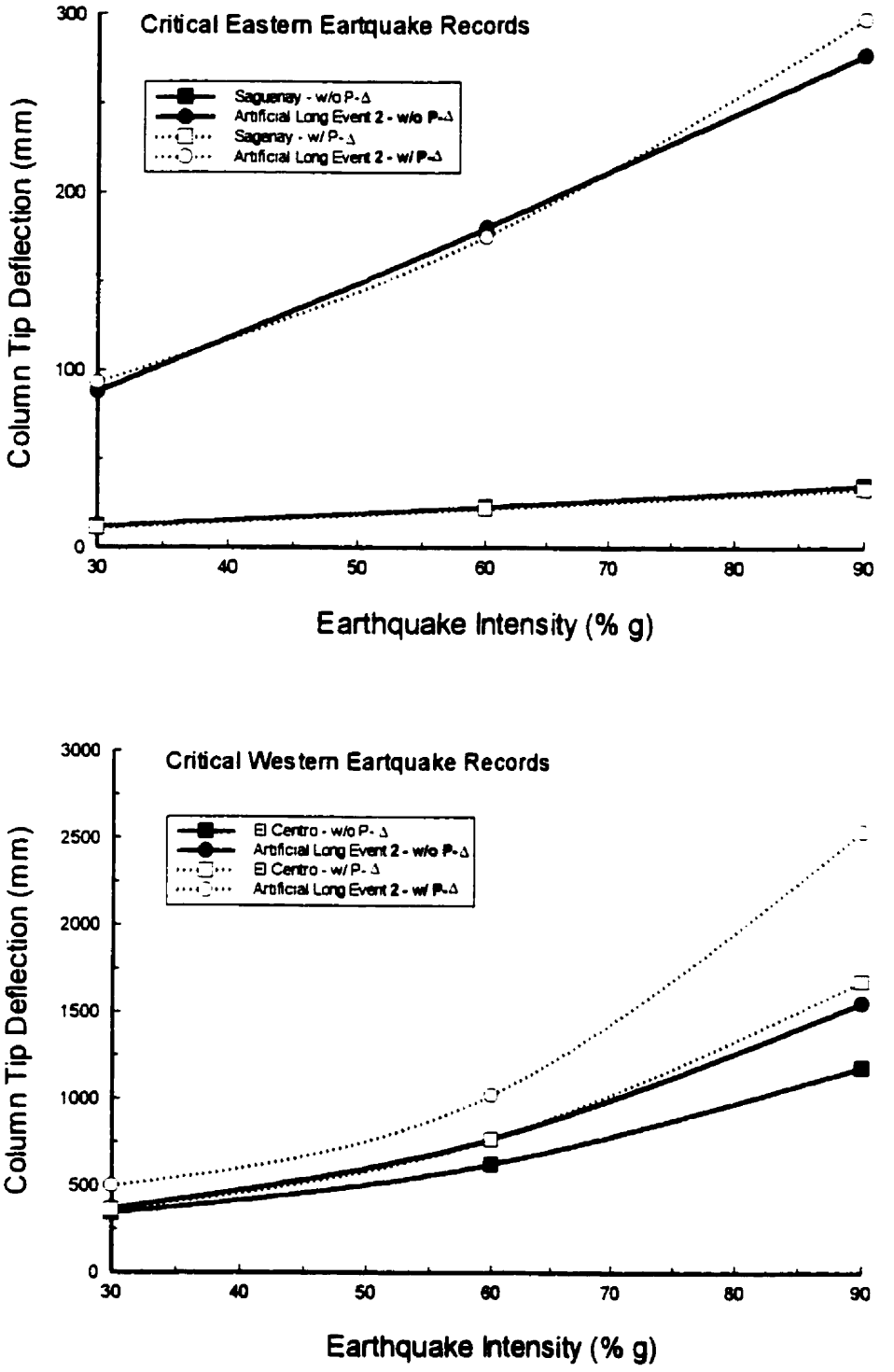

Figure 4.7 SDOF analysis of critical Eastern and Western Earthquake records at a period of 1.5 s and normalized to 30%, 60% and 90% of g.

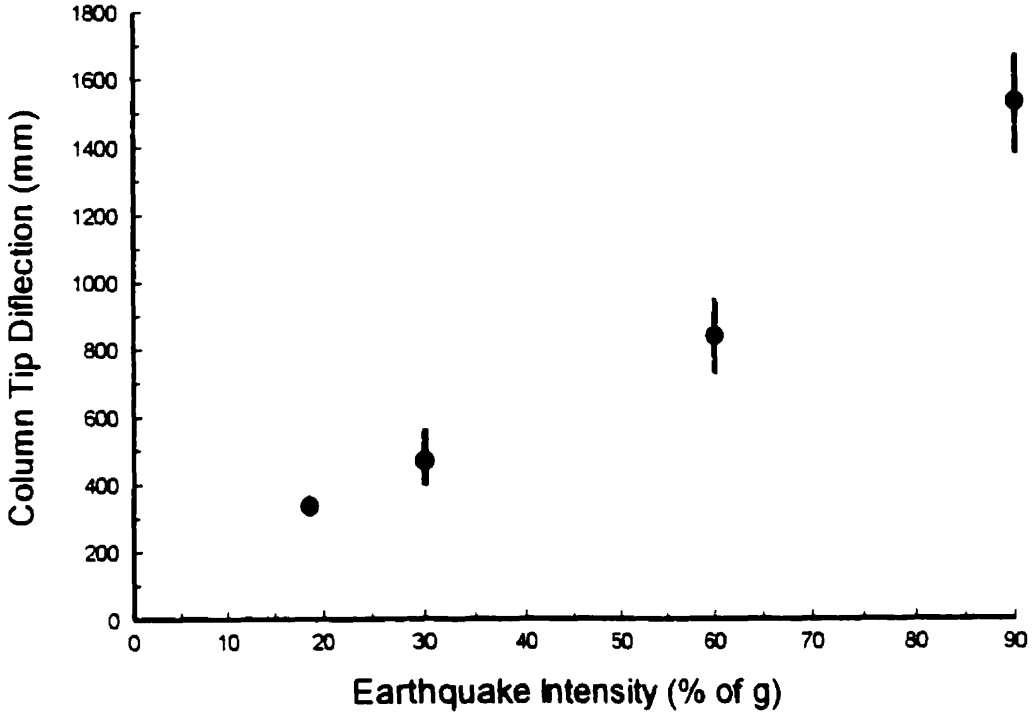

Figure 4.8 Average and variation of column tip displacements of different global bridge models subjected to El Centro at a period of 2.5 s and normalized to 30%, 60% and 90% of *g*.

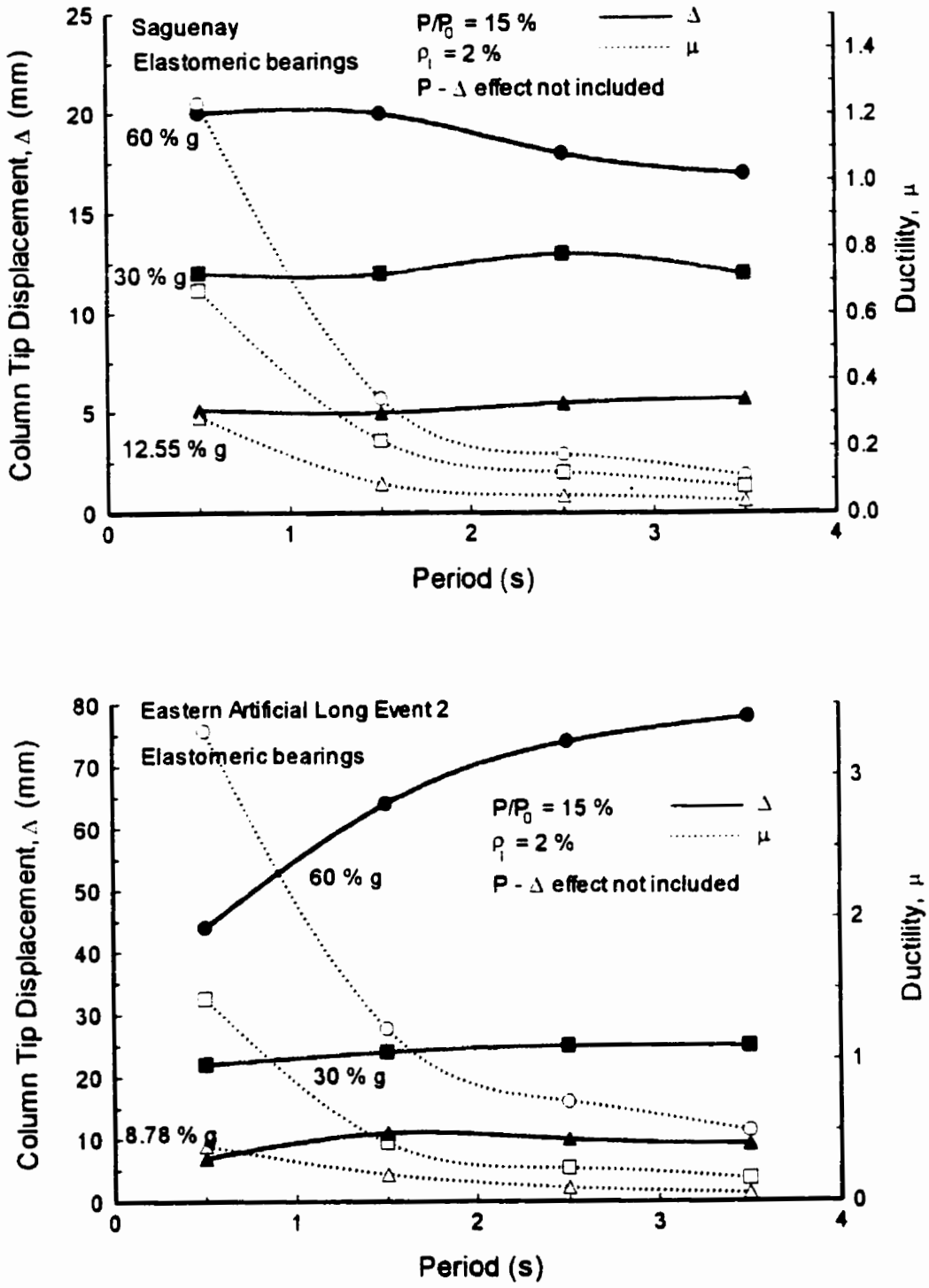

Figure 4.9 Eastern earthquake response of bridges with elastomeric bearings without P-Δ effect.

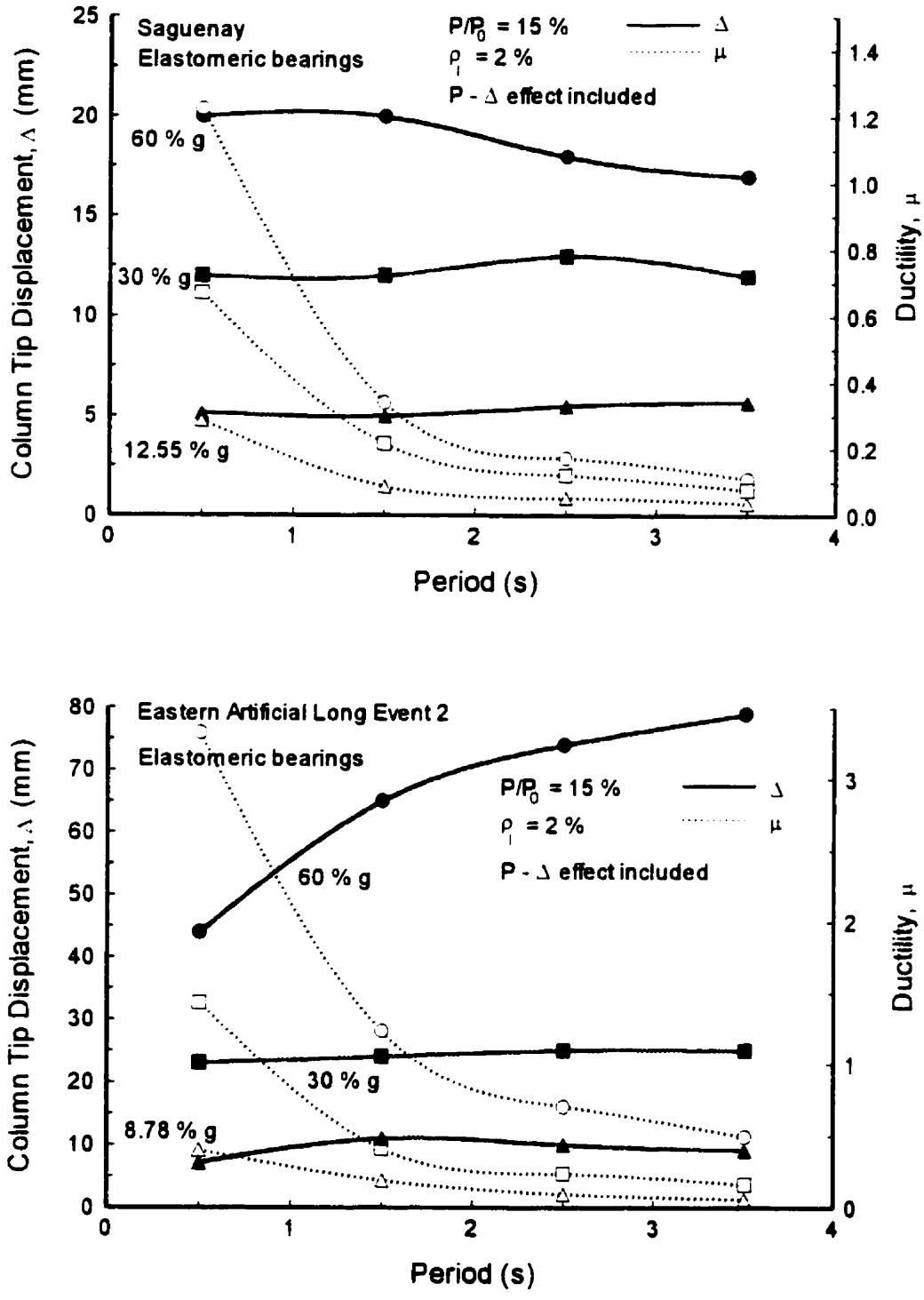

Figure 4.10 Eastern earthquake response of bridges with elastomeric bearings with P-Δ effect.

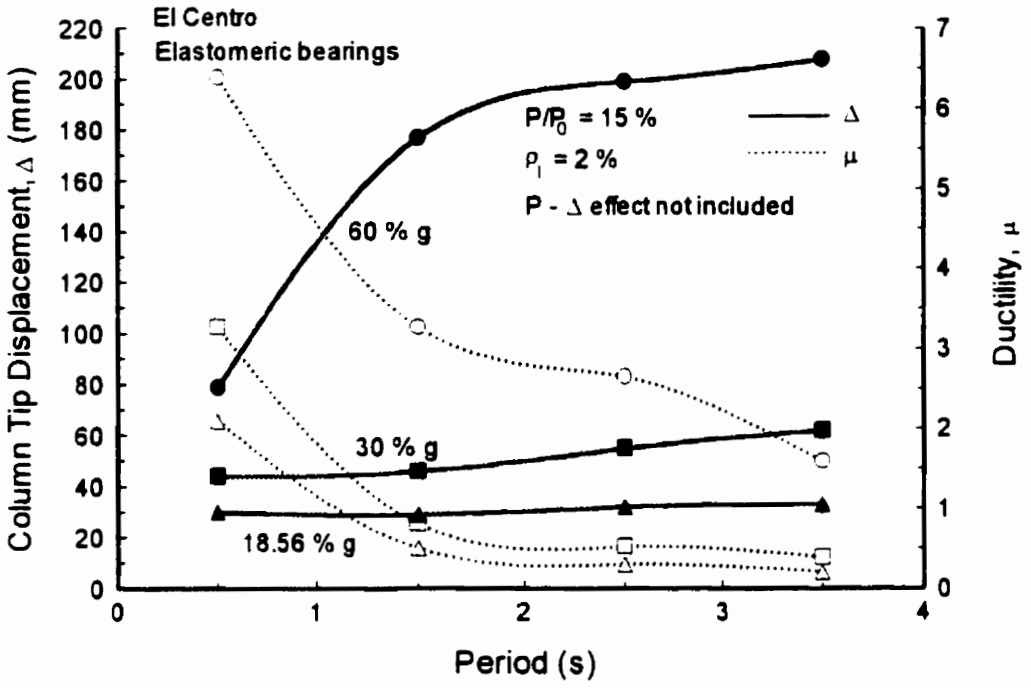

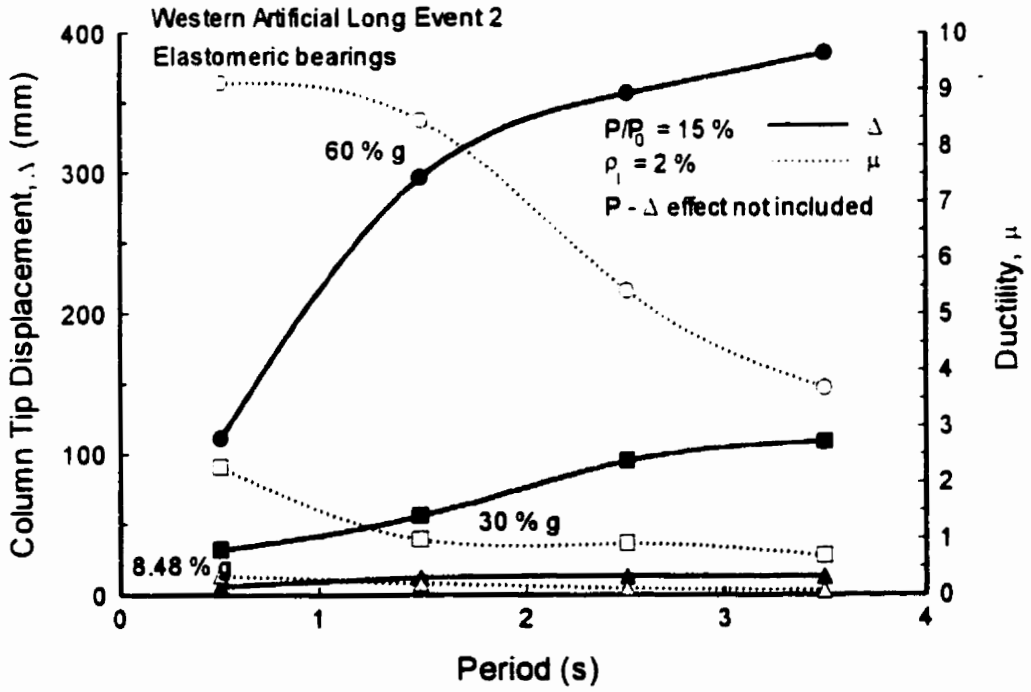

Figure 4.11 Western earthquake response of bridges with elastomeric bearings without P-Δ effect.

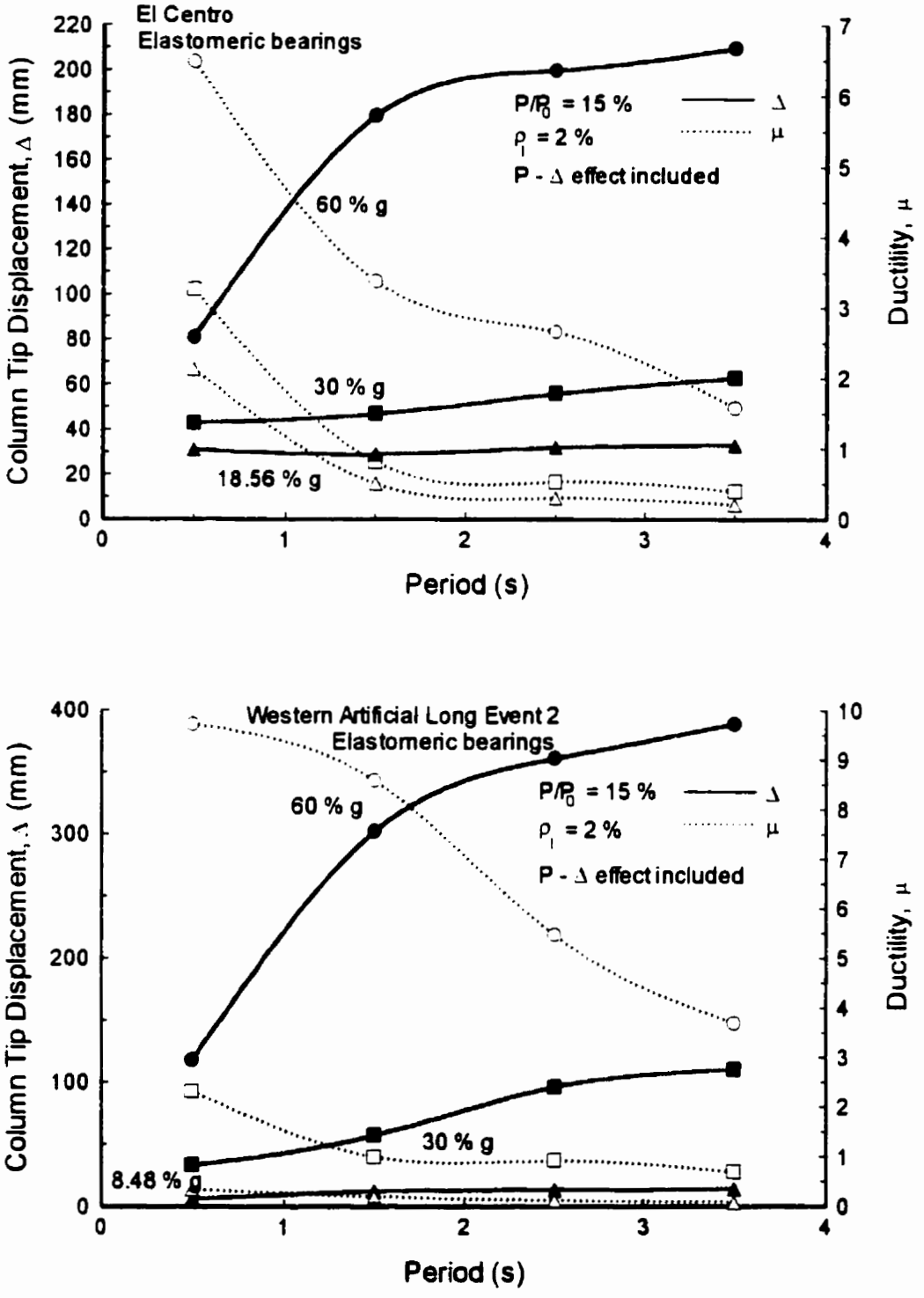

Figure 4.12 Western earthquake response of bridges with elastomeric bearings with P-Δ effect.

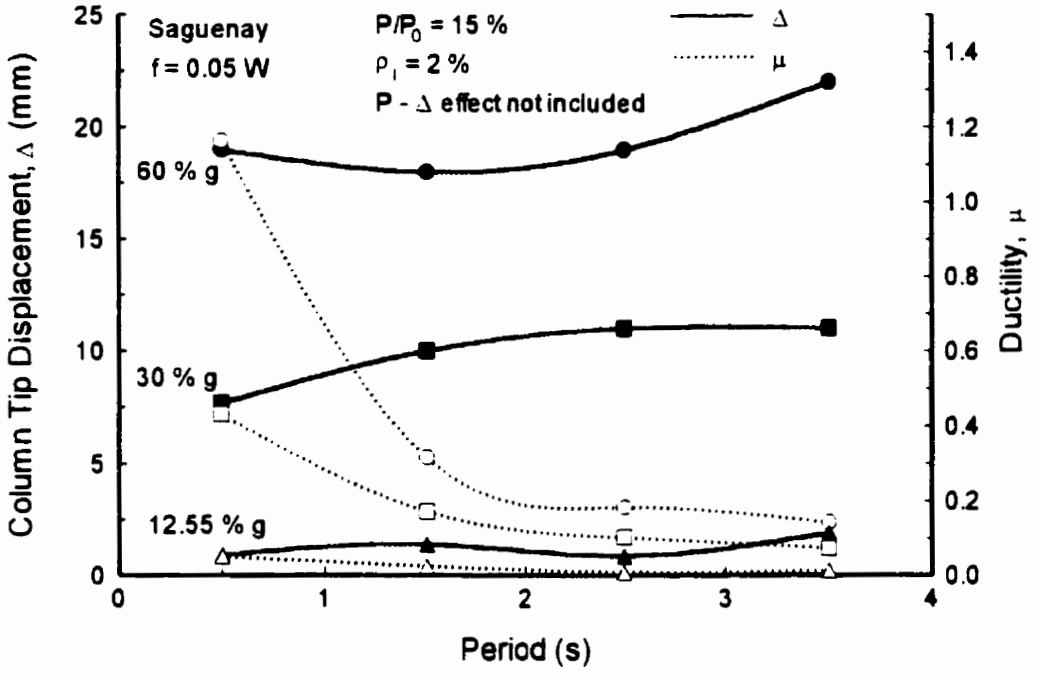

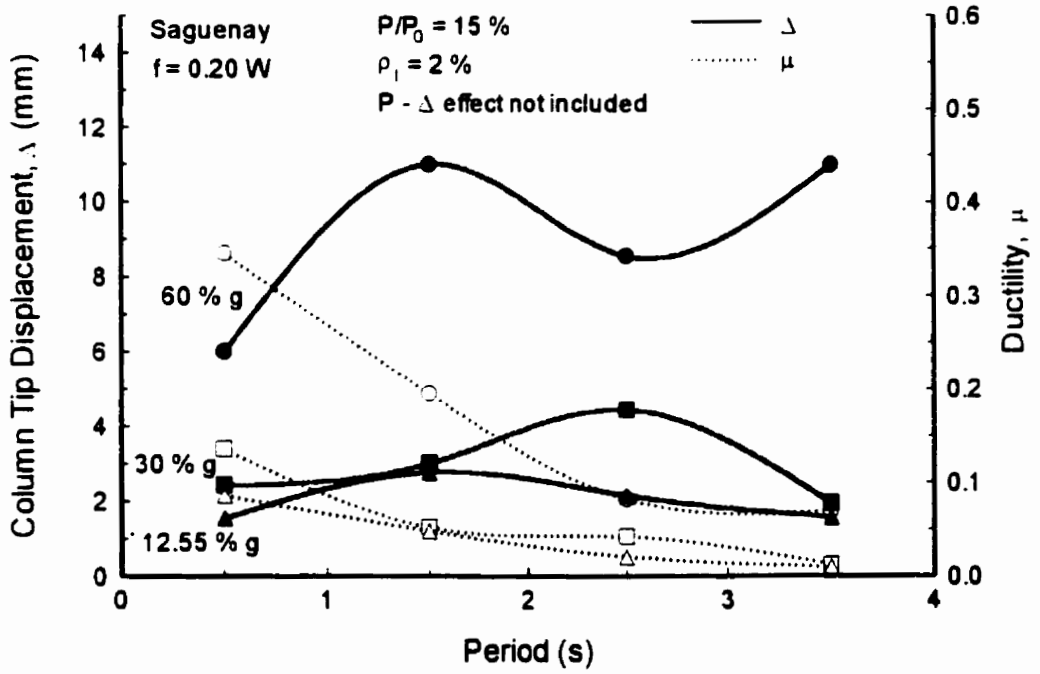

Figure 4.13 Saguenay Earthquake response of bridges with roller or rocker bearings without P-Δ effect.

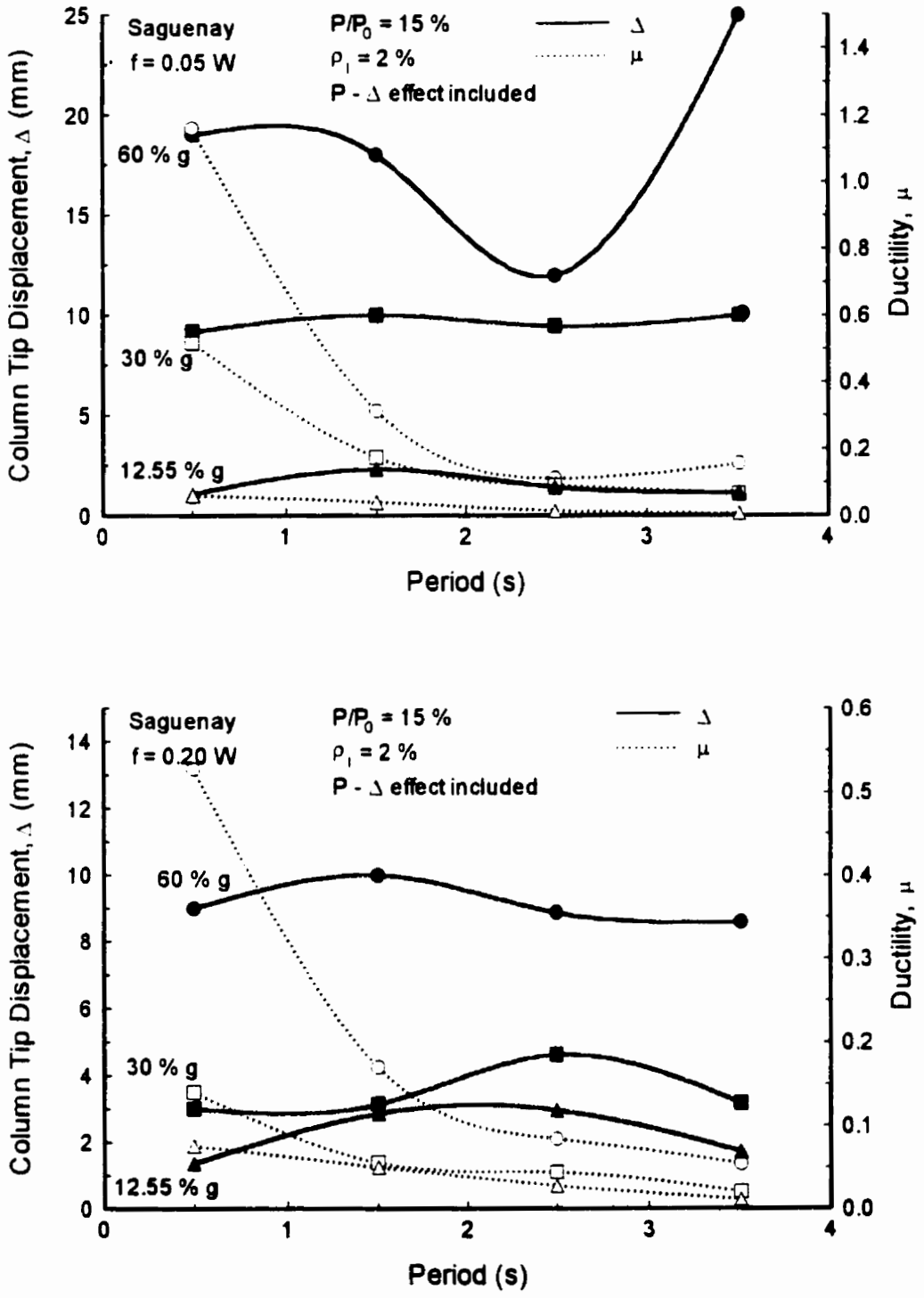

Figure 4.14 Saguenay Earthquake response of bridges with roller or rocker bearings with P-Δ effect.

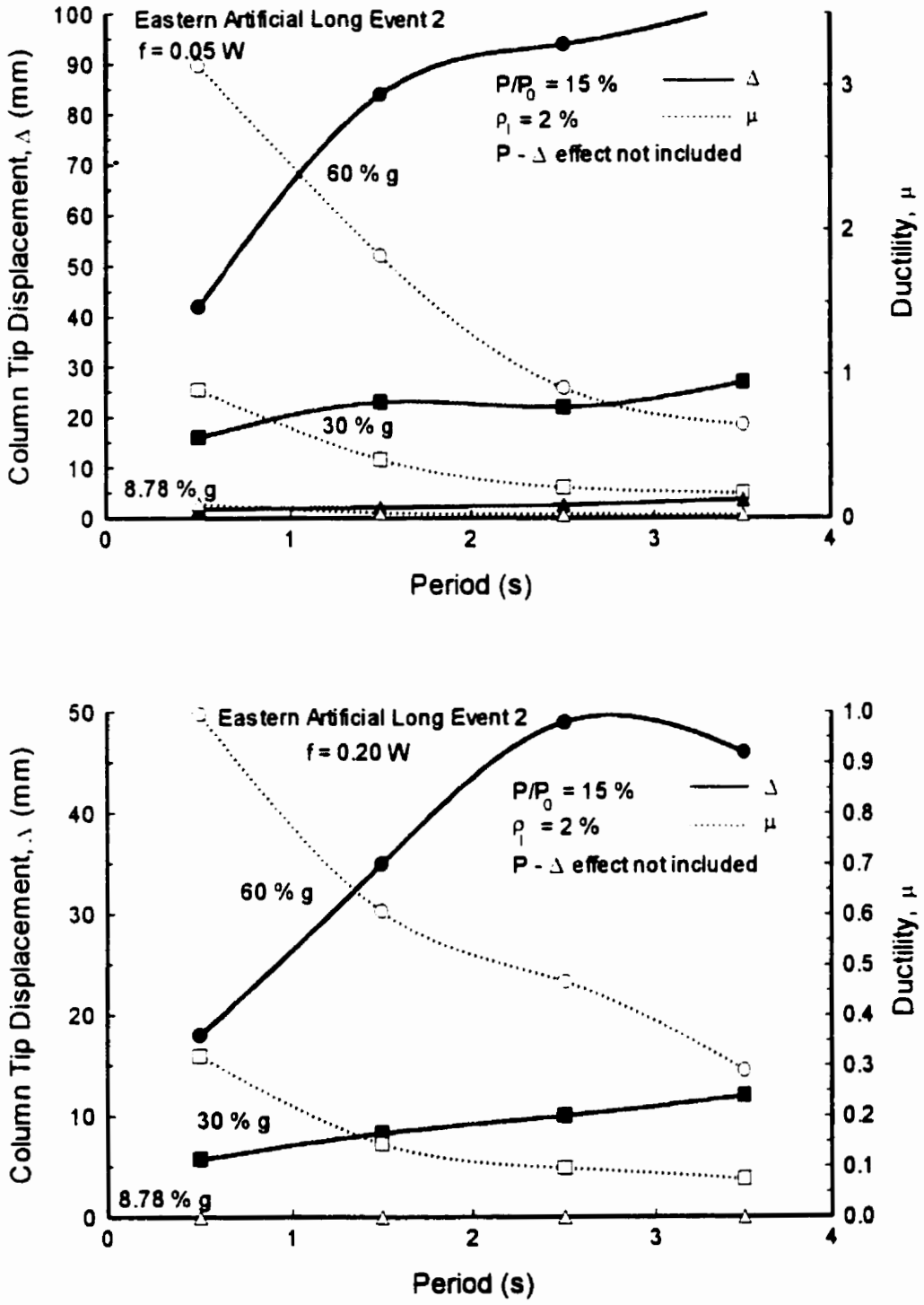

Figure 4.15 Eastern Artificial Long Event #2 Earthquake response of bridges with roller or rocker bearings without P-Δ effect.

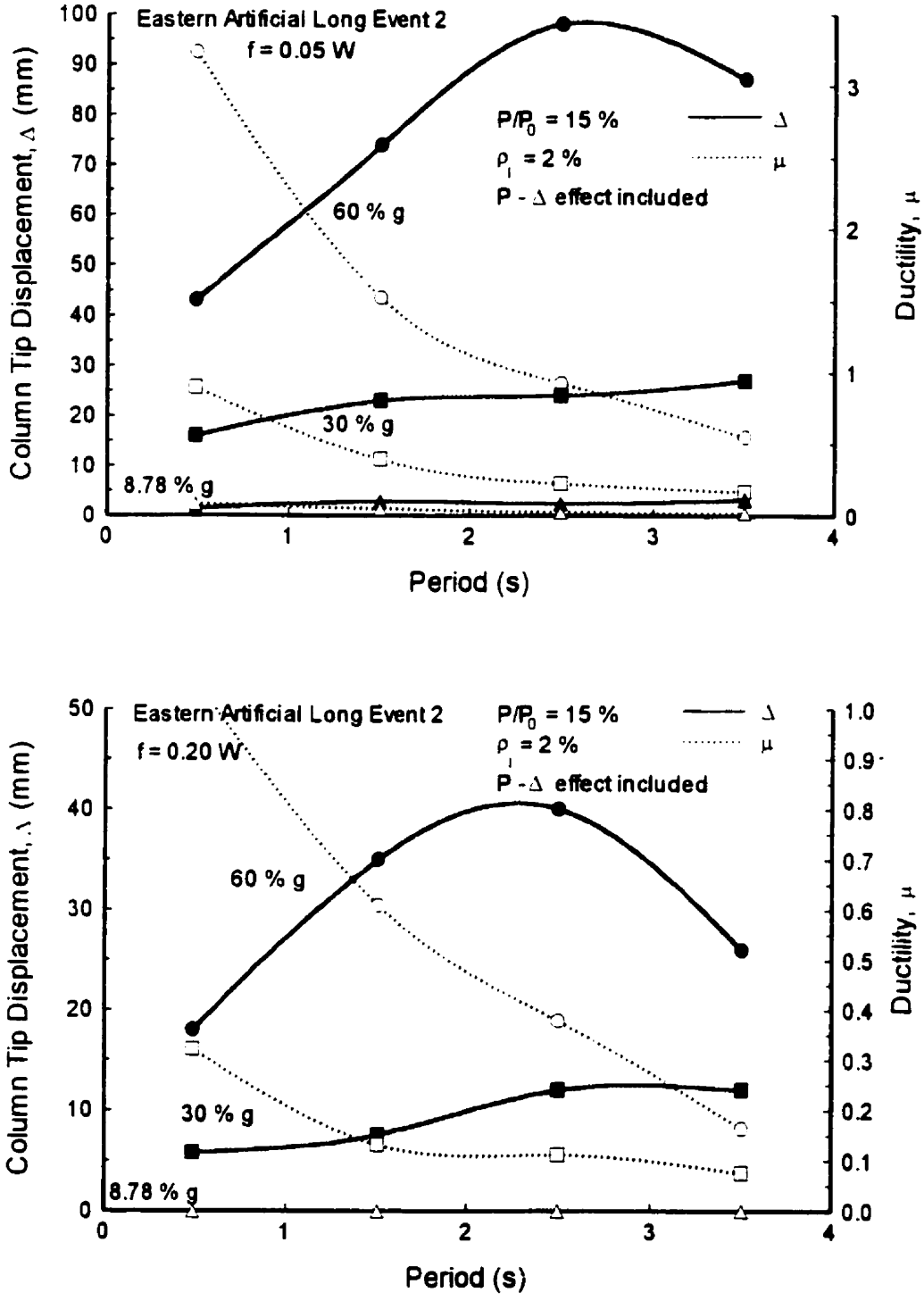

Figure 4.16 Eastern Artificial Long Event #2 Earthquake response of bridges with roller or rocker bearings with P-Δ effect.

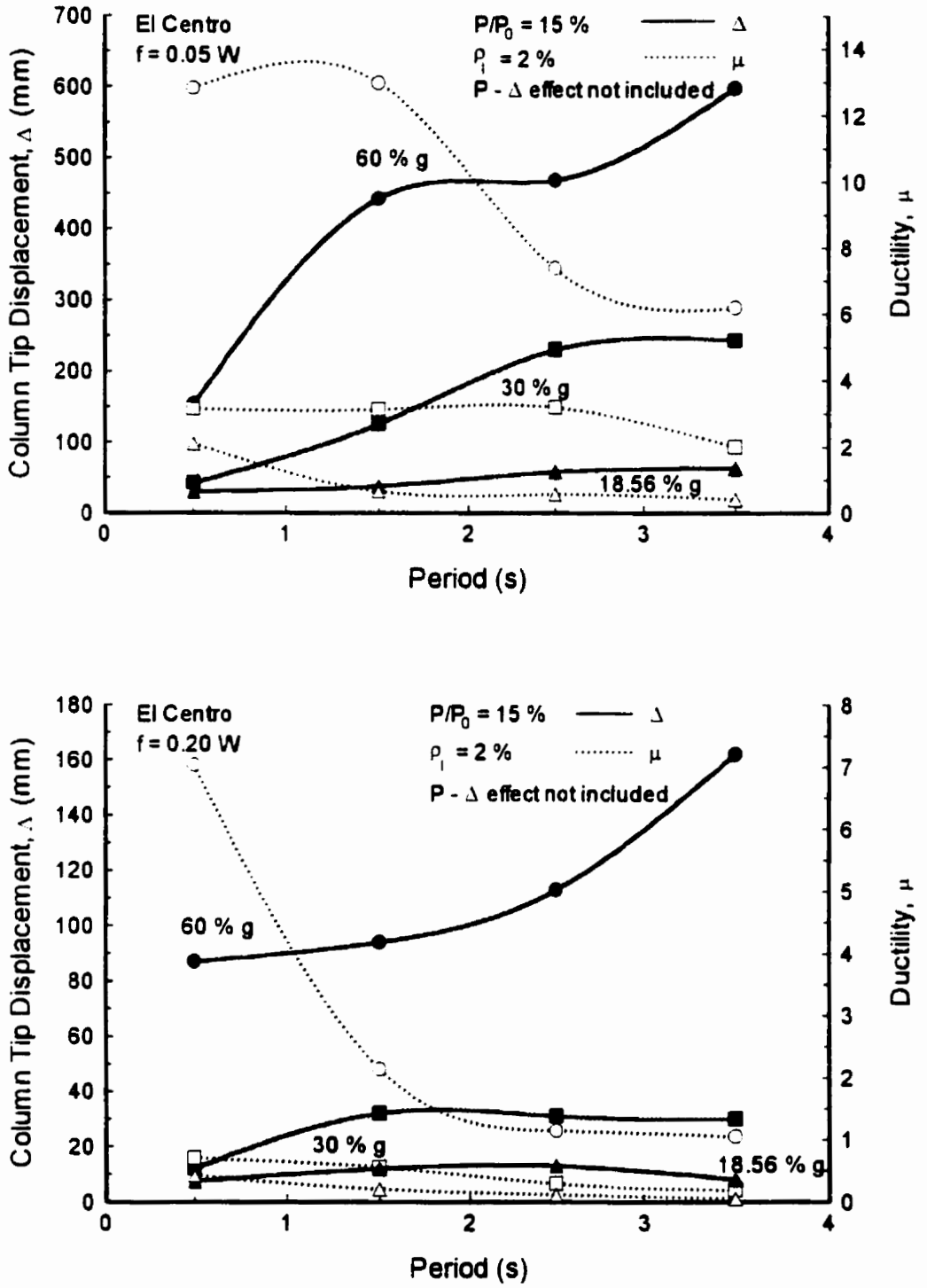

Figure 4.17 El Centro Earthquake response of bridges with roller or rocker bearings without P-Δ effect.

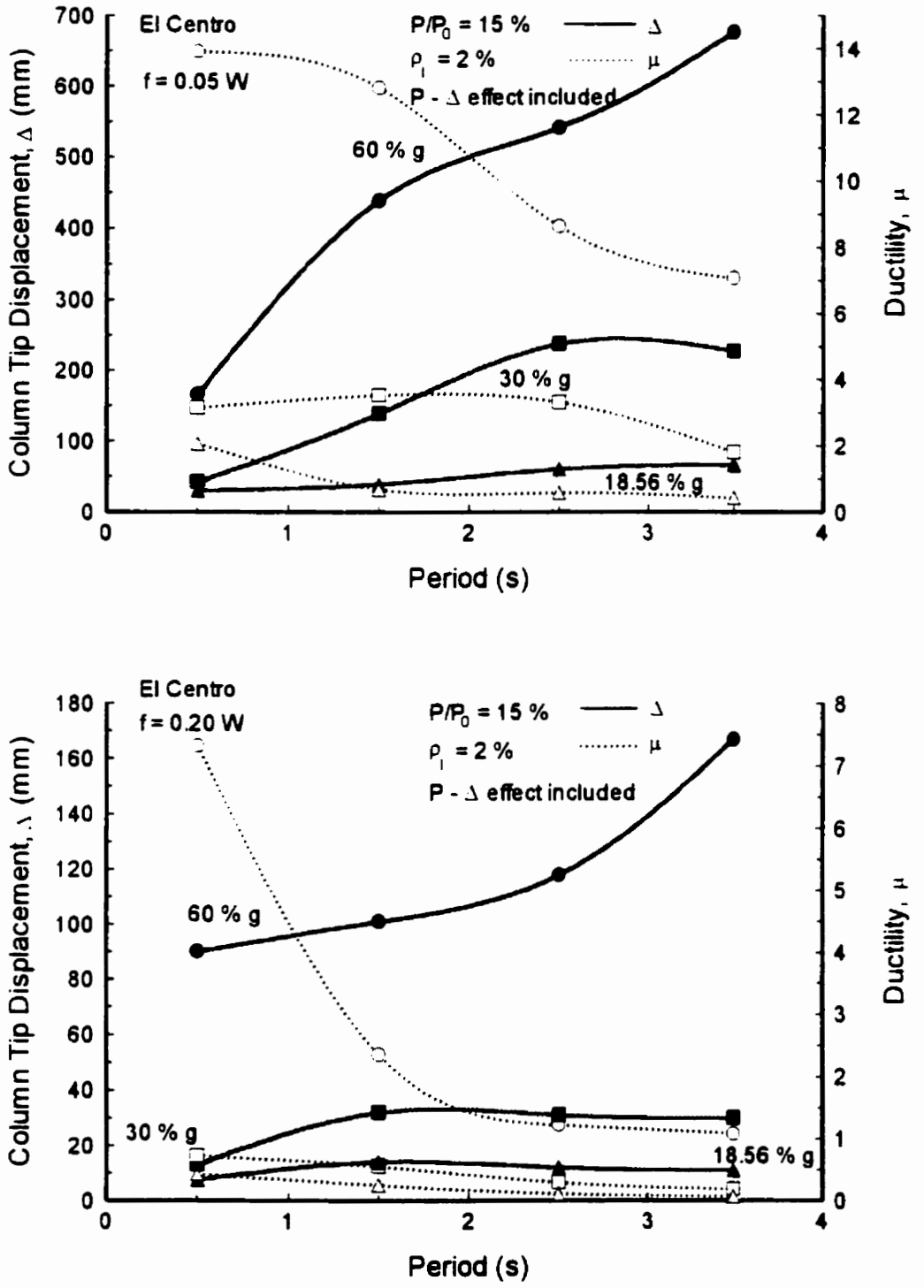

Figure 4.18 El Centro Earthquake response of bridges with roller or rocker bearings with P-Δ effect.

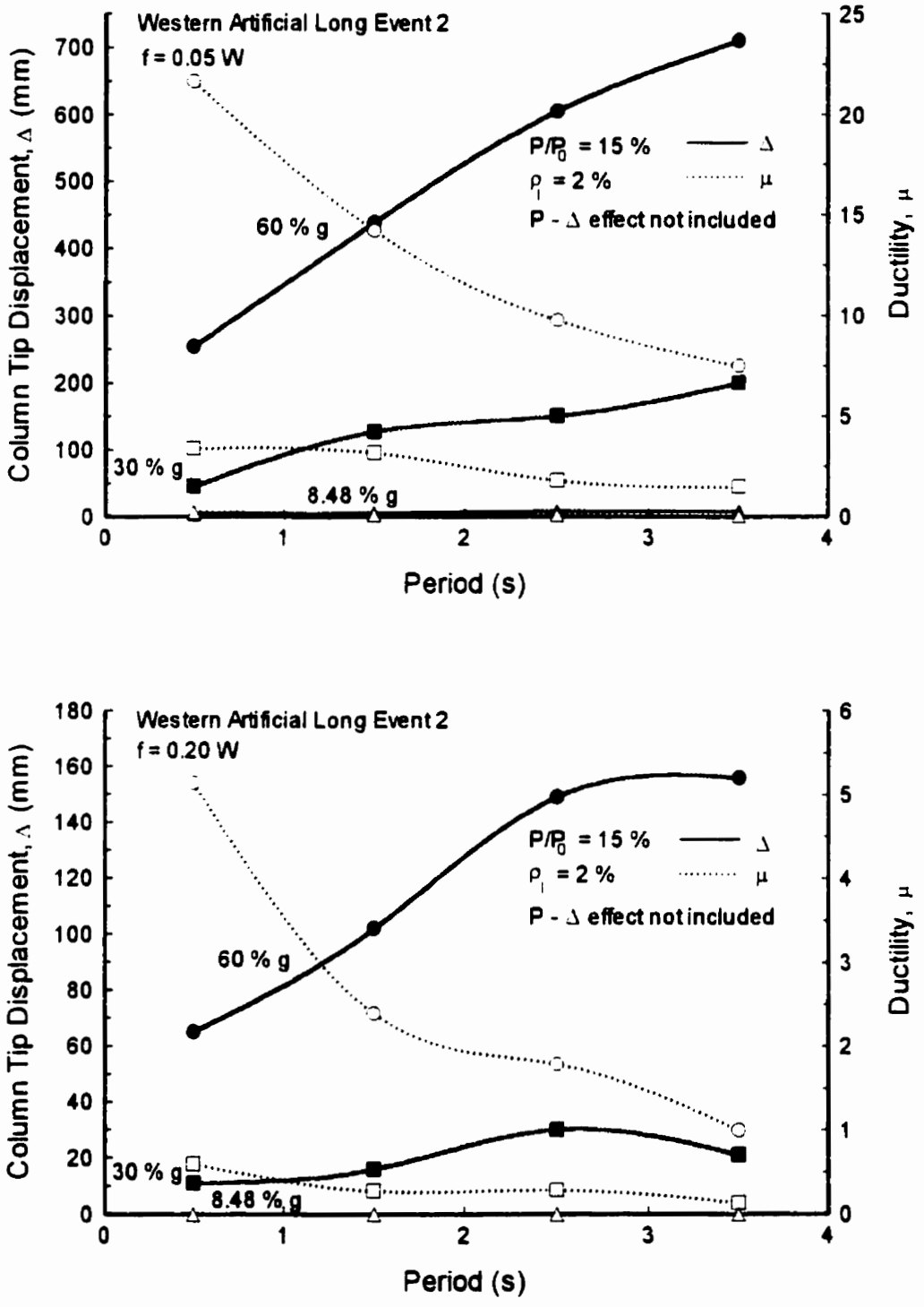

Figure 4.19 Western Artificial Long Event #2 Earthquake response of bridges with roller or rocker bearings without P-Δ effect.

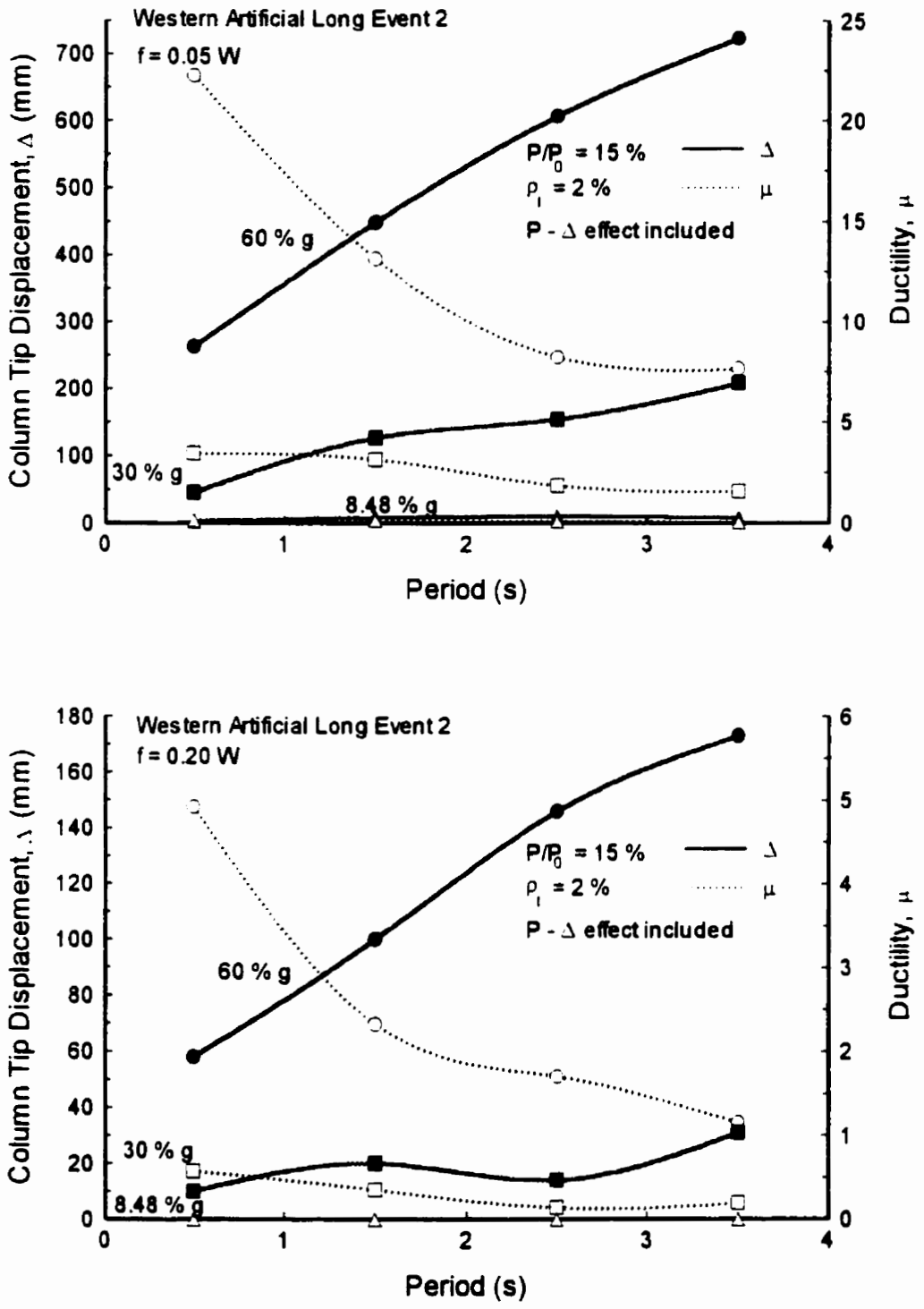

Figure 4.20 Western Artificial Long Event #2 Earthquake response of bridges with roller or rocker bearings with P-Δ effect.

Chapter 5

Experimental Research to Develop a Retrofit Technique

5.1 General

Experimental research was conducted to develop a rational and economical retrofit technique for concrete bridge columns. It involved testing seven full-scale reinforced concrete bridge columns under simulated seismic loading. The columns had either a circular or a square cross-section and represented pre-1970s design practice. The reinforcement arrangement consisted of 12 longitudinal bars with ties placed at 300 mm spacing. A circular and a square column were tested first prior to retrofitting to observe inelastic deformations and failure modes of existing bridge columns. Five companion columns; 4 circular and 1 square, were tested after being retrofitted. The retrofitted columns were tested to investigate the effectiveness of prestressing wires and high strength steel straps as external hoops with or without initial prestressing. The details of test specimens, material properties, test set-up, test procedure, observed behavior, test results, and analysis and evaluation of test data are presented in this chapter.

5.2 Description of Test Specimens

A total of 2 square and 5 circular columns were prepared for testing. The columns were labeled as BR-S or BR-C for square, and circular columns, respectively. The column

numbers followed the cross-sectional designation. For example, BR-S1 was square bridge column number 1. They represented the portion of a column between the point of inflection and column footing.

The square columns had a 550 mm square cross-section, and circular columns had a 610 mm diameter section with 1200 mm column height. Total height of cantilever column was 1485 mm including mid-height of loading beam, a distance of 285 mm from top of column to the application point of horizontal actuator. This translated into aspect ratios (ratio of cantilever length to diameter or width of column) of 2.43 and 2.70 for circular and square columns, respectively. They were cast from two batches of concrete in two stages. First all the footings were cast from the same batch. A few days later all the columns were cast from a second batch. Concrete with a specified strength of 30 MPa was ordered from a ready mix concrete company.

The reinforcing steel was of grade 400 MPa. Twelve No. 25 longitudinal reinforcement were uniformly distributed along the section perimeter. Ties, No. 10, were placed at 300 mm spacing with the first tie placed at 75 mm from the top of the footing. The circular ties had overlapping ends, whereas the square ties had 135 bends at the ends. This was done to reflect the pre-1970s construction practice. Figure 5.1 shows column geometry and typical reinforcement details. Figures 5.2 and 5.3 illustrate selected views of reinforcement cages during construction.

5.3 Material Properties

Properties of materials were established through standard tests. Concrete cylinders and steel coupons were tested to establish stress-strain relationships for the concrete and steel reinforcement. The properties of the prestressing steel were supplied by the manufacturer.

5.3.1 Concrete

Six standard concrete cylinders were tested to obtain the stress-strain relationship of the column concrete. The cylinder tests were conducted using a Forney testing machine with 2200 kN capacity. The average peak stress was found to be 45 MPa at 0.2% of strain. Figure 5.4 shows the stress-strain relationships obtained form the cylinder tests.

5.3.2 Reinforcing Steel

Coupon tests were performed to establish stress-strain characteristics of No. 25 and No. 10 reinforcement. The yield strength for No. 25 was found to be 445 MPa at a strain of 0.22%. The stress-strain relationship was observed to have a yield plateau, with strain hardening beginning at a strain of 1.18%. The ultimate strength was obtained as 658 MPa at a strain of 9.84%. Similarly, the yield strength of 10M reinforcement was found to be 425 MPa at a strain of 0.225%. Strain hardening started at 1.14% strain, and the ultimate point was obtained at 635 MPa stress and 9.85% strain. The coupon tests were performed using a Tinius Olsen testing machine with a capacity of 1300 kN. Figure 5.5 illustrates the stress-strain relationships of deformed reinforcement used.

5.3.3 Prestressing Wire

Seven-wire strands were used to retrofit the columns. A size designation of 9 was selected in order to provide the required force estimated to be needed for retrofitting. The size selected also provided the required flexibility for handling purposes. The strands had a nominal diameter of 9.53 mm, nominal area of 51.6 mm^2, and the grade of 1720 MPa. The stress-strain relationship of the prestressing wire was not established in the laboratory because of inadequate facilities. However, the Concrete Design Handbook (1995), indicates that the elastic modulus of a seven-wire strand is 200,000 MPa, with a yield strength of 1500 MPa. Figure 5.6 illustrates a typical stress-strain relationship of a Grade 1720 MPa 7-wire strand.

5.3.4 High Strength Steel Straps

High strength steel straps with cross-sectional dimensions of 19.05 mm by 1.12 mm (¾" by 0.044") were used in retrofitting one of the circular columns. Coupons were taken from this steel and tested to obtain its stress-strain relationship. The yield strength obtained was 911 MPa at 0.52% of strain. There was well-defined yield plateau, with an onset of strain hardening at a strain of 2.10%. The ultimate strength was 1014 MPa, and occurred at about 9% tensile strain. Figure 5.7 shows the stress-strain relationship of the high strength steel straps.

5.4 Instrumentation

The columns were well instrumented for displacement and strain measurements. Linear Variable Differential Transducers (LVDT) were used to measure displacements. Four LVDTs were attached on both sides of the column face to measure rotations due to flexure. The LVDTs were secured on treaded rods which had been cast in the concrete. The treaded rods were spaced at 300 mm and 600 mm from the bottom of column in order to measure flexural rotations within a distance equal to the cross-sectional dimension. Also, two Temposonic LVDTs were attached to measure the longitudinal column reinforcement extension and/or slip within the footing. An additional Temposonic LVDT was attached to the middle of the loading beam, 1485 mm from the footing base on top of the column, to measure the tip deflection of column. Figure 5.8 shows the instrumentation.

Strain gauges were placed on the reinforcing steel, prestressing cables and high strength steel straps, to measure steel strains during testing. The first and the second layer of stirrups had 4 strain gauges, while an additional 4 gauges were placed at the bottom of longitudinal bars inside the footing. Also, one strain gauge was placed on each external hoop to measure strains during loading. Figure 5.9 shows the strain gauge locations.

Two data acquisition systems were used to collect data, which consisted of steel strains, lateral deflections, and applied forces.

5.5 Description of Test Set-up

The tests were conducted using three computer servo-controlled MTS hydraulic actuators each with 1000 kN capacity in compression and tension. The specimen was secured on a large concrete foundation that had been fixed to the laboratory strong floor by means of 4 high-strength bolts. Two actuators were mounted vertically, one on either side of the column. These actuators were mounted on the foundation at one end, and on the steel loading beam at the other end to apply constant axial compression during testing. The third actuator was mounted horizontally on an A-frame which was also attached to the strong floor. Figure 5.10 shows a schematic diagram of the test set-up. Figure 5.11 illustrates side and front views of the test set-up.

5.6 Loading Program

The specimens were first subjected to a constant axial compression of 1800 kN, which corresponded to 15% of the axial capacity of columns under pure compression. The lateral force was then applied in the displacement control mode, consisting of incrementally increasing lateral drift cycles. The rate of applied cyclic lateral loading was slow and was controlled manually by the laboratory technician. The loading program used is shown in Figure 5.12. Three cycles were applied at each drift level, where the drift level was increased incrementally as 0.5%, 1.0%, 2.0%, etc. until the failure of column occurred.

5.7 Retrofitting Technique Used

The most common retrofitting scheme used for seismically deficient bridge columns is to increase strength and ductility of circular columns through steel jacketing. This is done in the form of providing a steel shell around the column, with a grout filling the gap between the two materials. Elliptic steel jackets have been proposed by researchers for square and rectangular columns. These procedures require extensive labor and material, and can be quite costly. One of the objective of this investigation was to achieve similar effectiveness of column retrofitting with an easier and less expensive technique. Thus, the new retrofitting technique must be economical in terms of labor and material, preferably using standard materials. The proposed retrofitting scheme consists of transverse prestressing steel or steel straps to externally reinforce columns for shear, while also improving concrete confinement. The effectiveness of these schemes were determined experimentally in the laboratory.

5.7.1 Proposed Retrofitting Technique for Circular Columns

Prestressing wires and high strength steel packaging straps were used to retrofit circular columns by providing lateral confinement. Prestressing wires were anchored using a newly developed twisted ring anchor by Dywidag-Systems International, a company which manufactures and installs prestressing materials. The plan dimensions of the twisted ring anchor is approximately 150 mm by 85 mm with a height of 65 mm. The effect of initial prestressing and spacing of these strands and straps are the parameters of this investigation, and

are discussed in Section 5.7. Figure 5.13 shows a schematic drawing of the retrofitting technique used for the circular columns. Figure 5.14 illustrates a typical view of a retrofitted circular column.

5.7.2 Proposed Retrofitting Technique for Square and Rectangular Columns

In order to enhance the confinement external pressure of a rectilinear column, the externally applied pressure must have components perpendicular to the column face, and be as uniform as possible for increased effectiveness. Thus, a hollow structural section (HSS) with a metric designation of HSS 31.8 x 31.8 x 6.35 was selected as external hoops to uniformly re-distribute forces exerted by the prestressing strands. The strand was placed directly on top of an HSS section and raised in 3 locations along each column side by means of half-disc shaped steel wire raisers to develop perpendicular force components. Figures 5.15 shows the retrofitting technique used for square columns. The height and location of steel wire raisers were calculated so that approximately equal perpendicular force components were generated at every point of connection of strands with the steel raisers. The number of wire raisers can be determined in the same manner as for internal cross ties used in columns, and have similar effect on column performance. Figure 5.16 illustrates a typical view of a retrofitted square column.

5.8 Test Results

A total of 7 column tests were performed in the laboratory. The results of these tests are reported in the following sections.

5.8.1 Square Column, Non-retrofitted (BR-S1)

This column was representative of a typical, full-scale bridge column, with No. 10 perimeter ties at 300 mm. This amount of transverse reinforcement produced nominal shear capacity, approximately equal to the shear force associated with flexural yielding, and hence was not sufficient to provide the required shear resistance for loads induced by seismic activity.

The column was first loaded with a constant axial compressive force of 1800 kN, prior to the application of lateral deformation reversals. Observations during testing indicated that

the first set of flexural cracks formed during the third cycle at 0.5% lateral drift. The recorded maximum lateral load at 0.5% drift level was 530 kN. Shear cracks were observed at the beginning of 1.0% drift. These cracks widened as new diagonal cracks appeared during the subsequent cycles at the same deformation level. Spalling of concrete cover was observed near the base. The maximum lateral load at 1.0% drift was 580 kN. The first cycle at 2.0% drift resulted in sudden formation of a wide diagonal crack which caused a drop in lateral load resistance to 370 kN. The cover concrete showed extensive spalling. The cover within the bottom 450 mm segment was completely spalled at the end of the second cycle at 2.0% drift. Longitudinal bars also started to buckle during this load stage, and the lateral load dropped to 50 kN. After the initial shear failure, the column continued to sustain approximately one half of its maximum resistance until the buckling of longitudinal reinforcement. Figure 5.17 shows views of testing at different drift levels. Figure 5.18 shows force-displacement hysteresis loops recorded during the experiment, indicating a brittle failure shortly after a lateral drift of 1.0%. Also, Figure 5.19 shows flexural and slip rotations, and Figure 5.20 shows strains in the reinforcing steel.

5.8.2 Circular Column, Non-retrofitted (BR-C1)

The column was subjected to the same loading program that was used for the previous square column, with observed behavior very similar to that described for the square column. However, the load resistance was different. The maximum lateral load recorded at 0.5% drift was 460 kN. It was increased up to 560 kN at 1.0% drift. The column could not survive the sudden diagonal shear crack that formed at the beginning of the 2.0% drift level. Crushing of concrete and buckling of longitudinal reinforcement were observed during the cycles at 2.0% drift. Shear failure was observed. Figure 5.21 shows views of testing at different drift levels. Figure 5.22 shows experimentally recorded force-displacement hysteresis loops. Also, Figure 5.23 shows flexural and slip rotations, and Figure 5.24 shows strains in the reinforcing steel.

5.8.3 Circular Column, Retrofitted, Type I (BR-C2)

One of the circular columns was retrofitted with 9 mm diameter 7-wire strands, placed as exterior hoops at every 150 mm starting at 75 mm from the column base. The strands had a

1760 MPa capacity, and were prestressed to 25 % of their tensile capacity prior to testing. The maximum load resistance at 0.5% and 1.0% drift levels were 500 kN and 615 kN, respectively. The cracks were completely eliminated during 1.0% drift cycles. Only after the first cycle of 2.0% drift level were some hairline flexural cracks observed. At the end of the 2.0% drift level, the maximum lateral load was increased to 650 kN, and concrete near the footing base started crushing. At 3.0% drift level, flexural cracks were more apparent between the first and second prestressing hoops from the footing base, and the cover concrete started to spall in the same region. The maximum lateral load resistance remained at 650 kN. It was clear that the behavior was no longer governed by shear, as observed in the companion non-retrofitted column, but by flexure. The prestressing strands not only functioned as shear reinforcement, but also confined the concrete, improving flexural behavior as well. At 4.0% drift the maximum lateral load dropped slightly to 630 kN, and more cover concrete spalled. At this load stage, the first two prestressing strands started to embed into the concrete as the concrete expanded. No major diagonal cracks were visible until 4.0% drift, with the exception of some minor hairline cracks. At 5.0% drift level flexural cracks started to widen and additional flexural cracks appeared around the third prestressing hoop from the base. The lateral load started dropping gradually during each cycle of the same drift level, from 600 kN to 450 kN. At the end of the cycles at 5.0% lateral drift, the concrete cover was completely spalled up to the second prestressing strand. At 6.0% drift, the longitudinal bars started buckling and the lateral load dropped sharply to 285 kN. Finally, the test was stopped. Figure 5.25 shows views of testing at different drift levels. Force-displacement hysteresis loops of this column is shown in Figure 5.26. Also, Figure 5.27 shows flexural and slip rotations, and Figures 5.28 and 5.29 show strains in the reinforcing steel and the prestressing wires.

5.8.4 Circular Column, Retrofitted, Type II (BR-C3)

This column was retrofitted the same way as the previously described type I retrofitted circular column with the exception of the level of prestressing in strands. This time the strands were prestressed to only about 5% of the ultimate strand capacity to make them just snug tight, to investigate the effect of low prestressing levels on column performance. Basically the same force-deformation characteristics as those for type I retrofitting were observed until the end of

4.0% drift. At later stages of loading, the force-displacement hysteresis loops showed some pinching indicating a shear contribution to the overall response. The pinching effect started with the formation of diagonal cracks. At 5.0% drift level the applied lateral load sharply decreased from 500 kN to 335 kN, and large diagonal cracks were observed. Finally, at 6.0% drift, the lateral load suddenly dropped to a level below 200 kN, with a subsequent drop to 50 kN at the second cycle of the same drift level. The test was aborted at this stage of loading. Figure 5.30 shows views of testing at different drift levels. Figure 5.31 shows force-displacement hysteresis loops recorded during testing. Also, Figure 5.32 shows flexural and slip rotations, and Figures 5.33 and 5.34 show strains in the reinforcing steel and prestressing wires.

5.8.5 Circular Column, Retrofitted, Type III (BR-C4)

The effect of hoop spacing was the parameter in this test, where the prestressing hoops were placed at 300 mm with the same cable the stressing as for column BR-C2, i.e. to 25% of the ultimate strength of prestressing strand. The behavior was identical to that of column BR-C2 until the end of 1.0% drift cycles. During the first cycle of 2.0% lateral drift, the cover concrete near the base started to crush as flexural cracks widened. By the end of the third cycle, the bottom cover concrete was completely spalled. Also, at 2.0% drift, the lateral load dropped from 580 kN to 520 kN. During the first at 3.0% drift, the second prestressing strand from the bottom started to fail, indicating that the lateral prestressing force was not sufficient to control diagonal cracking. With the rupture of one of the seven tendons, the cable relaxed, and the lateral load level dropped to 450 kN. The strength decay continued as bottom concrete continued crushing as the first prestressing wire started to sink in concrete. The test was terminated during the third cycle of 3.0% drift when all the longitudinal bars buckled and the column failed abruptly. Figure 5.35 shows views of testing at different drift levels. Figure 5.36 shows force-displacement hysteresis loops recorded during testing. Also, Figure 5.37 shows flexural and slip rotations, and Figures 5.38 and 5.39 show strains in reinforcing steel and prestressing wires.

5.8.6 Circular Column, Retrofitted, Type IV (BR-C5)

This retrofitting technique consisted of high-strength steel straps instead of prestressing straps. The straps were spaced at 150 mm and they were tied snug tight, as in the case for the type II column (BR-C3). The behavior was very similar to the column retrofitted with the type II scheme (BR-C3) until the end of 2.0% drift cycles. At the beginning of 3.0% drift cycles and after reaching a peak lateral load of 610 kN, the 4th and 5th straps from the bottom suddenly ruptured causing a sharp drop in lateral load resistance to 400 kN and below. Large diagonal cracks formed, and the concrete cover near the footing region cover spalled. The longitudinal bars buckled shortly after the rupture of the 2nd and 3rd straps at 3.0% drift. The test was then aborted. Figure 5.40 shows views of testing at different drift levels. Figure 5.41 shows the experimentally recorded force-displacement hysteretic relationship for this column. Also, Figure 5.42 shows flexural and slip rotations, and Figures 5.43 and 5.44 show strains in reinforcing steel and straps.

5.8.7 Square Column, Retrofitted (BR-S2)

This column was retrofitted using hollow steel sections, consisting of HSS 31.8 x 31.8 x 6.35 mm, as hoops with prestressing wire wrapped around each hoop. The strands were stressed up to 25% of the ultimate capacity of strands. The hoops were spaced at 150 mm, center-to-center, starting at 75 mm from the column base, the same way as retrofitted circular type I column (BR-C2). Some moderate flexural cracks were developed at the end of the cycles at 1.0% lateral drift. Neither shear cracks nor crushing of concrete were observed. The maximum lateral force at this stage of loading was approximately 600 kN. Concrete started to crush at the beginning of 2.0% drift cycles until spalling of concrete occurred at the end of 3.0% drift cycles. The maximum lateral load reached 650 kN. By the end of 5.0% drift, more concrete crushing and cover spalling was observed. Shear cracks were not wide; however, the lateral load started decaying to a level of 500 kN. During the first cycle at 6.0% drift, the first row of longitudinal bars that were in tension, abruptly ruptured and the lateral load dropped to 450 kN. The test was aborted after the tension failure of the longitudinal reinforcement. Figure 5.45 shows views of testing at different drift levels. Figure 5.46 shows experimentally recorded force-displacement hysteretic relationship for this column. Also, Figure 5.47 shows

flexural and slip rotations, and Figures 5.48 and 5.49 show strains in reinforcing steel and prestressing wires.

5.9 Effect of External Hoops on Shear Strength and Ductility of Columns

Bridge columns may need retrofitting to enhance shear capacity and inelastic deformability of columns. The shear capacity needs to be increased if the shear strength is lower than that corresponding to flexural capacity. This promotes flexural yielding and generally ductile flexural behavior. However, the column may not possess sufficient ductility, even in flexure, if the column concrete is not sufficiently confined by transverse reinforcement. The proposed retrofitting scheme, tested as part of this investigation, consists of external hoops, contributing to both the increase in shear (diagonal tension) strength, as well as concrete confinement. The increase in shear strength was achieved in two ways; first by providing additional transverse reinforcement against diagonal tension, second by improving concrete resistance to shear through transverse prestressing. The increase in flexural deformability was attained by confining column concrete through closely spaced external hoops.

The experimental research involved testing columns with a relatively low shear span-to-depth ratio so that, with the pre-1970 design practice, they would be critical in shear. The parameters that were investigated included the type and spacing of hoops, as well as the level of initial prestressing. Details of retrofitting schemes and column behavior during testing were discussed in the preceding section.

The strains in each external hoop were recorded and summarized in Tables 5.1 through 5.5. Figures 5.38 to 5.42 show the external hoop strain profile along the height of the columns. The analysis of test results of retrofitted columns was carried out using the incremental strains obtained from the hoops. The required prestressing force was then obtained at each drift level by calculating the difference between experimentally recorded lateral forces and the nominal values of shear contributions due to concrete and reinforcing steel. The concrete and steel contributions were calculated using Equations 3.40 through 3.47. The angle of inclination of diagonal tension cracks was taken as 30 degrees from the column axis, as suggested by Priestley et al. (1994). The contribution due to axial load was neglected since bridge columns

typically are not subjected to high axial compression. The analysis of test results are presented in Table 5.6.

5.10 Proposed Design Procedure for Column Retrofitting

A design procedure has been developed for bridge column retrofitting, based on the experimental observations and data evaluated in the previous section. Accordingly, a bridge column can be retrofitted by means of external hoops. The hoops may consist of prestressing strands or any other form of high-strength steel. The procedure outlined below is intended for shear critical columns, and leads to the determination of external hoop requirements for the purpose of retrofitting. Therefore, deformability capacity and demand of a column should first be checked by following the procedures presented in Chapters 3 and 4, respectively. If the column is found to be deficient in shear, then the procedure outlined below can be followed;

1. Calculate concrete contribution to shear resistance, V_c, using Equation 3.41, while considering the ductility ratio associated with drift demand.
2. Calculate the contribution of existing steel in the column, V_s, to shear resistance, using Equations 3.46 or 3.47.
3. Find shear force corresponding to probable flexural resistance, $V_{prob.}$, either by performing a sectional analysis or using a computer software (such as COLA) developed for this purpose. Probable flexural resistance is defined as 1.25 times the nominal flexural shear.
4. If $(\phi_c V_c + \phi_s V_s) \geq V_{prob}$; no need for retrofitting.
5. Otherwise retrofit by providing external hoops. The shear contribution, V_{hoop}, needed from external hoops can be computed as follows:

$$V_{hoop} = V_{prob} - (\phi_c V_c + \phi_s V_s) \tag{5.1}$$

where ϕ_c and ϕ_s are concrete and steel strength factors, and are expressed as 0.60 and 0.85, respectively.

The force developed by the external hoop can be calculated as;

$$V_{hoop} = 2A_{hoop}(1-\alpha_f)\phi_{hoop} f_{yh} \frac{b}{s_{hoop}} \cot\Theta$$

where A_{hoop} is the cross-sectional area of the external hoop; α_f is the ratio of initial prestressing strength to yield strength of the external hoop; ϕ_{hoop} is the external hoop strength factor; f_{yh} is the yield strength of external hoop; b is the diameter in circular columns or side dimension in rectilinear columns; s_{hoop} is the spacing of external hoops; Θ is the crack angle and it can be taken as 30 degrees.

Therefore, the cross-sectional area of the external hoop can be found as;

$$A_{hoop} = \frac{V_{hoop} s_{hoop}}{2(1-\alpha_f)\phi_{hoop} f_{yh} b} \tan\Theta \tag{5.2}$$

Substituting Equation 5.1 into 5.2 results the following relationship;

$$A_{hoop} = \frac{\left[V_{prob} - (\phi_c V_c + \phi_s V_s)\right] s_{hoop}}{2(1-\alpha_f)\phi_{hoop} f_{yh} b} \tan\Theta \tag{5.3}$$

6. Provide hoops at b/4 or 150 mm, whichever is less for confinement of concrete and stability of longitudinal reinforcement.

The above procedure is intended to increase resistance to diagonal tension by providing additional transverse reinforcement. Further improvement in shear resistance and hysteretic behavior, in terms of delayed strength decay and reduced pinching of hysteresis loops, may be achieved through prestressing. It was experimentally shown earlier in this chapter that an initial prestress of 25% f_{pu}, or approximately 30% f_{py} resulted in an enhancement of concrete shear resistance, as well as delayed strength decay under reversed cyclic loading. While the experimental evidence to this effect is limited, it is recommended that external hoops are pressed up to approximately 25% f_{pu}.

Table 5.1 Prestressing wire strains for retrofitted circular column (BR-C2).

P/S Wire #	Location From Bottom of Column (mm)	% Drift	Strain in P/S Wire (x 10^{-6})	Incremental P/S Strain
1	75	0	1500	0
		1	1550	50
		2	2100	600
		3	2400	900
		4	3100	1600
		5	-	-
2	225	0	1500	0
		1	1650	150
		2	1850	350
		3	2250	750
		4	2500	1000
		5	3000	1500
3	375	0	1500	0
		1	2150	650
		2	2650	1150
		3	2950	1450
		4	3400	1900
		5	5000	3500
4	525	0	1500	0
		1	2000	500
		2	2300	800
		3	2750	1250
		4	3300	1800
		5	4200	2700
5	675	0	1500	0
		1	1750	250
		2	1950	450
		3	2300	800
		4	2650	1150
		5	3500	2000
6	825	0	1500	0
		1	1600	100
		2	1850	350
		3	2050	550
		4	2300	800
		5	2900	1400
8	1050	0	1500	0
		1	1850	350
		2	1950	450
		3	2050	550
		4	2075	575
		5	2100	600

Table 5.2 Prestressing wire strains for retrofitted circular column (BR-C3).

P/S Wire #	Location From Bottom of Column (mm)	% Drift	Strain in P/S Wire (x 10^{-6})	Incremental P/S Strain
1	75	0	250	0
		1	350	100
		2	450	200
		3	600	350
		4	1800	1550
		5	2100	1850
2	225	0	100	0
		1	150	50
		2	200	100
		3	500	400
		4	1200	1100
		5	2500	2400
3	375	0	250	0
		1	700	450
		2	-	-
		3	-	-
		4	-	-
		5	-	-
4	525	0	250	0
		1	950	700
		2	1350	1100
		3	1700	1450
		4	2750	2500
		5	4000	3750
5	675	0	50	0
		1	500	450
		2	950	900
		3	1500	1450
		4	2400	2350
		5	3500	3450
7	975	0	50	0
		1	450	400
		2	770	720
		3	1100	1050
		4	1300	1250
		5	-	-
9	1125	0	10	0
		1	510	500
		2	750	740
		3	800	790
		4	900	890
		5	950	940

Table 5.3 Prestressing wire strains for retrofitted circular column (BR-C4).

P/S Wire #	Location From Bottom of Column (mm)	% Drift	Strain in P/S Wire (x 10^{-6})	Incremental P/S Strain
1	75	0	1725	0
		1	1800	75
		2	2100	375
		3	2800	1075
2	375	0	1350	0
		1	2750	1400
		2	3500	2150
		3	4100	2750
3	675	0	1800	0
		1	1800	0
		2	2750	950
		3	5000	3200
5	1125	0	1000	0
		1	1500	500
		2	1550	550
		3	1900	900

Table 5.4 Steel strap strains for retrofitted circular column (BR-C5).

Steel Strap #	Location From Bottom of Column (mm)	% Drift	Strain in Steel Strap (x 10^{-6})	Incremental Steel Strap Strain
1	75	0	100	0
		1	200	100
		2	800	700
		3	1700	1600
2	225	0	200	0
		1	400	200
		2	1000	800
		3	2200	2000
3	375	0	175	0
		1	250	75
		2	900	725
		3	1800	1625
4	525	0	200	0
		1	900	700
		2	1700	1500
		3	1900	1700
5	675	0	250	0
		1	750	500
		2	2000	1750
		3	3000	2750
6	825	0	50	0
		1	800	750
		2	2000	1950
		3	3000	2950
8	1050	0	320	0
		1	750	430
		2	-	-
		3	-	-

Table 5.5 Prestressing wire strains for retrofitted square column (BR-S2).

P/S Wire #	Location From Bottom of Column (mm)	% Drift	Strain in P/S Wire (x 10^{-6})	Incremental P/S Strain
2	225	0	1500	0
		1	1650	150
		2	1750	250
		3	1950	450
		4	2200	700
		5	2950	1450
		6	3800	2300
3	375	0	1500	0
		1	1750	250
		2	1950	450
		3	2200	700
		4	2500	1000
		5	3250	1750
		6	5000	3500
4	525	0	1500	0
		1	1750	250
		2	1800	300
		3	2000	500
		4	2250	750
		5	3000	1500
		6	4250	2750
6	825	0	1500	0
		1	1650	150
		2	1900	400
		3	2050	550
		4	2250	750
		5	2500	1000
		6	2700	1200

Table 5.6 Analysis of test results for retrofitted columns.

Column	Drift at Yield	Drift Level	Ductility	Ductility Factor	V_c	V_s	Inc. Hoop Strain (10^{-6})	V_{hoop}	$V_c+V_s+V_{hoop}$	$V_{experiment}$	Theory / Experiment
BR-C2	0.8	1.0	1.25	0.290	454,594	199,441	388	56,408	710,443	575,000	1.236
		2.0	2.50	0.243	380,135	199,441	688	100,022	679,598	632,500	1.074
		3.0	3.75	0.124	193,986	199,441	1,063	154,540	547,967	610,000	0.898
		4.0	5.00	0.085	133,243	199,441	1,463	212,693	545,377	572,500	0.953
		5.0	6.25	0.066	103,851	199,441	2,425	352,550	655,842	520,000	1.261
BR-C3	0.76	1.0	1.32	0.290	454,594	199,441	413	60,043	714,077	577,500	1.236
		2.0	2.63	0.230	360,540	199,441	700	101,767	661,748	620,000	1.067
		3.0	3.95	0.105	164,594	199,441	1,100	159,920	523,955	595,000	0.881
		4.0	5.26	0.081	127,055	199,441	1,983	288,291	614,787	560,000	1.098
		5.0	6.58	0.061	96,116	199,441	3,200	465,221	760,778	487,500	1.561
BR-C4	0.76	1.0	1.32	0.290	454,594	199,441	700	50,883	704,918	597,500	1.180
		2.0	2.63	0.230	360,540	199,441	1,550	112,671	672,651	570,000	1.180
		3.0	3.95	0.105	164,594	199,441	2,975	216,255	580,290	440,000	1.319
BR-C5	0.70	1.0	1.43	0.290	454,594	199,441	369	53,646	707,680	565,000	1.253
		2.0	2.86	0.209	326,949	199,441	1,194	173,585	699,976	600,000	1.167
		3.0	4.29	0.096	150,038	199,441	2,019	293,525	643,004	565,000	1.138
BR-S2	0.76	1.0	1.32	0.290	470,782	227,955	217	28,445	727,182	597,500	1.217
		2.0	2.63	0.230	373,379	227,955	333	43,650	644,984	645,000	1.000
		3.0	3.95	0.105	170,455	227,955	550	72,095	470,506	632,500	0.744
		4.0	5.26	0.081	131,580	227,955	817	107,094	466,629	610,000	0.765
		5.0	6.58	0.061	99,539	227,955	1,567	205,405	532,899	587,500	0.907
		6.0	7.89	0.042	67,499	227,955	2,850	373,583	669,036	430,000	1.556

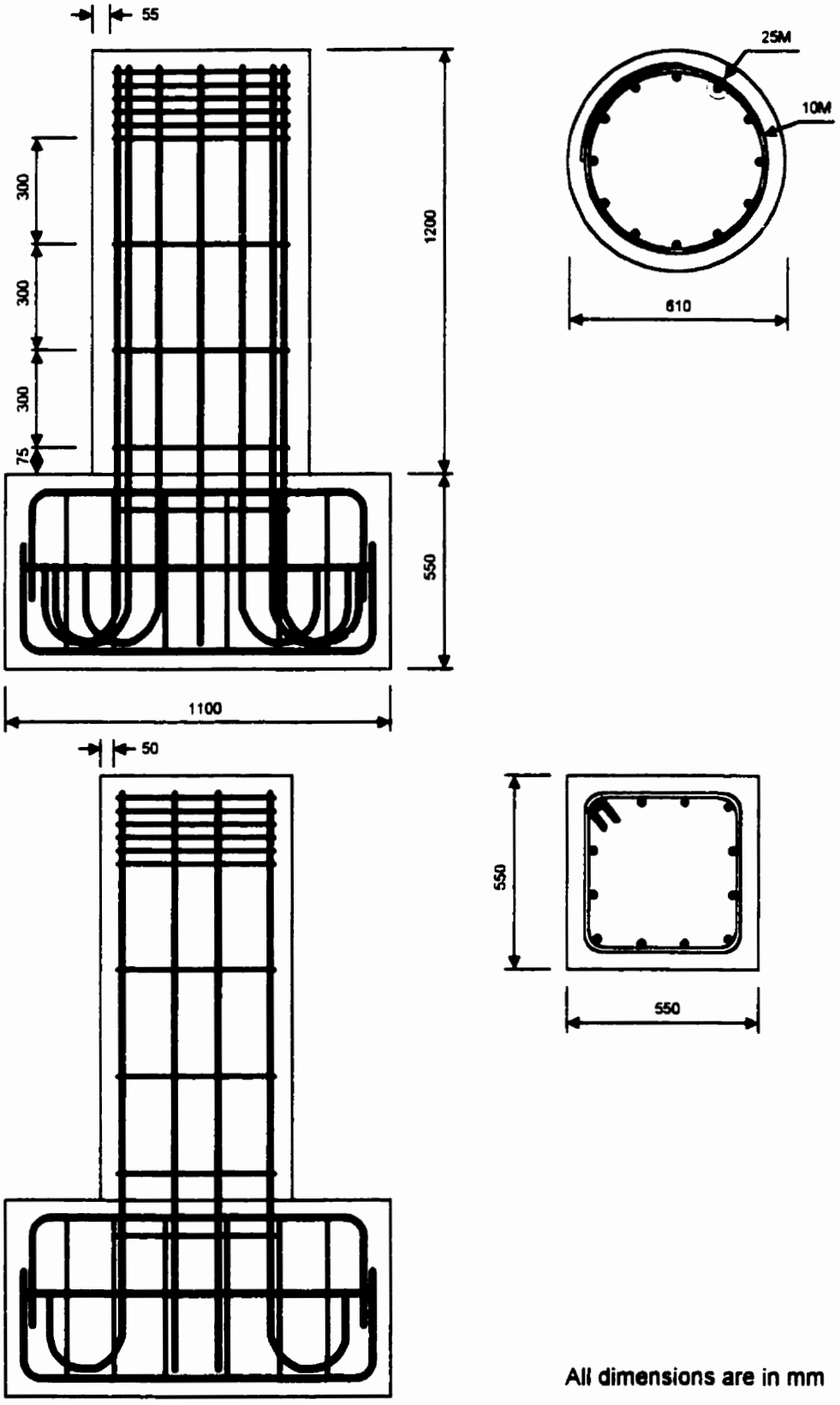

Figure 5.1 Column dimensions and reinforcement details.

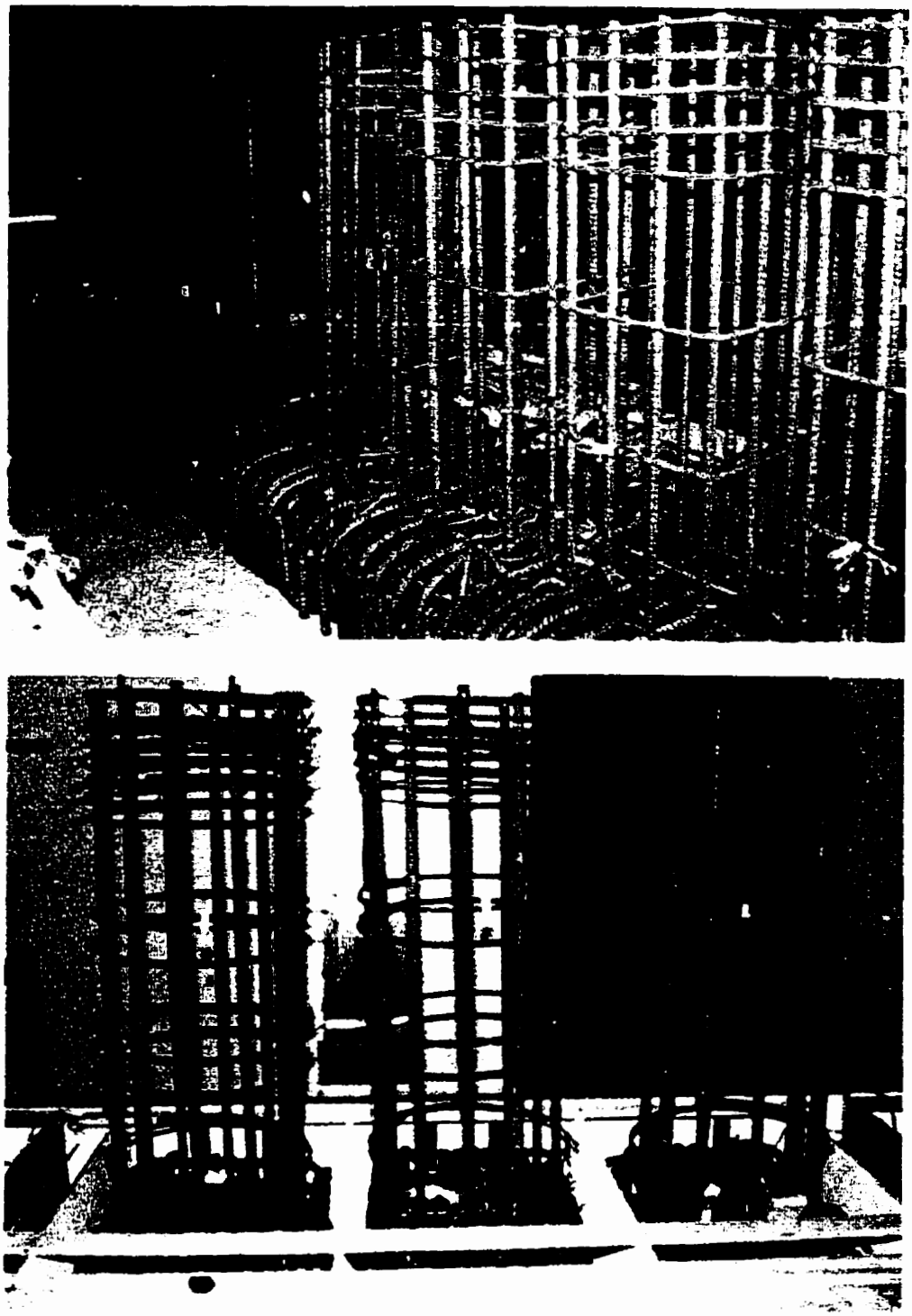

Figure 5.2 Reinforcement cages prior to casting of concrete.

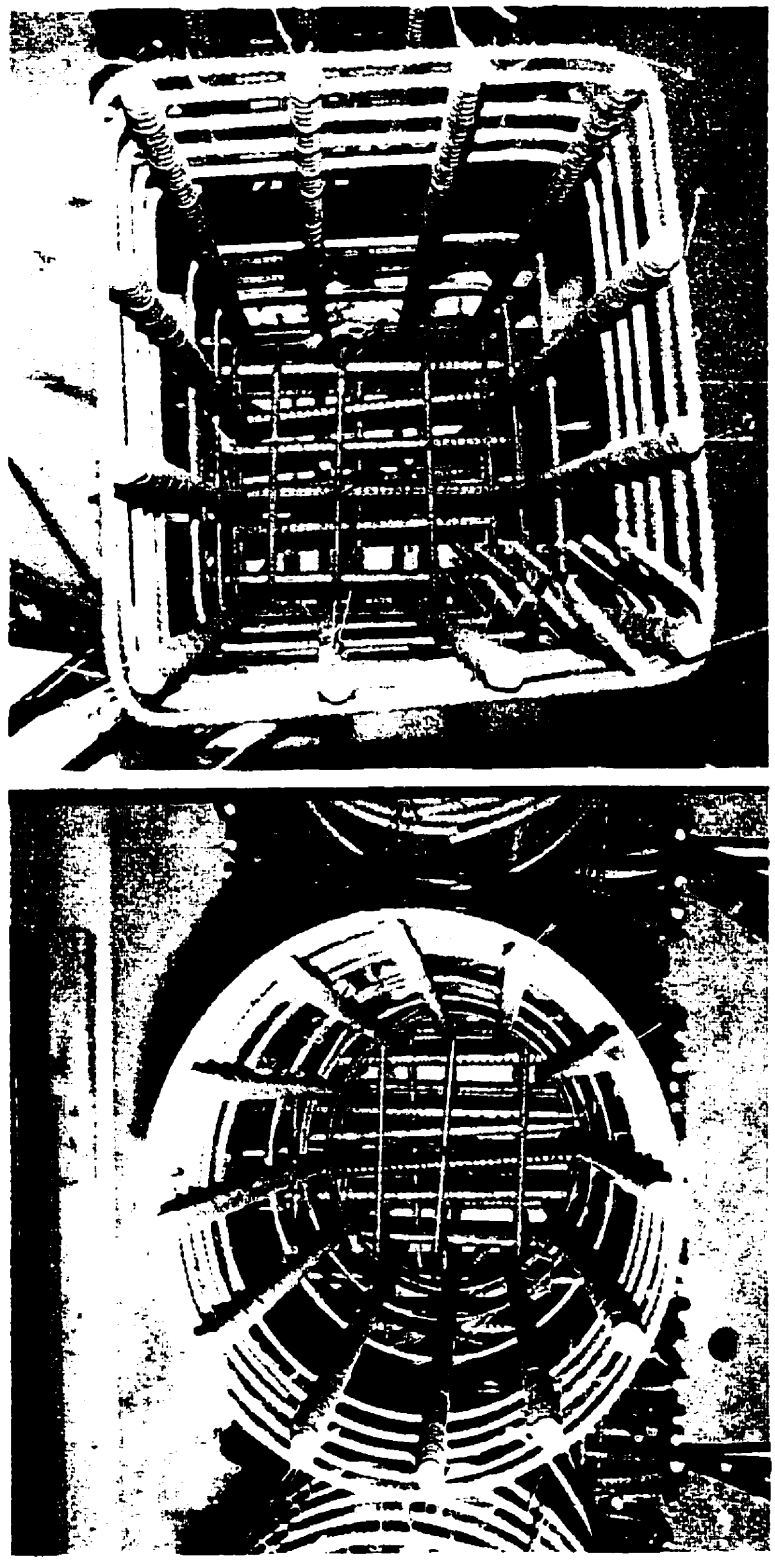

Figure 5.3 Typical cross-sectional views of column cages.

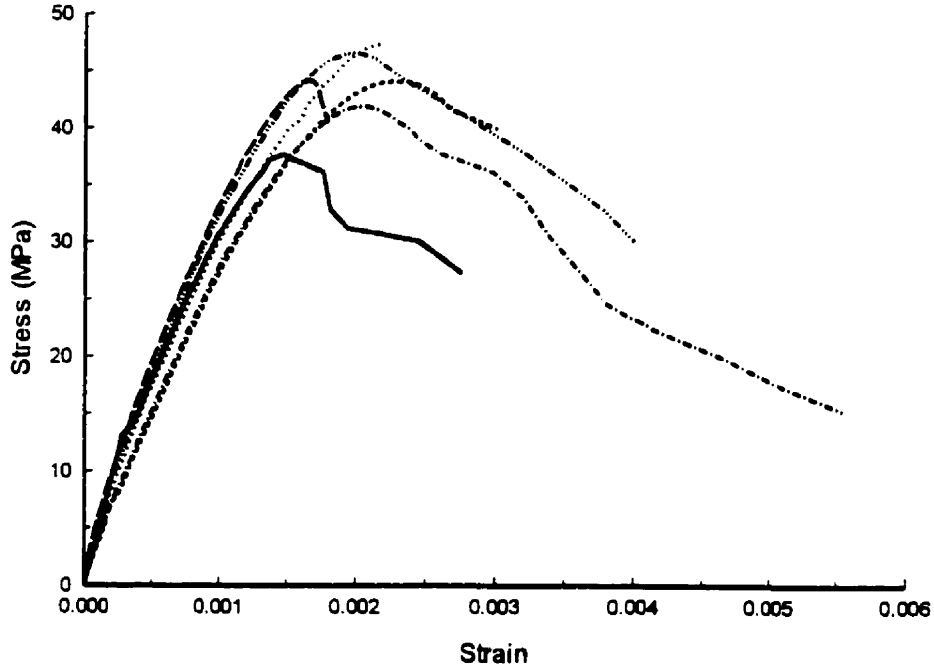

Figure 5.4 Stress-strain relationship of concrete cylinders.

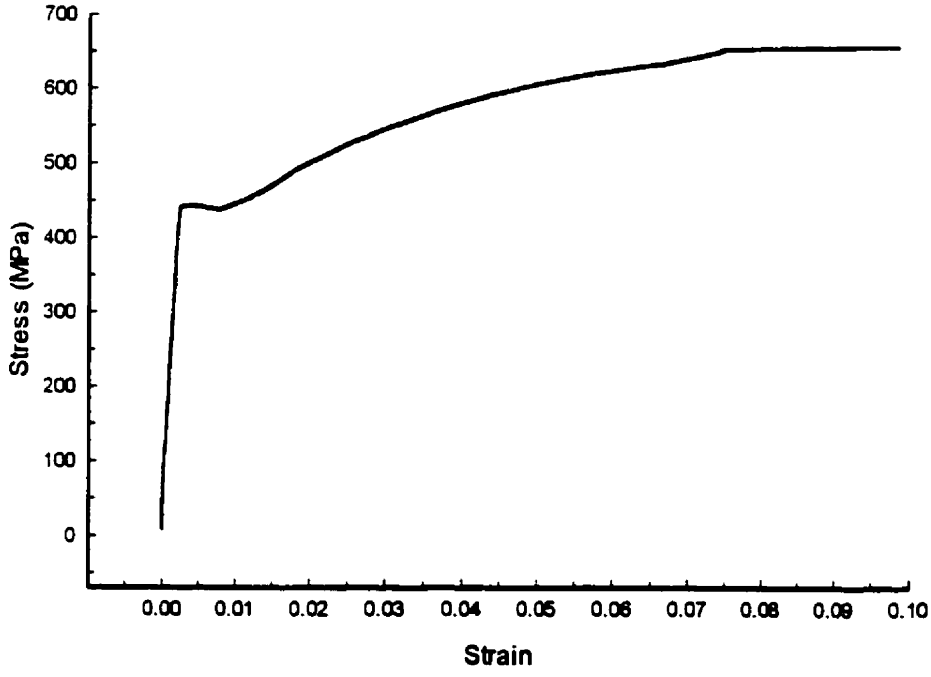

Figure 5.5 Stress-strain relationship of Grade 400, No. 25 deformed reinforcing steel.

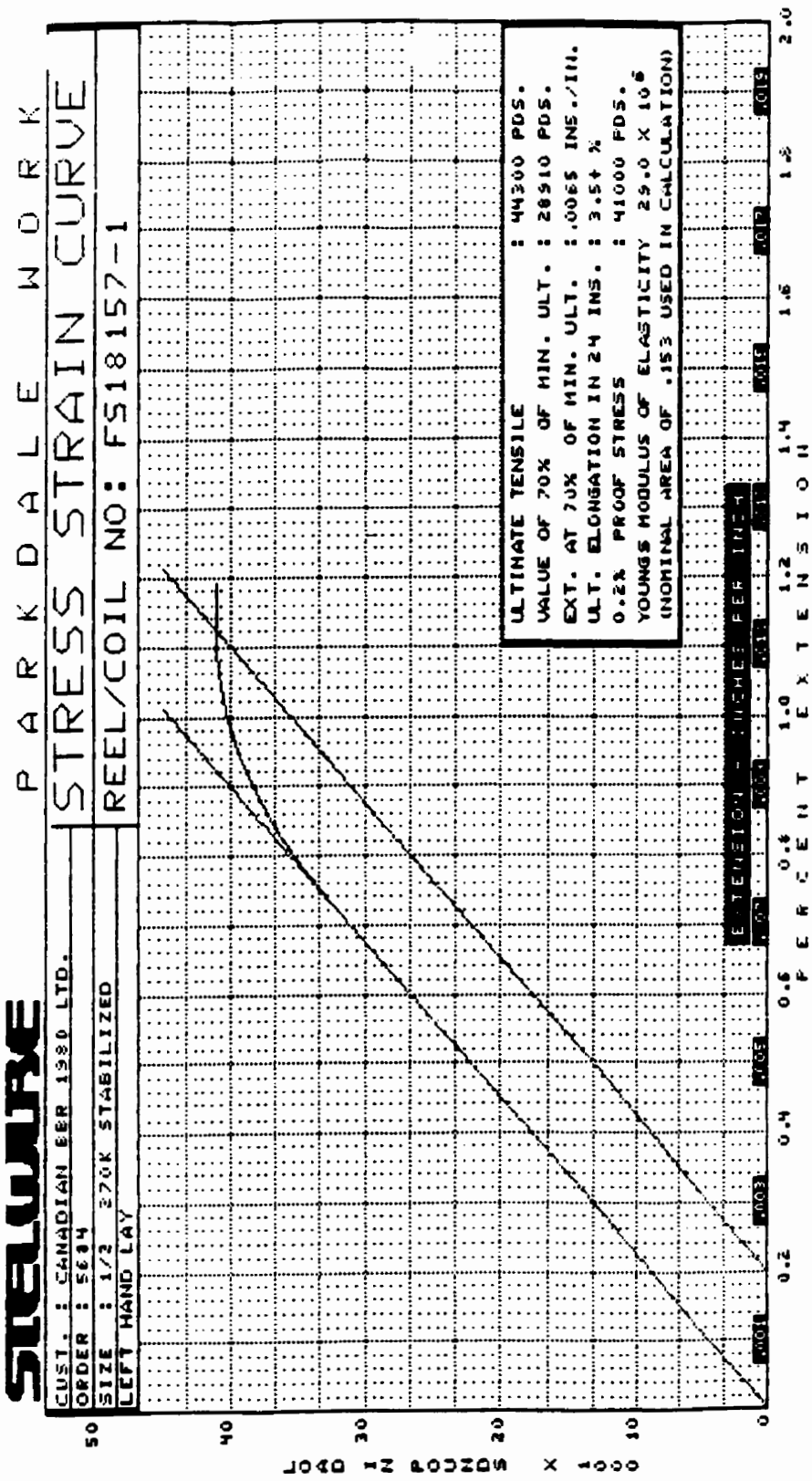

Figure 5.6 Stress-strain relationship of 7-wire prestressing strand.

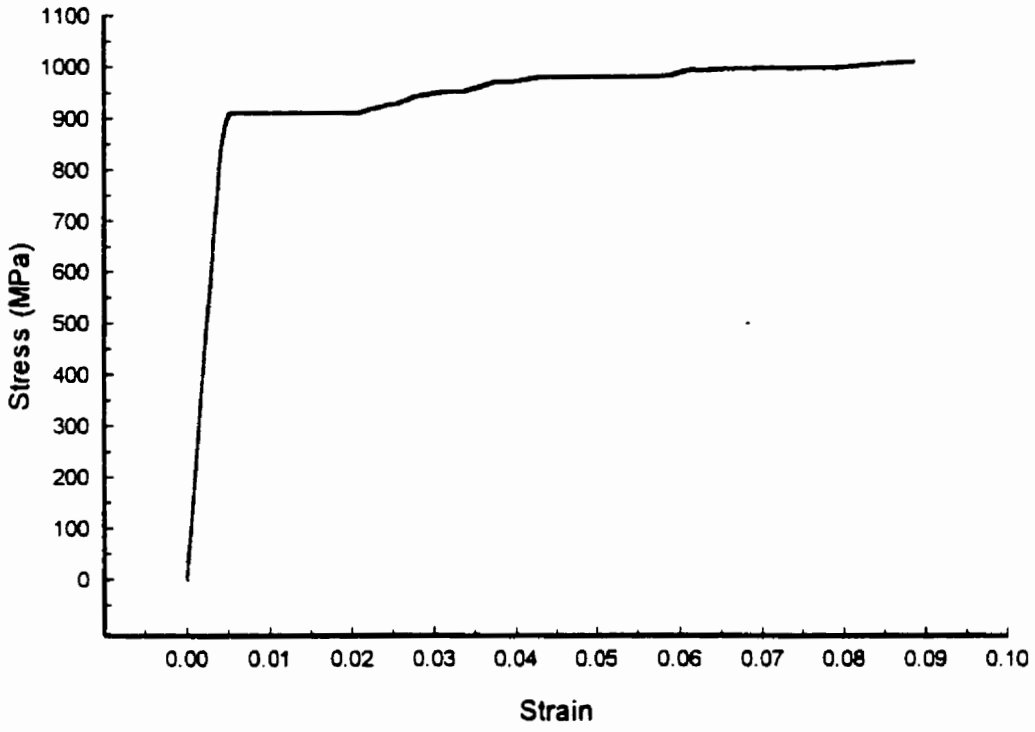

Figure 5.7 Stress-strain relationship of high strength steel strap.

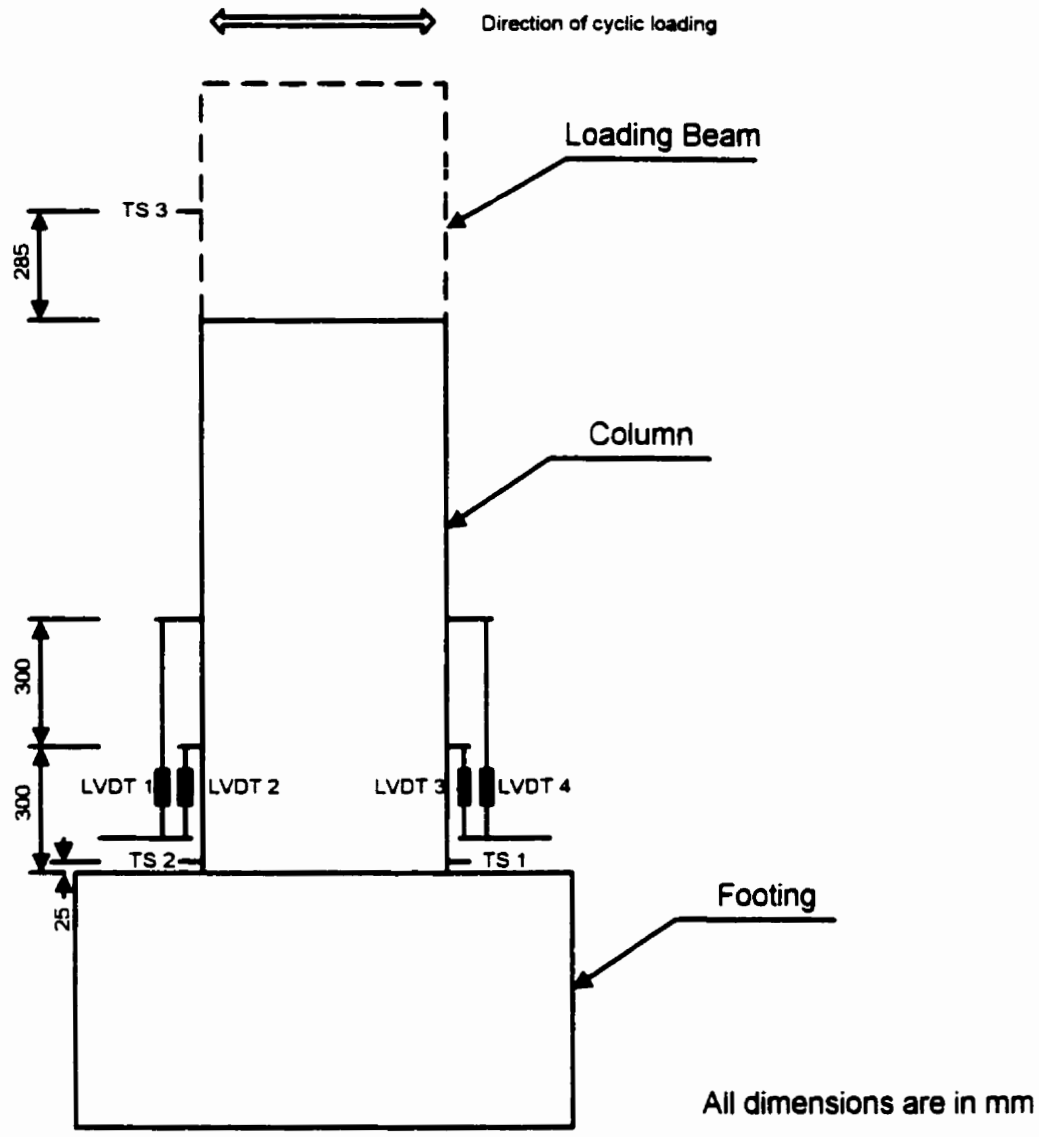

Figure 5.8 Column instrumentation.

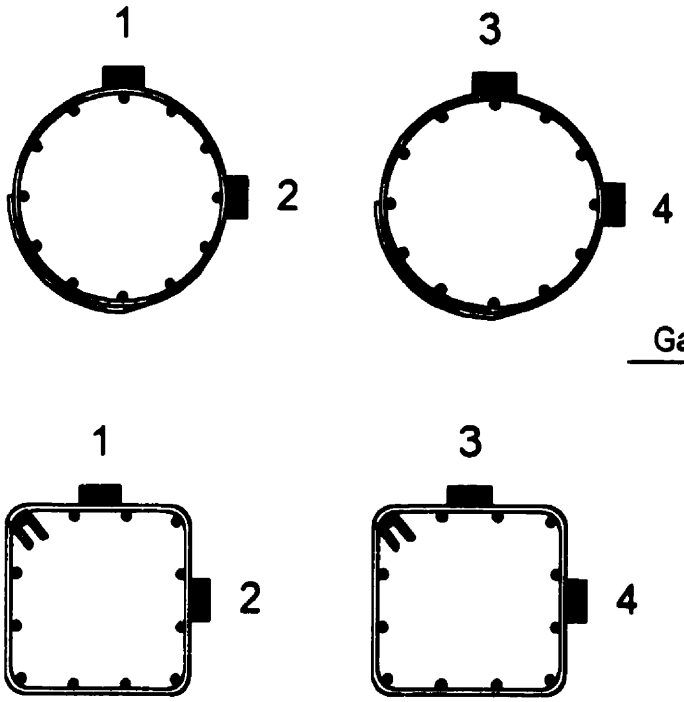

Gauge No.	Location
1, 2	Second stirrup layer
3, 4	First stirrup layer
5, 6	Back of footing
7, 8	Front of footing

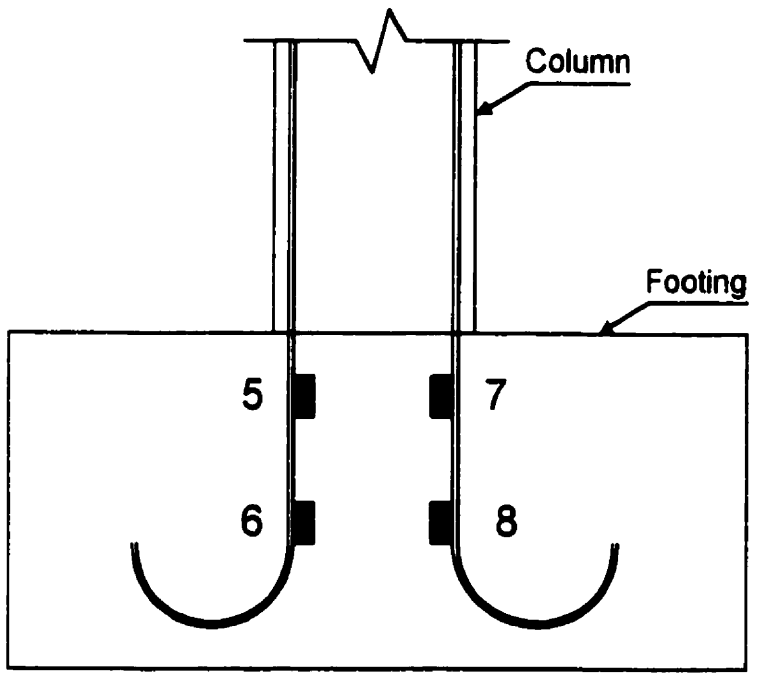

Figure 5.9 Strain gauge location on reinforcing steel.

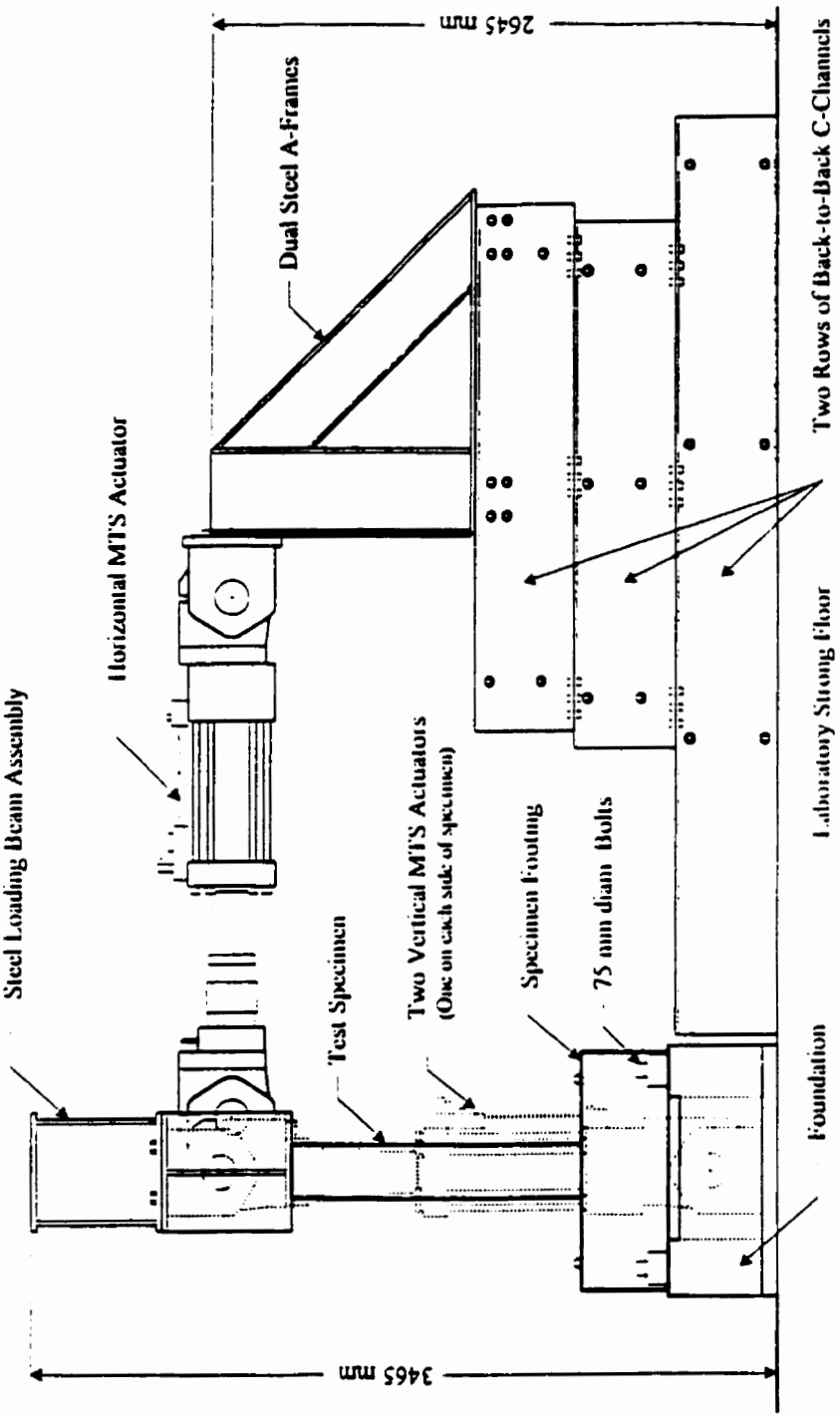

Figure 5.10 Schematic drawings of the test set-up.

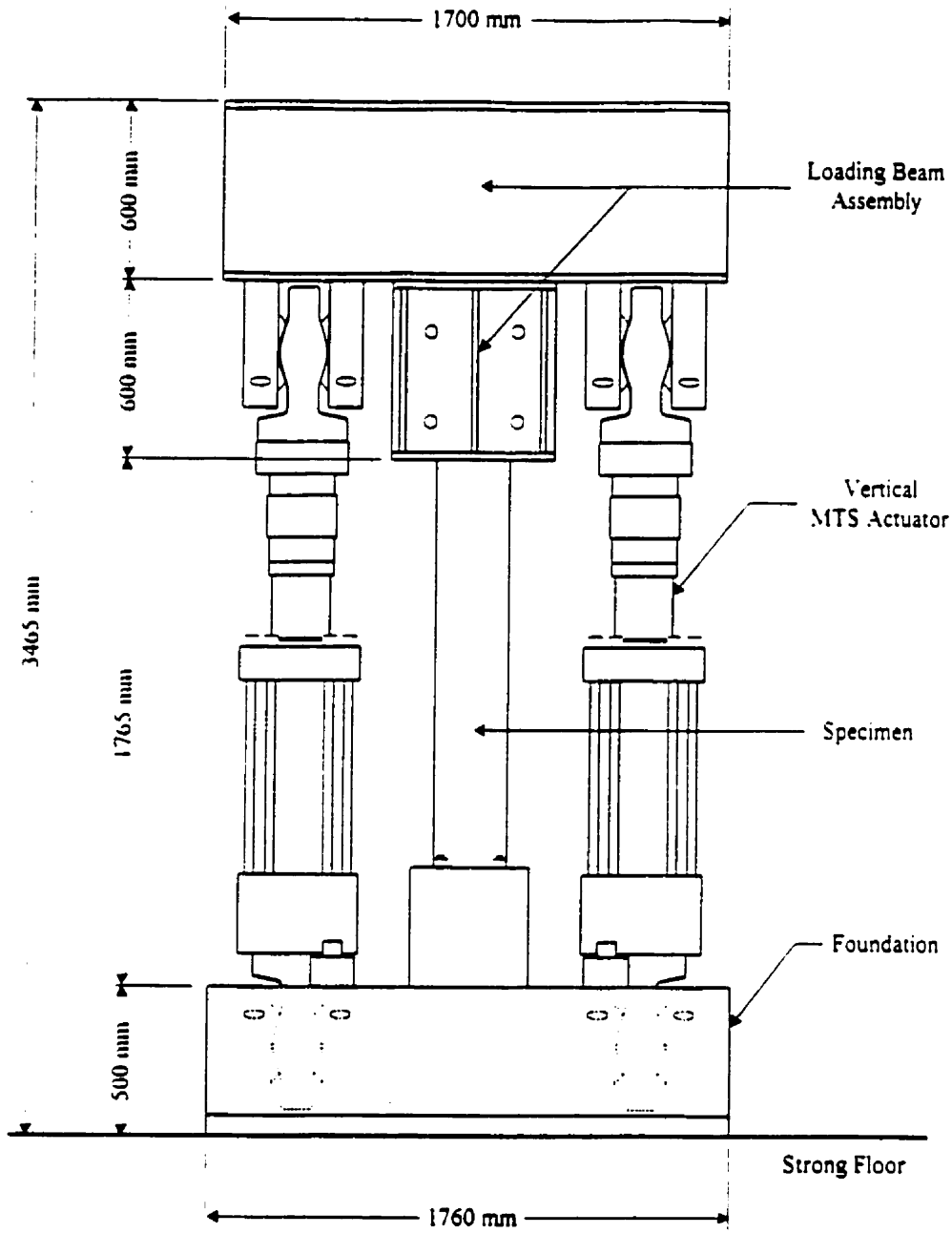

Front Elevation of the Test Setup

Figure 5.10 (Continued).

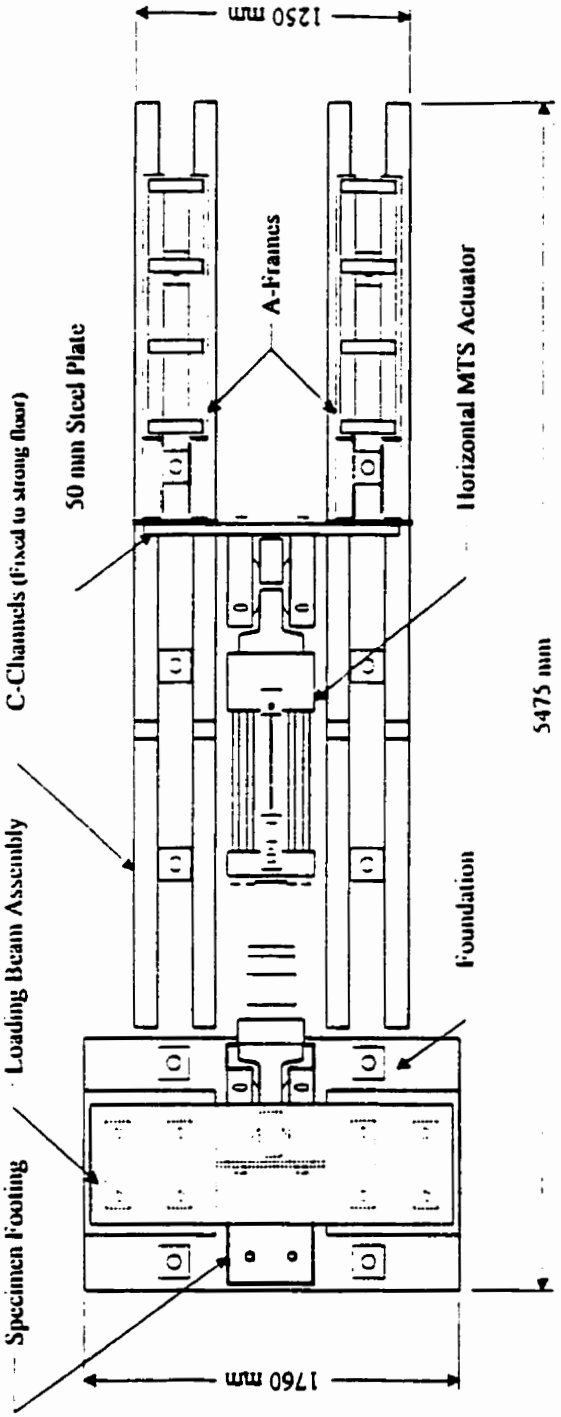

Plan View of Test Setup

Figure 5.10 (Continued).

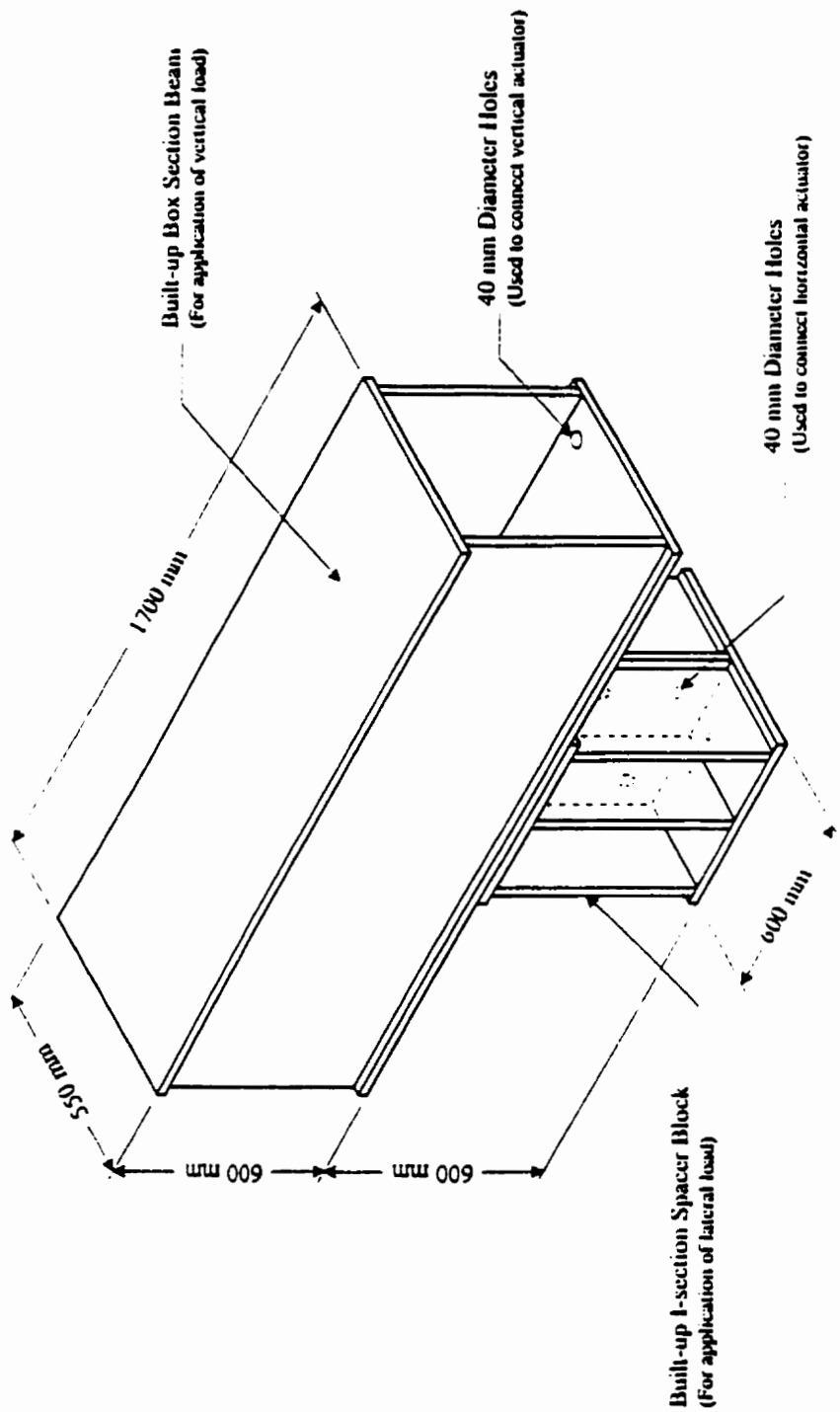

Details of Loading Beam Assembly

Figure 5.10 (Continued).

Figure 5.10 (Continued).

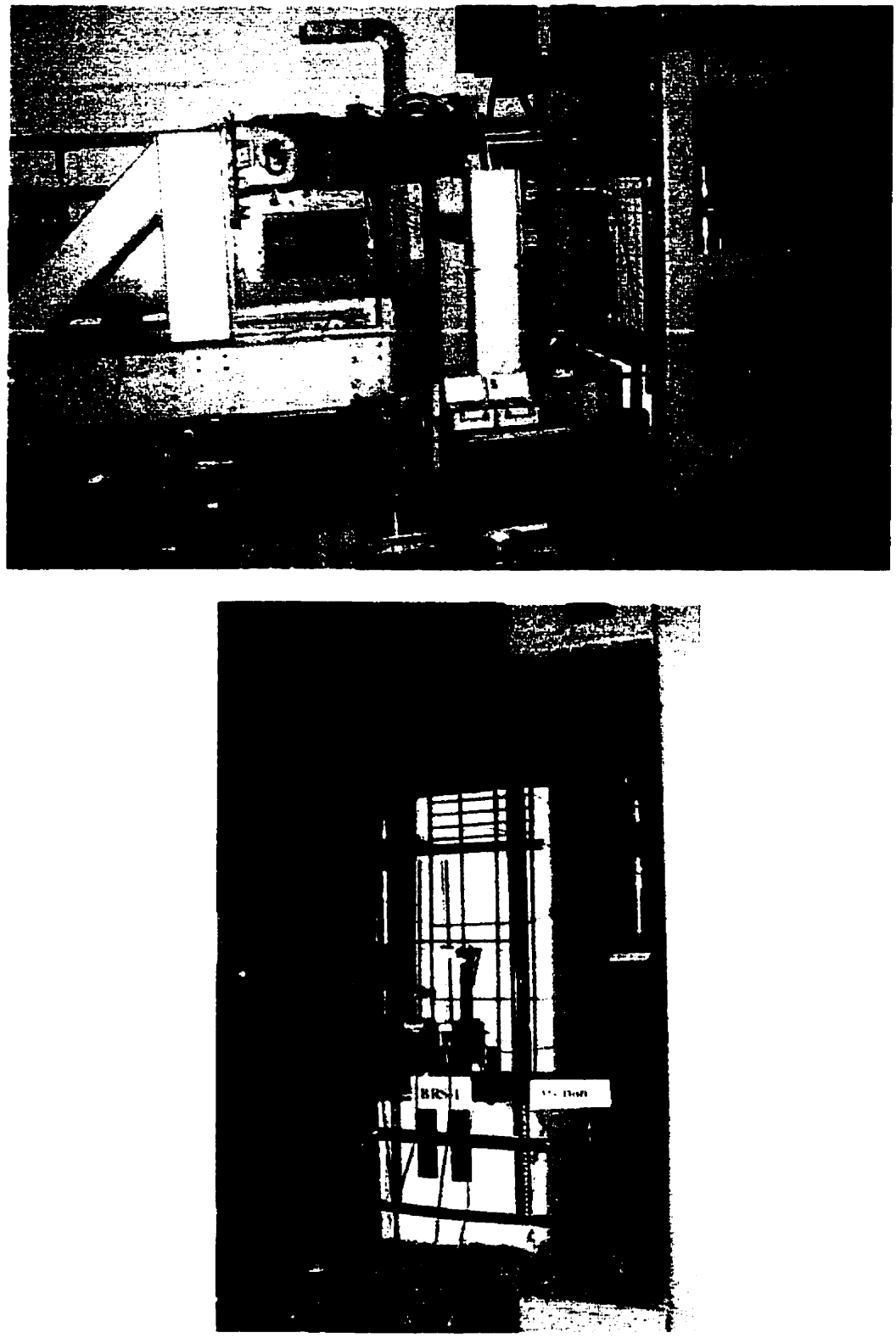

Figure 5.11 Side and front views of the test set-up.

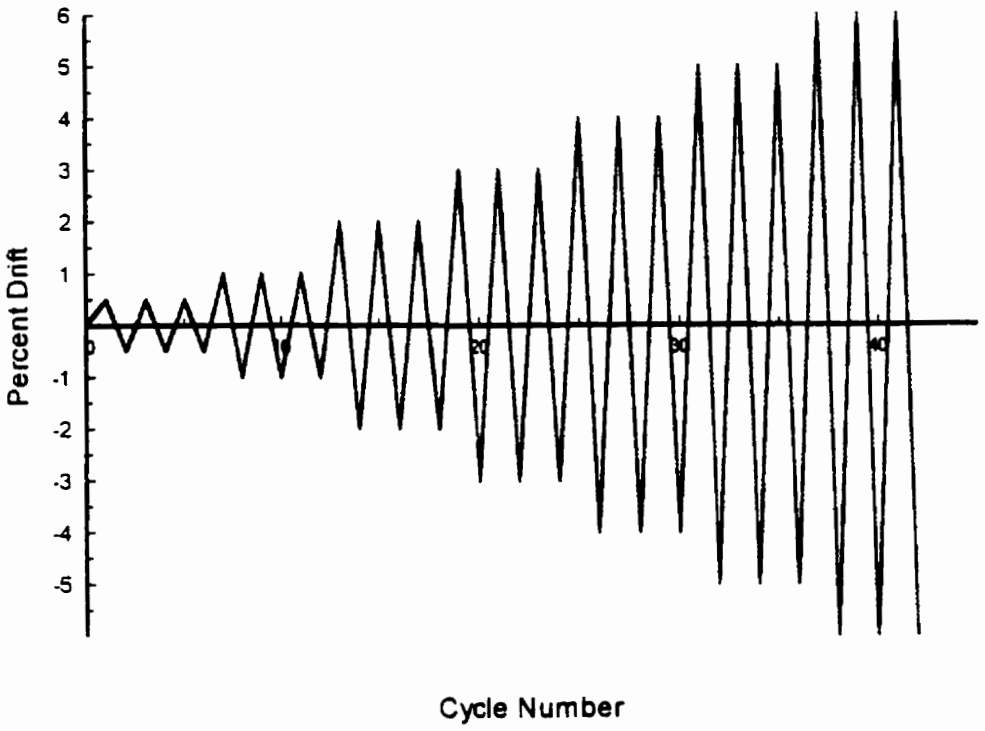

Figure 5.12 Loading program.

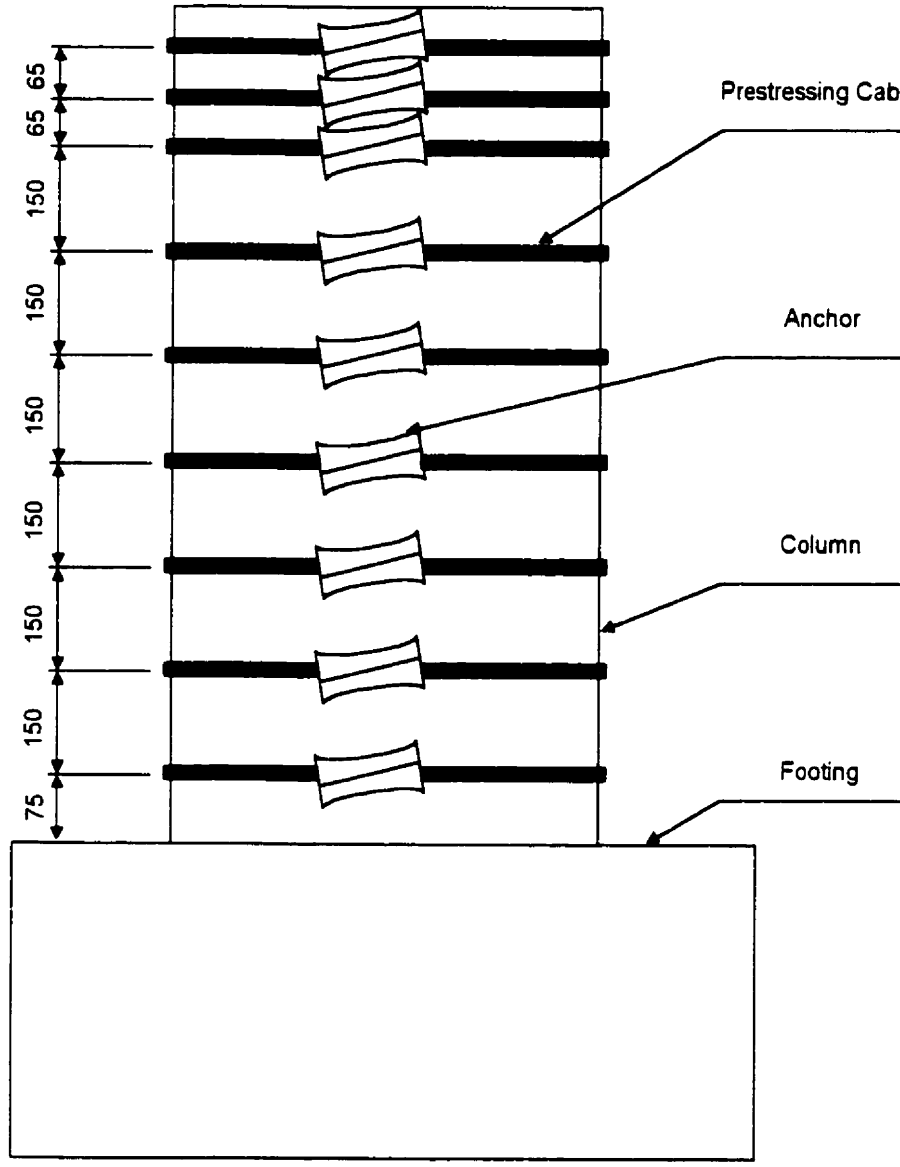

Figure 5.13 Retrofitting of circular column.

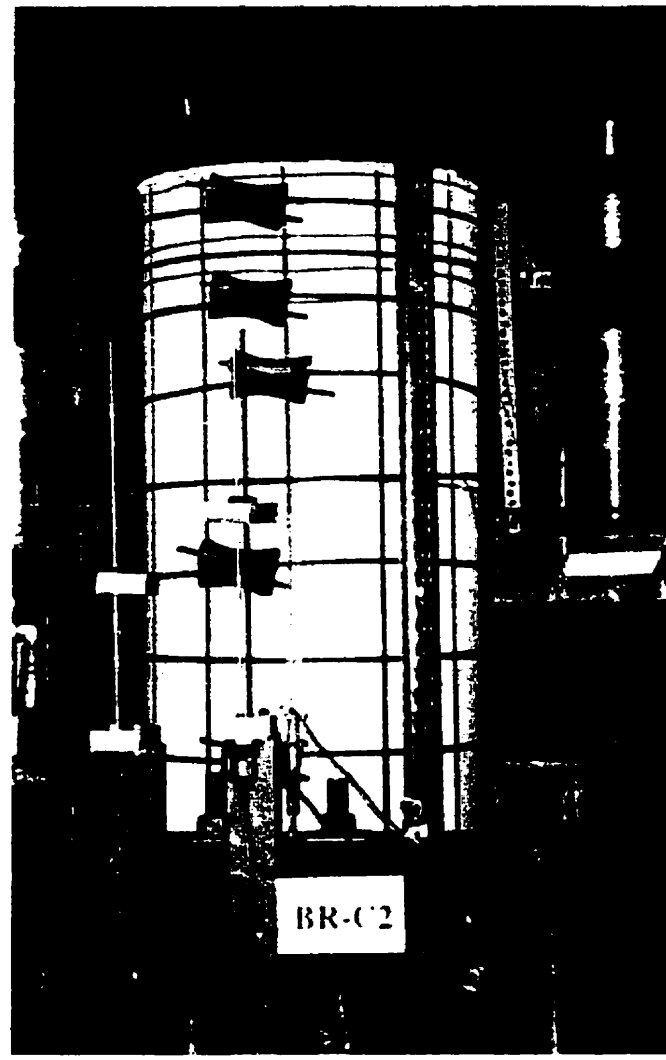

Figure 5.14 A typical view of retrofitted of circular column.

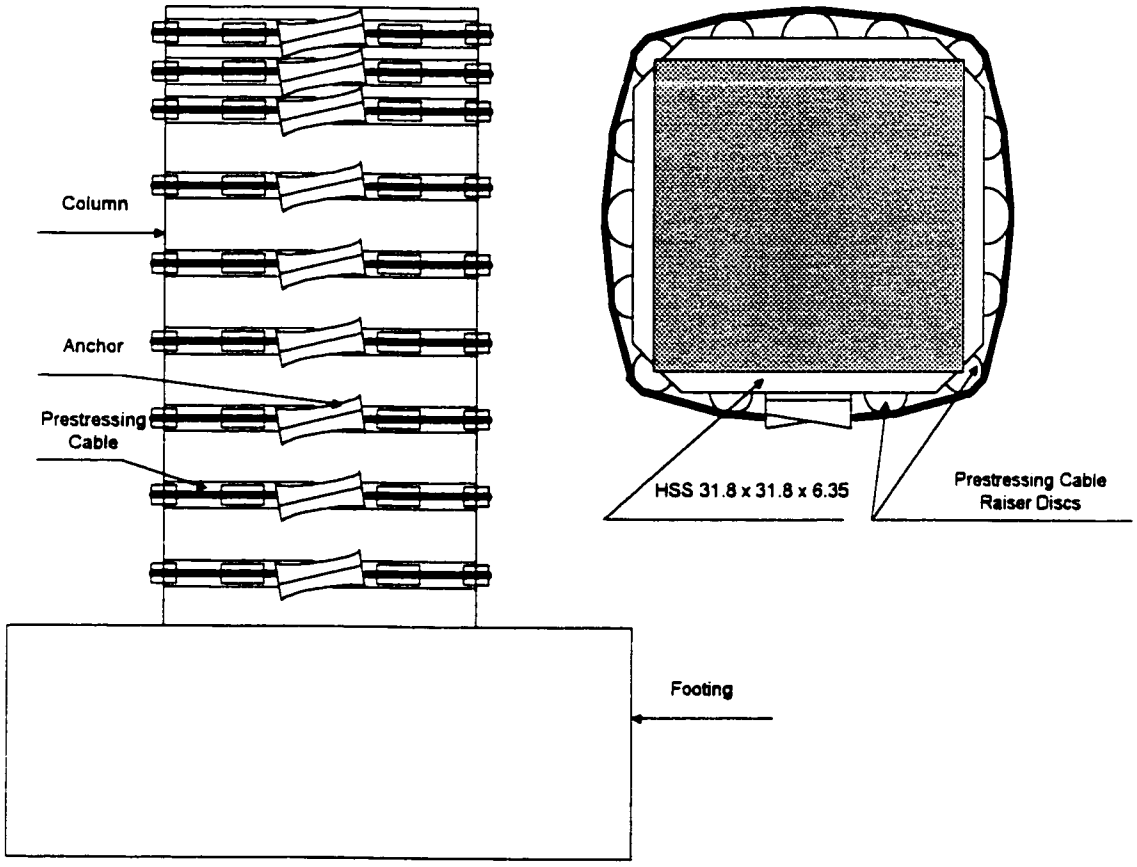

Figure 5.15 Retrofitting of square column.

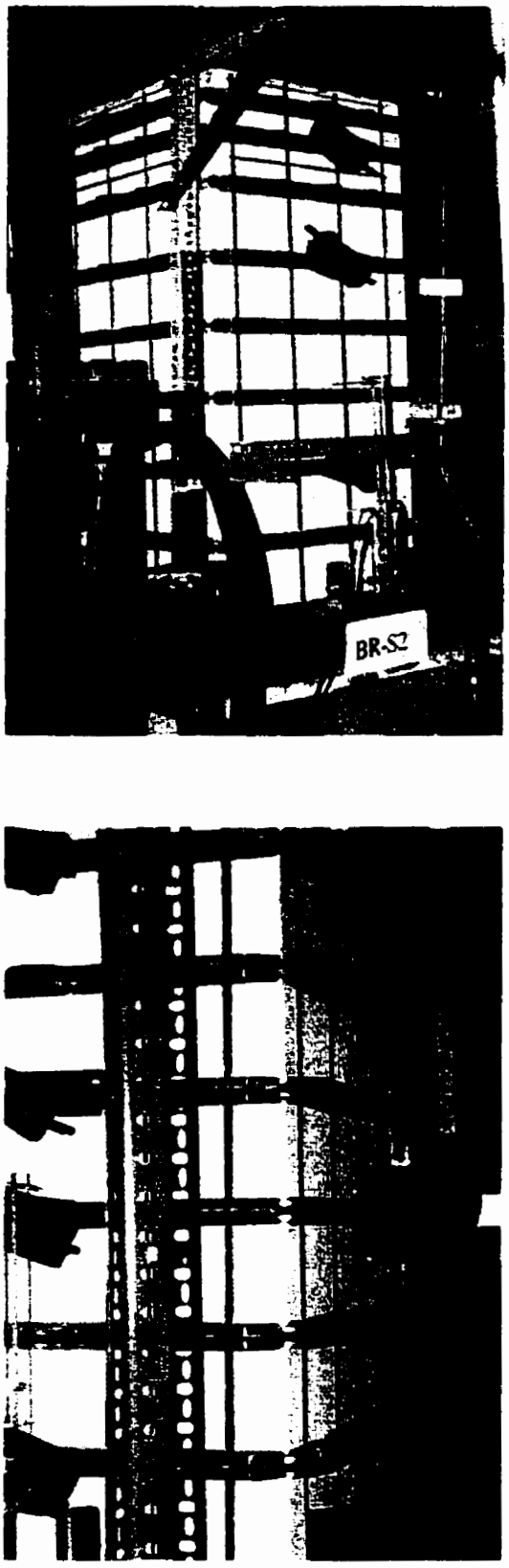

Figure 5.16 A typical view of retrofitted of square column.

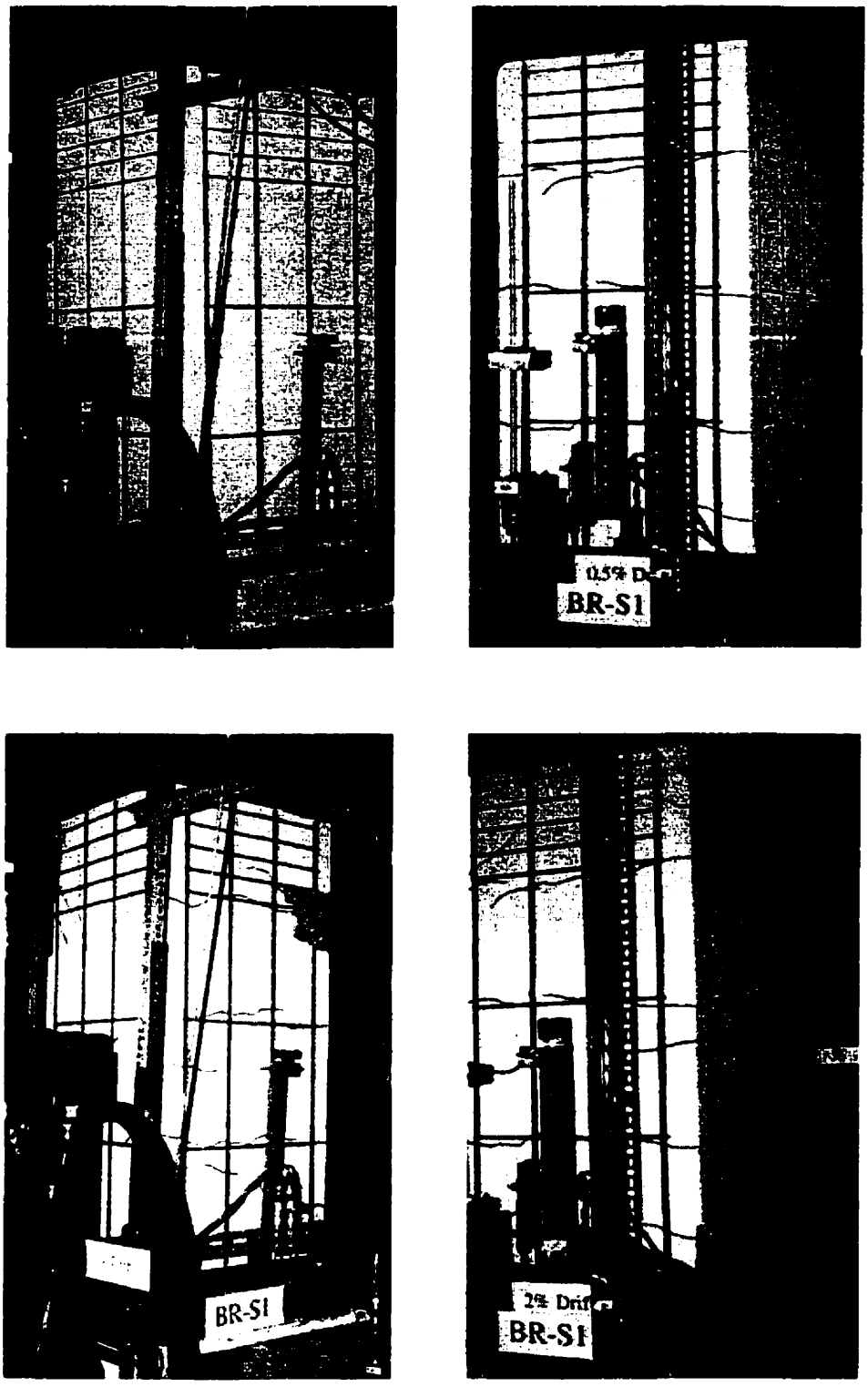

Figure 5.17 Various drift levels of non-retrofitted square column (BR-S1) specimen.

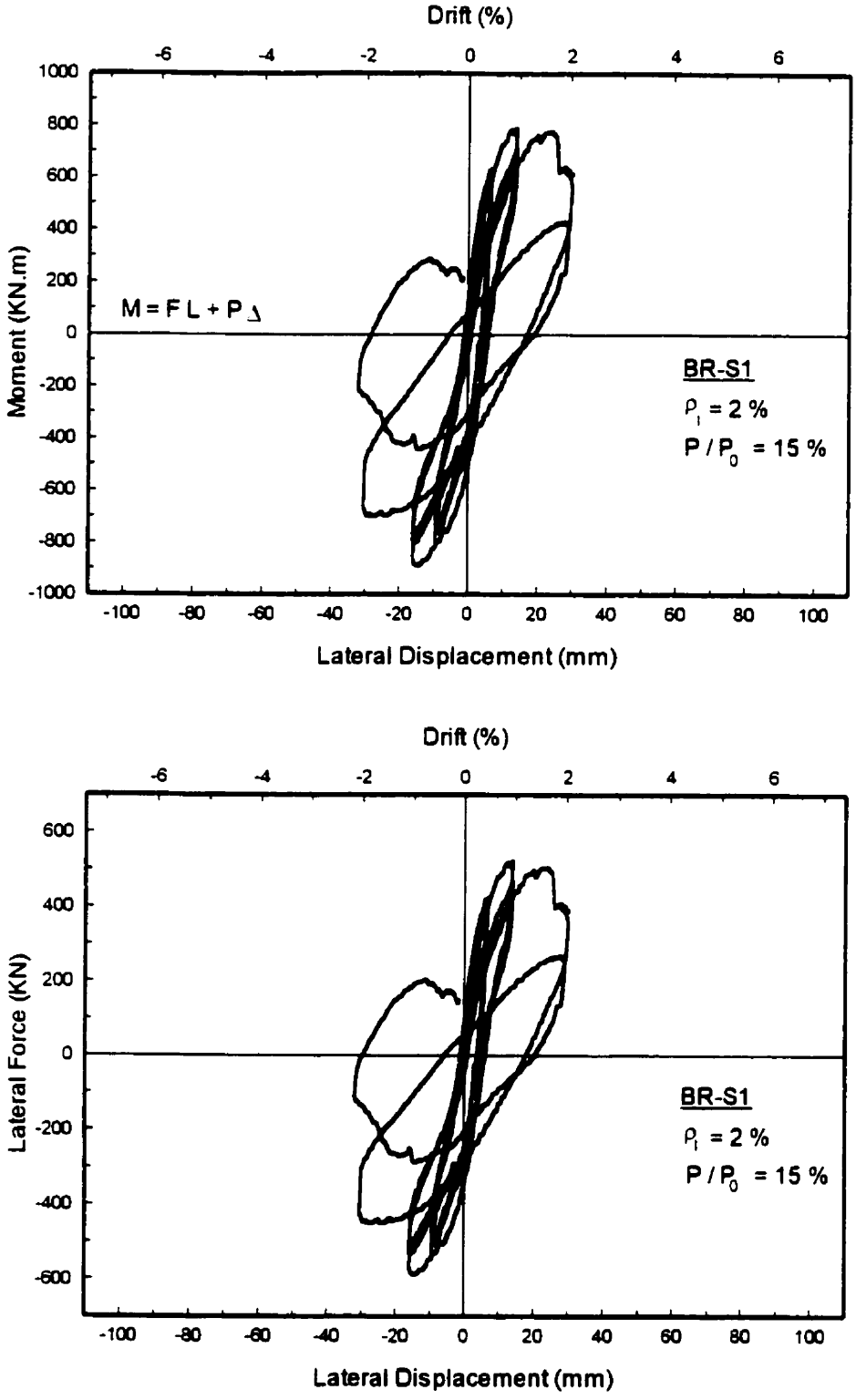

Figure 5.18 Moment-Displacement and Force-Displacement relationships for column BR-S1.

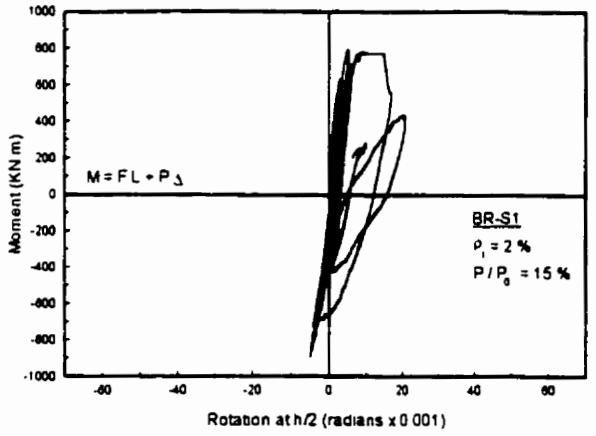

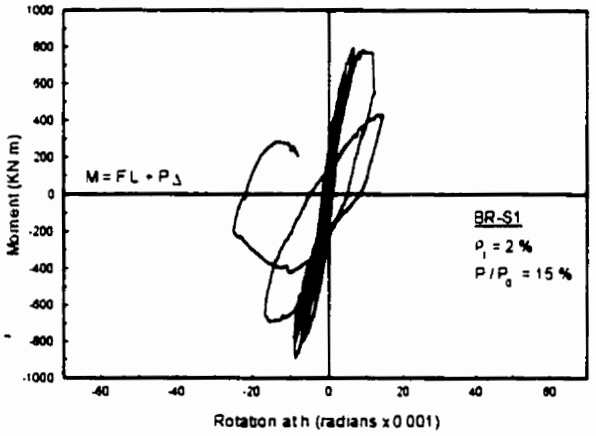

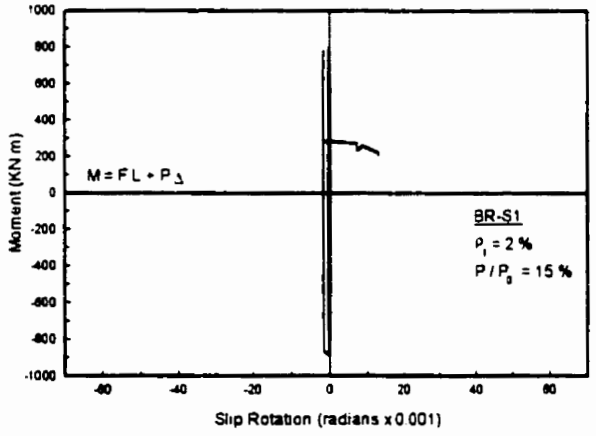

Figure 5.19 Moment-Rotation relationships for column BR-S1.

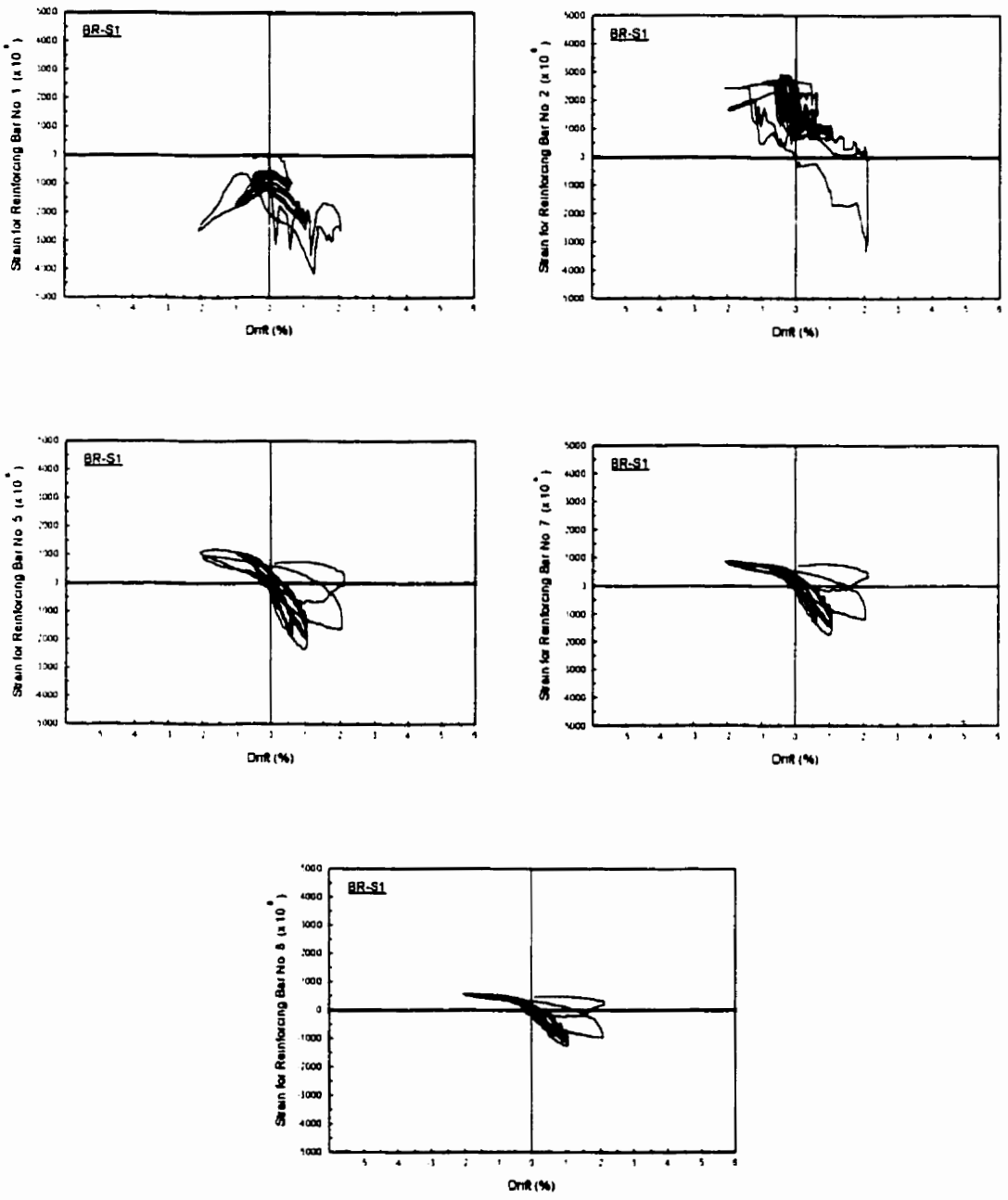

Figure 5.20 Reinforcing steel strains for column BR-S1.

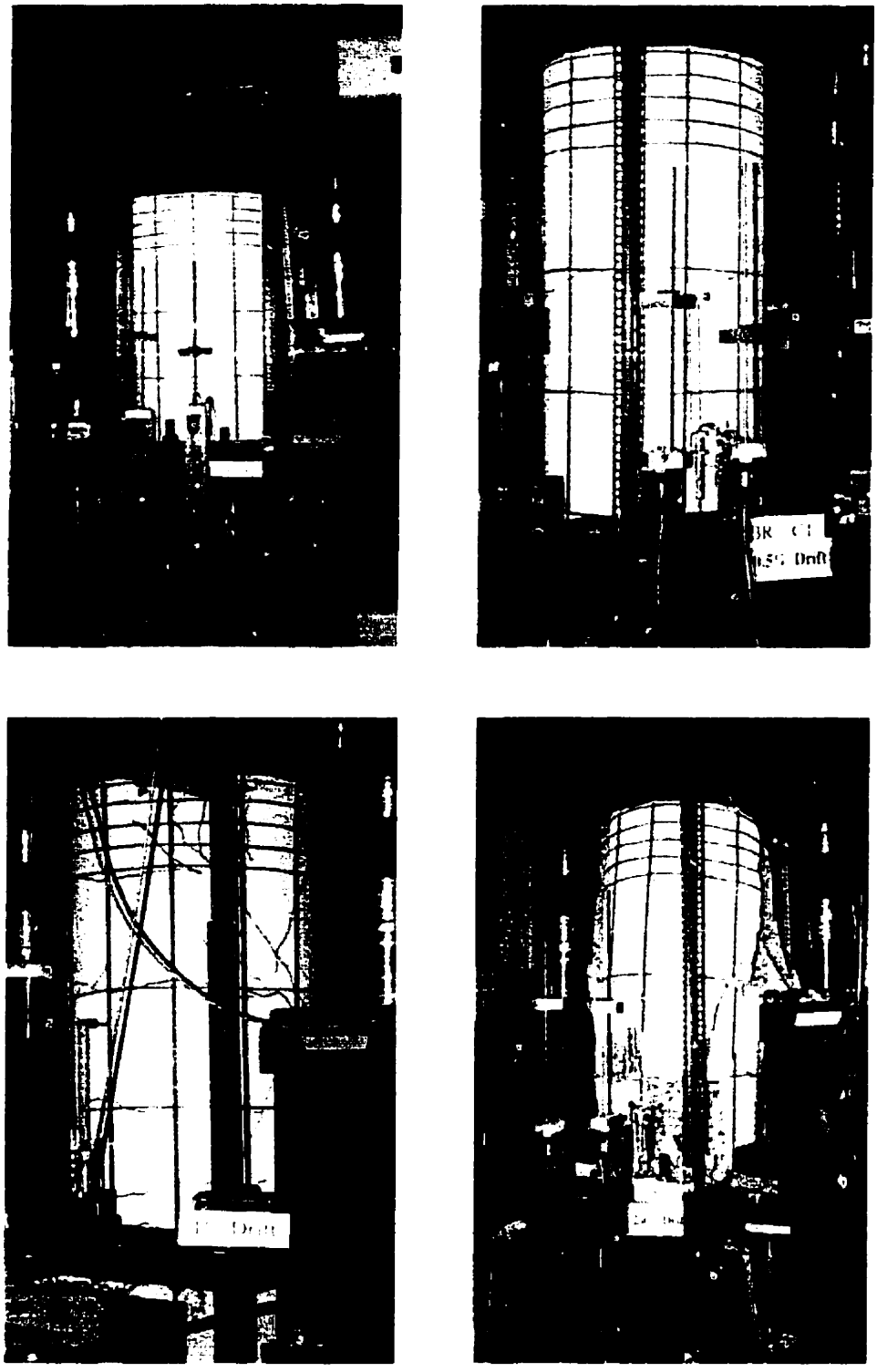

Figure 5.21 Various drift levels of non-retrofitted circular column (BR-C1) specimen.

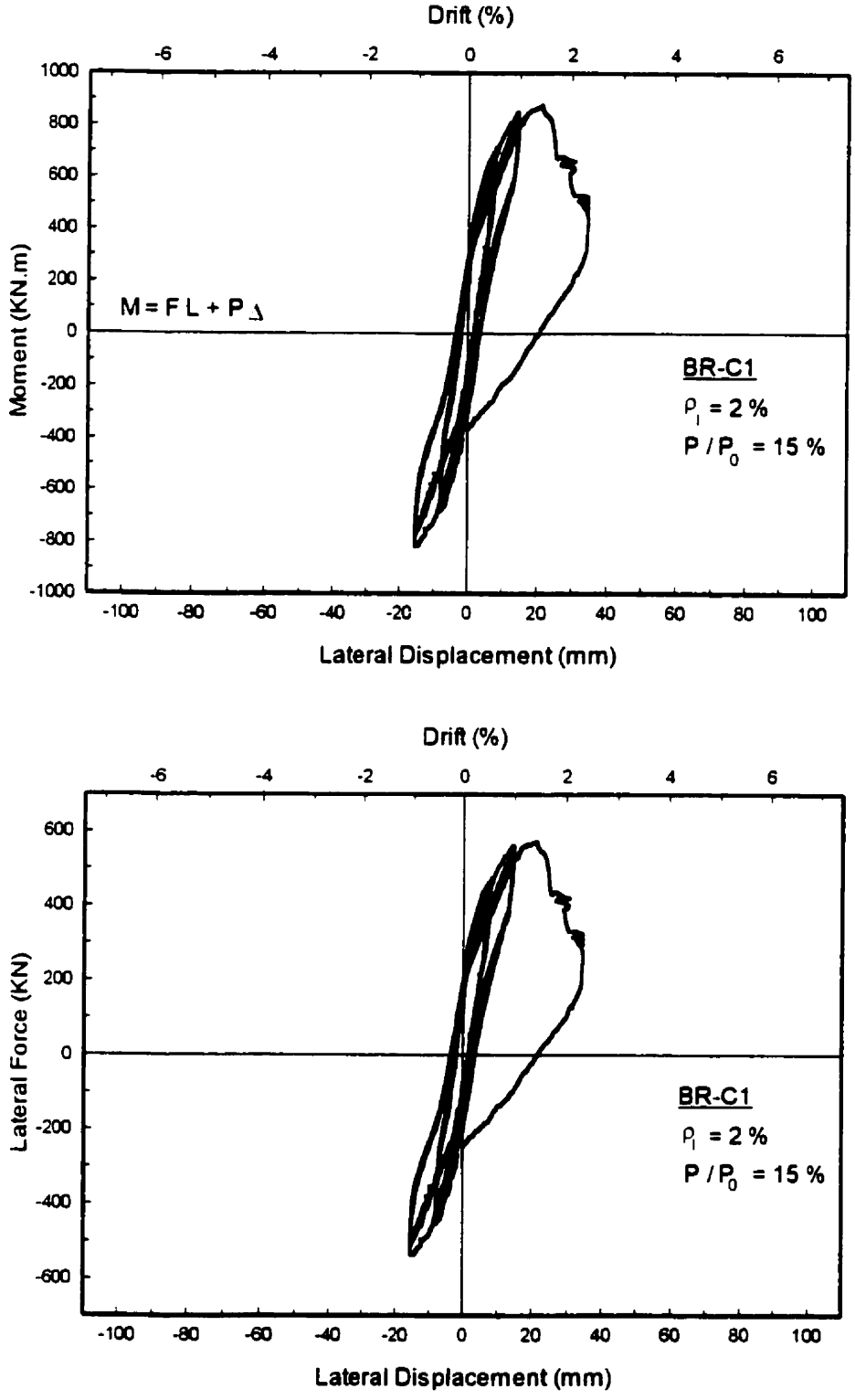

Figure 5.22 Moment-Displacement and Force-Displacement relationships for column BR-C1.

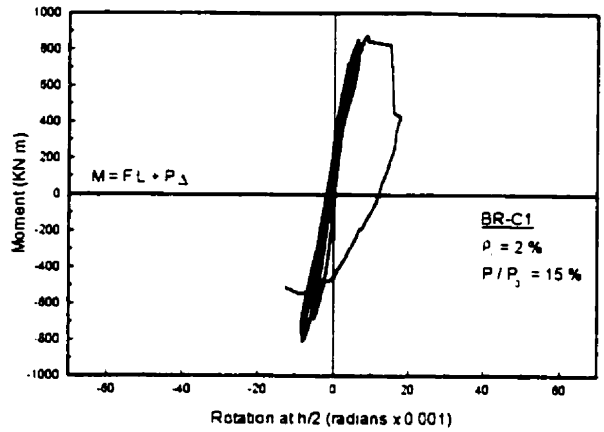

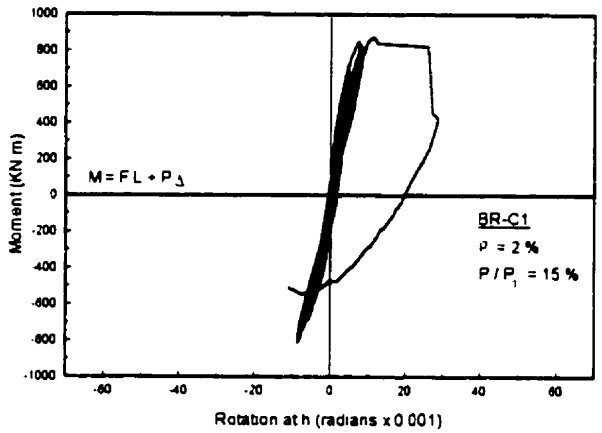

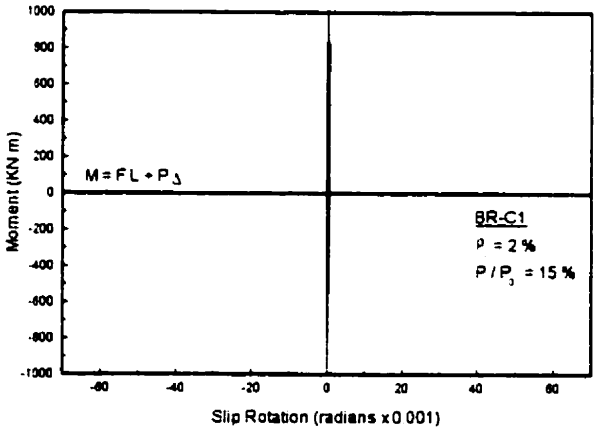

Figure 5.23 Moment-Rotation relationships for column BR-C1.

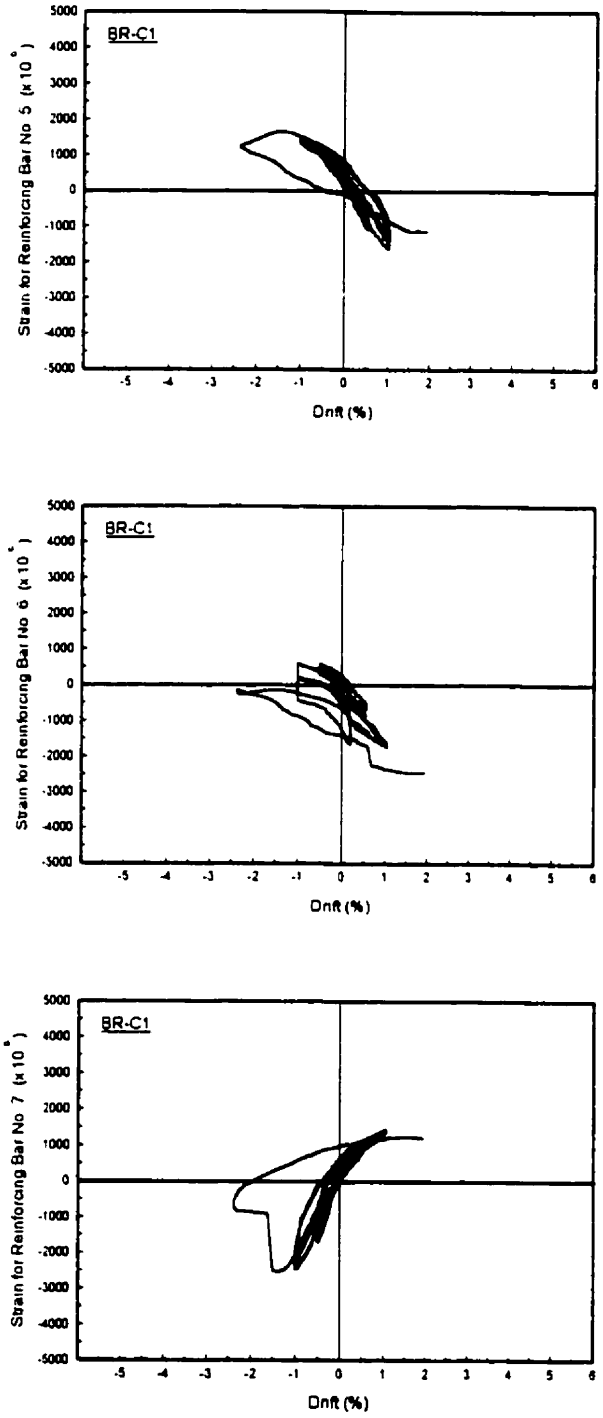

Figure 5.24 Reinforcing steel strains for column BR-C1.

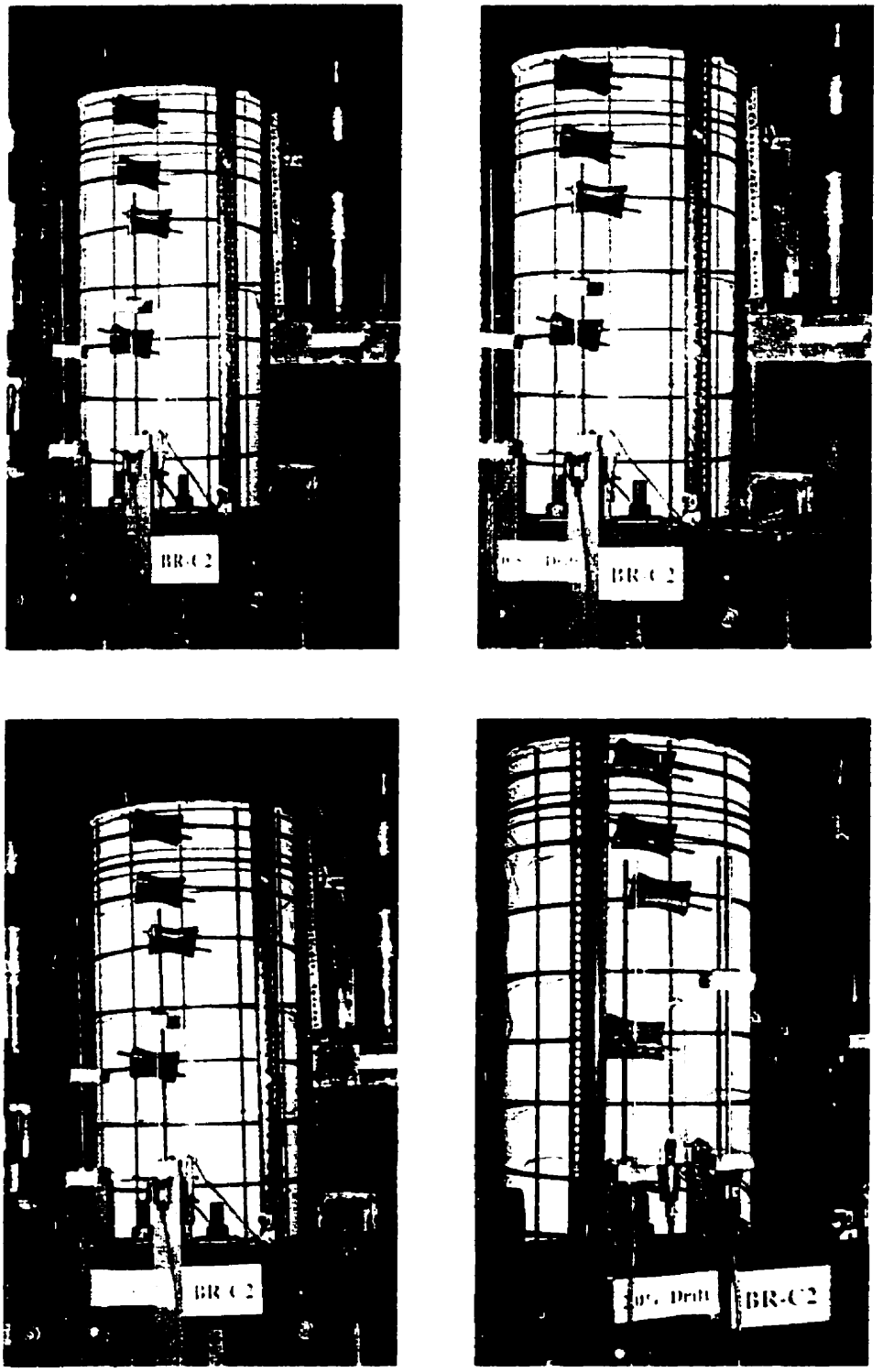

Figure 5.25 Various drift levels of retrofitted circular column (BR-C2) specimen.

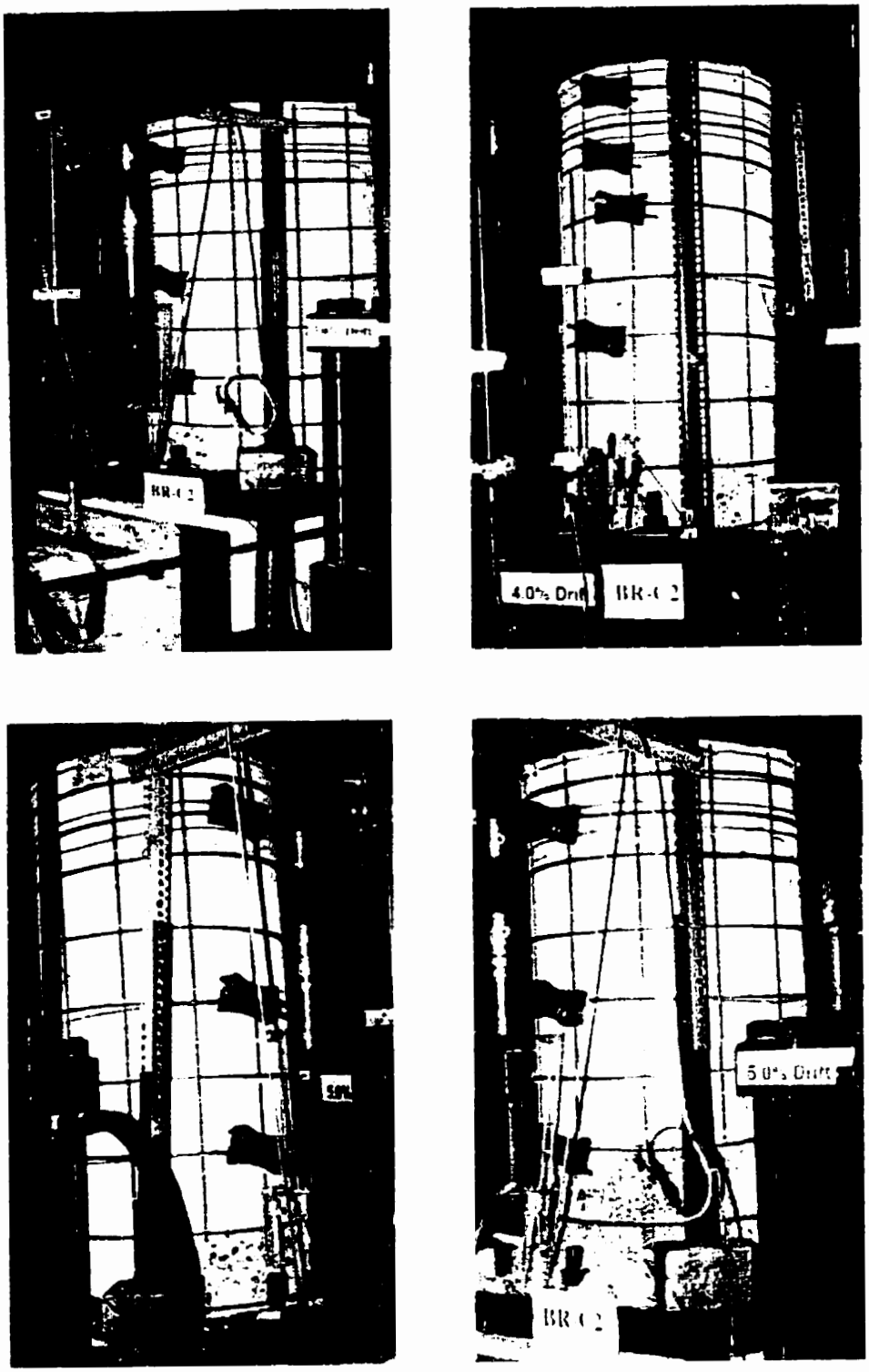

Figure 5.25 (Continued).

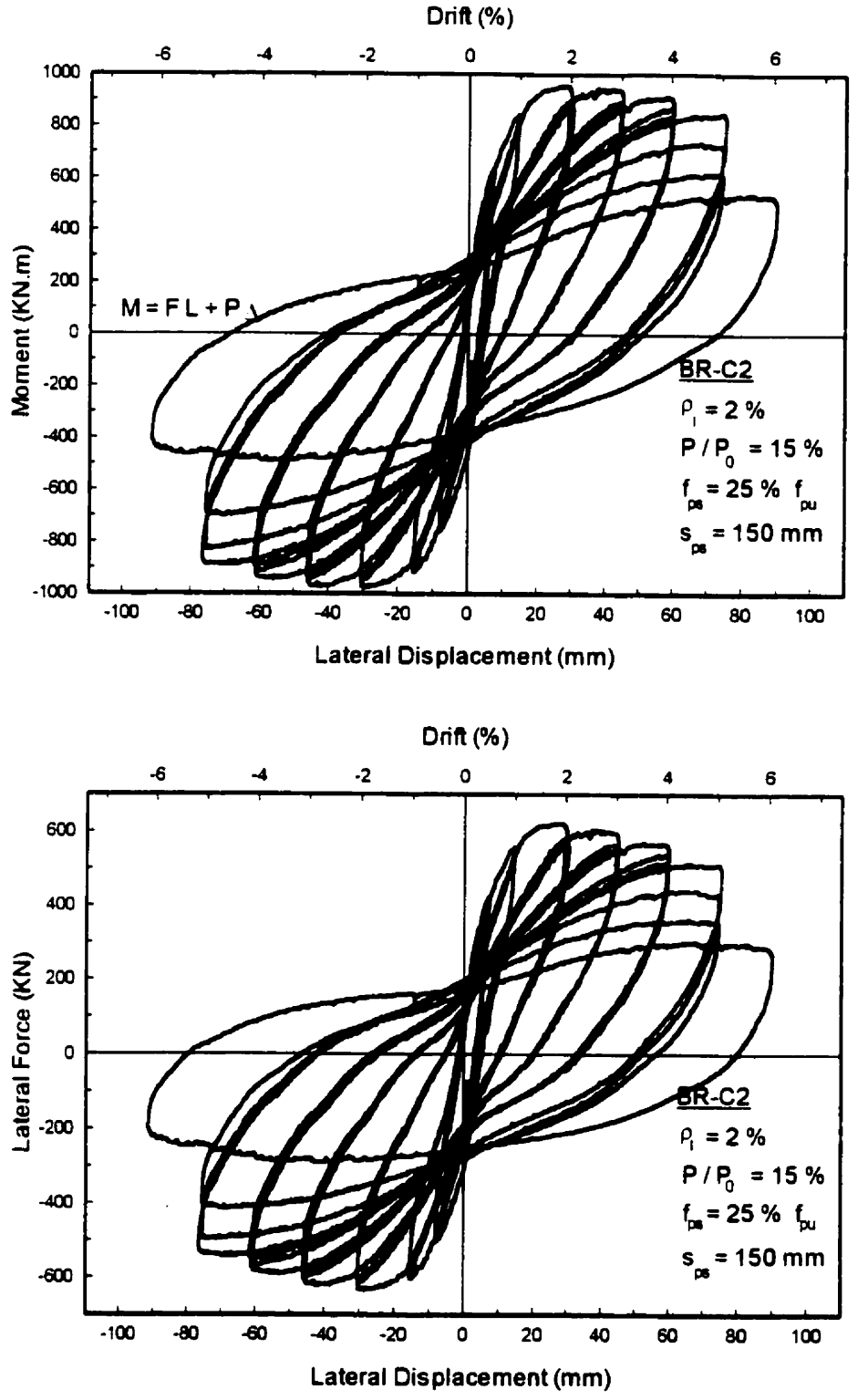

Figure 5.26 Moment-Displacement and Force-Displacement relationships for column BR-C2.

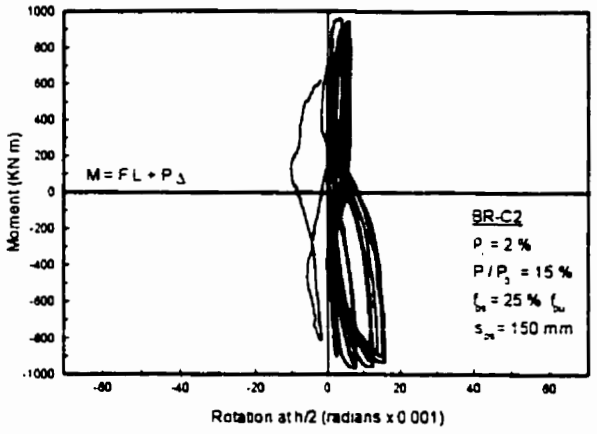

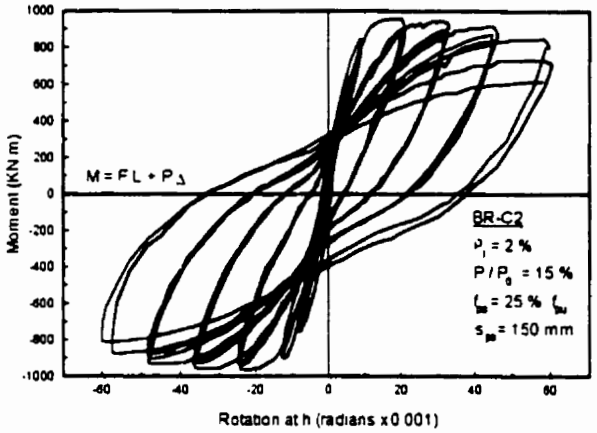

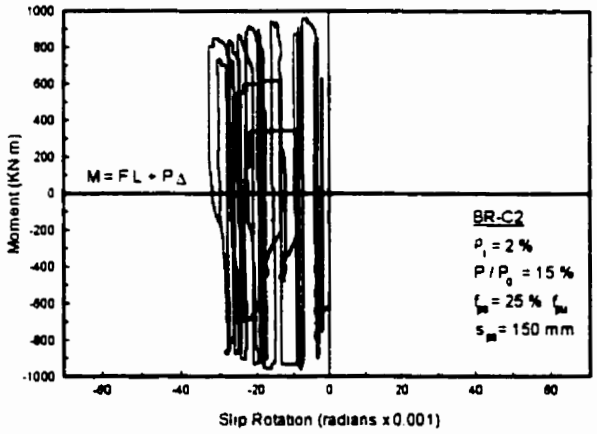

Figure 5.27 Moment-Rotation relationships for column BR-C2.

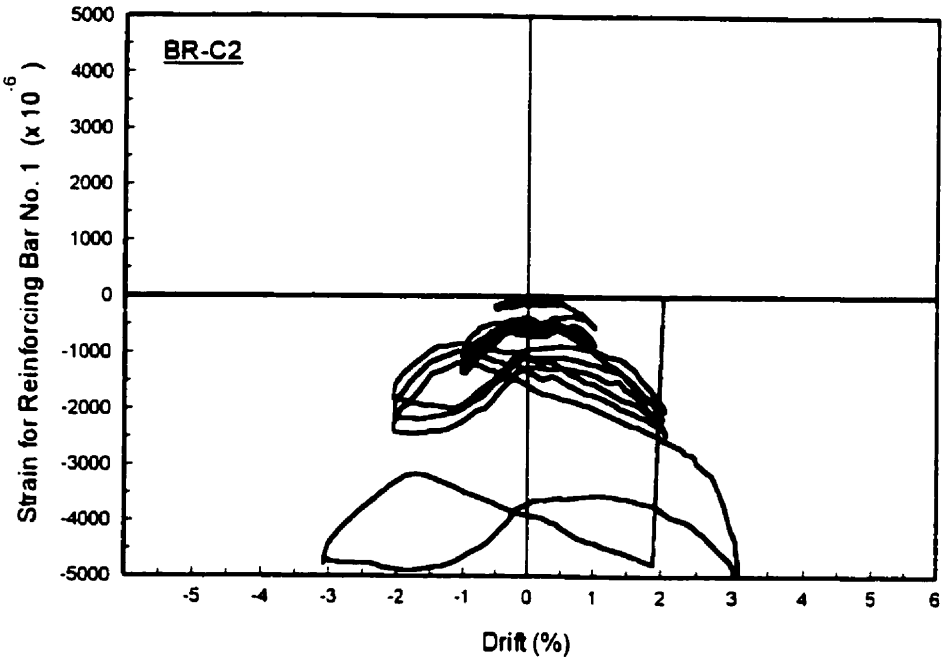

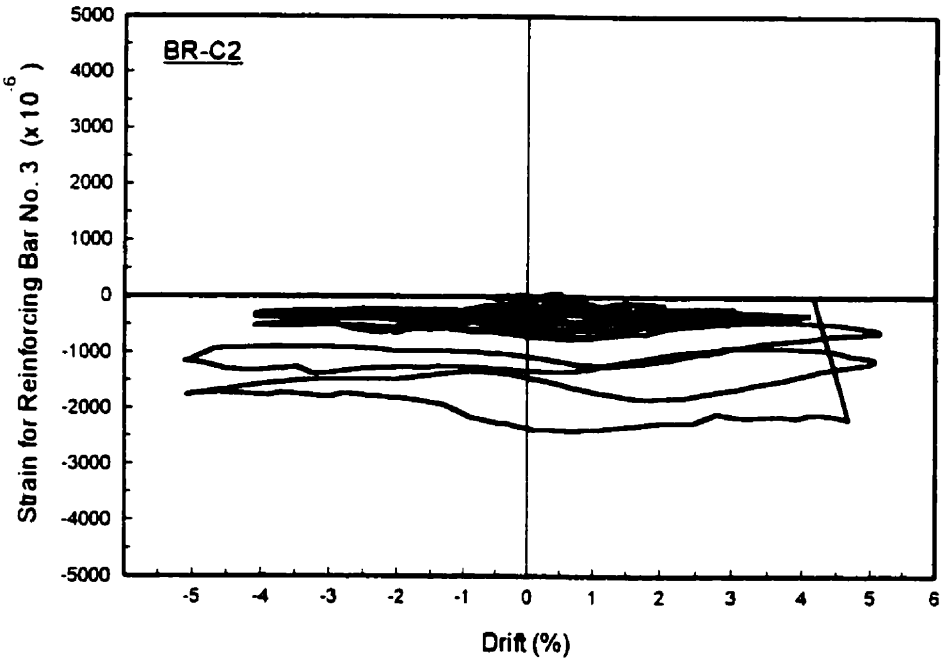

Figure 5.28 Reinforcing steel strains for column BR-C2.

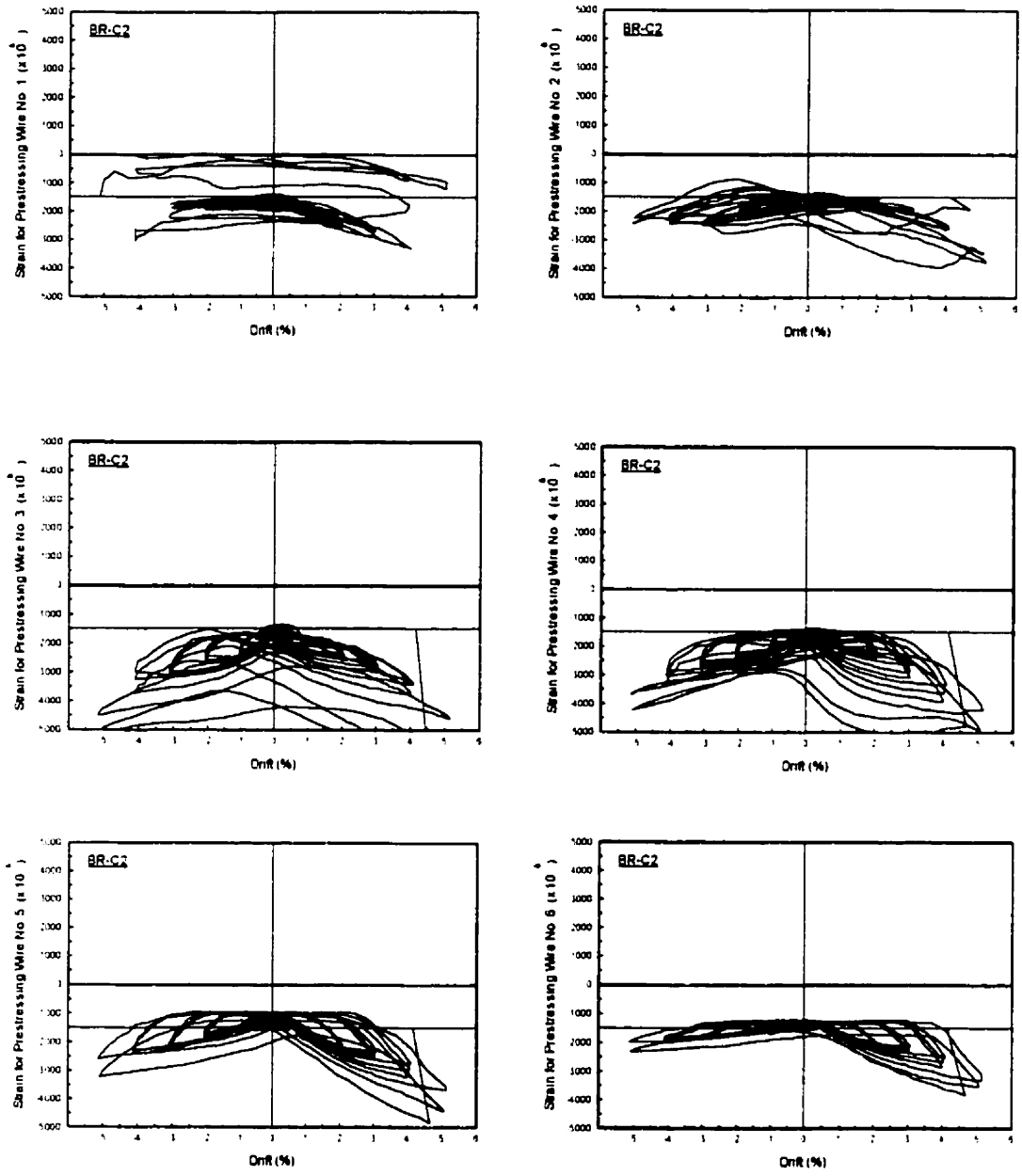

Figure 5.29 Prestressing wire strains for column BR-C2.

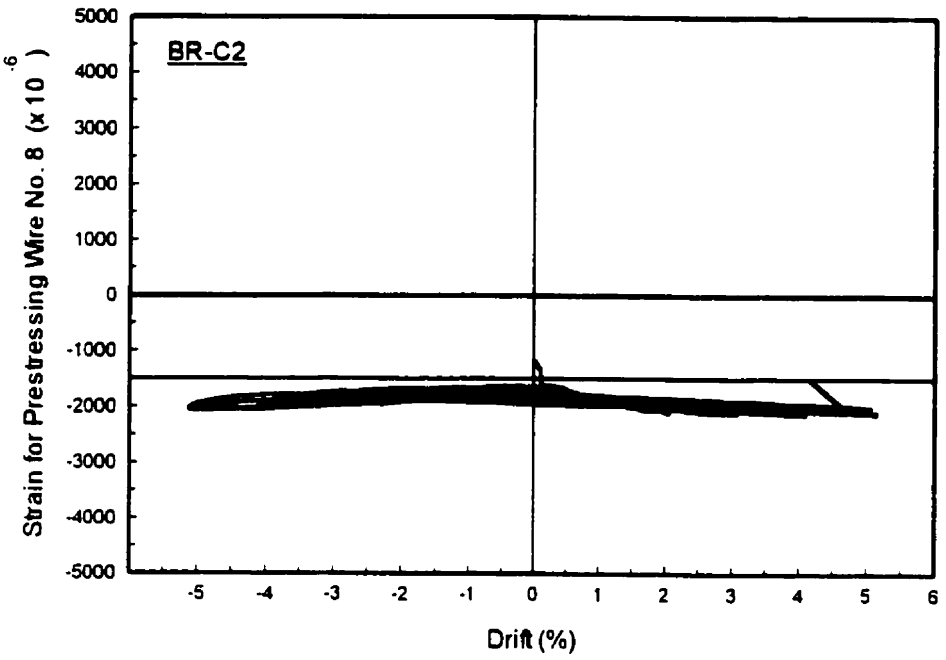

Figure 5.29 (Continued).

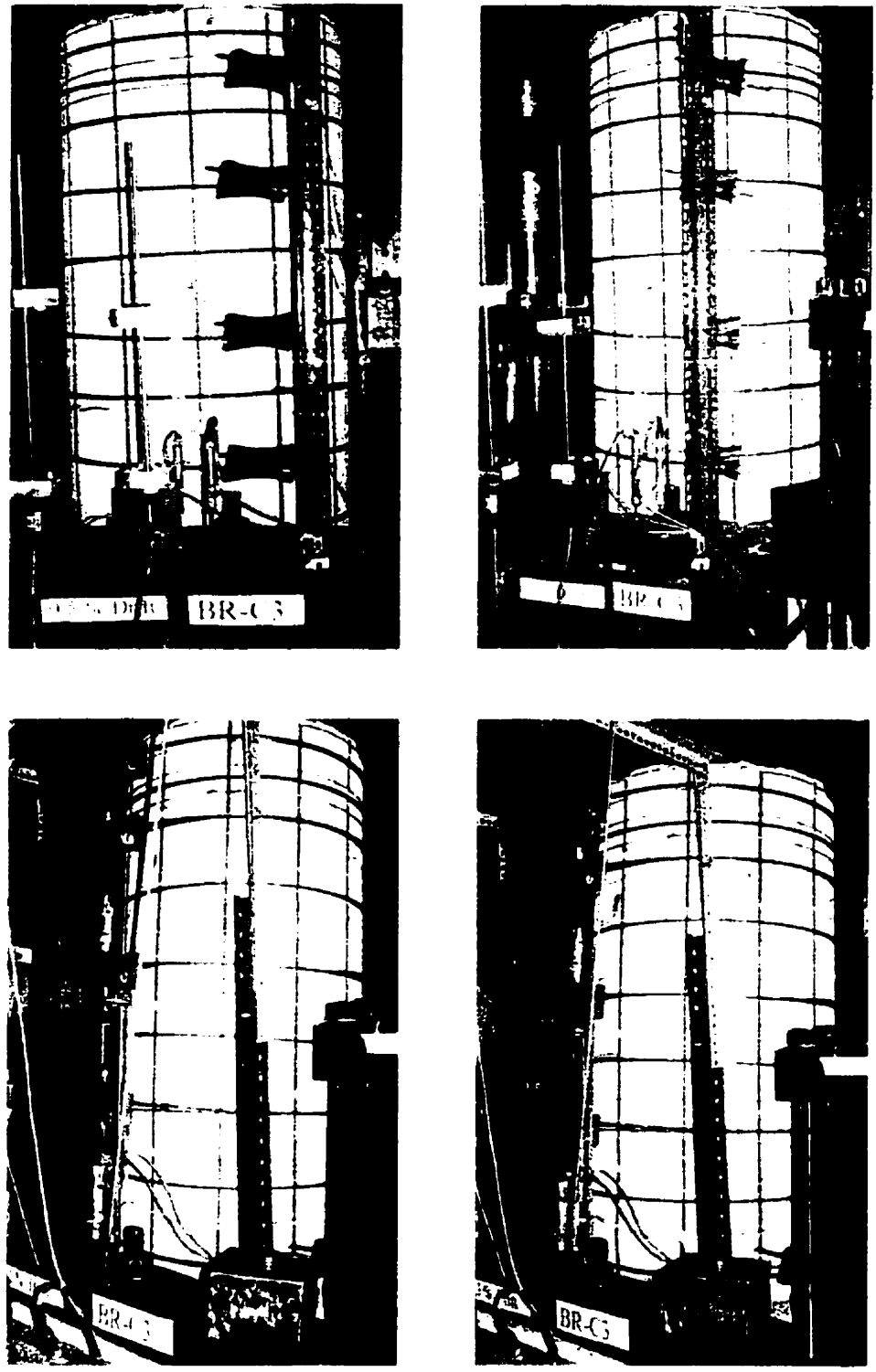

Figure 5.30 Various drift levels of retrofitted circular column (BR-C3) specimen.

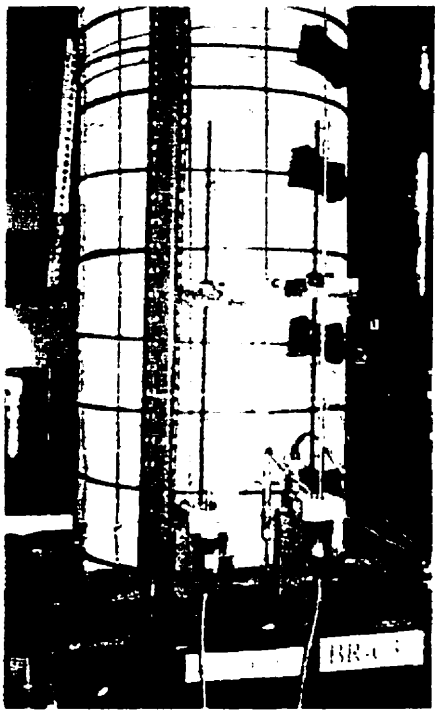

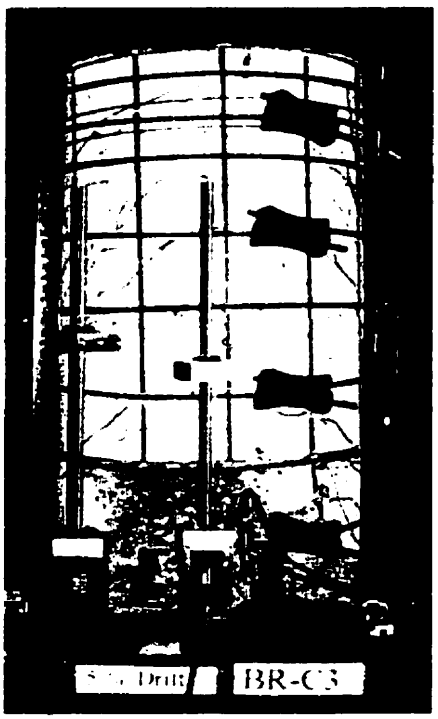

Figure 5.30 (Continued).

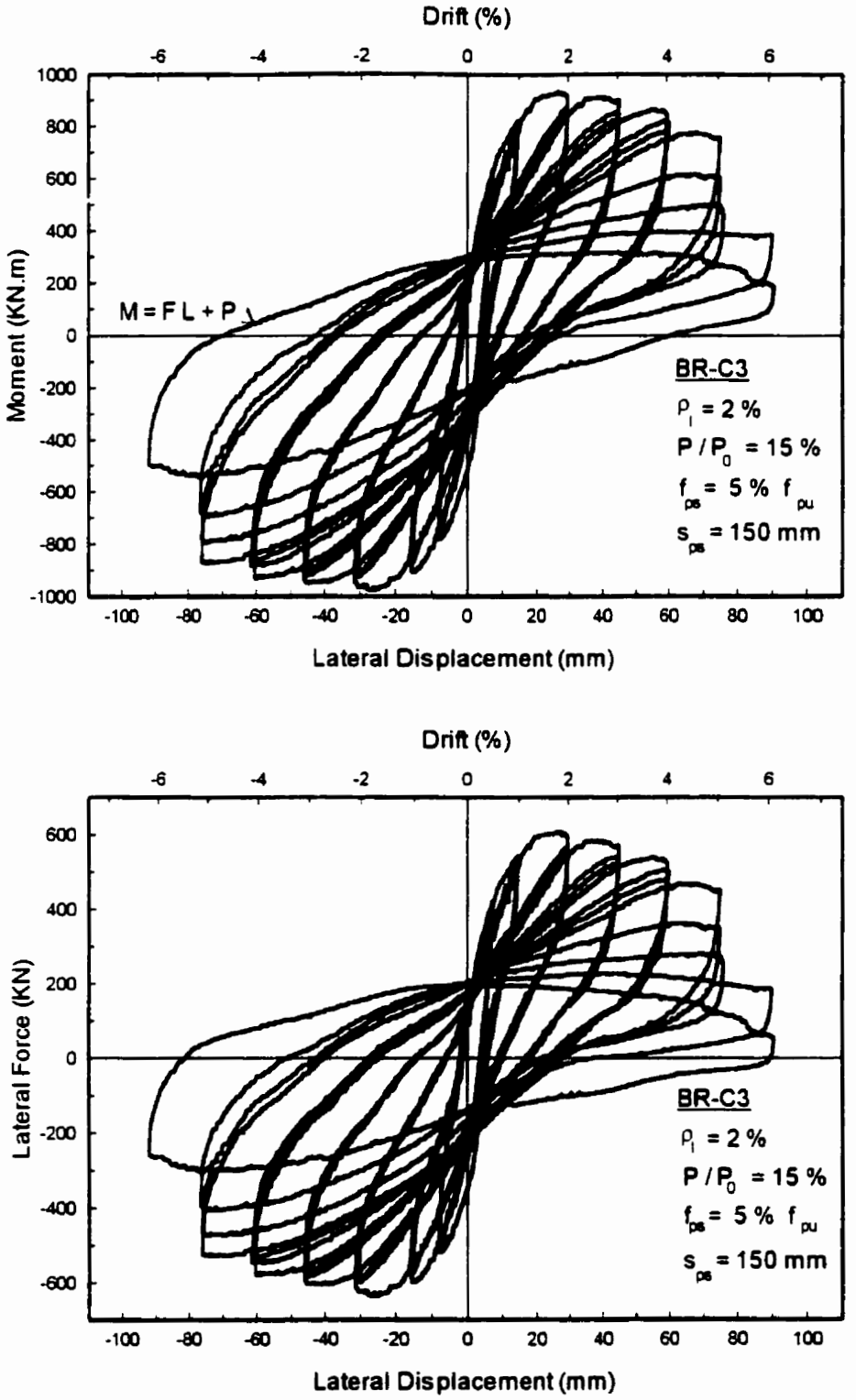

Figure 5.31 Moment-Displacement and Force-Displacement relationships for column BR-C3.

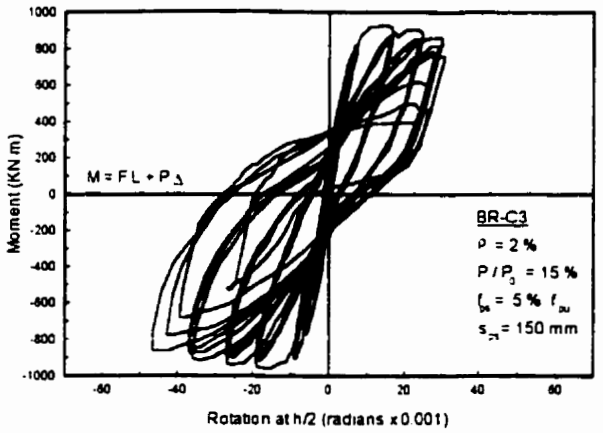

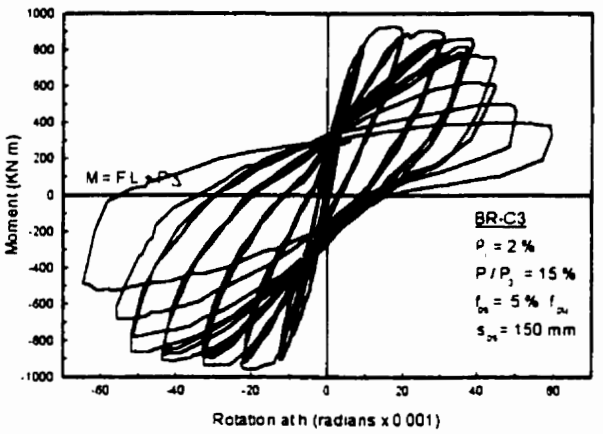

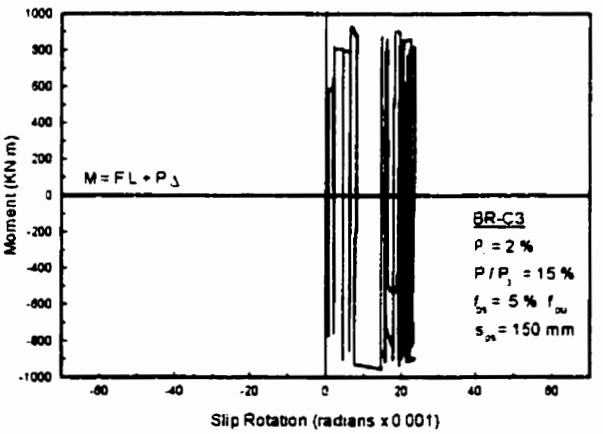

Figure 5.32 Moment-Rotation relationships for column BR-C3.

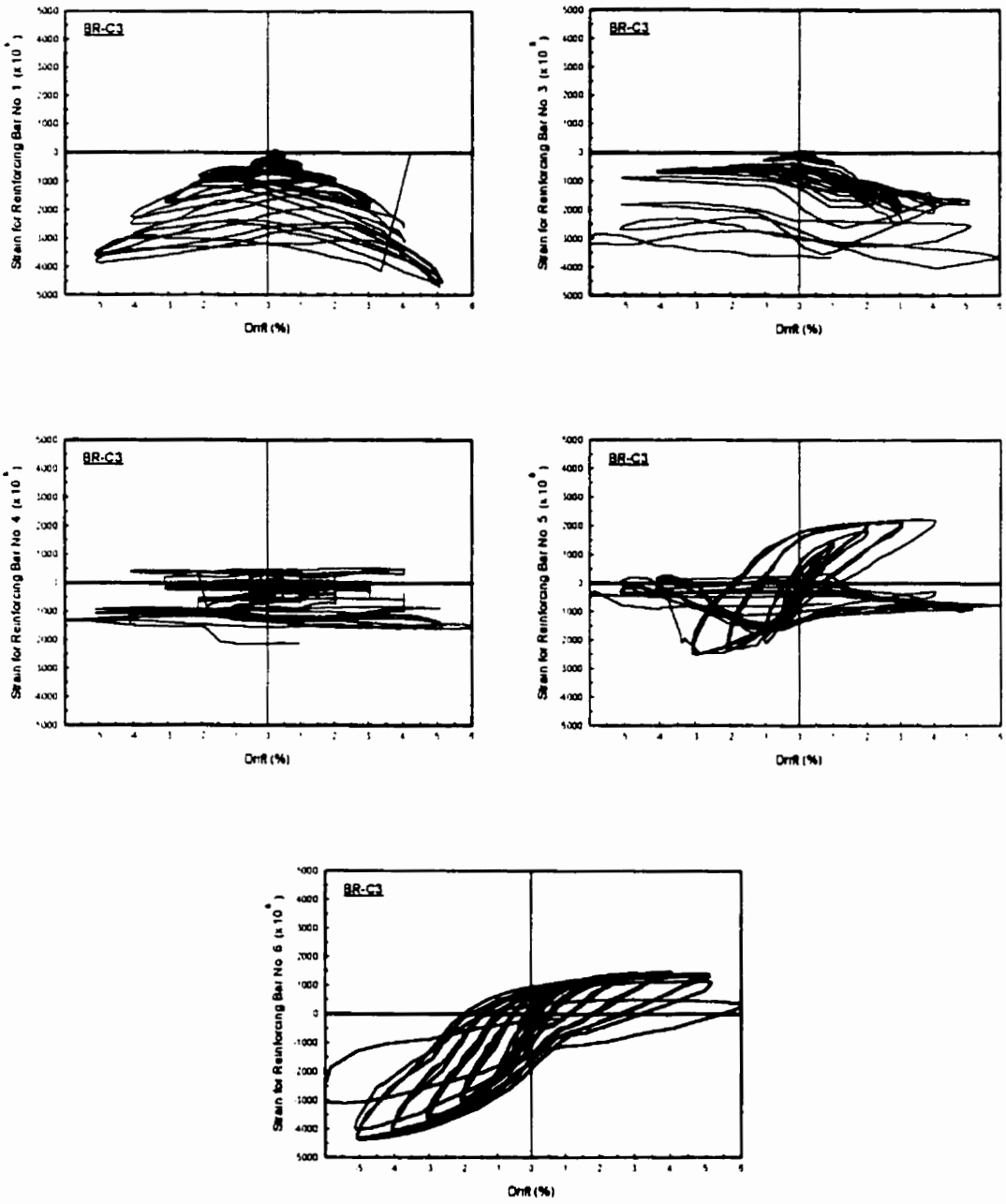

Figure 5.33 Reinforcing steel strains for column BR-C3.

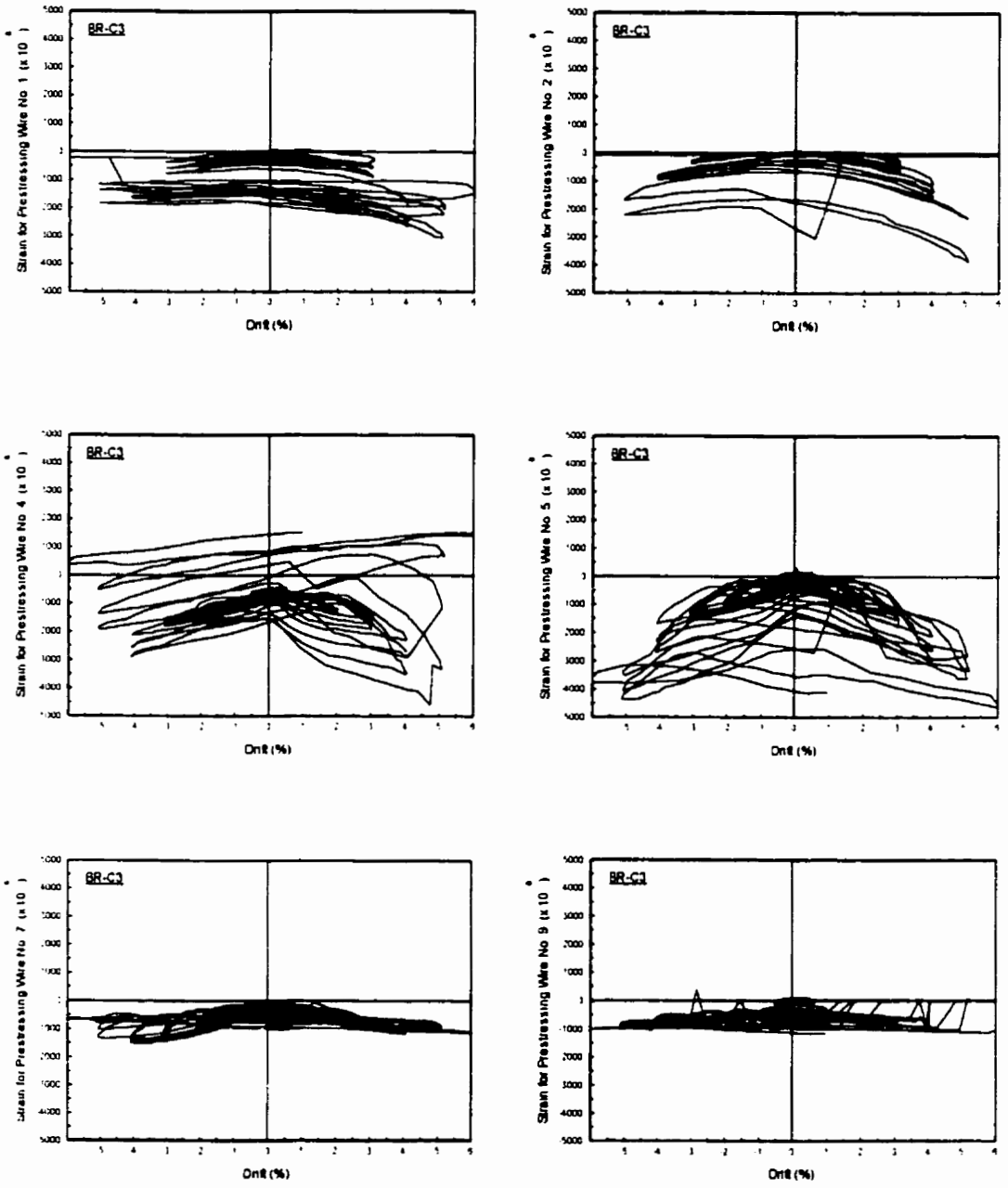

Figure 5.34 Prestressing wire strains for column BR-C3.

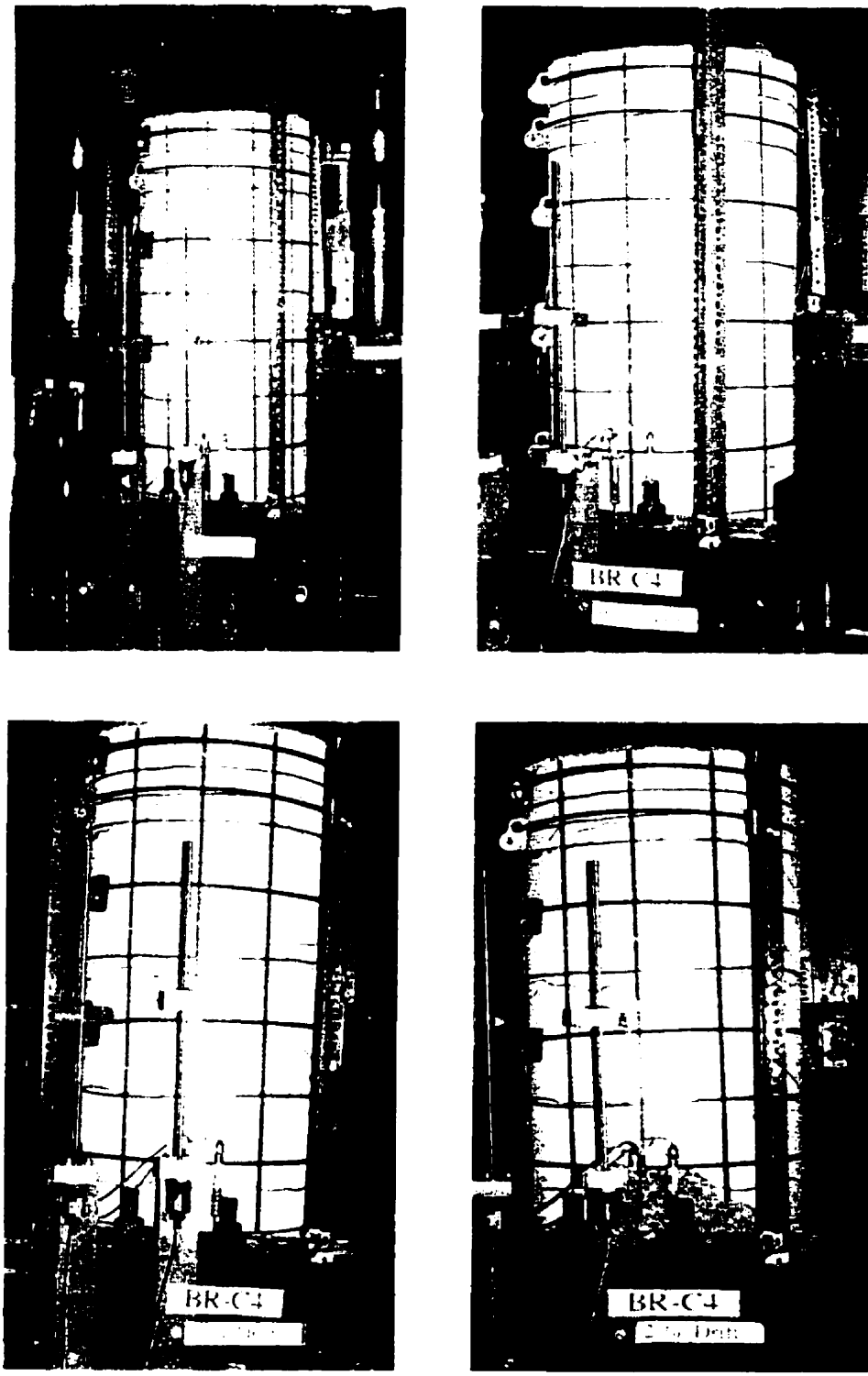

Figure 5.35 Various drift levels of retrofitted circular column (BR-C4) specimen.

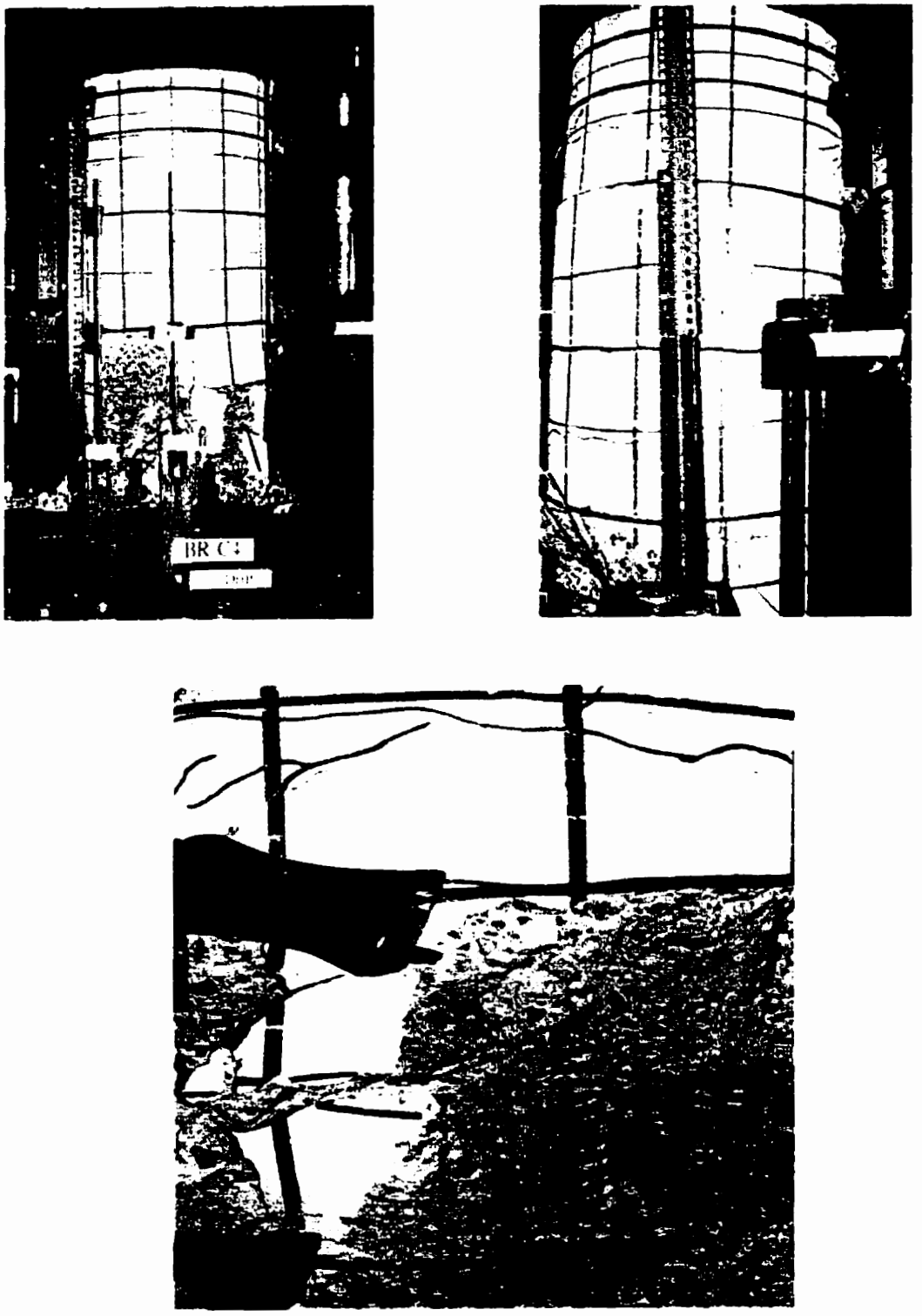

Figure 5.35 (Continued).

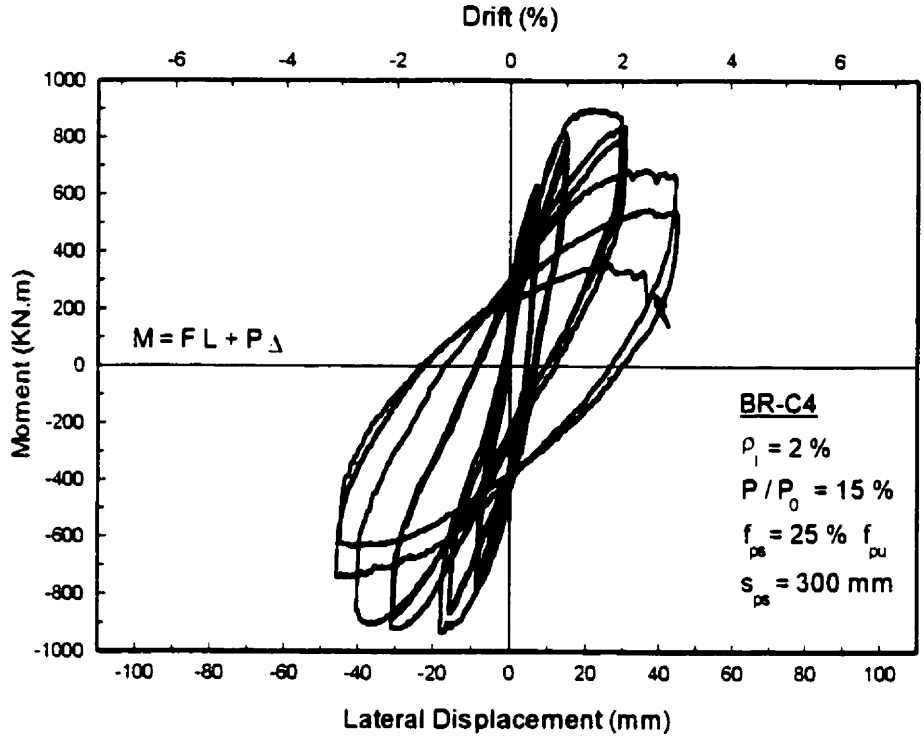

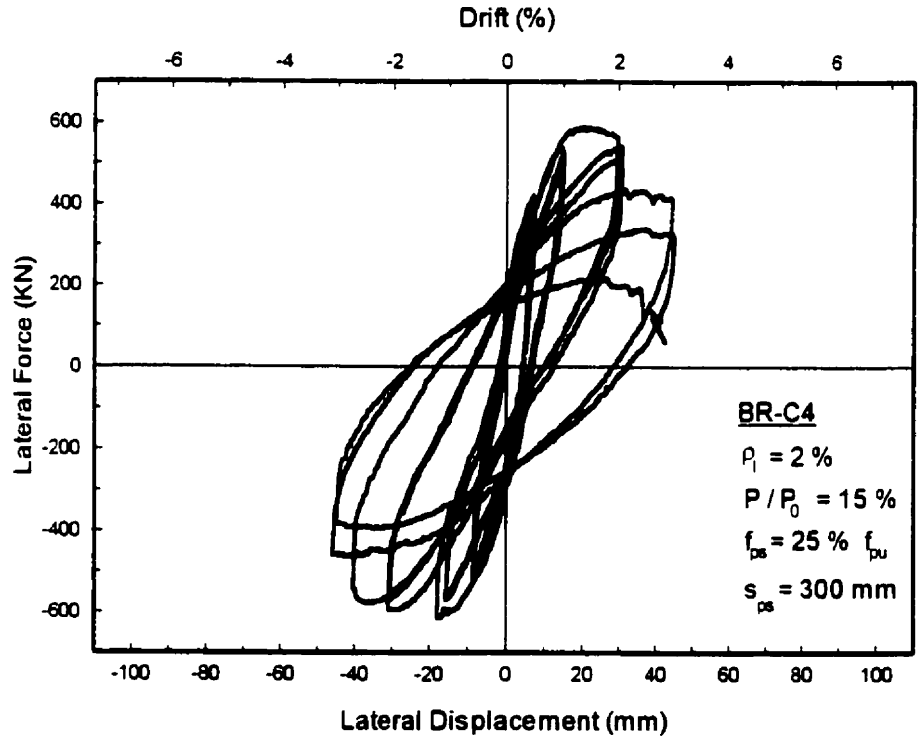

Figure 5.36 Moment-Displacement and Force-Displacement relationships for column BR-C4.

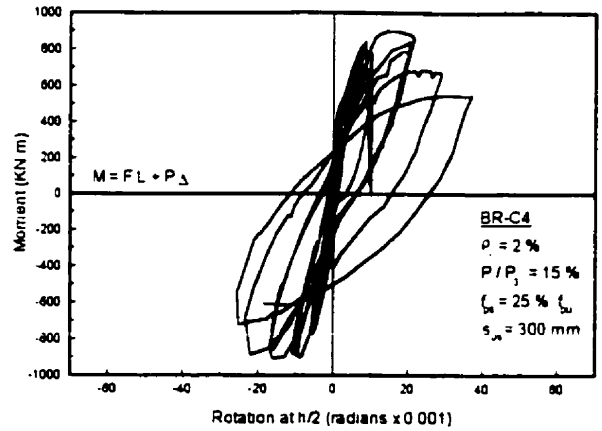

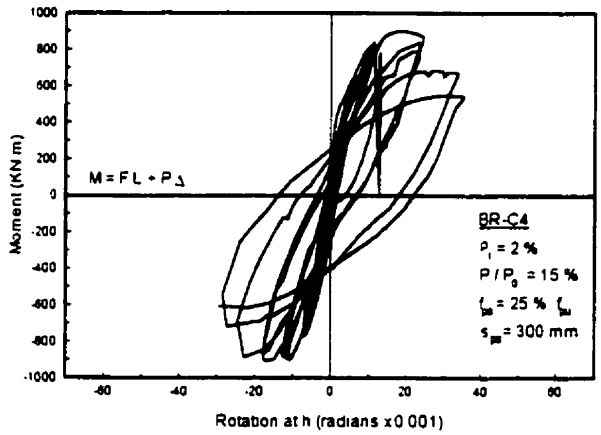

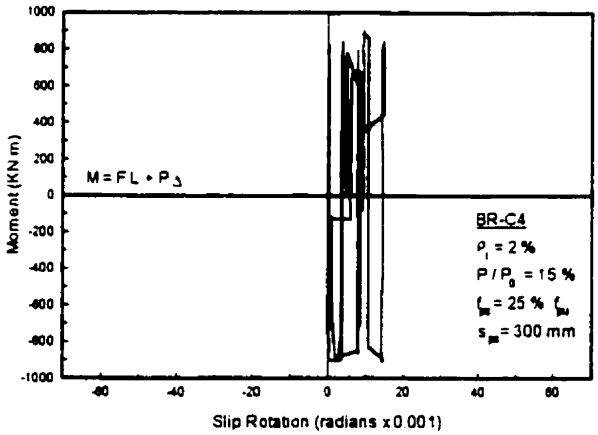

Figure 5.37 Moment-Rotation relationships for column BR-C4.

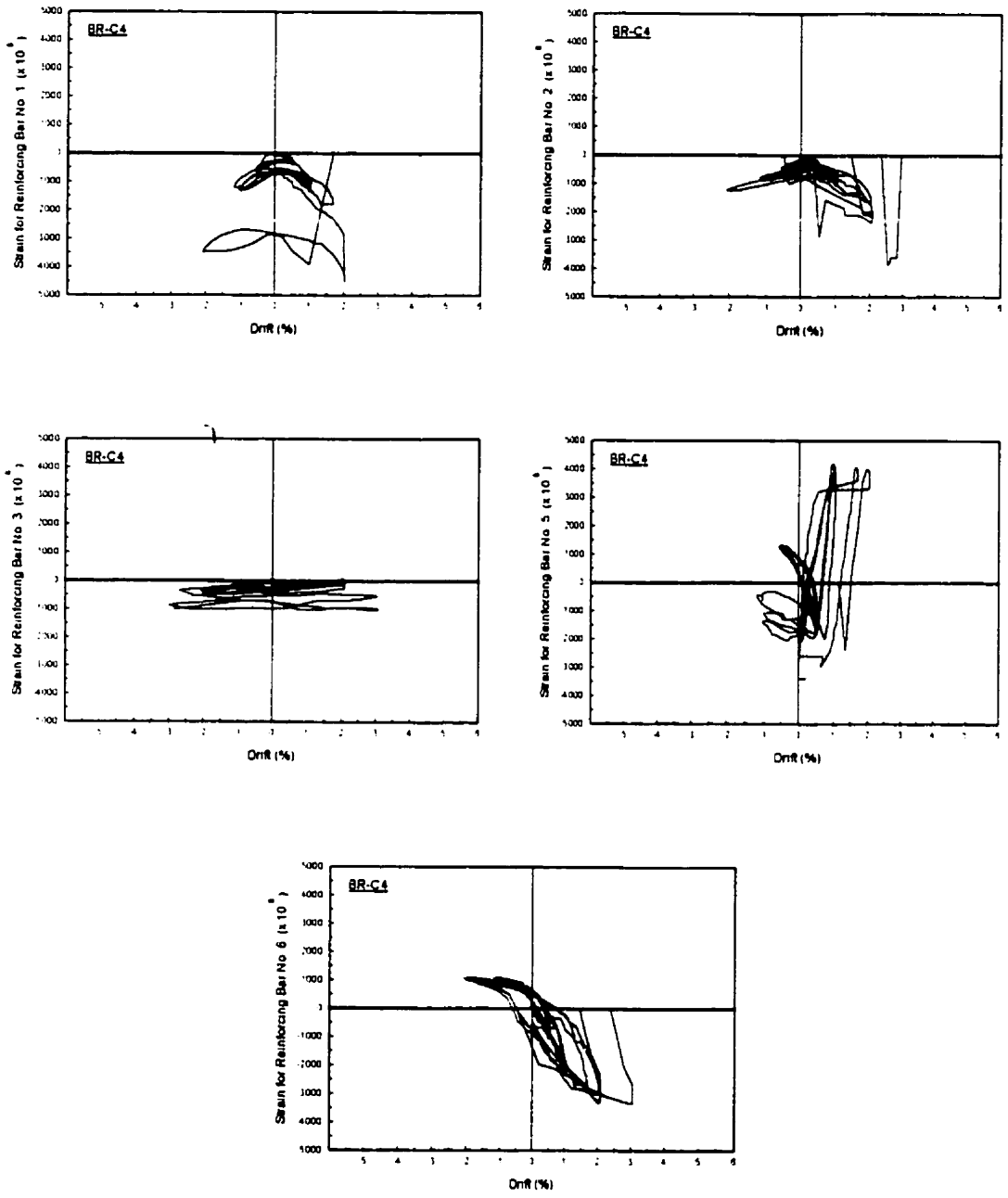

Figure 5.38 Reinforcing steel strains for column BR-C4.

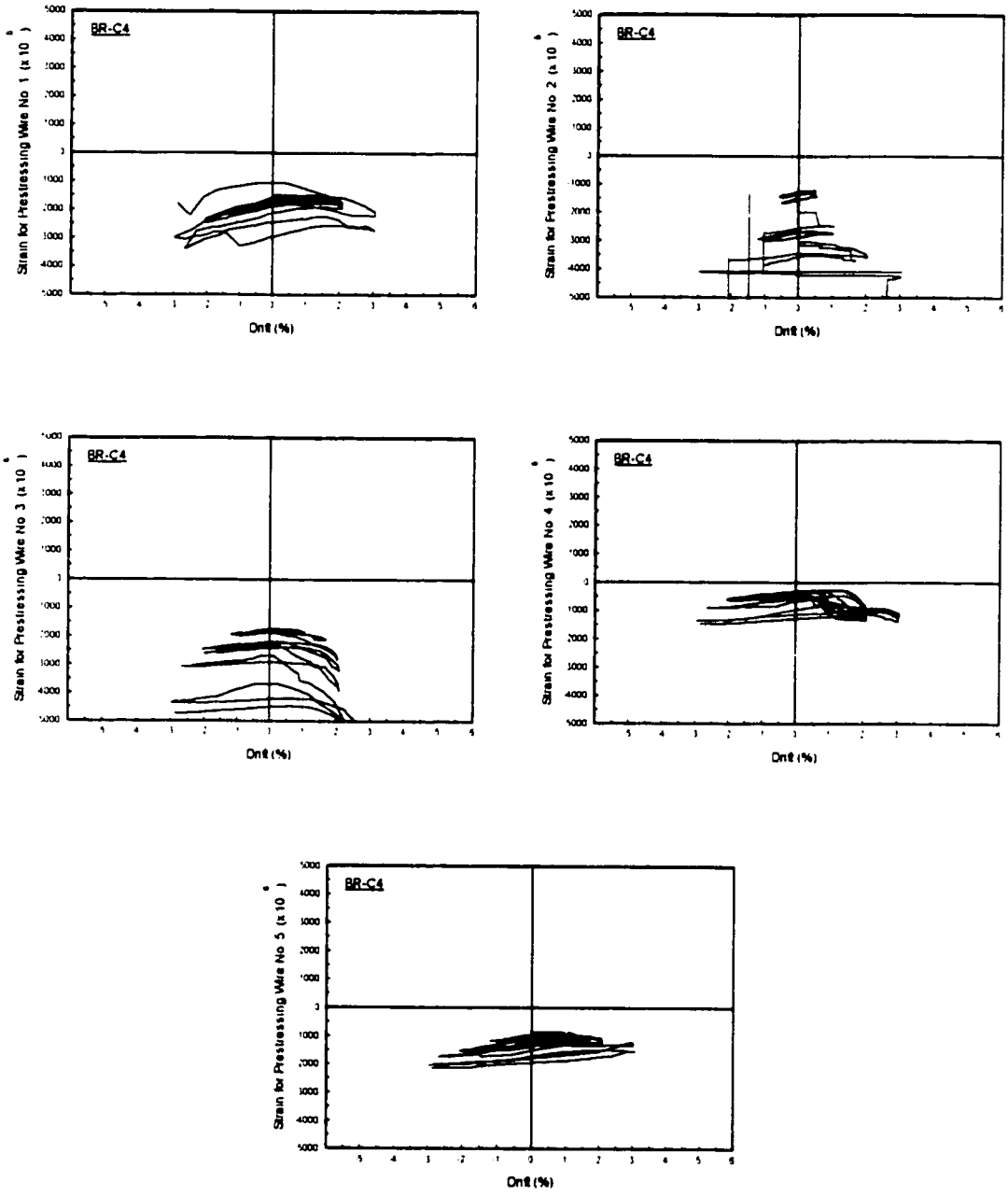

Figure 5.39 Prestressing wire strains for column BR-C4.

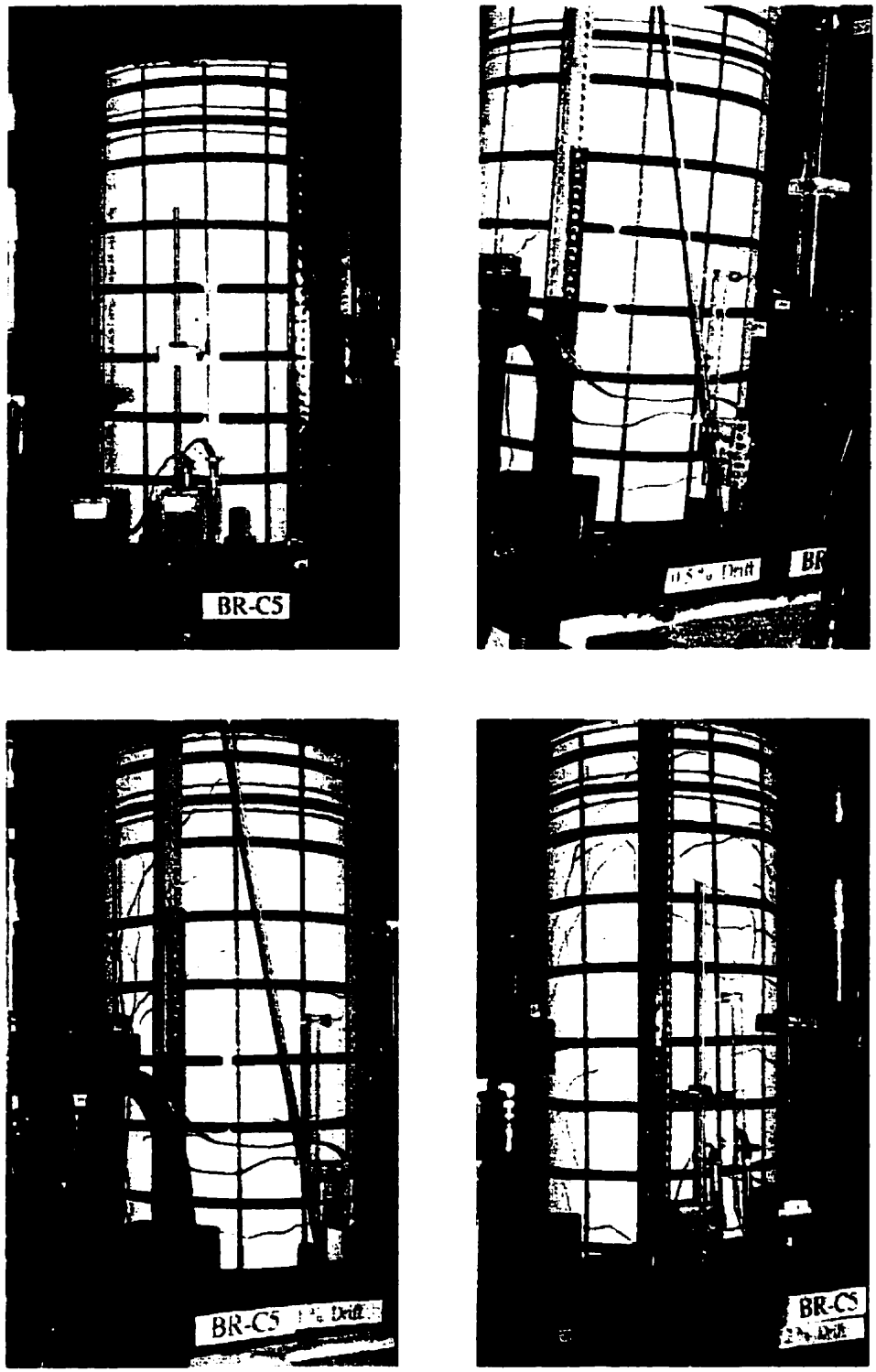

Figure 5.40 Various drift levels of retrofitted circular column (BR-C5) specimen.

Figure 5.40 (Continued).

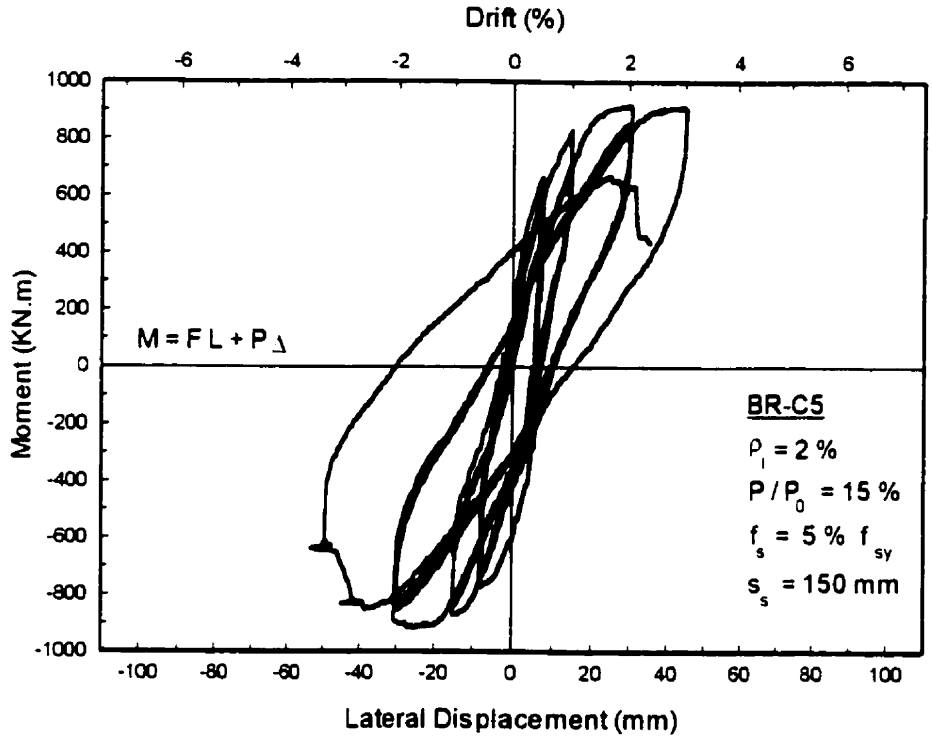

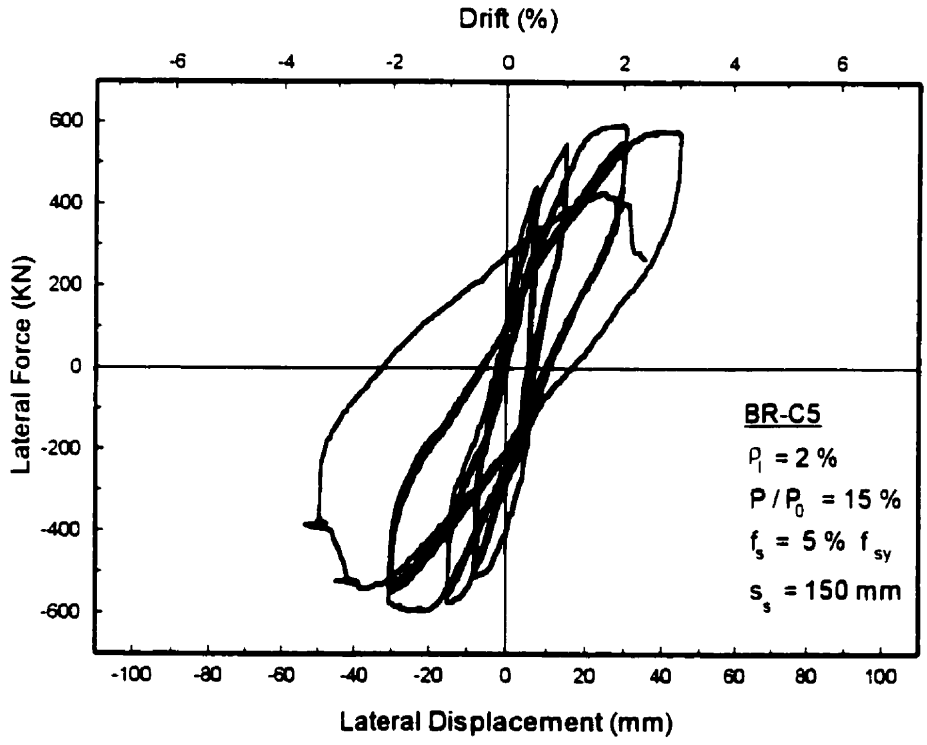

Figure 5.41 Moment-Displacement and Force-Displacement relationships for column BR-C5.

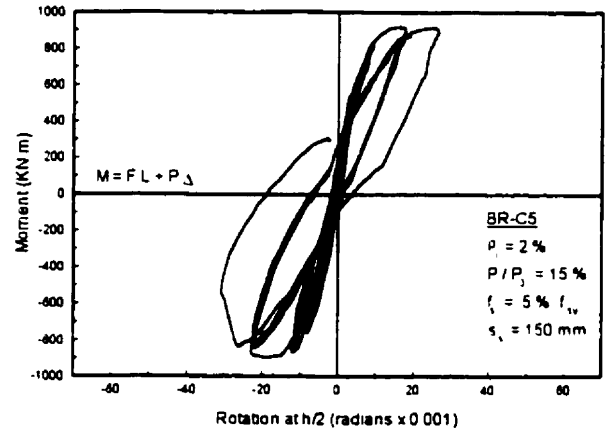

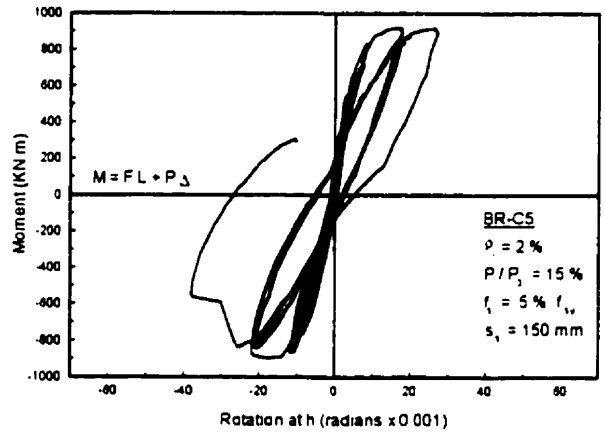

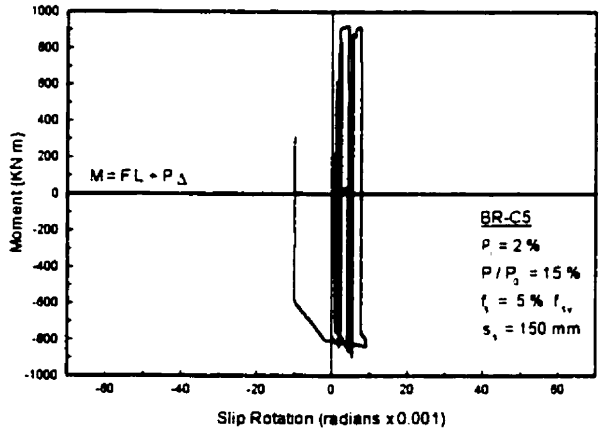

Figure 5.42 Moment-Rotation relationships for column BR-C5.

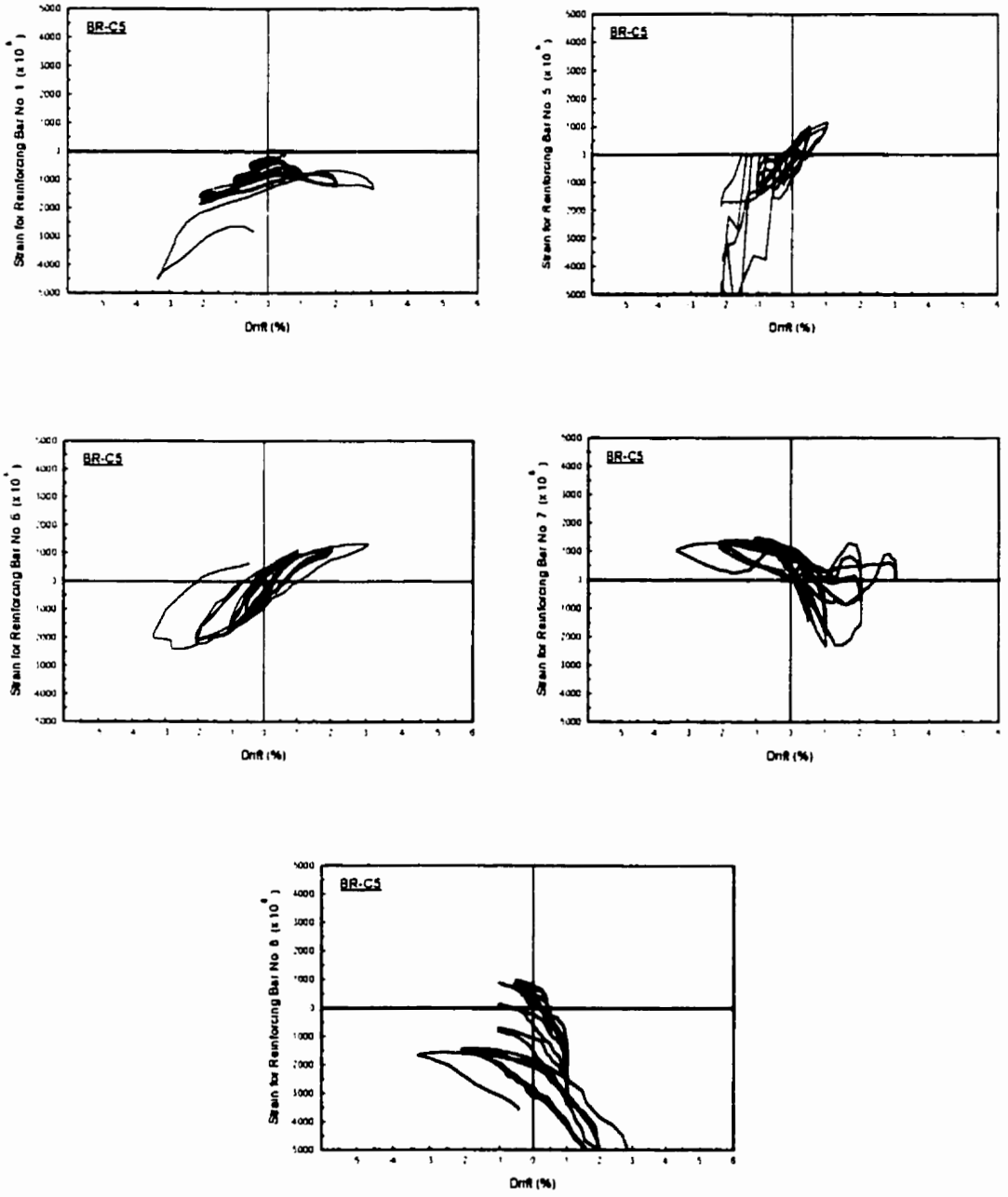

Figure 5.43 Reinforcing steel strains for column BR-C5.

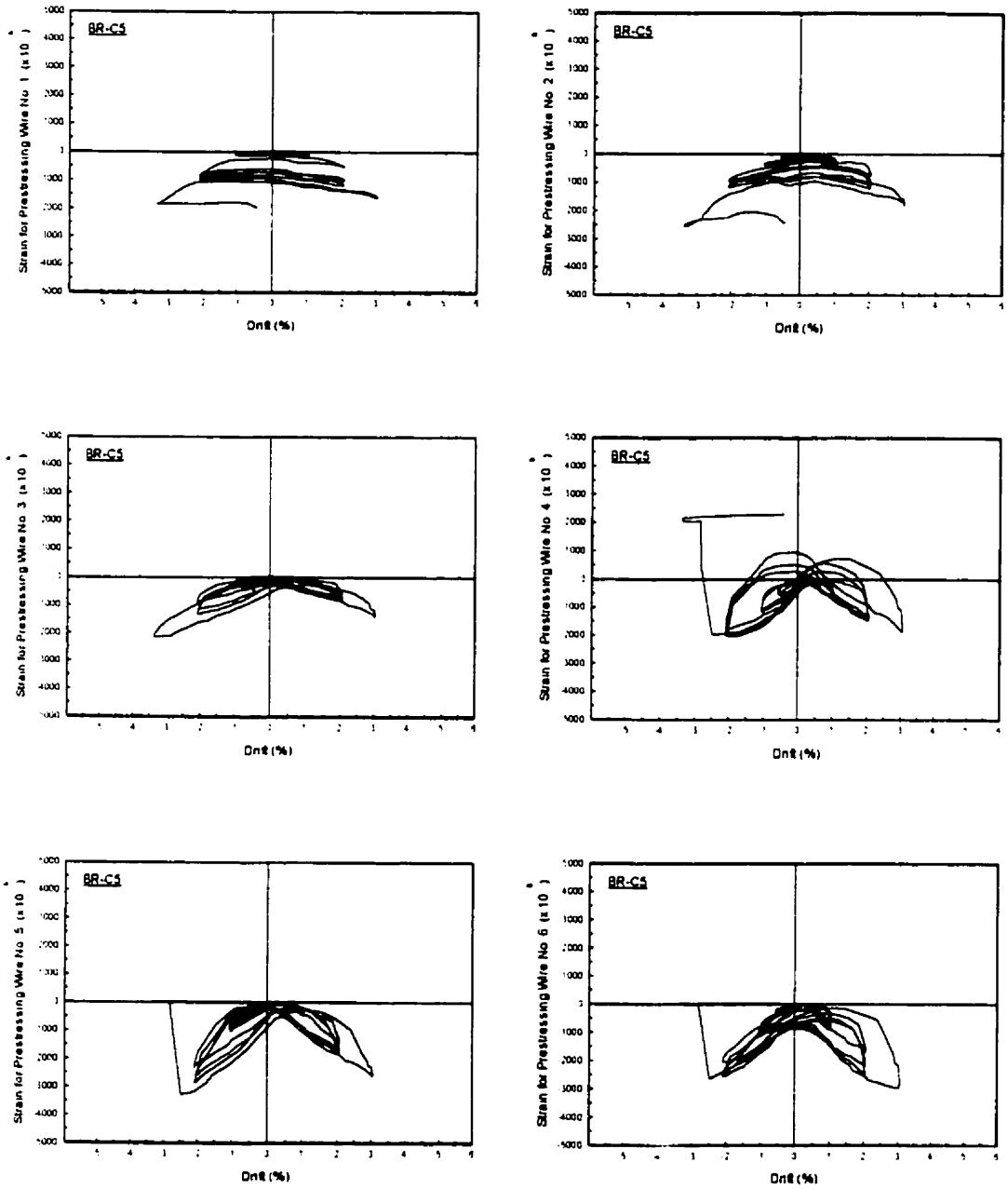

Figure 5.44 Steel strap strains for column BR-C5.

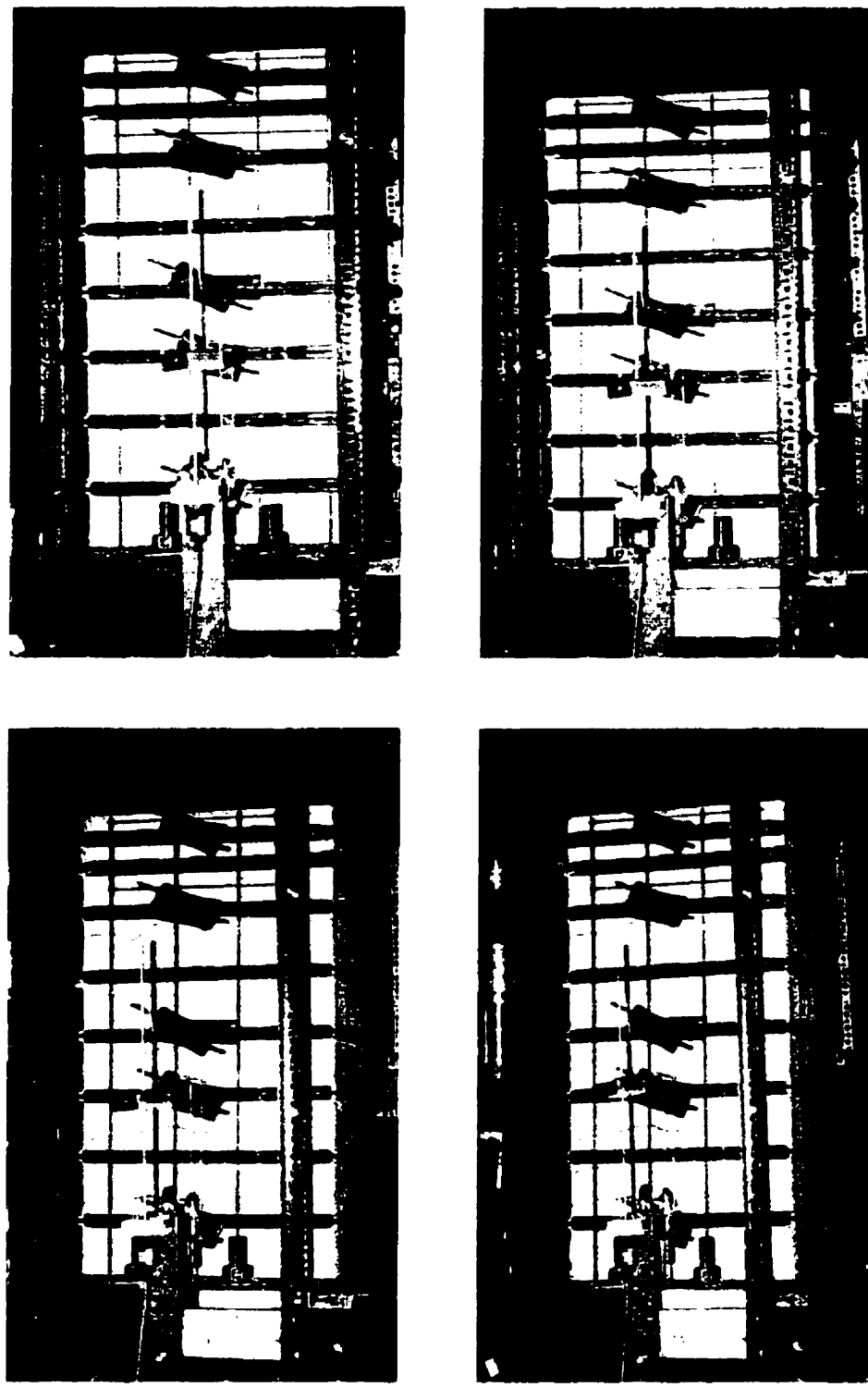

Figure 5.45 Various drift levels of retrofitted circular column (BR-S2) specimen.

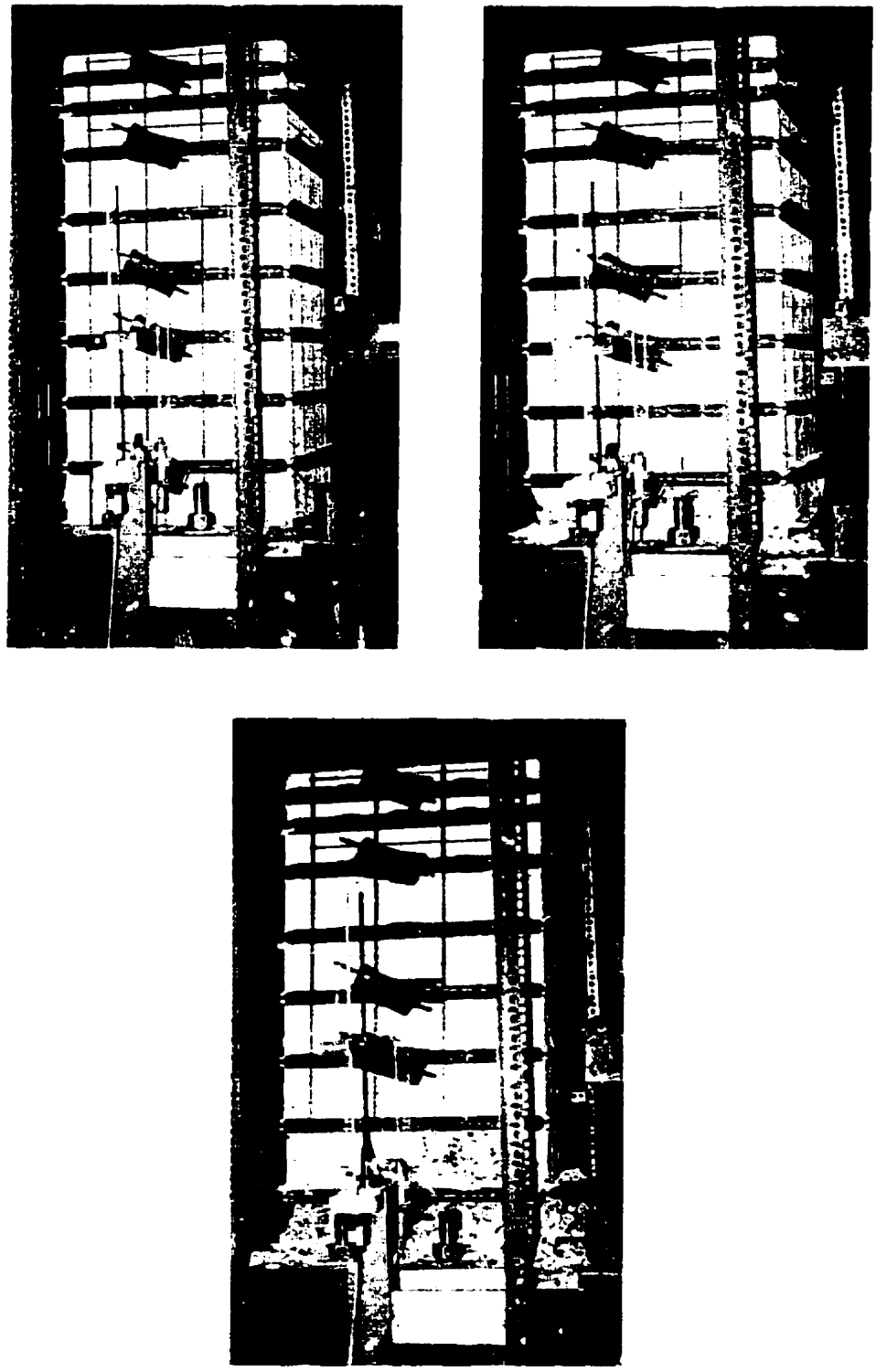

Figure 5.45 (Continued).

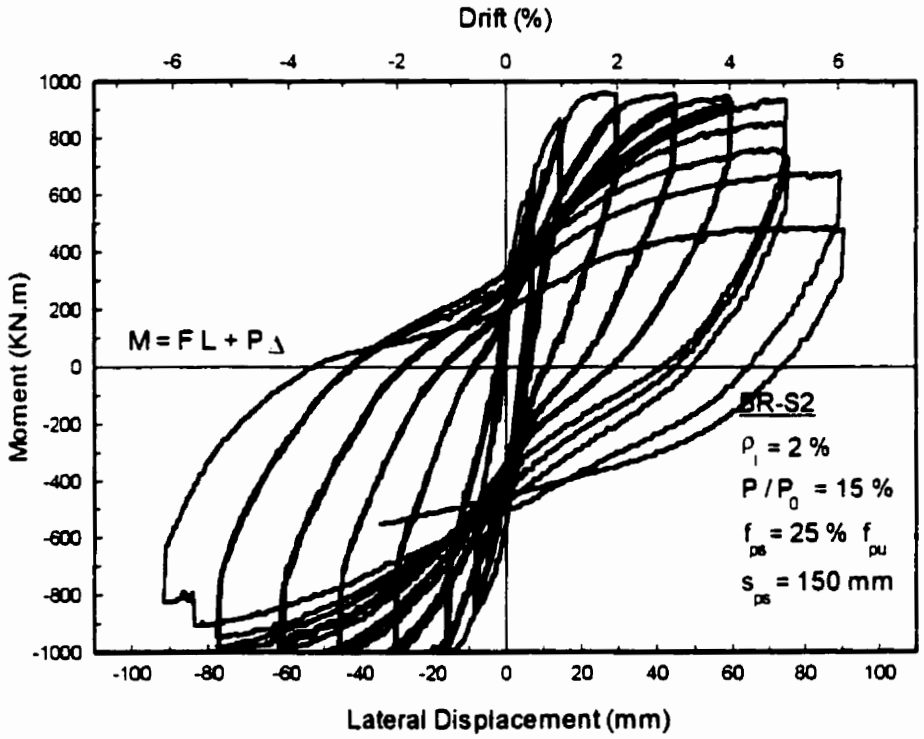

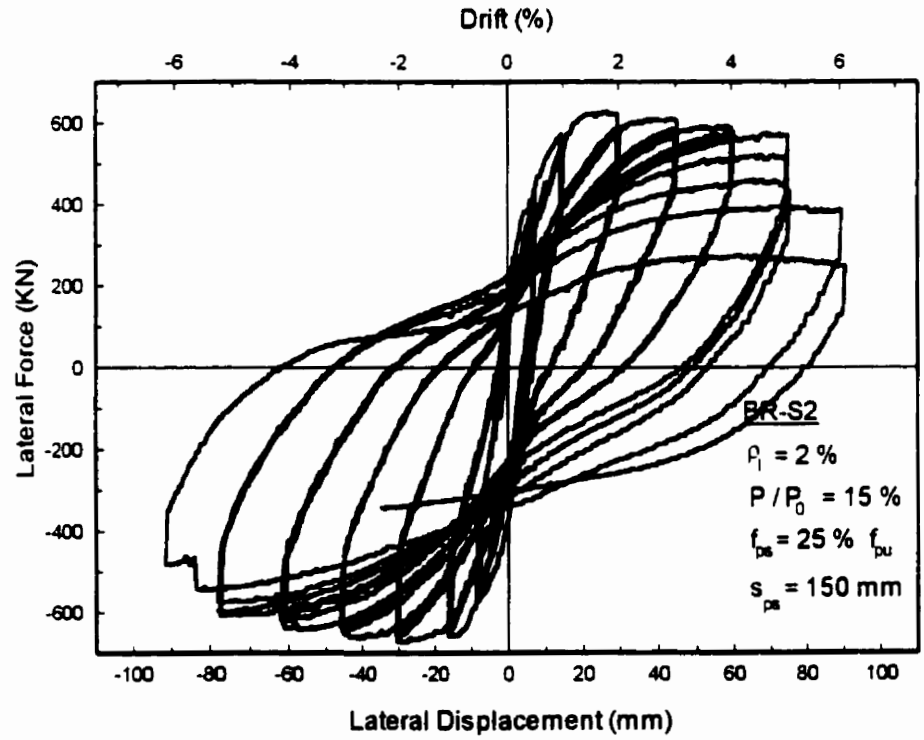

Figure 5.46 Moment-Displacement and Force-Displacement relationships for column BR-S2.

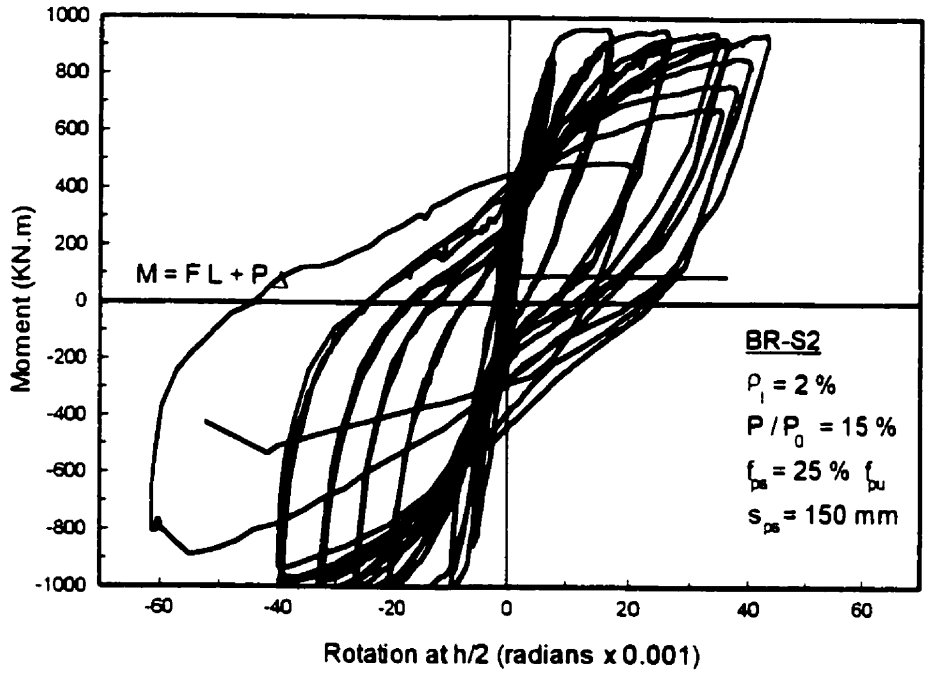

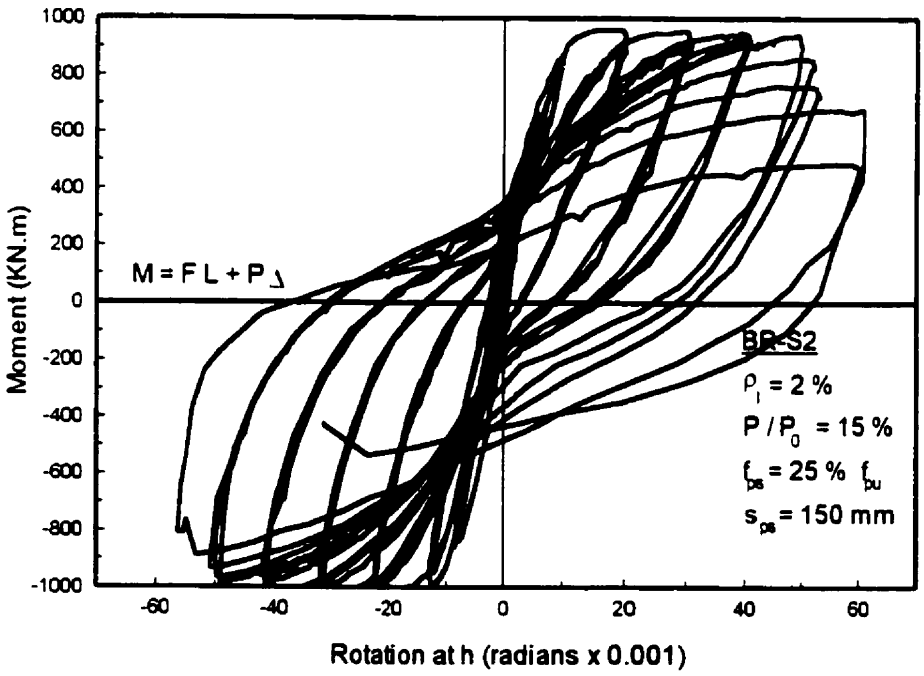

Figure 5.47 Moment-Rotation relationships for column BR-S2.

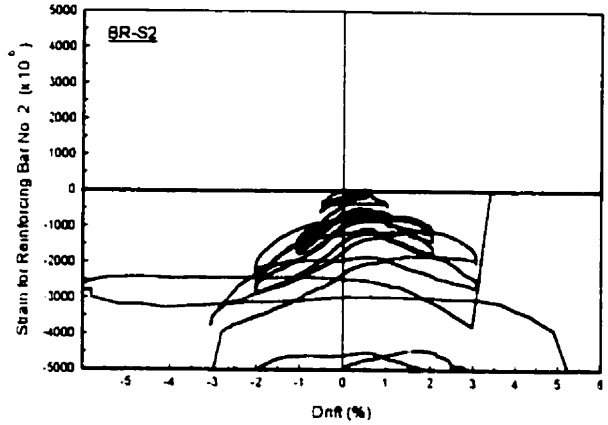

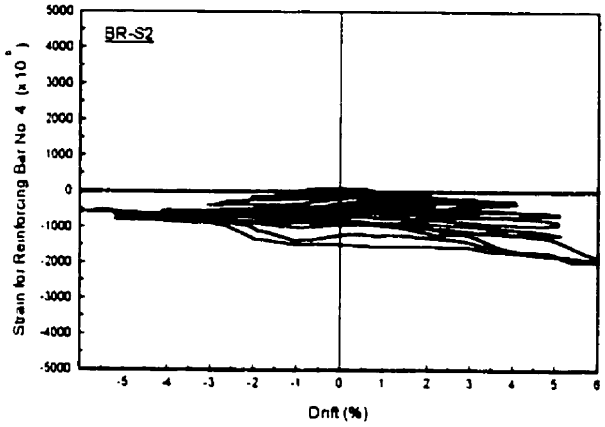

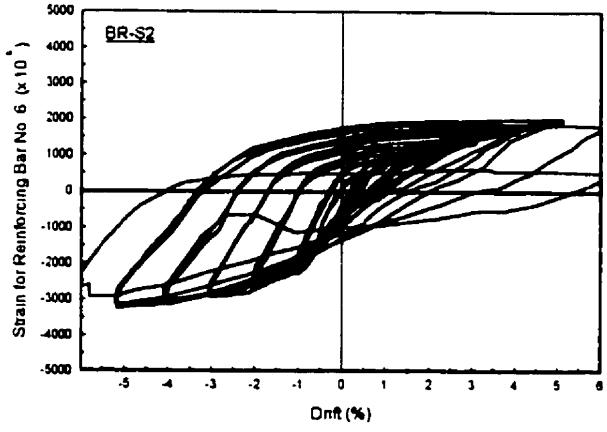

Figure 5.48 Reinforcing steel strains for column BR-S2.

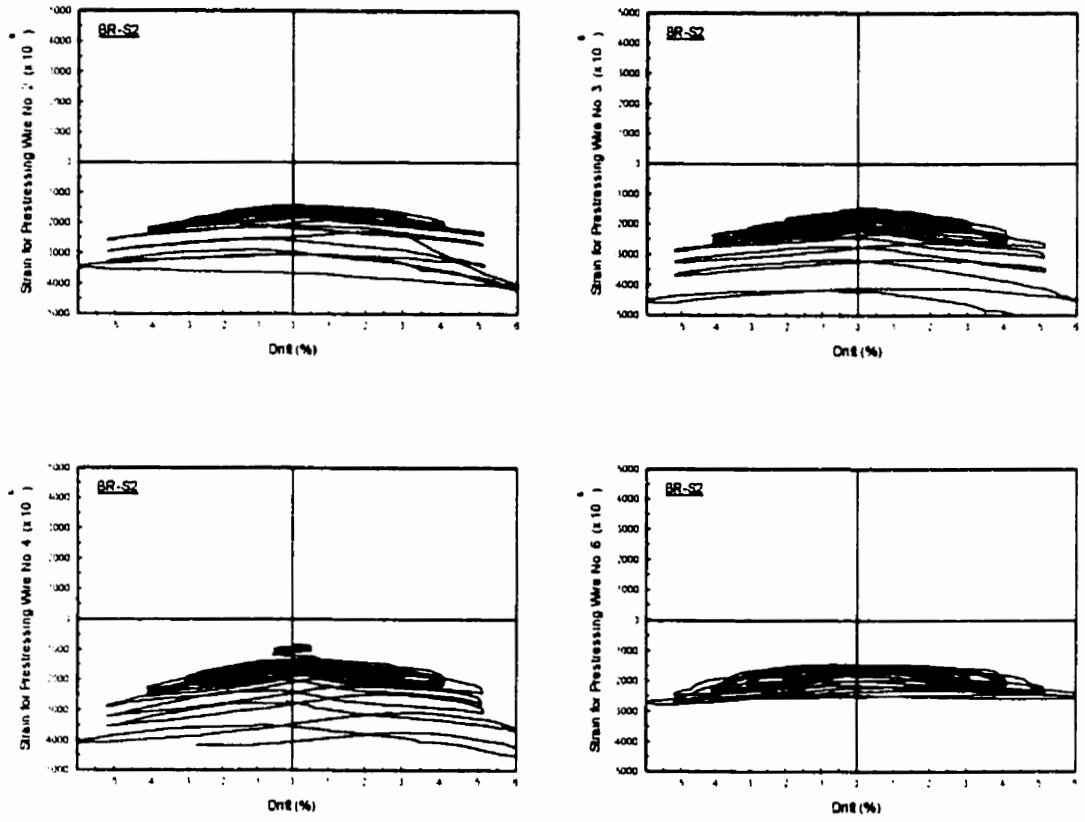

Figure 5.49 Prestressing wire strains for column BR-S2.

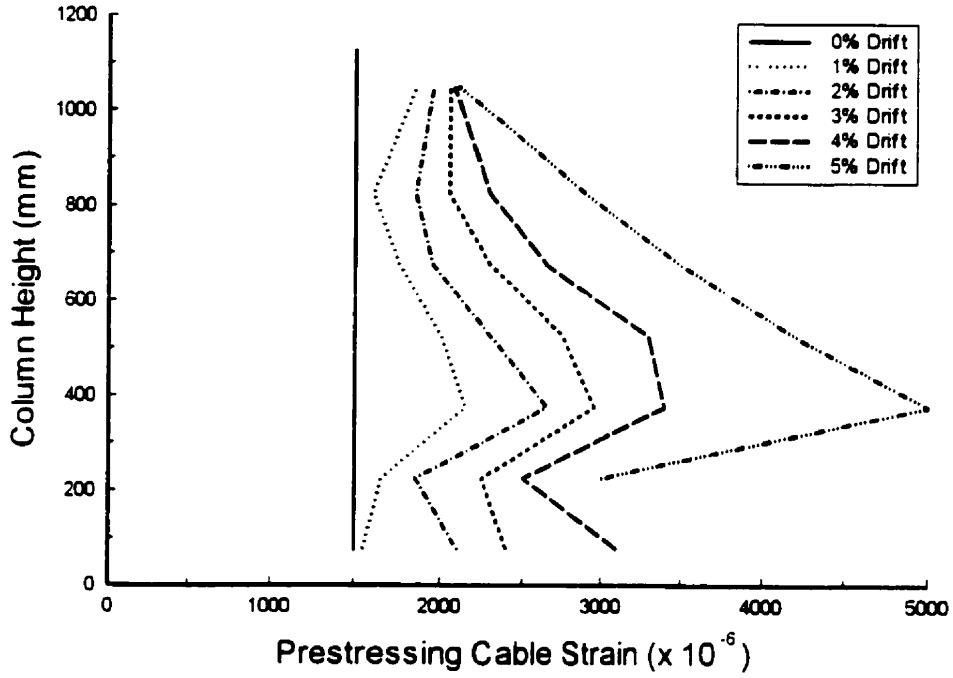

Figure 5.50 Prestressing wire strain profile for column BR-C2.

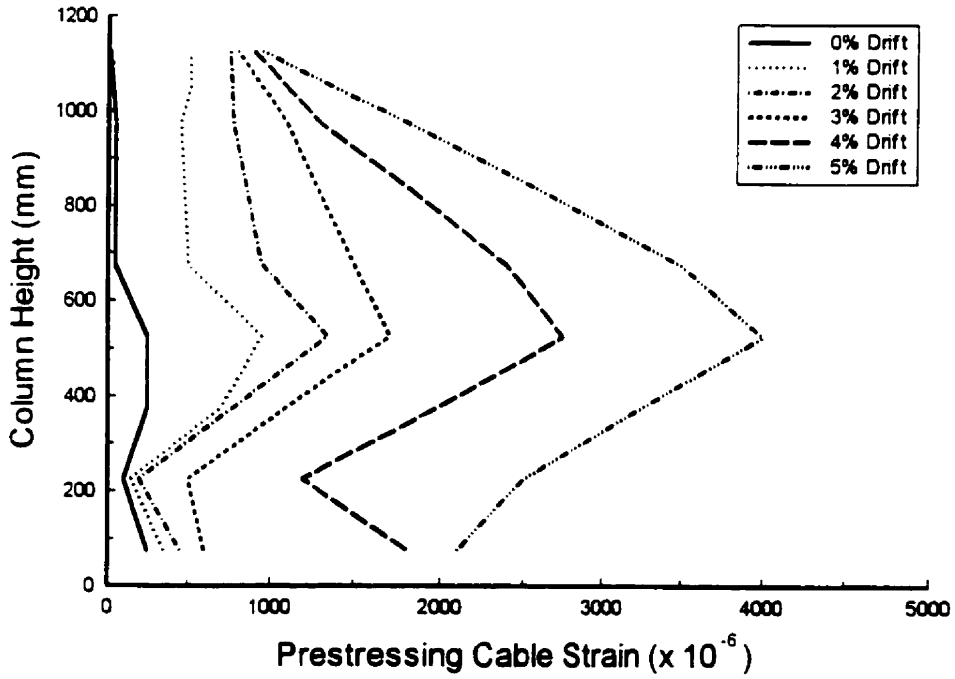

Figure 5.51 Prestressing wire strain profile for column BR-C3.

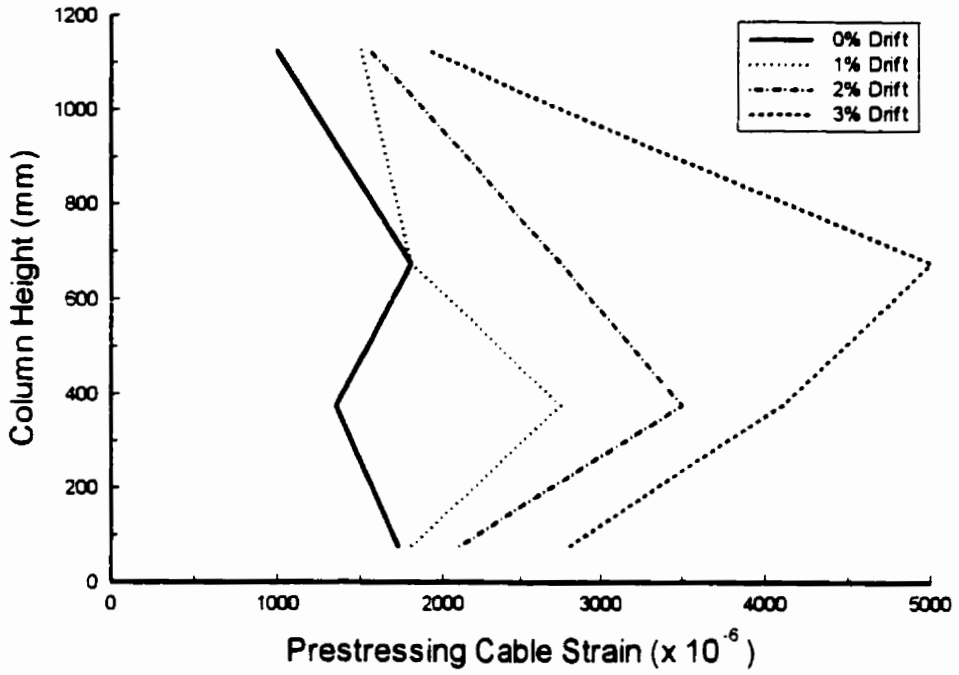

Figure 5.52 Prestressing wire strain profile for column BR-C4.

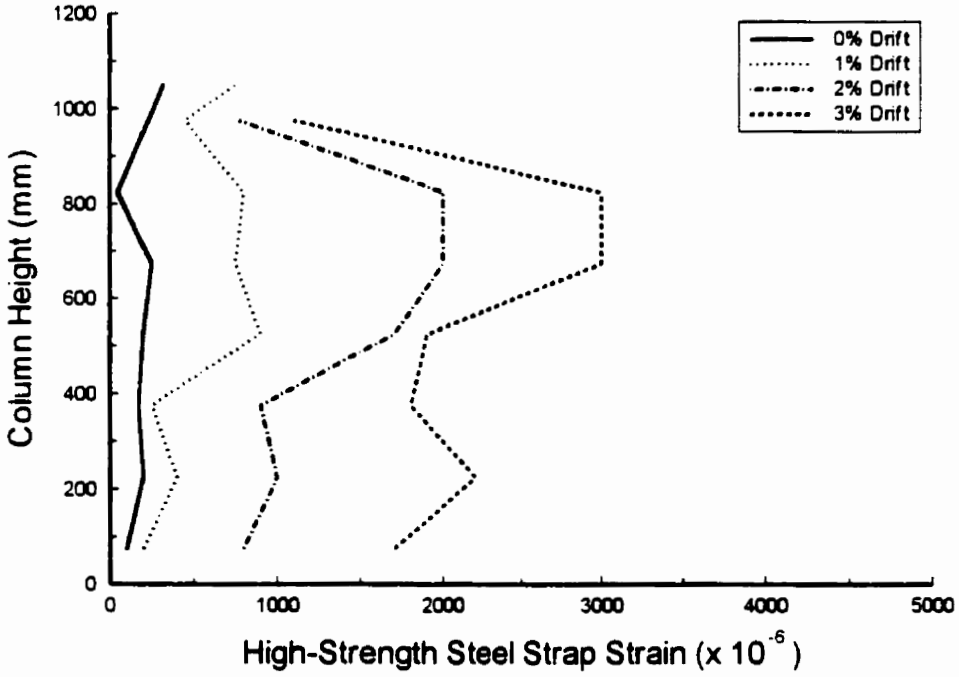

Figure 5.53 High-strength steel strap strain profile for column BR-C5.

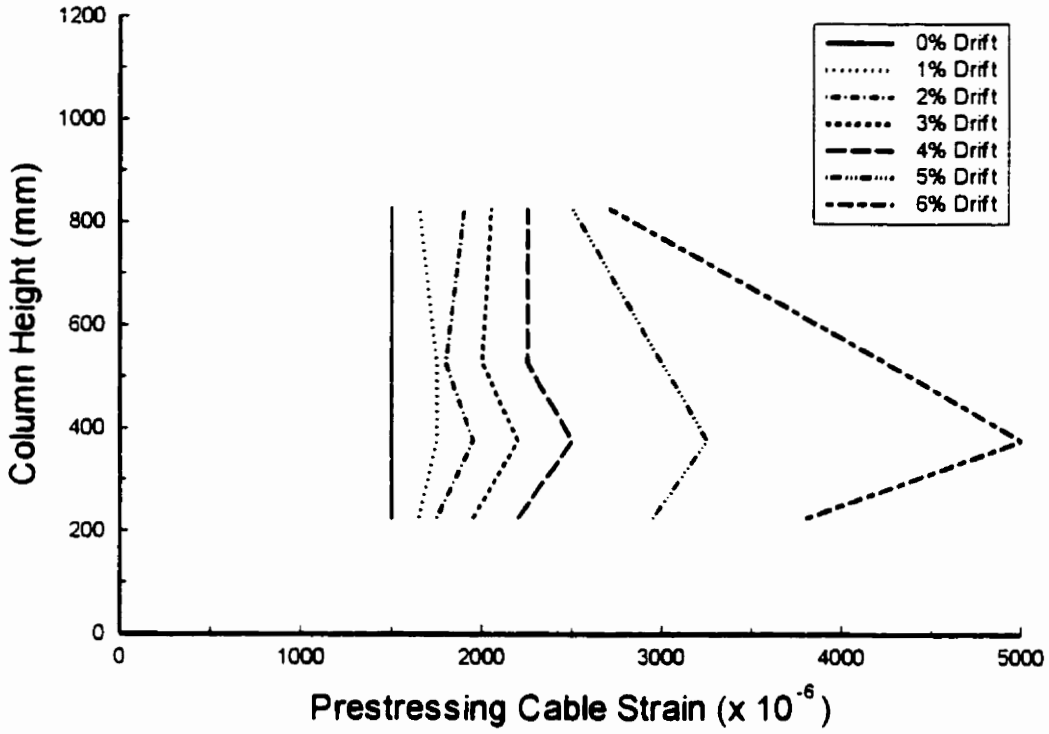

Figure 5.54 Prestressing wire strain profile for column BR-S2.

Chapter 6

Summary and Conclusions

6.1 Summary

A combined analytical and experimental investigation was conducted to study the capacity, demand and seismic retrofit of reinforced concrete bridge columns. A comprehensive literature review was first conducted on behavior, analysis and seismic retrofit of bridge structures. The literature survey demonstrated immediate research needs on the topic.

The research project consisted of four main tasks. The first task involved an extensive Canada-wide survey of bridge types, designs and column details. This information was necessary to classify the existing bridges in Canada in terms of their structural characteristics to be used in establishing seismic drift demands and capacities. The second task involved determination of inelastic deformation capacities of concrete bridge columns. A computer program was developed to conduct sectional and member analyses in the inelastic range of deformations. The program was verified against experimental data, and used to compute force-displacement relationships of reinforced concrete columns. A large volume of data was generated for columns with different design parameters. The data was presented in the form of tables and charts for an approximate determination of column drift capacities.

The third task of the project included prediction of drift demands for concrete bridge columns. Dynamic inelastic response history analyses of bridges were conducted to establish drift demands during earthquakes. Earthquake records were selected for Eastern and Western Canada. All the relevant components of inelastic deformations were considered through appropriate hysteretic models. Different support conditions were incorporated to simulate the

behavior of different types of bridge bearings. Both drift and ductility demands were computed. The results were presented in the form of tables and charts for bridges with different fundamental periods, geographic locations, support conditions and earthquake intensities.

The fourth task consisted of an experimental investigation, which involved design, preparation and testing of 7 near-full-size bridge columns under simulated seismic loading. A total of 5 circular and 2 square columns were tested for this purpose. A new retrofitting scheme was developed, consisting of external hoops, with or without initial prestressing. The test data provided invaluable information in terms of developing a design procedure for effective and practical retrofitting for seismic resistant bridge columns.

6.2 Conclusions

The following conclusions were drawn from this research project:

- A large proportion of the existing bridges in Canada was designed and built prior to the implementation of earthquake resistant design. This implies that most bridges in Canada were designed prior to 1970's, with potentially deficient column capacities for shear and inelastic deformability.
- Bridge columns designed prior to 1970's were typically reinforced with perimeter hoops spaced at 300 mm, regardless of the column size. In square and rectangular columns, 90-degree hooks were commonly used, while in circular columns lapped circular hoops were employed. Design yield strength of transverse reinforcement was approximately 250 MPa. Concrete strength ranged between 20-25 MPa.
- The majority of existing columns were reinforced with 1% to 2% longitudinal steel, and subjected to axial compression of approximately 10% to 20% of nominal concentric capacity. These columns had a wide range of height-to-width ratios, varying between 2.5 and 10, with a mean value of approximately 5.0.
- The computer software, COLA, developed to compute inelastic force-deformation response of concrete columns under monotonic loading, produce good correlation with experimental data. The features of inelastic material models, stability of longitudinal reinforcement, P-Δ effects, and anchorage slip were found to play important roles on non-linear drift capacity of columns.

- A parametric study was conducted using software COLA. It was found that inelastic drift capacities of columns depend on the shear span-to-depth ratio, axial load ratio, longitudinal reinforcement ratio, material strengths and concrete confinement. It was further observed that coefficient "r_c", defined as $\rho_s f_{yh}/f'_c(A_g/A_c-1)^{-1}$ could be used as a design parameter, reflecting the amount of lateral steel and concrete confinement. While typical drift capacities were found to vary between 1.5% and 5%, columns with shear span-to-depth ratios less then 2.5 were found to be potentially deficient in shear when r_c was below 0.5. The columns were able to develop at least 2% lateral drift when the axial load level was 10% of the nominal concentric capacity or lower. As the axial load level increased, column drift capacity decreased. Columns with aspect ratios of 5.0 and above were able to develop a minimum of 2% lateral drift, irrespective of concrete confinement. The same columns showed improved drift capacity of up to 3% when r_c was increased to 0.5 and 0.8 for columns with 2% and 1% longitudinal reinforcement, respectively.
- The fundamental period of bridge structures is the single most important parameter reflecting structural properties on displacement response, especially under intense earthquake records, when the displacement response is high. Column tip deflection increases approximately linearly with increasing peak ground acceleration. This is true even in the inelastic range of deformations.
- Bridge columns in Ottawa (representing columns in eastern Canada), with a fundamental period of 0.5 sec to 3.5 sec, are not expected to experience a tip deflection in excess of approximately 10 mm. This value was obtained form dynamic inelastic analyses of bridge structures with elastomeric bearings, subjected to a critical artificial earthquake record with 10% probability of occurrence in 50 years. Tip displacement response for the same bridge structures is limited to approximately 6 mm under the 1988 Saguenay record. Since these bridges show elastic response under these earthquake records, changing the bearing type to roller and rocker bearings has the effect of reducing maximum lateral displacement demand even further. Because the existing columns were found to have higher deformabilities than the above displacement demands, it may be concluded that concrete bridge columns in eastern Canada are not vulnerable to seismic damage, unless the ground motion is significantly more intense than those considered in this study. While increasing the peak ground acceleration to 30 % g increased the displacement demand to approximately 25

mm, a further increase to 60 % g produced a maximum displacement demand of approximately 100 mm.

- Bridge columns in Vancouver (representing columns in western Canada), with a fundamental period of 0.5 sec to 3.5 sec, show maximum tip deflection of 66 mm when subjected to the 1940 El Centro record. This value was obtained for bridges with roller or rocker bearings that roll or slide beyond the initial lateral resistance equal to 5% of the weight of the bridge superstructure. Elastomeric bearings reduce the maximum lateral displacement demand by a factor of 2 to 33 mm. The same bridges are not expected to deflect more than approximately 15 mm, when subjected to a critical artificial earthquake record with 10% probability of occurrence in 50 years. While increasing the peak ground acceleration to 30% g increased the displacement demand to approximately 240 mm, a further increase to 60% g produced a maximum displacement demand of approximately 725 mm. These results indicate that concrete bridge columns in western Canada may be vulnerable to seismic damage.
- The new retrofitting technique that was developed as part of this investigation resulted in significant improvements in column drift capacities. The drift capacity of retrofitted columns increased from 1% to 6% in most cases.
- The new retrofitting procedure developed was shown to be effective in eliminating shear failures in columns with shear span-to-depth ratios of 2.4 to 2.7. These columns changed their mode of behavior from a brittle shear dominant response to a ductile flexure dominant response. The external prestressing also provided improved concrete confinement, enhancing flexural deformability up to and exceeding 6% lateral drift.
- Prestressing external hoops was shown to improve column deformability. The initial prestressing of up to approximately 25% of ultimate steel strength improved inelastic deformability while also limiting diagonal shear cracking. However, this improvement was evident only after 5% lateral drift. Until then, external hoops without prestressing were sufficiently effective in controlling diagonal shear cracking and developing passive confinement pressure under laterally expanding concrete. The active lateral pressure produced by initial prestressing may be necessary for columns with very high drift demands.

- The spacing of external hoops was found to be an important parameter. The column with a hoop spacing of 300 mm (approximately 1/2 the column sectional dimension) could not maintain its strength beyond 2% of lateral drift even though it had sufficiently high prestressing. A companion column with an external hoop spacing of 150 mm developed a lateral drift of 5% without any significant strength decay.
- High-strength steel straps used as an alternative to prestressing strands proved to be effective during initial loading. However, their effectiveness seized beyond 2% lateral drift when the straps failed near the anchor locations. This shows that a stronger strap, or an improved anchorage technique may have produced a similar improvement in drift capacity as that obtained by using prestressing strands.
- The new retrofitting technique developed in this research program offers a number practical advantages, including ease, speed and economy of construction.

6.3 Recommendations for Future Research

The following are recommended for future research:

- Further column tests are needed to extend the retrofitting scheme developed in the current study to columns with different shear-span-to-depth ratios, especially to those that behave predominantly in the flexure mode.
- Additional tests are necessary to derive explicit relationships between the level of prestressing, spacing of hoops and lateral drift capacity.
- The proposed retrofitting procedure may be extended to building columns that are subjected to higher levels of axial compression with smaller cross-sectional dimensions. Both analytical and experimental researches are needed to further investigate this new application.
- Introducing a more elaborate analytical model for bar buckling may refine the analytical procedure used for the computation of drift capacity. Hence further analytical research is recommended with an improved model for bar buckling.
- Additional dynamic analyses of bridges under different ground motions and levels of probability of exceedence may be needed to establish seismic drift demands more accurately.

References

Akkari, M.; Hoffman, F. (1993), "San Francisco Bayshore Viaduct Seismic Retrofit," Structural Engineering in Natural Hazards Mitigation: Proceedings of Papers Presented at the Structures Congress '93 Published by ASCE, New York, NY, pp. 391-396

Alcocer, S. M. (1993), "RC Frame Connections Rehabilitated by Jacketing," Journal of Structural Engineering, v 119, n 5, pp. 1413-1431

Alcocer, S. M.; Jirsa J. O. (1993), "Strength of Reinforced Concrete Frame Connections Rehabilitated by Jacketing," ACI Structural Journal, v 90, n 3, pp. 249-261

Alsiwat, J. M.; Saatcioglu M. (1992), "Reinforcement Anchorage Slip Under Monotonic Loading", Journal of Structural Engineering, v 118, n 9, pp. 2421-2438

Astaneh-Asl, A.; Shen, J. (1993), "Rocking Behavior and Retrofit of Tall Piers," Structural Engineering in Natural Hazards Mitigation: Proceedings of Papers Presented at the Structures Congress '93, Published by ASCE, New York, NY, pp. 121-126

Bertero, V. V., (1985), "Earthquake Engineering," Structural Engineering Slide Library, Volume 4, Set Journal of International Structural Slides.

Buckle, I. G.; Mayes, R. L. (1989), "The Application of Seismic Isolation to Bridges," Seismic Engineering Research Practice, Published by ASCE, New York, NY, pp. 633-642

Bruneau, M. (1990), "Preliminary Report of Structural Damage From the Loma Prieta (San Francisco) Earthquake of 1989 and Pertinence to Canadian Structural Engineering Practice," Canadian Journal of Civil Engineering, v 17, pp. 198-208

Chai, Y. H.; Priestley, M. J. N.; Seible, F. (1991), "Seismic Retrofit of Circular Bridge Columns for Enhanced Flexural Performance, ACI Structural Journal, v 88, n 5, pp. 572-584

Chan, W. L. (1955), "The Ultimate Strength and Deformations of Plastic Hinges in Reinforced Concrete Frameworks," Magazine of Concrete Research, v 7, n 21, pp. 121-132

Coffman, H. L.; Marsh, M. L.; Brown, C. B. (1993), "Seismic Durability of Retrofitted Reinforced-Concrete Columns," Journal of Structural Engineering, v 119, n 5, pp. 1643-1661

Concrete Design Handbook, Canadian Portland Cement Association, 1985

Concrete Design Handbook, Canadian Portland Cement Association, 1995

Eberhard, M. O.; Stanton, J. F.; Trochalakis, P. (1996) "Design of Seismic Restrainers," Proceedings of the Fourth National Workshop on Bridge Research in Progress, June 17-19, Buffalo, New York, pp. 283-286

Ehsani, M. R.; Saadatmanesh, H. (1990), "Fiber Composite Plates for Strengthening Bridge Beams," Composite Structures, v 15, n 4, pp. 343-355

Ersoy, U.; Tankut, A. T.; Suleiman, R. (1993), "Behavior of Jacketed Columns," ACI Structural Journal, v 90, n 3, pp. 288-293

Gamble, W. L.; Hawkins, N. M.; Kaspar, I. I. (1996), "Seismic Retrofitting Experience and Experiments in Illinois," Proceedings of the Fourth National Workshop on Bridge Research in Progress, June 17-19, Buffalo, New York, pp. 247-250

Ghobarah, A.; Tso, W. K. (1974), "Seismic Analysis of Skewed Highway Bridges with Intermediate Supports," Earthquake Engineering and Structural Dynamics, v 2, pp. 235-248

Ghobarah, A.; Ali, H. M. (1988), "Seismic Performance of Highway Bridges," Engineering Structures, v 10, n 3, pp. 157-166

Harper, K. (1991), "Retrofitting Northwest Connector for Seismic Forces," Lifeline Earthquake Engineering: Proceedings of the Third US Conference, Published by ASCE, New York, NY, pp. 131-140

Hognestad, E. (1951), "A Study of Combined Bending and Axial Load in Reinforced Concrete Members," University of Illinois, Engineering Experimental station, Bulletin Series No. 399, pp. 128.

Jaradat, O. A.; McLean, D. I.; Marsh, M. L. (1996), "Strength Degradation of Existing Bridge Column," Proceedings of the Fourth National Workshop on Bridge Research in Progress, June 17-19, Buffalo, New York, pp. 253-256

Jones, R. M.; Schroeder, I. A. (1991), "Design and Construction Aspects of the Structure Research Tests at Cypress Viaduct," Lifeline Earthquake Engineering: Proceedings of the Third US Conference Published by ASCE, New York, NY, pp. 1013-1022

Kent, D. C.; Park, R. (1971), "Flexural Members with Confined Concrete," Journal of Structural Division, ASCE, v 97, pp. 1969-1990

King, J. W. H. (1946), "The effect of Lateral Reinforcement in Reinforced Concrete Columns," The Structural Engineer, v 24, n 7, pp. 355-388

Kunnath S. K., Reinhorn A. M., Park Y. J. (1990), "Analytical Modelling of Inelastic Seismic Response of R/C Structures," ASCE, Journal of Structural Engineering, v 116, n 4, pp. 996-1017

Kunnath, S. K.; Gross, J. L. (1996), "Inelastic Response of the Cypress Viaduct to the Loma Prieta Earthquake," Engineering Structures, v 17, n 7, pp. 485-493

Liu, W. D.; Nobari, F. S.; Imbsen, R. A. (1989), "Dynamic Response Prediction for Earthquake Resistance Design of Bridge Structures," Seismic Engineering Research Practice, Published by ASCE, New York, NY, pp. 1-10

Lobo, R. F.; Bracci, J. M.; Shen, K. L.; Reinhorn, A. M.; Soong, T. T. (1993), "Inelastic Response of Reinforced Concrete Structures with Viscoelastic Braces," Earthquake Spectra, v 9, n 3, pp. 419-446

Mau, S. T., El-Mabsout, M (1989), "Inelastic Buckling of Reinforcing Bars," Journal of Engineering Mechanics, ASCE, v 115, n 1, pp. 1-17

Mau, S. T. (1990), "Effect of Tie Spacing on Inelastic Buckling of Reinforcing Bars," ACI Structural Journal, v 87, n 6, pp. 671-677

Meyer, C.; Roufaiel, M. S. L.; Arzoumandis S. G. (1983), "Analysis of Damaged Concrete Frames for Cyclic Loads," Earthquake Engineering and Structural Dynamics, v 11, pp. 207-228

Meyer, C. (1989), "Inelastic Seismic Analysis of Concrete Buildings," Seismic Engineering Research Practice, Published by ASCE, New York, NY, pp. 837-846

Mitchell, D.; Tinawi, R.; Sexsmith, R. G (1991), "Performance of Bridges in the 1989 Loma Prieta Earthquake - Lessons for Canadian Designers," Canadian Journal of Civil Engineering, v 18, pp. 711-734

Mitchell, D.; Sexsmith, R. G; Tinawi, R. (1994), "Seismic Retrofitting Techniques for Bridges - A State-of-the-Art Report," Canadian Journal of Civil Engineering, v 21, pp. 823-835

Mitchell, D.; DeVall, R. H.; Saatcioglu, M.; Tinawi, R.; Tremblay, R. (1995), "Damage to Concrete Structures Due to the 1994 Northridge Earthquake," Canadian Journal of Civil Engineering, v 22, pp. 361-377

Mitchell, D.; Bruneau, M.; Williams, M.; Anderson, D.; Saatcioglu, M.; Sexsmith, R. G. (1995), "Performance of Bridges in the 1994 Northridge Earthquake," Canadian Journal of Civil Engineering, v 22, pp. 415-427

Ontario Highway Bridge Design Code, Ministry of Transportation and Communications, Highway Engineering Division, 1983

Ontario Highway Bridge Design Code, Ministry of Transportation, Quality and Standards Division, Third edition, 1991

Park, R., Paulay, T. (1975), "Reinforced Concrete Structures," John Wiley and Sons, pp. 769

Paulay T.; Priestley, M. J. N (1992), "Seismic Design of Reinforced Concrete and Masonry Buildings," John Wiley & Sons, Inc., USA, 744 p

Perry, S. H.; Cheong, H.; Armstrong, W. E. (1987), "Improved Strength and Ductility in Concrete Elements for Earthquake Resistance," Proceedings of the 4th Canadian Conference on Earthquake Engineering, University of British Columbia, Vancouver, pp. 92-101

Popovics, S. (1973), "Analytical Approach to Complete Stress-Strain Curves,' Cement and Concrete Research, v 3, n 5, pp. 583-599

Prakash, V.; Powell, G. H.; Campbell, S. (1993), "DRAIN-2DX Base Program Description and User Guide," Report No. UCB/SEMM-93-17, Department of Civil Engineering, University of California, Berkeley

Priestley, M. J. N.; Seible, F.; Anderson, D. L. (1993), "Proof Test of a Retrofit Concept for the San Francisco Double-Deck Viaducts: Part 2 - Test Details and Results," ACI Structural Journal, v 90, n 6, pp. 616-631

Priestley, M. J. N.; Verma R.; Xiao, Y. (1994), "Seismic Shear Strength of Reinforced Concrete Columns," ASCE, Journal of Structural Engineering, v 120, n 8, pp. 2310-2329

Razvi, S. R., Saatcioglu, M. (1996), "Design of R/C Columns for Confinement Based on Lateral Drift," Report No. OCEERC 96-02, Department of Civil Engineering, University of Ottawa

Richart, F. E., Brandtzaeg, A., Brown, R. L., (1928), "A Study of the Failure of Concrete Under Combined Compressive Stress," University of Illinois, Engineering Experimental Station, Bulletin No. 185, pp. 104

Richart, F. E., Brandtzaeg, A., Brown, R. L., (1929), "The Failure of Plain and Spirally Reinforced Concrete in Compression," University of Illinois, Engineering Experimental Station, Bulletin No. 190, pp. 74

Roberts, J. E. (1991), "Recent Advances in Seismic Design and Retrofit of California Bridges," Lifeline Earthquake Engineering: Proceedings of the Third US Conference, Published by ASCE, New York, NY, pp. 52-64

Rodriguez, M.; Park, R. (1991), "Repair and Strengthening of Reinforced Concrete Buildings for Seismic Resistance," Earthquake Spectra, v 7, n 3, pp. 439-459

Roy, H. E. M.; Sozen, M. A. (1963), "A Model to Simulate the Response of Concrete to Multi-Axial Loading," Structural Research Series No. 268, Civil Engineering Studies, University of Illinois

Saadeghvaziri, A. M.; Foutch, D. A. (1989), "Effects of Vertical Motion on the Inelastic Behavior of Highway Bridges," Seismic Engineering Research Practice, Published by ASCE, New York, NY, pp. 51-61

Saatcioglu, M. (1994), "Performance of Reinforced Concrete Structures During the 1994 Northridge Earthquake," Preliminary Report on the Northridge, California, Earthquake of January 17, 1994, Canadian Association for Earthquake Engineering, Vancouver, Canada, pp. 421-452.

Saatcioglu, M. and Razvi, S. (1992), "Strength and Ductility of Confined Concrete," Journal of Structural Engineering, ASCE, v 118, n 6, pp. 1590-1607

Saiidi, M.; Ghusn, G. (1989), "The Effect of Stiffness Degradation on the Three-Dimensional Seismic Response of Highway Bridges," Seismic Engineering Research Practice, Published by ASCE, New York, NY, pp. 21-30

Seim, C.; Rodriguez, S. (1993), "Seismic Performance and Retrofit of the Golden Gate Bridge," Structural Engineering in Natural Hazards Mitigation: Proceedings of Papers Presented at the Structures Congress '93, Published by ASCE, New York, NY, pp. 133-138

Selna, L. G.; Malvar, L. J.; Zelinski, R. J. (1989), "Bridge Retrofit Testing: Hinge Cable Restrainers," Journal of Structural Engineering, v 115, n 4, pp. 920-934

Selna, L. G.; Malvar, L. J.; Zelinski, R. J. (1989), "Box Girder Bar and Bracket Seismic Retrofit Devices," ACI Structural Journal, v 86, n 5, pp. 532-540

Sheikh , S. A. and Uzumeri, S. M. (1980), "Strength and Ductility of Tied Columns," Journal of Structural Engineering, ASCE, v 106, n 5, pp. 1077-1102

Sheikh, S. A. and Uzumeri, S. M. (1982), "Analytical Model for Concrete Confinement in Tied Columns," Journal of Structural Engineering, ASCE, v 108, n 5, pp. 2703-2723

Somani, D. R. (1987), "Seismic Behaviour of Girder Bridges for Horizontally Propagating Waves," Earthquake Engineering and Structural Dynamics, v 15, pp. 777-793

Spyrakos, C. C. (1990), "Assesment of SSI on the Longitudinal Seismic Response of Short Span Bridges," Engineering Structures, v 12, n 1, pp. 60-66

Stanton J. F.; MacRae, G. A.; Nosho, K. J. (1996), "Carbon Fiber Seismic Retrofit of Poorly Confined Square Reinforced Concrete Columns Subjected to Large Axial Forces," Proceedings of the Fourth National Workshop on Bridge Research in Progress, June 17-19, Buffalo, New York, pp. 265-268

Takizawa, H.; Aoyama, H. (1976), "Biaxial Effects in Modeling Earthquake Response of Reinforced Concrete Structures," Earthquake Engineering and Structural Dynamics, v 4, pp. 523-552

Tarakji, G. (1991), "Lessons Not Learned From the Catastrophic Collapse of Highway Structures in the 1989 Loma Prieta Earthquake," Lifeline Earthquake Engineering: Proceedings of the Third US Conference, Published by ASCE, New York, NY, pp. 1052-1060

Vallenas, J., Bertero, V., Popov, E. P. (1977), "Concrete Confined by Rectangular Hoops and Subjected to Axial Load," Report No. UCB/EERC-77/13, Earthquake Engineering Research Center, College of Engineering, University of California, Berkeley, pp. 14

Valluvan, R.; Kreger, M. E.; Jirsa, J. O. (1993), "Strengthening of Column Splices for Seismic Retrofit on Nonductile Reinforced Concrete Frames," ACI Structural Journal, v 90, n 4, pp. 432-433

Wilson, J. C. (1986), "Analysis of the Observed Seismic Response of a Highway Bridge," Earthquake Engineering and Structural Dynamics, v 14, pp. 339-354

Xiao, Y.; Ma, R. (1996), "Analysis and Design of Bridge Columns with Lap-Spliced Longitudinal Reinforcement," Proceedings of the Fourth National Workshop on Bridge Research in Progress, June 17-19, Buffalo, New York, pp. 259-262

Yashinsky, M. (1991), "The Seismic Retrofit of Bridge Foundations," Lifeline Earthquake Engineering: Proceedings of the Third US Conference, Published by ASCE, New York, NY, pp. 166-185

Zelinski, R. J. (1991), "San Francisco Double-Deck Viaduct Retrofits," Lifeline Earthquake Engineering: Proceedings of the Third US Conference, Published by ASCE, New York, NY, pp. 121-130

Zelinski, R. J.; Dubovik, A. T. (1991), "Seismic Retrofit of Highway Bridge Structures," Lifeline Earthquake Engineering: Proceedings of the Third US Conference, Published by ASCE, New York, NY, pp. 11-120

Appendix A

Source Code of COLA

```
{$D+,L+}
program sectional_analysis (input, output);

uses dos, crt, cit_core;

const n_1 = 100;
      n_2 = 275;
      n_3 = 50;
      n_4 = 500;
      n_5 = 500;

label 10, 20, 30;

type array_1 = array [1..n_1] of real;
     array_2 = array [1..n_2] of real;
     array_3 = array [1..n_3] of real;
     array_4 = array [1..n_4] of real;
     array_5 = array [1..n_5] of real;
     file_name = string[15];
     fail_message = string[52];

var r, cov, s, fco, eo, eo85, eo_ini, eou, fy, ey, fsh, esh, fu, esu,
    axial_load, euc, euc_inc, euc_max, sbd, lbd, t_l, lba, sba, cr_c, cr_mom,
    cr_cur, t_s, fcc, e1, e85, k_fac, accuracy, c_inc, alfa_inc, c,
    force_steel, force_conc, phi, diff, mom_arm, can_len, cr_strain, small_ss,
    final_t_ss, abs_small_ss, abs_big_ss, old_c_ss, old_t_ss, ext_ss, euc_in,
    ecc_in, es_in, sl, hl, bar_ext, r_d, strip_height, big_ss, rot, width,
    h_dim, v_dim, conc_strain, m_p_moment, area_conc_conf, area_conc_unconf,
    area_steel, phi_c, phi_s, comp_height_limit, percent_finish, final_c,
    po_code_with_conf, po_code_without_conf, po_real, m_p_force, tie_sp, sfy,
    final_strain, strain, strain_in, sp_v_tie, sp_h_tie, mr_bal, pr_bal,
    mr_ben, pr_ben, mom_zero_strain_before, mom_zero_strain_after,
    c_mom_zero_strain_before, c_mom_zero_strain_after, ecc_20_fcc,
    mom_zero_strain, final_c_ss, spacing, mom_ult, for_ult, z_m_euc_inc: real;

    dist_st_1, dist_st_2, force_st, strain_st, stress_st, area_st, str_con,
    exes_for: array_1;

    curvature, moment, el, pl, flex_def, slip_def, lat_for, lat_for_p_delta,
    slip_slope, tot_def, conf_conc_strain, unconf_conc_strain, fuc_array,
    fcc_array, es_t_p, es_c_p, es_c_p_neg, fs_t_array, fs_c_array,
    fs_c_array_neg: array_2;

    h_tie_angle, v_tie_angle: array_3;
```

```
  pr, mr: array_4;

  dcf, dcf_dist: array_5;

  nlb, lbn, sbn, c_m, cc, i, j, m_c, num_1, num_2, num_3, num_4, num_5,
  a_t_1, a_t_2, a_t_3, a_t_4, a_t_5, origmode, m_p, n_h_tie, n_v_tie,
  final_data_num, small_i, big_i: integer;

  out_1, out_2, st_dec, buc_dec, cover_dec, core_dec, m_p_dec: char;

  fm, fsl, ff, fd, func, fcon, fo, fp, fs_t, fs_c, fl, flpd, fp_1, fmp, fc,
  fsm: text;

  file_1_in, file_2_in, file_cur_mom, file_def_mom, file_slip_mom, file_out,
  col_type, file_euc_fuc, file_ecc_fcc, file_es_t_fs, file_es_c_fs,
  file_plot,file_flex_mom, file_def_lat_for, file_def_l_f_p_d, in_col_type,
  in_gen_data, gen_name, file_mom_axi_for, file_clean,
  file_slp_slo_mom: file_name;

  f_m: fail_message;

  c_flag, con_flag, st_c_flag, st_t_flag, d_flag, array_1_cond, mf_flag,
  array_2_cond, array_3_cond, array_4_cond, conc_strain_flag, st_b_flag,
  out_flag, final_cc_flag, z_m_flag_large, z_m_flag_small,
  z_m_flag: boolean;

{
  definition of variables used in the main program:

    area_st          : area of steel for each layer in rec. or sqr. columns
    axial_load       : axial loading in N
    a_t_1            : first array type
    array_1_cond     : true if num_1 <= limit in a_t_1, else false
    a_t_2            : second array type
    array_2_cond     : true if num_2 <= limit in a_t_2, else false
    a_t_3            : third array type
    array_3_cond     : true if num_3 <= limit in a_t_3, else false
    a_t_4            : first array type
    array_4_cond     : true if num_4 <= limit in a_t_4, else false
    accuracy         : limit to stop iteration
    alfa_inc         : incremental angle to calculate strip widths
    area_conc_conf   : confined concrete cross section area in sq. mm
    area_conc_unconf : unconfined concrete cross section area in sq. mm
    area_steel       : steel cross section area in sq. mm
```

big_ss : returns largest value of reinforcing bar stress
bar_ext : extension of bar due to yielding and slipping in mm

col_type : type of column (rectangular, square, or circular)
cov : concrete cover in mm
c_inc : incremental compresion height value in mm
c : compression height in mm
can_len : cantilever length of column in mm
c_m : counter
curvature : curvature of the column
c_flag : true until section's forces balance
cc : counter to count number of strips for a given c
con1_flag : true until core concrete strength falls below 20%
con2_flag : true until core concrete strength falls below 20%
c_array : compression height values for each concrete strain
cr_c : cracking neutral axis in mm
cr_mom : cracking moment in N.mm
cr_cur : cracking curvature
cr_strain : cracking strain
conc_strain : concrete strain used in M-P interaction calculation
comp_height_limit: compression heigth limit in M-P inter. calculation
conc_strain_flag : true until unconf. conc. strain exceeds the limit
cs : concrete strength at longitudinal bar level

dist_st_1 : dist. between surface and centerline of long. steel
dcf : concrete force at each strip
dcf_dist : dist. between the centroid of the section and strip
diff : sum of forces due to steel, concrete, and axial load
dist_st_2 : distance between top steel and others
d_flag : true if plastic hinge length is less than the width
flex_def : lateral deformation at top of column due to flexure

e1 : strain at maximum stress for core concrete
e85 : strain at 85% of maximum stress for core concrete
eo : strain at maximum stress for cover concrete
eo85 : strain at 85% of maximum stress for cover concrete
eo_ini : starting cover concrete strain
eou : ending cover concrete strain
ey : steel strain at yield
esh : steel strain at strain hardening
esu : steel strain at ultimate
euc : cover concrete strain
euc_inc : incremental cover concrete strain
euc_max : ending cover conctere strain
euc_array : cover concrete strain values

el : elastic length in hinging region of the column
euc_p : array of cover concrete strains for plotting
euc_in : cover concrete strain for plotting
ecc_p : array of confined core concrete strains for plotting
ecc_in : confined core concrete strains for plotting
es_p : array of steel strains for plotting
es_in : steel strain for plotting
exes_for : excess force in compression block due to long. reinf.

file_1_in : input file name for rec., square, or circular column
file_2_in : common input file name for rec., sqr., or cir. column
fcc : maximum core (confined) concrete stress in Mpa
fy : steel strength at yield in MPa
fsh : steel strength at strain hardening in MPa
fu : steel strength at ultimate in MPa
file_cur_mom : curvature vs moment file
file_flex_mom : top deflection due to flexure vs moment file
file_slip_mom : top deflection due to bar slip vs moment file
file_def_mom : total top deflection vs moment file
file_out : output file
file_euc_fuc : unconfined concrete model file
file_ecc_fcc : confined concrete model file
file_es_fs : steel model file
file_plot : plot files
file_def_lat_for : total deflection vs lateral force file
file_def_l_f_p_d : tot. def. w/ p - delta effect vs lateral force file
file_mom_axi_for : moment vs axial force interaction file
file_slp_slo_mom : rotation due to bar slip vs moment file
fco : maximum cover (unconfined) concrete stress in MPa
final_ss : returns final value of reinforcing bar stress
force_steel : section's force due to steel reinforcement
force_conc : section's force due to concrete (cover + core)
final _euc : final cover concrete strain value
final _ecc : final confined concrete strain value
fuc_array : array of max. cover concrete stresses for plotting
fcc_array : array of max. core concrete stresses for plotting
fs_array : array of steel strengths for plotting
func : file for unconfined concrete strain and stress values
fcon : file for confined concrete strain and stress values
fs : file for steel strain and stress values
fm : file for curvature and moment values
fsm : file for rotation due to slip vs moment values
fsl : file for top defl. due to bar slip and moment values
ff : file for top defl. due to flexure and moment values
fd : file for total top deformation and moment values

fl : file for total top def. and lateral force values
fmp : file for moment and axial force interaction values
fp_l : file name containing all plot file names
fp : file containing all plot file names
fo : file for output
f_t : concrete failure type
f_m : concrete failure message
file_clean : bacth file for erasing previously created data files
f_c : file containing data files for erasing

gen_name : common file indicator

hl : parameter of deformed bar
h_dim : horizontal dimension of a rectangular column
h_tie_angle : angle between horizontal tie and vertical plane

i : index
in_col_type : rectangular, square, or circular file indicator
in_gen_data : common file indicator

j : index

k_fac : ratio of confined to unconfined concrete stress

lbn : longitudinal bar number
lbd : logitudinal bar diameter
lba : longitudinal bar area
lat_for : lateral force at column base
lat_for_p_delta : lateral force at column base including P-Delta
large_c : compression heigth value used in M-P inter. calc.

moment : moment of the column
mom_arm : moment arm bet. centerline of steel and neutral axis
m : index
m_p : index for M-P calculation
m_p_moment : moment value in M-P calculation
mr : total moment in M-P calculation
m_p_force : total axial load in M-P calculation
mr_bal : balanced bending moment in N-mm

nlb : number of layers of bars in rec. or square columns
number of longitudinal bars in circular columns
num_1 : limit in the first array type
num_2 : limit in the second array type
num_3 : limit in the third array type

new_ss : initial value of small_ss
n_h_tie : number of horizontal ties in a stirrup
n_v_tie : number of vertival ties in a stirrup

origmode : original screen mode
old_ss : previous steel strength
out_1 : controls screen or file output
out_2 : controls another output to screen or file

phi : curvature
phi_c : concrete strength coefficient
phi_s : steel strength coefficient
pl : plastic length in hinging region of the column in mm
pr : total axial load in M-P calculation in N
po_code : code value of axial load capacity of column in N
po_real : real (calc.) value of axial load cap. of col. in N
percent_finish : percentage completed of M - P interaction calculation
pr_bal : balanced axial load in N

r : radius of circular column in mm
rot : orientation of top reinforcement (clockwise - degree)
r_d : reinforcement depth

s : spacing of stirrups (pitch) in cir. columns in mm
sbn : stirrup bar number
sf : steel force for each bar
ss : steel strain for each bar
strip_height : maximum strip width of concrete in mm
sbd : stirrup bar diameter
sba : stirrup bar area
sl : parameter of deformed bar
st_flag : true until steel strength goes beyond ultimate
small_ss : returns smallest value of reinforcing bar stress
slip_slope : slope of column due to extension of long. bars
sfy : stirrup steel yield strength
st_dec : input decision on bar no. or bar dia., and def. char.
sp_v_tie : center to center ver. tie spacing in a stirrup in mm
sp_h_tie : center to center hor. tie spacing in a stirrup in mm

t_l : dist. between surface and centerline of long. steel
t_s : dist. between surface and centerline of stirrup
slip_def : lateral deformation at top of column due to bar slip
tot_def : lat. def. at top of col. due to flex. and bar slip
tie_sp : spacing of stirrups in sqr. and rec. columns in mm

```
    v_dim          : vertical dimension of a rectangular column
    v_tie_angle    : angle between vertical tie and horizontal plane

    width          : width of square column in mm
}

procedure READ_GENERAL_INPUT (var f_in, input_general: file_name;
                        var lon_bar_num, stir_bar_num:integer;
                        var unconf_max_conc_str,
                           unconf_conc_strain_100fc,
                           unconf_conc_strain_85fc,
                           unconf_conc_strain_ult, steel_str_yield,
                           steel_strain_yield, steel_str_strain_hard,
                           steel_strain_strain_hard, steel_str_ult,
                           steel_strain_ult, strip_height, axial_load,
                           cantilever_length, conc_str_fac,
                           steel_str_fac, bar_diameter, hl, sl,
                           stir_bar_diameter, stir_steel_str_yield
                           : real;
                        var f_uc, f_cc, f_t_st, f_c_st, f_mc, f_fl,
                           f_fssm, f_sl, f_td, f_fd, f_fdpd, f_mp, f_p,
                           f_o, f_c: file_name;
                        var steel_decision, buckling_decision,
                           cover_model, core_model,
                           m_p_interaction_decision: char);
{
  reads general input values from a file

  called in main program
}
var fi: text;
   dummy_name: string[70];
begin
    assign(fi, f_in);
    reset(fi);
    readln(fi, input_general);
    if input_general = 'general' then
    begin
        for i:= 1 to 2 do readln(fi, dummy_name);
        readln(fi, dummy_name, cover_model);
        readln(fi, dummy_name, core_model);
        readln(fi, dummy_name, unconf_max_conc_str);
        readln(fi, dummy_name, unconf_conc_strain_100fc);
        readln(fi, dummy_name, unconf_conc_strain_85fc);
        readln(fi, dummy_name, unconf_conc_strain_ult);
```

```
readln(fi, dummy_name, conc_str_fac);
readln(fi, dummy_name);
readln(fi, dummy_name, steel_decision);
readln(fi, dummy_name, buckling_decision);
if steel_decision = 'Y' then
begin
    for i:= 1 to 2 do readln(fi, dummy_name);
    readln(fi, dummy_name, lon_bar_num);
    for i:= 1 to 5 do readln(fi, dummy_name)
end;
if steel_decision = 'N' then
begin
    for i:= 1 to 4 do readln(fi, dummy_name);
    readln(fi, dummy_name, bar_diameter);
    readln(fi, dummy_name);
    readln(fi, dummy_name, hl);
    readln(fi, dummy_name, sl)
end;
readln(fi, dummy_name, steel_str_yield);
readln(fi, dummy_name, steel_strain_yield);
readln(fi, dummy_name, steel_str_strain_hard);
readln(fi, dummy_name, steel_strain_strain_hard);
readln(fi, dummy_name, steel_str_ult);
readln(fi, dummy_name, steel_strain_ult);
readln(fi, dummy_name, steel_str_fac);
if steel_decision = 'Y' then
begin
    for i:= 1 to 2 do readln(fi, dummy_name);
    readln(fi, dummy_name, stir_bar_num);
    for i:= 1 to 2 do readln(fi, dummy_name)
end;
if steel_decision = 'N' then
begin
    for i:= 1 to 4 do readln(fi, dummy_name);
    readln(fi, dummy_name, stir_bar_diameter)
end;
readln(fi, dummy_name, stir_steel_str_yield);
readln(fi, dummy_name, axial_load);
readln(fi, dummy_name, cantilever_length);
readln(fi, dummy_name, strip_height);
readln(fi, dummy_name, m_p_interaction_decision);
readln(fi, dummy_name);
readln(fi, dummy_name, f_uc);
readln(fi, dummy_name, f_cc);
readln(fi, dummy_name, f_t_st);
```

```
        readln(fi, dummy_name, f_c_st);
        readln(fi, dummy_name, f_mc);
        readln(fi, dummy_name, f_fl);
        readln(fi, dummy_name, f_fssm);
        readln(fi, dummy_name, f_sl);
        readln(fi, dummy_name, f_td);
        readln(fi, dummy_name, f_fd);
        readln(fi, dummy_name, f_fdpd);
        readln(fi, dummy_name, f_mp);
        readln(fi, dummy_name, f_p);
        readln(fi, dummy_name, f_o);
        readln(fi, dummy_name, f_c)
    end;
    close(fi)
end;

procedure READ_CIRCULAR_INPUT (var f_in, input_column: file_name;
                        var cover, radius, rotation, spacing: real;
                        var num_lon_bar:integer);
{
  reads input values for circular columns from a file

  called in main program
}
var fi: text;
   dummy_name: string[70];
begin
    assign(fi, f_in);
    reset(fi);
    readln(fi, input_column);
    if input_column = 'circular' then
    begin
        readln(fi, dummy_name, cover);
        readln(fi, dummy_name, radius);
        readln(fi, dummy_name, num_lon_bar);
        readln(fi, dummy_name, spacing);
        readln(fi, dummy_name, rotation)
    end;
    close(fi)
end;

procedure READ_SQUARE_INPUT (var f_in, input_column: file_name;
                      var column_width, tie_spacing,
                        dist_ver_cross_ties, dist_hor_cross_ties
                        : real;
```

```
                    var num_hor_cross_ties, num_ver_cross_ties,
                      num_layer: integer;
                    var steel_area, steel_distance: array_1;
                    var hor_tie_angle, ver_tie_angle: array_3);
{
  reads input values for square columns from a file

  called in main program
}
var fi: text;
   dummy_name: string[70];
   i: integer;
begin
    assign(fi, f_in);
    reset(fi);
    readln(fi, input_column);
    if input_column = 'square' then
    begin
        readln(fi, dummy_name, column_width);
        readln(fi, dummy_name, tie_spacing);
        readln(fi, dummy_name, num_layer);
        for i:= 1 to num_layer do readln(fi, dummy_name, steel_area[i]);
        for i:= 1 to num_layer do readln(fi, dummy_name, steel_distance[i]);
        readln(fi, dummy_name, num_hor_cross_ties);
        for i:= 1 to num_hor_cross_ties do
           readln(fi, dummy_name, hor_tie_angle[i]);
        readln(fi, dummy_name, dist_ver_cross_ties);
        readln(fi, dummy_name, num_ver_cross_ties);
        for i:= 1 to num_ver_cross_ties do
           readln(fi, dummy_name, ver_tie_angle[i]);
        readln(fi, dummy_name, dist_hor_cross_ties);
    end;
    close(fi)
end;

procedure READ_RECTANGULAR_INPUT (var f_in, input_column: file_name;
                    var hor_dim, ver_dim, tie_spacing,
                      dist_ver_cross_ties, dist_hor_cross_ties
                      : real;
                    var num_hor_cross_ties, num_ver_cross_ties,
                      num_layer: integer;
                    var steel_area, steel_distance: array_1;
                    var hor_tie_angle, ver_tie_angle: array_3);
{
  reads input values for rectangular columns from a file
```

```
  called in main program
}
var fi: text;
   dummy_name: string[70];
   i: integer;
begin
    assign(fi, f_in);
    reset(fi);
    readln(fi, input_column);
    if input_column = 'rectangular' then
    begin
        readln(fi, dummy_name, hor_dim);
        readln(fi, dummy_name, ver_dim);
        readln(fi, dummy_name, tie_spacing);
        readln(fi, dummy_name, num_layer);
        for i:= 1 to num_layer do readln(fi, dummy_name, steel_area[i]);
        for i:= 1 to num_layer do readln(fi, dummy_name, steel_distance[i]);
        readln(fi, dummy_name, num_hor_cross_ties);
        for i:= 1 to num_hor_cross_ties do
           readln(fi, dummy_name, hor_tie_angle[i]);
        readln(fi, dummy_name, dist_ver_cross_ties);
        readln(fi, dummy_name, num_ver_cross_ties);
        for i:= 1 to num_ver_cross_ties do
           readln(fi, dummy_name, ver_tie_angle[i]);
        readln(fi, dummy_name, dist_hor_cross_ties);
    end;
    close(fi)
end;

procedure CLICK;
{
  makes sound

  called in NOFILE
         CHECK_ARRAY
         main program
}
begin
    sound(2000);
    delay(75);
    nosound
end;

function EXIST (filename: file_name): boolean;
```

```
{
  checks if the input file exists

  caled in main program
}
var f: file;
begin
    {$I-}
    assign(f, filename);
    reset(f);
    close(f);
    {$I+}
    if IOresult <> 0 then exist:= false
    else exist:= true
end;

procedure NOFILE (filename: file_name);
{
  displays message if the input file does not exist

  called in main program
}
begin
    clrscr;
    click;
    gotoxy(6, 13);
    textcolor(lightgreen);
    write(' File ', chr(174));
    textcolor(lightred + blink);
    write(filename);
    textcolor(lightgreen);
    writeln(chr(175), ' does not exist');
    textcolor(lightgray)
end;

procedure BEKLE;
{
  stops the program until a letter "c" or "C" is entered

  called in LIST_DIR_FILES
        CHECK_ARRAY
        main program
}
begin
    repeat
```

```
        gotoxy(6,24);
        textcolor(white);
        writeln('Enter < C > to continue...')
    until upcase(readkey) = 'C';
    textcolor(lightgray);
    clrscr
end;

procedure LIST_DIR_FILES (text: file_name);
{
  lists files in a directory

  called in main program
}
var
  DirInfo: SearchRec;
  i: integer;
procedure list_dir_files_heading;
begin
    textcolor(lightred);
    writeln('Please identify your filename for');
    gotoxy(15, 2);
    textcolor(lightgreen + blink);
    write(text);
    gotoxy(15, 3);
    textcolor(lightred);
    writeln(' input');
    writeln;
    textcolor(lightcyan)
end;
begin
    list_dir_files_heading;
    i:= 1;
    FindFirst('*.*', Archive, DirInfo);
    while DosError = 0 do
    begin
        gotoxy(13, i+4);
        writeln(DirInfo.Name);
        FindNext(DirInfo);
        i:= i + 1;
        if i > 18 then
        begin
            bekle;
            i:= 1;
            clrscr;
```

```
            list_dir_files_heading
        end
    end;
    textcolor(lightgray);
    bekle;
    clrscr
end;

procedure PRINT_DATE;
{
  prints current date

  called in main program
}
const days : array [0..6] of String[9] = ('Sunday','Monday','Tuesday',
                                'Wednesday','Thursday','Friday',
                                'Saturday');
var y, m, d, dow : Word;
begin
    GetDate(y,m,d,dow);
    WriteLn(fo,'Date: ', days[dow],', ', m:0, '/', d:0, '/', y:0)
end;

procedure PRINT_TIME;
{
  prints current time

  called in main program
}
var h, m, s, hund : Word;
function LeadingZero(w : Word) : String;
var s : String;
begin
    Str(w:0, s);
    if Length(s) = 1 then s := '0' + s;
    LeadingZero := s
end;
begin
    GetTime(h,m,s,hund);
    WriteLn(fo, 'Time: ', LeadingZero(h), ':', LeadingZero(m),':',
          LeadingZero(s), '.', LeadingZero(hund))
end;

procedure CHECK_ARRAY (var array_type, num, num_limit: integer;
                var cond: boolean);
```

```
{
  checks if the variables have enough memory

  called in CONCRETE_FORCE
        main program
}
var word: string[7];
begin
    cond:= true;
    case array_type of
        1 : word:= 'array_1';
        2 : word:= 'array_2';
        3 : word:= 'array_3';
        4 : word:= 'array_4';
        5 : word:= 'array_5'
    end;
    if num >= num_limit then
    begin
        textmode(co80);
        clrscr;
        click;
        gotoxy(13, 10);
        textcolor(lightcyan);
        write(char(201));
        for i:= 1 to 54 do write(char(205));
        write(char(187));
        gotoxy(13, 11);
        write(char(186));
        gotoxy(68, 11);
        writeln(char(186));
        gotoxy(13, 12);
        write(char(186));
        textcolor(lightgray);
        gotoxy(17, 12);
        write('Increase ',chr(174));
        textcolor(lightred + blink);
        write(word);
        textcolor(lightgray);
        write(chr(175), ' dimension in the source code');
        textcolor(lightcyan);
        gotoxy(68, 12);
        writeln(char(186));
        gotoxy(13, 13);
        write(char(186));
        gotoxy(68, 13);
```

```
        writeln(char(186));
        gotoxy(13, 14);
        write(char(200));
        for i:= 1 to 54 do write(char(205));
        write(char(188));
        textcolor(lightgray);
        cond:= false;
        bekle
    end
end;

procedure FAILURE_MESSAGES (var message: fail_message);
{
  displays error messsages depending on the type of column failure

  called in main program
}
begin
    textmode(co80);
    clrscr;
    click;
    gotoxy(13, 10);
    textcolor(lightcyan);
    write(char(201));
    for i:= 1 to 54 do write(char(205));
    write(char(187));
    gotoxy(13, 11);
    write(char(186));
    gotoxy(68, 11);
    writeln(char(186));
    gotoxy(13, 12);
    write(char(186));
    textcolor(lightred);
    gotoxy(15, 12);
    write(message);
    textcolor(lightcyan);
    gotoxy(68, 12);
    writeln(char(186));
    gotoxy(13, 13);
    write(char(186));
    gotoxy(68, 13);
    writeln(char(186));
    gotoxy(13, 14);
    write(char(200));
    for i:= 1 to 54 do write(char(205));
```

```
    write(char(188));
    textcolor(lightgray);
    bekle;
    textmode(co40)
end;

procedure HEADING;
{
  prints heading at the start of the program

  called in main program
}
begin
    clrscr;
    textcolor(lightred);
    gotoxy(15,8);
    click;
    for i:= 1 to 9 do write('C');
    for i:= 9 to 13 do
    begin
        gotoxy(14,i);
        writeln('C')
    end;
    gotoxy(15,14);
    for i:= 1 to 9 do write('C');
    delay(1000);
    gotoxy(30,8);
    click;
    for i:= 1 to 9 do write('O');
    for i:= 9 to 13 do
    begin
        gotoxy(29,i);
        writeln('O')
    end;
    gotoxy(30,14);
    for i:= 1 to 9 do write('O');
    for i:= 9 to 13 do
    begin
        gotoxy(39,i);
        writeln('O')
    end;
    delay(1000);
    click;
    for i:= 8 to 13 do
    begin
```

```
        gotoxy(45,i);
        writeln('L')
    end;
    gotoxy(45,14);
    for i:= 1 to 9 do write('L');
    delay(1000);
    click;
    gotoxy(58,8);
    writeln('   A');
    gotoxy(58,9);
    writeln('  A A');
    gotoxy(58,10);
    writeln(' A   A');
    gotoxy(58,11);
    writeln(' AAAAAAA');
    gotoxy(58,12);
    writeln('A      A');
    gotoxy(58,13);
    writeln('A      A');
    gotoxy(58,14);
    writeln('A      A');
    gotoxy(5, 19);
    textcolor(lightcyan);
    writeln('R E I N F O R C E D   C O N C R E T E   C O L U M N   A N A L Y S I
S');
    bekle;
    origmode:= lastmode;
    textmode(co40)
end;

procedure MENU (var column_type: file_name);
{
  prints column type selection menu

  called in main program
}
begin
    clrscr;
    repeat
    gotoxy(9, 10);
    textcolor(lightgreen);
    writeln('Enter type of column ...');
    gotoxy(12, 12);
    write('<');
    textcolor(lightred);
```

```
    write('square');
    textcolor(lightgreen);
    writeln('>');
    gotoxy(12, 13);
    write('<');
    textcolor(lightred);
    write('rectangular');
    textcolor(lightgreen);
    writeln('>');
    gotoxy(12, 14);
    write('<');
    textcolor(lightred);
    write('circular');
    textcolor(lightgreen);
    writeln('>');
    gotoxy(9, 18);
    delline;
    write(chr(196), chr(26), ' ');
    textcolor(lightgray);
    readln(column_type);
    if ((column_type <> 'square') or (column_type = 'circular')) and
    ((column_type = 'square') or (column_type <> 'circular')) and
    ((column_type <> 'square') or (column_type = 'rectangular')) and
    ((column_type = 'square') or (column_type <> 'rectangular')) and
    ((column_type <> 'rectangular') or (column_type = 'circular')) and
    ((column_type = 'rectangular') or (column_type <> 'circular')) then click
    until (column_type = 'square') or (column_type = 'circular')
    or (column_type = 'rectangular')
end;

procedure CHECK_FILE_NAME (var column_type, input_column_type: file_name);
{
  checks for correct input file name

  called in main program
}
begin
    if input_column_type <> column_type then
    begin
        clrscr;
        click;
        gotoxy(11, 10);
        textcolor(lightgreen);
        writeln('Wrong file name for');
        gotoxy(17, 12);
```

```
        textcolor(lightred);
        writeln(column_type);
        gotoxy(13, 14);
        textcolor(lightgreen);
        writeln(' column input');
        textcolor(lightcyan + blink);
        gotoxy(14, 17);
        writeln('Try again !!!');
        bekle
    end
end;

procedure CREATE_DATA_FILE_1 (var text_file_name: text;
                        var data_file_name: file_name;
                        var x_data, y_data: array_2;
                        var num_data: integer);
{
  creates a data file

  called in main program
}
var i: integer;
begin
    assign(text_file_name, data_file_name);
    rewrite(text_file_name);
    for i:= 1 to num_data  do
       writeln(text_file_name, x_data[i], '    ', y_data[i]);
    close(text_file_name)
end;

procedure CREATE_DATA_FILE_2 (var text_file_name: text;
                        var data_file_name: file_name;
                        var x_data, y_data: array_4;
                        var num_data: integer);
{
  creates a data file

  called in main program
}
var i: integer;
begin
    assign(text_file_name, data_file_name);
    rewrite(text_file_name);
    for i:= 1 to num_data  do
       writeln(text_file_name, x_data[i], '    ', y_data[i]);
```

```
    close(text_file_name)
end;

procedure clean_files;
{
  cleans data files

  called in main program
}
begin
    assign(fc, file_clean);
    rewrite(fc);
    writeln(fc, 'del ', file_euc_fuc);
    writeln(fc, 'del ', file_ecc_fcc);
    writeln(fc, 'del ', file_es_t_fs);
    writeln(fc, 'del ', file_es_c_fs);
    writeln(fc, 'del ', file_cur_mom);
    writeln(fc, 'del ', file_slp_slo_mom);
    writeln(fc, 'del ', file_slip_mom);
    writeln(fc, 'del ', file_flex_mom);
    writeln(fc, 'del ', file_def_mom);
    writeln(fc, 'del ', file_def_lat_for);
    writeln(fc, 'del ', file_def_l_f_p_d);
    writeln(fc, 'del ', file_mom_axi_for);
    writeln(fc, 'del ', file_plot);
    writeln(fc, 'del ', file_out);
    writeln(fc, 'del spock');
    close(fc)
end;

procedure BAR_AREAS (var bar_num: integer; var bar_area: real);
{
  finds area of a reinforcing bar

  called in main program
}
begin
    case bar_num of
        10 : bar_area:= 100;
        15 : bar_area:= 200;
        20 : bar_area:= 300;
        25 : bar_area:= 500;
        30 : bar_area:= 700;
        35 : bar_area:= 1000;
        45 : bar_area:= 1500;
```

```
        55 : bar_area:= 2500
    end
end;

procedure BAR_DIAMETERS (var bar_num: integer; var bar_diameter: real);
{
  finds diameter of a reinforcing bar

  called in main program
}
begin
    case bar_num of
        10 : bar_diameter:= 11.3;
        15 : bar_diameter:= 16.0;
        20 : bar_diameter:= 19.5;
        25 : bar_diameter:= 25.2;
        30 : bar_diameter:= 29.9;
        35 : bar_diameter:= 35.7;
        45 : bar_diameter:= 43.7;
        55 : bar_diameter:= 56.4
    end
end;

procedure DEFORMED_BAR_DIMENSIONS (var bar_num: integer; var sl, hl: real);
{
  finds deformed bar parameters

  called in main program
}
begin
    case bar_num of
        10 : sl:= 7.9;
        15 : sl:= 11.2;
        20 : sl:= 13.6;
        25 : sl:= 17.6;
        30 : sl:= 20.9;
        35 : sl:= 25.0;
        45 : sl:= 30.6;
        55 : sl:= 39.4
    end;
    case bar_num of
        10 : hl:= 0.45;
        15 : hl:= 0.72;
        20 : hl:= 0.98;
        25 : hl:= 1.26;
```

```
        30 : hl:= 1.48;
        35 : hl:= 1.79;
        45 : hl:= 2.20;
        55 : hl:= 2.55
    end
end;

procedure DIST_CONC_TO_LON_STEEL (var cover, stir_bar_dia, lon_bar_dia,
                                  dist_conc_to_lon_steel: real);
{
   calculates the distance from the surface of the column to the
   centerline of the longitudinal reinforcement

   called in main program
}
begin
    dist_conc_to_lon_steel:= cover + stir_bar_dia + lon_bar_dia / 2
end;

procedure DIST_CONC_TO_STIR_STEEL (var cover, stir_bar_dia,
                                   dist_conc_to_stir_steel: real);
{
   calculates the distance from the surface of the column to the
   centerline of the stirrup reinforcement

   called in main program
}
begin
    dist_conc_to_stir_steel:= cover + stir_bar_dia / 2
end;

function DIST_CONC_STR (var radius, alpha, comp_height: real): real;
{
   calculates the distance from the neutral axis
   to the strip in the circle

   called in CONCRETE_FORCE
             CRACKING
}
begin
    dist_conc_str:= radius * (cos(alpha) - 1) + comp_height
end;

function DIST_STEEL (var radius, dist_conc_to_lon_steel, angle, rotation
                     : real): real;
```

```
{
  calculates the distance between the top steel and any other steel

  called in DIST_STEEL_ARRAY
}
begin
   dist_steel:= (radius - dist_conc_to_lon_steel) * (1 - cos(angle
            + rotation))
end;

procedure DIST_STEEL_ARRAY (var num_lon_bar: integer;
                    var radius, dist_conc_to_lon_steel, rotation
                       :real;
                    var dist_st_array: array_1);
{
   stores the distances between top steel and others in an array

   called in main program
}
var angle, angle_inc, rot_angle: real;
   i: integer;
begin
    angle:= 0;
    angle_inc:= (360 / num_lon_bar) * pi /180;
    rot_angle:= rotation * pi / 180;
    for i:= 1 to num_lon_bar do
    begin
        dist_st_array[i]:= dist_steel (radius, dist_conc_to_lon_steel,
                                angle, rot_angle);
        angle:= angle + angle_inc
    end
end;

procedure DEPTH (var num_lon_bar: integer;
            var dist_st_array: array_1;
            var dist_conc_to_lon_steel, reinf_depth: real);
{
   calculates the distance from the surface of the column to the
   bottom steel

   called in main program
}
var i: integer;
begin
    reinf_depth:= dist_st_array[1];
```

```
    for i:= 2 to num_lon_bar do
      if dist_st_array[i] > reinf_depth then
        reinf_depth:= dist_st_array[i];
    reinf_depth:= reinf_depth + dist_conc_to_lon_steel
end;

function HOGNESTAD_PARABOLA (var max_conc_str, conc_strain, conc_strain_100fc
                        :real): real;
{
   calculates concrete strength using Hognestad's parabolic portion

   called in UNCONF_CONC_STR
         UNCONF_CONC_STR_PLOT
}
begin
    hognestad_parabola:= max_conc_str * (2 * (conc_strain
                  / conc_strain_100fc) - sqr(conc_strain
                  / conc_strain_100fc))
end;

function MODIFIED_HOGNESTAD_PARABOLA (var conf_max_conc_str,
                              conf_conc_strain_100fc, conc_strain,
                              k :real): real;
{
   calculates concrete strength using modified Hognestad's parabolic portion

   called in CONF_CONC_STR
         CONF_CONC_STR_PLOT
}
begin
    modified_hognestad_parabola:= exp(ln(conf_max_conc_str)
                        + (1 / (1 + 2 * k)) * ln(2 * (conc_strain
                        / conf_conc_strain_100fc) - sqr(conc_strain
                        / conf_conc_strain_100fc)))
end;

function POPOVICS_CURVE (var unconf_max_conc_str, conf_max_conc_str,
                     conf_conc_strain_100fc, conf_conc_strain: real)
                  : real;
{
   calculates concrete strength using Popovics' curve

   called in CONF_CONC_STR
         CONF_CONC_STR_PLOT
}
```

```
var mod_elas_unconf_conc, sec_mod_elas_conf_conc, r, numerator,
   denominator: real;
begin
    if conf_conc_strain <= 1E-05 then conf_conc_strain:= 1E-05;
    mod_elas_unconf_conc:= 3320 * sqrt(unconf_max_conc_str) + 6900;
    sec_mod_elas_conf_conc:= conf_max_conc_str / conf_conc_strain_100fc;
    r:= mod_elas_unconf_conc / (mod_elas_unconf_conc -
       sec_mod_elas_conf_conc);
    numerator:= conf_max_conc_str * (conf_conc_strain
            / conf_conc_strain_100fc) * r;
    denominator:= r - 1 + exp(r * ln(conf_conc_strain
             / conf_conc_strain_100fc));
    popovics_curve:= numerator / denominator
end;

function STRESS_STRAIN_LINEAR (var max_conc_str, conc_strain_85fc,
                          conc_strain_100fc, conc_strain:real): real;
{
   calculates concrete strength using Hognestad's linear portion

   called in UNCONF_CONC_STR
         UNCONF_CONC_STR_PLOT
         CONF_CONC_STR
         CONF_CONC_STR_PLOT
}
begin
    stress_strain_linear:= max_conc_str - (0.15 * max_conc_str)
                    / (conc_strain_85fc - conc_strain_100fc)
                    * (conc_strain - conc_strain_100fc)
end;

function UNCONF_CONC_STR (var unconf_conc_strain_100fc, unconf_max_conc_str,
                       curvature, dist_conc_str,
                       unconf_conc_strain_85fc: real;
                    var cover_model: char): real;
{
  calculates unconfined concrete stress using Hognestad's curve
  with the straight line portion

  called in CONCRETE_FORCE
}
var unconf_conc_strain, ucs, percent_fail: real;
begin
    percent_fail:= 0;
    unconf_conc_strain:= curvature * dist_conc_str;
```

```
    if unconf_conc_strain <= unconf_conc_strain_100fc then
    begin
        if cover_model = 'H' then
          unconf_conc_str:= hognestad_parabola (unconf_max_conc_str,
                                    unconf_conc_strain,
                                    unconf_conc_strain_100fc);
        if cover_model = 'P' then
          unconf_conc_str:= popovics_curve (unconf_max_conc_str,
                                  unconf_max_conc_str,
                                  unconf_conc_strain_100fc,
                                  unconf_conc_strain)
    end;
    if unconf_conc_strain > unconf_conc_strain_100fc then
    begin
        ucs:= stress_strain_linear (unconf_max_conc_str,
                            unconf_conc_strain_85fc,
                            unconf_conc_strain_100fc,
                            unconf_conc_strain);
        if ucs < percent_fail * unconf_max_conc_str then
          unconf_conc_str:= percent_fail * unconf_max_conc_str
        else unconf_conc_str:= ucs
    end
end;

function UNCONF_CONC_STR_PLOT (var unconf_conc_strain,
                          unconf_conc_strain_100fc,
                          unconf_max_conc_str,
                          unconf_conc_strain_85fc: real;
                       var cover_model: char): real;
{
  calculates unconfined concrete stress using Hognestad's curve
  with the straight line portion for plotting the stress - strain
  relationship

  called in main program
}
var ucs, percent_fail: real;
begin
    percent_fail:= 0;
    if unconf_conc_strain <= unconf_conc_strain_100fc then
    begin
        if cover_model = 'H' then
          unconf_conc_str_plot:= hognestad_parabola (unconf_max_conc_str,
                                      unconf_conc_strain,
                                      unconf_conc_strain_100fc);
```

```
        if cover_model = 'P' then
          unconf_conc_str_plot:= popovics_curve (unconf_max_conc_str,
                                    unconf_max_conc_str,
                                    unconf_conc_strain_100fc,
                                    unconf_conc_strain)
    end;
    if unconf_conc_strain > unconf_conc_strain_100fc then
    begin
        ucs:= stress_strain_linear (unconf_max_conc_str,
                          unconf_conc_strain_85fc,
                          unconf_conc_strain_100fc,
                          unconf_conc_strain);
        if ucs < percent_fail * unconf_max_conc_str then
          unconf_conc_str_plot:= percent_fail * unconf_max_conc_str
        else unconf_conc_str_plot:= ucs
    end
end;

procedure CONF_STRESS_STRAIN (var fle, conf_max_conc_str,
unconf_max_conc_str,
                        k, conf_conc_strain_100fc,
                        unconf_conc_strain_100fc, ro,
                        stir_steel_str_yield, conf_conc_strain_85fc,
                        unconf_conc_strain_85fc, k2: real);
{
  calculates confined stress-strain relationship paremeters

  called in CONF_CONC_STRESS_STRAIN_CIR
        CONF_CONC_STRESS_STRAIN_SQR_REC
}
var k1, k3, k4: real;
begin
    k1:= exp(ln(6.7) - 0.17 * ln(fle));
    conf_max_conc_str:= unconf_max_conc_str + (k1 * fle);
    k:= k1 * fle / unconf_max_conc_str;
    k3:= 40 / unconf_max_conc_str;
    if k3 >= 1.0 then k3:= 1.0;
    conf_conc_strain_100fc:= unconf_conc_strain_100fc * (1 + 5 * k3 * k);
    k4:= stir_steel_str_yield / 500;
    if k4 <= 1.0 then k4:= 1.0;
    conf_conc_strain_85fc:= 260 * k3 * ro * conf_conc_strain_100fc
                        * (1 + 0.5 * k2 * (k4 - 1))
                        + unconf_conc_strain_85fc
end;
```

```
procedure CONF_CONC_STRESS_STRAIN_CIR (var radius, dist_conc_to_stir_steel,
                                       bar_area, stir_steel_str_yield,
                                       pitch, unconf_max_conc_str,
                                       conf_max_conc_str,
                                       unconf_conc_strain_100fc,
                                       conf_conc_strain_100fc,
                                       unconf_conc_strain_85fc,
                                       conf_conc_strain_85fc, k: real);
{
  calculates confined stress-strain relationship paremeters of a circular
  cross section column using University of Ottawa model

  called in main program
}
var   bc, fl, k2, fle, ro: real;
begin
    bc:= 2 * (radius - dist_conc_to_stir_steel);
    fl:= (2 * bar_area * stir_steel_str_yield) / (bc * pitch);
    k2:= 1.0;
    fle:= k2 * fl;
    ro:= fle / stir_steel_str_yield;
    conf_stress_strain (fle, conf_max_conc_str, unconf_max_conc_str, k,
                  conf_conc_strain_100fc, unconf_conc_strain_100fc, ro,
                  stir_steel_str_yield, conf_conc_strain_85fc,
                  unconf_conc_strain_85fc, k2)
end;

procedure CONF_CONC_STRESS_STRAIN_SQR_REC (var input_column: file_name;
                                       var dist_conc_to_stir_steel,
                                          column_width, hor_dim, ver_dim,
                                          tie_spacing,
                                          dist_ver_cross_ties,
                                          dist_hor_cross_ties,
                                          bar_area, stir_steel_str_yield,
                                          unconf_max_conc_str,
                                          conf_max_conc_str,
                                          unconf_conc_strain_100fc,
                                          conf_conc_strain_100fc,
                                          unconf_conc_strain_85fc,
                                          conf_conc_strain_85fc, k: real;
                                       var num_hor_cross_ties,
                                          num_ver_cross_ties: integer;
                                       var hor_tie_angle, ver_tie_angle:
                                          array_3);
{
```

```
  calculates confined stress-strain relationship paremeters of a square and
  rectangular cross section column using University of Ottawa model

  called in main program
}
var   bcl, bcs, sum_hor_area_stir_steel, sum_ver_area_stir_steel,
      fll, fls, k2l, k2s, k2e, flle, flse, fle, ro: real;
      i: integer;
begin
    if input_column = 'square' then
    begin
        hor_dim:= column_width;
        ver_dim:= column_width
    end;
    bcl:= hor_dim - 2 * dist_conc_to_stir_steel;
    bcs:= ver_dim - 2 * dist_conc_to_stir_steel;
    sum_hor_area_stir_steel:= 0;
    sum_ver_area_stir_steel:= 0;
    for i:= 1 to num_hor_cross_ties do
       sum_hor_area_stir_steel:= sum_hor_area_stir_steel
                          + sin (hor_tie_angle[i] * pi / 180)
                          * bar_area;
    for i:= 1 to num_ver_cross_ties do
       sum_ver_area_stir_steel:= sum_ver_area_stir_steel
                          + sin (ver_tie_angle[i] * pi / 180)
                          * bar_area;
    fll:= (sum_ver_area_stir_steel * stir_steel_str_yield)
         / (bcl * tie_spacing);
    fls:= (sum_hor_area_stir_steel * stir_steel_str_yield)
         / (bcs * tie_spacing);
    k2l:= 0.26 * sqrt((bcl / tie_spacing) * (bcl / dist_ver_cross_ties)
         * (1 / 3));
    k2s:= 0.26 * sqrt((bcs / tie_spacing) * (bcs / dist_hor_cross_ties)
         * (1 / 3));
    flle:= k2l * fll;
    flse:= k2s * fls;
    fle:= ((flle * bcl) + (flse * bcs)) / (bcl + bcs);
    k2e:= ((k2l * bcl) + (k2s * bcs)) / (bcl + bcs);
    ro:= (sum_hor_area_stir_steel + sum_ver_area_stir_steel)
       / (tie_spacing * (bcl + bcs));
    conf_stress_strain (fle, conf_max_conc_str, unconf_max_conc_str, k,
                  conf_conc_strain_100fc, unconf_conc_strain_100fc, ro,
                  stir_steel_str_yield, conf_conc_strain_85fc,
                  unconf_conc_strain_85fc, k2e)
end;
```

```
function CONF_CONC_STR (var curvature, dist_conc_str, unconf_max_conc_str,
                        conf_max_conc_str, conf_conc_strain_100fc,
                        conf_conc_strain_85fc, k: real;
                      var core_model: char): real;
{
  calculates confined concrete stress using modified Hognestad's parabola or
  Popovics curve

  called in CONCRETE_FORCE
}
var conf_conc_strain, ccs, ecc_20_fcc: real;
begin
   conf_conc_strain:= curvature * dist_conc_str;
   ecc_20_fcc:= (conf_conc_strain_85fc - conf_conc_strain_100fc)
            * (0.8 * conf_max_conc_str) / (0.15 * conf_max_conc_str)
            + conf_conc_strain_100fc;
   if conf_conc_strain <= conf_conc_strain_100fc then
   begin
      if core_model = 'H' then
        conf_conc_str:= modified_hognestad_parabola (conf_max_conc_str,
                                        conf_conc_strain_100fc,
                                        conf_conc_strain, k);
      if core_model = 'P' then
        conf_conc_str:= popovics_curve (unconf_max_conc_str,
                                conf_max_conc_str,
                                conf_conc_strain_100fc,
                                conf_conc_strain)
   end;
   if conf_conc_strain > conf_conc_strain_100fc then
     conf_conc_str:= stress_strain_linear (conf_max_conc_str,
                                conf_conc_strain_85fc,
                                conf_conc_strain_100fc,
                                conf_conc_strain);
   if conf_conc_strain > ecc_20_fcc then
     conf_conc_str:= 0.2 * conf_max_conc_str
end;

function CONF_CONC_STR_PLOT (var unconf_max_conc_str, conf_max_conc_str,
                        conf_conc_strain_100fc, conf_conc_strain,
                        conf_conc_strain_85fc, k: real;
                      var core_model: char): real;
{
  calculates confined concrete stress using modified Hognestad's parabola or
  Popovics curve for plotting the stress - strain relationship
```

```
  called in main program
}
var ccs, ecc_20_fcc: real;
begin
    ecc_20_fcc:= (conf_conc_strain_85fc - conf_conc_strain_100fc)
              * (0.8 * conf_max_conc_str) / (0.15 * conf_max_conc_str)
              + conf_conc_strain_100fc;
    if conf_conc_strain <= conf_conc_strain_100fc then
    begin
        if core_model = 'H' then
          conf_conc_str_plot:= modified_hognestad_parabola (conf_max_conc_str,
                                                conf_conc_strain_100fc,
                                                conf_conc_strain, k);
        if core_model = 'P' then
          conf_conc_str_plot:= popovics_curve (unconf_max_conc_str,
                                    conf_max_conc_str,
                                    conf_conc_strain_100fc,
                                    conf_conc_strain)
    end;
    if conf_conc_strain > conf_conc_strain_100fc then
      conf_conc_str_plot:= stress_strain_linear (conf_max_conc_str,
                                    conf_conc_strain_85fc,
                                    conf_conc_strain_100fc,
                                    conf_conc_strain);
    if conf_conc_strain > ecc_20_fcc then
      conf_conc_str_plot:= 0.2 * conf_max_conc_str
end;

function CHORD (var radius, alpha: real): real;
{
  calculates length of strip in the circle

  called in CONCRETE_FORCE
           CRACKING
}
begin
    chord:= 2 * radius * sin(alpha)
end;

function SIDE_CHORD (var radius, dist_conc_to_stir_steel, alfa: real): real;
{
  calculates length of strip outside the core - one side only

  called in CONCRETE_FORCE
```

```
}
var term, beta: real;
begin
    if abs(alfa - pi / 2) < 0.0001 then
      side_chord:= dist_conc_to_stir_steel
    else
    begin
        term:= radius * cos(alfa) / (radius - dist_conc_to_stir_steel);
        beta:= alfa - arccos(term);
        side_chord:= (radius - dist_conc_to_stir_steel) * sin(beta)
                / sin(pi / 2 - alfa)
    end
end;

function LIMITING_ANGLE (var section_radius, strip_angle:real): real;
{
  calculates compression height at strip level

  called in CONCRETE_FORCE
        CRACKING
}
begin
    limiting_angle:= section_radius * (1 - cos(strip_angle))
end;

function AVERAGE_STRIP_WIDTH (var first_width, second_width: real): real;
{
  calculates average strip widthbetween two chord lines

  called in CONCRETE_FORCE
        CRACKING
}
begin
    average_strip_width:= (first_width + second_width) / 2
end;

procedure CONCRETE_FORCE (var conc_force, curvature, unconf_conc_strain,
                          comp_height, dist_conc_to_stir_steel,
                          dist_conc_to_lon_steel, radius, width, hor_dim,
                          ver_dim, unconf_conc_strain_100fc,
                          unconf_max_conc_str, unconf_conc_strain_85fc,
                          alfa_inc, strip_height, conf_conc_strain_100fc,
                          conf_max_conc_str, conf_conc_strain_85fc,
                          k: real;
                      var steel_dist, conc_str: array_1;
```

```
                    var delta_conc_force_array,
                      delta_conc_force_dist_array: array_5;
                    var conc_count, num_lon_bar: integer;
                    var con_array: boolean;
                    var column: file_name;
                    var cover_model, core_model: char);
{
  calculates force in concrete for unconfined and confined
  portion of concrete section

  called in main program
}
var   alfa, condition, max_condition, b1_u, dfc1, fc1_u, b2_u, dfc2, fc2_u,
      alfa_max, delta_dfc, b1, b2, b1_c, fc1_c, b2_c, fc2_c, alfa_side_chord,
      area_cir_strip_u, area_sqr_strip_u, area_cir_strip_c, area_rec_strip_u,
      area_sqr_strip_c, area_rec_strip_c, steel_distance, zero_force_region,
      factor: real;
      alfa_count, num, a_t, i: integer;
      con1: boolean;
function average_strength (var first_strength, second_strength: real): real;
begin
     average_strength:= (first_strength + second_strength) / 2
end;
begin
    a_t:= 5;
    num:= n_5;
    conc_force:= 0;
    alfa_max:= 0;
    curvature:= unconf_conc_strain / comp_height;
    conc_count:= 1;
    alfa_count:= 1;
    max_condition:= 0;
    condition:= max_condition;
    if condition = max_condition then
    begin
        alfa:= alfa_max;
        max_condition:= dist_conc_to_stir_steel;
        repeat
            condition:= limiting_angle (radius, alfa);
            b1_u:= chord (radius, alfa);
            dfc1:= dist_conc_str (radius, alfa, comp_height);
            if dfc1 <= 1 then dfc1:= 1;
            fc1_u:= unconf_conc_str (unconf_conc_strain_100fc,
                                     unconf_max_conc_str,
                                     curvature, dfc1,
```

```
                    unconf_conc_strain_85fc, cover_model);
alfa:= alfa_count * alfa_inc;
condition:= limiting_angle (radius, alfa);
if condition >= comp_height then
begin
   condition:= comp_height;
   b2_u:= 2 * sqrt(sqr(radius) - sqr(radius - condition));
   dfc2:= comp_height - condition;
   if dfc2 <= 1 then dfc2:= 1;
   fc2_u:= unconf_conc_str (unconf_conc_strain_100fc,
                    unconf_max_conc_str,
                    curvature, dfc2,
                    unconf_conc_strain_85fc, cover_model)
end
else
if condition >= max_condition then
begin
   condition:= max_condition;
   b2_u:= 2 * sqrt(sqr(radius) - sqr(radius - condition));
   dfc2:= comp_height - condition;
   if dfc2 <= 1 then dfc2:= 1;
   fc2_u:= unconf_conc_str (unconf_conc_strain_100fc,
                    unconf_max_conc_str,
                    curvature, dfc2,
                    unconf_conc_strain_85fc, cover_model);
   alfa_max:= arctan(0.5 * b2_u / (radius - condition))
end
else
begin
   b2_u:= chord (radius, alfa);
   dfc2:= dist_conc_str (radius, alfa, comp_height);
   if dfc2 <= 1 then dfc2:= 1;
   fc2_u:= unconf_conc_str (unconf_conc_strain_100fc,
                    unconf_max_conc_str,
                    curvature, dfc2,
                    unconf_conc_strain_85fc, cover_model)
end;
delta_dfc:= dfc1 - dfc2;
if delta_dfc > strip_height then alfa_inc:= alfa_inc / 2;
area_cir_strip_u:= average_strip_width (b1_u, b2_u)
            * delta_dfc;
if column = 'circular' then
   delta_conc_force_array[conc_count]:= area_cir_strip_u
                        * average_strength (fc1_u, fc2_u);
if column = 'square' then
```

```
        begin
            area_sqr_strip_u:= area_cir_strip_u * width
                        / average_strip_width (b1_u, b2_u);
            delta_conc_force_array[conc_count]:= area_sqr_strip_u
                                    * average_strength (fc1_u, fc2_u)
        end;
        if column = 'rectangular' then
        begin
            area_rec_strip_u:= area_cir_strip_u * hor_dim
                        / average_strip_width (b1_u, b2_u);
            delta_conc_force_array[conc_count]:= area_rec_strip_u
                                    * average_strength (fc1_u, fc2_u)
        end;
        conc_force:= conc_force + delta_conc_force_array[conc_count];
        delta_conc_force_dist_array[conc_count]:= (dfc1 + dfc2) / 2;
        conc_count:= conc_count + 1;
        check_array (a_t, conc_count, num, con_array);
        alfa_count:= alfa_count + 1
    until (condition = max_condition) or (condition = comp_height)
        or (con_array = false)
end;
if condition = max_condition then
begin
    alfa:= alfa_max;
    max_condition:= 2 * radius - dist_conc_to_stir_steel;
    repeat
        if alfa > pi / 2 then alfa_side_chord:= pi - alfa
        else alfa_side_chord:= alfa;
        condition:= limiting_angle (radius, alfa);
        b1:= chord (radius, alfa);
        b1_u:= 2 * side_chord (radius, dist_conc_to_stir_steel,
                        alfa_side_chord);
        b1_c:= b1 - b1_u;
        dfc1:= dist_conc_str (radius, alfa, comp_height);
        if dfc1 <= 1 then dfc1:= 1;
        fc1_u:= unconf_conc_str (unconf_conc_strain_100fc,
                        unconf_max_conc_str, curvature, dfc1,
                        unconf_conc_strain_85fc, cover_model);
        fc1_c:= conf_conc_str (curvature, dfc1, unconf_max_conc_str,
                        conf_max_conc_str,
                        conf_conc_strain_100fc,
                        conf_conc_strain_85fc, k, core_model);
        alfa:= alfa_count * alfa_inc;
        if alfa > pi / 2 then alfa_side_chord:= pi - alfa
        else alfa_side_chord:= alfa;
```

```
condition:= limiting_angle (radius, alfa);
if condition >= comp_height then
begin
    condition:= comp_height;
    b2:= 2 * sqrt(sqr(radius) - sqr(radius - condition));
    alfa_side_chord:= arcsin(b2 / (2 * radius));
    b2_u:= 2 * side_chord (radius, dist_conc_to_stir_steel,
                    alfa_side_chord);
    b2_c:= b2 - b2_u;
    dfc2:= comp_height - condition;
    if dfc2 <= 1 then dfc2:= 1;
    fc2_u:= unconf_conc_str (unconf_conc_strain_100fc,
                     unconf_max_conc_str, curvature,
                     dfc2, unconf_conc_strain_85fc,
                     cover_model);
    fc2_c:= conf_conc_str (curvature, dfc2,
                    unconf_max_conc_str,
                    conf_max_conc_str,
                    conf_conc_strain_100fc,
                    conf_conc_strain_85fc, k, core_model);
end
else
if condition >= max_condition then
begin
    condition:= max_condition;
    b2:= 2 * sqrt(sqr(radius) - sqr(radius - condition));
    alfa_side_chord:= arcsin(b2 / (2 * radius));
    b2_u:= 2 * side_chord (radius, dist_conc_to_stir_steel,
                    alfa_side_chord);
    b2_c:= b2 - b2_u;
    dfc2:= comp_height - condition;
    if dfc2 <= 1 then dfc2:= 1;
    fc2_u:= unconf_conc_str (unconf_conc_strain_100fc,
                     unconf_max_conc_str, curvature,
                     dfc2, unconf_conc_strain_85fc,
                     cover_model);
    fc2_c:= conf_conc_str (curvature, dfc2,
                    unconf_max_conc_str,
                    conf_max_conc_str,
                    conf_conc_strain_100fc,
                    conf_conc_strain_85fc, k, core_model);
    alfa_max:= pi - arctan(0.5 * b2_u / (condition - radius))
end
else
begin
```

```
    b2:= chord (radius, alfa);
    b2_u:= 2 * side_chord (radius, dist_conc_to_stir_steel,
                  alfa_side_chord);
    b2_c:= b2 - b2_u;
    dfc2:= dist_conc_str (radius, alfa, comp_height);
    if dfc2 <= 1 then dfc2:= 1;
    fc2_u:= unconf_conc_str (unconf_conc_strain_100fc,
                  unconf_max_conc_str, curvature,
                  dfc2, unconf_conc_strain_85fc,
                  cover_model);
    fc2_c:= conf_conc_str (curvature, dfc2,
                  unconf_max_conc_str,
                  conf_max_conc_str,
                  conf_conc_strain_100fc,
                  conf_conc_strain_85fc, k, core_model);
end;
delta_dfc:= dfc1 - dfc2;
if delta_dfc > strip_height then alfa_inc:= alfa_inc / 2;
area_cir_strip_u:= average_strip_width (b1_u, b2_u)
            * delta_dfc;
area_cir_strip_c:= average_strip_width (b1_c, b2_c)
            * delta_dfc;
if column = 'circular' then
delta_conc_force_array[conc_count]:= area_cir_strip_u
                        * average_strength (fc1_u, fc2_u)
                        + area_cir_strip_c
                        * average_strength (fc1_c, fc2_c);
if column = 'square' then
begin
   area_sqr_strip_u:= area_cir_strip_u
               * 2 * dist_conc_to_stir_steel
               / average_strip_width (b1_u, b2_u);
   area_sqr_strip_c:= area_cir_strip_c
               * (width
               - 2 * dist_conc_to_stir_steel)
               / average_strip_width (b1_c, b2_c);
   delta_conc_force_array[conc_count]:= area_sqr_strip_u
                        * average_strength (fc1_u, fc2_u)
                        + area_sqr_strip_c
                        * average_strength (fc1_c, fc2_c)
end;
if column = 'rectangular' then
begin
   area_rec_strip_u:= area_cir_strip_u
               * 2 * dist_conc_to_stir_steel
```

```
                    / average_strip_width (b1_u, b2_u);
        area_rec_strip_c:= area_cir_strip_c
                    * (hor_dim
                    - 2 * dist_conc_to_stir_steel)
                    / average_strip_width (b1_c, b2_c);
        delta_conc_force_array[conc_count]:= area_rec_strip_u
                                * average_strength (fc1_u, fc2_u)
                                + area_rec_strip_c
                                * average_strength (fc1_c, fc2_c)
      end;
      conc_force:= conc_force + delta_conc_force_array[conc_count];
      delta_conc_force_dist_array[conc_count]:= (dfc1 + dfc2) / 2;
      conc_count:= conc_count + 1;
      check_array (a_t, conc_count, num, con_array);
      alfa_count:= alfa_count + 1
   until (condition = max_condition) or (condition = comp_height)
      or (con_array = false)
end;
if condition = max_condition then
begin
   alfa:= alfa_max;
   max_condition:= 2 * radius;
   repeat
      condition:= limiting_angle (radius, alfa);
      b1_u:= chord (radius, alfa);
      dfc1:= dist_conc_str (radius, alfa, comp_height);
      if dfc1 <= 1 then dfc1:= 1;
      fc1_u:= unconf_conc_str (unconf_conc_strain_100fc,
                    unconf_max_conc_str, curvature, dfc1,
                    unconf_conc_strain_85fc, cover_model);
      alfa:= alfa_count * alfa_inc;
      if condition >= comp_height then
      begin
         condition:= comp_height;
         b2_u:= 2 * sqrt(sqr(radius) - sqr(radius - condition));
         dfc2:= comp_height - condition;
         if dfc2 <= 1 then dfc2:= 1;
         fc2_u:= unconf_conc_str (unconf_conc_strain_100fc,
                       unconf_max_conc_str, curvature,
                       dfc2, unconf_conc_strain_85fc,
                       cover_model)
      end
      else
      if abs(condition - max_condition) < 1.0E-3 then
      begin
```

```
    condition:= max_condition;
    b2_u:= 2 * sqrt(sqr(radius) - sqr(radius - condition));
    dfc2:= comp_height - condition;
    if dfc2 <= 1 then dfc2:= 1;
    fc2_u:= unconf_conc_str (unconf_conc_strain_100fc,
                    unconf_max_conc_str, curvature,
                    dfc2, unconf_conc_strain_85fc,
                    cover_model)
end
else
begin
    b2_u:= chord (radius, alfa);
    dfc2:= dist_conc_str (radius, alfa, comp_height);
    if dfc2 <= 1 then dfc2:= 1;
    fc2_u:= unconf_conc_str (unconf_conc_strain_100fc,
                    unconf_max_conc_str, curvature,
                    dfc2, unconf_conc_strain_85fc,
                    cover_model)
end;
delta_dfc:= dfc1 - dfc2;
if delta_dfc > strip_height then alfa_inc:= alfa_inc / 2;
area_cir_strip_u:= average_strip_width (b1_u, b2_u)
            * delta_dfc;
if column = 'circular' then
delta_conc_force_array[conc_count]:= area_cir_strip_u
                        * average_strength (fc1_u, fc2_u);
if column = 'square' then
begin
    area_sqr_strip_u:= area_cir_strip_u * width
                / average_strip_width (b1_u, b2_u);
    delta_conc_force_array[conc_count]:= area_sqr_strip_u
                            * average_strength (fc1_u, fc2_u)
end;
if column = 'rectangular' then
begin
    area_rec_strip_u:= area_cir_strip_u * hor_dim
                / average_strip_width (b1_u, b2_u);
    delta_conc_force_array[conc_count]:= area_rec_strip_u
                            * average_strength (fc1_u, fc2_u)
end;
conc_force:= conc_force + delta_conc_force_array[conc_count];
delta_conc_force_dist_array[conc_count]:= (dfc1 + dfc2) / 2;
conc_count:= conc_count + 1;
check_array (a_t, conc_count, num, con_array);
alfa_count:= alfa_count + 1
```

```
        until (condition = max_condition) or (condition = comp_height)
            or (con_array = false)
    end;
    if condition = max_condition then
    begin
        zero_force_region:= comp_height - 2 * radius;
        if zero_force_region > 0 then
        begin
            max_condition:= comp_height;
            factor:= 0.1;
            repeat
                condition:= 2 * radius + zero_force_region * factor;
                if condition > comp_height then condition:=max_condition;
                delta_conc_force_array[conc_count]:= 0;
                conc_force:= conc_force
                        + delta_conc_force_array[conc_count];
                delta_conc_force_dist_array[conc_count]:= comp_height
                                                - condition;
                conc_count:= conc_count + 1;
                check_array (a_t, conc_count, num, con_array);
                factor:= factor + 0.1
            until (condition = max_condition) or (con_array = false)
        end
    end;
    for i:= 1 to nlb do
    begin
        steel_distance:= comp_height - steel_dist[i] - dist_conc_to_lon_steel;
        if (steel_distance > 0) and (steel_distance <= comp_height) then
          conc_str[i]:= conf_conc_str (curvature, steel_distance,
                                unconf_max_conc_str,
                                conf_max_conc_str,
                                conf_conc_strain_100fc,
                                conf_conc_strain_85fc, k, core_model)
        else
          conc_str[i]:=0
    end
end;

function STEEL_STRAIN (var unconf_conc_strain, comp_height, dist_steel,
                    dist_conc_to_lon_steel : real) : real;
{
  calculates strain in longitudinal reinforcement

  called in STEEL_FORCE
}
```

```
begin
    steel_strain:= unconf_conc_strain * ((comp_height - dist_steel
            - dist_conc_to_lon_steel)) / comp_height
end;

function TENSION_STEEL_STR (var steel_strain, steel_str_yield,
                        steel_strain_yield, steel_str_strain_hard,
                        steel_strain_strain_hard, steel_str_ult,
                        steel_strain_ult : real) : real;
{
  calculates tensile stress in longitudinal reinforcement

  called in COMPRESSION_STEEL_STR
        STEEL_FORCE
        SLIP_EXTENSION
        main program
}
var strain, term_1, term_2: real;
begin
    strain:= abs(steel_strain);
    if strain <= steel_strain_yield then
      tension_steel_str:= (steel_str_yield / steel_strain_yield) * strain;
    if (strain > steel_strain_yield) and
    (strain <= steel_strain_strain_hard) then
      tension_steel_str:= steel_str_yield + ((steel_str_strain_hard
                    - steel_str_yield)
                    / (steel_strain_strain_hard - steel_strain_yield))
                    * (strain - steel_strain_yield);
    if (strain > steel_strain_strain_hard) and
    (strain <= steel_strain_ult) then
    begin
        term_1:= steel_str_ult - steel_str_strain_hard;
        term_2:= (strain - steel_strain_strain_hard)
              / (steel_strain_ult - steel_strain_strain_hard);
        tension_steel_str:= steel_str_strain_hard + term_1 * (2 * term_2
                    - sqr(term_2))
    end;
    if strain > steel_strain_ult then tension_steel_str:= steel_str_ult
end;

function COMPRESSION_STEEL_STR (var steel_strain, steel_str_yield,
                        steel_strain_yield, steel_str_strain_hard,
                        steel_strain_strain_hard, steel_str_ult,
                        steel_strain_ult, bar_diameter,
                        spacing: real;
```

```
                    var comp_flag: boolean): real;
{
  calculates compressive stress in longitudinal reinforcement

  called in STEEL_FORCE
        main program
}
var strain, aspect_ratio, fs_limit, es_limit, plastic_modulus, term_1,
   term_2: real;
begin
    strain:= abs(steel_strain);
    aspect_ratio:= spacing / bar_diameter;
    if aspect_ratio < 4.5 then
      compression_steel_str:= tension_steel_str (strain, steel_str_yield,
                                    steel_strain_yield,
                                    steel_str_strain_hard,
                                    steel_strain_strain_hard,
                                    steel_str_ult,
                                    steel_strain_ult);
    if (aspect_ratio >= 4.5) and (aspect_ratio < 8) then
    begin
       fs_limit:= steel_str_strain_hard
             + (steel_str_ult - steel_str_strain_hard)
             * (47.98 * exp(-0.8782 * aspect_ratio));
       es_limit:= steel_strain_strain_hard
             + (steel_strain_ult - steel_strain_strain_hard)
             * (6.079 * exp(-0.4369 * aspect_ratio));
       if strain <= steel_strain_strain_hard then
         compression_steel_str:= tension_steel_str (strain, steel_str_yield,
                                    steel_strain_yield,
                                    steel_str_strain_hard,
                                    steel_strain_strain_hard,
                                    steel_str_ult,
                                    steel_strain_ult);
       if strain > steel_strain_strain_hard then
       begin
          term_1:= fs_limit - steel_str_strain_hard;
          term_2:= (strain - steel_strain_strain_hard)
                / (es_limit - steel_strain_strain_hard);
          compression_steel_str:= steel_str_strain_hard + term_1
                        * (2 * term_2 - sqr(term_2))
       end;
       if strain > es_limit then
       begin
          compression_steel_str:= 0;
```

```
            comp_flag:= false
        end
    end;
    if aspect_ratio >= 8 then
    begin
        plastic_modulus:= -23140 + 11130 * ln(aspect_ratio);
        fs_limit:= steel_str_yield * 27.95
                * exp(-1.743 * ln (aspect_ratio));
        es_limit:= steel_strain_yield
                * (40.47 - 5.94 * ln (aspect_ratio));
        if strain <= steel_strain_yield then
          compression_steel_str:= tension_steel_str (strain, steel_str_yield,
                                        steel_strain_yield,
                                        steel_str_strain_hard,
                                        steel_strain_strain_hard,
                                        steel_str_ult,
                                        steel_strain_ult);
        if strain > steel_strain_yield then
          compression_steel_str:= steel_str_yield - (strain - steel_strain_yield)
                            * plastic_modulus;
        if strain > es_limit then
        begin
            compression_steel_str:= 0;
            comp_flag:= false
        end
    end
end;

procedure STEEL_FORCE (var buckling_decision: char;
                var input_column: file_name;
                var num_lon_bar: integer;
                var unconf_conc_strain, comp_height,
                   dist_conc_to_lon_steel, steel_str_yield,
                   steel_strain_yield, steel_str_strain_hard,
                   steel_strain_strain_hard, steel_str_ult,
                   steel_strain_ult, st_force, bar_diameter, pitch,
                   tie_spacing, bar_area: real;
                var dist_st_array, steel_force_array,
                   steel_strain_array, steel_area,
                   steel_stress_array: array_1;
                var buckling_flag: boolean);
{
  calculates force in longitudinal reinforcement

  called in main program
```

```
}
var  i: integer;
     spacing, sd, es, fs: real;
begin
    buckling_flag:= true;
    st_force:=0;
    if (input_column = 'rectangular') or (input_column = 'square') then
          spacing:= tie_spacing;
    if input_column = 'circular' then spacing:= pitch;
    for i:= 1 to num_lon_bar do
    begin
        sd:= dist_st_array[i];
        es:= steel_strain (unconf_conc_strain, comp_height, sd,
                    dist_conc_to_lon_steel);
        steel_strain_array[i]:= es;
        if es < 0 then
        fs:= tension_steel_str (es, steel_str_yield, steel_strain_yield,
                        steel_str_strain_hard, steel_strain_strain_hard,
                        steel_str_ult, steel_strain_ult);
        if es >= 0 then
        begin
            if buckling_decision = 'Y' then
              fs:= compression_steel_str (es, steel_str_yield,
                                steel_strain_yield,
                                steel_str_strain_hard,
                                steel_strain_strain_hard,
                                steel_str_ult, steel_strain_ult,
                                bar_diameter, spacing,
                                buckling_flag);
            if buckling_decision = 'N' then
              fs:= tension_steel_str (es, steel_str_yield, steel_strain_yield,
                                steel_str_strain_hard, steel_strain_strain_hard,
                                steel_str_ult, steel_strain_ult);
        end;
        steel_stress_array[i]:= fs;
        if (input_column = 'rectangular') or (input_column = 'square') then
          steel_force_array[i]:= steel_area[i] * fs;
        if input_column = 'circular' then
          steel_force_array[i]:= bar_area * fs;
        if es < 0 then steel_force_array[i]:= -1 * steel_force_array[i];
        st_force:= st_force + steel_force_array[i]
    end
end;

function TOTAL_EXCESS_FORCE (var num_lon_bar: integer;
```

```
                    var input_column: file_name;
                    var excess_force, conc_str_steel, steel_area
                       : array_1;
                    var bar_area: real): real;
{
  calculates total excess force due to steel area

  called in main program
}
var tot_excess_force: real;
   i: integer;
begin
    tot_excess_force:= 0;
    for i:= 1 to num_lon_bar do
    begin
        if input_column = 'circular' then
          excess_force[i]:= conc_str_steel[i] * bar_area;
        if (input_column = 'square') or (input_column = 'rectangular') then
          excess_force[i]:= conc_str_steel[i] * steel_area[i];
        tot_excess_force:= tot_excess_force + excess_force[i]
    end;
    total_excess_force:= tot_excess_force
end;

procedure TENSION_STEEL_CHECK (var strain, steel_strain_ult, final_tension_strain,
                          old_tension_strain, extension_strain: real;
                       var message: fail_message;
                       var steel_tension_flag: boolean);
begin
    if strain > steel_strain_ult then
    begin
        steel_tension_flag:= false;
        final_tension_strain:= old_tension_strain;
        message:= '      REINFORCING STEEL FAILED IN TENSION';
        failure_messages(message)
    end;
    final_tension_strain:= strain;
    old_tension_strain:= final_tension_strain;
    extension_strain:= strain
end;

procedure COMPRESSION_STEEL_CHECK (var strain, steel_strain_ult,
                              final_compression_strain,
                              old_compression_strain,
                              extension_strain: real;
```

```
                        var message: fail_message;
                        var steel_compression_flag: boolean);
begin
   if strain > steel_strain_ult then
   begin
      steel_compression_flag:= false;
      final_compression_strain:= old_compression_strain;
      message:= '     REINFORCING STEEL FAILED IN COMPRESSION';
      failure_messages(message)
   end;
   final_compression_strain:= strain;
   old_compression_strain:= final_compression_strain;
   extension_strain:= 0
end;

procedure CRACKING (var steel_str_yield, steel_strain_yield,
                    unconf_max_conc_str, radius, comp_height,
                    dist_conc_to_lon_steel, bar_area, crack_moment,
                    crack_curvature, axial_load, crack_strain, alfa_inc,
                    column_width, hor_dim, ver_dim, max_tension_strain
                    : real;
                 var dist_st_array, steel_area: array_1;
                 var num_lon_bar: integer;
                 var column: file_name);
{
  calculates cracked moment and curvature

  called in main program
}
var  i: integer;
    accuracy, c_inc, result_1, result_2, term_1, term_2, term_3,
    term_4, tr_inertia, crack_stress, conc_mod_elas, steel_mod_elas,
    reinf_ratio, tr_sec_area, tr_bar_area, condition, max_condition,
    alfa, width_1, dist_1, width_2, dist_2, average_dist, delta_dist,
    area_cir_strip, area_sqr_strip, diff, sum_a1, beta_inc, beta_1, beta_f1,
    b_1, beta_2, b_2, b_avg, t, y, sum_a2, beta_f2: real;
    steel_strain: array [1..80] of real;
begin
   accuracy:= 0.001;
   c_inc:= 10;
   comp_height:= 0;
   result_1:= 1.0E+30;
   conc_mod_elas:= 3320 * sqrt(unconf_max_conc_str) + 6900;
   steel_mod_elas:= steel_str_yield / steel_strain_yield;
   reinf_ratio:= steel_mod_elas / conc_mod_elas;
```

```
repeat
    comp_height:= comp_height + c_inc;
    if column = 'circular' then
    begin
        term_1:= pi * sqr(radius) * comp_height;
        term_2:= pi * sqr(radius) * radius;
        term_3:= 0;
        for i:= 1 to num_lon_bar do
            term_3:= term_3 + comp_height
                - (dist_conc_to_lon_steel + dist_st_array[i]);
        result_2:= term_1 - term_2 + (reinf_ratio - 1) * bar_area
                * term_3
    end;
    if column = 'square' then
    begin
        term_1:= column_width * sqr(comp_height);
        term_2:= column_width * sqr(column_width - comp_height);
        term_3:= 0;
        for i:= 1 to num_lon_bar do
            term_3:= term_3 + steel_area[i] * (reinf_ratio - 1)
                * (comp_height - dist_st_array[i]
                - dist_conc_to_lon_steel);
        result_2:= term_1 - term_2 + 2 * term_3
    end;
    if column = 'rectangular' then
    begin
        term_1:= hor_dim * sqr(comp_height);
        term_2:= hor_dim * sqr(ver_dim - comp_height);
        term_3:= 0;
        for i:= 1 to num_lon_bar do
            term_3:= term_3 + steel_area[i] * (reinf_ratio - 1)
                * (comp_height - dist_st_array[i]
                - dist_conc_to_lon_steel);
        result_2:= term_1 - term_2 + 2 * term_3
    end;
    if abs(result_1) <= abs(result_2) then
    begin
        comp_height:= comp_height - c_inc;
        c_inc:= c_inc / 10
    end;
    diff:= abs(result_1) - abs(result_2);
    result_1:= result_2
until abs(diff) <= accuracy;
if column = 'circular' then
begin
```

```
    term_4:= 0;
    for i:= 1 to num_lon_bar do
       term_4:= term_4 + sqr(comp_height
             - (dist_conc_to_lon_steel + dist_st_array[i]));
    tr_bar_area:= 0;
    for i:= 1 to num_lon_bar do
       tr_bar_area:= tr_bar_area + (reinf_ratio - 1) * bar_area;
    tr_sec_area:= tr_bar_area;
    condition:= 0;
    max_condition:= 2 * radius;
    alfa:= 0;
    tr_inertia:= (reinf_ratio - 1) * bar_area * term_4;
    repeat
        condition:= limiting_angle (radius, alfa);
        width_1:= chord (radius, alfa);
        dist_1:= dist_conc_str (radius, alfa, comp_height);
        alfa:= alfa + alfa_inc;
        condition:= limiting_angle (radius, alfa);
        diff:= max_condition - condition;
        if abs(diff) < 0.001 then
        begin
            condition:= max_condition;
            width_2:= 0;
            dist_2:= comp_height - condition
        end
        else
        begin
            width_2:= chord (radius, alfa);
            dist_2:= dist_conc_str (radius, alfa, comp_height)
        end;
        average_dist:= (dist_1 + dist_2) / 2;
        delta_dist:= dist_1 - dist_2;
        area_cir_strip:= average_strip_width (width_1, width_2)
                    * delta_dist;
        tr_inertia:= tr_inertia + average_strip_width (width_1, width_2)
                  * delta_dist * sqr(delta_dist) / 12
                  + area_cir_strip * sqr(average_dist);
        tr_sec_area:= tr_sec_area + area_cir_strip;
    until condition = max_condition
end;
if column = 'square' then
begin
    tr_sec_area:= sqr(column_width);
    for i:= 1 to num_lon_bar do
       tr_sec_area:= tr_sec_area + steel_area[i] * (reinf_ratio - 1);
```

```
        tr_inertia:= sqr(sqr(column_width)) / 12 + sqr(column_width)
                * sqr((column_width / 2 - comp_height));
        for i:= 1 to num_lon_bar do
          tr_inertia:= tr_inertia + steel_area[i] * (reinf_ratio - 1)
                  * sqr(comp_height - dist_st_array[i])
    end;
    if column = 'rectangular' then
    begin
        tr_sec_area:= hor_dim * ver_dim;
        for i:= 1 to num_lon_bar do
          tr_sec_area:= tr_sec_area + steel_area[i] * (reinf_ratio - 1);
        tr_inertia:= hor_dim * sqr(ver_dim) * ver_dim / 12
                + hor_dim * ver_dim * sqr((ver_dim / 2 - comp_height));
        for i:= 1 to num_lon_bar do
          tr_inertia:= tr_inertia + steel_area[i] * (reinf_ratio - 1)
                  * sqr(comp_height - dist_st_array[i])
    end;
    crack_stress:= 0.6 * sqrt(unconf_max_conc_str);
    crack_moment:= (crack_stress + axial_load / tr_sec_area) * tr_inertia
            / (2 * radius - comp_height);
    crack_curvature:= crack_moment / (conc_mod_elas * tr_inertia);
    crack_strain:= crack_curvature * comp_height;
    for i:= 1 to num_lon_bar do
       steel_strain[i]:= crack_strain *(comp_height-(dist_conc_to_lon_steel
                + dist_st_array[i])) / comp_height;
    max_tension_strain:= steel_strain[1];
    for i:= 2 to num_lon_bar do
      if steel_strain[i] < steel_strain[i-1] then max_tension_strain
                                    := steel_strain[i]
end;

procedure FLEX_DEFLECTION (var m, c, el, pl, def: array_2;
                    var cantilever_length: real;
                    var data_num: integer);
{
  calculates the deflection and plastic length of the member

  called in main program
}
var y: array_2;
  l, m_min, m_max, m_pl, m_pl_1, m_pl_2, m_end, m_begin, c_pl, pl_1, pl_2,
  max_mom, el_len, pl_len: real;
  i, j, k: integer;
  flag: boolean;
begin
```

```
l:= cantilever_length;
i:= 1;
el[i]:= 0;
pl[i]:= 0;
def[i]:= 0;
y[i]:= 0;
m_min:= m[i];
i:= 2;
while (m[i] > m[i-1]) and (i <= data_num) do
begin
    def[i]:= 0;
    m_max:= m[i];
    y[i]:= l;
    for j:= i-1 downto 2 do
       y[j]:= (m[j] / m[j+1]) * y[j+1];
    for j:= 1 to i-1 do
       def[i]:= def[i] + ((c[j] + c[j+1]) / 2) * (y[j+1] - y[j])
             * (y[j] + (y[j+1] - y[j]) / 2);
    el[i]:= 0;
    pl[i]:= 0;
    i:= i + 1
end;
max_mom:= m_max;
while (m[i] < m[i-1]) and (i <= data_num) do
begin
    def[i]:= 0;
    pl[i]:= (1- (m[i] / max_mom)) * l;
    el[i]:= l - pl[i];
    el_len:= el[i];
    pl_len:= pl[i];
    m_pl:= sqr(m[i]) / max_mom;
    k:= 0;
    flag:= true;
    repeat
        k:= k + 1;
        if m[k] > m_pl then
        begin
            m_end:= m[k];
            m_begin:= m[k-1];
            j:= k;
            flag:= false
        end
    until flag = false;
    c_pl:= ((c[k] - c[k-1]) / (m_end - m_begin)) * (m_pl - m_begin)
        + c[k-1];
```

```
    y[j]:= el[i];
    for k:= j-1 downto 2 do
       y[k]:= (m[k] / m_pl) * el[i];
    for k:= 1 to j-2 do
       def[i]:= def[i] + ((c[k] + c[k+1]) / 2) * (y[k+1] - y[k])
             * (y[k] + (y[k+1] - y[k]) / 2);
    def[i]:= def[i] + ((c[j-1] + c_pl) / 2) * (el[i] - y[j-1])
          * (y[j-1] + (el[i] - y[j-1]) / 2);
    def[i]:= def[i] + pl[i] * c[i] * (1 - pl[i] / 2);
    i:= i + 1
end;
while i <= data_num do
begin
    if m[i] > m[i-1] then
    begin
        def[i]:= 0;
        m_max:= m[i];
        m_pl:= el_len * m[i] / l;
        k:= 0;
        flag:= true;
        if m_pl < max_mom then
        begin
            repeat
                k:= k + 1;
                if m[k] > m_pl then
                begin
                    m_end:= m[k];
                    m_begin:= m[k-1];
                    c_pl:= ((c[k] - c[k-1]) / (m_end - m_begin))
                          * (m_pl - m_begin) + c[k-1];
                    j:= k;
                    flag:= false
                end
            until flag = false;
            el[i]:= el_len;
            pl[i]:= pl_len;
            y[j]:= el[i];
            for k:= j-1 downto 2 do
               y[k]:= (m[k] / m_pl) * el[i];
            pl_1:= l - el[i] - pl_len;
            pl_2:= pl_len;
            pl[i]:= pl_1 + pl_2;
            for k:= 1 to j-2 do
               def[i]:= def[i] + ((c[k] + c[k+1]) / 2)
                     * (y[k+1] - y[k]) * (y[k] + (y[k+1] - y[k])
```

```
                / 2);
        def[i]:= def[i] + ((c[j-1] + c_pl) / 2)
                * (y[j] - y[j-1]) * (y[j-1] + (y[j] - y[j-1])
                / 2);
        def[i]:= def[i] + ((c_pl + c[i]) / 2) * pl_1
                * (pl_1 / 2 + el[i]);
        def[i]:= def[i] + pl_2 * c[i] * (1 - pl_2 / 2)
    end
    else
    begin
        repeat
            k:= k + 1
        until m[k] = max_mom;
        j:= k;
        repeat
            k:= k + 1;
            if m[k] > m_pl then
            begin
                j:= j + 1;
                flag:= false
            end
        until flag = false;
        el[i]:= (m[j-1] / m[i]) * l;
        y[j-1]:= el[i];
        for k:= j-2 downto 2 do
            y[k]:= (m[k] / m[j-1]) * el[i];
        pl_1:= l - el[i] - pl_len;
        pl_2:= pl_len;
        pl[i]:= pl_1 + pl_2;
        for k:= 1 to j-2 do
            def[i]:= def[i] + ((c[k] + c[k+1]) / 2)
                * (y[k+1] - y[k]) * (y[k] + (y[k+1] - y[k])
                / 2);
        def[i]:= def[i] + ((c[i] + c[j-1]) / 2) * pl_1
                * (pl_1 / 2 + el[i]);
        def[i]:= def[i] + pl_2 * c[i] * (pl_2 / 2 + pl_1 + el[i])
    end;
    i:= i + 1
end
else
begin
    def[i]:= 0;
    if max_mom < m_max then max_mom:= m_max;
    pl[i]:= (1- (m[i] / max_mom)) * l;
    if pl[i] < pl_len then pl[i]:= pl_len;
```

```
pl_len:= pl[i];
el[i]:= l - pl[i];
m_pl:= m[i] * el[i] / l;
if el[i] >= el[i-1] then
begin
    pl_2:= pl[i];
    pl_1:= l - el[i-1] - pl_2;
    pl[i]:= pl_1 + pl_2;
    el[i]:= l - pl[i];
    m_pl_1:= m[i] * el[i] / l;
    m_pl_2:= m_pl;
    k:= 0;
    flag:= true;
    repeat
        k:= k + 1;
        if m[k] > m_pl_1 then
        begin
            m_end:= m[k];
            m_begin:= m[k-1];
            c_pl:= ((c[k] - c[k-1]) / (m_end - m_begin))
                * (m_pl_1 - m_begin) + c[k-1];
            j:= k;
            flag:= false
        end
    until flag = false;
    y[j]:= el[i];
    el_len:= el[i];
    for k:= j-1 downto 2 do
       y[k]:= (m[k] / m_pl_1) * el[i];
    for k:= 1 to j-2 do
       def[i]:= def[i] + ((c[k] + c[k+1]) / 2)
             * (y[k+1] - y[k]) * (y[k] + (y[k+1] - y[k])
             / 2);
    def[i]:= def[i] + ((c[j-1] + c_pl) / 2) * (y[j] - y[j-1])
          * (y[j-1] + (y[j] - y[j-1]) / 2);
    def[i]:= def[i] + ((c_pl + c[i]) / 2) * pl_1
          * (pl_1 / 2 + el[i]);
    def[i]:= def[i] + pl_2 * c[i] * (l - pl_2 / 2)
end
else
begin
    m_pl:= sqr(m[i]) / max_mom;
    k:= 0;
    flag:= true;
    repeat
```

```
                k:= k + 1;
                if m[k] > m_pl then
                begin
                    m_end:= m[k];
                    m_begin:= m[k-1];
                    c_pl:= ((c[k] - c[k-1]) / (m_end - m_begin))
                        * (m_pl - m_begin) + c[k-1];
                    j:= k;
                    flag:= false
                end
            until flag = false;
            el[i]:= l - pl[i];
            el_len:= el[i];
            y[j]:= el[i];
            for k:= j-1 downto 2 do
            y[k]:= (m[k] / m_pl) * el[i];
            for k:= 1 to j-2 do
              def[i]:= def[i] + ((c[k] + c[k+1]) / 2)
                    * (y[k+1] - y[k]) * (y[k] + (y[k+1] - y[k])
                    / 2);
            def[i]:= def[i] + ((c[j-1] + c_pl) / 2) * (y[j] - y[j-1])
                * (y[j-1] + (y[j] - y[j-1]) / 2);
            def[i]:= def[i] + pl[i] * c[i] * (l - pl[i] / 2)
        end;
        i:= i + 1
      end
  end
end;

procedure SLIP_EXTENSION (var steel_strain, steel_str_yield,
                    steel_strain_yield, steel_str_strain_hard,
                    steel_strain_strain_hard, steel_str_ult,
                    steel_strain_ult, bar_area, bar_diameter,
                    unconf_max_conc_str, sl, hl, extend: real);
{
  calculates extension in the reinforcing bar

  called in main program
}
var k, es, ld, fs, le, lyp, lsh: real;
procedure elastic (var steel_str, steel_str_yield, bar_diameter, dev_length,
                elastic_length: real);
var ue: real;
begin
   ue:= steel_str_yield * bar_diameter / (4 * dev_length);
```

```
    if ue = 0 then ue:= 1000000;
    elastic_length := steel_str * bar_diameter / (4 * ue)
end;
procedure plastic (var steel_str_1, steel_str_2, bar_diameter, sl, hl,
                   unconf_max_conc_str, plastic_length: real);
var uf: real;
begin
    uf:= (5.5 - 0.07 * sl / hl) * sqrt(unconf_max_conc_str / 27.6);
    plastic_length := (steel_str_1 - steel_str_2) * bar_diameter / (4 * uf)
end;
begin
    es:=abs(steel_strain);
    k:= 3 * bar_diameter;
    ld:= 440 * bar_area * steel_str_yield / (k * sqrt(unconf_max_conc_str)
        * 400);
    if ld < 300 then ld:= 300;
    fs:= tension_steel_str (es, steel_str_yield, steel_strain_yield,
                        steel_str_strain_hard, steel_strain_strain_hard,
                        steel_str_ult, steel_strain_ult);
    if es <= steel_strain_yield then
    begin
        elastic (fs, steel_str_yield, bar_diameter, ld, le);
        extend:= 0.5 * es * le
    end;
    if (es > steel_strain_yield) and  (es <= steel_strain_strain_hard) then
    begin
        elastic (steel_str_yield, steel_str_yield, bar_diameter, ld, le);
        plastic (fs, steel_str_yield, bar_diameter, sl, hl,
              unconf_max_conc_str, lyp);
        extend:= 0.5 * steel_strain_yield * le + 0.5
              * (steel_strain_yield + es) * lyp
    end;
    if es > steel_strain_strain_hard then
    begin
        elastic (steel_str_yield, steel_str_yield, bar_diameter, ld, le);
        plastic (steel_str_strain_hard, steel_str_yield, bar_diameter, sl, hl,
              unconf_max_conc_str, lyp);
        plastic (fs, steel_str_yield, bar_diameter, sl, hl,
              unconf_max_conc_str, lsh);
        extend:= 0.5 * steel_strain_yield * le + 0.5
              * (steel_strain_yield + steel_strain_strain_hard) * lyp
              + 0.5 * (steel_strain_strain_hard + es) * lsh
    end
end;
```

```
procedure LATERAL_FORCE (var cantilever_length: real;
                         var moment, lat_for: array_2;
                         var data_num: integer);
{
   calculates lateral force at the base of the column due to moment

   called in main program
}
begin
    for i:= 1 to data_num do
       lat_for[i]:= moment[i] / cantilever_length
end;

procedure LATERAL_FORCE_P_DELTA (var cantilever_length, axial_load: real;
                                 var moment, total_deformation,
                                 lat_for_p_delta: array_2;
                                 var data_num: integer);
{
   calculates lateral force at the base of the column due to
   moment including P-Delta effect

   called in main program
}
begin
    for i:= 1 to data_num do
       lat_for_p_delta[i]:= (moment[i] - axial_load * total_deformation[i])
                            / cantilever_length
end;

procedure INITIALS_EUC (var unconf_conc_strain, unconf_conc_strain_initial,
                        unconf_conc_strain_inc, unconf_conc_strain_max,
                        unconf_conc_strain_ult, unconf_conc_strain_100fc
                        : real);
{
  initilizes concrete strain limits

  called in main program
}
begin
    unconf_conc_strain_initial:= unconf_conc_strain_100fc;
    unconf_conc_strain:= unconf_conc_strain_initial;
    unconf_conc_strain_inc:= 0.0005;
    unconf_conc_strain_max:= unconf_conc_strain_ult
end;
```

```
procedure INITIALS_C (var accuracy, cover, comp_height_inc, comp_height,
                      alfa_inc, radius:real);
{
  initilizes height of compresion block limits

  called in main program
}
begin
   comp_height_inc:= 0.1 * 2 * radius;
   comp_height:= cover;
   accuracy:= 1;
   alfa_inc:= 1 * pi / 180
end;

begin  {main program}
   heading;
   menu (col_type);
   repeat
       clrscr;
       list_dir_files (col_type);
       gotoxy(9, 9);
       textcolor(lightgreen);
       writeln('Enter input file name for');
       gotoxy(17, 11);
       textcolor(lightred);
       writeln(col_type);
       gotoxy(17, 13);
       textcolor(lightgreen);
       writeln(' column ');
       gotoxy(9, 18);
       write(chr(196), chr(26), ' ');
       textcolor(lightgray);
       readln(file_1_in);
       if not exist (file_1_in) then
       begin
          clrscr;
          click;
          nofile (file_1_in);
          bekle
       end
   until exist (file_1_in);
   repeat
       clrscr;
       gen_name:= 'general';
       list_dir_files (gen_name);
```

```
      gotoxy(6, 12);
      textcolor(lightgreen);
      write('Enter');
      textcolor(lightred);
      write(' general');
      textcolor(lightgreen);
      writeln(' input file name ');
      gotoxy(6, 18);
      write(chr(196), chr(26), ' ');
      textcolor(lightgray);
      readln(file_2_in);
      if not exist (file_2_in) then
      begin
         clrscr;
         click;
         nofile (file_2_in);
         bekle
      end
until exist (file_2_in);
if col_type = 'square' then
begin
   read_square_input (file_1_in, in_col_type, width, tie_sp, sp_v_tie,
                sp_h_tie, n_h_tie, n_v_tie, nlb, area_st,
                dist_st_1, h_tie_angle, v_tie_angle);
   check_file_name (col_type, in_col_type)
end;
if col_type = 'rectangular' then
begin
   read_rectangular_input (file_1_in, in_col_type, h_dim, v_dim,tie_sp,
                     sp_v_tie, sp_h_tie, n_h_tie, n_v_tie, nlb,
                     area_st, dist_st_1, h_tie_angle,
                     v_tie_angle);
   check_file_name (col_type, in_col_type)
end;
if col_type = 'circular' then
begin
   read_circular_input (file_1_in, in_col_type, cov, r, rot, s, nlb);
   check_file_name (col_type, in_col_type)
end;
read_general_input (file_2_in, in_gen_data, lbn, sbn, fco, eo, eo85,
               eou, fy, ey, fsh, esh, fu, esu, strip_height,
               axial_load, can_len, phi_c, phi_s, lbd, hl, sl, sbd,
               sfy, file_euc_fuc, file_ecc_fcc, file_es_t_fs,
               file_es_c_fs, file_cur_mom, file_flex_mom,
               file_slp_slo_mom, file_slip_mom, file_def_mom,
```

```
                file_def_lat_for, file_def_l_f_p_d, file_mom_axi_for,
                file_plot, file_out, file_clean, st_dec, buc_dec,
                cover_dec, core_dec, m_p_dec);
if in_gen_data <> 'general' then
begin
    clrscr;
    click;
    gotoxy(11, 10);
    textcolor(lightgreen);
    writeln('Wrong file name for');
    gotoxy(16, 12);
    textcolor(lightred);
    writeln('general');
    gotoxy(13, 14);
    textcolor(lightgreen);
    writeln(' column input');
    textcolor(lightcyan + blink);
    gotoxy(14, 17);
    writeln('Try again !!!');
    bekle;
    textmode(origmode);
    exit
end;
if (col_type = 'square') and (in_col_type <> 'square') then
begin
    textmode(origmode);
    exit
end;
if (col_type = 'rectangular') and (in_col_type <> 'rectangular') then
begin
    textmode(origmode);
    exit
end;
if (col_type = 'circular')and (in_col_type <> 'circular') then
begin
    textmode(origmode);
    exit
end;
clrscr;
if axial_load <= 0 then axial_load:= 0.001;
a_t_1:= 1;
num_1:= n_1;
a_t_2:= 2;
num_2:= n_2;
a_t_3:= 3;
```

```
num_3:= n_3;
a_t_4:= 4;
num_4:= n_4;
a_t_5:= 5;
num_5:= n_5;
check_array (a_t_1, nlb, num_1, array_1_cond);
if array_1_cond = false then exit;
if st_dec = 'Y' then
begin
    bar_diameters (lbn, lbd);
    bar_diameters (sbn, sbd);
    bar_areas (lbn, lba);
    bar_areas (sbn, sba);
    deformed_bar_dimensions (lbn, sl, hl)
end;
if st_dec = 'N' then
begin
    lba:= pi * sqr(lbd) / 4;
    sba:= pi * sqr(sbd) / 4
end;
if col_type = 'circular' then
begin
    dist_conc_to_lon_steel (cov, sbd, lbd, t_l);
    dist_conc_to_stir_steel (cov, sbd, t_s);
    dist_steel_array (nlb, r, t_l, rot, dist_st_2);
    depth (nlb, dist_st_2, t_l, r_d);
    conf_conc_stress_strain_cir (r, t_s, sba, sfy, s, fco, fcc, eo, el,
                        eo85, e85, k_fac)
end;
if (col_type = 'square') or (col_type = 'rectangular') then
begin
    t_l:= dist_st_1[1];
    cov:= t_l - lbd / 2 - sbd;
    t_s:= cov + sbd / 2;
    for i:= 1 to nlb do dist_st_2[i]:= dist_st_1[i] - t_l;
    depth (nlb, dist_st_2, t_l, r_d);
    conf_conc_stress_strain_sqr_rec (col_type, t_s, width, h_dim, v_dim,
                        tie_sp, sp_v_tie, sp_h_tie, sba,
                        sfy, fco, fcc, eo, el, eo85, e85,
                        k_fac, n_h_tie, n_v_tie,
                        h_tie_angle, v_tie_angle)
end;
if col_type = 'square' then r:= width / 2;
if col_type = 'rectangular' then r:= v_dim / 2;
initials_euc (euc, eo_ini, euc_inc, euc_max, eou, eo);
```

```
c_m:= 1;
curvature[c_m]:= 0;
moment[c_m]:= 0;
slip_slope[c_m]:= 0;
slip_def[c_m]:= 0;
conf_conc_strain[c_m]:= 0;
unconf_conc_strain[c_m]:= 0;
fuc_array[c_m]:= 0;
fcc_array[c_m]:= 0;
es_t_p[c_m]:= 0;
fs_t_array[c_m]:= 0;
es_c_p[c_m]:= 0;
fs_c_array[c_m]:= 0;
old_c_ss:= esu;
old_t_ss:= esu;
z_m_euc_inc:= euc;
c_m:= 2;
initials_c (accuracy, cov, c_inc, c, alfa_inc, r);
cracking (fy, ey, fco, r, cr_c, t_l, lba, cr_mom, cr_cur, axial_load,
        cr_strain, alfa_inc, width, h_dim, v_dim, final_t_ss, dist_st_2,
        area_st, nlb, col_type);
ecc_20_fcc:= (e85 - e1) * (0.8 * fcc) / (0.15 * fcc) + e1;
conc_strain_flag:= true;
con_flag:= true;
mf_flag:= true;
z_m_flag_large:= true;
z_m_flag_small:= true;
z_m_flag:= true;
st_b_flag:= true;
final_cc_flag:= true;
repeat   {euc}
    initials_c (accuracy, cov, c_inc, c, alfa_inc, r);
    repeat    {c}
        c_flag:= true;
        textcolor(lightcyan);
        gotoxy(2,14);
        write('    ',char(238),'uc = ', euc:1:5);
        write('    C = ', c:1:3);
        textcolor(lightgray);
        steel_force (buc_dec, col_type, nlb, euc, c, t_l, fy, ey,
                fsh, esh, fu, esu, force_steel, lbd, s, tie_sp,
                lba, dist_st_2, force_st, strain_st, area_st,
                stress_st, st_b_flag);
        concrete_force (force_conc, phi, euc, c, t_s, t_l, r, width,
                h_dim, v_dim, eo, fco, eo85, alfa_inc,
```

```
                    strip_height, e1, fcc, e85, k_fac, dist_st_2,
                    str_con, dcf, dcf_dist, cc, nlb, array_2_cond,
                    col_type, cover_dec, core_dec);
            if array_2_cond = false then exit;
            if ecc_20_fcc < (euc * (c - t_s) / c) then con_flag:= false;
            diff:= force_conc - total_excess_force (nlb, col_type,
                 exes_for, str_con, area_st, lba) + force_steel
                 - axial_load;
            if diff > 0 then
            begin
                accuracy:= accuracy * 10;
                if accuracy <= 1E+6 then
                begin
                    c:= c - c_inc;
                    c_inc:= c_inc / 10
                end
                else c_flag:= false;
            end
            else c:= c + c_inc;
            if c > 50000 then
            begin
                f_m:= ' CONVERGENCE CANNOT BE ACHIEVED - CHECK YOUR
INPUT';
                failure_messages (f_m);
                exit
            end;
            clrscr
        until c_flag = false;
        st_c_flag:= true;
        st_t_flag:= true;
        small_ss:= strain_st[1];
        small_i:= 1;
        for i:= 2 to nlb do
        begin
            if strain_st[i] < small_ss then
            begin
                small_ss:= strain_st[i];
                small_i:= i
            end
        end;
        abs_small_ss:= abs(small_ss);
        if small_ss < 0 then
        begin
            es_t_p[c_m]:= abs_small_ss;
            fs_t_array[c_m]:= stress_st[small_i]
```

```
end
else
begin
    es_t_p[c_m]:= 0;
    fs_t_array[c_m]:= 0
end;
big_ss:= strain_st[1];
big_i:= 1;
for i:= 2 to nlb do
begin
    if strain_st[i] >= big_ss then
    begin
        big_ss:= strain_st[i];
        big_i:= i
    end
end;
abs_big_ss:= abs(big_ss);
if big_ss >= 0 then
begin
    es_c_p[c_m]:= abs_big_ss;
    fs_c_array[c_m]:= stress_st[big_i]
end
else
begin
    es_c_p[c_m]:= 0;
    fs_c_array[c_m]:= 0
end;
if small_ss >= 0 then
begin
    if buc_dec = 'Y' then final_c_ss:= abs_big_ss;
    if buc_dec = 'N' then
    begin
        compression_steel_check (abs_big_ss, esu, final_c_ss,
                                 old_c_ss, ext_ss, f_m, st_c_flag);
        if st_c_flag = false then goto 10
    end
end;
if (big_ss >= 0) and (small_ss < 0) then
begin
    if buc_dec = 'Y' then final_c_ss:= abs_big_ss;
    if buc_dec = 'N' then
    begin
        compression_steel_check (abs_big_ss, esu, final_c_ss,
                                 old_c_ss, ext_ss, f_m, st_c_flag);
        if st_c_flag = false then goto 10
```

```
    end;
    tension_steel_check (abs_small_ss, esu, final_t_ss, old_t_ss,
                    ext_ss, f_m, st_t_flag);
    if st_t_flag = false then goto 10
end;
if big_ss < 0 then
begin
    tension_steel_check (abs_small_ss, esu, final_t_ss, old_t_ss,
                    ext_ss, f_m, st_t_flag);
    if st_t_flag = false then goto 10
end;
slip_extension (ext_ss, fy, ey, fsh, esh, fu, esu, lba, lbd, fco,
            sl, hl, bar_ext);
slip_slope[c_m]:= bar_ext / (r_d - c);
slip_def[c_m]:= can_len * tan(slip_slope[c_m]);
if (c > r_d) then
begin
    slip_slope[c_m]:= 0;
    slip_def[c_m]:= 0
end;
moment[c_m]:= axial_load * (r - c);
curvature[c_m]:= phi;
conf_conc_strain[c_m]:= euc * (c - t_s) / c;
unconf_conc_strain[c_m]:= euc;
if (ecc_20_fcc < conf_conc_strain[c_m])
and (final_cc_flag = true) then
begin
    final_data_num:= c_m -1;
    final_cc_flag:= false
end;
for i:= 1 to nlb do
begin
    mom_arm:= c - dist_st_2[i] - t_l;
    moment[c_m]:= moment[c_m] + (force_st[i] - exes_for[i])
            * mom_arm
end;
for i:=1 to cc - 1 do
   moment[c_m]:= moment[c_m] + dcf[i] * dcf_dist[i];
if (c > r_d) and (abs(c - r_d) > 1) and (z_m_flag = true) then
begin
    if z_m_flag_large = false then z_m_euc_inc:= z_m_euc_inc / 2;
    euc:= euc + z_m_euc_inc;
    z_m_flag_small:= false
end;
if (c < r_d) and (abs(c - r_d) > 1) and (z_m_flag = true) then
```

```
      begin
         if z_m_flag_small = false then z_m_euc_inc:= z_m_euc_inc / 2;
         euc:= euc - z_m_euc_inc;
         while euc <= 0 do
         begin
            euc:= euc + z_m_euc_inc;
            z_m_euc_inc:= z_m_euc_inc / 2;
            euc:= euc - z_m_euc_inc
         end;
         z_m_flag_large:= false
      end;
      if (abs(c - r_d) <= 1) then
      begin
         mom_zero_strain:= moment[c_m];
         z_m_flag:= false
      end;
      if (z_m_flag = false) then
      begin
         c_m:= c_m + 1;
         check_array (a_t_2, c_m, num_2, array_2_cond);
         if array_2_cond = false then
         begin
            textmode(origmode);
            exit
         end;
         euc:= euc + euc_inc
      end
until (euc >= euc_max) or (moment[c_m-1] < 0);
if moment[c_m-1] < 0 then
begin
   c_m:= c_m - 3;
   f_m:= '        NEGATIVE MOMENT WAS CALCULATED';
   failure_messages (f_m);
   mf_flag:= false;
end;
if euc > euc_max then
begin
   conc_strain_flag:= false;
   f_m:= ' UNCONFINED CONCRETE STRAIN EXCEEDED MAXIMUM LIMIT';
   failure_messages (f_m)
end;
10 : c_m:= c_m - 1;
mom_ult:= moment[1];
for i:= 2 to c_m do
  if moment[i] > mom_ult then mom_ult:= moment[i];
```

```
flex_deflection (moment, curvature, el, pl, flex_def, can_len, c_m);
for i:= 1 to c_m do tot_def[i]:= slip_def[i] + flex_def[i];
d_flag:= true;
for i:= 1 to c_m do if pl[i] > 2 * r then d_flag:= false;
lateral_force (can_len, moment, lat_for, c_m);
lateral_force_p_delta (can_len, axial_load, moment, tot_def,
                lat_for_p_delta, c_m);
for_ult:= lat_for_p_delta[1];
for i:= 2 to c_m do
   if lat_for_p_delta[i] > for_ult then for_ult:= lat_for_p_delta[i];
clrscr;
for i:= 2 to c_m do
begin
    strain_in:= unconf_conc_strain[i];
    fuc_array[i]:= unconf_conc_str_plot (strain_in, eo, fco, eo85, cover_dec);
    strain_in:= conf_conc_strain[i];
    fcc_array[i]:= conf_conc_str_plot (fco, fcc, e1, strain_in, e85,
                                k_fac, core_dec)
end;
textcolor(lightcyan);
if m_p_dec = 'Y' then
begin
    c:= 1;
    c_inc:= 0.02 * 2 * r;
    conc_strain:= 0.0035;
    m_p:= 1;
    comp_height_limit:= 10 * r;
    final_c:= 1E+6;
    if col_type = 'circular' then
    begin
        area_conc_conf:= pi * sqr(r - t_s);
        area_conc_unconf:= pi * sqr(r) - area_conc_conf
    end;
    if (col_type = 'square') then
    begin
        area_conc_conf:= sqr(width - t_s);
        area_conc_unconf:= sqr(width) - area_conc_conf
    end;
    if (col_type = 'rectangular') then
    begin
        area_conc_conf:= (h_dim - t_s) * (v_dim - t_s);
        area_conc_unconf:= (h_dim * v_dim) - area_conc_conf
    end;
    area_steel:= 0;
    for i:= 1 to nlb do
```

```
begin
   if col_type = 'circular' then area_steel:= area_steel + lba;
   if (col_type = 'square') or (col_type = 'rectangular') then
     area_steel:= area_steel + area_st[i]
end;
while c <= comp_height_limit do
begin
   if c = comp_height_limit then c:= final_c;
   steel_force (buc_dec, col_type, nlb, conc_strain, c, t_l, fy,
            ey, fsh, esh, fu, esu, force_steel, lbd, s,
            tie_sp, lba, dist_st_2, force_st, strain_st,
            area_st, stress_st, st_b_flag);
   concrete_force (force_conc, phi, conc_strain, c, t_s, t_l, r,
              width, h_dim, v_dim, eo, fco, eo85, alfa_inc,
              strip_height, el, fcc, e85, k_fac, dist_st_2,
              str_con, dcf, dcf_dist, cc, nlb, array_2_cond,
              col_type, cover_dec, core_dec);
   if array_2_cond = false then goto 30;
   m_p_force:= phi_s * force_steel + phi_c * (force_conc -
           total_excess_force (nlb, col_type, exes_for,
           str_con, area_st, lba));
   m_p_moment:= 0;
   for i:= 1 to nlb do
      m_p_moment:= m_p_moment + phi_s * (force_st[i] -
              exes_for[i]) * (r - dist_st_2[i] - t_l);
   for i:= 1 to cc - 1 do
      m_p_moment:= m_p_moment + phi_c * dcf[i]
              * (dcf_dist[i] + r - c);
   if c = final_c then
   begin
      pr[m_p]:= m_p_force;
      mr[m_p]:= m_p_moment;
      if m_p_moment < 0 then
      begin
         pr[m_p]:= pr[m_p] - (abs(mr[m_p]) * (pr[m_p] -
                pr[m_p-1])) / (mr[m_p-1] + abs(mr[m_p]));
         mr[m_p]:= 0
      end;
      po_real:= pr[m_p];
      goto 30
   end;
   pr[m_p]:= m_p_force;
   mr[m_p]:= m_p_moment;
   m_p:= m_p + 1;
   check_array (a_t_4, m_p, num_4, array_4_cond);
```

```
        if array_4_cond = false then exit;
        percent_finish:= 100 - 100 * (comp_height_limit - c)
                    / comp_height_limit;
        gotoxy(2,14);
        writeln(' Calculating M-P interaction    ',percent_finish:1:0,' %');
        c:= c + c_inc;
        if c > comp_height_limit then c:= comp_height_limit
    end;
    30 : po_code_without_conf:= 0.85 * phi_c * fco * (area_conc_unconf
                    + area_conc_conf - area_steel)
                    + phi_s * area_steel * fy;
    po_code_with_conf:= 0.85 * phi_c * (fco * area_conc_unconf
                + fcc * area_conc_conf - fcc * area_steel)
                + phi_s * area_steel * fy;
    for i:= 1 to m_p do
      if (pr[i] < 0) and (pr[i+1] >= 0) then
      begin
          mr_ben:= mr[i] + abs(pr[i]) * (mr[i+1] - mr[i])
                / (pr[i+1] + abs(pr[i]));
          pr_ben:= 0
      end;
    mr_bal:= mr[2];
    for i:= 3 to m_p do
      if (mr[i] > mr_bal) and ((abs(mr[i] - mr[i-1]) / mr[i-1]) < 0.05) then
      begin
          mr_bal:= mr[i];
          pr_bal:= pr[i]
      end;
    clrscr
end;
if m_p_dec = 'N' then
begin
    m_p:= 5;
    mr[1]:= 0;
    pr[1]:= 0;
    mr[2]:= 1;
    pr[2]:= 1;
    mr[3]:= 1;
    pr[3]:= 0;
    mr[4]:= 0;
    pr[4]:= 1;
    mr[5]:= 1;
    pr[5]:= 1
end;
for i:= 1 to c_m do
```

```
begin
    es_c_p_neg[i]:= -1 * es_c_p[i];
    fs_c_array_neg[i]:= -1 * fs_c_array[i]
end;
create_data_file_1 (fs_t, file_es_t_fs, es_t_p, fs_t_array, c_m);
create_data_file_1 (fs_c, file_es_c_fs, es_c_p_neg, fs_c_array_neg, c_m);
create_data_file_1 (func, file_euc_fuc, unconf_conc_strain, fuc_array, c_m);
create_data_file_1 (fcon, file_ecc_fcc, conf_conc_strain, fcc_array, c_m);
create_data_file_1 (fm, file_cur_mom, curvature, moment, c_m);
create_data_file_1 (fsm, file_slp_slo_mom, slip_slope, moment, c_m);
create_data_file_1 (fsl, file_slip_mom, slip_def, moment, c_m);
create_data_file_1 (ff, file_flex_mom, flex_def, moment, c_m);
create_data_file_1 (fd, file_def_mom, tot_def, moment, c_m);
create_data_file_1 (fl, file_def_lat_for, tot_def, lat_for, c_m);
create_data_file_1 (flpd, file_def_l_f_p_d, tot_def, lat_for_p_delta, c_m);
create_data_file_2 (fmp, file_mom_axi_for, mr, pr, m_p);
assign(fp_1, 'spock');
rewrite(fp_1);
writeln(fp_1, file_plot);
close(fp_1);
assign(fp, file_plot);
rewrite(fp);
writeln(fp, file_euc_fuc);
writeln(fp, file_ecc_fcc);
writeln(fp, file_es_t_fs);
writeln(fp, file_es_c_fs);
writeln(fp, file_cur_mom);
writeln(fp, file_slip_mom);
writeln(fp, file_flex_mom);
writeln(fp, file_def_mom);
writeln(fp, file_def_lat_for);
writeln(fp, file_def_l_f_p_d);
writeln(fp, file_mom_axi_for);
close(fp);
clrscr;
20 : repeat
    gotoxy(8, 13);
    textcolor(lightcyan);
    writeln('Output to screen, or file');
    gotoxy(17, 15);
    writeln('[S, F] ?');
    out_1:= upcase(readkey)
until (out_1 = 'S') or (out_1 = 'F');
if out_1 = 'S' then
begin
```

```
      textmode(origmode);
      assigncrt(fo)
    end;
    if out_1 = 'F' then assign(fo, file_out);
    rewrite(fo);
    print_date;
    print_time;
    writeln(fo);
    textcolor(lightred);
    if col_type = 'circular' then
    begin
      writeln(fo, '              Circular Cross-Section Analysis');
      writeln(fo, '              ==============================')
    end;
    if col_type = 'square' then
    begin
      writeln(fo, '              Square Cross-Section Analysis');
      writeln(fo, '              ==============================')
    end;
    if col_type = 'rectangular' then
    begin
      writeln(fo, '              Rectangular Cross-Section Analysis');
      writeln(fo, '              ==============================')
    end;
    writeln(fo);
{
    textcolor(lightcyan);
    writeln(fo, ' INPUT:');
    writeln(fo, '*******');
    textcolor(lightgray);
    writeln(fo);
    if col_type = 'circular' then
    begin
       writeln(fo, ' --> Radius            = ', r:1:1, ' mm');
       writeln(fo);
       writeln(fo, ' --> Stirrup pitch     = ', s:1:1, ' mm')
    end;
    if col_type = 'square' then
    begin
       writeln(fo, ' --> Width of column   = ', width:1:1, ' mm');
       writeln(fo);
       writeln(fo, ' --> Spacing of ties   = ', tie_sp:1:1, ' mm')
    end;
    if col_type = 'rectangular' then
    begin
```

```
    writeln(fo, ' --> Horizontal dimension = ', h_dim:1:1,
          ' mm');
    writeln(fo);
    writeln(fo, ' --> Vertical dimension   = ', v_dim:1:1,
          ' mm');
    writeln(fo);
    writeln(fo, ' --> Spacing of ties      = ', tie_sp:1:1, ' mm')
end;
writeln(fo);
writeln(fo, ' --> Clear cover          = ', cov:1:1, ' mm');
writeln(fo);
writeln(fo, ' --> Axial load           = ', axial_load:1:1, ' N');
writeln(fo);
writeln(fo, ' --> Cantilever length    = ', can_len:1:1, ' mm');
writeln(fo);
if out_1 = 'S' then bekle;
writeln(fo, ' --> Stirrup steel:');
if st_dec = 'Y' then writeln(fo, '       Bar number       = ',
  sbn, 'M');
if st_dec = 'N' then writeln(fo, '       Bar diameter     = ',
  sbd:1:1, ' mm');
writeln(fo);
writeln(fo, ' --> Longitudinal steel:');
if st_dec = 'Y' then writeln(fo, '       Bar number       = ',
  lbn, 'M');
if st_dec = 'N' then writeln(fo, '       Bar diameter     = ',
  lbd:1:1, ' mm');
writeln(fo);
out_flag:= true;
writeln(fo, ' --> Reinforcement location from top of cross section:');
if col_type = 'circular' then
  for i:= 1 to nlb do
  begin
     if (i > 15) and (out_flag = true) then
     begin
        if out_1 = 'S' then bekle;
        out_flag:= false
     end;
     writeln(fo, '       Bar # ', i, '          = ',
          (dist_st_2[i] + t_l):1:1, ' mm')
  end;
if (col_type = 'square') or (col_type = 'rectangular') then
begin
   for i:= 1 to nlb do
      writeln(fo, '       Layer # ', i, '        = ', dist_st_1[i]
```

```
            :1:1, ' mm');
        writeln(fo);
        writeln(fo, ' --> Reinforcement area:');
        for i:= 1 to nlb do
          writeln(fo, '       Layer # ', i, '       = ',
              area_st[i]:1:1, ' mm',char(253))
    end;
    writeln(fo);
    if buc_dec = 'Y' then writeln(fo, ' --> Buckling of longitudinal reinforcement is
considered');
    if buc_dec = 'N' then writeln(fo, ' --> Buckling of longitudinal reinforcement is not
considered');
    writeln(fo);
    if cover_dec = 'H' then writeln(fo, ' --> Hognestad model is used for cover concrete');
    if cover_dec = 'P' then writeln(fo, ' --> Popovics model is used for cover concrete');
    writeln(fo);
    if core_dec = 'H' then writeln(fo, ' --> Hognestad model is used for core concrete');
    if core_dec = 'P' then writeln(fo, ' --> Popovics model is used for core concrete');
    writeln(fo);
    if out_1 = 'S' then bekle;
    writeln(fo, ' --> Unconfined concrete parameters:');
    writeln(fo, '       Fuc             = ', fco:1:1, ' MPa');
    writeln(fo, '       ',char(238),'01             = ', eo:1:5);
    writeln(fo, '       ',char(238),'085            = ', eo85:1:5);
    writeln(fo);
    writeln(fo, ' --> Concrete strength factor:');
    writeln(fo, '       ',char(237),'c              = ', phi_c:1:2);
    writeln(fo);
    writeln(fo, ' --> Longitudinal steel parameters:');
    writeln(fo, '       Fy              = ', fy:1:1, ' MPa');
    writeln(fo, '       ',char(238),'y              = ', ey:1:5);
    writeln(fo, '       Fsh             = ', fsh:1:1, ' MPa');
    writeln(fo, '       ',char(238),'sh             = ', esh:1:5);
    writeln(fo, '       Fu              = ', fu:1:1, ' MPa');
    writeln(fo, '       ',char(238),'u              = ', esu:1:5);
    writeln(fo);
    writeln(fo, ' --> Transverse steel parameter:');
    writeln(fo, '       Fy - stirrup    = ', sfy:1:1, ' MPa');
    writeln(fo);
    writeln(fo, ' --> Steel strength factor:');
    writeln(fo, '       ',char(237),'s              = ', phi_s:1:2);
    writeln(fo);
    if out_1 = 'S' then bekle;
}
    textcolor(lightcyan);
```

```
    writeln(fo, ' OUTPUT:');
    writeln(fo, '********');
    textcolor(lightgray);
    writeln(fo);
    writeln(fo, ' --> Cracking moment      = ', cr_mom:1:1, ' N-mm');
    writeln(fo);
    writeln(fo, ' --> Cracking curvature   = ', cr_cur);
    writeln(fo);
    writeln(fo, ' --> Cracking strain      = ', cr_strain:1:5);
    writeln(fo);
    writeln(fo, ' --> Confined concrete parameters:');
    writeln(fo, '       Fcc              = ', fcc:1:1, ' MPa');
    writeln(fo, '       ',char(238),'1               = ', e1:1:5);
    writeln(fo, '       ',char(238),'85              = ', e85:1:5);
    writeln(fo);
    writeln(fo, ' --> Plastic hinge length = ', pl[c_m]:1:1, ' mm');
    writeln(fo);
    if out_1 = 'S' then bekle;
    writeln(fo, ' --> Failure mode(s):');
    if st_c_flag = false then
      writeln(fo, '       Reinforcing steel failed in compression');
    if st_t_flag = false then
      writeln(fo, '       Reinforcing steel failed in tension');
    if st_b_flag = false then
      writeln(fo, '       Reinforcing steel failed in buckling');
    if con_flag = false then
      writeln(fo, '       Core conc. dropped below 20% of confined compression strength');
    if conc_strain_flag = false then
      writeln(fo, '       Unconf. conc. strain exceeded the limit specified in input file');
    if mf_flag = false then
      writeln(fo, '       Negative moment was calculated');
    if d_flag = false then
      writeln(fo, '       Plastic hinge length exceeded column x-section dimension');
    if final_cc_flag = false then
      writeln(fo, '       Data row number when core conc. dropped below 20% fcc = ',
final_data_num:1);
    writeln(fo);
    if array_4_cond = true then
    begin
       writeln(fo, ' --> Code axial load cap. = ', po_code_without_conf:1:1, ' N');
       writeln(fo, '     (without the effect of confinement)');
       writeln(fo);
       writeln(fo, ' --> Code axial load cap. = ', po_code_with_conf:1:1, ' N');
       writeln(fo, '     (with the effect of confinement)');
       writeln(fo);
```

```
      writeln(fo, ' --> Real axial load cap. = ', po_real:1:1, ' N');
      writeln(fo);
      writeln(fo, ' --> Bending Moment - Axial load interaction curve:');
      writeln(fo, '      Pure Tensile :  P = ', pr[1]:11:1, ' N',
              '      M = ', mr[1]:13:1, ' N-mm');
      writeln(fo, '      Pure Bending :  P = ', pr_ben:11:1, ' N',
              '      M = ', mr_ben:13:1, ' N-mm');
      writeln(fo, '      Balance Point:  P = ', pr_bal:11:1, ' N',
              '      M = ', mr_bal:13:1, ' N-mm');
      writeln(fo, '      Pure Compr. :  P = ', pr[m_p]:11:1, ' N',
              '      M = ', mr[m_p]:13:1, ' N-mm');
      writeln(fo)
   end;
   if out_1 = 'S' then bekle;
   writeln(fo, ' --> Moment at reinforcement depth (zero strain moment):');
   writeln(fo, '      Mo              = ', mom_zero_strain:1:1, ' N-mm');
   writeln(fo);
   writeln(fo, ' --> Ultimate moment     = ', mom_ult:1:1, ' N-mm');
   writeln(fo);
   writeln(fo, ' --> Ultimate Lat. Force  = ',for_ult:1:1, ' N');
   writeln(fo);
   if out_1 = 'S' then bekle;
{
   writeln(fo, ' --> Data files:');
   writeln(fo, '      Unconf. Conc. Strain - Stress values are stored in  "',
       file_euc_fuc, '"');
   writeln(fo, '      Conf. Conc. Strain - Stress values are stored in    "',
       file_ecc_fcc, '"');
   writeln(fo, '      Tension Steel Strain - Stress values are stored in  "',
       file_es_t_fs, '"');
   writeln(fo, '      Compr. Steel Strain - Stress values are stored in   "',
       file_es_c_fs, '"');
   writeln(fo, '      Curvature - Moment values are stored in             "',
       file_cur_mom, '"');
   writeln(fo, '      Moment - Flexural Deformation values are stored in  "',
       file_flex_mom, '"');
   writeln(fo, '      Moment - Slip Rotation values are stored in         "',
       file_slp_slo_mom, '"');
   writeln(fo, '      Moment - Slip Deflection values are stored in       "',
       file_slip_mom, '"');
   writeln(fo, '      Moment - Total Deflection values are stored in      "',
       file_def_mom, '"');
   writeln(fo, '      Total Deflection - Shear values are stored in       "',
       file_def_lat_for, '"');
   writeln(fo, '      Tot. Def. (w/ P-Delta) - Shear values are stored in "',
```

```
        file_def_l_f_p_d, '');
    writeln(fo, '      Moment - Axial force values are stored in      ',
        file_mom_axi_for, '');
    if out_1 = 'S' then bekle;
}
    close(fo);
    clrscr;
    textmode(co40);
    repeat
        gotoxy(14, 13);
        textcolor(lightcyan);
        writeln('Another output');
        gotoxy(17, 15);
        writeln('[Y, N] ?');
        out_2:= upcase(readkey)
    until (out_2 = 'Y') or (out_2 = 'N');
    if out_2 = 'Y' then goto 20;
    clean_files;
    textmode(origmode)
end.
```

Appendix B

Reinforcement Details of Existing Bridges

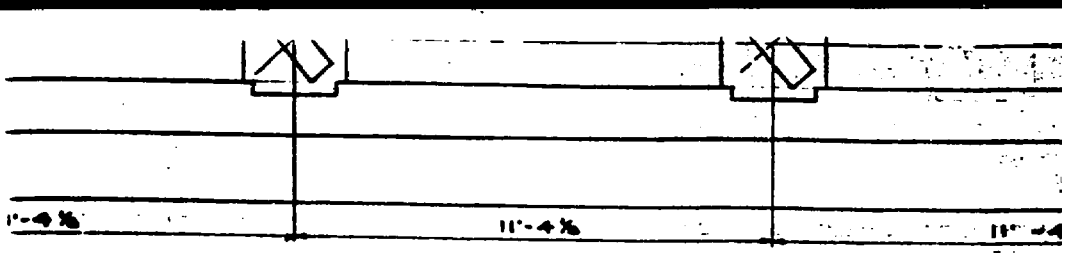

HALF PLAN

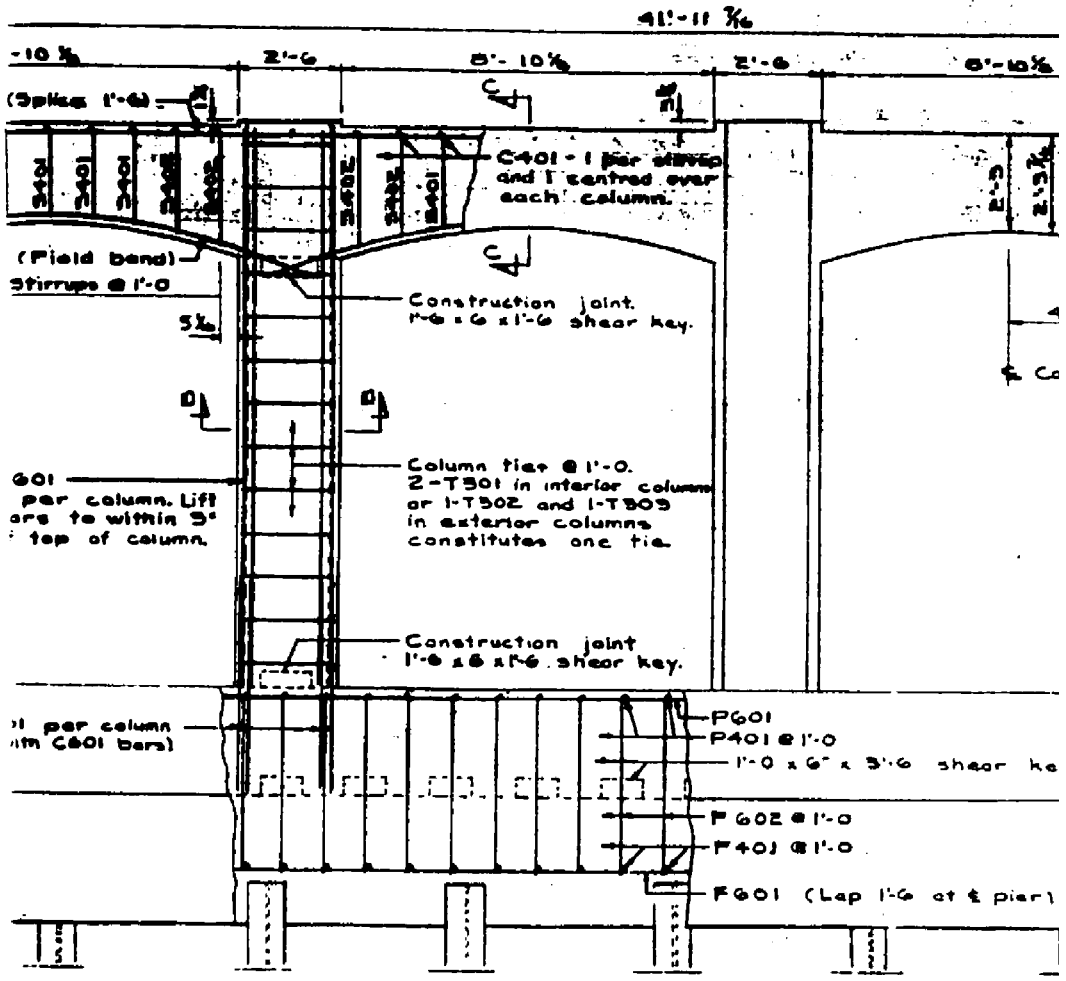

HALF ELEVATION

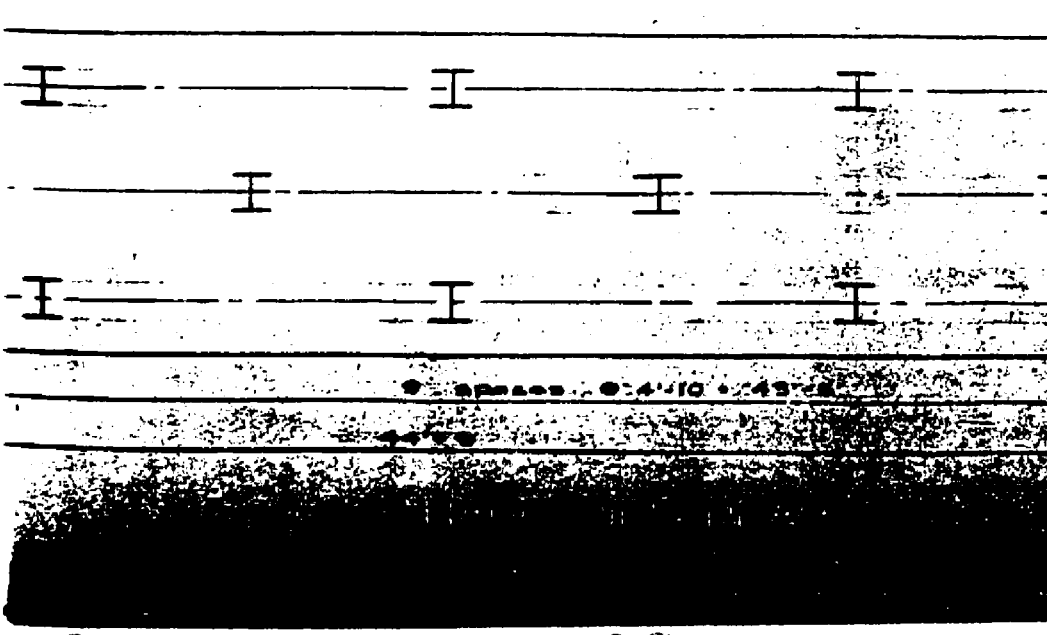

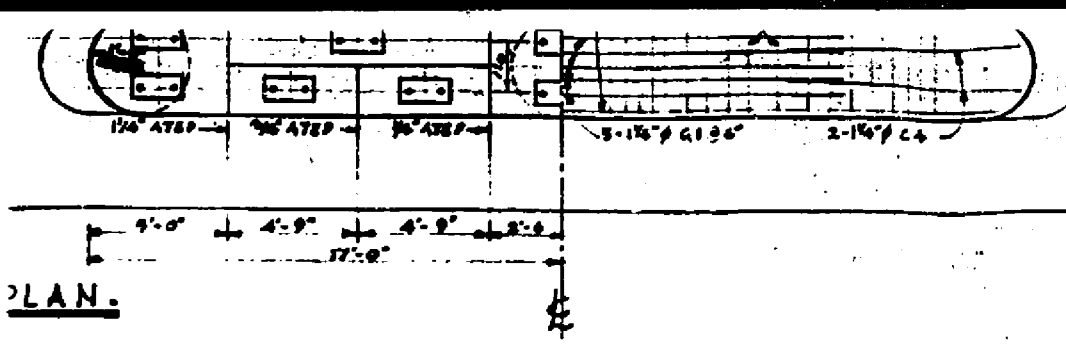

PLAN.

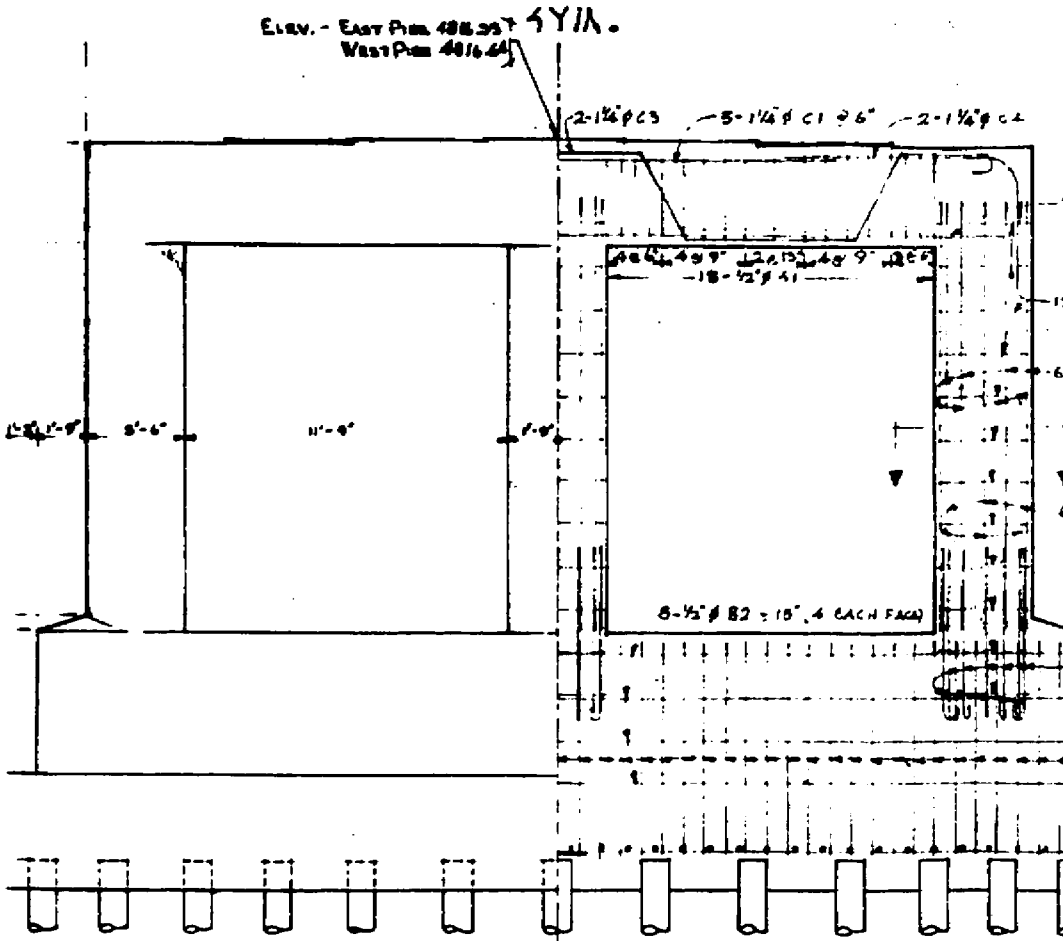

ELEVATION

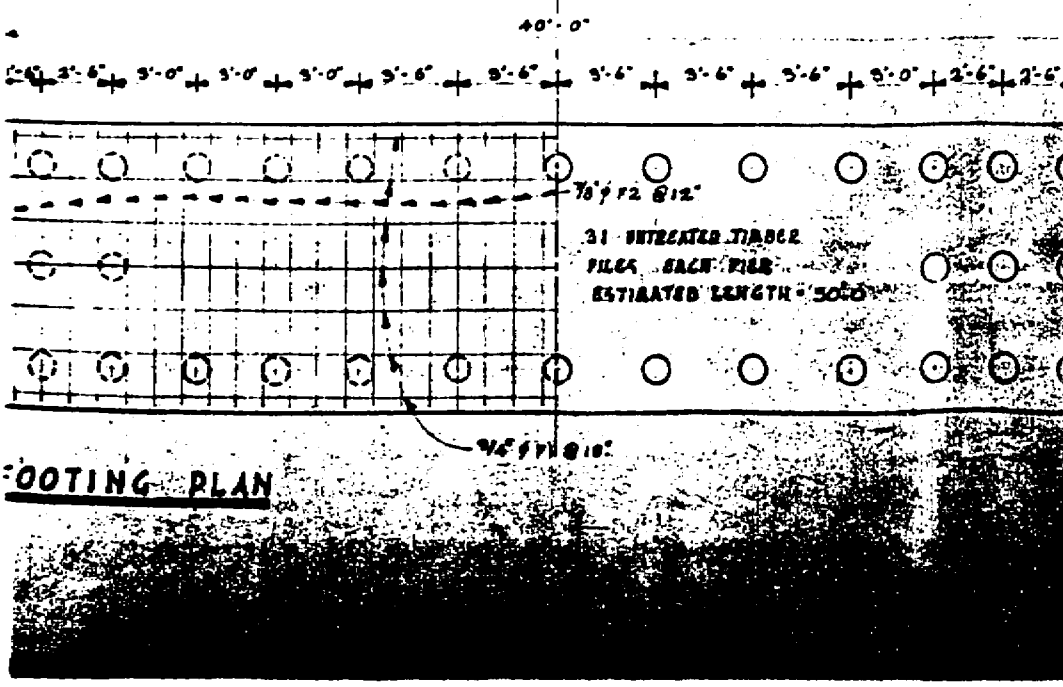

FOOTING PLAN

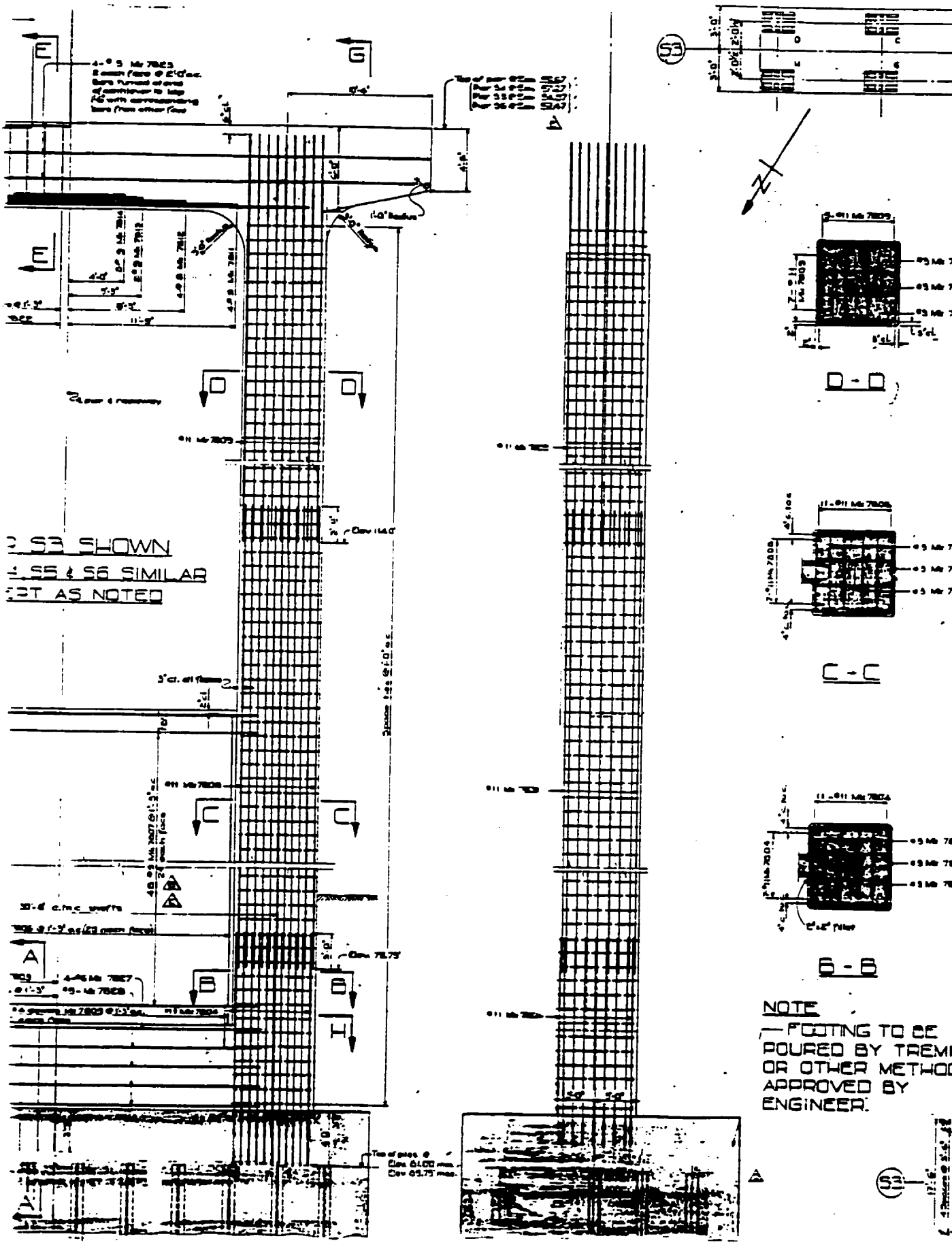
S3 SHOWN
S5 & S6 SIMILAR
T AS NOTED
D - D
C - C
B - B
NOTE
FOOTING TO BE
POURED BY TREMI
OR OTHER METHOD
APPROVED BY
ENGINEER.

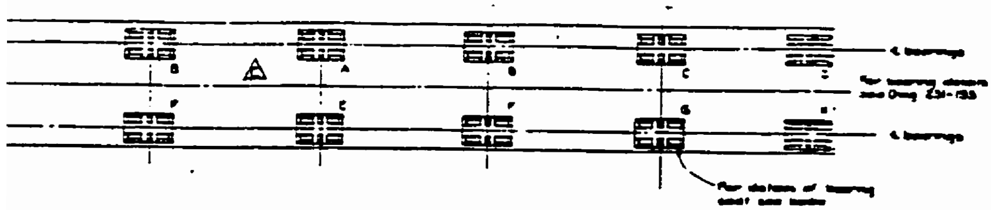

PLAN OF PIER TOP

Bearing seat	Pier 53	Pier 54	Pier 55	Pier 56
A	160.45	158.05	155.65	153.25
B	160.36	157.96	155.56	153.16
C	160.27	157.87	155.47	153.07
D	160.04	157.54	155.24	152.84
E	160.53	158.13	155.73	153.33
F	160.44	158.04	155.64	153.24
G	160.35	157.95	155.55	153.15
H	160.12	157.72	155.32	152.92

BEARING SEAT ELEVATIONS

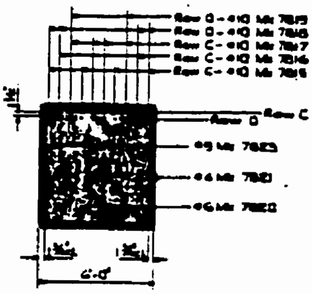

F - F

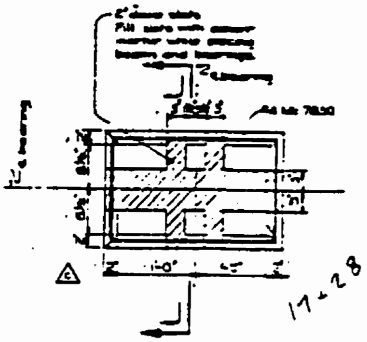

TYPICAL BEARING SEAT

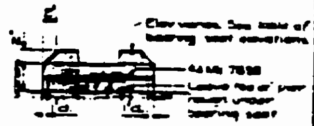

J - J

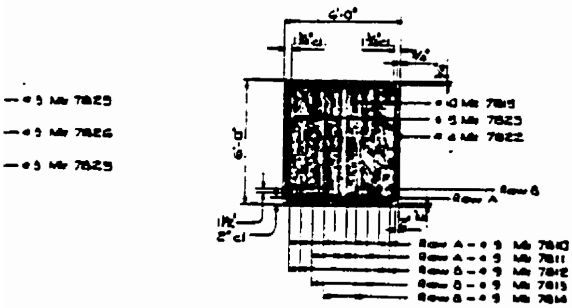

E - E

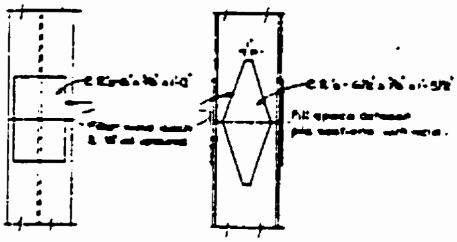

'H' PILE SPLICE

NOTES

Piers are located centrally on bridge ℄ and at right angles to ℄, centered on numbered piers except for N15, N16, N28, N44, 342, 349, 356 & 373. Pier shafts can be located from the Cruise [illegible] drawings.

All concrete to be 3000 psi ultimate strength at 28 days.

Reinforcement cover, chamfers & fillets are as typically noted.

Reinforcement notes see dwg. # 231-M2.

[illegible] shall be placed in all footings corresponding to the main vertical steel in the structure immediately above and arranged for [illegible].

A layer of gravel may be required by the Engineer for [illegible] where the soil condition is unsuitable for receiving fresh concrete.

[illegible] are untreated fir without shoes. Piles are to be not longer than [illegible] below cut-off and are to be driven to a supporting value of [illegible] kips as computed by the 'Engineering News' formula (with adjustment for friction, [illegible] etc.)

Steel bearing and anchor piles shall be driven to a supporting value of [illegible] kips as computed by the 'Engineering News' formula (with adjustment for friction, [illegible] etc.) Splices shall be as shown on the drawing.

Elevations to underside of footings and ground fill are [illegible] values. Changes in elevations must be approved by the Engineer.

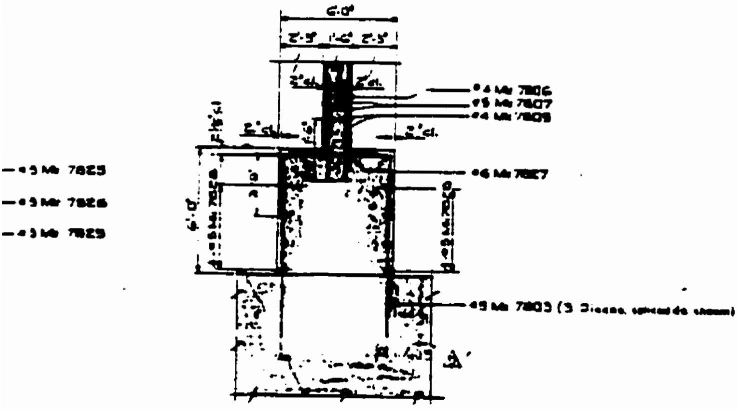

A - A

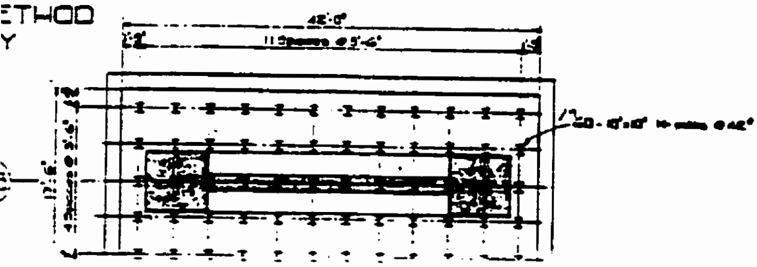

	Date	By	Description
3	[illegible]	J.B. / F.R.R.	Joint footing changed to [illegible]
2	June 1959	P.S. / D.B.	Bearing & pier top elev. changed. Bearing seat elev. [illegible]
1	[illegible]	N.O. / [illegible]	[illegible]

OAK STREET BRIDGE

PROVINCIAL GOVERNMENT OF BRITISH COLUMBIA
DEPARTMENT OF PUBLIC WORKS

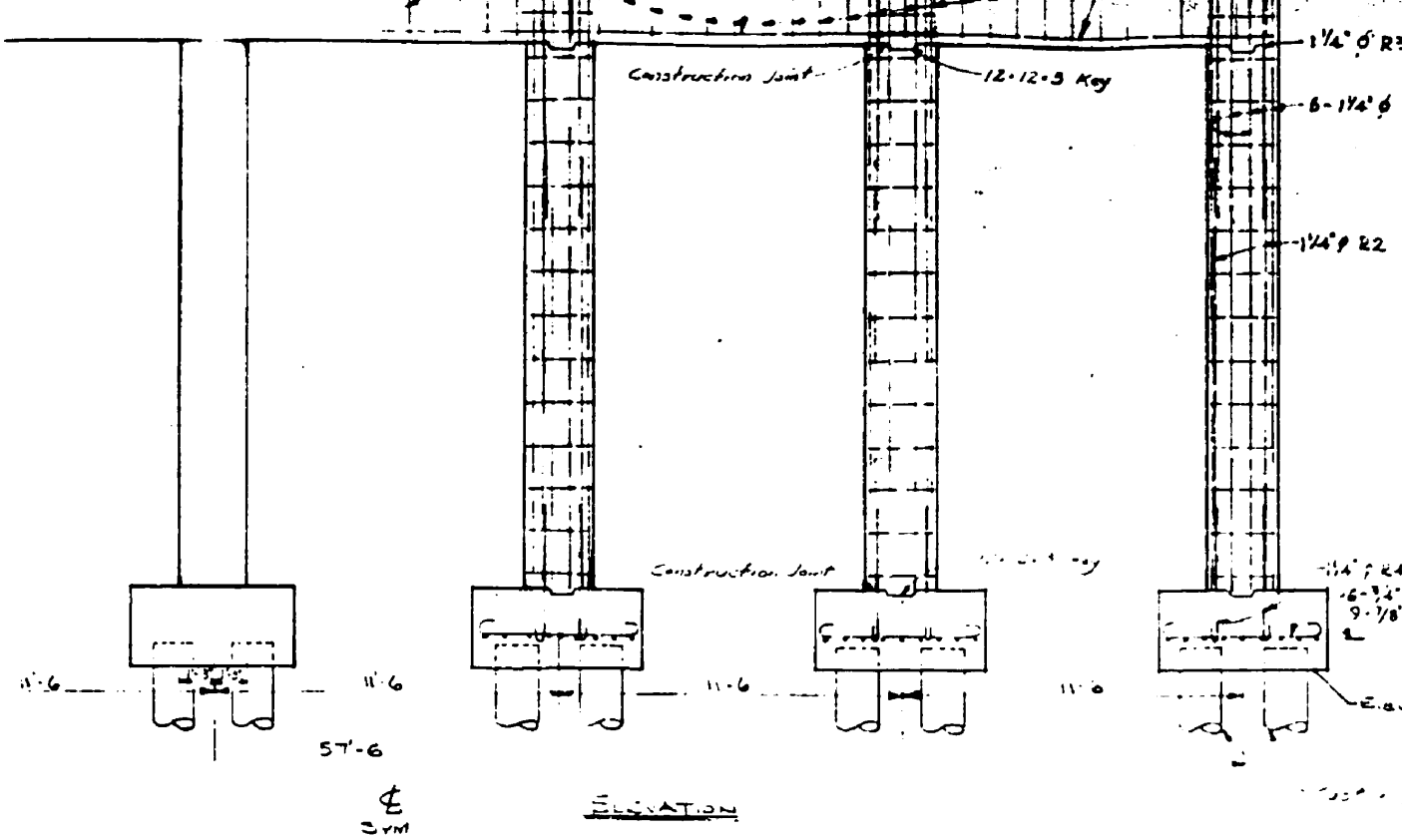

ELEVATION

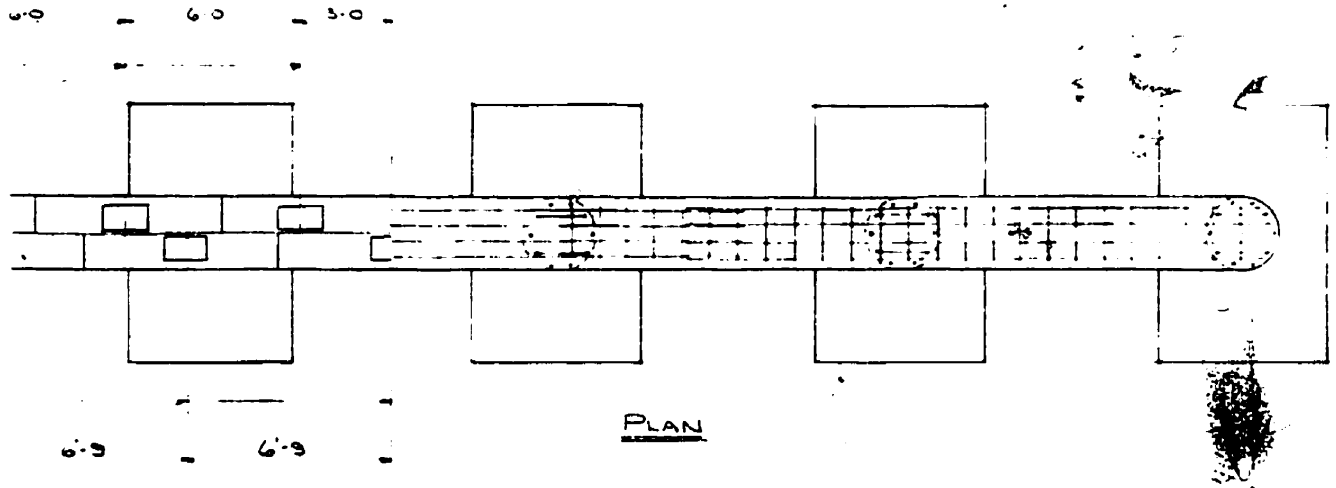

PLAN

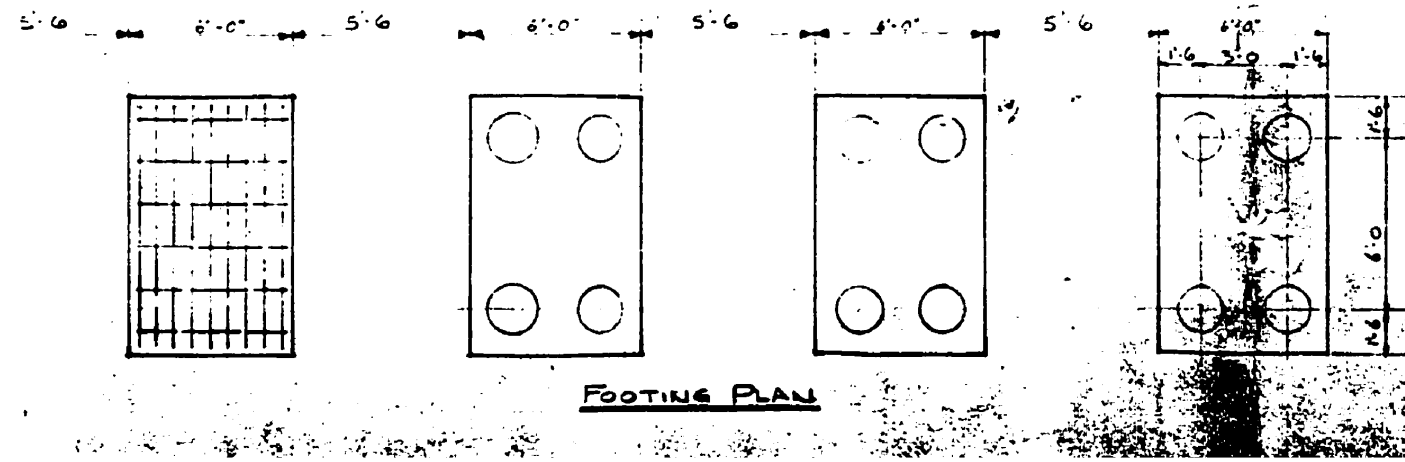

FOOTING PLAN

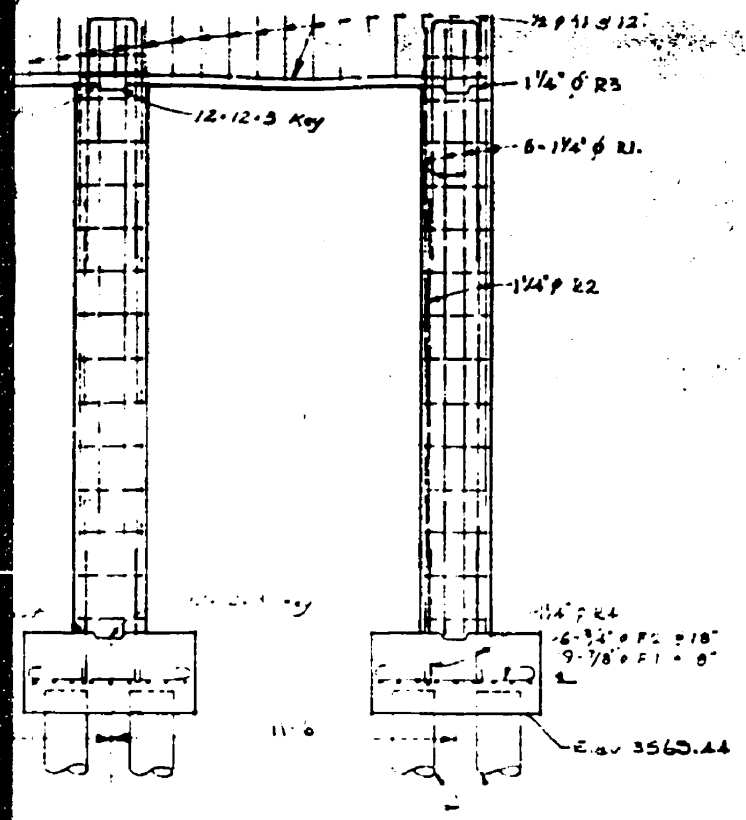

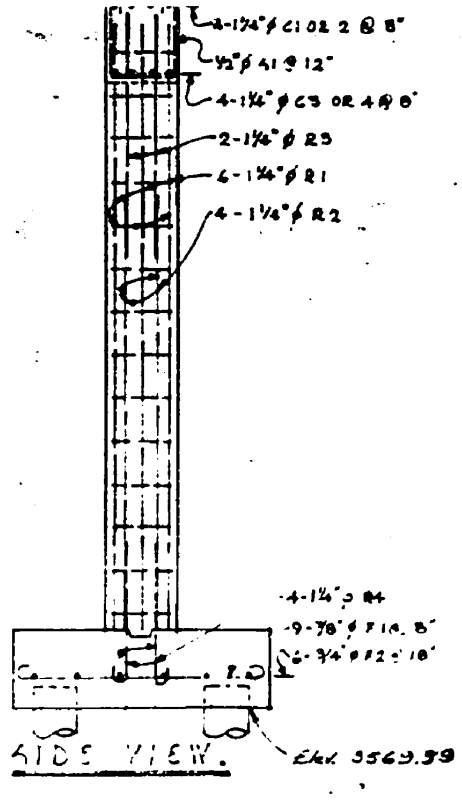

MARK	No. REQD	SIZE N
C 1	8	10
C 2	16	10
C 3	8	10
C 4	16	10
R1	118	4
R1	72	10
R2	48	10
R3	24	10
R4	48	10
F 1	108	7
F 2	72	6
T 1	168	2
P-1	288	6
P-2	288	2

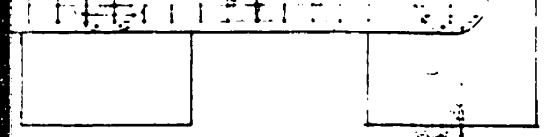

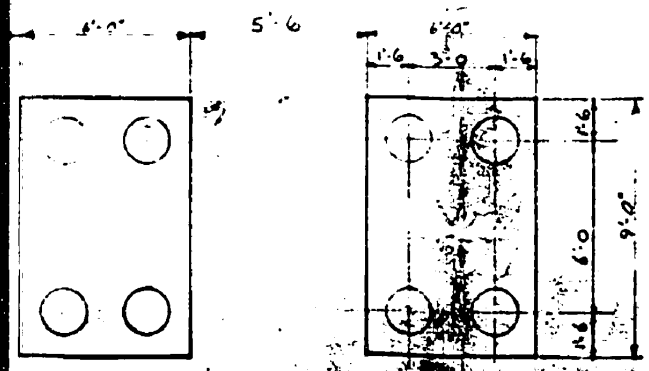

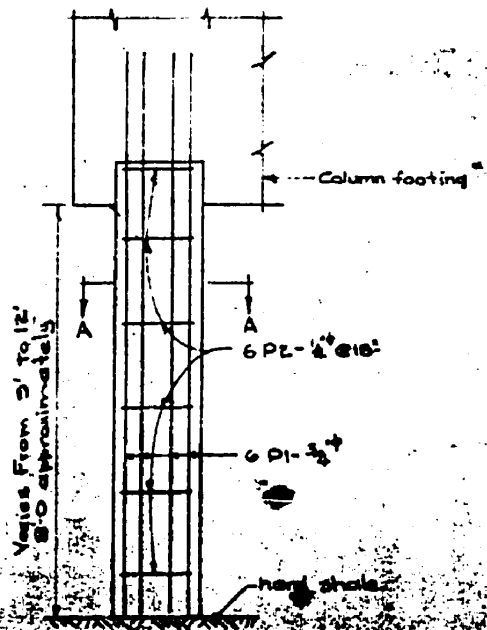

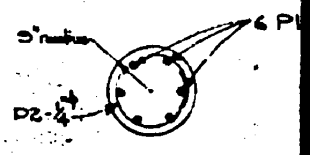

SECT A-A

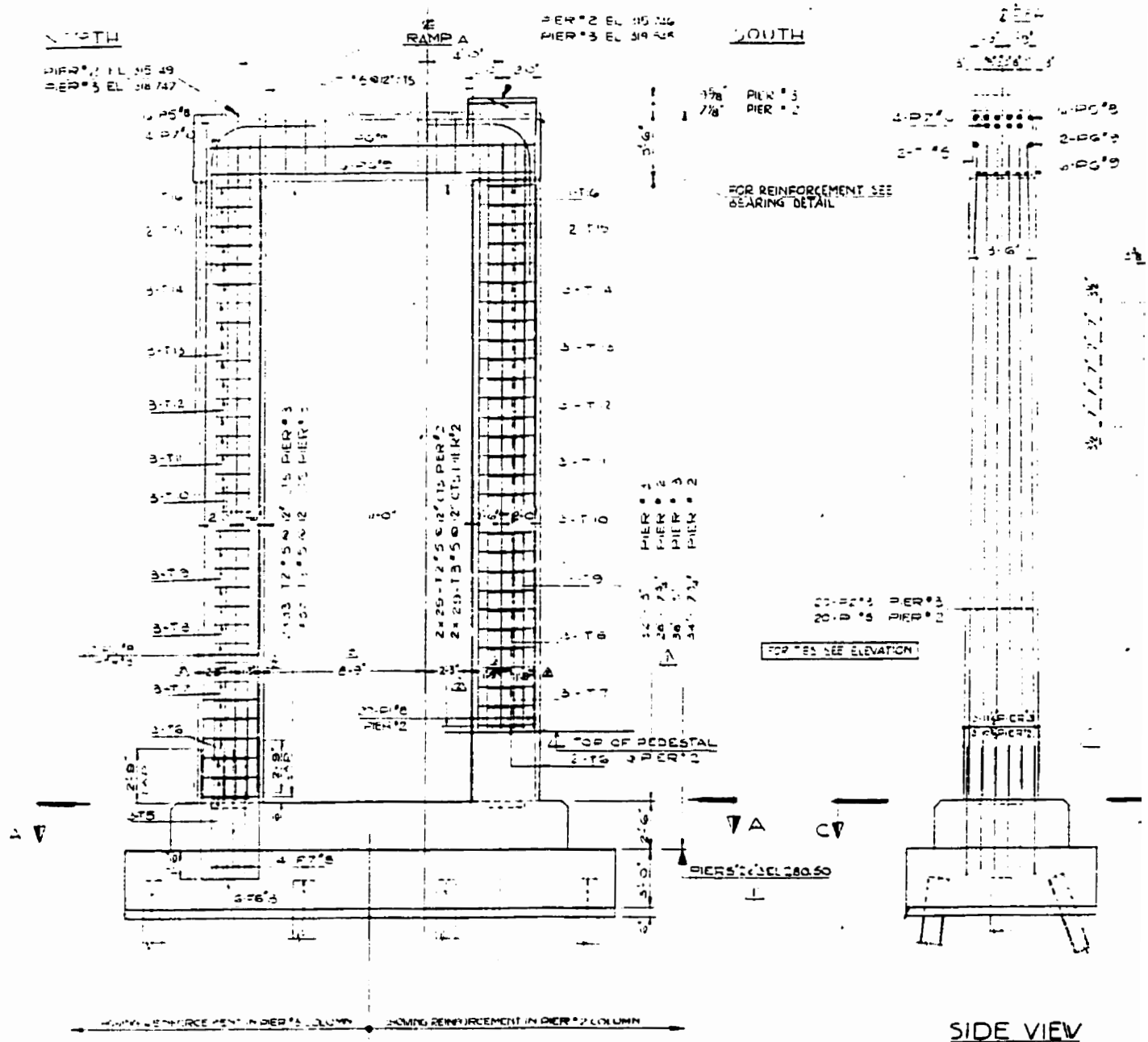

ELEVATION OF PIER #3

REINFORCEMENT STEEL IN PIER #2 SIMILAR

SCALE 3/4" = 1'-0"

SIDE VIEW

SCALE 3/4" = 1'-0"

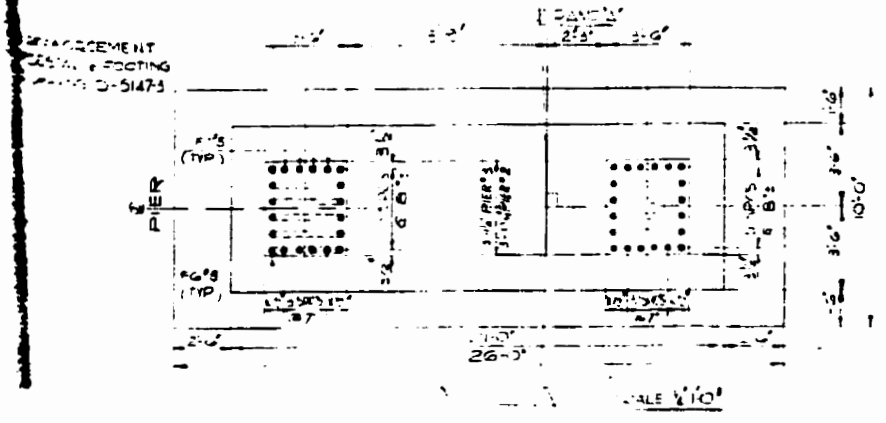

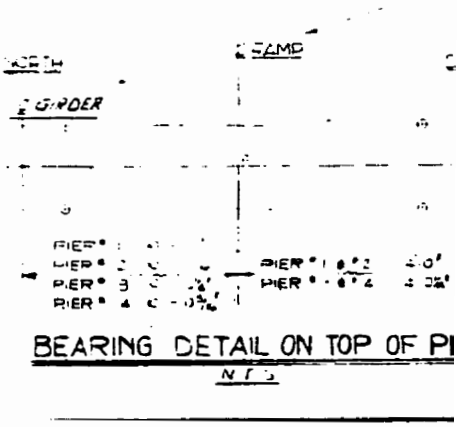

BEARING DETAIL ON TOP OF PI

N.T.S.

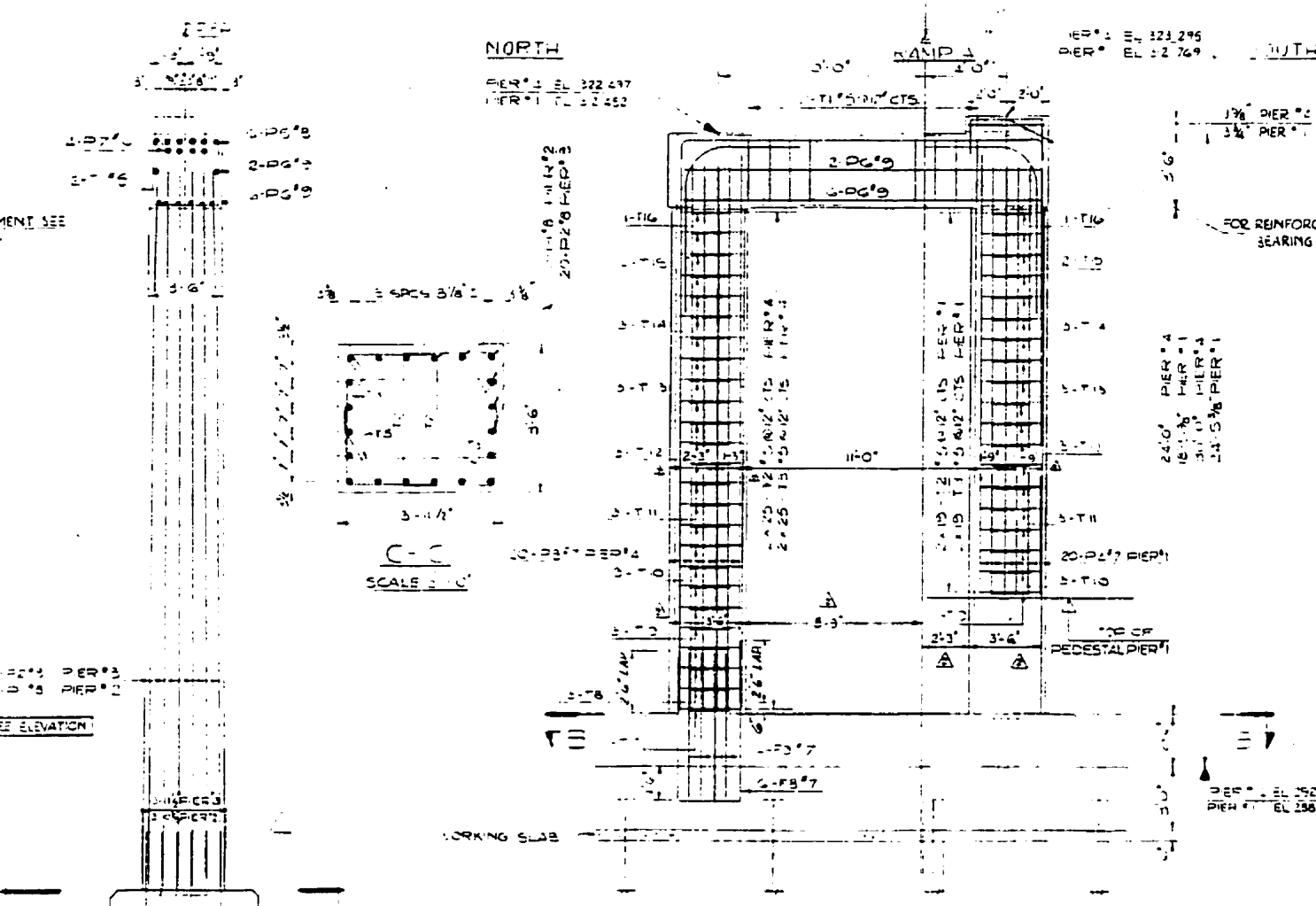

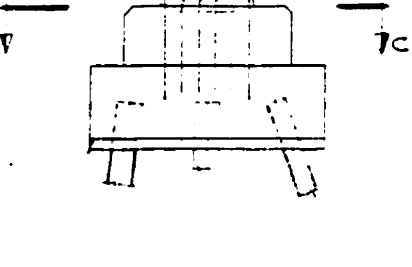

SIDE VIEW
SCALE 1" = 1'-0"

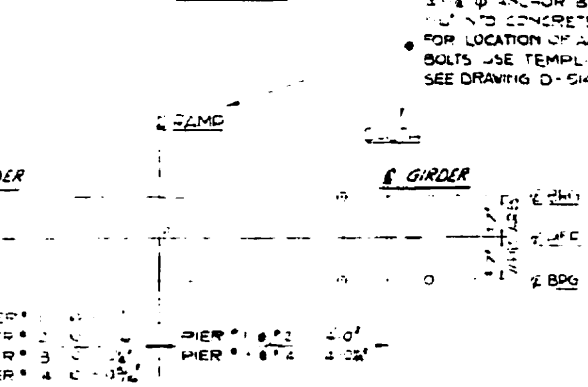

ARING DETAIL ON TOP OF PIER CAPS
N T S

ELEVATION OF PIER #4
REINFORCEMENT STEEL IN PIER #1 SIMILAR
SCALE 1" = 1'-0"

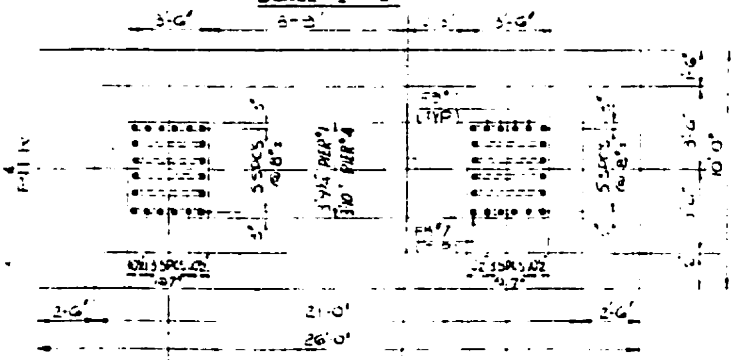

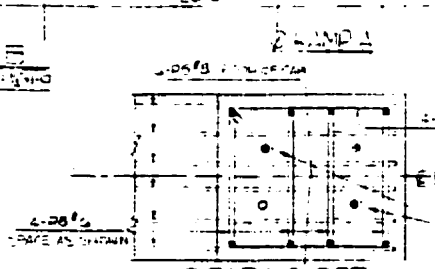

BEARING DETAIL
SHOWING REINFORCEMENT
SCALE 1" = 1'-0"

FOR REINFORCEMENT
PEDESTAL & FOOTING
SEE DRAWING D-5147-3

4 ANCHOR BOLTS
IN CONCRETE
FOR LOCATION OF ANCHOR
BOLTS USE TEMPLATE
SEE DRAWING D-5147-

REVISIONS

KING CO.

APPR
DESIGN
DRAWING
DATE

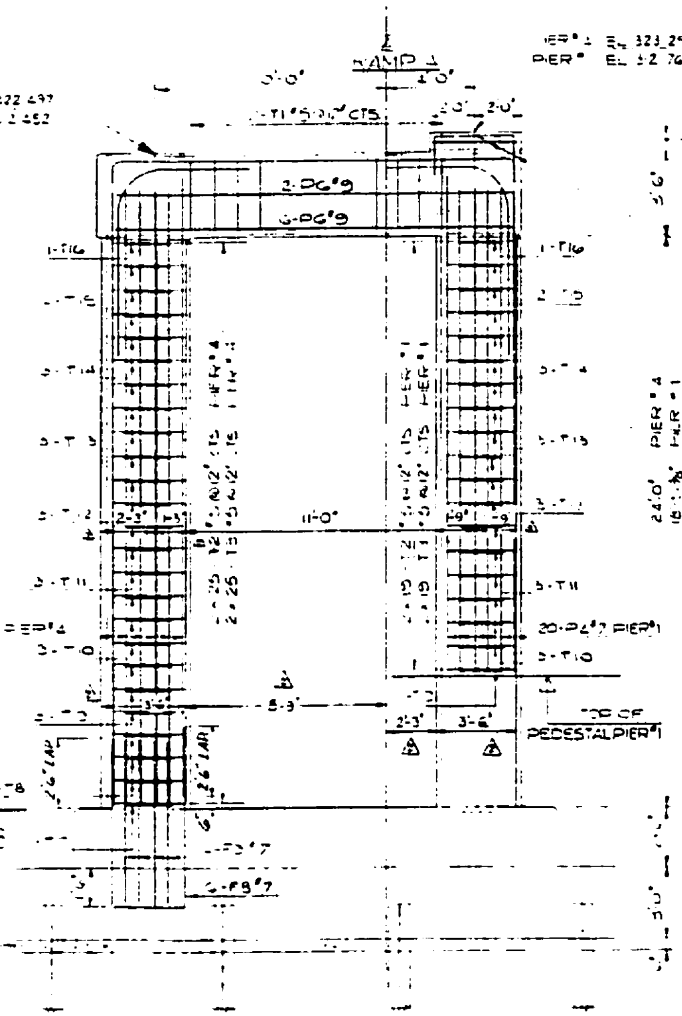

ELEVATION OF PIER #4

REINFORCEMENT STEEL IN PIER #1 SIMILAR
SCALE 1/4"=1'-0"

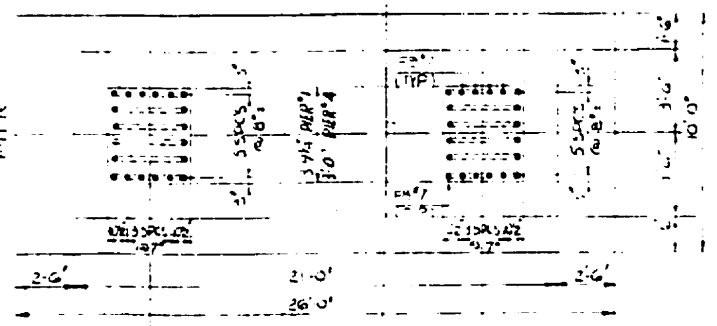

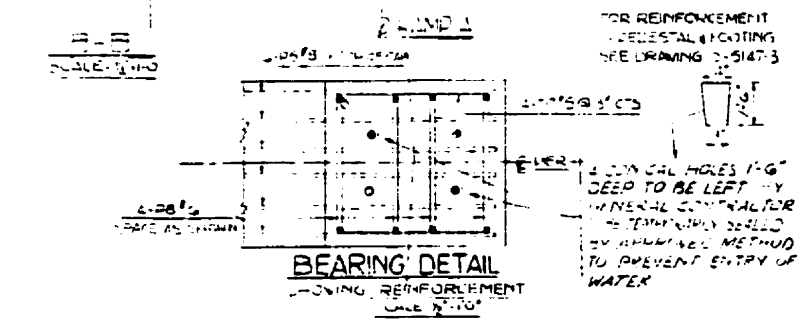

BEARING DETAIL

SHOWING REINFORCEMENT
SCALE 1"=1'-0"

FOR REINFORCEMENT OF PEDESTAL & FOOTING SEE DRAWING S-5147-3

4 CORRUGATED HOLES 1'-6" DEEP TO BE LEFT EMPTY IN CONCRETE FOR REMOVABLE STEEL BOLTS BY APPROVED METHOD TO PREVENT ENTRY OF WATER

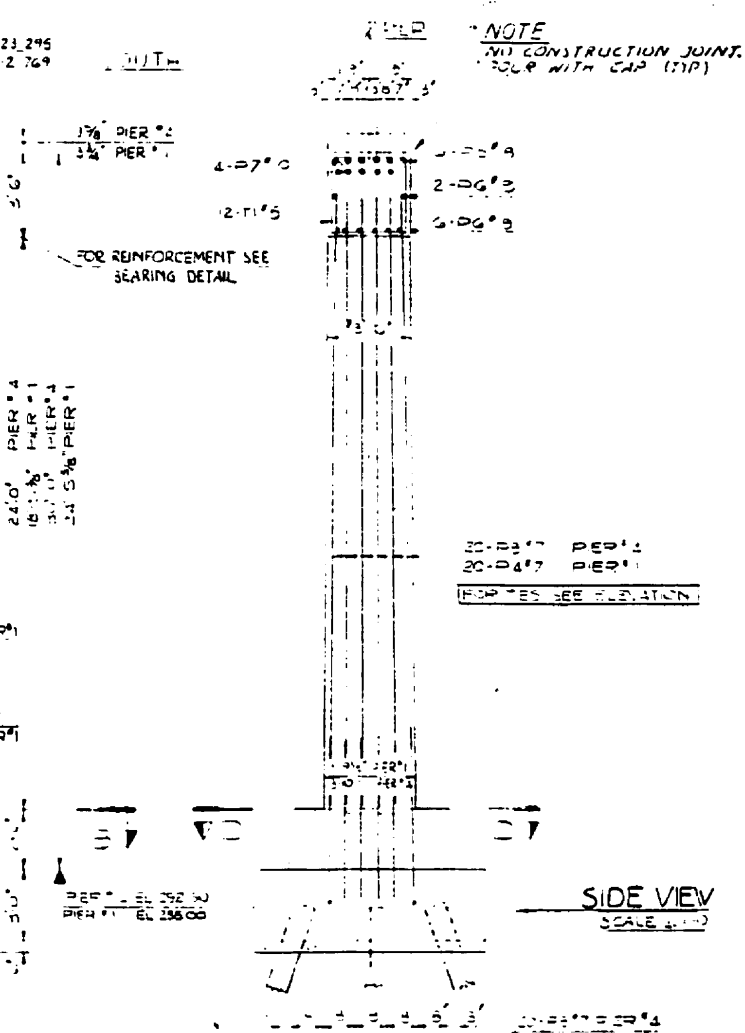

SIDE VIEW

SCALE 1/4"=1'-0"

NOTE
NO CONSTRUCTION JOINT. TOP WITH CAP (TYP.)

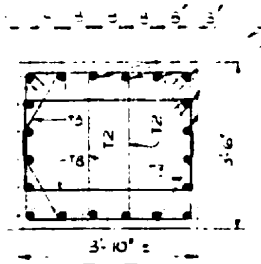

D-D

SCALE ½"=1'-0"

REVISIONS			
NOV 69	E.T.	DIMENSIONS REVISED AS-CONSTR.	
29 6/73	A.U.	PREV ELEV PIER 3 SIDE VIEW SECT D-D ADD	
DATE	BY	DESCRIPTION	

DEPARTMENT OF HIGHWAYS ONTARIO
BRIDGE DIVISION

BRIDGE OVER OLD WELLAND CANAL

CONNECTION BETWEEN HWY No 406 AND GENEVA ST IN ST. CATHARINES

KING'S HIGHWAY No. ____ DIST No. 1
CO. LINCOLN
CITY OF ST CATHARINES LOT ____ CON. ____

PIERS

APPROVED				SITE No. 79-152	W.P. No. 274-6	
DESIGN	A.U.	CHECK	J.S.	CONTRACT No.	6405	6429
DRAWING	N.T.	CHECK	J.S.			
DATE	MAY 69	LOADING	H-20 S-16	DRAWING No.	D-5147	

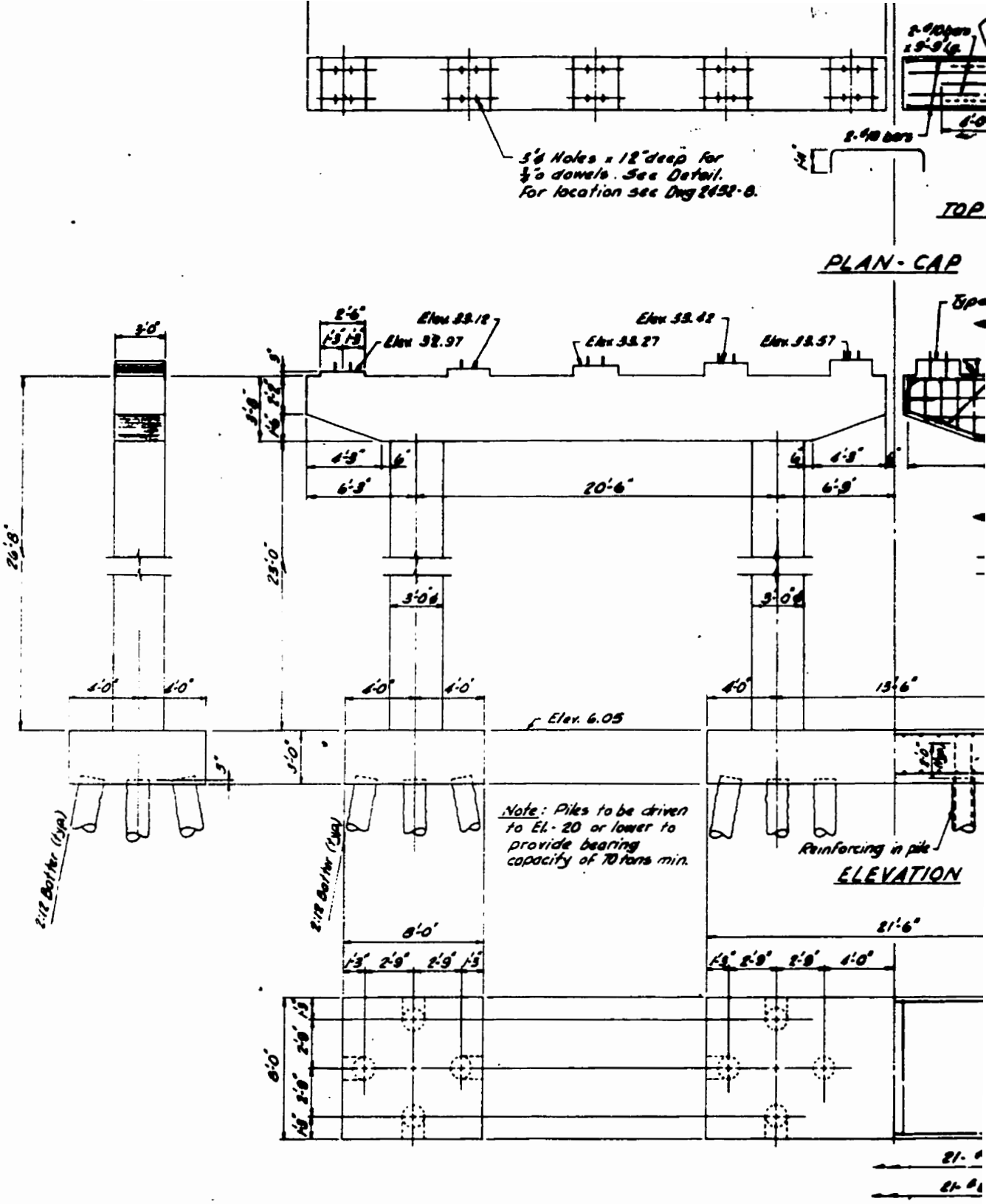
5/8 Holes x 12" deep for
3/4" o dowels. See Detail.
For location see Dwg 2452-B.
TOP
PLAN - CAP
Elev 32.18
Elev 32.97
Elev 33.27
Elev 33.42
Elev 33.57
2'-6"
3'-0"
3'-0"
6'-3"
6'-3"
20'-6"
6'-3"
6'-3"
26'-8"
23'-0"
3'-0"
9'-0"
4'-0"
4'-0"
6'-0"
4'-0"
4'-0"
13'-6"
Elev. 6.05
3'-0"
3"
2:1 Batter (typ)
2:1 Batter (typ)
Note: Piles to be driven
to El. - 20 or lower to
provide bearing
capacity of 70 tons min.
Reinforcing in pile
ELEVATION
8'-0"
21'-6"
1'-3" 2'-9" 2'-9" 1'-3"
1'-3" 2'-9" 2'-9" 4'-0"
8'-0"
PLAN - FOOTING

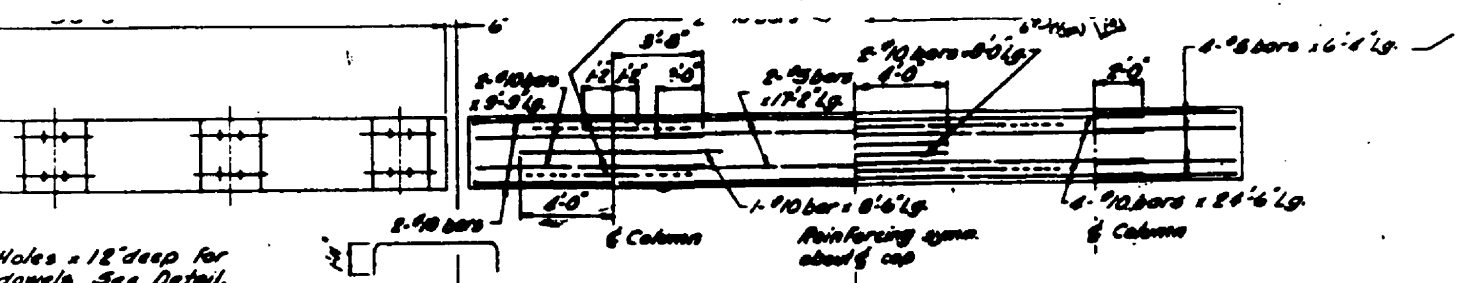

PLAN - CAP

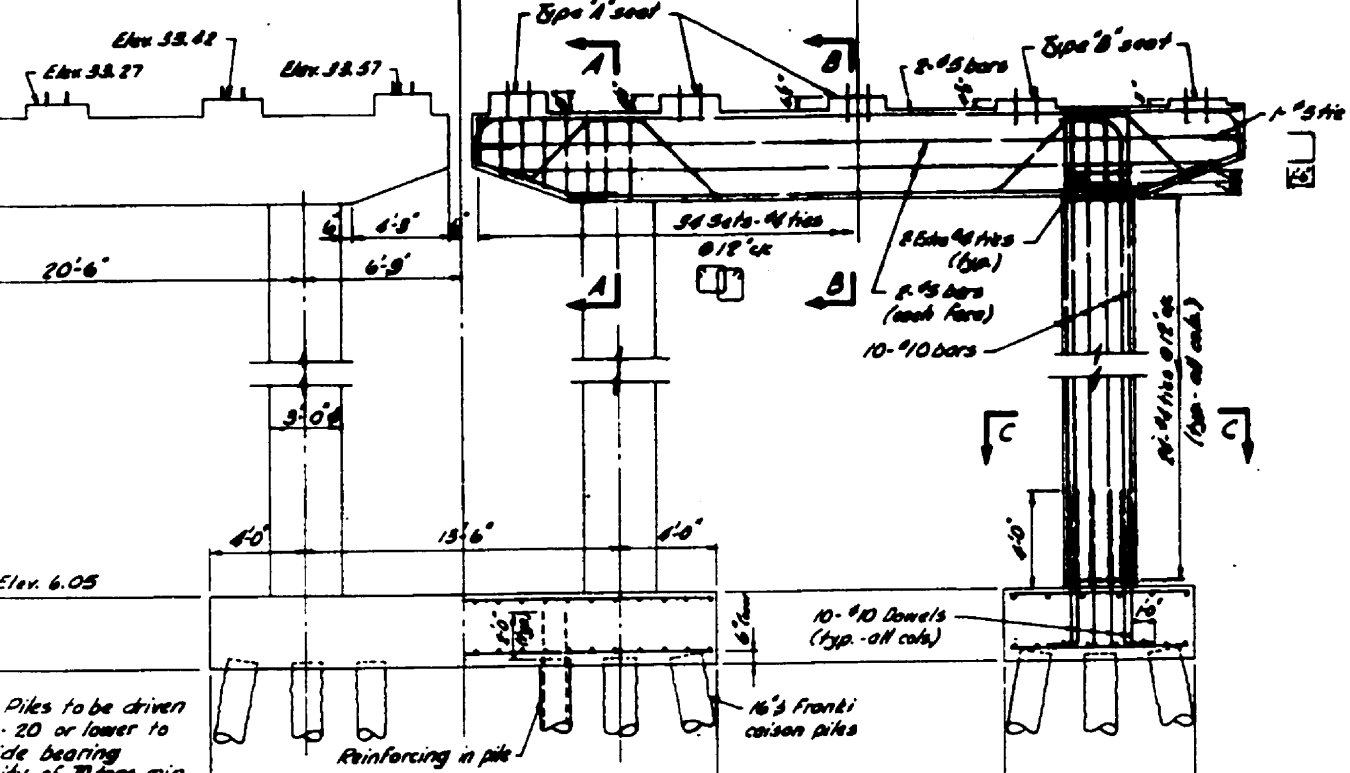

ELEVATION

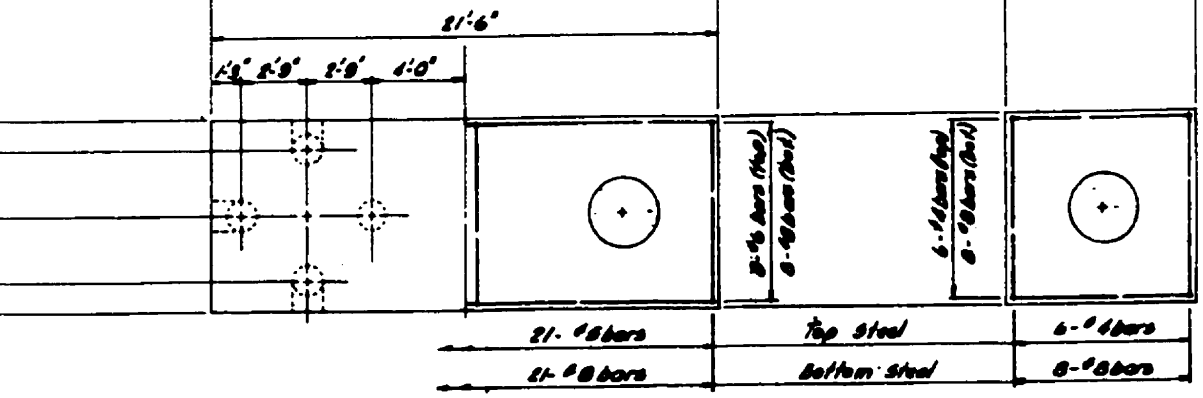

PLAN - FOOTINGS

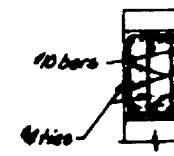

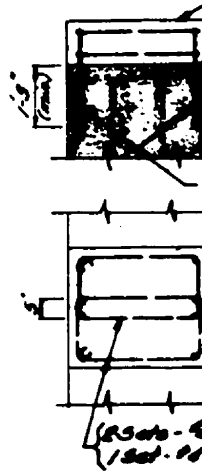

BRIDGE SEAT

Notes

1. Concrete to be Class 'A' throughout.
2. Exposed edges to have except as noted.
3. Reinforcing steel to be "Intermediate" grade.
4. Reinforcing steel to have cover except as noted.
5. Lap of bars for splices 40 x 'd'. Splices to be st

ESTIMATED QUANTITIES				
Location	Concrete Class 'A'	Reinforcing	[illegible]	Anchor Bolts
Abut'mt	65 cu.yds.	5117 lbs.	[illegible]	16

D	
C	
B	
A	Quantities revised

REVISIONS

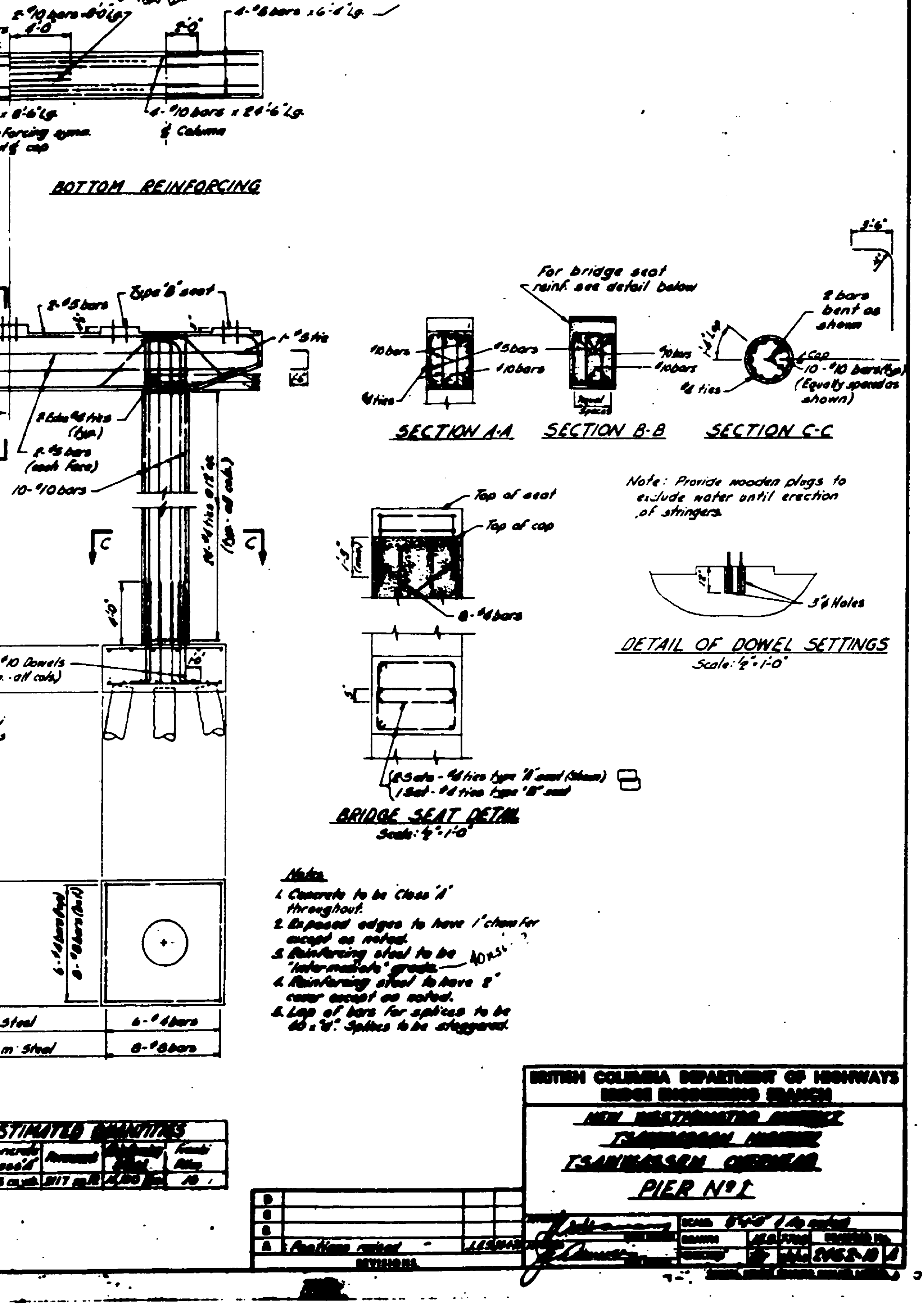

BOTTOM REINFORCING
4-#10 bars x 24'-6" Lg.
℄ Column
For bridge seat reinf. see detail below
Type 'B' seat
SECTION A-A
SECTION B-B
SECTION C-C
2 bars bent as shown
10 - #10 bars (typ.) (Equally spaced as shown)
10-#10 bars
Note: Provide wooden plugs to exclude water until erection of stringers.
Top of seat
Top of cap
8-#4 bars
3"φ Holes
DETAIL OF DOWEL SETTINGS
Scale: ½"=1'-0"
BRIDGE SEAT DETAIL
Notes
1. Concrete to be Class 'A' throughout.
2. Exposed edges to have 1" chamfer except as noted.
3. Reinforcing steel to be "intermediate" grade.
4. Reinforcing steel to have 2" cover except as noted.
5. Lap of bars for splices to be 40 x "d". Splices to be staggered.
6-#4 bars
8-#8 bars
ESTIMATED QUANTITIES
BRITISH COLUMBIA DEPARTMENT OF HIGHWAYS
PIER Nº 1
REVISIONS

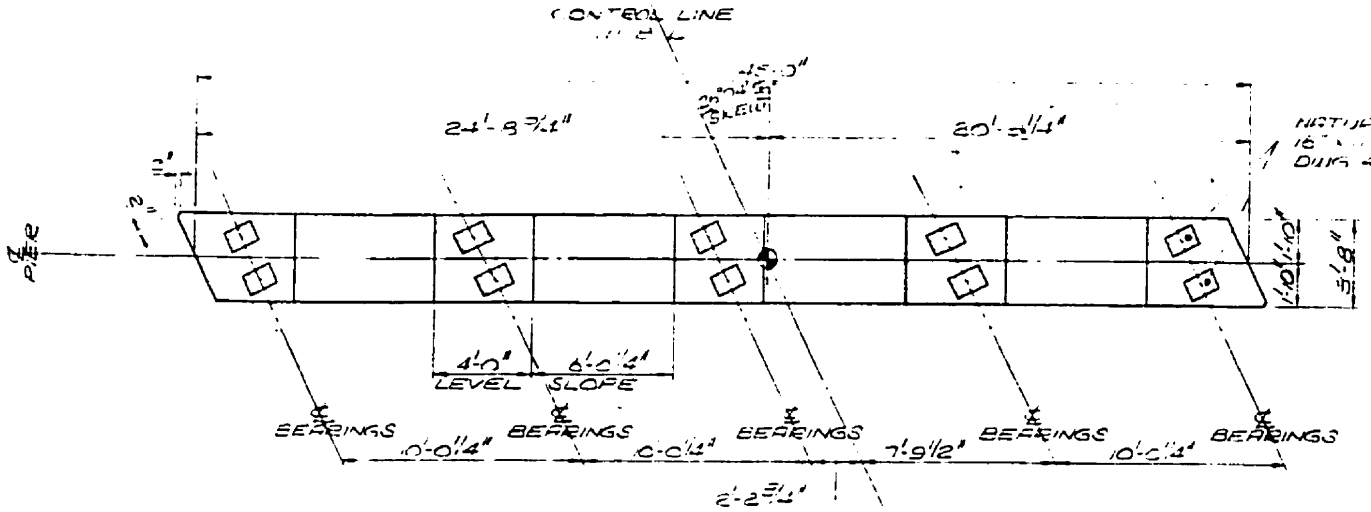

PLAN

SCALE 1/4"=1'-0"

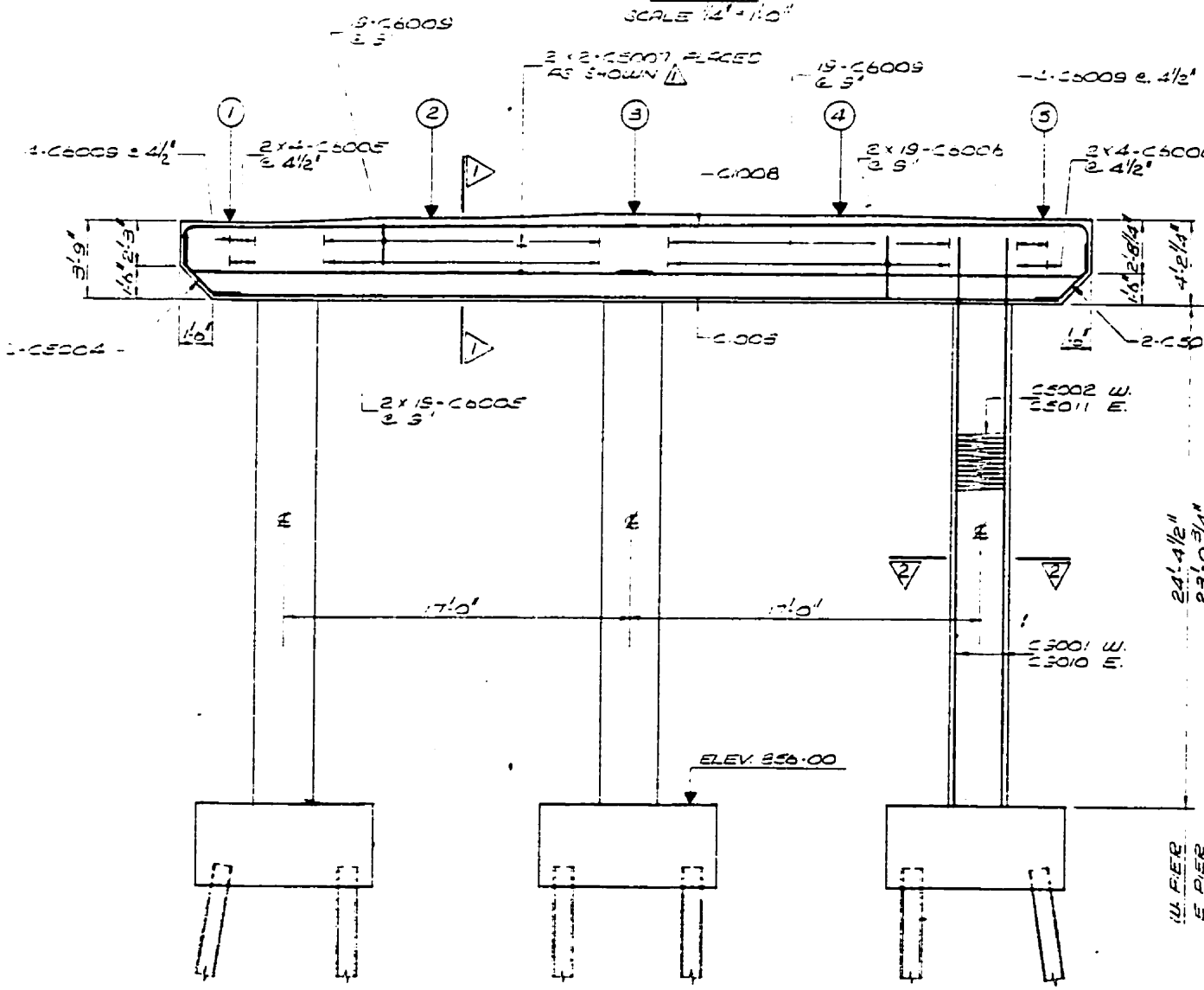

ELEVATION

SCALE 1/4"=1'-0"

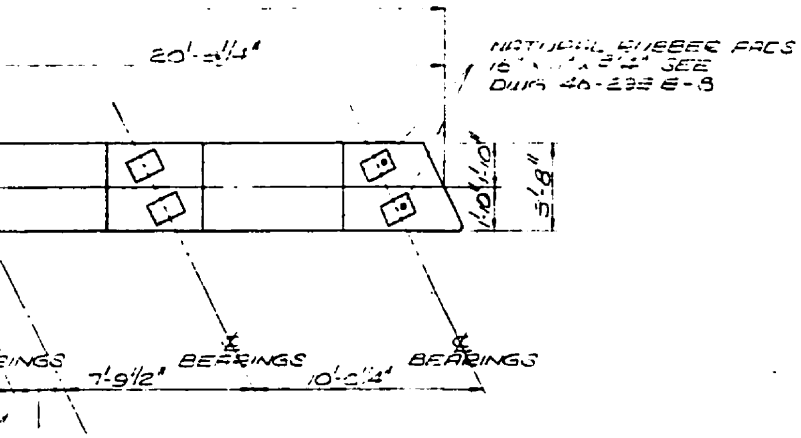

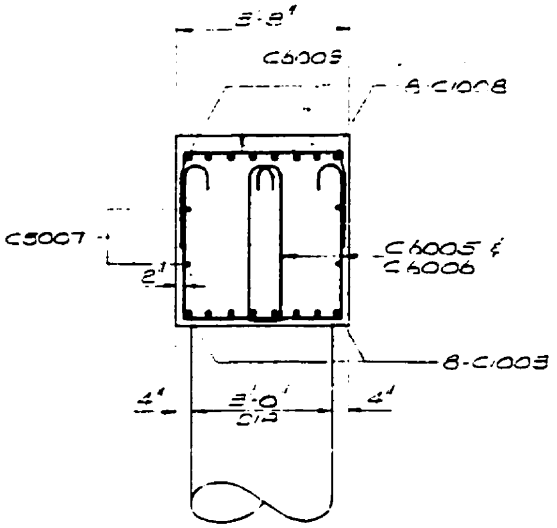

1
SCALE 1/2" = 1'-0"

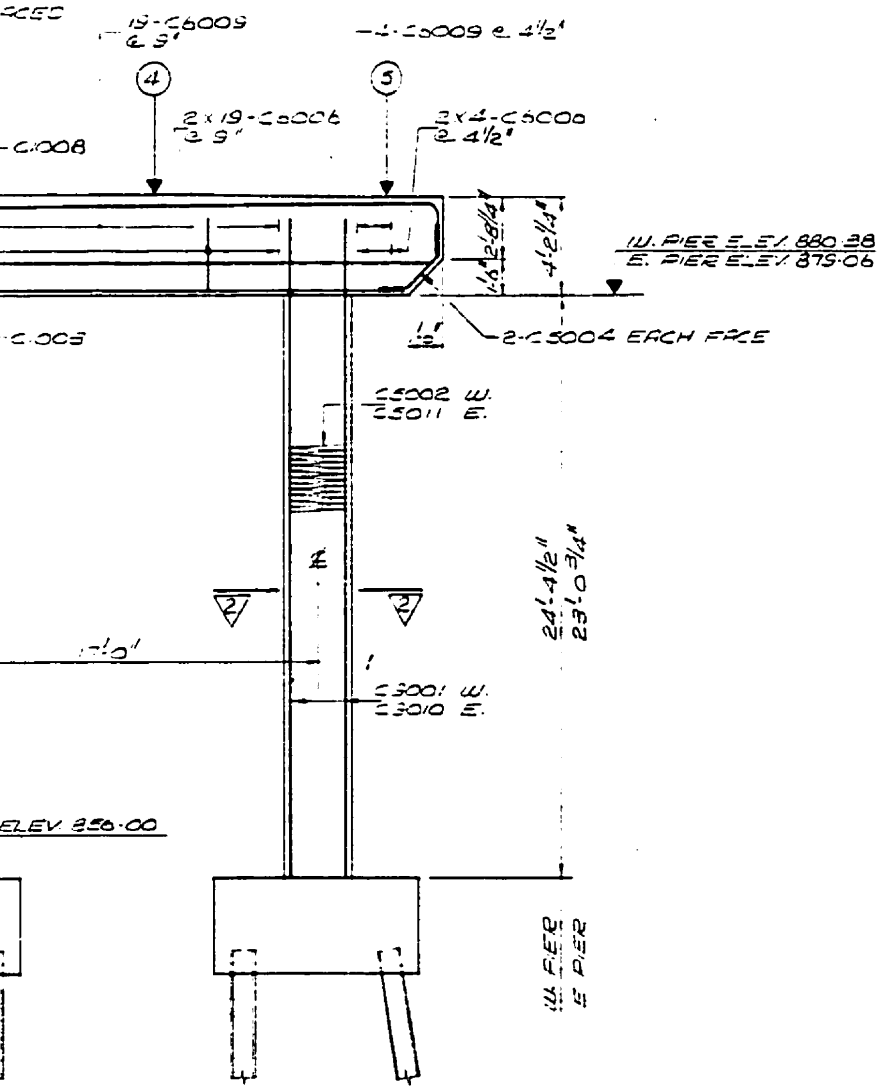

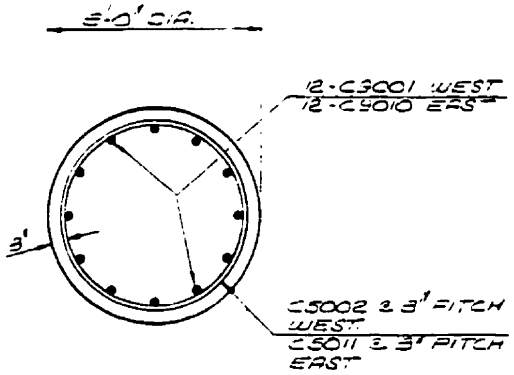

2
SCALE 3/4" = 1'-0"

FOR REDU

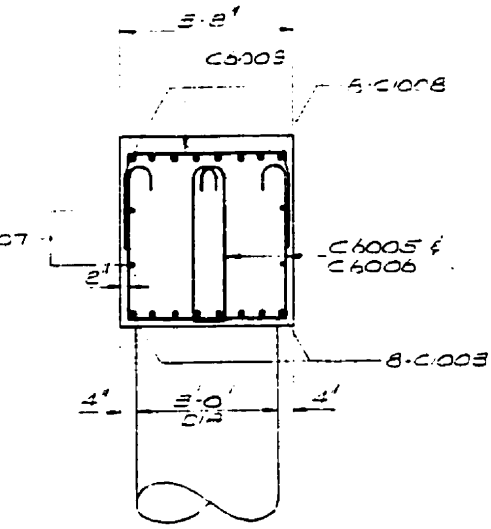

1
SCALE 1/2" = 1'-0"

BEARING SEAT ELEVATIONS					
LOCATION	1	2	3	4	5
WEST PIER	884.13	884.40	884.66	884.65	884.56
EAST PIER	882.81	883.08	883.35	883.34	883.25

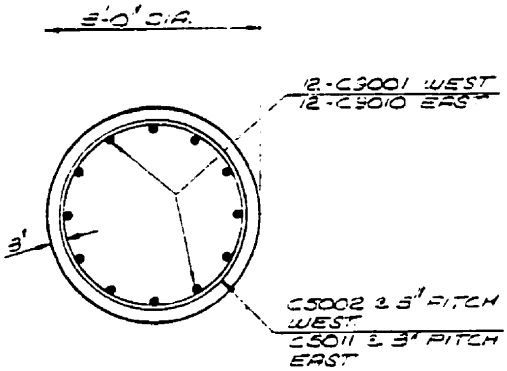

2
SCALE 3/4" = 1'-0"

REVISIONS			
	DATE	BY	DESCRIPTION

MINISTRY OF TRANSPORTATION AND COMMUNICATIONS
ONTARIO

C.P.R. OVERHEAD
W.B.L.

KING'S HIGHWAY No. 17N DIST. No. 17
REGIONAL MUNICIPALITY OF SUDBURY
TWP. WATERS LOT 5 CON. 5

PIERS

APPROVED _____ STRUCTURAL ENGINEER
DESIGN J.S. CHECK
DRAWING E.O.N. CHECK
DATE DEC '81

CONTRACT No. 78-37
W.P. No. 62-74-09
STATE No. 44-209 A SHEET 7

CIVIL
JOSEPH SEQUEC
REGISTERED PROFESSIONAL ENGINEER
PROVINCE OF ONTARIO

FOR REDUCED PLAN
USE SCALE BELOW
0 1 2 3
1 INCHES ON ORIGINAL PLAN

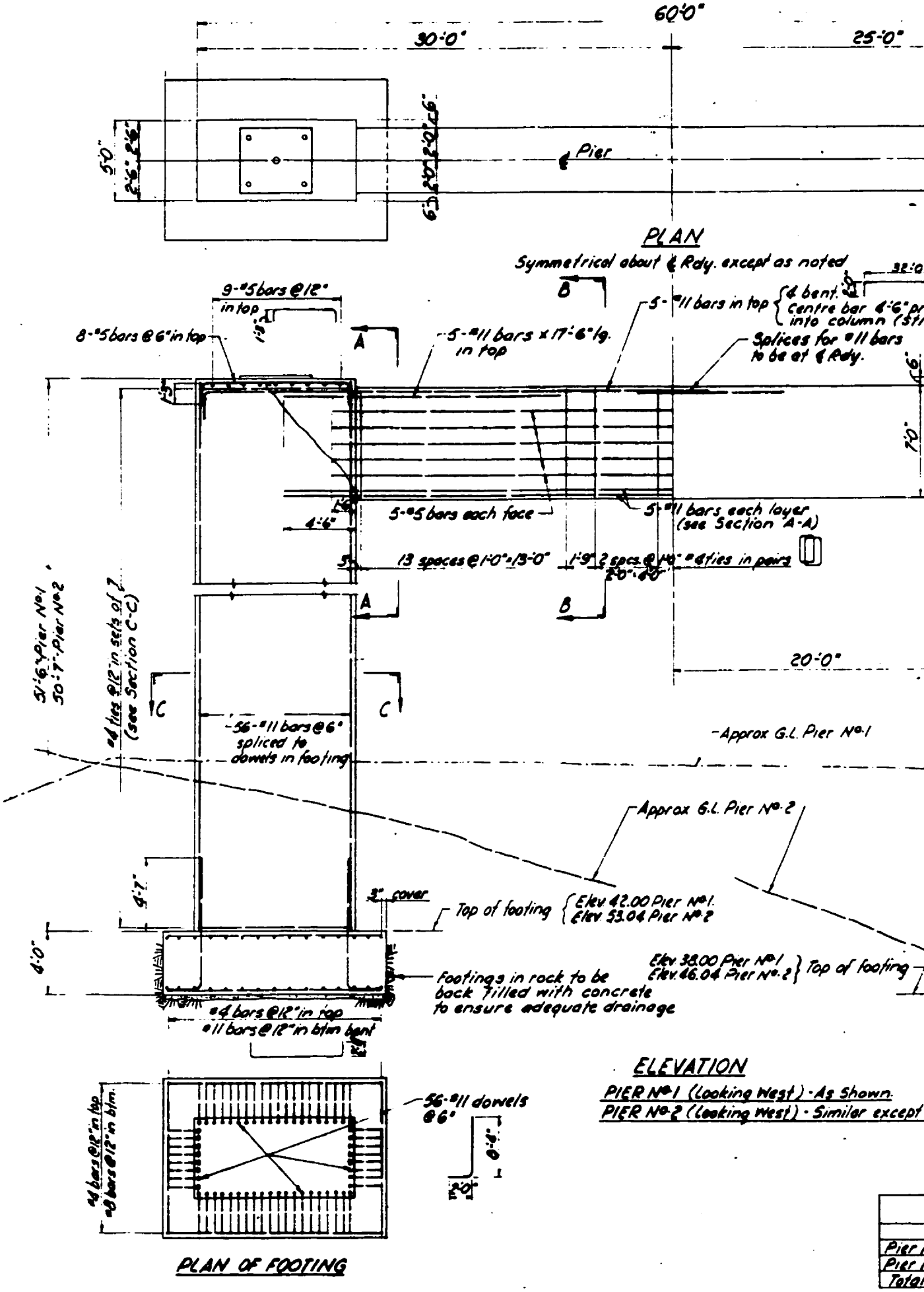
60'-0"
30'-0"
25'-0"
Pier
PLAN
Symmetrical about ℄ Rdy. except as noted
9-#5 bars @12" in top
8-#5 bars @6" in top
5-#11 bars x 17'-6" lg. in top
5-#11 bars in top
Splices for #11 bars to be at ℄ Rdy.
5-#5 bars each face
5-#11 bars each layer (see Section A-A)
13 spaces @1'-0" = 13'-0"
2 spcs @ 4" = #6 ties in pairs
20'-0"
#4 ties @12" in sets of 2 (see Section C-C)
56-#11 bars @6" spliced to dowels in footing
Approx G.L. Pier No.1
Approx G.L. Pier No.2
3" cover
Top of footing Elev 42.00 Pier No.1 Elev 53.04 Pier No.2
Elev 38.00 Pier No.1 Elev 46.04 Pier No.2 Top of footing
Footings in rock to be back filled with concrete to ensure adequate drainage
#4 bars @12" in top
#11 bars @12" in btm bent
ELEVATION
PIER No.1 (Looking West) - As Shown
PIER No.2 (Looking West) - Similar except
#4 bars @12" in top
#8 bars @12" in btm.
56-#11 dowels @6"
PLAN OF FOOTING

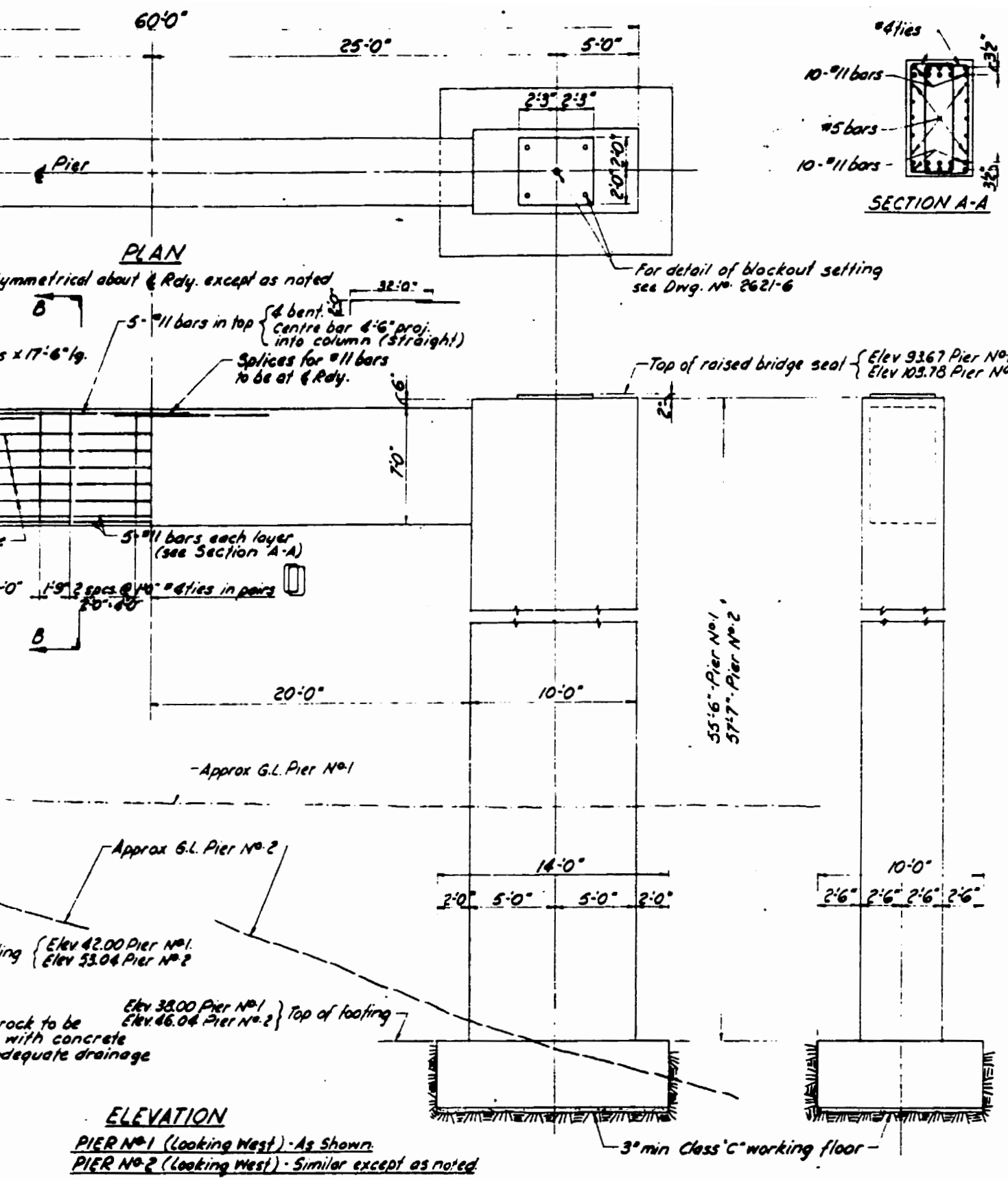

ESTIMATED QUANTITIES

	Formwork	C1'T conc.	C1'C conc.	Reinforcing
Pier No.1	3,900 sq.ft	281 cu.yd	3 cu.yd	59,250 lbs.
Pier No.2	3,950 sq.ft	283 cu.yd	3 cu.yd	59,700 lbs.
Totals	7,850 sq.ft.	564 cu.yd.	6 cu.yd.	118,950 lbs.

D	
C	
B	
A	
REVISIONS	

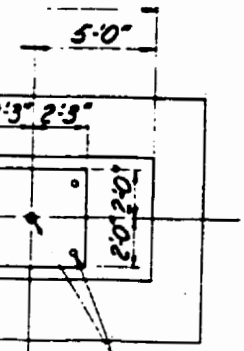

For detail of blockout setting see Dwg. No. 2621-6

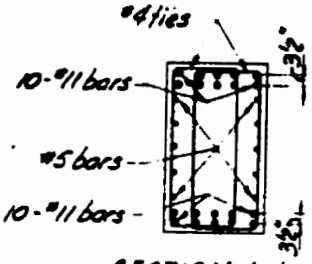

SECTION A-A

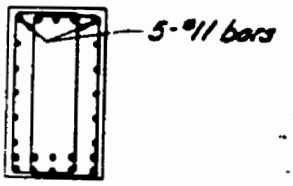

SECTION B-B

Note: All not shown similar to Section A-A

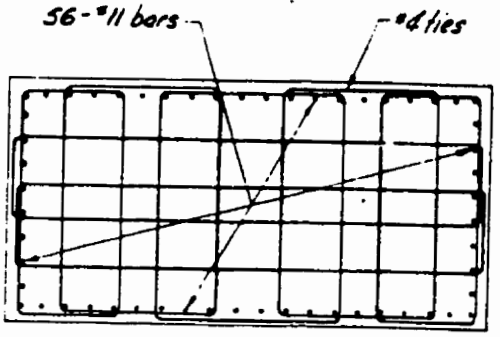

SECTION C-C
Scale: 1/2"=1'-0"

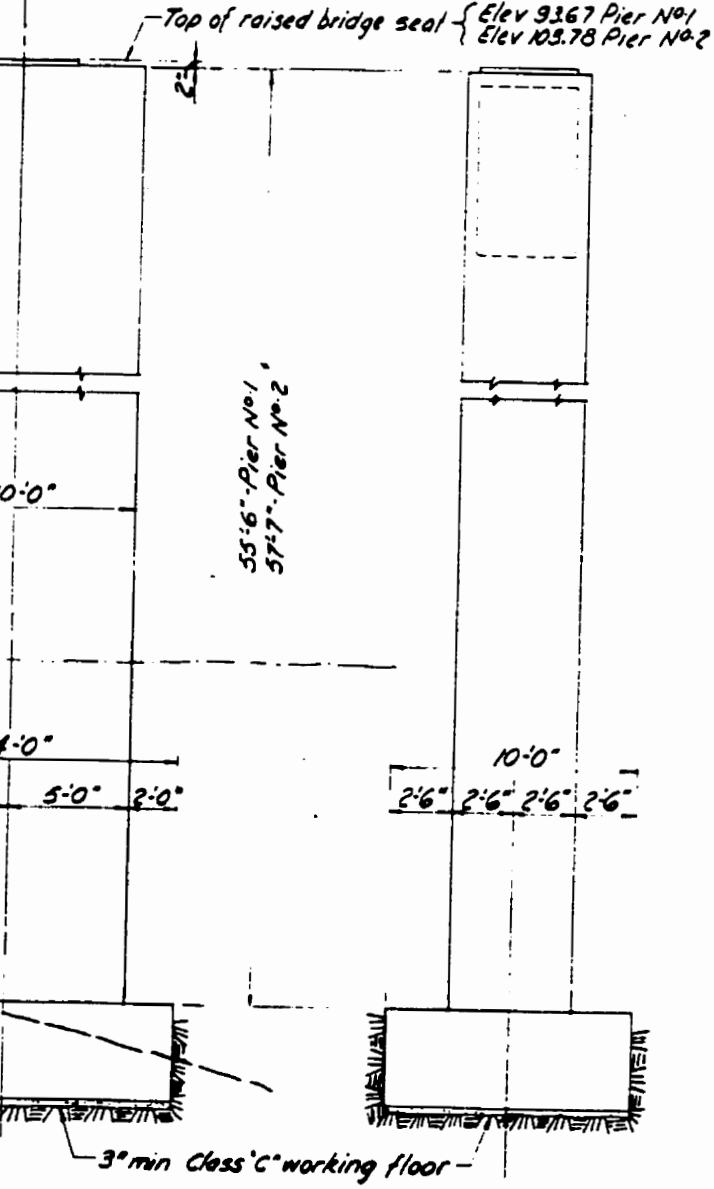

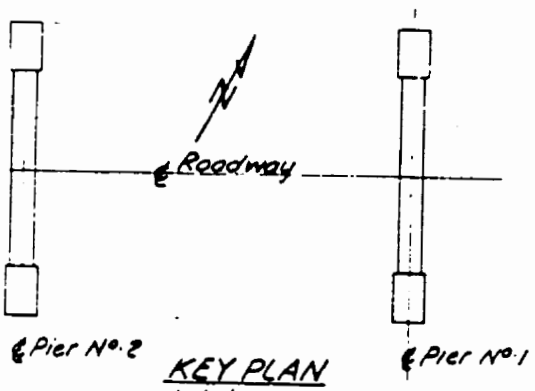

KEY PLAN
Not to Scale

NOTE:
For general notes see Dwg. No. 2621-5

QUANTITIES		
Cl"A" conc.	Cl"C" conc.	Reinforcing
281 cu.yd.	3 cu.yd.	59,250 lbs.
283 cu.yd.	3 cu.yd.	59,700 lbs.
564 cu.yd.	6 cu.yd.	118,950 lbs.

REVISIONS	
D	
C	
B	
A	

BRITISH COLUMBIA DEPARTMENT OF HIGHWAYS
BRIDGE DESIGN
NANAIMO DISTRICT
ISLAND HIGHWAY

ENGLISHMAN RIVER BRIDGE
PIERS

RECOMMENDED
RECOMMENDED
SCALE: 1/4" = 1'-0" AND AS NOTED
DRAWN PYC CHECKED
APPROVED
DRAWING NO. 2621-7

CANCEL PRINTS BEARING EARLIER LETTERS

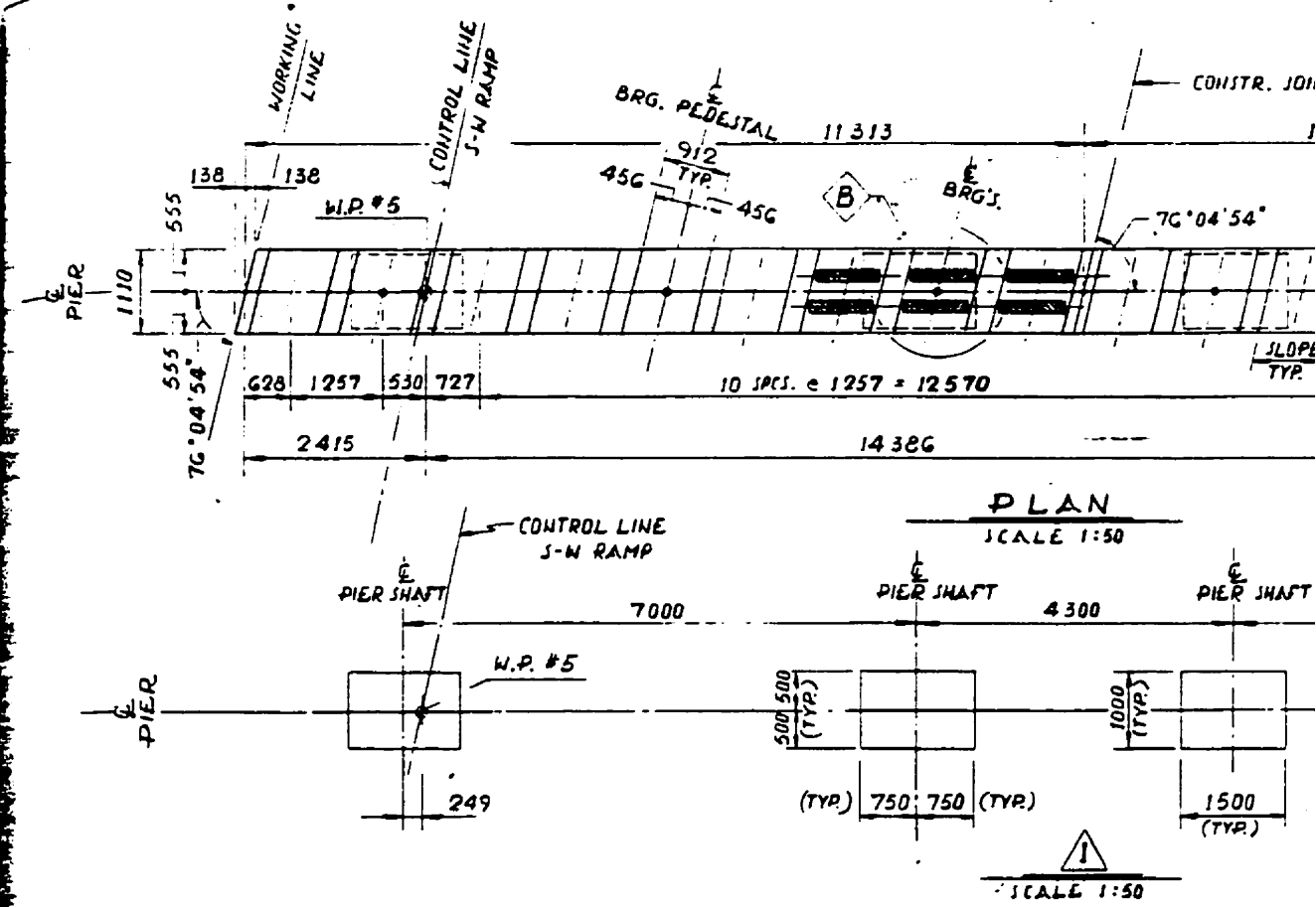

PLAN
SCALE 1:50

1
SCALE 1:50

t	s	r	q	p	o	n	m	l	k	h	g
71.830	71.856	71.883	71.909	71.935	71.962	71.988	72.015	72.041	72.067	72.094	72.12

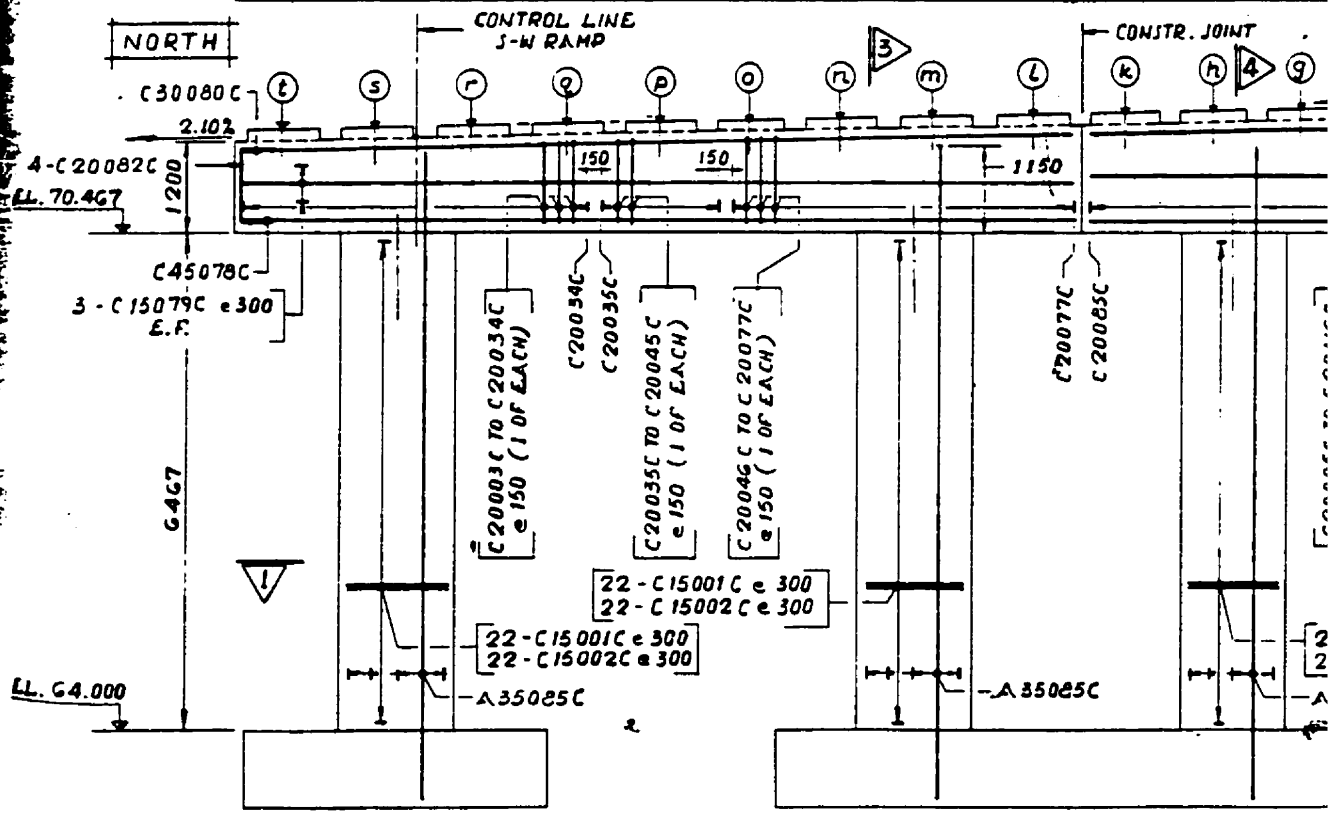

ELEVATION
SCALE 1:50

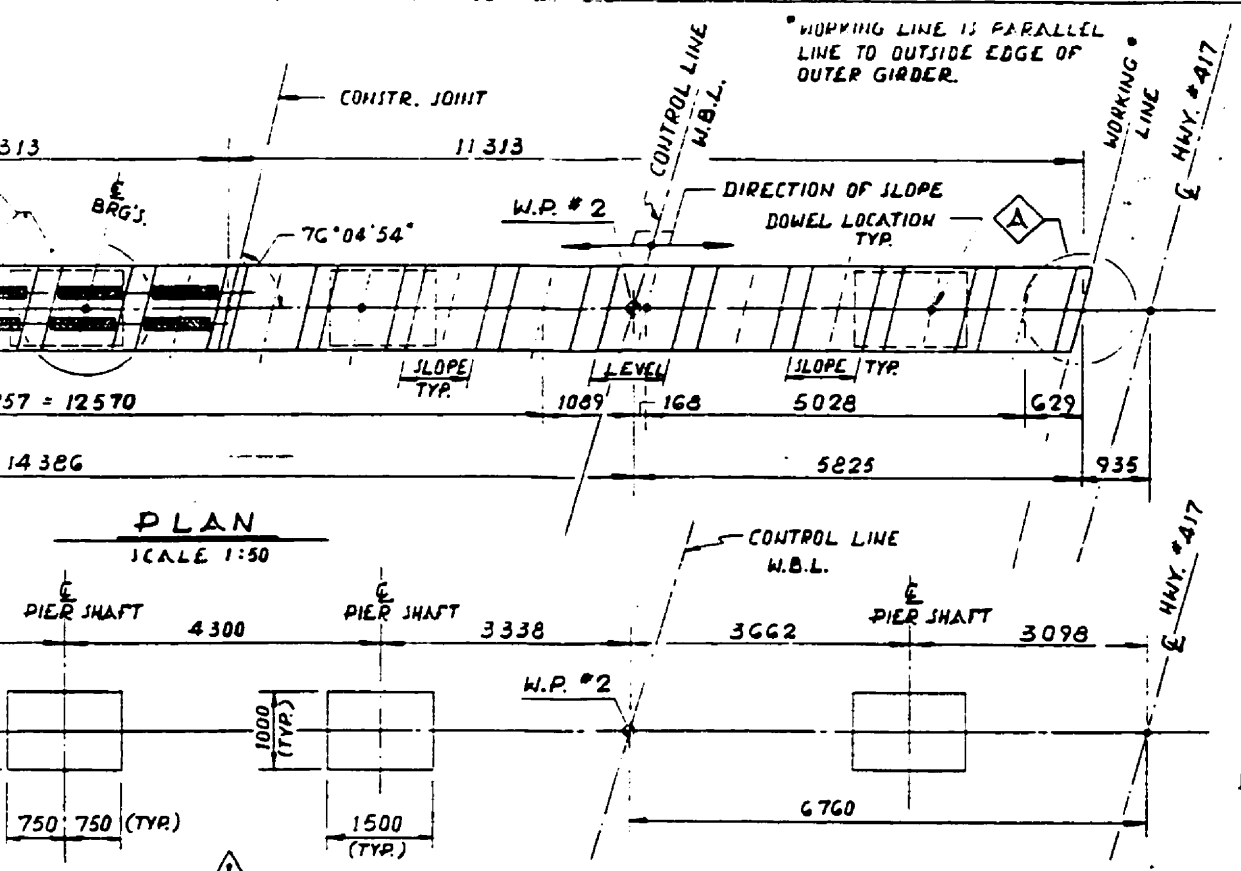

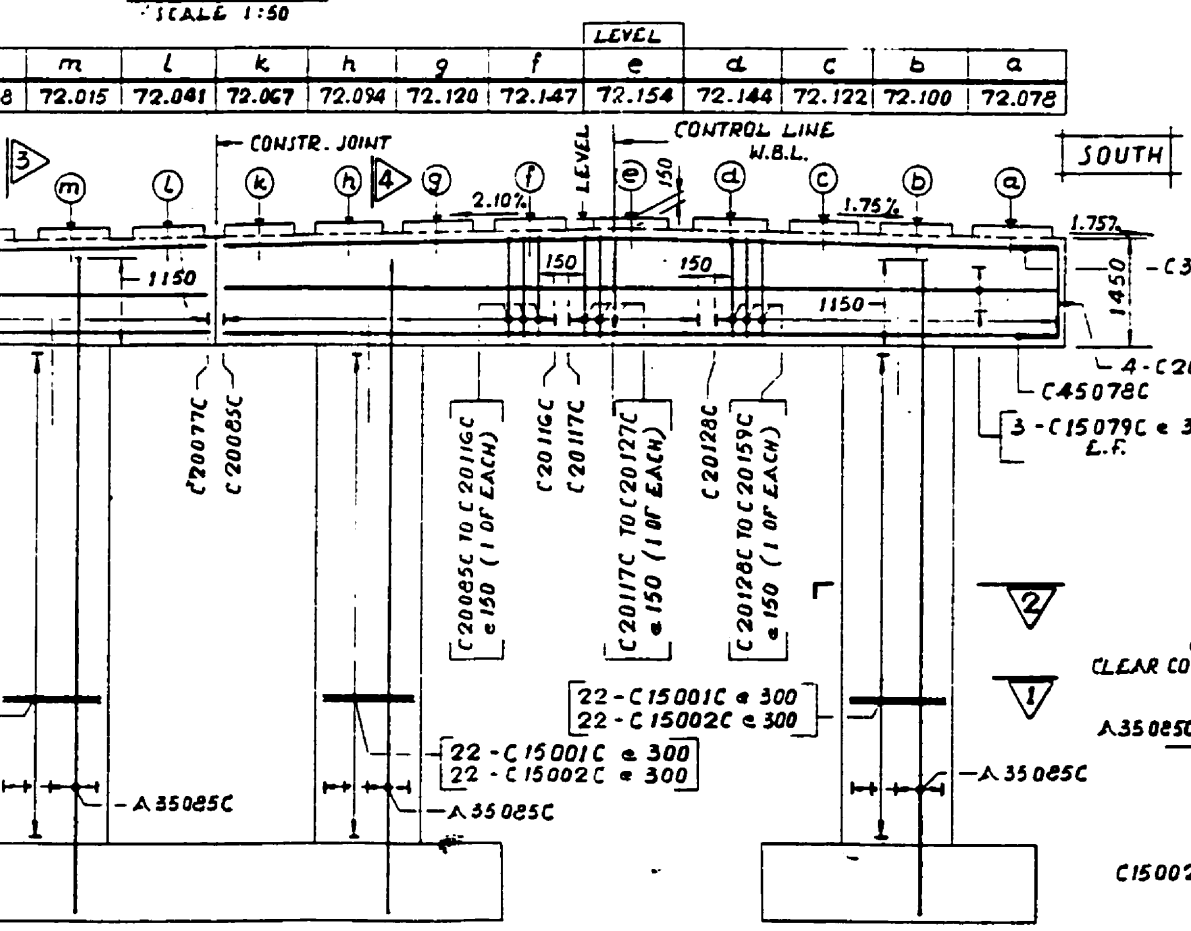

ELEVATION
SCALE 1:50

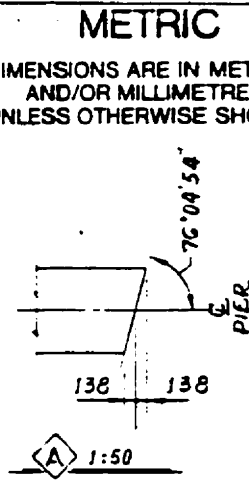

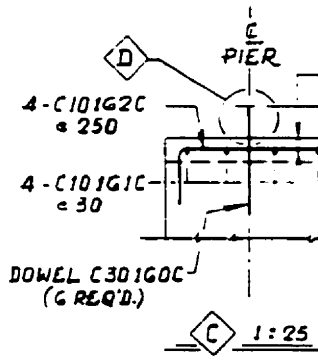

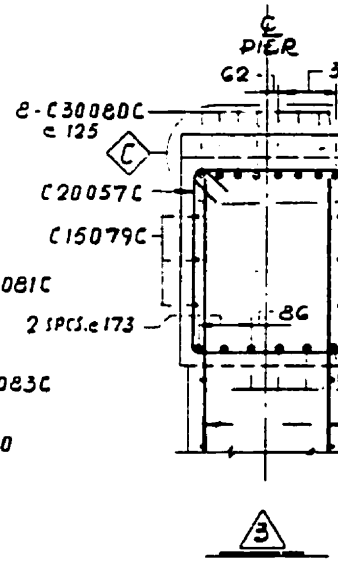

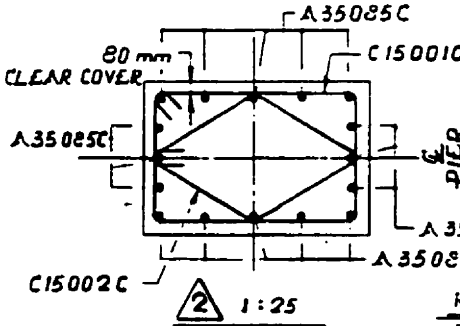

METRIC

DIMENSIONS ARE IN METRES AND/OR MILLIMETRES UNLESS OTHERWISE SHOWN

CONT No 86-40
WP No 62-82-02

ST. LAURENT BOULEVARD
INTERCHANGE OVERPASS
NORTH STRUCTURE
PIER

SHEET 223

*WORKING LINE IS PARALLEL LINE TO OUTSIDE EDGE OF OUTER GIRDER.

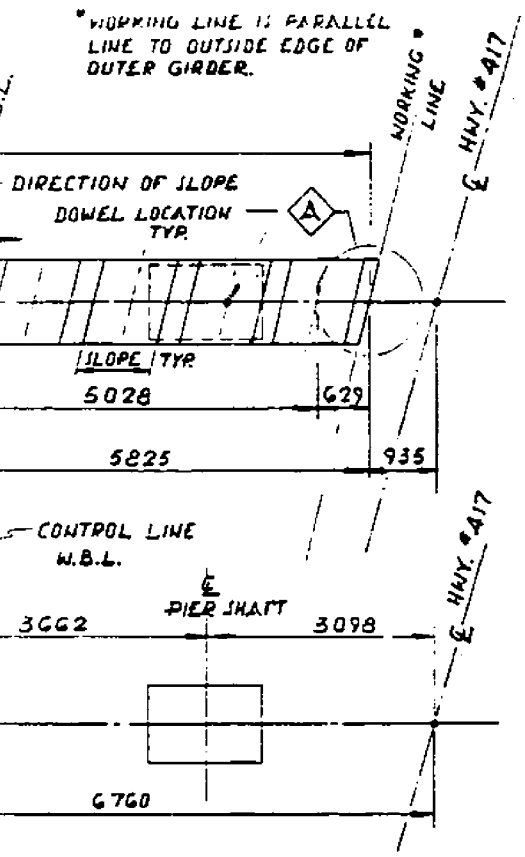

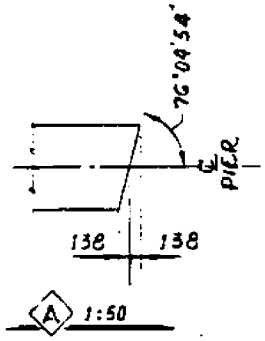

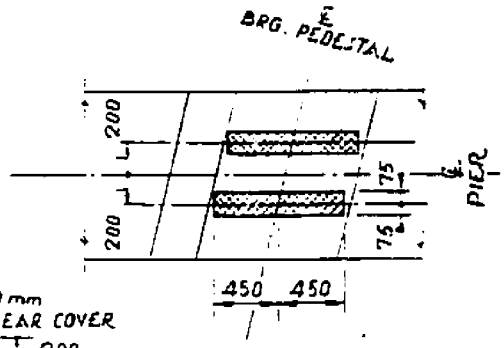

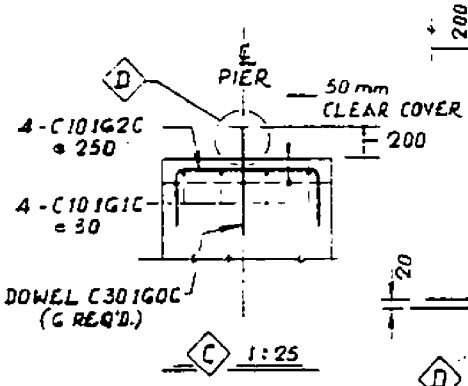

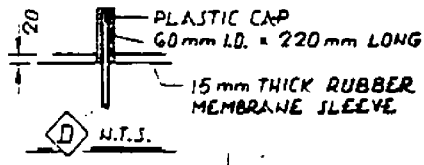

d	c	b	a
2.144	72.122	72.100	72.078

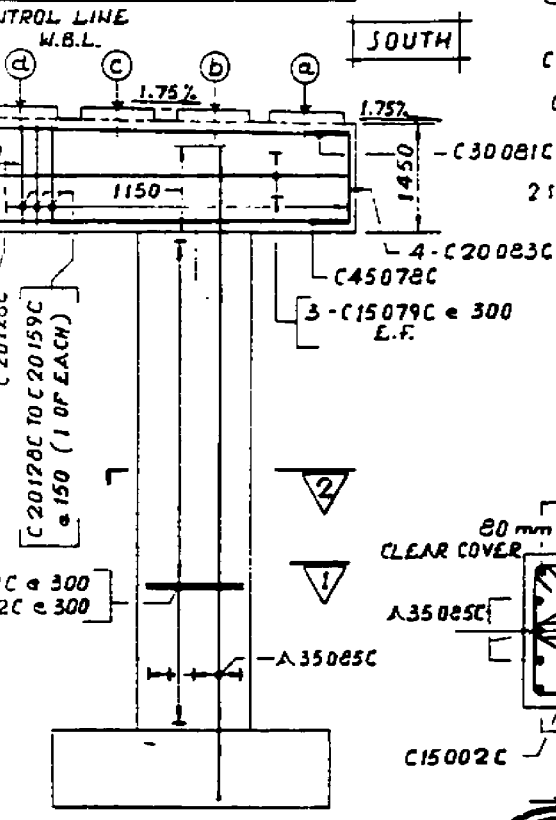

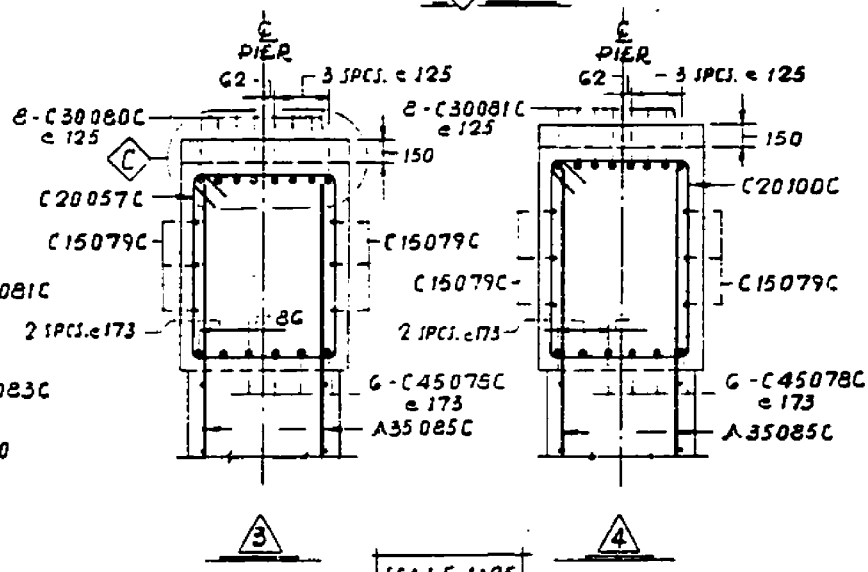

SCALE 1:25

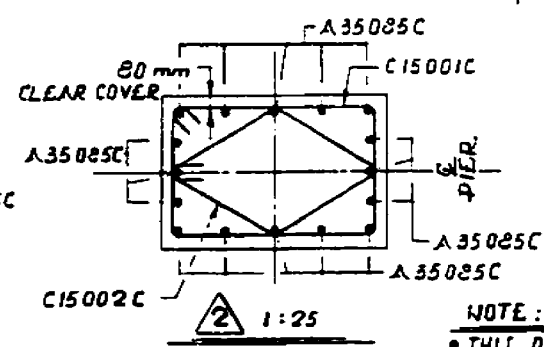

NOTE:

- THIS DRAWING TO BE READ IN CONJUNCTION WITH DWG. #4.
- FOR COMPLETE BRG. DETAILS SEE DWG. #14.

DRAWING NOT TO BE SCALED
100 mm ON ORIGINAL DRAWING

REVISIONS	DATE	BY	DESCRIPTION

DESIGN M.G.	CHECK G.M.	LOADING OHBDC - A - B3	DATE May '85
DRAWING A.A.	CHECK M.G.	SITE No 03-72	DWG A

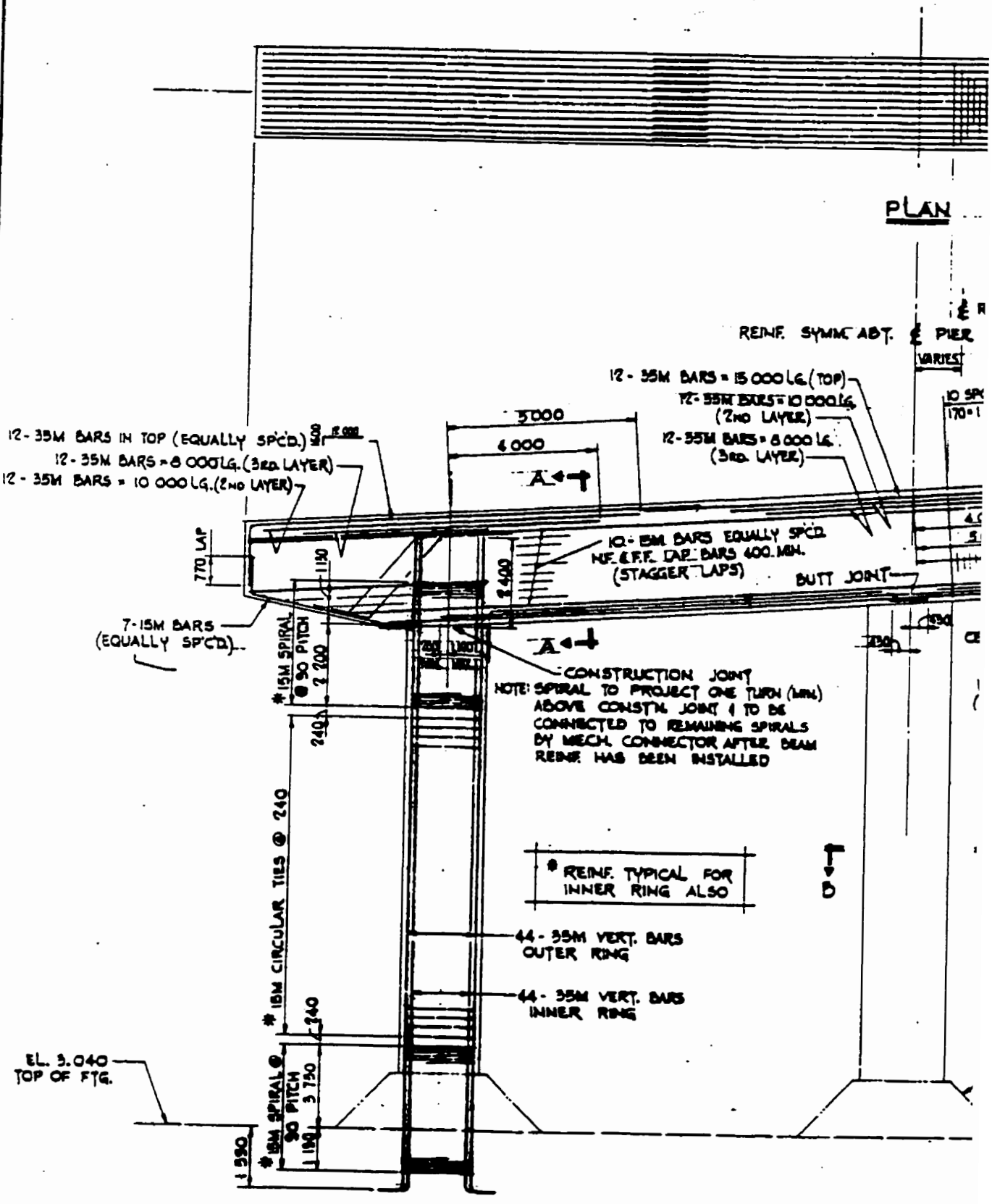

ELEVATION - LOOKI

G - 15M HORIZ. B
LAP 400 MI

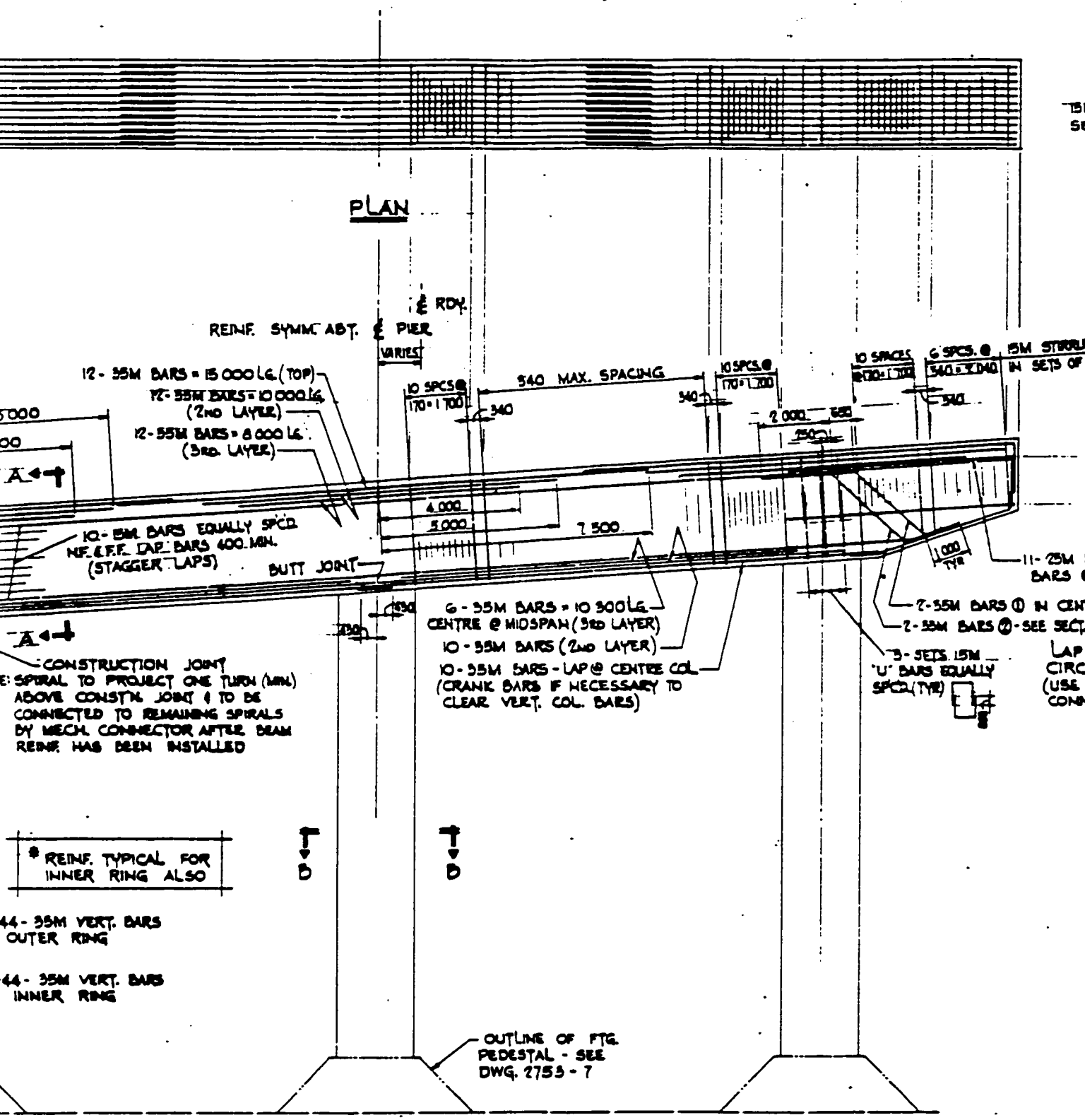

ELEVATION - LOOKING NORTH

D	
C	
B	

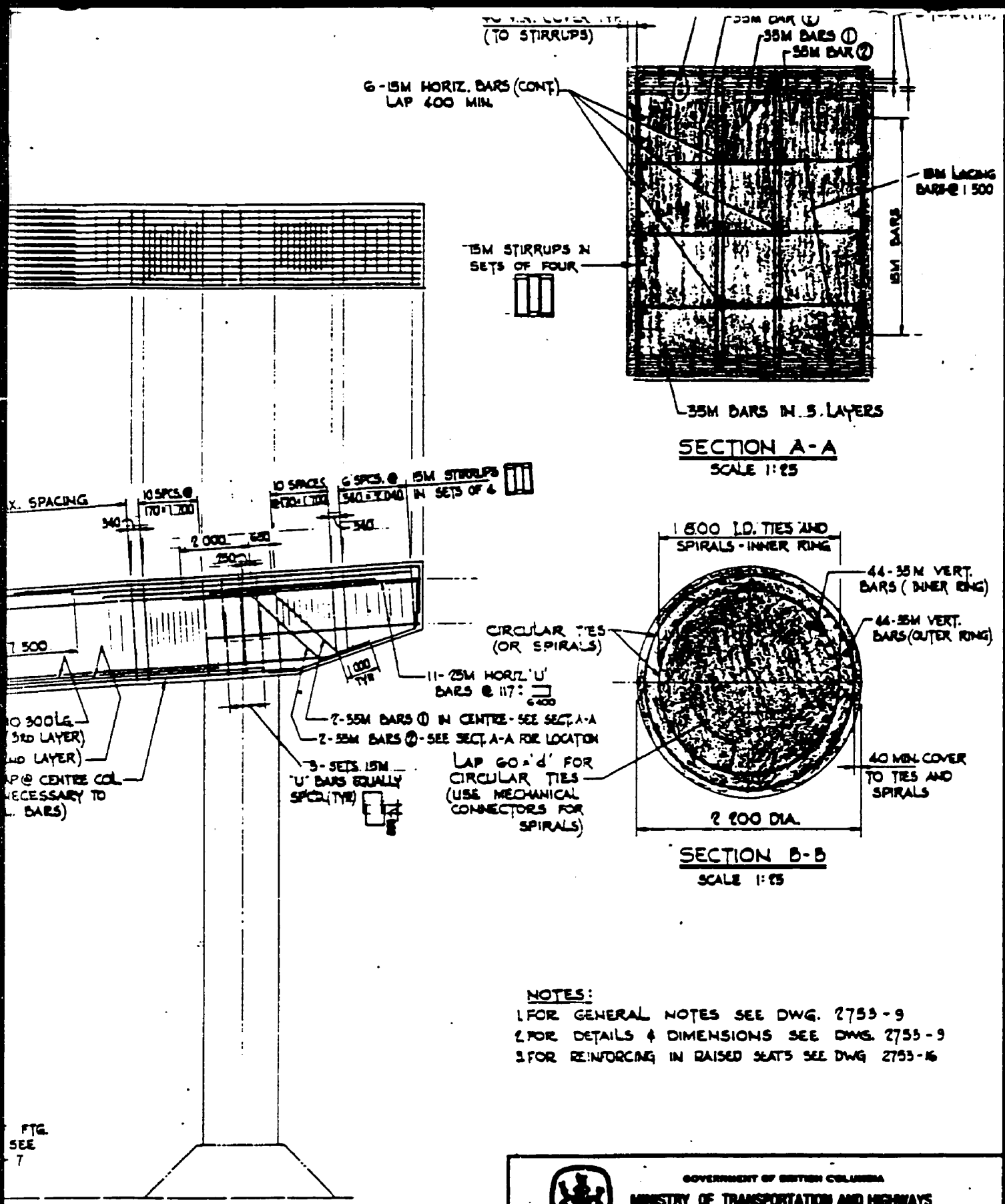

NOTES:

1. FOR GENERAL NOTES SEE DWG. 2753-9
2. FOR DETAILS & DIMENSIONS SEE DWG. 2753-9
3. FOR REINFORCING IN RAISED SEATS SEE DWG 2753-16

GOVERNMENT OF BRITISH COLUMBIA
MINISTRY OF TRANSPORTATION AND HIGHWAYS
BRIDGE ENGINEERING BRANCH

NEW WESTMINSTER DISTRICT

ANNACIS HIGHWAY

ANNACIS BRIDGE NORTH APPROACH PIERS N15 & N16-SHEET Nº2

D			PREPARED UNDER THE DIRECTION OF	DATE	SCALE: 1:75 & AS NOTED			
C			T.K.E. Vickers		DRAWN	D.C.	DEC '85	CHECKED	G.P.	M.R.P.
B			APPROVED FOR USE IN CONSTRUCTION	DATE	EXAMINED AND ACCEPTED		DATE	

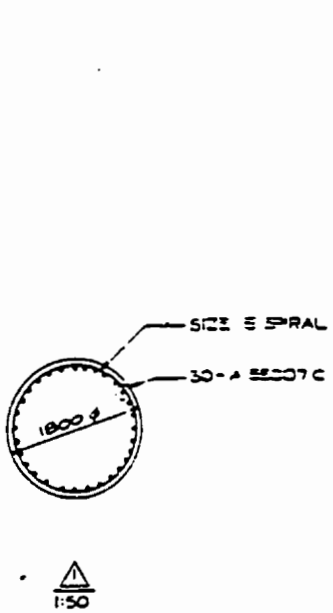

1:50

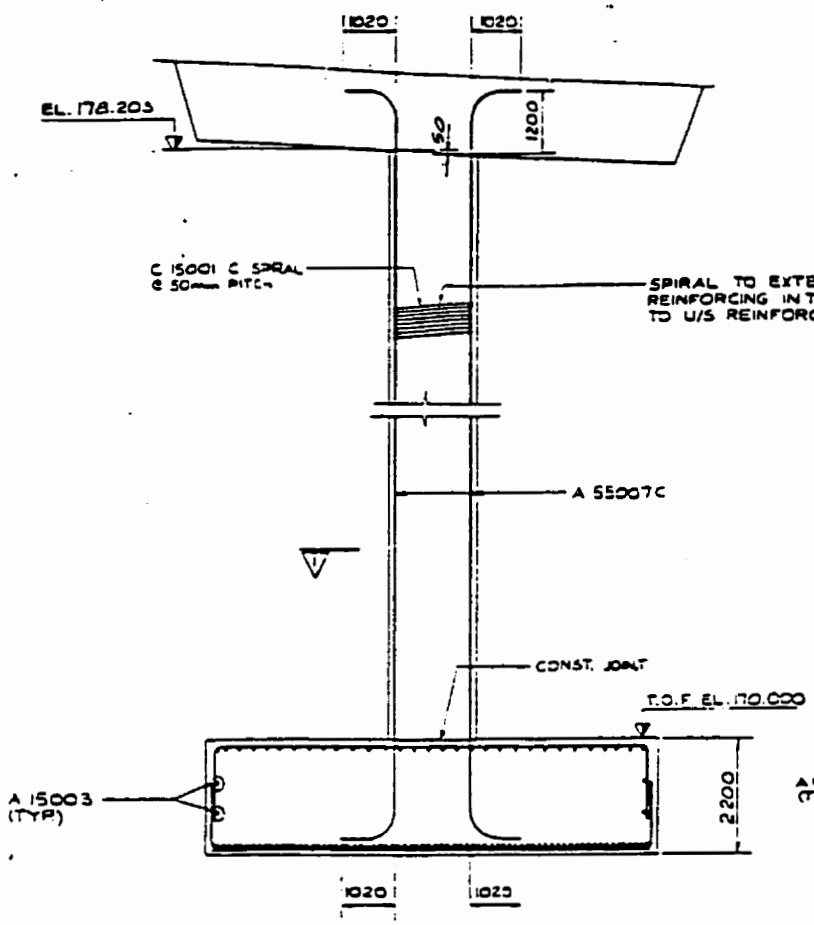

3
1:75

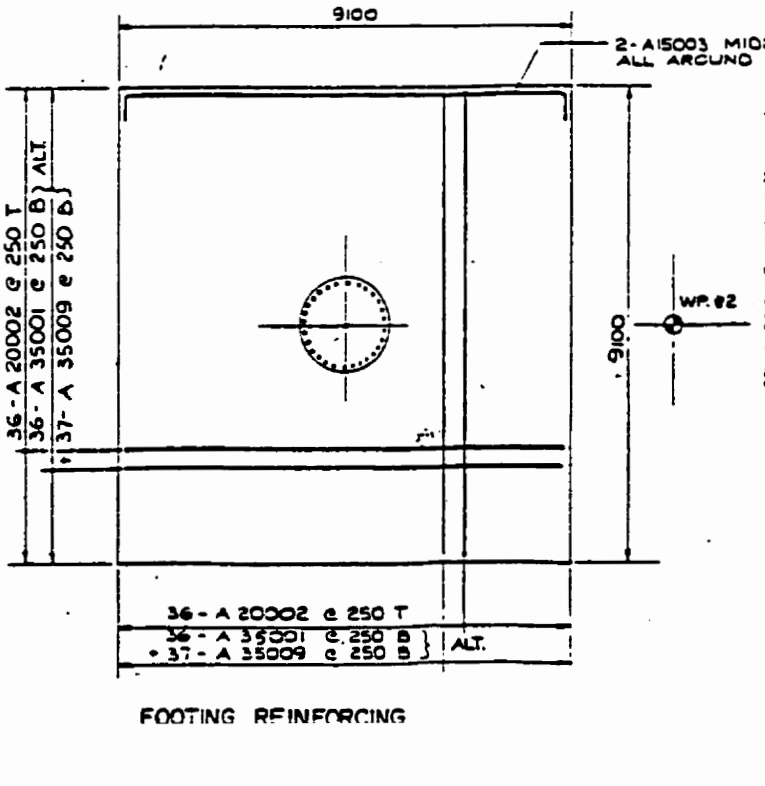

FOOTING REINFORCING

METR

DIMENSIONS ARE
AND/OR MILLI
UNLESS OTHERW

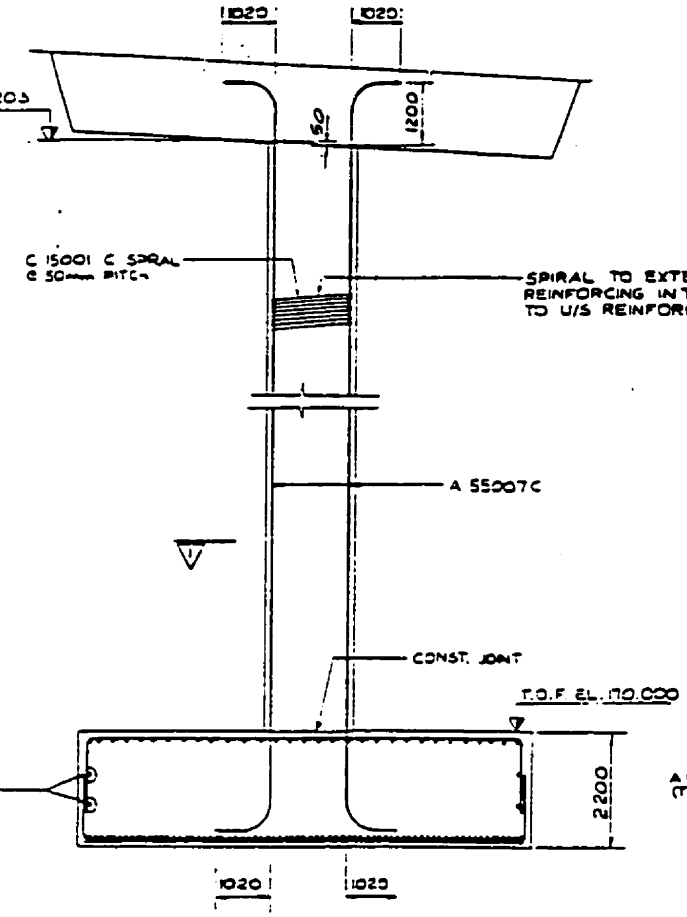

3
1:75

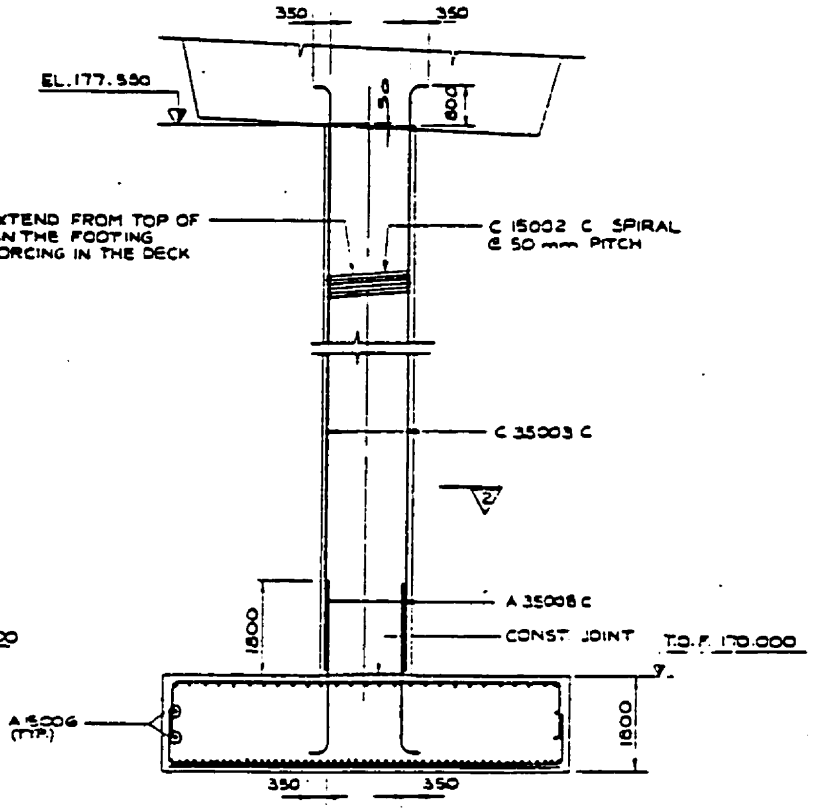

4
1:75

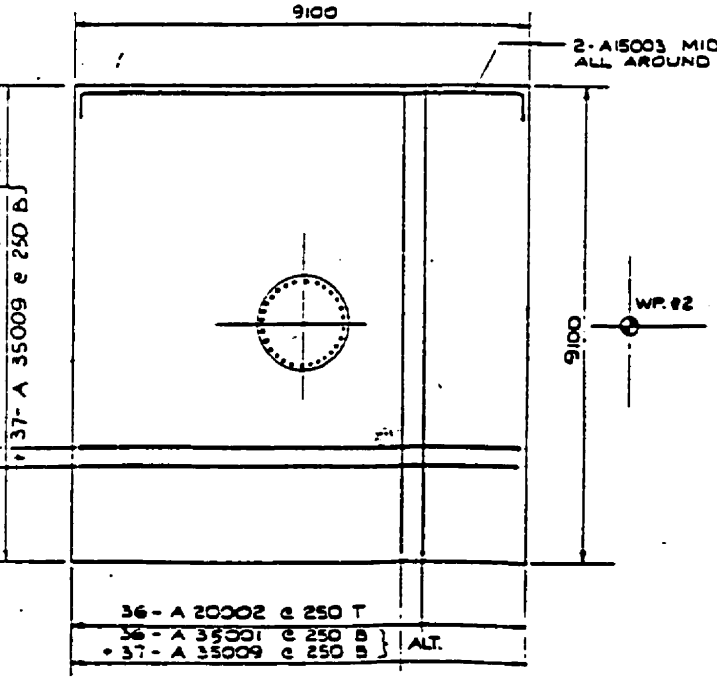

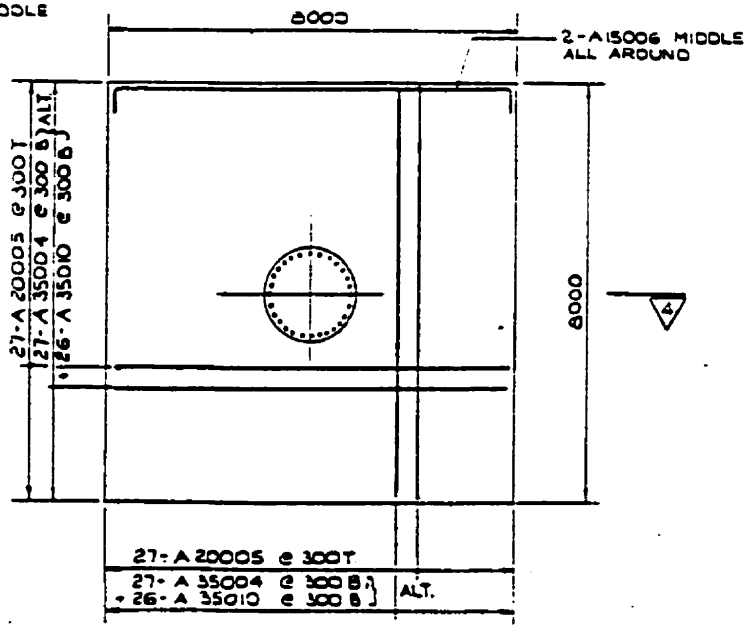

METRIC

DIMENSIONS ARE IN METRES AND/OR MILLIMETRES UNLESS OTHERWISE SHOWN

CONT No 93-100
WP No 369-87-09 (NB) 369-87-10 (SB)

HWY 50 UNDERPASS AT HWY 407

PIER DETAILS

SHEET 169

MARSHALL MACKLIN MONAGHAN LIMITED
CONSULTING ENGINEERS SURVEYORS PLANNERS

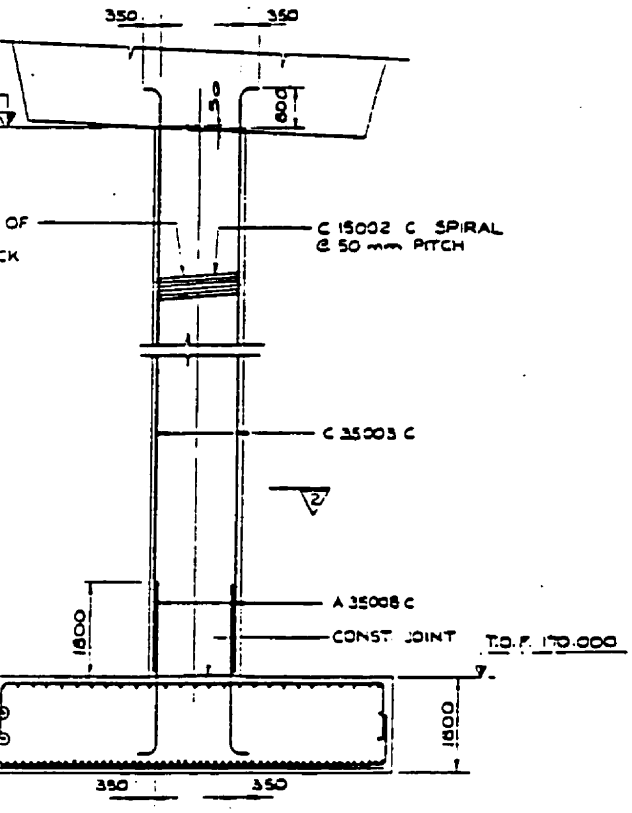

4
1:75

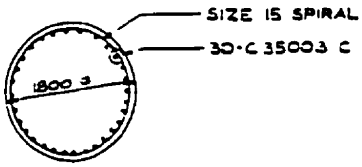

2
1:50

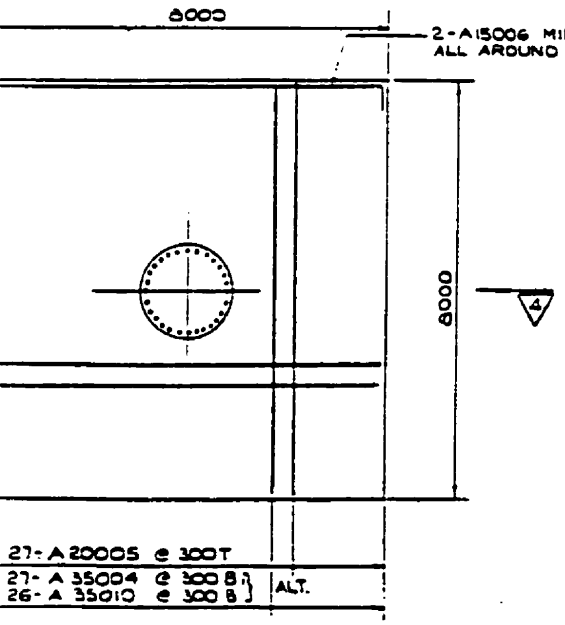

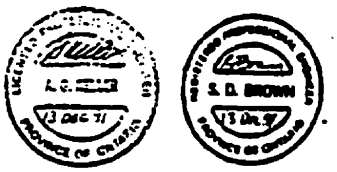

REVISIONS